A Comprehensive Report on Rare Earth Elements in Wyoming

Wayne M. Sutherland and Elizabeth C. Cola



Report of Investigations No. 71 • 2016

WYOMING STATE GEOLOGICAL SURVEY
Thomas A. Drean, Director and State Geologist

Director and State Geologist Thomas A. Drean



Design and layout by:
Elizabeth C. Cola

Calcium phosphate concretions in the Cloverly-Morrison Formations at North Sheldon Gulch. Of all the samples collected during this study, this sample (20150812LC-3A) contained some of the highest rare earth element concentrations.

Cover photo: A north-northwest view of the variegated Cloverly-Morrison Formations at the North Sheldon Gulch locale.

A Comprehensive Report on Rare Earth Elements in Wyoming

Wyoming State Geological Survey (WSGS) Report of Investigations No. 71, 2016

Citation: Sutherland, W.M. and Cola, E.C., 2016, A comprehensive report on rare earth elements in Wyoming: Wyoming State Geological Survey Report of Investigations No. 71, 137 p.

The WSGS encourages fair use of its material. We request that credit be expressly given to the "Wyoming State Geological Survey" when citing information from this publication. Please contact the WSGS at 307-766-2286, ext. 224, or by email at wsgs-info@wyo.gov, if you have any questions about citing materials, preparing acknowledgments, or extensive use of this material. We appreciate your cooperation.

Any use of trade, product, or firm names in this publication is for descriptive purposes only and does not imply endorsement or approval by the State of Wyoming or the WSGS. Individuals with disabilities who require an alternate form of this publication should contact the WSGS. TTY relay operator 800-877-9975.

For additional information about the WSGS or to order publications and maps, log on to http://www.wsgs.wyo.gov, call 307-766-2286, ext. 224, or email wsgs-info@wyo.gov.

A Comprehensive Report on Rare Earth Elements in Wyoming

Wyoming State Geological Survey
Report of Investigations No. 71
2016

Wayne M. Sutherland and Elizabeth C. Cola

Wyoming State Geological Survey, Laramie, Wyoming 82071

Table of Contents

Abstract 1

Introduction 1

Scope and Results of Project 2

Access 2

Samples and Analyses 3

Rare Earth Elements Defined 4

REE Uses. 7

Politics and Supplies 7

REE Prices. 10

Extraction of REE 10

General Geology of REE 12

REE Minerals 12

REE Exploration and Production in Wyoming. 15

Geologic Occurrences of Wyoming REE 16

Bear Lodge Mountains Rare Earth Element Deposit. 18

Precambrian Occurrences 21

Pegmatites 21

Tie Siding Pegmatites 23

Medicine Bow Mountains 28

Many Values Area 28

Big Creek Pegmatite District 30

Sierra Madre 33

Wind River Mountains 34

Owl Creek Mountains. 36

Other Precambrian Occurrences 38

Medicine Bow Mountains and Sierra Madre 39

Granite Mountains, Green Mountain, Ferris-Seminoe Mountains, Pedro Mountains, and Shirley Mountains 44

Bighorn Mountains 51

Wind River Mountains 55

Union Pass–Warm Spring Area 55

Gros Ventre Range. 59

Tertiary-aged Igneous Occurrences . . . 59
Absaroka Mountains and Vicinity . . . 59
Black Hills . . . 59
Rattlesnake Hills . . . 66
Leucite Hills . . . 68
Other Tertiary-aged Igneous Occurrences . . . 69
Sedimentary Occurrences . . . 69
Quaternary Placers . . . 71
White River Formation . . . 72
Green River Formation: Wilkins Peak Member . . . 72
Wind River Formation . . . 77
Battle Spring Formation . . . 80
Lance Formation . . . 82
Fox Hills Sandstone and Lewis Shale . . . 82
Mesaverde Formation . . . 83
Rock Springs Formation . . . 87
Frontier Formation . . . 89
Thermopolis Shale . . . 91
Cloverly-Morrison Formations . . . 92
Phosphoria Formation . . . 94
Flathead Sandstone . . . 100
REE Associated with Uranium Deposits . . . 105
REE Associated with Coal . . . 106
Occurrences of Other Elements and Minerals . . . 112
Conclusions . . . 118
Acknowledgements . . . 118
References . . . 120

List of Figures

Figure 1. Periodic Table of the Elements 5

Figure 2. Sample localities across Wyoming. 17

Figure 3. FMR hand sample photo 19

Figure 4. Sample locations and geology of the Laramie Range. 22

Figure 5. Sample locations and geology of the Tie Siding area.. 24

Figure 6. Tie Siding pegmatites photos 26

Figure 7. Sample locations and geology of the Big Creek pegmatite district and eastern Sierra Madre 29

Figure 8. Big Creek pegmatite photos. 31

Figure 9. Platt Mine euxenite photo. 33

Figure 10. Blackhall Mountain photos. 34

Figure 11. Sample location and geology of the Anderson Ridge area 35

Figure 12. Anderson Ridge garnet photo 36

Figure 13. Sample locations and geology of the Owl Creek Mountains and northern Wind River Basin 37

Figure 14. Sherman Granite photo 42

Figure 15. Sample locations and geology of the Medicine Bow Mountains. 43

Figure 16. Sample locations and geology of the western Granite Mountains area. 45

Figure 17. Jade-related photos.. 47

Figure 18. Sample locations and geology of the western Shirley and Pedro Mountains. 50

Figure 19. Sample locations and geology of The Horn area. 52

Figure 20. Stove Leg prospect photos. 54

Figure 21. Sample locations and geology of the Union Pass-Warm Spring area. 57

Figure 22. Wildcat Road photos. 58

Figure 23. Geology of the Gros Ventre Range 60

Figure 24. Sample locations and geology of the Pilot Knob area. 61

Figure 25. Pilot Knob photos. 62

Figure 26. Sample locations and geology of northeastern Wyoming. 63

Figure 27. Phonolitic rock photos 64

Figure 28. Sample locations and geology of the Rattlesnake Hills area 65
Figure 29. Rattlesnake Hills carbonatite photos 66
Figure 30. Stratigraphic column of Wyoming 70
Figure 31. Sample locations and geology of southeast Green River Basin. 73
Figure 32. Sample locations and geology along the southwestern edge of the Casper Arch 78
Figure 33. Sample locations and geology of the northern Great Divide Basin. 81
Figure 34. Sample locations and geology of black sandstone deposits in Wyoming. 84
Figure 35. Richard's Gap photos 88
Figure 36. Dahllite concretion photos 91
Figure 37. Sample locations and geology of northeast Bighorn Basin. 93
Figure 38. North Sheldon Gulch photos. 94
Figure 39. Sample locations and geology of western Wyoming. 95
Figure 40. Phosphoria Formation photos 98
Figure 41. Geology and sample and drill hole locations near Bald Mountain. 102
Figure 42. Conglomerate of the lower Flathead Sandstone photos. 104
Figure 43. NURE sample localities across Wyoming 107
Figure 44. Tiger Stripe chert photos. 117

List of Tables

Table 1. Rare earth elements 6
Table 2. REE uses.. 8
Table 3. Estimated global mine production and reserves from 2010-15. 9
Table 4. Rare earth element prices from 2013-15. 11
Table 5. Rare earth bearing minerals in Wyoming 14
Table 6. Rare Element Resources, Ltd., Bear Lodge Project 45 year plan. 20
Table 7. Concentration of REE from the Tie Siding area. 25
Table 8. Concentration of REE from the Weddle claims 28
Table 9. Concentration of REE from Big Creek pegmatite district. 32
Table 10. Concentration of REE from Blackhall Mountain. 34
Table 11. Concentration of REE from the Anderson Ridge area 36
Table 12. Concentration of REE from the Allie claims 38
Table 13. Concentration of REE from the Onemile Creek area. 40
Table 14. Concentration of REE from the Broadway mine 41
Table 15. Concentration of REE in Sherman Granite from the Albany area 42
Table 16. Concentration of REE from the Clarence Wood lode claims 46
Table 17. Concentration of REE from jade-related locales. 47
Table 18. Concentration of REE from the Gap claims. 48
Table 19. Concentration of REE from the Babbs mine 49
Table 20. Concentration of REE from the Omega claims 49
Table 21. Concentration of REE from the Bull Camp prospects 53
Table 22. Concentration of REE from the Stove Leg prospect. 54
Table 23. Locations and host rock of samples from the Wind River Range 56
Table 24. Analyses of historic samples from the Wind River Range. 56
Table 25. Concentration of REE from the Union Pass-Warm Spring area 58
Table 26. Concentration of REE from Pilot Knob. 62
Table 27. Concentration of REE from the Mineral Hill area 64

Table 28. Concentration of REE from carbonatite and potentially related rocks in the Rattlesnake Hills area . . 67
Table 29. Concentration of REE from the Leucite Hills area. 69
Table 30. Measured section of the lower part of the Wilkins Peak Member of the Green River Formation 74
Table 31. Concentration of REE from South Firehole Canyon 75
Table 32. Concentration of REE from Southwest Pine Mountain 77
Table 33. Concentration of REE from the northern Wind River Basin 79
Table 34. Concentration of REE from the Deacon's Prayer group claims. 79
Table 35. Concentration of REE from the Poison Spider deposit 82
Table 36. Concentration of REE from black sandstone deposits 85
Table 37. Concentration of REE from Richard's Gap 88
Table 38. Concentration of REE from Spring Gap area and Frontier Formation 90
Table 39. Concentration of REE in dahllite near the Wyo-Ben Mine 91
Table 40. Concentration of REE from North Sheldon Gulch 94
Table 41. Concentration of REE from the Phosphoria Formation. 97
Table 42. Concentration of REE from the Rawlins Red deposit 101
Table 43. Concentration of REE from Bald Mountain 103
Table 44. Concentration of REE from the western Rattlesnake Hills. 104
Table 45. Concentration of REE from coal and coal-related rocks in Wyoming. 109
Table 46. Concentration of REE from coal and coal-related rocks internationally 110
Table 47. Concentration of REE from coal and coal-related rocks in Kentucky. 111
Table 48. Major element oxide composition of the Tensleep Sandstone in Bison Basin 115

ABSTRACT

The rare earth elements (REE) are a group of 17 metals with similar physical and chemical properties that include the lanthanide series elements plus scandium and yttrium. Sixteen REE occur in nature, while promethium (Pm) is highly-unstable and does not occur naturally on Earth. REE are considered strategic metals in the United States and are necessary for energy generation, transportation, data transmission, and national defense. However, production of REE has been negligible in the United States since the early 2000s. Production increased briefly with the 2010 re-opening of Molycorp's Mountain Pass Mine in California, but since the closure of this operation in 2015, there has been no domestic production.

Planned mining and processing of the Bear Lodge REE deposit by Rare Earth Element Resources, Ltd. in northeastern Wyoming held promise for significant new United States production until poor market conditions forced the company to temporarily halt operations in early 2016. A restart of that project could replace production formerly provided by Molycorp and reduce dependence on China, which has accounted for more than 90 percent of the global supply in the past decade. Exploration for REE that began several years ago, when prices were high, continues across the country, although at a reduced level due to current low REE prices.

In Wyoming, investigations in the mid-20th century identified many sites that either hosted REE or were later interpreted to be potential REE occurrences. Unfortunately, these studies lacked complete elemental analyses. In 2012–13, the Wyoming State Geological Survey (WSGS) collected samples from many known, suspected, and potential REE host rocks and analyzed them for REE content and other potential economic elements. That data was published in WSGS Report of Investigations 65 by Sutherland and others (2013). Many samples were collected and analyzed for RI-65, and the aim of the RI-71 study is not only to analyze additional sites but to provide further information on sites that showed higher REE concentrations in the 2012–13 investigation. This report contains data from the 2015 field season and summarizes previous studies to produce a comprehensive report on the investigations of REE in Wyoming.

REE enrichment occurs in a variety of geologic environments across Wyoming. These environments include carbonatites, granites, pegmatites, epidosite dikes, calc-silicate pods and dikes, iron-rich silicate pods, paleoplacers in marginal marine sandstones, phosphatic horizons in marine shales and lacustrine mudstones, and apparent secondary mineralization from fluid movement within porous sandstones. The WSGS has developed a publicly accessible online database, the Wyoming Database of Geology (WyoDOG), which contains locations, geologic settings, and analyses for all samples in this and earlier reports. This database may aid mineral exploration across the state by identifying REE and other potentially economic elements.

INTRODUCTION

Rare earth elements (REE) are a group of metallic elements with similar physical and chemical properties. REE are a vital resource to industrialized societies worldwide. In the last 15 years, REE production and processing have centered in China, which by 2010 provided 95 to 97 percent of the world's supply (Northern Miner, 2010; Els, 2015). When China reduced REE exports by 40 percent in 2010, as compared to 2009, world demand exceeded the supply (Bradsher, 2010; Davis, 2011; Grace, 2010). This inspired heightened REE exploration and development by other countries to meet demand and offset the elevated price. The 2010 reopening of Molycorp's Mountain Pass Mine in California increased the United States' supply for a short time. However, its recent closure and China's stronghold on global supply has continued driving interest in securing REE resources to maintain U.S. national security. Development of REE in Wyoming would contribute to the diversification of the state's economy and benefit the national supply.

REE occurrences have been documented statewide since the 1930s. However, early exploration primarily focused on uranium and thorium, and REE were only an interesting association. Marzell (1932) reported production of 363 kg (800 lbs) of samarskite in 1930 but gave no source location. REE mineralization associated with thorium from the Bear Lodge Mountains was reported in 1949 (Rare Element Resources, Ltd., 2011). Radioactive monazite, a thorium- and REE-hosting mineral, was found in paleoplacers of the northern Bighorn Mountains in 1950 (Wilson, 1951; McKinney and Horst, 1953a). The U.S. Bureau of Mines (USBM) and the U.S. Atomic Energy Commission (USAEC) investigated these monazite paleoplacers between 1951 and 1953 (Klein and Winkel, 1952; McKinney and Horst, 1953a; b), but no REE analyses were reported. Between 1952 and 1955, allanite-bearing ore was reportedly mined in the southern Bighorn Mountains (Bromley, 1955), and a small amount of REE-bearing minerals were mined from a pegmatite in Carbon County during the 1950s (King and Harris, 2002).

Most early REE studies identified the potential for REE occurrences based on other elements and environmental factors but did not produce detailed analyses due to high analytical costs. Modern technology has significantly reduced the cost of high quality, detailed analyses, but historically, follow up studies in Wyoming have been slow

due to time and budget constraints. The Wyoming State Geological Survey (WSGS) compiled an open file report on REE and yttrium in Wyoming in 1987, which was updated in 1991 and 2002 (King and Harris, 1987; 2002; King, 1991). These reports were based on literature searches and did not include any original sampling or analyses. Between 2009 and 2012, the WSGS began to verify and expand on these reports by sampling and analyzing potential REE host rocks within the state. Using WSGS Open File Report 91-3 (King and Harris, 2002) as a foundation, the WSGS compiled data from existing sources, collected and analyzed more than 300 samples, and re-analyzed some samples collected at earlier dates. This information was released in WSGS Report of Investigations 65 (Sutherland and others, 2013).

The Wyoming State Legislature, in 2014, allocated approximately $94,000 of Abandoned Mine Reclamation (AML) funds to the WSGS to continue its investigations into REE occurrences within Wyoming. These funds are the unspent remainder from $200,000 in legislatively-approved funding that financed the RI-65 study. Due to time constraints of the initial grant, numerous potential REE occurrences were not sampled. This investigation fills in gaps and provides additional information where the original report left off. It also encompasses synopses of previous reports to create a comprehensive summary of REE in Wyoming. Results from the current investigation include a written summary report, related maps, and new entries, including elemental analyses, into the WSGS's publicly available online database, Wyo-DOG. Overall, more than 275 new samples were collected and analyzed for this investigation from known and potential host rocks for REE and other minerals. Another 45 samples previously collected by the WSGS for other projects were analyzed and are included in the results of this study (appendix 1) along with analyses from RI-65 (appendix 2). Thousands of data points from the National Uranium Resource Evaluation (NURE) database were also evaluated. The NURE program's primary goal was to identify uranium resources in the United States, during which extensive sampling of water, sediments, and rocks took place in the 1970s and 1980s. This study assessed the NURE data for samples with elevated REE content (appendix 3).

SCOPE AND RESULTS OF PROJECT

The current project continues the investigation of REE where RI-65 (Sutherland and others, 2013) left off. This report expands on the material found in RI-65, includes more extensive historical source material, and provides additional comprehensive evaluation of REE occurrences and their environments. These include carbonatites and related rocks in central Wyoming, REE associated with Wyoming coal deposits, and REE occurrences in association with uranium deposits. The report also significantly increases the number of analyses for REE and other elements across Wyoming.

Information provided from this project should be useful to individuals, consultants, legislative constituents, and industry as a base for initiating exploration not only for REE but for other industrial/economic metals and elements as well. Anomalous concentrations of certain elements may be pathfinders that lead to the discovery of other economic deposits. For example, an abundance of arsenic in some geological settings is considered a pathfinder for gold. A database of our sample analyses, locations, and geologic settings may aid in exploration to identify these anomalous occurrences. It is hoped that educational institutions may also use these data to better understand the often complex geologic environments in Wyoming. Decision makers at state and community levels may find this information useful in identifying potential areas of economic development or environmental concern.

The findings of this investigation, related maps, and analyses are also available on the WSGS website at http://www.wsgs.wyo.gov. The Wyo-DOG online database includes all elemental analyses along with brief write-ups and photographs for most samples, making the results of this study available to a wide audience for exploration, evaluation, and education. Data from Wyo-DOG can be displayed in several formats, including ArcGIS and Google Earth.

ACCESS

Many locations described in this report may not be publicly accessible based on land ownership. Private lands may not be accessed without permission from the landowner. Descriptions of sites that occur on private land or on the Wind River Indian Reservation are compiled from historical sources, or access was granted by the landowner. Access to the reservation can only be granted from reservation officials. No sites were visited within the Wind River Indian Reservation during this study. The WSGS does not investigate mineral rights, nor does it provide economic evaluation for specific properties. Evaluation of mineral rights and the economics of specific properties are left to private companies and individuals.

Mining claims may cover some areas of interest, and prospecting cannot be conducted on claims without the claimant's permission. Mining claim information, along with claimant contact information, should be available in the courthouse for the county in which the claim is staked. That information is also available at the U.S. Bureau of Land Management (USBLM) Wyoming State Office in Cheyenne. The phone number for the USBLM in Cheyenne is (307) 775-6200, and the web page is http://

www.blm.gov/wy/st/en.html. Contact information for claimants may also be found on claim posts that mark the claim's location on the ground.

Public lands administered by the State of Wyoming, the U.S. Forest Service (USFS), or the USBLM each have sets of rules governing these activities in specific areas. Check with the proper agency before proceeding. USBLM information about exploration and development regulations for locatable minerals are found at http://www.blm.gov/wy/st/en/programs/mineral_resources/Surface.html.

Both the USBLM and USFS produce maps that show general land ownership. The WSGS publications sales desk carries many of these maps; contact (307) 766-2286 or visit https://sales.wsgs.wyo.gov/catalog/index.php. Up-to-date land ownership information can only be relied upon from the courthouse for a particular county.

SAMPLES AND ANALYSES

This investigation is a survey of grab samples (i.e. small, unmeasured samples, not considered to be representative of a larger volume of material) from various sites across Wyoming. Analyses of these grab samples can neither confirm nor deny the presence or absence of economic concentrations of REE or other elements. A grab sample only represents one small piece of evidence for the occurrence of a mineral concentration or deposit and is not associated with, nor does it indicate a volume of material greater than the size of the individual sample. The elemental concentrations associated with a grab sample may or may not extend into the outcrop from which it was collected.

No single sample can define or eliminate the possibility of an economic deposit. A thorough evaluation of a deposit, as opposed to a survey of occurrences as presented in this report, requires multiple samples be evaluated across the range of geologic environments that occur at a specific location. Each of those samples must represent a specific volume of relatively uniform material such that elemental concentrations, coupled with deposit modeling and other factors, can be converted to tonnage estimates across the deposit. Only then can the economic tenor of the deposit be estimated.

Not all samples are equal. The analysis of a panned concentrate from a placer sample is not equivalent to that of a grab sample. A panned concentrate results from washing disaggregated minerals in the field with water to separate out the heavier ones from lighter ones. Analytical results may show relatively high values for some elements in the concentrate. To provide proper perspective, a panned concentrate analysis must be diluted to represent the original larger volume of material from which the concentrate was derived. This dilution may reduce reported values by a factor of 10 to 100 or more, depending on techniques and equipment used during sampling.

All sample analyses for this project were conducted by ALS Chemex of Reno, Nev. Analytical methods for historic samples, included within Wyo-DOG or this report, are referred to as generic if either the laboratory or the method of analysis is unknown. Geochemical analyses of samples include whole rock analyses (major element concentrations in the form of oxides) by inductively coupled plasma (ICP), atomic emission spectrometry, mass spectrometry, and atomic adsorption. These methods, when preceded by effective preparation techniques, can generally detect most elements present in a sample from very low concentrations, in the range of less than 0.1 to 5 parts per million (ppm), up to ore-grade concentrations. To put this in perspective, 1.0 percent is equal to 10,000 ppm.

Analyses cited here from other published sources, such as King and Harris (2002) or National Uranium Resource Evaluation (NURE) program data compiled by Smith (2001) are assumed to be reasonably accurate for the purposes of this survey of REE in Wyoming. For serious exploration of any occurrences described here in, geologists and prospectors should verify analyses through their own sampling and analytical procedures.

Samples from the NURE program with any REE analyses were reviewed for this report. NURE was initiated in 1973 by the Atomic Energy Commission, now the U.S. Department of Energy (USDOE), primarily to identify uranium resources in the United States. A large amount of chemical data was amassed from sediment, soil, and water samples collected across the United States in the late 1970s and early 1980s. Sediment and soil samples from Wyoming specifically were collected by contractors for the Los Alamos Scientific Laboratory from 1976 to 1979. This part of the NURE program was known as the Hydrogeochemical and Stream Sediment Reconnaissance (HSSR). Analysis for up to 52 different elements were made for various sediment and soil samples, although no individual sample was analyzed for all 52.

The NURE HSSR program, intended to cover the entire United States, began in 1975 and ended in 1980, before the project could be completed. Samples were analyzed and resultant geochemical data were released in several publications. In 1985, the NURE HSSR sample archive, original field maps, field notes, and data tapes became the responsibility of the U.S. Geological Survey (USGS). A copy of the NURE HSSR database was released as two CD-ROM publications (Hoffman and Buttleman, 1994; 1996). The

USGS began a new effort to recompile the NURE HSSR data in 1995, which was released as an online open file report (Smith, 2001).

The NURE data released by the USGS and accessed for this REE investigation is organized in 1 degree x 2 degree quadrangles that cover Wyoming and can be found at: http://mrdata.usgs.gov/nure/sediment/select.php?place=fUS56&div=quad.
An online manual describing the intricacies of the data is found at: http://mrdata.usgs.gov/nure/sediment/NURE_Manual.html.
Detailed discussions of NURE data for each 1 degree x 2 degree quadrangle in Wyoming are found at: http://pubs.usgs.gov/of/1997/ofr-97-0492/state/nure_wy.htm.
Cumulatively, we reference these interrelated hosts for the NURE data as (Smith, 2001).

The USGS online database includes 18,527 records of geochemical analyses for sediment samples collected within the State of Wyoming. This NURE HSSR data was used to augment the current REE investigation and to help verify, if possible, historic reports of REE occurrences and occurrences of other elements. A search of that database found 113 samples that showed greater than five times the average crustal abundance of one or more REE. The locations of these elevated samples can be found both in figures within this report and in the appendix 3.

RARE EARTH ELEMENTS DEFINED

Rare earth elements (a.k.a. rare earth metals) are a group of metallic elements with similar physical and chemical properties. Fifteen of these, known as the lanthanide series, are listed in the periodic table in succession from atomic numbers 57 through 71 (fig. 1). However, one highly unstable element, promethium, does not occur naturally on Earth, has a half-life of 17.7 years, and decays into neodymium-145 through a type of radioactive decay called electron capture.

Two other elements not within the lanthanide series, scandium (atomic number 21) and yttrium (atomic number 39), are generally included within the group of REE because of their shared occurrence in nature with the lanthanides. Within this report, the acronym "REE" is inclusive of these elements except in our discussion of coal, because most coal-centered investigations refer to "REE plus Y"; this terminology will be used where appropriate. With the inclusion of scandium and yttrium, there are 16 naturally-occurring REE.

Rare earths were named from perceived scarcity during the 18th and 19th centuries, *rare*, and an obsolete term for oxide, *earth* (Hedrick, 2004; Long and others, 2010). REE are now known to be relatively common within the earth's crust. Even the two least abundant REE, thulium (Tm) and lutetium (Lu), are nearly 140 to 180 times more common in the crust than gold. However, economically mineable concentrations of REE are not common. REE range in crustal abundances from cerium, the 25th most abundant of the 78 common elements in the earth's crust at 60 ppm, to thulium and lutetium, the least abundant REE at about 0.5 ppm (table 1). Estimates of crustal abundances vary depending on the reference source.

REE are arbitrarily subdivided into Light Rare Earth Elements (LREE) and Heavy Rare Earth Elements (HREE) based on their atomic weight (table 1; Hedrick, 2004). LREE include the elements lanthanum (atomic number 57, atomic weight 138.91) through samarium (atomic number 62, atomic weight 150.36); while HREE are europium (atomic number 63, atomic weight 151.96) through lutetium (atomic number 71, atomic weight 174.97).

In their elemental form, REE are iron gray to silver, malleable, ductile, and soft metals that are unstable in the presence of oxygen and readily react to form metal oxides. Chemically, REE are generally trivalent, but exceptions occur with cerium, europium, and ytterbium. Cerium forms compounds with a valence of +4. Europium can be divalent and oxidizes much more readily than the trivalent REE, forming a yellow surface coating of Eu(OH) within minutes after exposure to moist air. Ytterbium has a closed shell electron configuration, making it reluctant to share electrons with oxygen or other elements and relatively inert; thus, it can be handled in air without any difficulty (Borzone and others, 1999).

The reactivity of most REE is problematic for shipping and long-term storage in elemental form. Because of this, REE are often reported in metric tons (1 tonne = 1,000 kilograms [kg]) of Rare Earth Oxide (REO) with all REE lumped together. The designation Total Rare Earth Oxides (TREO) is used in mining and exploration to describe the total REE content in a deposit or sample in an equivalent oxide form, even though their mineral occurrence may not be in the form of an oxide. By convention, TREO only addresses the 15 lanthanide series elements plus yttrium; scandium is not included in TREO (Rare Element Resources, Ltd., 2011). A mixture of REE in metallic form, usually admixed with iron, is called misch metal or mischmetal (Hedrick, 1985).

REE with even atomic numbers, such as ^{58}Ce and ^{60}Nd, have greater cosmic and terrestrial abundances than adjacent REE with odd atomic numbers, like ^{57}La and ^{59}Pr.

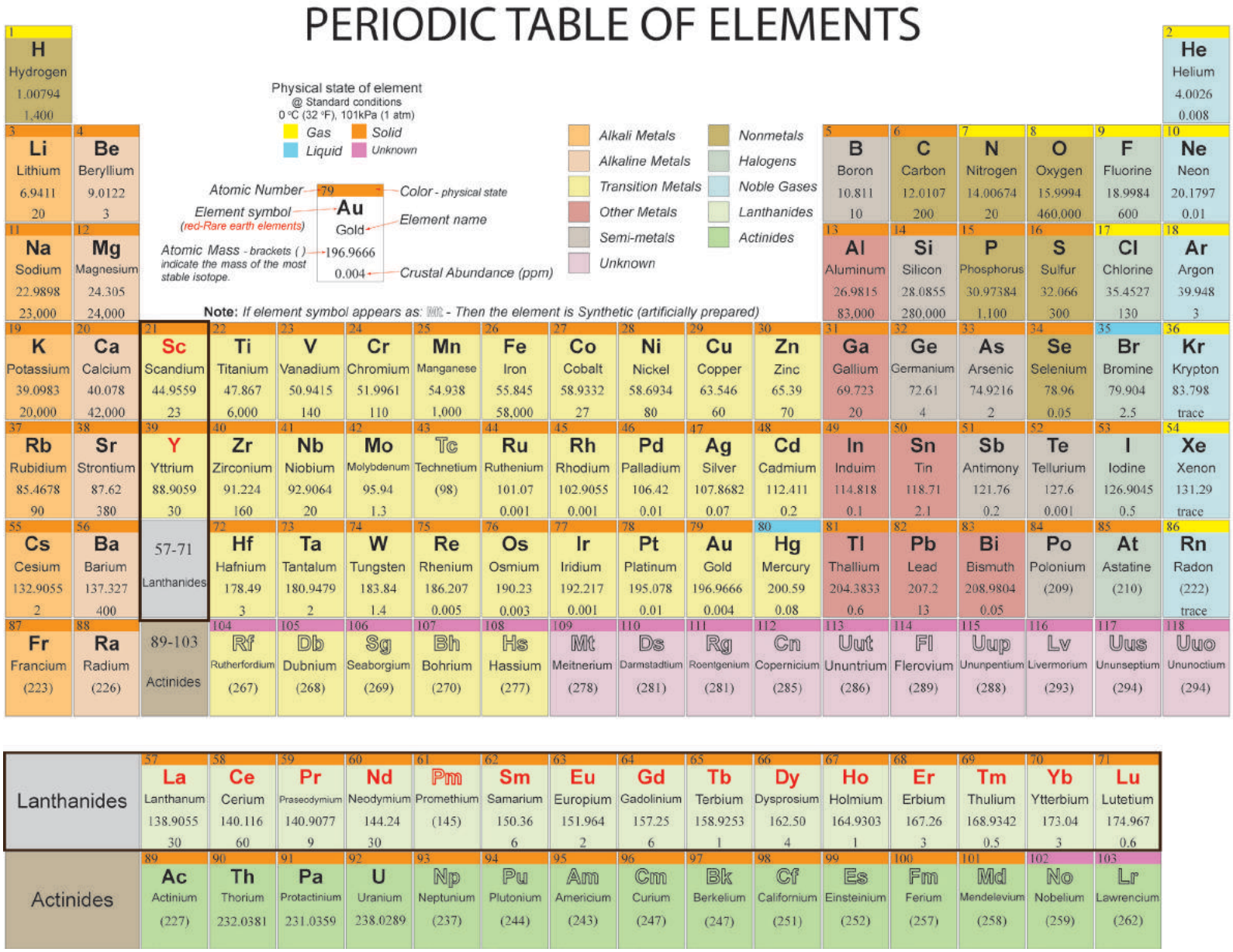


Figure 1. Periodic Table of the Elements with REE outlined in black. (Chart by James R. Rodgers, Wyoming State Geological Survey.)

Table 1. A list of the REE divided into LREE and HREE as well as associated elements. The average crustal concentration and the cut-off for elevated REE at five times the crustal abundance are shown.

Element (chemical Symbol)	Atomic Number	Crustal Concentration[a] (ppm)	Crustal Concentration[b] (ppm)	Five Times Crustal Concetration[a] (ppm)	Element Group
Lanthanum (La)	57	34	30	170	LREE
Cerium (Ce)	58	60	64	300	
Praseodymium (Pr)	59	8.7	7.1	43.5	
Neodymium (Nd)	60	33	26	165	
Promethium (Pm)	61	0	-	0	
Samarium (Sm)	62	6	4.5	30	
Europium (Eu)	63	1.8	0.88	9	HREE
Gadolinium (Gd)	64	5.2	3.8	26	
Terbium (Tb)	65	0.94	0.64	4.7	
Dysprosium (Dy)	66	6.2	3.5	31	
Holmium (Ho)	67	1.2	0.8	6	
Erbium (Er)	68	3	2.3	15	
Thulium (Tm)	69	0.45	0.33	2.25	
Ytterbium (Yb)	70	2.8	2.2	14	
Lutetium (Lu)	71	0.56	0.32	2.8	
Scandium (Sc)	21	26	13.6	130	
Yttrium (Y)	39	29	22	145	
Cumulative Total REEs		**218.85**	**181.97**	**1,094**	
Iron (Fe)	26	63,000.00	-	315,000	Associated Elements
Copper (Cu)	29	68	-	340	
Silver (Ag)	47	0.08	-	0.4	
Platinum (Pt)	78	0.037	-	0.185	
Gold (Au)	79	0.003	-	0.016	
Lead (Pb)	82	10	-	50	
Thorium (Th)	90	6	-	30	
Uranium (U)	92	1.8	-	9	

After Sutherland and others (2013)

[a]http://www.webelements.com/periodicity/abundance_crust/; described as estimates of the average composition continental crust derived by a consensus and averaging process for data abstracted from five different references.

[b]Taylor and McLennan (1985) apply to the upper continental crust.

Cerium is the most abundant with a continental crustal abundance of about 60 ppm, followed by lanthanum at 34 ppm and neodymium at 33 ppm. The cumulative total abundance of REE in the earth's crust, including scandium and yttrium, ranges from about 20 ppm to 219 ppm, depending on the reference cited (Long and others, 2010; WebElements.com, 2012).

To depict low REE concentrations and compare slight deviations between samples, this report addresses concentrations in parts per million (ppm). However, commercial REE assay values are, by convention, reported in terms of TREO. The difference between reported ppm in assay values and reported TREO will vary with the specific geochemistry of individual deposits. TREO equivalents found in Rare Element Resources' Bear Lodge project are approximately 15.6 percent higher than the combined raw metal assay values (Rare Element Resources, Ltd., 2011). Using the Bear Lodge deposit as a general indication, 3,000 ppm in raw metal assay would give an estimated TREO of about 0.34 percent, and 10,000 ppm would be about 1.15 percent TREO.

Total REE values greater than 3,000 ppm may be indicative of potential for an economic deposit, depending on the type of sample. The selection of 3,000 ppm resulted from study of REE reported as TREO grades in various active exploration projects outside of Wyoming (Saywell, 2011; Grace, 2010). Reported TREO in exploration projects varied from 0.33 percent in drill core intercepts (the low end of positive indications for further exploration) to more commonly cited figures in the vicinity of 1 percent. Values of 1 to 2 percent are considered good, and values greater than 2 percent are great. This assumes favorable mineability and economic factors, including sufficient deposit size and tenor, consistency of ore grades, uniform mineralogy, favorable chemistry for metal extraction, mine siting, and transportation. It is not often that samples yielded greater than 3,000 ppm REE in Wyoming, but all samples with elevated occurrences are reported.

In contrast to base (such as copper, lead, or iron) and precious metals, REE have very little tendency to become concentrated in exploitable ore deposits (Haxel and others, 2002). LREE are more incompatible with many minerals because they have larger ionic radii and are therefore more strongly concentrated in the continental crust than HREE. In most rare earth deposits, lanthanum, cerium, praseodymium, and neodymium constitute 80 to 99 percent of the total. Because of this, deposits containing relatively high grades of the less common and more valuable HREE (europium through lutetium and yttrium) are particularly desirable (Sutherland and others, 2013).

REE USES

Consumer products that rely on integral use of REE include catalytic converters, cell phones, digital cameras, and computers. Additionally, neodymium, samarium, gadolinium, dysprosium, and praseodymium are used in high-power permanent magnets where weight and space are of concern. These applications range from computer hard drive motors and MRI scanners to wind generators. A typical 2-megawatt wind turbine requires 60 kg (132 lbs) of dysprosium and 372 kg (820 lbs) of neodymium, which, at October 2011 prices would cost $301,680 only for the REE (Grushkin, 2011). A typical hybrid car, such as a Toyota Prius, contains around 11.3 kg (25 lbs) of REE, mostly lanthanum, in its rechargeable battery (McDermott, 2009) and about 2 kg (4.5 lbs) of neodymium and dysprosium in its drive motor (Grushkin, 2011). Smart phones and LED lights each contain less than a gram of REE (Molycorp, 2015a).

Lanthanum and neodymium are also used as catalysts in refining heavy crude oil into usable forms. Gadolinium, which has the highest neutron capture cross section of all the elements, is the material of choice for absorbing high-energy neutrons. Erbium-doped fiber functions as laser amplifiers for transmitting signals in fiber-optic cables. Europium is used in semiconductor technology and as a phosphor activator in optical sensors, which creates the red color viewed on cathode ray tubes (Wilburn, 2012). Cerium, lanthanum, neodymium, and praseodymium are incorporated into mischmetal, which is a pyrophoric that gives off sparks when scratched. It is commonly used in cigarette lighters and automatic gas-lighting devices, and can also be used in making some types of steel, aluminum alloys, and magnesium alloys (Sutherland and others, 2013). Various uses of REE, listed by element, are shown in table 2.

As listed above, REE have a wide range of applications varying from lighters and cell phones to wind energy, but they are also used for national security purposes. The United States Department of Defense(USDOD) uses REE in lasers, precision-guided munitions, communications and radar systems, avionics, night-vision equipment, satellites, range finders, and control systems (Hedrick, 2004; 2010). These security related uses make China's control of REE a subject of concern to many nations.

POLITICS AND SUPPLIES

The largest known REE deposits occur in China, Australia, and North America, with much smaller deposits found in India, Brazil, Malaysia, and South Africa. Production has been dominated by China, with additional production from Australia, India, Malaysia, Russia, and Thailand

Table 2. A variety of REE uses.

Element	Typical Uses	Element Group
Lanthanum	lanthanum oxide additive in optical lenses increases light refraction and decreases dispersion, catalysts in heavy crude oil reformation, lighting phosphors, batteries, metal alloys, polishing compounds, ceramics	LREE
Cerium	polishing compounds for optical lenses, lighting phosphors, batteries, metal alloys, catalysts, glass additives, ceramics	
Praseodymium	high-power permanent magnets, batteries, metal alloys, catalysts, polishing compounds, glass additives, ceramics	
Neodymium	catalysts in heavy crude oil reformation, high-power permanent magnets, neodymium-yttrium-aluminum-garnet lasers, neodymium-iron-boron permanent magnets, batteries, metal alloys, glass additives, ceramics	
Samarium	samarium-cobalt permanent magnets, batteries	
Europium	phosphor activator for red color in a color television tube	HREE
Gadolinium	high-power permanent magnets, paint or coating against neutron radiation, phosphors	
Terbium	terbium-iron-nickel alloy with dysprosium (Terfenol-D) used in stealth technology, lighting phosphors, high-power permanent magnets	
Dysprosium	high-power permanent magnets, ceramics, nanotechnology research	
Holmium	high-power permanent magnets, nuclear control rods, lasers, optical coatings	
Erbium	doped fiber laser amplifiers, metal alloys	
Thulium	Few uses due to rarity and properties similar to other REEs	
Ytterbium	radiation source in portable X-ray equipment, stress gauges, lasers, metal alloys, catalysts	
Lutetium	few uses due to rarity and properties similar to other REEs	
Scandium	high-strength light-weight metallurgical applications	Associated Elements
Yttrium	neodymium-yttrium-aluminum-garnet lasers, lighting phosphors, ceramics	

After Sutherland and others (2013)

(table 3; Hedrick, 2004). China's reserves (currently economically extractable material) are the largest with an estimate of about 42 percent of the world's reserves. Russia and Vietnam combined contain about 30 percent of the reserves. Brazil comes in third, with approximately 17 percent, while Australia and India together have nearly 2.4 percent of global reserves. The United States only has about 1.4 percent (Gambogi, 2015a; 2015b; 2016).

Prior to the 1990s, the United States produced sufficient REE for domestic use. However, low prices and overproduction from the mid-1990s through 2003 closed most mines and plants outside of China (Saywell, 2011). Since then, China has had control of the market, producing 97 percent of the world's REE in 2012 (Niles, 2012) and is currently producing nearly 90 percent (Els, 2015). In 2010, China drastically reduced its REE exports and hiked export taxes to a range of 15 to 25 percent. Many concluded this was done to strengthen China's hold on the resource (Davis, 2011). This was problematic, as substitutes for many REE applications are available but tend to be inferior (Cordier, 2011). Thus, these actions resulted in a scramble for resources throughout the rest of the world (Bradsher, 2010; Grace, 2010; Davis, 2011). China con-

Table 3. Estimated mine production and reserves by country from 2010-15.

Country	Mine Production (tons) 2010	2011	2012	2013	2014	2015[e]	Reserves (tons)
United States	-	-	800	5,500	5,400	4,100	1,800,000
Australia	-	-	3,200	2,000	8,000	10,000	3,200,000
Brazil	550	550	140	330	0	0	22,000,000
China	130,000	130,000	100,000	95,000	105,000	105,000	55,000,000
India	2,800	3,000	2,900	2,900	NA	NA	3,100,000
Malaysia	30	30	100	180	240	200	30,000
Russia	-	-	2,400	2,500	2,500	2,500	*
Thailand	-	-	NA	800	2,100	2,000	NA
Vietnam	-	-	200	220	-	-	*
other countries	NA	NA	NA	NA	NA	NA	41,000,000
World total (rounded)	133,000	133,500	110,000	110,000	123,000	123,000	126,000,000

From: Rare Earths U.S. Geological Survey, Mineral Commodity Summaries, prepared by Joseph Gambogi (2015a; 2016)

[e]estimated; NA means not available

*included with "other countries"

tinued to restrict the world supply of REOs through 2014 (Gambogi, 2014) until August of that year. At that time, the World Trade Organization upheld a ruling in favor of the United States, European Union, and Japan's claims that China was violating trade rules with respect to the unfair imposition of export restrictions on rare earths. China's claims that the controls were aimed at protecting the environment and conserving resources were dismissed.

Today, China continues efforts to consolidate its rare earths industry in order to curb pollution as well as illegal production and exports (Gambogi, 2015a; 2015b). Ways to block and trace illicit extraction and exports have been suggested by the Chinese Vice Minister of Industry and Information Technology. However, with 90 percent of the nation's REE producers operating at a loss, according to the Association of China Rare Earth Industry, many closures are expected to occur in the near future (Jamasmie, 2016a).

China's state-owned mines kept rare earth prices artificially low during most of the past 15 years, which drove other suppliers out of business. The United States had the expertise but lacked the manufacturing infrastructure to refine REO to metals. Rebuilding the United States REE supply chain has begun but could take as long as 15 years to complete (Long and others, 2010; Hsu, 2010). Achieving a secure strategic supply of REE seems to be more important now than the economic impact of developing the necessary supply chain.

In 2010, Molycorp Mineral, LLC's Mountain Pass Mine recommenced operations for the first time since 2002 (Molycorp, 2015c). Upon completion of the expansion and modernization project, it was expected to produce about 19,050 tonnes (21,000 tons) of REO equivalent per year beginning in mid-2013 and expand to 40,000 tonnes (44,090 tons) of REO per year (Molycorp, 2013). This became the only active REE operation in the United States and slightly reduced dependence on China's supply. However, a drop in the price of REE and financial problems in 2015 plagued the company, forcing Molycorp to file for Chapter 11 (Molycorp, 2015b). In February 2016, creditors reached a deal to divide up the value of the company in order to clear a path to exit bankruptcy. It is possible that reorganization could still occur; although, persisting disputes between Molycorp's primary lender and unsecured creditors continue to be an issue (Hals, 2016).

It has been suggested that alternative technologies and recycling of REE may help reduce market demand in the future (Elmquist, 2011). Other hypothesized sources for REE include processing of waste material from both coal (Jamasmie, 2015a) and uranium mining (Lottermoser, 2015), which are addressed later in this report. Only 1 percent of all REE are currently estimated to be recycled today; this is a fraction of what could be used especially when fluorescent lights and computer parts can be easily recovered and reprocessed (Molycorp, 2015a). Recently, U.S. Rare Earths, Inc. announced a plan to collect REE by recycling electronics, including batteries, magnets, and catalytic converters, using a new membrane solvent extraction system developed by the USDOE's Critical Materials

Institute (Jamasmie, 2015b). In addition, a patent-pending method was developed by researchers at Worchester Polytechnic Institute to extract REE from discarded electric and hybrid car parts (Mining.com, 2015).

High-technology REE applications are diverse and expanding, which drives increasing technological, economic, and strategic needs in the United States (Long and others, 2010). A 2010 study by the U.S. Department of Energy (USDOE) addressed the supply of critical minerals in the United States. They used the term critical as a measure of importance to the economy, availability of clean energy, and risk of supply disruption. Among other minerals and elements addressed, they considered five REE, Dy, Nd, Tb, Eu, and Y, as most critical in the short-term future of the United States.

With the closure of the Molycorp Mountain Pass operation there are currently no active REE mines in the United States. Until recently, the Bear Lodge deposit in northeast Wyoming was to have mining and processing facilities running by 2017 under the operation of Rare Element Resources, Ltd. However, due to a difficult market, the company has temporarily suspended its permitting activities (Rare Element Resources, Ltd., 2016). The Bear Lodge deposit will be discussed further in a later section of this report. Due to the lack of domestic REE suppliers, other REE projects are being investigated for exploration or development purposes in the United States including Bokan, Alaska; La Paz, Ariz.; Diamond Creek, Idaho; Lemhi Pass, Idaho and Mont.; Pea Ridge, Mo.; Elk Creek, Nebr.; Thor, Nev.; and Round Top, Tex. (Gambogi, 2015a; 2015b; 2016).

REE PRICES

REE prices have risen substantially in the last decade. Between October 2009 and June 2011, prices for all REE rose 1,500 percent, then retreated significantly during the latter part of 2011 (Saywell, 2011). Prices retreated further during 2012 but remained substantially higher than in 2010 (U.S. Geological Survey, 2013). In 2013 and 2014, domestic consumption of REE imports increased due to improved economic conditions and lower prices of REE (Gambogi, 2014). Prices and imports rely heavily on global economic conditions, excess inventory, and increased efficiency of material usage. For example, prices continued to decline in 2014 because of decreased use of REE in the phosphor industry due to increased use of LED lighting, which requires less REE than fluorescent lighting. New regulations in China may influence prices in the near future as the government curtails illegal producers and exporters, enacts resource taxes, and continues to try and maintain its monopoly on REE (Saefong, 2015).

Although there have been major fluctuations in the past, prices are expected to remain relatively high until a chain of supply, processing, and manufacturing have been established outside of China. Table 4 shows the slight fluctuations in REO price from 2013 to early 2015. Prices from 2008 through 2011 can be found in RI-65 (Sutherland and others, 2013).

Relative market values for REE are highly variable and depend in part on the source quoted. Prices also depend on the level of purity, which is determined by the specifications for any particular application (Lynas Corporation, 2011). Pricing occasionally addresses individual metallic elements. However, most references cite REE in oxide form, reported as REO. REO concentrates vary in their elemental mixes based on the composition of the source deposit. REO prices vary accordingly and may not be comparable between one deposit and another. Concentrates range from nearly 40 percent REO to 99 percent REO. One of the best sources for current REE price information is Metal-Pages (http://www.metal-pages.com/metalprices/rareearths/), which requires a subscription to view (Sutherland and others, 2013).

EXTRACTION OF REE

Concentrations of REE found in their host rocks and minerals are generally low, and the cost of separation of the individual elements is quite high compared to other metals. REE ores are mineralogically and chemically complex and often radioactive (Long and others, 2010). Isolation of individual REE by ordinary metallurgical means is difficult because of their similar chemical properties. Currently, separation is a long and complex process that involves multiple and repetitive steps in solvent extraction and/or ion exchange. Other extraction methods may involve iterative fractional crystallization, fusion, volatilization, or a combination of selective reduction and vacuum distillation of halides (Hedrick, 1985; Uda and others, 2000). Recent proprietary technology developed by Rare Element Resources for its Bear Lodge project increased projected recovery of REE to greater than 99.9 percent, significantly helping its economic outlook (Rare Element Resources, Ltd., 2015a).

The presence of two or more mineral phases in many deposits requires a different extraction technology for each mineral, compounding both complexity and cost (Long and others, 2010). The cost of building a plant to separate the individual REE is also high and must be tailored to the unique mineralogy of a specific ore. Construction of a new mine, with attached separation plant, was estimated in 2010 to cost between $500 million and $1 billion (Hsu,

Table 4. REE prices from 2013-15.

Element/ Mineral	Oxide FOB ex-China Q2 2013[a]	Oxide (≥99.9%) 2013[b]	Oxide (≥99.9%) 2014[b]	Oxide (99%) FOB ex-China April 2014[c]	Oxide (≥99.0%) FOB ex-China Nov. 2014[e]	Oxide (≥99.9%) FOB ex-China Nov. 2014[e]	Oxide (≥99.5%) FOB ex-China Dec. 2014[d]	Oxide (≥99.0%) FOB ex-China Feb. 2015[e]	Oxide (≥99.9%) FOB ex-China Feb. 2015[e]	Oxide (99.5-99.9%) FOB ex-China Feb. 2015[f]
lanthanum	5.43	6.00	5.00	7.66	2.18	6.61	4.80	2.09	6.28	2.14
cerium	5.44	5.50	4.50	3.22	2.01	6.44	4.40	1.93	5.80	2.05
praseodymium	57.91			94.19	77.33		105.00	63.64		63.66
neodymium	45.30	67.50	58.00	50.47	44.31		59.00	47.53		49.56
promethium				-	-	-	-	-	-	-
samarium	5.88			3.06	2.82			2.66		2.74
europium	636.24	975.00	705.00	645.61	350.67		680.00	265.84		282.05
gadolinium				23.39	14.66	25.78	39.00	13.29	17.72	13.06
terbium	481.80	825.00	615.00	491.86		420.35	600.00		620.30	636.63
dysprosium	246.74	465.00	340.00	264.52	228.70		340.00	277.93		282.05
holmium					44.15*			39.47		
erbium					43.42		77.00	39.20		41.10
thulium										
ytterbium						48.66			30.61	
lutetium						1,122.82			990.86	
yttrium		25.00	16.50	7.91		6.28	15.00		5.40	5.48
scandium					3,302.88*		7,200.00	3,302.88		

[a]From Statista.com, average Chinese domestic prices in the 2nd quarter of 2013

[b]From USGS 2015 Mineral Commodity Summaries on REE and Yttrium. Average price source Metal-Pages (2015). Yttrium price for 99.999% purity (Gambogi, 2015b)

[c]From Metal Prices (2015), price listed is the average for April 2014, subscription needed for most recent prices

[d]From Mineral Prices (2015) HEFA Rare Earth prices

[e]From the Association of China Rare Earth Industry, average spot ton price for November 2014 and February 2015 (Shen, 2015). *Sc and Ho reported at ≥99.5%

[f]From Shanghai Metals Market (2015), price listed is the average spot price for February 2015, subscription needed for most recent prices

Prices from previous years (2000-2011) can be found in WSGS RI-65 (Sutherland and others, 2013)

Prices above in USD/kg. Conversion factor: 1 USD = 0.16 CNY (RMB or Yuan)

2010), with a lead time up to 15 years for full-capacity completion (Long and others, 2010; Hsu, 2010).

As with the extraction of many natural resources, pollution can be a problem without proper planning. In China, where regulation is lacking, the mining of REE contributes to high levels of air and water pollution in the vicinity of the operation (Kaiman, 2014). With increased technology and innovation, it is possible that the process can become less expensive and more eco-friendly. In fact, Rare Earth Salts Separations and Refining, LLC, a company based in Nebraska, recently announced plans for a pilot facility capable of separating, refining, and selling rare earth products. Initial work has demonstrated an environmentally-friendly process, industry leading recovery rates, and extremely low operating costs. Design and construction were reported to have begun in the first half of 2015 and to be completed within 18 months of groundbreaking (Rare Earth Salts, 2014; 2015).

GENERAL GEOLOGY OF REE

REE minerals and deposits are often classified as either LREE or HREE. Since both types usually occur together, the designation is often a statement relating to the economic dominance of either the light or the heavy elements. HREE deposits are generally less common than LREE deposits, making them more valuable (Long and others, 2010).

Awareness of the diversity of REE deposit types is beneficial to exploration efforts. Economically exploitable concentrations of REE are primarily derived from crystalline rocks (Long and others, 2010). REE are more common in alkaline igneous rocks and carbonatites than in mafic rocks (Long and others, 2010). REE typically occur as trivalent cations in rock-forming minerals in carbonates, oxides, phosphates, and silicates (Hedrick, 2004). They are chemically similar to thorium and are often found in minerals and rocks in association with thorium (Hedrick and Templeton, 1988). Economic concentrations of REE host minerals occur in alkaline igneous rocks, carbonatites, and a wide variety of dikes and veins that cross-cut alkaline intrusions and surrounding rocks (Long and others, 2010).

Sedimentary rocks that may be enriched in REE include phosphatic rocks, coarse clastic rocks, and shales (Hedrick, 1985). Phosphate deposits may be sources for yttrium and lanthanum (Long and others, 2010). Sediments derived from rocks that contain even small amounts of HREE-bearing minerals may produce both placer and paleoplacer concentrations.

Ion-adsorption clays, or laterites that develop as residuum from chemical weathering, may be enriched in REE from intensive leaching of igneous and other rocks. Economic REE concentrations in ion-adsorption clays are known in southern China and Kazakhstan (Long and others, 2010). Such clays tend to have a greater enrichment in HREE than other deposit types (Hedrick, 2004).

REE MINERALS

Numerous minerals are known to contain REE as essential constituents, and a greater number contain REE as accessory elements. Only a few of these minerals host large enough concentrations of REE to be considered ore minerals (Hedrick, 1985). Allanite and monazite occur as relatively common accessory minerals within many types of felsic igneous rocks (Deer and others, 1967). Other REE-bearing minerals can be uncommon and are often hosted in generally uncommon rock types. Worldwide, the principal commercial sources of REE are the minerals bastnasite, loparite, monazite, and xenotime, and rare earth ion-adsorption clays (Hedrick, 2004). When discussing principal REE-bearing minerals specific to the United States, Long and others (2010) omit loparite and ion-adsorption clays but add euxenite and allanite, although other REE-bearing minerals are also present. Table 5 lists minerals reported in Wyoming that contain REE. Mineral formulas shown in the following discussions are variable depending on the source cited and on subvarieties that may contain differing elemental substitutions.

Of the principal REE-bearing minerals, allanite, bastnasite, euxenite, monazite, and xenotime are known to occur in Wyoming (King and Harris, 2002). Ewaldite and mckelveyite, although not primary REE sources, were actually discovered with association to trona beds in the Green River Formation in Sweetwater County, Wyoming (Anthony and others, 2001; webmineral.com, 2015).

Allanite $Ca(Ce,La,Y,Ca)Al_2(Fe^{2+},Fe^{3+})(SiO_4)(Si_2O_7)O(OH)$

Allanite is a member of the epidote mineral group, where some calcium atoms are replaced by REE, particularly cerium. It is also the only member of the epidote group in which ferrous (Fe^{2+}, reduced) iron is an essential constituent. Cerium- or REE-epidotes may contain 0.35 to 2.23 percent radioactive components (Deer and others, 1967). The REE content of allanite is typically about 5 percent REO but can vary widely from 3 to 51 percent, depending on its geologic source (Gupta and Krishnamurthy, 2005).

Allanite is most commonly found as an accessory mineral in igneous rocks but rarely in sufficient concentration to be economically mined. Typically, these igneous rocks include granites, syenites, diorites, and their associated pegmatites. The mineral usually occurs as black to dark-

brown and brownish-violet tabular grains. It has a conchoidal fracture and is often metamict, meaning its crystal lattice is disrupted, due to radioactive decay of thorium, while the mineral grain retains its original morphology; this can weaken the crystal structure. Microscopic dark halos or rings seen inside of allanite mineral grains are also an effect caused by radioactivity (Long and others, 2010). The specific gravity of allanite is 3.4 to 4.2 and its hardness is between 5 to 6.5 Mohs scale (Deer and others, 1967); these characteristics suggest a possibility for placer concentrations. However, metamict varieties may weather rapidly. Weathering of allanite produces a reddish-brown, iron-rich, earthy crust deficient in REE compared to unweathered allanite (Deer and others, 1967).

Ancylite $Sr_3(Ce,La,Dy)_4(CO_3)_7(OH)_4{\cdot}3H_2O$

Ancylite is part of a group of hydrous carbonates containing strontium and varying amounts of REE. It is an uncommon accessory mineral found in carbonatites and some nepheline syenites (MinDat.org, 2016). Ancylite is one of the ore minerals in Rare Element Resources' Bear Lodge carbonatite-hosted REE deposit (Jim Clark, Rare Element Resources, Ltd., personal communication, 2013). The radioactive mineral forms in brittle, pyramidal or bladed crystals at a Mohs scale hardness of 4.5. They can appear brown, gray, colorless, or pinkish with vitreous to greasy luster.

Bastnasite $(Ce,La,Y)CO_3F$

Bastnasite, also spelled bastnaesite or bastnäsite, is an uncommon REE-bearing carbonate mineral classified as a cerium-lanthanum-yttrium carbonate fluoride; it occurs in a mineral series with hydroxyl-bastnasite [$(Ce,La)CO_3(OH,F)$] and is also closely related to parisite [$Ca(Ce,La)_2(CO_3)_3F_2$]. Bastnasite may form replacement crystals after allanite (Long and others, 2010). Although bastnasite is not common, it is the most abundant REE-bearing mineral (MinDat.org, 2016).

Bastnasite is primarily mined from rare, carbonate-rich, igneous rocks called carbonatites. Carbonatites contain greater than 50 percent carbonate minerals and are usually associated with alkaline igneous complexes. Bastnasite is one of the world's primary sources for REE and is dominated by LREE (Hedrick, 2004). Bastnasite theoretically can contain about 75 percent REO but averages about 60 percent. The yttrium content is generally very low at about 0.05 percent (Hedrick, 1985). In addition to being found in carbonatites, bastnasite is an accessory mineral in some alkaline igneous rocks and in some hydrothermal deposits (Hedrick, 2004).

Bastnasite may be massive or granular and typically forms small, rounded hexagonal or short prismatic crystals; it may also occur as spheres or rosettes (Long and others, 2010). It is translucent with a vitreous to greasy or pearly luster. Its color varies from colorless to shades of yellow, reddish-brown, and pink. Bastnasite is relatively heavy with a specific gravity of 4.7 to 5.0. However, a low Mohs scale hardness of 4.0 to 4.5 (MinDat.org, 2016) combined with brittleness and a prominent basal cleavage suggest little possibility for placer concentrations.

Euxenite $(Y,Ca,Ce,U,Th)(Nb,Ti,Ta)_2O_6$

Euxenite is a slightly radioactive oxide mineral in a series with polycrase [$(Y,Ca,Ce,U,Th)(Ti,Nb,Ta)_2O_6$]. Euxenite has similar properties to other REE-bearing oxide minerals such as fergusonite and samarskite, both uranium minerals, and to aeschynite, a minor REE-bearing mineral. Euxenite is typically found in granite pegmatites in association with quartz, feldspars, columbite (ferrocolumbite), tantalite (ferrotantalite or manganocolumbite), and monazite (Long and others, 2010; MinDat.org, 2016).

Euxenite may form black to yellow- or green-tinged, greasy to submetallic, tabular to prismatic crystals. The mineral may also be granular to massive or form radial aggregates. It is brittle, exhibits a conchoidal fracture, appears glassy, and has no cleavage. It is often metamict, giving an amorphous X-ray pattern due to radiation damage (Webmineral.com, 2016). Its Mohs scale hardness of 5.5 to 6.5 and specific gravity of 5.3 to 5.9 facilitate its concentration in placer deposits such as in detrital black sands (Long and others, 2010; MinDat.org, 2016). Euxenite is the only REE-bearing mineral with historically notable production from Wyoming in the Platt Mine of the Big Creek area discussed later.

Ewaldite $(Ba,Sr)(Ca,Y,Ce,Na,K)(CO_3)_2$ *and*
McKelveyite $NaCa(Ba,Sr)_3(Y,REE)(CO_3)_6{\cdot}3H_2O$

McKelveyite and ewaldite are not major sources for REE but are significant because they were discovered in Wyoming in 1965 and 1971, respectively (Milton and others, 1965; Mineral Data Publishing, 2001-2005). Both are carbonate minerals associated with Eocene-aged lacustrine deposits, trona deposits, and hydrothermal carbonate veins. They were originally found in the Green River Formation in Sweetwater County, Wyoming. Ewaldite contains about eight percent REE in the form of cerium and yttrium. McKelveyite contains almost seven percent yttrium and two percent lanthanum, cerium, praseodymium, neodymium, and samarium. These minerals are radioactive and come in a variety of colors from yellowish-, greenish-, bluish-gray to reddish-brown. McKelveyite has a hardness of 3.5–4 and forms tabular to pyramidal, prismatic crystals. Ewaldite does not have a recorded hardness

Table 5. Minerals reported in Wyoming commonly bearing REE.

Mineral	Chemical Formula[a,b]	REE as primary or accessory constituents
Allanite[c]	$Ca(Ce,La,Y,Ca)Al_2(Fe^{2+},Fe^{3+})(SiO_4)(Si_2O_7)O(OH)$	Minerals with REE as essential constituents
Ancylite	$Sr_3(Ce,La,Dy)_4(CO_3)_7(OH)_4{\cdot}3H_2O$	
Bastnasite	$(Ce,La,Y)CO_3F$	
Brannerite	$(U,Ca,Y,Ce)(Ti,Fe)_2O_6$	
Brockite	$(Ca,Th,Ce)PO_4{\cdot}H_2O$	
Burbankite	$(Na,Ca)_3(Sr,Ba,Ce)_3(CO_3)_5$	
Calkinsite	$(Ce,La)_2(CO_3){\cdot}4H_2O$	
Cerianite	$(Ce,Th)O_2$	
Carbocernaite	$(Ca,Na)(Sr,Ce,Ba)CO_3$	
Euxenite	$(Y,Ca,Ce,U,Th)(Nb,Ta,Ti)_2O_6$	
Ewaldite[d]	$(Ba,Sr)(Ca,Y,Ce,Na,K)(CO_3)_2$	
Fergusonite	$(Y,Er,Ce,Nd,La,Fe)(Nb,Ta,Ti)O_4$	
Gadolinite	$(Y,Ce,La,Nd)_2FeBe_2Si_2O_{10}$	
McKelveyite[d]	$NaCa(Ba,Sr)_3(Y,REE)(CO_3)_6{\cdot}3H_2O$	
Parisite	$Ca(Ce,La)_2(CO_3)_3F_2$	
Monazite	$(Ce,La,Y,Th)PO_4$	
Rhabdophane	$(Ce,La,Nd)PO_4{\cdot}H_2O$	
Samarskite	$(Y,Ce,U,Ca,Th,Fe)(Nb,Ta,Ti)_2(O,OH)_6$	
Synchysite	$(Ce,La,Nd,Y)Ca(CO_3)_2F$	
Xenotime	YPO_4	
Apatite	$Ca_5(PO_4)_3(F,OH,Cl)_3$	Minerals with REE as accessory constituents
Columbite-Tantalite	$(Fe,U,Ca)(Nb,Ta)O_4$	
Fluorite	CaF_2	
Huttonite-thorite	$ThSiO_4$	
Pycrochlore-Microlite	$(Na,Ca)_2(Nb,Ta,Ti)O_6(OH,F)$	
Sphene	$CaTiSiO_5$	
Zircon	$ZrSiO_4$	

[a]After King and Harris (2002); Rare Element Resources (2011); Sutherland and others (2013), formulas vary with citation source

[b]REEs not listed may substitute into some formulas for specific occurrences

[c]Chemical formula after Long and others (2010)

[d]Chemical formula after webmineral.com (2015)

but also forms prismatic, pyramidal, and hexagonal crystals (Anthony and others, 2001; webmineral.com, 2015).

Monazite $(Ce,La,Y,Th)PO_4$

Monazite is a REE-thorium phosphate mineral that can be LREE ore, similar to bastnasite. However, it hosts slightly more of the HREE, especially yttrium, dysprosium, and gadolinium (Hedrick, 2004). Monazite can theoretically contain 70 percent REO, including about two percent yttrium oxide. In reality, most concentrates contain about 55 to 65 percent REO (Hedrick, 1985) with typical values in the 60 to 62 percent range (Long and others, 2010). Monazite's high thorium content (4.5 to 10 percent ThO_2 equivalent) and thorium's naturally-occurring radioactivity is considered an impediment to mining and processing. This causes world monazite production to be relatively small (Hedrick, 2004).

Monazite forms translucent, brownish-red to yellow, equant to tabular prismatic crystals with wedge-shaped terminations and a vitreous to adamantine luster. It has a good planar cleavage, a conchoidal fracture, and may be found in both granular and massive forms. Metamict alteration due to radioactive decay of thorium is usually present in monazite and shifts its luster to resinous (Hedrick, 2004; Long and others, 2010; MinDat.org, 2016).

Monazite is a rare accessory mineral in alkaline igneous and metamorphic rocks such as granites, syenites, gneisses, and related pegmatites (Deer and others, 1967). Economic concentrations are typically found in placers and paleoplacers (Hedrick, 1985). Placer occurrences derive from monazite's high specific gravity of 4.8 to 5.5 and a Mohs scale hardness of 5, which contributes a moderate resistance to weathering. Monazite is recovered from placers as a byproduct during processing for other resistant, heavy minerals, including cassiterite, ilmenite, magnetite, rutile, and zircon (Hedrick, 2004; Long and others, 2010).

Xenotime YPO_4

Xenotime is a yttrium-dominated phosphate related to monazite that allows for the possibility of REE substitutions in its structure. It can contain about 67 percent REO, most of which is HREE dominated by Y_2O_3, but concentrates average about 25 percent REO (Hedrick, 1985; Gupta and Krishnamurthy, 2005).

Xenotime generally forms yellowish- to reddish-brown prismatic crystals with vitreous to resinous lusters. Occasionally, it may be gray, green, or pink, and its crystal form may vary from equant or pyramidal to radial aggregates and rosettes. Xenotime's similarities in crystal habit and overall appearance to zircon confound identification. However, its Mohs scale hardness is only 4 to 5, compared to zircon's 7.5, and xenotime has a distinct cleavage (Long and others, 2010; MinDat.org, 2016).

Xenotime occurs as an accessory mineral in acidic and alkaline igneous rocks as well as some mica schists and quartz-rich gneisses (Long and others, 2010). As an REE ore mineral, xenotime is a byproduct of tin mining and, to a lesser extent, is recovered as a detrital byproduct from the mining of heavy-mineral sands (Hedrick, 2004). Its specific gravity of 4.4 to 5.1 favors concentration in placers.

REE EXPLORATION AND PRODUCTION IN WYOMING

REE mineralization in Wyoming was discovered in the Bear Lodge Mountains in 1949 (Rare Element Resources, Ltd., 2011). Record of a telephone conversation between H.D. Thomas and C.C. Towle of the USAEC in 1951 states that the USAEC examined the "Sundance deposit," which was first reported in the spring of 1950, and that it was "mainly rare earths" with negligible uranium content in the monazite (Thomas, 1951). Wilmarth and Johnson (1953) of the U.S. Geological Survey (USGS) found iron-manganese veins in two locations hosting REOs as high as 12.99 percent. However, these authors concluded the limited size of the veins and the high cost of mining detered commercial mining of the rare-earth ore, but additional deposits were likely to be found in the area (Wilmarth and Johnson, 1953).

After early interest in the Bear Lodge deposit, exploration was renewed in 1972 by the Duval Corporation, which found high-grade copper, molybdenum, and precious and rare earth metals within an altered carbonatite-alkaline-intrusive complex. Duval's drilling encountered combined REO intercepts ranging from 1 to 15 percent. In the 1980s, carbonatite-hosted thorium and REE deposits in the Bear Lodge Mountains were thought to be "the largest resource of disseminated rare earth elements in North America" (Staatz, 1983). Exploration involving numerous companies continued in the Bear Lodge through the mid-1990s when lower Chinese prices began to weaken incentive for REE exploration in the United States. In 2004, Rare Element Resources, Ltd. began exploration drilling in the Bear Lodge REE deposit. The deposit, located northwest of Sundance, is the largest known REE deposit in Wyoming and is currently well-advanced in exploration, including metallurgical and environmental studies directed toward mine development (Rare Element Resources, Ltd., 2013a). Planning, permitting, and licensure were underway for a small open pit mine, physical upgrade plant, hydrometallurgical plant, and the handling of naturally-occurring radioactive materials (Business Wire, 2015). Unfortunately, a lull in the market has prompted Rare Element Resources,

Ltd. to temporarily suspend all actions, beginning in late January 2016, for 6 to 12 months until the venture becomes economical again (Rare Element Resources, Ltd., 2016).

Exploration in other parts of Wyoming, similarly focused first on uranium and thorium, resulted in identification of REE or REE-bearing minerals. Paleoplacers in the Bald Mountain area of the Bighorn Mountains were initially examined for low-grade gold in the latter half of the 19th century. During late summer of 1950, paleoplacers in the lower part of the Flathead Sandstone were found to host radioactive monazite and were investigated by the USBM in 1951 (Klein and Winkel, 1952). Evaluation of the Bald Mountain area paleoplacers for monazite and thorium content by the USAEC in 1952 (McKinney and Horst, 1953a; b) showed a significant resource, but the study concluded that it could only be mined economically if the price per ton for the monazite was significantly higher. No analyses for REE accompanied reports from these investigations since the focus was on uranium and thorium even though the same minerals hosted REE as well. A few years later, the USBM reported in the 1956 Minerals Yearbook that U.S. Yttrium, Inc., based in Laramie, Wyoming, was conducting exploration and research in rare earth metals in the Bald Mountain area.

Minor amounts of REE-bearing minerals were reportedly mined in Wyoming from at least three locations. Marzell (1932) reported production of 363 kg (800 lbs) of samarskite from Wyoming in 1930 but left the source of the material unknown. Allanite-bearing ore was reportedly extracted from the Beaver Creek prospect in the Bighorn Mountains, in southern Johnson County, between 1952 and 1955, but neither production nor processing records exist (Bromley, 1955; King and Harris, 2002). The Platt Mine, in the Big Creek district on the west side of the Medicine Bow Mountains, produced approximately 4,500 kg (10,000 lbs) of euxenite from a pegmatite between 1956 and 1958 (Houston, 1961). Other sources reduce this figure to 1,800 kg (4,000 lbs) and state that 5,900 kg (13,000 lbs) of ore produced from this mine in 1956 was for uranium (King and Harris, 2002).

Recent REE exploration in Wyoming, beyond the Bear Lodge deposit, began in 2009 and continues to the present. Targets of renewed interest include placers, paleoplacers of several ages, alkaline igneous complexes, pegmatites, and carbonatites (Sutherland and others, 2013).

GEOLOGIC OCCURRENCES OF WYOMING REE

REE occur in a variety of rock units across Wyoming. Reported Precambrian REE occurrences are hosted by pegmatites, veins and dikes, faults and shear zones, metacarbonate rocks, disseminated minerals in generally alkalic igneous rocks, and metasediments. Sedimentary occurrences in paleoplacers are found primarily in the Cambrian Flathead Sandstone and the Cretaceous Mesaverde Formation as well as local, smaller deposits in numerous units. Disseminations of REE are also reported within phosphate-rich rock of the Permian Phosphoria Formation. Tertiary-aged hosts include alkali igneous rocks, carbonatite veins, dikes, hydrothermal zones, paleoplacers, and apparent depositions from solution movement within sandstones. Quaternary REE hosts can be found in alluvial placers and paleoplacers (King and Harris, 2002; Sutherland and others, 2013).

The most significant REE occurrence in Wyoming to date is the carbonatite-hosted Bear Lodge deposit currently under evaluation by Rare Element Resources, Ltd. The Bear Lodge REE deposit is centered on carbonatite dikes associated with Eocene (46 to 50 Ma) alkalic intrusive rocks. In this deposit, the minerals ancylite and bastnasite contain most of the REE, which are dominated by the LREE: cerium, lanthanum, neodymium, and praseodymium; HREE-enriched targets have also been determined in the western part of the property (Rare Element Resources, Ltd., 2014). Potential for the discovery of carbonatites that host REE also exists in other parts of Wyoming.

WSGS investigations RI-65 (Sutherland and others, 2013) and RI-67 (Sutherland and Cola, 2015) identified 15 locations that contained five times the average crustal abundance of REE. These included paleoplacer deposits in the Flathead Sandstone at Bald Mountain and in the Western Rattlesnake Hills, black sandstone paleoplacers of the Mesaverde Formation at the Dugout Creek, Grass Creek, Cottonwood Creek, and Lovell deposits, and other placer deposits at Spring Gap, Poison Spider, and the Deacon's Prayer group claims. Other locations included the Rawlin's Red deposit, Wyo-Ben Mine, the Phosphoria Formation at Hoback, the Wilkins Peak Member at South Firehole Canyon, and episodic dikes at the Clarence Wood lode claims. Veins and pegmatites with REE-bearing mineralization were found at the Union Pass-Warm Spring area, Platt Mine, Tie Siding area, and Holiday Place deposit. The descriptions and chemistry are discussed later.

All samples analyzed from previous studies and the current study are shown in figure 2. Samples with greater than five times the average continental crustal abundance of one or more REE are especially noted. These occurrences do not imply economic deposits. However, they do indicate sites that may be of interest for further exploration with possibilities for locating previously unknown REE deposits. *Many samples analyzed for this project that yielded low*

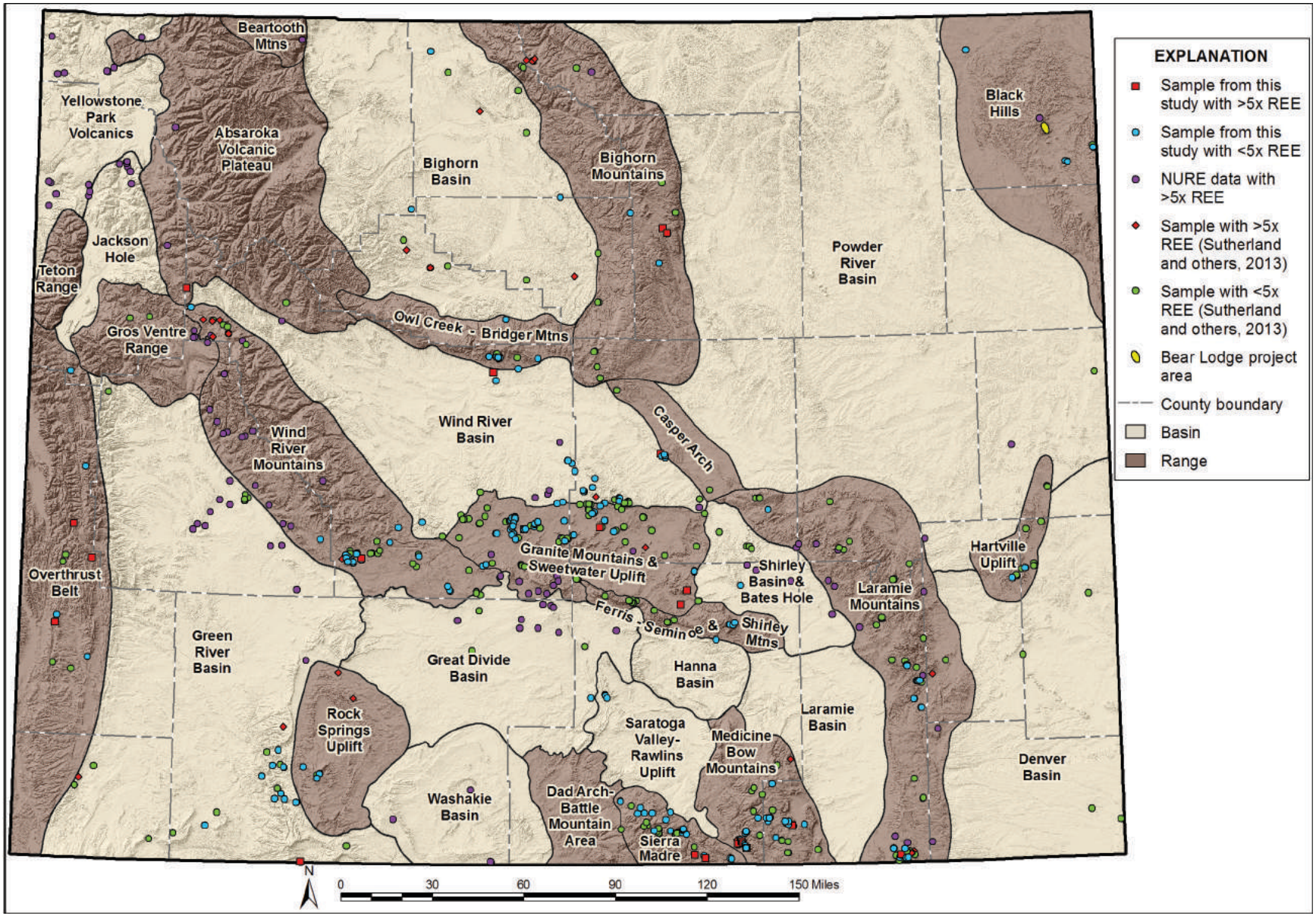


Figure 2. Sample localities across Wyoming. This map includes sample locations from the current study, RI-65 (Sutherland and others, 2013), and NURE data (Smith, 2001). Samples with REE elevated above five times the crustal concentration are noted as well as the Bear Lodge project area. The NURE locations shown contain elevated REEs.

values for REE and other elements of economic interest were not addressed in the text. The results of these analyses are included on the appendix CD, detailed site and sample descriptions can be found in Wyo-DOG.

Bear Lodge Mountains Rare Earth Element Deposit, Crook County, Wyo.

The Bear Lodge Mountains REE deposit was not directly investigated during this study or during RI-65, as it is privately owned, and evaluation by Rare Element Resources, Ltd. exceeds that of the WSGS. Access was granted by Rare Element Resources, Ltd. to view the site and the core-logging facilities to better understand the deposit. An overview of the geology and current development is included here since it is the most advanced REE project in Wyoming. An understanding of the Bear Lodge project can provide perspective for comparison and the evaluation of other potential REE deposits.

The Bear Lodge Mountains are along the northwestern edge of the Black Hills uplift and adjacent to the northeastern part of the Powder River Basin (fig. 2). They are the largest of several domal uplifts in the region, with exposed cores composed of Tertiary alkalic intrusions and flanked by steeply dipping Paleozoic and Mesozoic sediments (Sutherland, 2007; 2008). These intrusions and the resulting uplifts have exposed Precambrian crystalline rocks both in the Bear Lodge Mountains and in the Tinton-Mineral Hill area near the South Dakota border. Other domes in the region, such as Green Mountain, Strawberry Mountain, and Lime Buttes, are thought to have unexposed igneous cores.

Prospecting in the Bear Lodge began in 1875, following the discovery of gold in feldspar porphyry near Warren Peak. Recent exploration in the area has been fostered by both historically known mineralization and by similarities this Tertiary intrusive complex shares with the 30 Ma gold-hosting Cripple Creek igneous complex in Colorado. In addition to gold, historic mineral values in the Bear Lodge have included Ba, Cu, Ag, Pb, Zn, Mn, Nb, Ta, Th, F, P_2O_5, and REE (DeWitt and others, 1986; Hausel and Sutherland, 1988; Hausel, 1989; Hausel, 1997; Sutherland and others, 2013).

REE mineralization in the Bear Lodge Mountains is part of the Paleocene and Eocene alkalic igneous intrusive and volcanic rocks that crop out in northeastern Wyoming. These rocks form sills, plugs, dikes, and irregular bodies that intrude rocks ranging from Precambrian to Cretaceous in age. Outcrops are exposed in the Bear Lodge Mountains, Missouri Buttes, Devils Tower, Mineral Hill, Black Buttes, Inyan Kara Mountain, and Sundance Mountain (Sutherland, 2007; 2008). Most of these rocks are porphyritic, exhibit flow banding, and show evidence of shallow emplacement and rapid cooling (Staatz, 1983). Extrusive flows and pyroclastic deposits are found in limited areas where magma reached the surface in the Bear Lodge Mountains.

Magmatism progressed from east to west in three pulses beginning in the South Dakota Black Hills about 58 Ma, with later pulses about 55–54 Ma near the Wyoming-South Dakota border, and about 50–46 Ma in the Bear Lodge Mountains, Devils Tower, and Missouri Buttes (Duke, 2005). Carbonatite dikes, which contain rare-earth mineralization, represent the last phase of igneous intrusive activity in the area. Accompanying the east to west trend is a transition from subalkalic magmatism in the east to extremely alkalic in the west. Alteration is common and includes fenitization, silicification, carbonate enrichment, and sericitization (Duke, 2005). The largest volume of intrusive rocks is either trachyte or phonolite, accompanied by lesser amounts of latite, syenite, nepheline syenite, lamprophyre, pseudoleucite porphyry, agglomerate, intrusive breccias, and carbonatite (Robinson and others, 1964; Staatz, 1983; Sutherland and others, 2013).

Historically, one carbonatite dike that cuts intrusive breccia was exposed in an old exploration trench on top of the Bear Lodge Mountains in the SE¼ sec. 7 and SW¼ sec. 8, T. 52 N., R. 63 W. (Staatz, 1983; Sutherland, 2008). Carbonatite has since been recognized at the surface in trenches located in the Carbon target and directly south of Bull Hill (Rare Element Resources, Ltd., 2011).

Carbonatite is mostly calcite but may also contain accessory minerals commonly associated with REE enrichment, including strontianite, fluorite, pyrite, pyrrhotite, sphalerite, galena, and locally-abundant acmite and actinolite. Although Thomas (1951) mentioned monazite, the most common REE-bearing minerals reported by Staatz (1983) were brown bastnasite and pink ancylite. The exposed carbonatite is brown to yellowish-brown and mottled, while unweathered carbonatite, encountered in drill holes, appears light-gray to white and is banded with accessory minerals. Similar carbonatite dikes were subsequently intersected by drill holes at other locations and were found to occur in swarms of several closely spaced, relatively narrow dikes accompanied by one thick main dike (Staatz, 1983).

REE mineralization occurs in unaltered carbonatite and in deeply weathered carbonatite dikes referred to as FMR dikes (fig. 3). FMR references the major iron-manganese-rare-earth-element constituents of the highly oxidized, carbonatite dikes. These FMR [F (FeO_x), M (MnO_x), and R (REE minerals)] dikes, veins, and stockworks extend

to depths of 150 m (500 ft) or more as shown by exploration drilling. Carbonatite and FMR dikes encountered in drill holes and trenches range from narrow veinlets to more than 15 m (50 ft) in width and generally dip steeply to the southwest along northwest strikes (Rare Element Resources, Ltd., 2014).

FMR dikes contain altered silicates, amorphous silica, and variable amounts of REE minerals dominated by bastnasite. Additionally, FMR veins within the oxidized zone host REE mineralization as cerianite [$(CeTh)O_2$], parisite [$Ca(REE)_2(CO_3)_3F_2$], and fine-grained fibrous clusters of synchysite [$Ca(REE)(CO_3)_2F$]. FMR bodies generally have higher concentrations of REE than the carbonatites; but, the oxidized material tends to be very fine-grained and may require more complex beneficiation methods. Common accessory minerals in FMR dikes include barite, fluorite, apatite, with varying amounts of sanidine and quartz. These veins are typically vuggy, rusty to black in color, and also occur as sheeted zones and stockworks (Rare Element Resources, Ltd., 2011). REE mineralization within the dikes can reach more than 20 percent and appears to



Figure 3. FMR hand sample from the Rare Element Resources, Ltd. Bear Lodge deposit.

be uniform both along strike and at depth. Mineralization within the stockworks varies from about 0.5 percent to 3 percent TREO (Rare Element Resources, Ltd., 2014).

The carbonatite and FMR dikes are classified as either sovite- or silico-carbonatite. REE mineral abundances in both types reportedly range from trace amounts to greater than 50 percent. Sovite-carbonatite consists of fine to coarse crystalline calcite with accessory biotite, potassium feldspar, augite, strontianite, dolomite, and sulfides. As much as 30 percent sulfide and oxide components include pyrite, pyrrhotite, chalcopyrite, galena, sphalerite, molybdenite, hematite, rutile, and ilmenite. Silico-carbonatite contains 30 to 50 percent silicate minerals (biotite or phlogopite and potassium feldspar) with calcite and accessory aegirine, apatite, strontianite, barite, and celestite (Rare Element Resources, Ltd., 2011; 2014).

LREE dominate the Bear Lodge deposit. However, drilling between 2010 and 2012 encountered HREE-enriched FMR veins and stockwork. These localities are referred to as the Whitetail Ridge, East Taylor, and Carbon target areas. Continued drilling through 2012 updated the Whitetail Ridge resources to 2.04 million tonnes (2.25 million tons) at a grade of 2.61 percent TREO (Rare Element Resources, Ltd., 2013b). Further drilling in 2013 expanded this indicated resource to 4.26 million tons (3.86 million tonnes) at 2.49 percent TREO. This is reported to be about 2.5 times the enrichment in overall HREE element grade compared to the Bull Hill resource. The Carbon and Taylor targets, which are in close vicinity to Bull Hill and Whitetail Ridge, also contain strong REE mineralization with HREE enrichment, elevating them to a higher priority than originally thought (Rare Element Resources, Ltd., 2014).

In October 2014, Rare Element Resources reported an NI 43-101-compliant[1] total high-grade Measured and Indicated (M&I) mineral resource of 15.7 million tonnes (17.3 million tons) averaging 3.11 percent TREO at a 1.5 percent cutoff grade, which included M&I resources of 5.4 million tonnes (6 million tons) grading 4.51 percent REO at 3 percent cutoff grade. An inferred resource of 26.2 million tonnes (29.3 million tons) averaging 2.58 percent TREO was also announced (Rare Element Resources, Ltd., 2014). The relative order in decreasing abundance of REOs include Ce_2O_3, La_2O_3, Nd_2O_3, Pr_2O_3, Sm_2O_3, Gd_2O_3, Y_2O_3, Eu_2O_3, Dy_2O_3, Tb_2O_3, and others (Rare Element Resources, Ltd., 2014). The continuing expansion of the identified Bear Lodge REE deposit through drilling seems to confirm Staatz's 1983 claim that Bear Lodge may be "the largest resource of disseminated rare-earth elements in North America."

[1] National Instrument 43-101 is a Standards of Disclosure for Mineral Projects rule issued by the Canadian Securities Administrators, which governs the public disclosure of scientific and technical information by publicly-traded mining companies, including oral statements, written documents, and websites. NI 43-101 requires that all disclosure be based on advice by a "qualified person" (engineer or geologist) who, in some cases, must be independent of the mining company and the property. Its purpose is to ensure public confidence in mining-related stocks by enhancing the accuracy and integrity of public disclosure in the mining sector.

Gold mineralization occurs within the same large alkaline-igneous complex as the REE mineralization and is comingled with REE in places. The East Taylor target area was primarily a gold exploration area until a thick FMR zone was intersected in 2010. One hole intersected high-grade REE mineralization that also averaged 1.3 g/tonne (0.038 oz/ton) gold[2] from the surface to a depth of 62.5 m (205 ft). On March 15, 2011, the company released an NI 43-101-compliant inferred mineral resource estimate of 26,850 kg (947,000 oz) of gold contained in 69.3 million tonnes (76.4 million tons) averaging 0.42 ppm (0.42 g/tonne; 0.122 oz/ton) using a 0.15 ppm (0.15 g/tonne; 0.004 oz/ton) cutoff grade. A February 2012 news release reported some of Rare Element Resources' best gold drilling assays, including 24.4 m (80 feet) of 4.5 ppm (4.5 g/tonne; 0.131 oz/ton) in one hole (Rare Element Resources, Ltd., 2012). Gold exploration was suspended and there is no plan for future development as it is not currently economic (Rare Element Resources, Ltd., 2014).

Rare Element Resources' REE project is about 3,898.7 hectares (9,634 acres), which includes 499 unpatented lode mining claims and one state lease. Between 2004 and the end of October 2013, 309 drill holes amounting to 69,171.5 m (226,940.5 ft) and 20,829 assay samples had been completed (Rare Element Resources, Ltd., 2014). An October 2014 pre-feasibility report predicts the project life to be about 45 years using current mineral reserves. Once mining is underway, the physical upgrade plant will utilize gravity separation, screening, and wash processes designed to recover REE-bearing fines. The hydometallurgical plant will process the pre-concentrate through acid-leaching to produce selective precipitation of REE. This creates a high-purity, nearly thorium-free, bulk TREO concentrate (Rare Element Resources, Ltd., 2014). Projections for mine production, the physical upgrade plant, and hydrometallurgical plant can be found in table 6.

Rare Element Resources announced in December 2015 its patent-pending, zero-discharge solvent extraction separation technology was a success. The advantages of this process included a 99 percent pure lanthanum oxide product, 99 percent cerium removal, 100 percent thorium removal, easily separated light and heavy rare earths as well as a 99.7 percent pure light rare earths stream. Also, the process did not generate waste effluent nor did it require acid-stripping mixers/settlers or strong acids to recover separated REE, making the process more environmentally sound and cost efficient (Rare Element Resources, Ltd., 2015b; 2015c).

Unfortunately, continuing weak market conditions in the past few years, coupled with lengthy permitting and regulating processes, have forced Rare Element Resources to temporarily suspend permitting and licensing efforts for its Bear Lodge REE project. The temporary suspension was announced in January 2016, and the hiatus is expected to last for six months to a year (Rare Element Resources, Ltd., 2016). Details of Rare Element Resources, Ltd. recent

Table 6. A 45-year plan for the Rare Element Resources Bear Lodge Project as of 2014.

Process	Years 1-9	Years 10-38	Years 39-45
Mine Production	Average mining rate of 199,600 tonnes (220,000 tons) per year	Average mining rate of 332,000 tonnes (336,000 tons) per year	Remaining low grade stock piles
	Years 1-9	LOM	
Physical Upgrade Plant	92.8% average recovery of ore averaging 4.7% TREO	87.9% average recovery of ore averaging of 2.8% TREO	-
Hydrometallurgical Plant	88.3% approximate recovery rate with TREO production rate of 7,732 tonnes (8,523 tons) per year	89.9% approximate recovery with TREO production rate of approximately 6,813 tonnes (7,510 tons) per year	-

From Rare Element Resources (2014)

[2] By convention, ounces (oz) always means Troy ounces when referring to gold or other precious metals.

activity related to the Bear Lodge project can be found on their website at http://www.rareelementresources.com.

PRECAMBRIAN OCCURRENCES

In general, Precambrian rocks across Wyoming are potential REE hosts. Granitic igneous rocks and metamorphic rocks of various compositions contain known REE occurrences. These host concentrations and dispersions of REE-bearing minerals include allanite, euxenite, and xenotime. REE enrichment is reported in the Laramie Anorthosite Complex and the Sherman Granite in the Laramie Mountains as well as in granites and gneisses in the Medicine Bow Mountains (King and Harris, 2002). Enrichment of REE also occurs in calc-silicate pods and dikes within Archean granitic gneiss in the southern Bighorn Mountains. Alteration, such as epidotization, at some of these locales can also be an important process in concentrating REE. However, the most important Precambrian REE-host rocks in Wyoming are granitic pegmatites and other pods and dikes within granitic igneous and metamorphic units (Sutherland and others, 2013). Allanite and euxenite-bearing pegmatites have been reported within the Mesoproterozoic Sherman Granite near Tie Siding in the southern Laramie Mountains and within Paleoproterozoic granite gneiss in the Big Creek district on the west flank of the Medicine Bow Mountains.

Pegmatites

Globally, granitic pegmatites host important deposits of strategic resources. Strategic resources are elements that are important for a country's economy or defense and have substantial risk of supply disruptions (Adams and others, 1980; Linnen and others, 2012). Strategic resources commonly hosted in granitic pegmatites include Ta, Nb, Be, Sb, W, Co, and REE (Sutherland and others, 2013). Two general types of pegmatites that are important hosts of strategic resources are: Lithium-Cesium-Tantalum (LCT) pegmatites, which contain high concentrations of Li, Cs, Ta, P, B, Rb, Be, Nb, and Sn; and Niobium-Yttrium-Fluorine (NYF) pegmatites, which are enriched in niobium, yttrium, and fluorine as well as REE (Linnen and others, 2012). The LCT pegmatites currently have greater economic importance than the NYF pegmatites (Linnen and others, 2012). Yet, the economic potential of the NYF pegmatites to produce REE resources is demonstrated by the Strange Lake pegmatite in Canada, which hosts more than 140 million tonnes (154.3 million tons) of ore with an average grade of 0.9 percent TREO (Quest Rare Minerals, 2013).

LCT and NYF pegmatites typically occur within granitic intrusive complexes (Linnen and others, 2012). Although, REE-bearing pegmatites are also present within metamorphic terrains as pods and dikes that can be discordant to foliation as well as small lenses concordant to foliation (Houston, 1961; Adams and others, 1980).

The concentration and distribution of REE in natural deposits are dependent on several petrogenetic processes, including enrichment and complexing in late-stage magmatic or hydrothermal fluids, fractionation into mineral phases, oxidation or reduction, and redistribution during weathering (Castor and Hedrick, 2006). Thus, not all pegmatites may contain REE. Many combinations of factors affect whether or not the conditions are suitable for mineral crystallization or precipitation. Across Wyoming, some granitic pegmatites are potential hosts for both high- and low-grade REE-mineralization, but many do not contain REE, because the necessary conditions for formation were not met.

Significant REE enrichment is present in the Big Creek (Medicine Bow Mountains) and Tie Siding (Laramie Mountains) districts, and interesting REE or other element anomalies occur in the Weddle claims (Laramie Mountains), Many Values area (Medicine Bow Mountains), Allie claims (Bighorn Mountains), and Blackhall Mountain area (Sierra Madre). For granitic pegmatites hosted within intrusive rocks, post-emplacement processes may be important factors controlling the concentration of REE. In the Tie Siding area, post-emplacement hydrothermal activity was apparently responsible for further concentration of REE within alteration zones (Sutherland and others, 2013). In the Weddle claims, the only notable REE enrichment is associated with a granite dikelet, which reinforces the importance of post-emplacement processes in concentrating REE. In contrast, when the host is metamorphic rock, the secondary processes appear to be less important for REE enrichment in pegmatites. Field relations in the Allie claims suggest that the pegmatite bodies are the product of partial melting of the host-rock gneiss (Sutherland and others, 2013).

The Laramie Mountains are an asymmetrical, north-trending, Precambrian-cored, anticlinal uplift of Laramide age in southeastern Wyoming (fig. 4). The uplift is flanked by Paleozoic and Mesozoic sedimentary rocks and, in some locations, partially overlain by Tertiary sediments. The core of the southern part of the mountains is dominated by the 1.4 Ga Sherman Granite, other related igneous rocks, and minor metasedimentary and metavolcanic rocks (Houston, 1993). These units are cut by pegmatites, quartz veins, and mafic dikes as well as kimberlites of Late Proterozoic and Early Devonian age (Hausel, 1998). The Sherman Granite flanks the eastern and southern edges of the related, but slightly older, 1.4 Ga Laramie Anorthosite Complex (Frost and others, 1993). The anorthosite was emplaced across the northeasterly trend of the Cheyenne belt in the

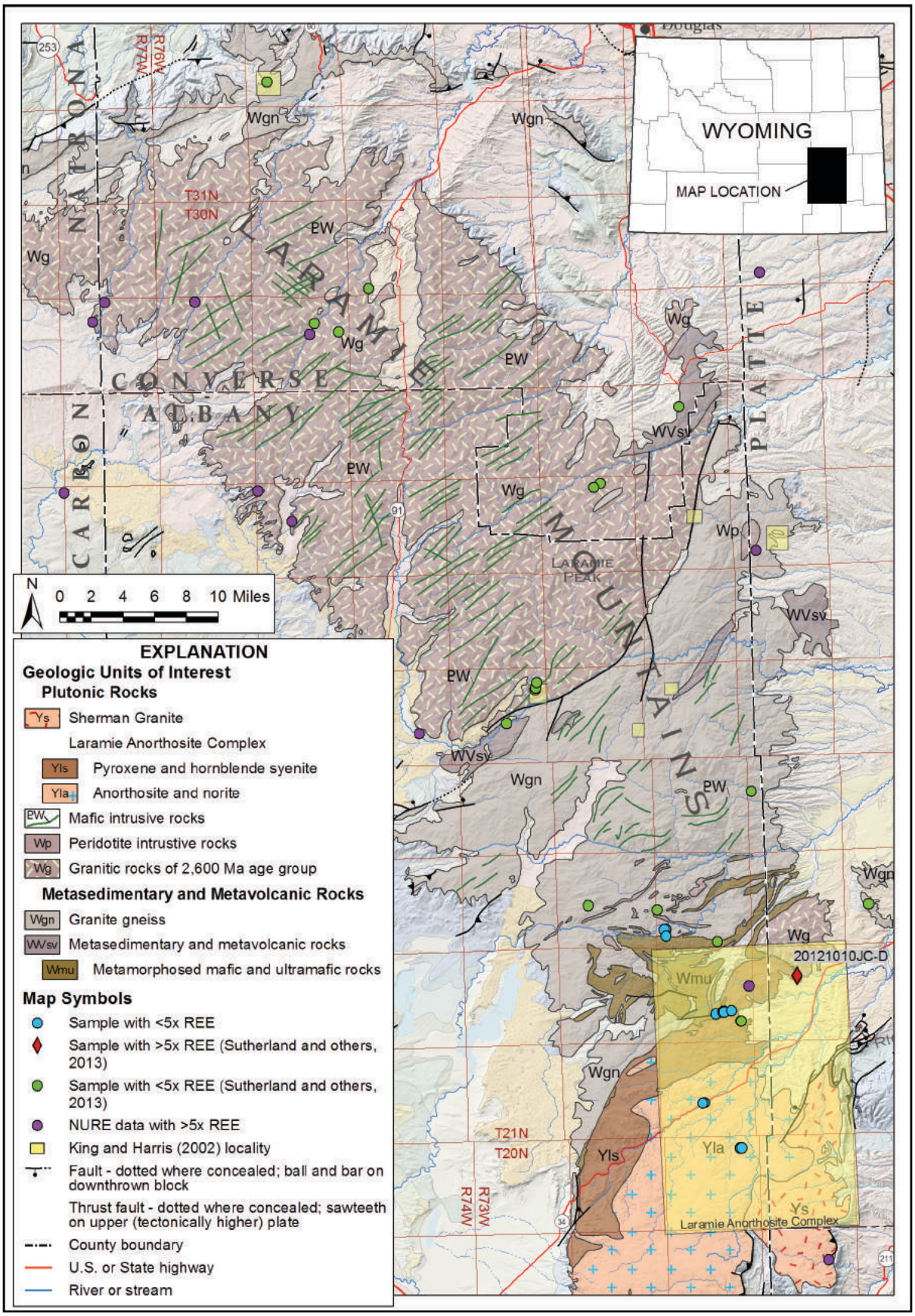


Figure 4. Sample locations and geology of the Laramie Mountains. Sampling focused in Precambrian rocks; these units are bold compared to surrounding geology. Map modified from Love and Christiansen (1985).

central Laramie Mountains, obscuring many of its features. The Cheyenne belt suture represents a continental collision zone and is the boundary between the Archean Wyoming Province to the north and the cratonized (1.7 Ga) Proterozoic rocks of the Colorado Province to the south (Graff, 1978; Hills and Houston, 1979; Houston and others, 1979). North of the anorthosite complex, the core of the range is dominated by granitic gneisses but includes a variety of mafic dikes, ultramafic intrusions, metasedimentary and metavolcanic rocks, along with pegmatites and quartz veins.

Tie Siding Pegmatites

The Tie Siding area is at the southern end of the Laramie Basin, where the Laramie Mountains broaden westward into Boulder Ridge and merge with the Medicine Bow Mountains in the south and west to become part of the Colorado Front Range. Samples that host elevated REE in this area are associated with pegmatites that cut the Sherman Granite. These pegmatites are either adjacent to northeast-trending outcrops of Lincoln Granite, or are in the vicinity of north-trending mafic dikes. Both the Lincoln Granite and the mafic dikes are interpreted to be slightly younger than the Sherman Granite (fig. 5; Frost and others, 1999).

Pegmatite pods within the Sherman Granite southeast of Tie Siding (fig. 5) can be highly radioactive and enriched in some REE (King and Harris, 2002). The Tie Siding pegmatites are typically zoned, and have an overall alkali feldspar granite composition. Zonation consists of an outer zone of biotite, microcline, and quartz, a central zone that is more than 90 percent microcline, and an inner core of quartz (Griffin and Warner, 1982). Many of these pegmatites are freshly exposed due to mining of potassium feldspar in the 1940s (fig. 6A; Osterwald and others, 1966; Griffin and Warner, 1982).

The REE-bearing minerals within some of these pegmatites are uncertain, but allanite (fig. 6B) is present in at least one locality, and zones of elevated radioactivity (7 – 500 times background) are present at all of the studied pegmatites (Griffin and Warner, 1982). The highest levels of radioactivity are associated with biotite (Sutherland and others, 2013), and Griffin and Warner (1982) suggest that the source of this radioactivity is zircon hosted within the biotite. However, a sample of biotite (Sample 20121107JC-E) associated with high radioactivity was not radioactive and contained very little zircon. Radioactivity associated with several large biotite seams exhibits significant variability along the seam, suggesting that the source of the radioactivity is not disseminated uniformly throughout. Most of the high REE concentrations in the Tie Siding pegmatites (table 7) are associated with alteration zones on the margins of the pegmatites. However, the highest concentration of REE is found in large, 0.3-0.6 m (1-2 ft) diameter, allanite nodules within alkali feldspar (fig 6B; Sutherland and others, 2013).

Tie Siding pegmatite #1, sec. 35, T. 13 N., R. 72 W. and NE¼NW¼ sec. 2, T. 12 N., R. 72. W., Albany County

Outcrops in this area are dominated by pink, very coarse-grained to pegmatitic, epidote-pyroxene monzonite of the Sherman Granite. Moderate to abundant magnetite plus moderate hematite and limonite staining (Sample 20121107JC-A) are present. This monzonite is enriched in all of the REE as well as yttrium and niobium (table 7; Sutherland and others, 2013).

Smith (1954) identified pyrochlore in this pegmatite and reported a sample with 4.1 percent ThO_2, 0.35 percent chemical uranium[3] (cU_3O_8), and 1.23 percent equivalent uranium[3] (eU_3O_8). He also noted radioactivity up to 900 times background and a vitreous radioactive mineral (Smith, 1953a). Subsequent workers were unable to locate this pegmatite (Griffin and Warner, 1982), and the reported location in sec. 35, T. 13 N., R. 72 W. (Smith, 1953a; 1954) is probably incorrect. However, a biotite alkali-feldspar granite to granite pegmatite is exposed in a group of small prospect pits in the SE¼NW¼ sec. 2, T. 12 N., R. 72 W. to the south of the location cited by Smith (1953a; 1954).

Feldspars in the pegmatite exhibit graphic texture, and a zone of feldspar to clay alteration is associated with radioactivity up to eight times background (3,800 counts per minute [cpm] with background of 500 cpm). When isolated, a sample of this material (Sample 20121107JC-B) exhibited only slightly anomalous radioactivity. It is enriched in all of the REE, yttrium, and niobium to concentrations greater than five times the crustal abundance except for europium, which is present at more than three times crustal abundance. This sample also contains more than 0.04 percent uranium and 0.065 percent thorium (table 7; Sutherland and others, 2013).

A sample of granitic pegmatite with biotite (Sample 20121107JC-C) adjacent to the alteration zone exhibits minor to moderate epidote, hematite, and limonite staining but no anomalous radioactivity. It is also weakly

[3] Chemical uranium, cU_3O_8 or cU, is defined as uranium assay or grade determined from chemical analysis of a sample. Equivalent uranium, eU_3O_8 or eU, refers to the grade or assay of uranium determined from gamma logging. Thorium may also be determined this way and is reported as eTh.

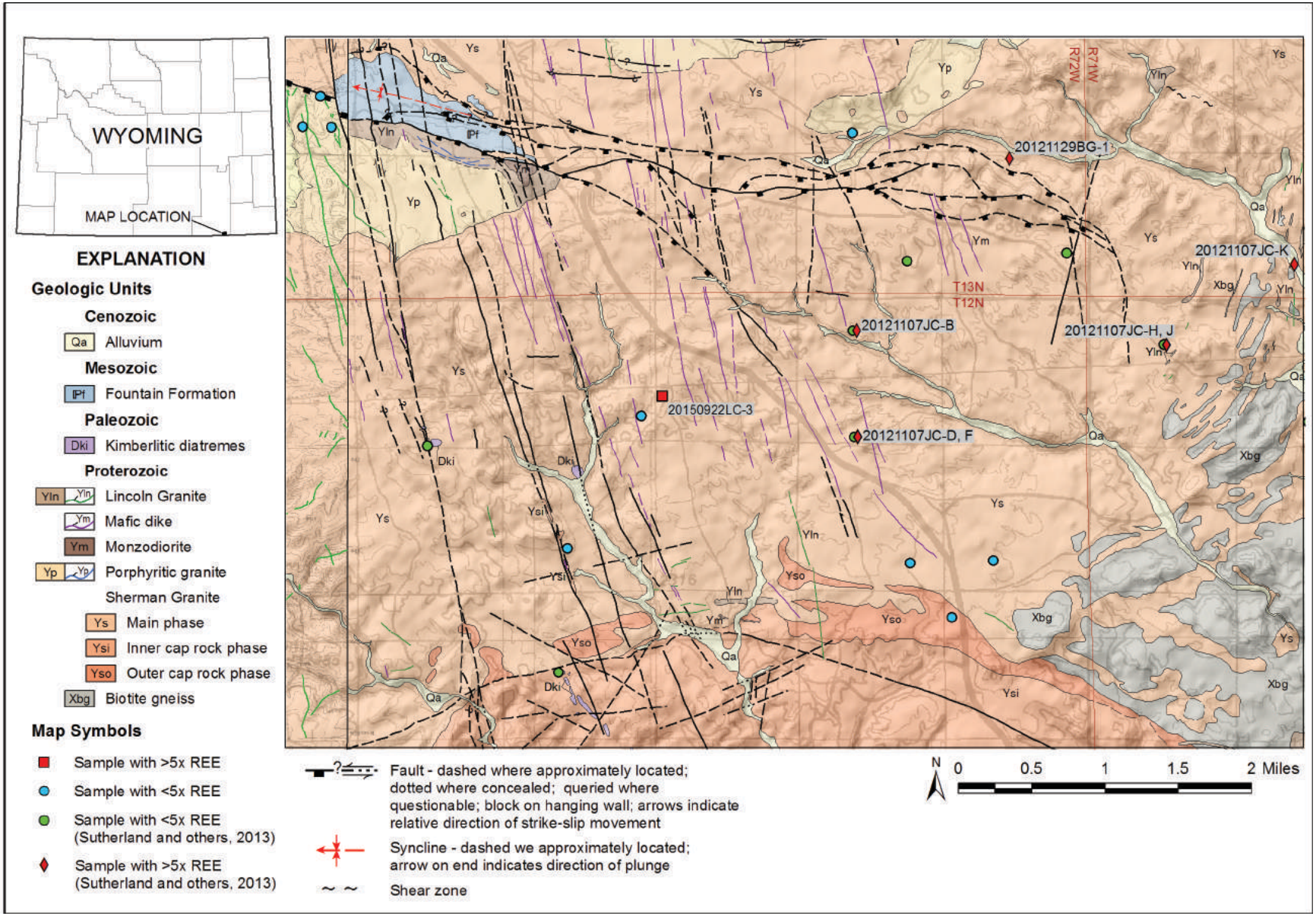


Figure 5. Sample locations and geology of the Tie Siding area. Sampling done during this study and RI-65 (Sutherland and others, 2013) was primarily in Sherman Granite and Lincoln Granite with many dikes, veins, and faults. Map modified from Ver Ploeg and others (2011) and Carnes and others (2013).

enriched in lanthanum, cerium, and praseodymium (table 7; Sutherland and others, 2013).

Tie Siding pegmatite #2, NE¼SE¼ sec. 36, T. 13 N., R. 72 W., Albany County

Uraniferous zircon (crytolite) was reported in this pegmatite (Smith, 1954), as was a vitreous radioactive mineral with radioactivity up to 35 times background (Smith, 1953b). Griffin and Warner (1982) associated the high radioactivity with biotite and reported an analysis of 200 ppm lanthanum, 50 ppm yttrium, <10 ppm niobium, 500 ppm zirconium, and 20 ppm cU_3O_8.

Background radiation in the area is about 500 cpm and about 1,650 cpm inside a prospect pit where the pegmatite, similar in composition to pegmatite #1, is exposed. The pegmatite is cut by a small dike of white to pink, medium- to coarse-grained biotite granite (Sample 20121107JC-G) associated with elevated radioactivity more than 15 times background (7,600 cpm). When isolated, this sample is not anomalously radioactive. The granite is enriched in Eu, Er, Tm, Yb, Lu, and Nb (table 7; Sutherland and others, 2013).

Tie Siding pegmatite #3, SW¼NE¼ sec. 6, T. 12 N., R. 71 W., Albany County

Smith (1953c) reported radioactivity up to 35 times background and a vitreous radioactive mineral at this location. Griffin and Warner (1982) associated the high radioactivity with biotite and reported an analysis of 50 ppm lanthanum, 1,000 ppm niobium, >200 ppm yttrium, and 127 ppm cU_3O_8.

Table 7. Concentration of REE from the Tie Siding area. Bold values indicate concentrations greater than five times the crustal abundance.

	Tie Siding area								
Element	La (ppm)	Ce (ppm)	Pr (ppm)	Nd (ppm)	Sm (ppm)	Eu (ppm)	Gd (ppm)	Tb (ppm)	Dy (ppm)
20121107JC-B	**2,110**	**4,670**	**384**	**1,185**	**122.5**	6.1	**58.8**	**7.44**	**36.2**
20121107JC-D	9.7	14.1	3	13.4	4.87	0.33	7.38	1.59	11.6
20121107JC-E	27	32	5.2	20.8	5.3	<0.2	7.3	1.26	9.4
20121107JC-F	4.9	5.9	1.28	6.1	3.15	0.29	6.83	1.59	13
20121107JC-G	12.4	4.4	2.49	9	1.74	2.29	2.14	0.43	3.27
20121107JC-H	5.8	29.4	2.37	12.1	7.32	0.16	15.7	4.05	**32.1**
20121107JC-J	**821**	**1285**	**187.5**	**661**	**119**	8.77	**96.2**	**11.65**	**56.9**
20121107JC-K	**23,200**	**60,300**	**8,400**	**35,200**	**7,800**	**63.7**	**5,400**	**674**	**2,830**
20121129BG-1	10.9	17.6	3.28	14.4	6.11	1.96	9.67	2.37	18.3
20150922LC-3*	**194**	**504**	**68**	**301**	**61.5**	1.85	**52.7**	**8.04**	**45.5**

Element	Ho (ppm)	Er (ppm)	Tm (ppm)	Yb (ppm)	Lu (ppm)	Sc (ppm)	Y (ppm)	Cumulative REE (ppm)
20121107JC-B	**7.33**	**22.5**	**3.86**	**28.7**	**5.47**	2	**252**	**8,902**
20121107JC-D	2.73	9.8	1.97	**16.2**	**2.95**	1	81.9	182.5
20121107JC-E	2.37	9.5	1.77	**15.5**	2.57	2.2	68	210.2
20121107JC-F	3.56	13.2	**2.47**	**18.1**	**3.34**	<1	118	201.7
20121107JC-G	0.91	3.54	0.75	6.53	1.36	<1	23.8	75.05
20121107JC-H	**8.36**	**28.3**	**4.85**	**32.2**	**5.25**	3	**225**	416.0
20121107JC-J	**10.25**	**25.1**	**3.37**	**20.2**	**3.3**	7	**301**	**3,617**
20121107JC-K	**437**	**915**	**106.5**	**578**	**83.3**	9	**9,540**	**155,537**
20121129BG-1	4.61	**17.3**	**3.43**	**29.1**	**5.31**	1	137	282.3
20150922LC-3*	**9.13**	**24.8**	**3.4**	**22.8**	**3.36**	49	**229**	**1,578.08**

Samples containing elevated REE from Sutherland and others (2013)

*From this study

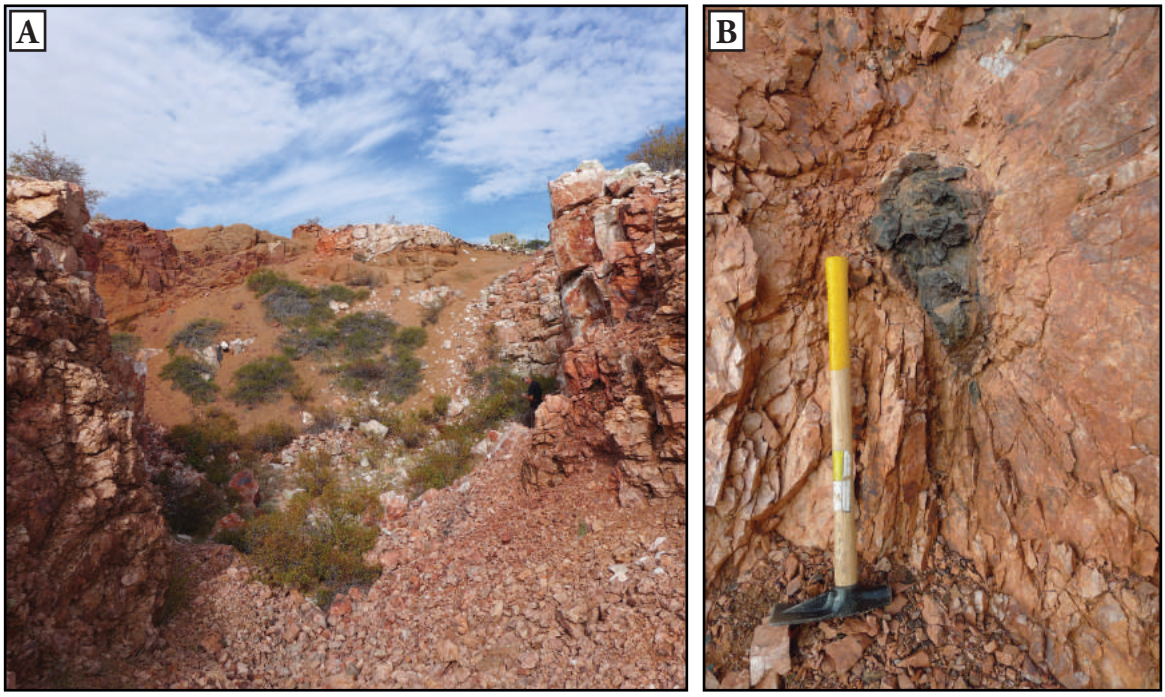


Figure 6. Tie Siding pegmatites. A) A large pegmatite prospect in the Tie Siding area. Pegmatite is cross cut by a rusty shear zone shown in the upper left (Sample 20150922LC-1). B) Allanite nodule in the Holiday Place pegmatite, sampled during RI-65 (Sample 20121107JC-K; Sutherland and others, 2013).

This pegmatite is exposed in an abandoned quarry owned by Adventure Stone, LLC, a producer of construction aggregate and decorative stone in the 1990s and early 2000s. Background radiation outside of the quarry is about 500 cpm but increases to about 1,650 cpm within the quarry. The exposed pegmatite here is similar to that of pegmatite #1, except that it hosts 1.8 m (6 ft) long and up to 15 cm (5.9 in) thick seams of biotite associated with hematite. High radioactivity (20,000 cpm), up to 40 times background, is associated with a large biotite seam near a granite pegmatite that exhibits clay alteration of feldspars (Sample 20121107JC-H). The sample itself is not anomalously radioactive (Sutherland and others, 2013). The contact between the granite pegmatite and enclosing monzonite is filled by a green, fine-grained to aphanitic mafic dike with plagioclase phenocrysts, very-fine grained hornblende, biotite, quartz, and dendritic pyrolusite fracture coating (Sample 20121107JC-I). The monzonite-mafic dike contact hosts a zone where feldspars have been altered to clay (Sample 20121107JC-J; Sutherland and others, 2013).

The altered pegmatite (Sample 20121107JC-H) is enriched in the HREE, except europium, as well as samarium, yttrium, and niobium, and it contains greater than five times the crustal abundance of Dy, Ho, Er, Tm, Yb, Lu, and Y. The mafic dike near the margin of the pegmatite (Sample 20121107JC-I) is enriched in all of the HREE as well as neodymium, samarium, and yttrium. The altered zone (Sample 20121107JC-J) is enriched in all of the REE as well as yttrium; only europium and niobium are present at lower concentrations (table 7; Sutherland and others, 2013).

Tie Siding pegmatite #4, SE¼SW¼ sec. 2, T. 12 N., R. 72 W., Albany County

High radioactivity at this location is associated with biotite, and a biotite-bearing sample of this pegmatite contained 500 ppm lanthanum, 200 ppm niobium, 150 ppm yttrium, and 57 ppm cU_3O_8. A sample of altered granite southwest of the pegmatite yielded 230 ppm lanthanum, 100 ppm niobium, 36 ppm yttrium, 30 ppm cU_3O_8, and a trace of allanite (Griffin and Warner, 1982).

Background radiation outside of the pegmatite quarry is about 500 cpm but increases to about 1,650 cpm within the quarry. The pegmatite is compositionally similar to pegmatite #3. Biotite in this pegmatite occurs both as seams with associated hematite and as radiating groups of biotite books. Elevated radioactivity (5,000 cpm) is present in an altered, extensively fractured part of the pegmatite associated with a biotite seam and a hematite seam (Sample 20121107JC-D). About 20 m (65 ft) east of this sample, high radioactivity (13,000 cpm) is associated with the

west end of a 10 x 60 cm (4 x 24 in) biotite seam (Sample 20121107JC-E). The biotite itself did not register above background (approximately 1,650 cpm) and neither did a sample of biotite granite pegmatite located just above the biotite books (Sample 20121107JC-F; Sutherland and others, 2013).

The biotite seam (Sample 20121107JC-E) exhibits weak to moderate HREE enrichment, with ytterbium enriched greater than five times the crustal abundance. Furthermore, the biotite contains more than 0.05 percent niobium, the highest value for niobium of any of the samples collected from the Tie Siding pegmatites. The altered pegmatite (Sample 20121107JC-D) is also enriched in yttrium and all of the HREE, except europium. Ytterbium and lutetium are present above five times the crustal abundance, and the pegmatite contains more than 0.02 percent thorium and nearly 0.03 percent niobium. The unaltered biotite granite pegmatite (Sample 20121107JC-F) is similarily enriched in yttrium and the HREE, except europium, and contains more than five times the crustal abundance of thulium, ytterbium, and lutetium; it also contains more than 0.03 percent thorium (table 7; Sutherland and others, 2013).

Holiday Place pegmatite, SE¼SW¼ sec. 32, T. 13 N., R. 71 W., Albany County

Griffin and Warner (1982) found a trace of allanite here and reported up to 1,000 ppm lanthanum, >200 ppm yttrium, 50 ppm niobium, and 198 ppm cU_3O_8. This pegmatite is exposed in a prospect pit in a hill on the east side of Dale Creek. Background radioactivity near the pit was about 1,000 cpm. The pegmatite is similar to pegmatites #3 and #4, but it lacks the radiating biotite books and hosts 30 x 60 cm (12 x 24 in) nodules of allanite (Sample 20121107JC-K; fig. 6B; Sutherland and others, 2013).

The allanite nodules exhibit radioactivity up to 50,000 cpm and are centers for radial fractures that extend into the surrounding alkali feldspar. The sampled allanite nodule contains more than 15 percent REE and yttrium, nearly 0.1 percent uranium, and more than 0.5 percent thorium (table 7). As observed in outcrop, the nodules appear to account for 1 percent or less of the entire volume of the pegmatite (Sutherland and others, 2013). Although the REE content within the allanite is high, its makeup of 1 percent or less of the outcrop combined with the small size of the pegmatite is not encouraging for economic development.

Unnamed pegmatite, NE¼NW¼ sec. 36, T. 13 N., R. 72 W., Albany County

A granitic pegmatite, not previously mentioned in the literature, is exposed in a prospect pit at this location. This pegmatite is similar in composition to pegmatite #1 but has biotite- and hematite-rich seams similar to those present in pegmatite #4. These biotite- and hematite-rich seams are associated with altered pegmatitic alkali-feldspar with inclusions of hematite, biotite, and a vitreous black mineral (Sample 20121129BG-1) that is enriched to greater than five times the average crustal abundance in Er, Tm, Yb, and Lu as well as Nb and Ta (table 7; Sutherland and others, 2013).

Tie Siding area, center of S½NW¼SW¼ sec. 3, T. 12 N., R. 72 W., Albany County

The Sherman Granite is widespread in this area and contains veins, pegmatites, fractures, and faults. Most of the pegmatites sampled in the vicinity did not contain elevated REE. However, at this location, a low-lying outcrop in the middle of a two-track road contained elevated concentrations of almost every REE. This outcrop is a severely weathered, rusty, granitic gneiss. Fractures cross-cutting the gneiss are filled with an unidentifiable, dense, black, slightly metallic, non-magnetic mineral. The sample (20150922LC-3) contained REE commonly at or above eight times the crustal abundance. Europium was the only REE that showed no elevation (table 7). Similar rusty weathering granite (20150922LC-4) was found in the area and contained 819 ppm Mo, 105.5 ppm Se, 40.9 ppm Te, >250 ppm Bi, 0.41 ppm Au, and 37.5 percent Fe_2O_3 but no REE enrichment. Another sample (20150922LC-7B) to the north that did not have elevated REE contained 2,000 ppm Sr.

Weddle claims, SE¼NE¼ sec. 2, T. 15 N., R. 71 W. and SW¼NW¼ sec. 1, T. 15 N., R. 71 W., Albany County

This location, in the Laramie Mountains, is about 17 miles northeast of the Tie Siding area where the Sherman Granite is cut by pegmatites and granitic dikes (King and Harris, 2002). Samples of beryl- and possibly euxenite-bearing pegmatite, analyzed by Griffin and Warner (1982), contained up to 700 ppm lanthanum, 50 ppm niobium, 367 ppm U_3O_8, and 70 ppm Y. High radioactivity within the pegmatite was found to be associated with biotite. Because of the possible occurrence of euxenite and the association between radioactivity and biotite, King and Harris (2002) suggested that these pegmatites are related to those near Tie Siding.

Two large prospect pits are present within a granitic pegmatite containing abundant biotite in section 2. The pegmatite is cut by granite dikes and quartz veins up to 60 cm (24 in) thick. Hematite staining is abundant throughout the pegmatite (Sample 20120921BG-1), but unstained portions are also present (Sample 20120921BG-2). In places this pegmatite is extremely biotite-rich (up to 50 percent; Sample 20120921BG-3). The cross-cutting granitic dikes are pink

and coarse-grained with moderate biotite and Fe-staining as well as minor epidote alteration (Sample 20120921BG-4). Two of the samples taken here (20120921BG-1 and 20120921BG-4) are slightly enriched in HREE, but the amount of enrichment found by Griffin and Warner (1982) was not encountered (table 8); neither beryl nor euxenite were observed (Sutherland and others, 2013).

The pegmatite in section 1 is similar in composition to the pegmatite in section 2 but contains biotite pods up to about 30 cm (12 in) across and orange, pegmatitic, alkali feldspar (Sample 20120921BG-5). A thin, biotite-granite dikelet that cuts both the pegmatite and a quartz vein includes an unidentified, fine-grained, black mineral (Sample 20120921BG-6); this sample exhibits weak enrichment in HREE, notably thulium and ytterbium. A medium- to coarse-grained granite at this location is weakly enriched in some of the HREE (Sample 20120921BG-7; Sutherland and others, 2013).

Medicine Bow Mountains

The Medicine Bow Mountains and Sierra Madre are Precambrian-cored Laramide uplifts that are cut by the Cheyenne belt (fig. 7). The Mullen Creek-Nash Fork shear zone, which forms part of the Cheyenne belt cuts the Precambrian of the southern Medicine Bow Mountains along a northeast trend, while similar shear zones and faults cut easterly across the southern Sierra Madre. The Cheyenne belt in the Medicine Bow Mountains and Sierra Madre is characterized by highly fractured cataclastic rocks accompanied by numerous faults and shear zones. North of the Cheyenne belt, amphibolite grade schists and gneisses are overlain by younger Archean and Proterozoic metasedimentary and metaigneous rocks (Sutherland and Hausel, 2005). Metaconglomerates, found in several of these rock units, host occurrences of uranium, thorium, and REE. Similarities between these rocks and the gold-rich quartz-pebble metaconglomerates of the Witwatersrand, in South Africa, suggest that they also have potential to host gold (Houston and others, 1978). South of the Cheyenne belt, the Colorado Province consists of volcanogenic island-arc basement rocks, intrusive granites, and gabbroic complexes.

Many Values Area

The Many Values area covers the E½ sec. 32 and W½ sec. 33, T. 13 N., R. 78 W. along Forest Service Road 544 in the southern Medicine Bow Mountains. Local rocks consist of Paleoproterozoic felsic gneiss intruded by the Mesoproterozoic Sherman Granite, both of which are cut

Table 8. Concentration of REE from the Weddle claims. Bold values indicate concentrations greater than five times the crustal abundance.

	Weddle claims								
Element	La (ppm)	Ce (ppm)	Pr (ppm)	Nd (ppm)	Sm (ppm)	Eu (ppm)	Gd (ppm)	Tb (ppm)	Dy (ppm)
20120921BG-1	5.4	4.82	6.57	6.1	2.35	0.1	4.32	0.86	6.57
20120921BG-2	0.8	1.14	0.14	0.4	0.09	0.09	0.1	0.02	0.014
20120921BG-3	2.5	3.9	0.63	2.7	0.8	0.38	1.07	0.2	1.28
20120921BG-4	2.8	3.7	0.8	3.7	1.66	0.16	2.51	0.54	3.74
20120921BG-5	1.1	1.15	0.33	0.6	0.17	0.08	0.27	0.05	0.33
20120921BG-6	9.5	18.5	2.34	9.4	2.99	0.27	4.79	1.2	9.09
20120921BG-7	16.6	42.1	4.81	17.6	3.79	0.57	3.96	0.75	4.82

Element	Ho (ppm)	Er (ppm)	Tm (ppm)	Yb (ppm)	Lu (ppm)	Sc (ppm)	Y (ppm)	Cumulative REE (ppm)
20120921BG-1	1.7	6.39	1.23	10.4	1.67	0.3	67.5	126.3
20120921BG-2	0.03	0.012	0.02	0.17	0.03	0.2	1	4.3
20120921BG-3	0.3	1.14	0.21	1.45	0.25	0	11.5	28.3
20120921BG-4	0.82	2.95	0.58	4.17	0.66	0	23.3	52.1
20120921BG-5	0.08	0.27	0.05	0.33	0.05	0.1	2.4	6.8
20120921BG-6	2.21	8.36	1.6	11.35	1.87	0	63.1	146.6
20120921BG-7	1.16	4.1	0.73	5.24	0.87	0	35.7	142.8

From Sutherland and others (2013)

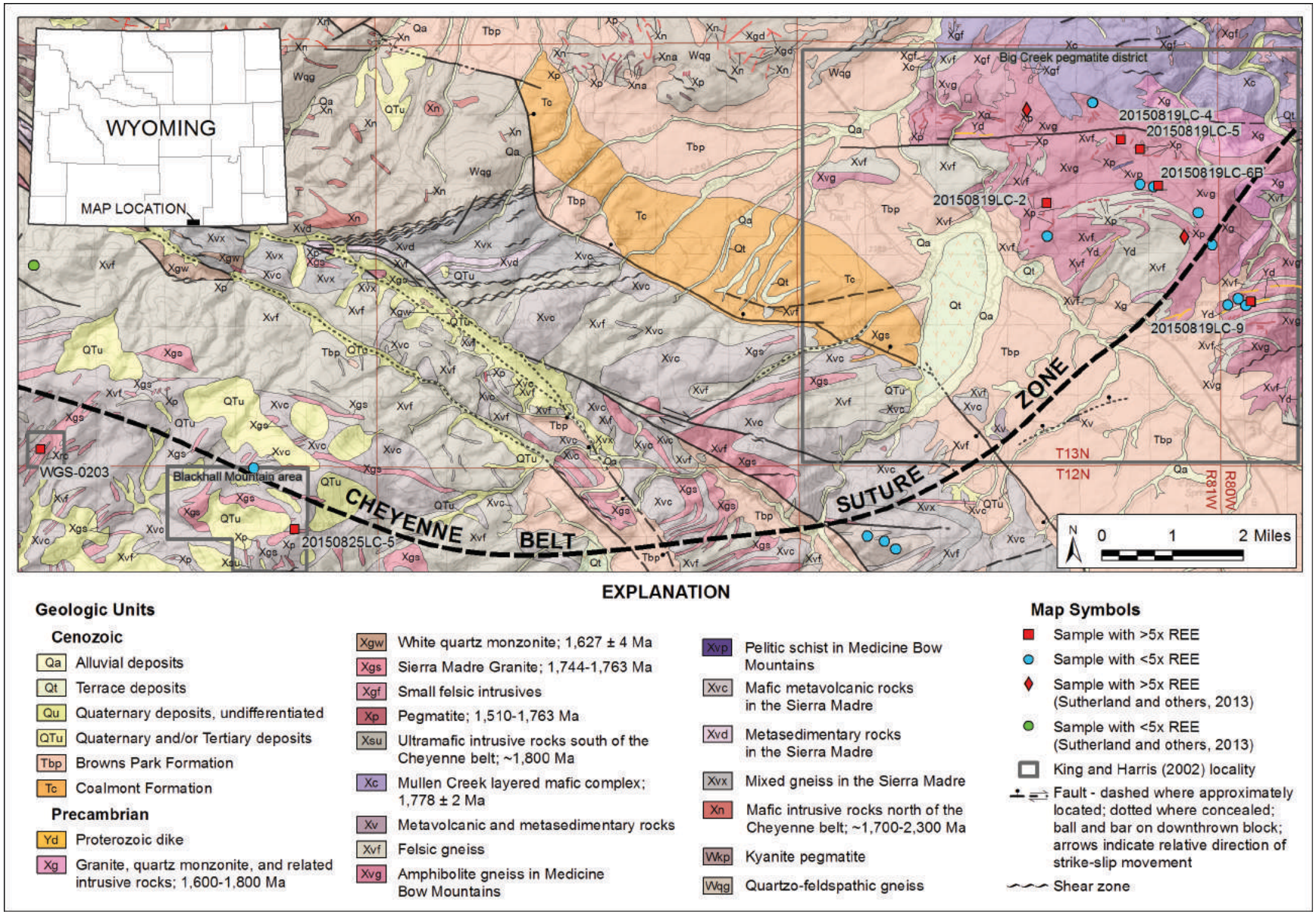


Figure 7. Sample locations and geology of the Big Creek pegmatite district and eastern Sierra Madre. The geology sampled is primarily Precambrian metamorphic rock with veins and pegmatites. The Cheyenne belt crosses this area, affecting the regional structure (Houston, 1993). Map modified from Sutherland and Hausel (2005).

by granitic pegmatites (Sutherland and Hausel, 2005). Tantalum, mica, and beryl were produced from a mine within the Many Values area in the early 1940s (King and Harris, 2002).

Many Values mine, SE¼NE¼ sec. 32, T. 13 N., R. 78 W., Albany County

Two shallow shafts and several prospect pits, developed in Paleoproterozoic, tourmaline-rich, mica schist and gneiss host rock, are cut by pegmatites striking 230˚ and dipping 85˚ NW. The pegmatites are muscovite-rich, granite to granodiorite with rapakivi texture, minor euhedral garnet, and minor iron staining. Through the early 1940s, 18,600 kg (41,000 lbs) of mica, 1.8 tonnes (2 tons) of beryl, and 39 kg (85 lbs) of tantalite were produced from two of the granitic, cross-cutting pegmatites (Osterwald and others, 1966). Additionally, Adams and others (1980) found euxenite, fergusonite, allanite, and cleavelandite within the Many Values pegmatites; they noted that tantalite typically occurs as inclusions in cleavelandite. A representative sample of the Many Values pegmatite (20120911WS-D) yielded 75.8 ppm niobium (4.5 times crustal abundance) and 10.3 ppm tantalum (6.1 times crustal abundance), but no other significant enrichment is present (Sutherland and others, 2013).

Many Values prospect pits, SE¼NE¼ sec. 32 and NE¼SE¼ sec. 33, T. 13 N., R. 78 W., Albany County

A prospect pit about 0.8 km (0.5 mi) east of the Many Values Mine exposes a granitic pegmatite that cuts gneiss; this pegmatite (Sample 20120911WS-B) is weakly graphitic and exhibits minor epidote alteration but is not enriched in any of the REE or other elements of economic interest. A prospect pit about 107 m (350 ft) east of the Many Values Mine exposes a pegmatite that cuts the Sherman Granite; the pegmatite (Sample 20120911WS-C) contains 62.7 ppm tantalum (36.9 times the crustal abundance; Sutherland and others, 2013).

Big Creek Pegmatite District

The Big Creek pegmatite district (fig. 7), on the west side of the Medicine Bow Mountains, was investigated and mapped by Houston (1961). The district is located within the E½ of T. 13 N., R. 81 W. and W¼, T. 13 N., R. 80 W. It covers an area of the Colorado Province several miles wide about 3.2 to 10 km (2 to 6 mi) south of the Mullen Creek-Nash Fork shear zone, which is part of the Cheyenne belt; northwest-southeast-trending structures control the location of outcrops. One of the larger layered mafic complexes in the western U.S., the Mullen Creek complex, lies along the northern edge of the Big Creek pegmatite district. In the mid-1950s, conflicting records showed that between 2,700 and 9,070 tonnes (3,000 and 10,000 tons) of REE-bearing material were removed from pegmatite in the Platt Mine (Houston, 1961; Adams and others, 1980; King and Harris, 2002). This was one of the few historic economic REE operations in Wyoming.

Houston (1961) described two types of granite pegmatites that cut Early Proterozoic amphibolite gneiss in close proximity to both a medium- to coarse-grained, pink to gray, foliated, granitic intrusion and a well-foliated amphibolite of the 1,778 ± 2 Ma, Mullen Creek layered mafic igneous complex. He noted that the distinctions between the two types were arbitrary and that the they were gradational with each other. In the vicinity of known REE occurrences, the amphibolite gneiss is dominated by hornblende gneiss and schist, with lesser, alternating layers of feldspar-quartz-biotite gneiss.

The most common type of pegmatite is unzoned with feldspar and quartz that is roughly conformable in direction and attitude to the amphibole gneiss. These pegmatites tend to be long and narrow, with widths rarely greater than 3 m (10 ft) and lengths exceeding 0.8 km (0.5 mi). Their contacts with the country rock are sharp and exhibit no decrease in grain size along the margins. Mineralogy is simple and is dominated by feldspar accompanied by minor quartz and accessory biotite, muscovite, garnet, magnetite, and ilmenite (Houston, 1961).

The second type of pegmatite can have poorly developed zoning, has cross-cutting relationships with the amphibole gneiss, and tends to be elliptical in plan view, with lengths averaging three times their widths. Similar to the first type, these pegmatites have sharp contacts and show no decrease in grain size toward contacts with the country rock. However, the mineralogy is more complicated and includes garnet, biotite, muscovite, tourmaline, fluorite, and rarely monazite, allanite, euxenite, and columbite along with feldspar and quartz (Houston, 1961).

Houston (1961) described these pegmatites as either copper-bearing or REE-bearing. In the district he noted five pegmatites of the type two variety that are known to host one or more of the REE-bearing minerals monazite, allanite, and euxenite. Only the Platt pegmatite contained economic quantities of these minerals. Numerous other pegmatites in the district were not examined but have the potential to host REE mineralization (King and Harris, 2002). The nearby Big Creek mine hosted copper mineralization but no primary REE minerals or columbite. Columbite [$(Fe,Mn)(Nb,Ta)_2O_6$] may contain REE and uranium as accessory constituents (King and Harris, 2002; MinDat.org, 2016).

Big Creek pegmatite 2, N½SW¼NE¼ sec. 15, T. 13 N., R. 81 W., Carbon County

Sample 20150819LC-2B contained epidote and garnet in a rusty granitic gneiss and pegmatite. The outcrop was widespread and the sample was collected from a 0.28 square meter (3 sq-ft) prospect. A collapsed prospect or shaft was also near the location. The garnet-rich sample contained elevated Er, Lu, Tm, and Yb (table 9).

Big Creek pegmatite 4, SW¼NE¼ sec. 11, T. 13 N., R. 81 W., Carbon County

This prospect was composed of plagioclase-quartz-muscovite gneiss with rusty, subhedral garnets and chalky feldspars. The sample (20150819LC-5) contained elevated lutetium and ytterbium (table 9).

Big Creek pegmatite 5, NE¼SE¼ sec. 11, T. 13 N., R. 81 W., Carbon County

Sample 20150819LC-5 was taken from an extensive, low-lying outcrop (fig. 8A) of light colored gneiss and pegmatite. The gneiss, graphic in part, is primarily plagioclase and quartz with some potassium feldspar. Red garnet and magnetite grains ranging from a few millimeters to centimeters (less than 0.1 to 1.0 in) in diameter are present. A yellowish-orange halo around the magnetite grains stains the gneiss (fig. 8B). Er, Lu, Tm, Y, and Yb were all present at more than five times the crustal abundance, and Ho was also elevated (table 9).

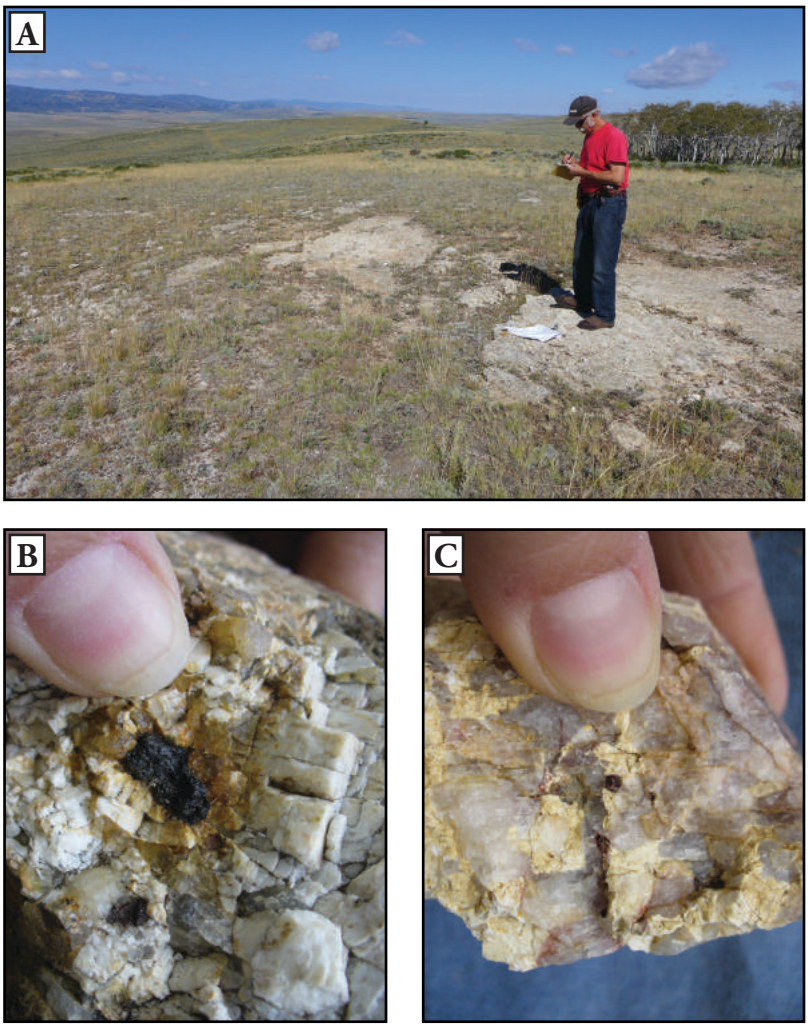


Figure 8. Pegmatites in the Big Creek pegmatite district. A) The low-lying outcrop of pegmatite 5 (Sample 20150819LC-5). B) Magnetite with a rusty halo and garnet from pegmatite 5. C) Yellow, chalky plagioclase with garnet and quartz in pegmatite 9 (Sample 20150819LC-9).

Big Creek pegmatite 6, NE¼NE¼ sec. 13, T. 13 N., R. 81 W., Carbon County

Many prospects were cut into granite and pegmatite along a low ridge about 0.8 km (0.5 mi) southeast of Big Creek pegmatite 5, and the outcrop sampled has similar characteristics as the previous location. The gneiss and pegmatite were primarily composed of plagioclase, quartz, and k-feldspar with rusty garnets. Sample 20150819LC-6B contained more than quintuple the crustal abundance of Lu, Tm, Yb, and slightly elevated Y (table 9).

Big Creek pegmatite 9, SW¼NW¼SE¼ sec. 19, T. 13 N., R. 80 W., Carbon County

Sample 20150819LC-9 contained granitic gneiss and pegmatite with k-feldspar, yellowish chalky plagioclase (fig. 8C), rusty quartz veins, garnet, and magnetite. This sample in particular contained the same REE as the previous locations but at much higher concentrations. Europium was 21 times the average crustal content, Ho 11 times, Lu 35 times, Tm 30 times, Y 12 times, and Yb 40 times the average. Many large prospects were located in the area in close proximity to mapped Proterozoic dikes and felsic gneiss (Sutherland and Hausel, 2005). Table 9 compares the chemistry of the Big Creek pegmatite area.

Multiple samples from the Big Creek area and on Blackhall Mountain contain magnetite as well as REE enrichment. This suggested to the authors that there may be a relationship between the two. It should be noted that there were also samples with magnetite that were not enriched in

Table 9. Concentration of REE from Big Creek pegmatite district. Bold values indicate concentrations greater than five times the crustal abundance.

	Big Creek pegmatite district								
Element	La (ppm)	Ce (ppm)	Pr (ppm)	Nd (ppm)	Sm (ppm)	Eu (ppm)	Gd (ppm)	Tb (ppm)	Dy (ppm)
20120917BW-A*	2	3.8	0.65	3.4	3.18	0.61	12.6	**5.06**	**56.9**
20120917JC-A*	51.4	72.5	13.5	52.7	12.8	0.6	12.4	2.4	17
20150819LC-2B	1.4	3.4	0.46	2.2	1.14	0.28	1.89	0.65	7.22
20150819LC-4	2.2	4	0.66	3.7	3.57	0.11	7.22	1.86	13.15
20150819LC-5	0.05	0.9	0.012	0.5	0.36	0.2	2.21	1.19	14.45
20150819LC-6B	3.8	6.7	1	4.25	1.82	0.31	6.15	2.01	15.5
20150819LC-9	6.8	11.8	1.77	6.5	1.74	0.37	4.8	2.35	32.1

Element	Ho (ppm)	Er (ppm)	Tm (ppm)	Yb (ppm)	Lu (ppm)	Sc (ppm)	Y (ppm)	Cumulative REE (ppm)
20120917BW-A*	**18.15**	**79.2**	**17.25**	**142**	**26.6**	30	**697**	**1,098.4**
20120917JC-A*	4	**16.5**	**4**	**36.2**	**6.8**	9.2	**261**	573.0
20150819LC-2B	2.87	**14.05**	**2.79**	**25.4**	**4.98**	3	73.2	144.93
20150819LC-4	2.81	8.84	1.6	**13.75**	**2.1**	10	105	180.57
20150819LC-5	5.2	**22.8**	**4.61**	**40.2**	**7.12**	6	**168**	273.80
20150819LC-6B	3.71	12.45	**2.39**	**21.1**	**3.41**	8	127.5	220.10
20150819LC-9	**13.55**	**63.9**	**12.65**	**110**	**19.95**	11	**350**	649.28

*Samples from Sutherland and others (2013). REE in sample 20120917JC-A are normalized for silica.

REE, yet the number of samples with both magnetite and enriched REE was noticeable. Hydrothermal deposits can commonly have REE, magnetite, and apatite, but there is a lack of evidence for a direct correlation between the REE with magnetite. No apatite was noted in our cursory investigation of these pegmatites, nor was it described by Houston (1961). Studies of magnetite-rich pegmatites in Saudi Arabia and Alaska, found multiple magnetite specimens were enriched in niobium, yttrium, lanthanum, scandium, and other trace elements (Overstreet and others, 1985; 1978). They suggested that, although the number of analyses were too small for broader implications, it is possible that magnetite either scavenges trace elements from the surrounding host rock during crystallization or contains inclusions rich in trace elements. Further in-depth investigation would need to be done to examine the chemistry of the magnetite in the samples collected by the WSGS to make a similar correlation.

Platt Mine (Platt pegmatite, Uranium King Mine), SW¼SE¼ sec. 3, T. 13 N., R. 81 W., Carbon County

The Platt Mine was excavated to a depth of 23 m (75 ft) in a zoned, cross-cutting type pegmatite 21 m (70 ft) wide by 49 m (160 ft) long. The outer part of the pegmatite is feldspar, and the central part is quartz-mica-feldspar-rare earth minerals. Euxenite is the most abundant REE-bearing mineral followed by monazite and columbite as the least abundant (Houston, 1961). These occur as large individual crystals (fig. 9) and crystal aggregates both in the central pegmatite and in gash fractures. Uranium accounted for most of the production from the Platt Mine in 1956 with 12 tonnes (13 tons) of ore (King and Harris, 2002). Approximately 4,500 kg (10,000 lbs) of euxenite were reported as extracted from the mine between 1956 and 1958 (Houston, 1961; Adams and others, 1980); although the USBM recorded only 1,413 kg (3,115 lbs) for 1957 and 450 kg (1,000 lbs) for 1958 (King and Harris, 2002).

The euxenite was reported by Houston (1961) to be metamict to the extent that it gave no X-ray diffraction pattern. His X-ray fluorescence studies of the euxenite showed, in order of decreasing abundance, the presence of Nb, Y, Fe, Ta, U, and Zr. These were accompanied by minor amounts of Pb, Mn, Zn, Er, Eu, Ac, Ho, Ti, Th, Sm, and Rn. King and Harris (2002) suggested that the euxenite crystals, reported to be up to 7.6 cm (3 in) long, might have been misidentified and were probably samarskite or niobium-rich, yttrium-bearing tantalite. However, a 1980 USDOE report (Adams and others, 1980) also described both euxenite and allanite in several samples from the Platt pegmatite. Sample analyses in that report did not show any lanthanum or yttrium concentrations higher than average

concentrations. Scandium exceeded the quintupled crustal abundance at 200 ppm. No other REE were evaluated in samples from the Platt pegmatite by Adams and others (1980).

X-ray fluorescence of monazite from the Platt Mine showed, in order of abundance: Ce, Nd, Y, Th, and La. These were accompanied by minor amounts of Pr, Sm, and Gd. Although phosphorus is a major constituent of monazite, its presence could not be examined by the type of analysis used (Houston, 1961).



Figure 9. Euxenite from the Platt Mine pegmatite.

The Platt Mine pegmatite dike trends approximately 50˚. A sample collected during the first phase of this study (Sample 20120917JC-A) is composed of granitic pegmatite dominated by muscovite, quartz, microcline, and perthite, with lesser plagioclase and hematite with limonite staining. It contains minor garnet, dendritic pyrolusite, epidote alteration, and a glassy black mineral, possibly euxenite or columbite-tantalite. The dike intrudes granitic gneiss (Sutherland and Hausel, 2005) with minor biotite; banding in the gneiss trends 342˚ and dips 59˚ E. Analysis of sample 20120917JC-A shows enrichment in lutetium and ytterbium greater than five times the crustal abundance (table 9); HREE are slightly enriched above average. The sample is also enriched in niobium and tantalum. Values in this sample are a minimum estimate for concentrations in this pegmatite dike, because the relatively high silica content of the sample suggests dilution by excess quartz. When the analysis is normalized to the global average silica content of granite, 72.04 percent, (Blatt and Tracy, 1997) Er, Lu, Tm, Yb and Y are enriched above five times the average abundance, as are niobium and tantalum. The high niobium and tantalum concentrations support the presence of euxenite or columbite-tantalite within the pegmatite (Sutherland and others, 2013).

Additional Platt pegmatites

N½NE¼ sec. 8, T. 13 N., R. 81 W., Carbon County

Several pegmatites occur in this area (Houston, 1961). One of these was discussed in a 1982 USDOE National Uranium Resource Evaluation (NURE) report (Dribus and Nanna, 1982). The report identified a 0.3 to 0.9 m (1 to 3 ft) wide, 30° trending garnet-bearing granite pegmatite that cut Early Proterozoic biotite schist. The pegmatite exhibited 2 to 17 times background radioactivity (Geslin, 1954; Dribus and Nanna, 1982) and contained black, metallic minerals identified as euxenite and allanite by Scanning Electron Microscope-Energy Dispersive Spectroscopy (SEM-EDS). Various early analyses reported up to 0.1 percent uranium (King and Harris, 2002).

S½ sec. 13, T. 13 N., R. 81 W., Carbon County

A similar pegmatite dike in this area, exposed in both outcrop and a prospect pit, cuts granitic gneiss near a contact with pelitic schist (Sutherland and Hausel, 2005). The dike is granite pegmatite with abundant biotite and hematite as well as moderate garnet, columbite-tantalite (or possibly euxenite), allanite, and limonite staining (Sample 20120917BW-A). This pegmatite sample is enriched in all of the HREE, except for europium. The elements Dy, Er, Ho, Lu, Tb, Tm, and Yb as well as Y, Nb, and Ta exhibit greater than five times the crustal abundance (table 9). The high niobium and tantalum concentrations suggest the pegmatite hosts euxenite or columbite-tantalite (Sutherland and others, 2013).

SE¼SW¼ sec. 2, T. 13 N., R. 81 W., Carbon County

In this area, a quartz vein cross-cutting amphibolite is exposed in a prospect pit. The vein, about 2 m (6.6 ft) wide, vuggy, and exhibiting abundant hematite and limonite staining, was sampled during this and past investigations. Samples 20150819LC-3 and 20120917JC-B did not contain any significant element enrichment besides arsenic and tellurium (table 9).

Sierra Madre

Prospects in the Sierra Madre dot the landscape in various rock types. Pegmatites dating 1,510-1,763 Ma cross cut amphibolite gneisses, felsic gneisses, and various other metamorphic rocks (Sutherland and Hausel, 2005). Although much of the focus in the past was on copper and gold, REE were found to be elevated in some of the prospects.

Blackhall Mountain Lookout, SE¼SE¼ sec. 2, T. 12 N., R. 83 W., Carbon County

Blackhall Mountain is located in an area consisting of mafic metavolcanics, the Sierra Madre granite, felsic gneiss, and pegmatites dated 1,510-1,763 Ma (Sutherland and Hausel, 2005). At the forest service lookout (fig. 10A), a massive outcrop of granitic pegmatite caps the mountain and nearby crests. DeNault (1967) reported the pegma-

Table 10. Concentration of REE from Blackhall Mountain. Bold values indicate concentrations greater than five times the crustal abundance.

	Blackhall Mountain								
Element	La (ppm)	Ce (ppm)	Pr (ppm)	Nd (ppm)	Sm (ppm)	Eu (ppm)	Gd (ppm)	Tb (ppm)	Dy (ppm)
20150825LC-5A	**490**	**873**	**79.1**	241	23.3	2.25	7.68	0.63	2
	Ho (ppm)	Er (ppm)	Tm (ppm)	Yb (ppm)	Lu (ppm)	Sc (ppm)	Y (ppm)	Cumulative REE (ppm)	
	0.31	0.47	0.05	0.25	0.03	1	5.6	**1,726.67**	

tites contained a metamict, REE-bearing mineral in thin section thought to be allanite. X-ray fluorescence of this mineral showed 1 percent or less each of cerium, lanthanum, praseodymium, neodymium, and thorium (DeNault, 1967). King and Harris (2002) suggest the granitic rock in the area is similar in age to those of the Mullen Creek mafic complex to the east (after Love and Christiansen, 1985). The pegmatite sampled for this study contains coarse, cohesive, biotite books that exhibit a rusty weathering halo (fig. 10B); magnetite is also found in the area. Cerium, lanthanum, and praseodymium are all elevated beyond five times the crustal abundance (table 10; Sample 20150825LC-5A). Many of the samples taken near Blackhall Mountain also contained elevated barium ranging from 676 ppm to 4,210 ppm (Samples 20150825LC-4A, 4B, 5A, 5B).



Figure 10. Blackhall Mountain. A) Resistant pegmatite forms ridges where the lookout is located and in the shadow behind. B) Large biotite flakes within the pegmatite below the lookout (Sample 20150825LC-5B).

Wind River Mountains

The Wind River Mountains are a northwest-trending, Precambrian-cored, asymmetric, Laramide anticline that was thrust southwestward at the end of the Paleocene. The southern tip of the Wind Rivers is known as the South Pass granite-greenstone belt, which comprises an Archean synclinorium of metamorphosed volcanic, sedimentary, and plutonic rocks intruded by granitic plutons extensively exposed to the north (Hausel, 1991). In the southern part of the range, granitic pegmatites within Precambrian crystalline rocks are potential hosts for REE and associated elements. Many small prospects and mines in the area reportedly host beryl, tourmaline, and garnet; of these, only tourmaline was seen in the field. A large, inactive, iron mine, the Atlantic City Iron Mine, is also located in this area. Banded iron formation (BIF) was sampled during RI-67, but it contained no elevated REE (Sutherland and Cola, 2015). Access is limited in the central part of the range because of designated wilderness, so no sampling was carried out in that area during this study.

Anderson Ridge, SW¼SW¼ sec. 26 and NW¼NW¼ sec. 35, T. 29 N., R. 101 W., Fremont County

The Anderson Ridge area, near the southeast end of the Wind River Range (fig. 11), contains many veins and peg-

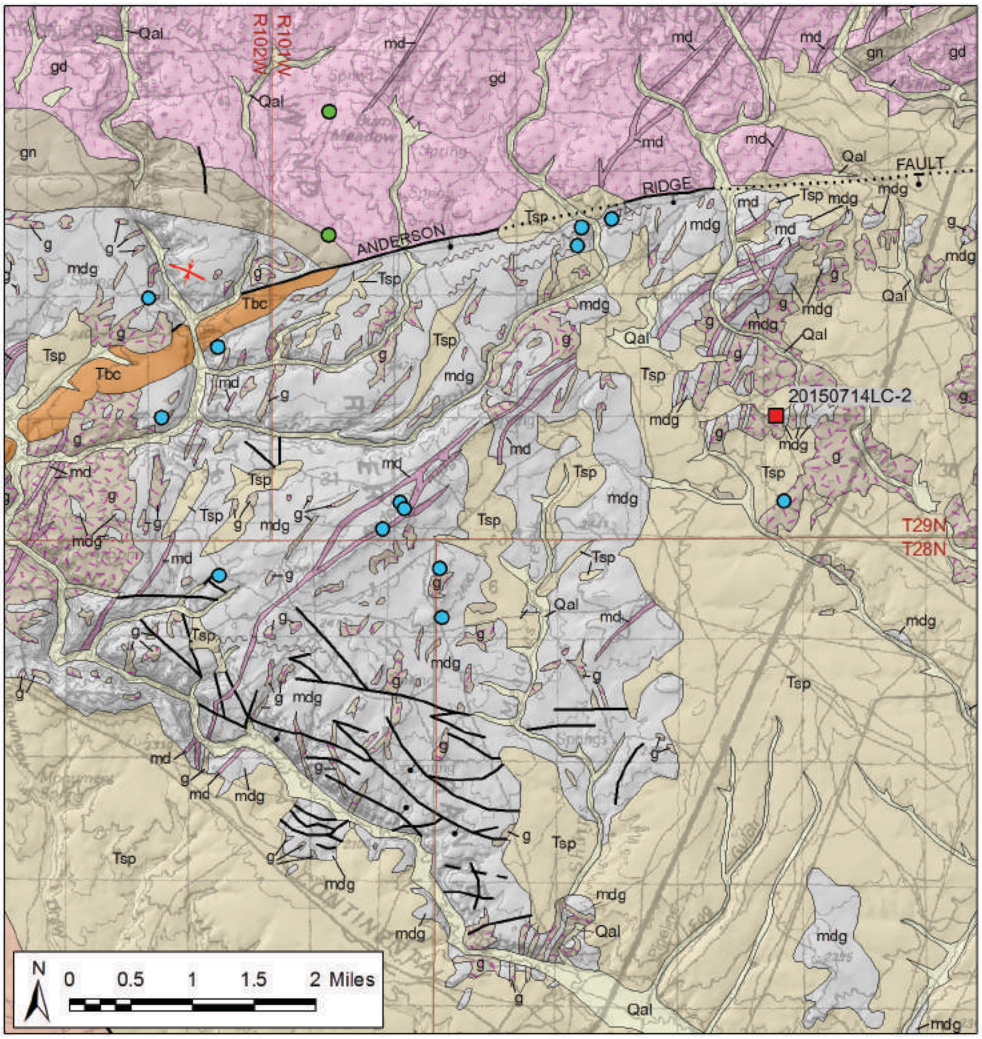


Figure 11. Sample locations and geology of the Anderson Ridge area. Samples were taken from igneous and metamorphic units in and near Anderson Ridge Fault shear zones. Map modified from Sutherland and Hausel (2006)

matites. The host rock is 2.8 Ga foliated metagraywacke, which was intruded by granite and pegmatites around 2.5 to 2.6 Ga (Harris and Hausel, 1986; Stuckless and others, 1985). The pegmatites and veins vary in size and shape and can reach up to 610 m (2,000 ft) in width and length (El-Etr, 1963; Proctor and El-Etr, 1968; Harris and Hausel, 1986). Mineralogy and texture also vary in the area with layered pegmatites ranging from equigranular to coarse-grained and containing magnetite, tourmaline, garnet, beryl, and biotite (El-Etr, 1963; Proctor and El-Etr, 1968). Harris and Hausel (1986) reported many occurrences of beryl and tourmaline as well as the possibility of elevated REE in the various outcrops and prospects. Sample 20150714LC-2 was taken from a pegmatite in the South Pass Granite (Hausel, 2007) that contained primarily feldspar and quartz. Although beryl has been reported near here, none was found. A dense, black garnet, typically anhedral with some well-formed faces, was present in this sample (fig. 12). The garnet contained elevated yttrium and ytterbium just below five times the average crustal abundance (table 11).

Several samples in this area that were barren of REE contained elevated concentrations of other elements of interest. Maroon breccia with rusty, limonitic, and metallic coatings in the Anderson Ridge Fault Zone (20150714LC-3) contained elevated copper at 4,620 ppm, and a nearby prospect in granite with copper mineralization (20150714LC-4) showed 1.085 percent Cu. Samples taken from a large pegmatite with quartz, feldspar, muscovite and tourmaline (20150714LC-7A) contained elevated Rb at 844 ppm. Rusty-stained portions of the pegmatite (20150714LC-7B) had 984 ppm Rb as well as >250 ppm As, >250 ppm Bi, and 0.46 ppm Au. Another grayish-white quartz vein with a prospect exposing muscovite-rich, rusty rock (20150714LC-14) had 1.05 ppm Au, 5.8 ppm Ag, >250 ppm As and Bi, 635 ppm Rb, and 5.08 ppm Te.



Figure 12. Dense garnet with elevated REE in the Anderson Ridge area (Sample 20150714LC-2).

Owl Creek Mountains

The Owl Creek Mountains (fig. 13) are an east-trending, Precambrian-cored, Laramide uplift that has been thrust southward over Phanerozoic sediments of the Wind River Basin. Copper Mountain is an area of exposed east-northeast-trending, steeply south-dipping, Archean supracrustal and granitic rocks in the southeastern part of the Owl Creek Mountains. These rocks were folded, intruded by Archean granitic rocks including pegmatites, metamorphosed about 2.7 Ga, and later cut by Archean (and possibly Proterozoic) mafic dikes (Hausel and others, 1985). Similar to the Wind River Mountains, Precambrian units with granitic pegmatites are potential hosts for REE. Archean gneiss and tonalite also host columbite-tantalite-bearing pegmatites (Sample 20150804LC-1; Hausel and others, 1985). Prospects and small mines that were sampled contain beryl, tourmaline, muscovite, feldspar, and other minerals. The samples that did not show elevated REE, but contained other interesting elements and minerals, are detailed in the "occurrences of other elements and minerals" section.

Whippet and Zimmerman mines area, SE¼NE¼ sec. 28 and NW¼ sec. 27, T. 40 N., R. 93 W., Fremont County

Dikes of Archean granitic rocks intruded the margins of an Archean supracrustal belt in the Copper Mountain area

Table 11. Concentration of REE from the Anderson Ridge area. Bold values indicate concentrations greater than five times the crustal abundance.

	Anderson Ridge area								
Element	La (ppm)	Ce (ppm)	Pr (ppm)	Nd (ppm)	Sm (ppm)	Eu (ppm)	Gd (ppm)	Tb (ppm)	Dy (ppm)
20150714LC-2	2	3.1	0.42	1.4	1.13	0.04	4.59	2.52	21
	Ho (ppm)	Er (ppm)	Tm (ppm)	Yb (ppm)	Lu (ppm)	Sc (ppm)	Y (ppm)	Cumulative REE (ppm)	
	3.66	9.61	1.74	**13.7**	1.42	12	138.5	216.83	

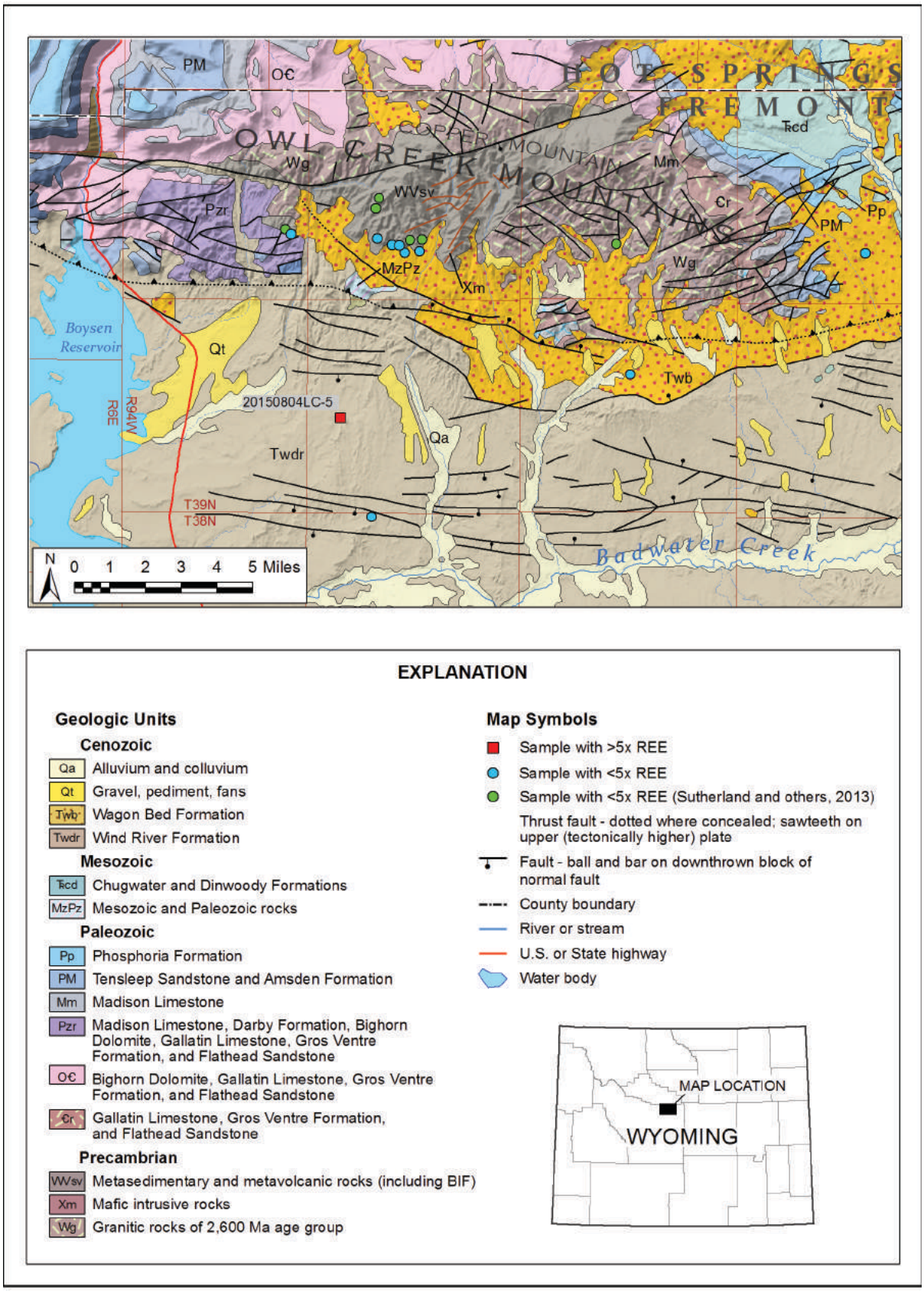


Figure 13. Sample locations and geology of the Owl Creek Mountains and northern Wind River Basin. Most samples were taken in Precambrian rock except one taken in the Wind River Formation. Map modified from Love and Christiansen (1985).

of the Owl Creek Mountains (Thaden, 1980; Hausel and others, 1985). Tungsten, tantalum, beryllium, lithium, and potassium feldspar were produced from pegmatites within these Archean granitic rocks at Whippet mine #8 (Hausel and others, 1985).

The Zimmerman beryl mine is 0.5 km (0.33 mi) southeast of the Whippet #8 mine and targets a northeast-trending felsic dike (Thaden, 1980; Hausel and others, 1985). At the Zimmerman mine, the outcrop is dominated by granitic rocks, mostly white to light-gray, very fine-grained to pegmatitic, muscovite tonalite with moderate hematite, epidote, and black tourmaline. One individual tourmaline crystal was at least 9 cm (3.5 in) long. The tonalite is banded in places, and exhibits both modal and size grading from quartz to plagioclase and pegmatitic to very fine-grained (Sample 20121011JC-F). The tonalite is not significantly enriched in any of the REE but contains 24 ppm tantalum (more than 14 times the average abundance), 122.5 ppm cesium (more than 64 times the average), 12 ppm tungsten (nearly 11 times the average), and 480 ppm lithium (more than 28 times the average). The high concentrations of lithium, cesium, and tantalum in this pegmatite suggest that it is an LCT-type pegmatite. If other pegmatites in the Owl Creek Mountains are mostly LCT-type, the prospect of REE enrichment should be considered relatively low (Sutherland and others, 2013).

Allie (Parlett-Adams) claims, SW¼NW¼ sec. 12, T. 39 N., R. 88 W., Natrona County

Russell and DeVore (1948) reported radioactive allanite within lenses of granitic pegmatite enclosed in Precambrian gneiss at this locality. Radioactivity at the pegmatite lenses was reported to be 2 to 12 times background and the individual radioactive mineral grains ranged from 0.6 to 7.6 cm (0.25 to 3 in) long (Russell and DeVore, 1948). King and Harris (2002) listed this site as an unverified occurrence.

The dominant lithology in the area is pink to gray, medium- to coarse-grained, biotite hornblende quartzofeldspathic gneiss with abundant small, tight folds. Small pockets of biotite granite pegmatite are common within the gneiss and one lens of biotite granite pegmatite contains allanite with some grains up to 1.3 cm (0.5 in) in length (Sample 20121017JC-D). The pegmatite lens is weakly-to moderately-enriched in all of the LREE and some of the HREE as shown in table 12 (Sutherland and others, 2013).

Other Precambrian Occurrences

In addition to pegmatites, REE also occur in other Precambrian units such as quartz-pebble conglomerates, alkali igneous rocks, and various metamorphic rocks. The following section describes these known or suspected REE-hosted occurrences by region.

Proterozoic and Neoarchean radioactive quartz-pebble conglomerates in the Medicine Bow Mountains and in the Sierra Madre were mapped by Houston and others (1978). Paleoplacers within these conglomerates hosted both U- and Th-bearing minerals and minor gold. Later drilling also identified the presence of REE (Karlstrom and others, 1981b). Occurrences within igneous and metamorphic rocks often coincide with alteration zones related to faults, fractures, and various dikes.

While allanite characteristically crystallizes as an accessory mineral from acidic, intermediate, and some alkaline rocks and their related pegmatites, epidote generally crystallizes in lower temperature environments related to low- to medium-grade metamorphism and late-stage magmatic fluids (Deer and others, 1967). Epidote ($Ca_2Fe^{+3}Al_2O\cdot OH\cdot Si_2O_7\cdot SiO_4$) is often notable in alteration zones and is related to allanite but is not known as an ore mineral for REE. However, because of epidote's structure, REE can substitute for Ca, Th, and to a lesser extent U. Thus, some epidote-rich rocks such as epidosite, a rock composed primarily of epidote accompanied by a small amount of quartz and other minerals, can host anomalous amounts of REE.

Late-stage magmatic fluids associated with igneous intrusions have left varying amounts of epidotization along zones of alteration in the Precambrian cores of many Wyoming mountain ranges. These zones are particularly

Table 12. Concentration of REE from the Allie claims. Bold values indicate concentrations greater than five times the crustal abundance.

	Allie claims								
Element	La (ppm)	Ce (ppm)	Pr (ppm)	Nd (ppm)	Sm (ppm)	Eu (ppm)	Gd (ppm)	Tb (ppm)	Dy (ppm)
20121017JC-D	66.8	174.5	20.6	85.8	27.4	0.85	16	1.89	7.69
	Ho (ppm)	Er (ppm)	Tm (ppm)	Yb (ppm)	Lu (ppm)	Sc (ppm)	Y (ppm)	Cumulative REE (ppm)	
	1.1	2.67	0.38	2.54	0.39	3.4	29.6	441.61	

prevalent along a broad east-west trend in central Wyoming referred to as the Oregon Trail structural belt. In this area, continents collided during the Archean approximately 2.65 to 2.63 billion years ago (Chamberlain and others, 2003; Frost and others, 2006; Grace and others, 2006). This collision resulted in widespread shear zones, extensive emplacement of granitic intrusions, and late-stage magmatic fluids, which produced numerous epidotized zones and were responsible for central Wyoming's nephrite jade deposits. It is also worth noting that elevated REE, chromium, and nickel are common in jade-related deposits due to substitution of elements in epidote and the ferroactinolite-tremolite amphibole series. Further chemistry can be found in appendix 2.

Medicine Bow Mountains and Sierra Madre

Onemile Creek area, sec. 6 and N½ sec. 7, T. 18 N., R. 78 W., Carbon County

The Onemile Creek area contains Early Proterozoic Magnolia Formation with radioactive conglomerates hosting potential REE resources (King and Harris, 2002). Pyrite as well as the radioactive minerals coffinite, uranothorite, thorogummite, and brannerite were identified by Houston and Karlstrom (1981). Surface sampling and drill holes were conducted with a focus on radioactive layers. Of the six units in the Magnolia Formation, units 1, 2, 4, 5a, and 5b contained significant radioactive rocks (Karlstrom and others, 1981b; Graff and Houston, 1977; Houston and others, 1978; 1979; King and Harris, 2002). The units are primarily quartzite or quartz-pebble conglomerates, occasionally arkosic, varying in grain size. Table 13 displays the chemistry, unit information, and drill hole information for the samples summarized in King and Harris (2002). The Magnolia Formation was not sampled by the WSGS, but descriptions show it may be a potential REE resource since many samples contained five times the crustal abundance or more in lanthanum, cerium, and yttrium.

Rock Creek (Threemile Creek) area, NW¼ and W½SW¼ sec. 19, T. 18 N., R. 78 W., Carbon County

Quartz-pebble conglomerate in the upper granular quartzite of the Early Proterozoic Magnolia Formation exhibits 20 times the background radiation in this area. Samples contained up to 122 ppm U and 130 ppm Th, with 70 ppm Y in the most uraniferous sample. Drill holes encountered conglomerates with up to 365 ppm U, 344 ppm Th, 905 ppm La, 610 ppm Ce, and 45 ppm Y. The most thorium- and REE-rich units were at depths greater than 214 m (703 ft). Other conglomerates in the drill holes contained no REE enrichment (Karlstrom and others, 1981b).

Cooper Creek area, center S½ and SE¼ sec. 33, T. 18 N., R. 78 W., Carbon County

The Proterozoic Magnolia Formation in this area showed about five to six times background radioactivity at the surface. Samples of the quartz-pebble conglomerate contained 34 to 485 ppm Th with at most 13 ppm U. The sample with the most thorium also contained 150 ppm Y. A drill hole that intersected Lindsey Quartzite and Bow River Quartzite did not encounter elevated REE (Karlstrom and others, 1981b; King and Harris, 2002). No analyses were conducted for other REE.

Vagner Formation, NE¼NE¼ sec. 6, T. 14 N., R. 78 W., Carbon County

Early Proterozoic quartzite from the Vagner Formation contained 150 ppm Y, 25 ppm U, and 24 ppm Th (Karlstrom and others, 1981b). The source of the yttrium is unknown (King and Harris, 2002).

Medicine Peak Quartzite, E½SW¼ sec. 8, T. 16 N., R. 79 W., Albany County

A sample of Proterozoic Medicine Peak Quartzite conglomerate reportedly contained 2,000 ppm Y, 500 ppm Zr, 28 ppm U, and 46 ppm Th (Karlstrom and others, 1981b). King and Harris (2002) point out that the yttrium content may be a typographical error and could be 200 ppm rather than 2,000 ppm.

Rock Mountain Conglomerate, S½ sec. 2 and NE¼NW¼ sec. 11, T. 18 N., R. 79 W., Carbon County

Out of 18 samples of Archean Rock Mountain Conglomerate from section 2, only one, a coarse-grained quartzite, contained elevated REE at 396 ppm Ce, 30 ppm La, and 11 ppm Y. A drill hole in section 11 did not intersect any elevated radioactivity. However, one sample of arkosic paraconglomerate in the Rock Mountain Conglomerate at 159.4 m (523 ft) depth contained 150 ppm La, 127 ppm Ce, 55 ppm Y, 327 ppm Zr, 190 ppm U, and 86 ppm Th (Karlstrom and others, 1981b).

Unnamed (Sample 160402), NE¼NE¼ sec. 15, T. 16 N., R. 80 W., Carbon County

This sample was taken from the Lindsey Quartzite. It contained only 2 ppm U but 150 ppm Y. No other data was collected (Karlstrom and others, 1981b; King and Harris, 2002).

Hubbell Ditch area, center S½ sec. 11, T. 14 N., R. 80 W., Carbon County

At this locale, Precambrian chlorite schist contained 500 ppm La. Stream sediments near here also had at least 150

Table 13. Concentration of REE from the Onemile Creek area. Bold values indicate concentrations greater than five times the crustal abundance.

		Onemile Creek area							
		Element							
Section	Unit	La (ppm)	Ce (ppm)	Y (ppm)	Nb (ppm)	Th (ppm)	U (ppm)	drill hole #	depth (ft)
	Average 143 surface samples	163	159	12	23	99	25	-	-
7	unit 2 conglomerate	**657**	**457**	41		371	177	-	-
7	unit 1 paraconglomerate	164	116	9		229	26	-	-
7	unit 1 paraconglomerate	**261**	195	9		131	15	-	-
6	unit 2 coarse-grained quartzite		248	13		270	71	-	-
6	unit 4 qtz-pebble conglomerate		**781**			214	104	-	-
6	unit 4 qtz-pebble conglomerate	**454**	**381**	28		365	370	-	-
6	unit 4 qtz-pebble conglomerate	**685**	**566**	27		422	52	-	-
6	unit 4 qtz-pebble conglomerate	**975**	**825**	27		657	43	-	-
6	unit 4 qtz-pebble conglomerate		**667**	31		650	37	-	-
6	unit 5a qtz-pebble conglomerate	**333**	269	14		15	269	-	-
6	unit 5a qtz-pebble conglomerate†		**3,952**	137	757	915	102	-	-
6	unit 5b qtz-pebble conglomerate		**533**	38		315	64	-	-
	Average: 335 subsurface samples	101	102	17	21	112	118	-	-
7	unit 1 arkosic paraconglomerate	**196**	147	23		104	236	MB-16	121-125
7	unit 1 quartz conglomerate	**286**	226	19		212	84	MB-16	142
7	unit 1	**484**	**440**	29		8	36	MB-16	170
7	unit 1	**179**	133	12		53	63	MB-16	181
7	unit 2 pebbly quartzite	**347**	245	28		212	273	MB-16	272
7	unit 2 pebbly quartzite	133	88	56		79	940	MB-16	390
7	unit 2 pebbly quartzite	**189**	124	40		110	1620	MB-16	390
6	quartzite		90	30		257	217	EMB-1	393-403
6	unit 3*	**242**	244	25		272	129	EMB-1	453-475
6	unit 5 quartzite	**409**	286	42		142	96	EMB-2	169
6	unit 3*		**436**	19		402	29	EMB-4	34
6	unit 5 qtz-pebble conglomerate*	**495**	**466**	75		725	792	EMB-6	93, 141, 236-245, 295-305
6	unit 5*		>150				>200	EMB-7	
6	unit 5*	**535**	**719**	97				EMB-8	
6	pebble conglomerate*		**921**	**142**		1143	545	EMB-9	284-285

From Karlstrom and others (1981b); Graff and Houston (1977); Houston and others (1978; 1979); King and Harris (2002)

All samples from the Magnolia Formation

*only maximum concentration shown from unit thickness

†sample also contained 923 ppm Zr

ppm La (McCallum and Kluender, 1983). The origin of the elevated lanthanum could be related to Archean quartzofeldspathic gneiss or quartzite from the Proterozoic Heart Formation and shearing within the Cheyenne belt (King and Harris, 2002).

Broadway mine, center of SW¼ sec. 32, T. 13 N., R. 83 W., Carbon County

This site was investigated during previous WSGS studies. Located in the southeastern Sierra Madre, the reclaimed mine originally targeted a shear zone at the contact between Sierra Madre granite and a complex of gneiss, amphibolite, pyroxenite, gabbro, and diorite (Osterwald, 1947; DeNault, 1967; Sutherland and Hausel, 2005). The outcrop is composed of very coarse grained black pyroxene and epidote with extensive limonitic alteration in places. All but two of the REE were elevated beyond five times the crustal abundance in sample WGS-0203. Lutetium and scandium were also elevated above normal (table 14). Additionally, thorium, cadmium, and selenium were present in elevated concentrations. Another sample of green, medium- to coarse-grained, diopside-spessertine hornfels with minor actinolite and moderate to abundant limonite staining and grain-coatings (20121203WSGS-A) contained 2.75 percent zinc but no REE enrichment (Sutherland and others, 2013).

Dexter Peak, SW¼SW¼ sec. 21 and center N½ sec. 28, T. 15 N., R. 87 W., Carbon County

The strongly radioactive Archean Jack Creek Quartzite crops out near the top of the peak in an overturned section. Samples contained 3 to 131 ppm U and 16 to 664 ppm Th. Drill holes and surface samples in the area did not encounter elevated REE (Houston and Karlstrom, 1981; Houston and others, 1978; Graff and Houston, 1977). King and Harris (2002) also list this locale as an unverified REE locality based on the common occurrence of elevated REE with elevated thorium. The WSGS was unable to sample the Dexter Peak area due to limited access; many roads in the area have been closed or reclaimed by the USFS.

Carrico Ranch, E½ sec. 12, T. 15 N., R. 88 W.; SW¼ sec. 6 and NW¼ sec. 7, T. 15 N., R. 87 W., Carbon County

An overturned, radioactive, quartz-pebble conglomerate layer in the Archean Deep Gulch Conglomerate Member of the basal Jack Creek Quartzite is traceable for about 2 km (1.2 mi). Radioactive, thorium-rich minerals include monazite, zircon, and possibly huttonite. Pyrite is the most abundant heavy-mineral. In section 12, surface samples contained as much as 151 ppm Ce, 24 ppm Y, and 524 ppm Th. Other samples showed up to 208 ppm La, 181 ppm Ce, 150 ppm Y, 1,129 ppm Th, and 72 ppm U (Karlstrom and others, 1981b; King and Harris, 2002). A drill hole in the area encountered a quartz-pebble conglomerate between 49.7 and 54.9 m (163 and 180 ft) depth that contained 2,596 ppm Th, 718 ppm U, 223 ppm La, 185 ppm Ce, 122 ppm Y, 78 ppm Nb, and 2,133 ppm Zr. Another two drill holes intersected zones with up to 167 ppm La, 77 and 65 ppm Y, 133 and 121 ppm Ce, 546 and 960 ppm Th, and 209 and 269 ppm U (Karlstrom and others, 1981b). The WSGS was unable to sample this area due to lack of access across private land and washed-out roads.

Manning Ranch, NW¼ sec. 29 and NW¼ sec. 30, T. 16 N., R. 87 W., Carbon County

On the Manning Ranch, an overturned, radioactive, quartz-pebble conglomerate in Deep Gulch Conglomerate of the basal Jack Creek Quartzite contains up to 21 ppm U and 406 ppm Th. Drill holes encountered conglomerate with up to 653 ppm Th and 48 ppm U but no elevated REE (Karlstrom and others, 1981b). King and Harris (2002) list this locale as an unverified REE locality, because REE are common with high thorium concentrations in placers.

Deep Gulch, sec. 36, T. 16 N., R. 88 W.; SW¼ sec. 30, T. 16 N., R. 87 W., Carbon County

Radioactive Archean Deep Gulch Conglomerate, of the basal Jack Creek Quartzite, is traceable for 1.5 km (0.9 mi) and overturned. Surface samples contained up to 206 ppm U and 844 ppm Th but were not enriched in REE

Table 14. Concentration of REE from the Broadway mine. Bold values indicate concentrations greater than five times the crustal abundance.

	Broadway mine								
Element	La (ppm)	Ce (ppm)	Pr (ppm)	Nd (ppm)	Sm (ppm)	Eu (ppm)	Gd (ppm)	Tb (ppm)	Dy (ppm)
WGS-0203	**937**	**1,860**	**198.5**	**713**	**112.5**	**10**	**71.4**	**9.53**	**49.8**
	Ho (ppm)	Er (ppm)	Tm (ppm)	Yb (ppm)	Lu (ppm)	Sc (ppm)	Y (ppm)	Cumulative REE (ppm)	
	8.42	**21.4**	**2.59**	**14.95**	1.86	44	**214**	**4,268.95**	

(Karlstrom and others, 1981b; Houston and others, 1978; Graff and Houston, 1977). In drill holes here, conglomerates vary in composition. One, at a depth of 125.3 m (411 ft), contained 494 ppm U, 483 ppm Th, and 2.5 ppm Au but no REE. Another contained 107 ppm Y, 337 ppm Th, 241 La, 192–1,000 ppm Ce, and 110 ppm Y (Karlstrom and others, 1981b). Also near this area, a radioactive arkosic conglomerate in the Phantom Lake Group contained 100 ppm Y, 393 ppm Th, and 11 ppm U (Karlstrom and others, 1981b). The few locations of elevated radioactivity, lanthanum, and yttrium may warrant further investigation into the area (King and Harris, 2002).

Albany area, SE¼NE¼SE¼ sec. 15, T. 14 N., R. 78 W., Albany County

Near Albany, the Sherman Granite was reported to contain disseminated allanite (Dribus and Nanna, 1982; Mussard, 1982; Sanford and Stone, 1914). The allanite varies from trace amounts to 0.6 percent by volume, with one sample containing 2.8 percent by volume (Dribus and Nanna, 1982; Mussard, 1982). King and Harris (2002) analyzed 17 samples, which contained elevated cerium, up to 328 ppm, and lanthanum, up to 198 ppm. The most lanthanum-rich sample also contained 0.60 percent allanite. Further investigation of road cuts containing typical Sherman Granite (fig. 14) near Albany (sample 20150818LC-1) verified the presence of elevated lanthanum as well as the other LREE (table 15). However, this was the only sample in the area that yielded elevated REE out of five taken in this part of the Medicine Bow Mountains (fig. 15).



Figure 14. Sherman Granite with elevated REE in an altered zone near Albany, Wyo., (Sample 20150818LC-1).

Keystone, S½ sec. 35, T. 14 N., R. 79 W., Albany County

Two samples taken in the Proterozoic Keystone quartz diorite, 1.6 to 3.2 km (1 to 2 mi) northwest of the Lake Resort area, contained 0.33 and 0.63 percent allanite by volume (Mussard, 1982; King and Harris, 2002). A sample (201508LC-12) was collected by the WSGS about 0.8 km (0.5 mi) south of the area from a prospect pit exposing a dense, felsic gneiss with iron stain and epidote. No elevated REE were present.

Gaps trondhjemite, center S½ sec. 8 and NE¼NW¼ sec. 17, T. 16 N., R. 79 W., Albany County

A sample of Early Proterozoic Gaps trondhjemite contained 114 ppm Th and 1 ppm U. Fractures in the rock hosted uraninite with up to 1,000 ppm U. Yttrium enrichment occurs in the Gaps granite and a quartz vein in the granite. The granite showed 200 ppm and 150 ppm Y, and the vein contained 1,500 ppm Y (Karlstrom and others, 1981a, b). The elevated yttrium in the vein appears to be related to other metals in the rock, while it seems to be natural in the trondhjemite. Sheared granite in the area also exhibited 10 times the background radiation (Houston and others, 1978). King and Harris (2002) note the possibility of a typographical error where yttrium may be 150 ppm rather than 1,500 ppm.

Mullen Creek area, T. 14 N., R. 80 W., Carbon County

A vein in a fault cutting gabbroic rocks contains 1,000 ppm La in the center W½NW¼ of section 11 (McCallum and Kluender, 1983). The Mullen Creek area is an Early Proterozoic mafic complex that was intruded by granitic rock (fig. 15). The high lanthanum content may be related to the intrusion rather than the mafic complex (King and Harris, 2002). Allanite was reported at 1 percent by volume in younger granitic rock in the W½SE¼ of section 11 (Mussard, 1982), and others samples of granitic rock within the mafic complex contained up to 0.88 percent

Table 15. Concentration of REE in Sherman Granite from the Albany area. Bold values indicate concentrations greater than five times the crustal abundance.

	Albany area								
Element	La (ppm)	Ce (ppm)	Pr (ppm)	Nd (ppm)	Sm (ppm)	Eu (ppm)	Gd (ppm)	Tb (ppm)	Dy (ppm)
20150818LC-1	**280**	**584**	**49.9**	**164**	21.3	3.8	11.2	1.19	5.72
	Ho (ppm)	Er (ppm)	Tm (ppm)	Yb (ppm)	Lu (ppm)	Sc (ppm)	Y (ppm)	Cumulative REE (ppm)	
	0.99	3.05	0.41	2.77	0.45	9	28.3	**1,166.08**	

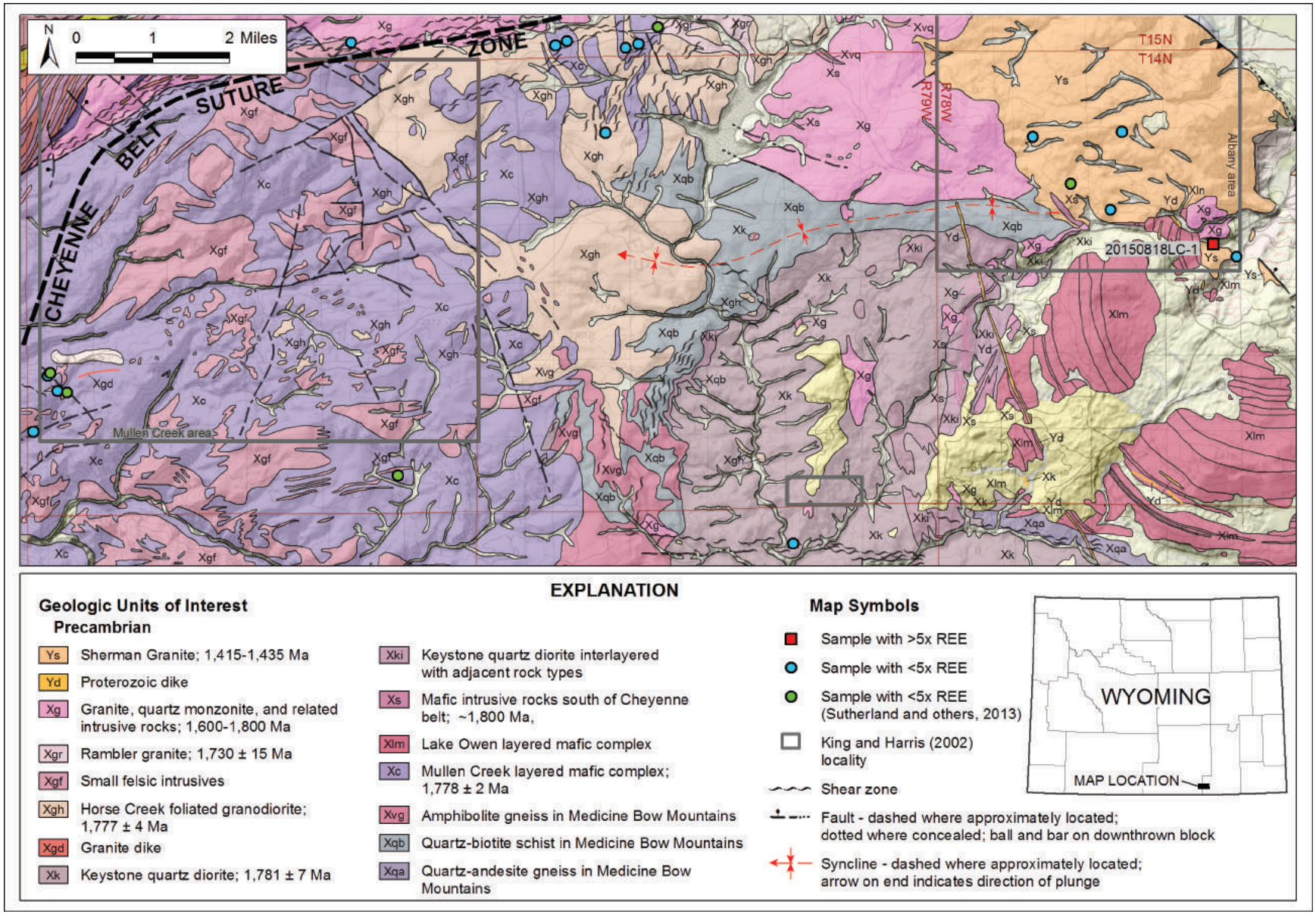


Figure 15. Sample locations and geology of the southern Medicine Bow Mountains. Most samples were collected from Precambrian igneous and metamorphic rocks. The Cheyenne belt suture zone crosses the northwestern corner of this area (Houston, 1993). Map modified from Sutherland and Hausel (2005).

allanite. Chemical analyses showed up to 244 ppm La, 475 ppm Ce, 13 ppm Y, 3 ppm Yb, and 685 ppm Zr (Mussard, 1982; King and Harris, 2002).

Granite Mountains, Green Mountain, Ferris-Seminoe Mountains, Pedro Mountains, and Shirley Mountains

The Granite Mountains (fig. 16) are a west-trending, Precambrian-cored, anticlinal uplift formed during the Laramide orogeny. The 80 km (50 mi) long Emigrant Trail Thrust Fault, with a throw to the south and west of more than 4,572 m (15,000 ft), defines their western and southern boundary. The east-trending North Granite Mountains Fault approximates their northern boundary. The Pedro Mountains, dominated by Archean granite and gneiss, mark the far eastern end of the Granite Mountains and are bordered on the east by a north- to northwest-trending normal fault.

Near the end of the Early Eocene, the Granite Mountains block was uplifted as much as 1,524 m (5,000 ft) along the North Granite Mountains Fault and an even greater amount along its southern edge. This extensive normal faulting cut the southern part of the thrust plate along the South Granite Mountains Fault system, particularly east of Crooks Gap along the north side of Green Mountain (Love, 1970). Minor Precambrian and Paleozoic outcrops occur along the trace of the normal fault, while the bulk of Green Mountain consists of Eocene arkosic sandstones and conglomerates of the Battle Spring Formation. During Miocene time, synclinal subsidence that exceeded 914 m (3,000 ft) began along the Granite Mountains trend. During the Pliocene, both the North and South Granite Mountains fault systems reactivated with reversed movements, dropping the Granite Mountains downward by as much as 305 m (1,000 ft) along the northern fault and 610 m (2,000 ft) along the southern fault (Love, 1970).

The Granite Mountains comprise a metamorphic complex of Archean gneisses, schists, and fragments of supracrustal rocks that have been metamorphosed to amphibolite grade, intruded by medium- to coarse-grained granites, and subsequently intruded by diabase dikes (Peterman and Hildreth, 1978). Numerous pervasive, dominantly ductile, east-trending shear zones with steep southerly dips cut the Archean rocks in the Oregon Trail structural belt. Archean deformation was generally ductile, whereas Laramide deformation was typically brittle; some Archean structures were reactivated during the Laramide orogeny (Hausel, 1996). The Granite Mountain batholith intruded the area around 2.62 Ga (Frost and others, 1998). East- to northeast-trending mafic dikes intruded during two intervals at approximately 2.4 to 2.6 Ga (Langstaff, 1995) and 1.47 to 1.45 Ga (Chamberlain and Frost, 1995; Chamberlain and others, 2000; 2003).

Sampling in this region focused on the areas with intense metamorphism. This often included highly epidotized areas associated with jade-related deposits (fig. 17). The fluid movement along sheared and fractured zones facilitated mineralization and the concentration of REE in, or related to, the epidote.

The Ferris Mountains, east of Green Mountain, are a very steep and faulted, Precambrian-cored, anticlinal uplift on the south side of the South Granite Mountains Fault system. To the southeast of the Ferris Mountains, the Seminoe Mountains form a northwest-trending, Laramide-uplifted thrust wedge cored by Archean metamorphic and igneous rocks. The highly folded and faulted uplift is flanked on the southwest by steeply dipping Paleozoic and Mesozoic strata and the northeast-dipping, low-angle Bradley Peak Thrust Fault (Blackstone and Hausel, 1992). The Seminoes are bounded on the northeast by a normal fault, the Kortes Fault (Hausel, 1994), which is the southeastern extension of the South Granite Mountains Fault system. The Shirley Mountains (fig. 18) are a Precambrian-cored, complexly faulted, irregular uplift east of the Seminoe Mountains. Normal faulting and steep folds separate the Shirley Mountains from the Seminoes.

Clarence Wood lode claims, SW¼SW¼ sec. 5, T. 29 N., R. 85 W., Natrona County

A moderately radioactive, irregularly shaped epidosite (80 percent epidote) dike is present within Archean quartz monzonite in this vicinity of the eastern Granite Mountains (King and Harris, 2002). Griffin and Milton (1982) reported a sample analysis from this dike of 700 ppm La, 100 ppm Y, 200 ppm Zr, 114 ppm eU, and 70 ppm eTh. The epidosite sample (20121023WS-B) showed enrichment at greater than five times the average crustal abundance in all of the naturally-occurring LREE and gadolinium and weak to moderate enrichment in the remaining HREE, except for ytterbium (table 16; Sutherland and others, 2013). King and Harris (2002) noted similar dikes are present in the surrounding areas in Carbon, Fremont, and Natrona Counties.

Sage Creek prospect, NW¼NE¼SE¼ sec. 12, T. 26 N., R. 83 W., Carbon County

In this area of the western Shirley Mountains, prospects within Precambrian granite and gneiss (Jones and Gregory, 2011) follow small areas of exposed nephritic alteration. The Sage Creek prospect contains abundant epidote, while minor nephrite is exposed about 91 m (300 ft) south of the pit (W. Sutherland, personal field notes, 2008). In the

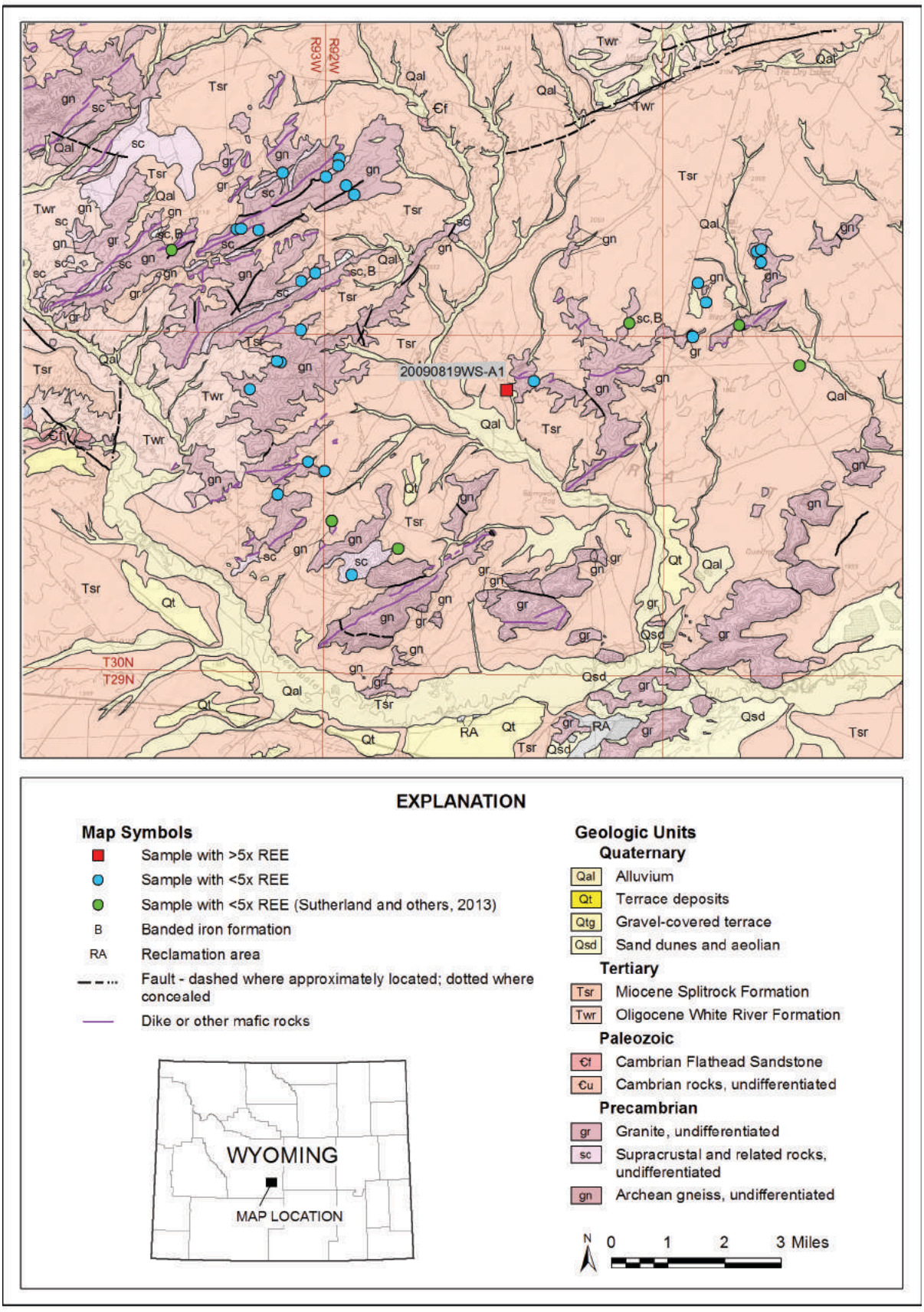


Figure 16. Sample locations and geology of the western Granite Mountains area. Sampling focused on Precambrian units and jade-related outcrops. The area shown is within the Oregon Trail structural belt (Grace and others, 2006). Map modified from Sutherland and Hausel (2003).

Table 16. Concentration of REE from the Clarence Wood lode claims. Bold values indicate concentrations greater than five times the crustal abundance.

	Clarence Wood lode claims								
Element	La (ppm)	Ce (ppm)	Pr (ppm)	Nd (ppm)	Sm (ppm)	Eu (ppm)	Gd (ppm)	Tb (ppm)	Dy (ppm)
20121023WS-B	**571**	**944**	**98.6**	**330**	**57.2**	7.1	**33.2**	3.4	15.1
	Ho (ppm)	Er (ppm)	Tm (ppm)	Yb (ppm)	Lu (ppm)	Sc (ppm)	Y (ppm)	Cumulative REE (ppm)	
	2.5	5.3	0.62	2.9	0.45	7.7	66	**2,145.07**	

From Sutherland and others (2013)

epidote (sample 20081029-Leo-Ep), Ce and La are present in concentrations greater than the quintupled average. Gd, Nd, and Pr also exhibit some REE elevation (table 17).

Fiesta #2 prospect, W½NW¼ sec. 2, T. 30 N., R. 87 W., Natrona County

This jade prospect, occurring in sheared and altered granitic gneiss in the east-central Granite Mountains (Sutherland and Hausel, 2003), hosts nephrite alteration with abundant epidote. The epidote contains many elevated REE, but none indicate economic enrichment (table 17). Epidote is widespread throughout the area.

Rhoads Jade mine, SW¼SE¼SW¼ sec. 3, T. 30 N., R. 92 W., Fremont County

The Rhoads Jade mine, in the western Granite Mountains, is located in epidotized, amphibolitic, gabbroic, ultramafic rocks as mapped by McLaughlin and others (2013). Jade, along with dark-green epidote and minor pink coloration, are located at this prospect. The epidote, sample 20090819WS-A1, contains elevated concentrations of HREE and lanthanum (table 17), whereas most jade-related alterations (fig. 17) are not elevated in REE (appendix 1 and 2).

Tin Cup mine area, T. 31 N., R. 92–93 W., Fremont County

Two samples in the Tin Cup area, in the western Granite Mountains (fig. 16), contained elevated scandium. Sample 20150603LC-1, sheared granitic material near an abandoned adit, and 20150603LC-6A, a quartz vein with hornblende and tourmaline, yielded 36 and 40 ppm Sc, respectively; the latter also contained 2.28 ppm Tl. A second, large pit of massive tourmaline (20150603LC-4) was examined, but no elements of interest were elevated. Another sample of massive, rust-stained quartz vein in a prospect to the northwest of the Tin Cup mine (20150603LC-2) contained 8.7 ppm Se. Jasper prospects are also scattered across the area with one (20150603LC-9A) containing 2.53 ppm Te.

Unnamed (Sample 23), SE corner sec. 25, T. 30 N., R. 90 W., Fremont County

Near Lankin Dome in the central Granite Mountains, an epidosite vein in quartz monzonite contained 150 ppm La, 100 ppm Y, 153 ppm U, and 37 ppm Th (Griffin and Milton, 1982). This site does not have the characteristic thorium enrichment relative to uranium like other epidosites in the area (King and Harris, 2002). About 4.8 km (3 mi) northwest of this location, in the SW¼NE¼SW¼ of section 22, T. 30 N., R. 90 W., a NURE stream sediment sample (prime id W15379) showed 32.1 ppm Sm along with slightly elevated Ce at 148 ppm, La at 137 ppm, Yb at 6.3 ppm, and Th at 58.4 ppm.

Samples collected in the Moonstone Formation about 4.8 km (3 mi) east of this location contained elevated REE. The uppermost tuffaceous unit of the area (Sample 20150604DB-3) is equivalent to unit 44 from Love (1961). Sample 20150604DB-4 was a yellow to tan, limey, tuffaceous bed equivalent to the lowest member of unit 44 from Love (1961). See appendix 2 for details.

Gap claims, NW¼ sec. 25, T. 28 N., R. 90 W., Fremont County

Samples taken from Archean quartz monzonite, on the northeast side of Green Mountain, contained 150–300 ppm La, 70 ppm Y, 70 ppm Nb, 70–100 ppm Zr, 62–100 ppm U, and 90 ppm Th (Griffin and Milton, 1982; King and Harris 2002). This location is along the South Granite Mountains Fault, which may have provided a conduit for fluid movement and mobilization of REE, Th, U, and some other elements. A NURE soil sample (prime id W15010) in sec. 5, T. 28 N., R. 92 W. is close to Precambrian outcrops along the fault trace, as is the NURE sample (prime id W15255) in sec. 29, T. 28 N., R. 90 W., both of which host at least one REE greater than five times average crustal abundance. One WSGS sample (20120824WS-E), collected several kilometers farther east along the fault in sec. 32, T. 28 N., R. 89 W., also hosted enriched REE along with elevated Th and U. Although the South Granite Mountains Fault may in part be responsible

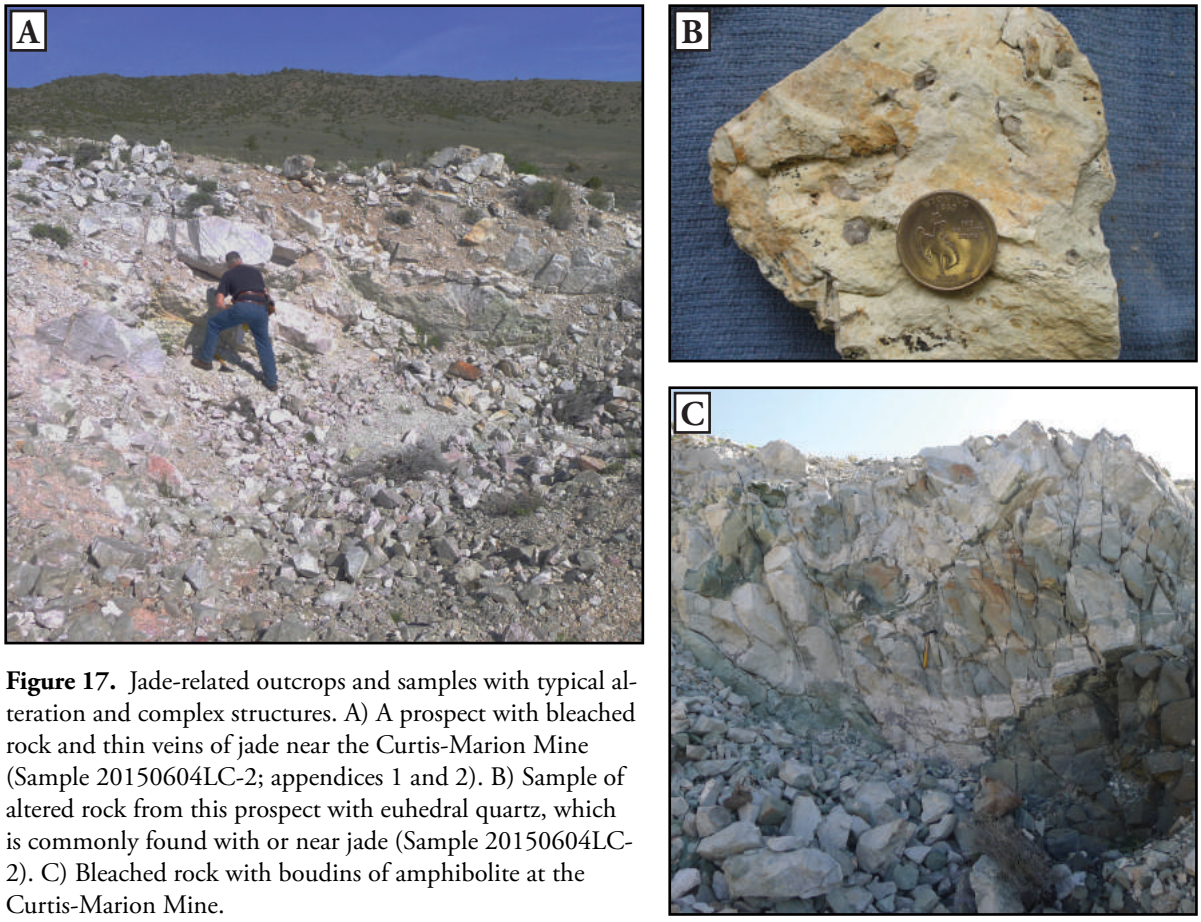


Figure 17. Jade-related outcrops and samples with typical alteration and complex structures. A) A prospect with bleached rock and thin veins of jade near the Curtis-Marion Mine (Sample 20150604LC-2; appendices 1 and 2). B) Sample of altered rock from this prospect with euhedral quartz, which is commonly found with or near jade (Sample 20150604LC-2). C) Bleached rock with boudins of amphibolite at the Curtis-Marion Mine.

Table 17. Concentration of REE from jade-related locales. Bold values indicate concentrations greater than five times the crustal abundance.

Sage Creek prospect									
Element	La (ppm)	Ce (ppm)	Pr (ppm)	Nd (ppm)	Sm (ppm)	Eu (ppm)	Gd (ppm)	Tb (ppm)	Dy (ppm)
20081029-Leo-Ep	**242**	**410**	39.9	135.5	23.6	3.21	20	3	16.2
	Ho (ppm)	Er (ppm)	Tm (ppm)	Yb (ppm)	Lu (ppm)	Sc (ppm)	Y (ppm)	Cumulative REE (ppm)	
	3.14	8.55	1.1	6.34	0.91	12	81.6	**1,007.05**	
Fiesta #2 prospect									
Element	La (ppm)	Ce (ppm)	Pr (ppm)	Nd (ppm)	Sm (ppm)	Eu (ppm)	Gd (ppm)	Tb (ppm)	Dy (ppm)
20090413WS-A1	163	298	29.2	102.5	20.4	3.22	20	3.53	22.4
	Ho (ppm)	Er (ppm)	Tm (ppm)	Yb (ppm)	Lu (ppm)	Sc (ppm)	Y (ppm)	Cumulative REE (ppm)	
	4.49	12.95	1.96	12.95	1.9	15	127.5	839.0	
Rhoads Jade Mine									
Element	La (ppm)	Ce (ppm)	Pr (ppm)	Nd (ppm)	Sm (ppm)	Eu (ppm)	Gd (ppm)	Tb (ppm)	Dy (ppm)
20090819WS-A1	144.5	215	21.4	78.6	20.5	6.84	**58.8**	**5.66**	**38**
	Ho (ppm)	Er (ppm)	Tm (ppm)	Yb (ppm)	Lu (ppm)	Sc (ppm)	Y (ppm)	Cumulative REE (ppm)	
	8.16	23	**3.14**	**19.75**	**2.79**	13	**227**	886.14	

Table 18. Concentration of REE from the Gap claims. Bold values indicate concentrations greater than five times the crustal abundance.

	Gap claims								
Element	La (ppm)	Ce (ppm)	Pr (ppm)	Nd (ppm)	Sm (ppm)	Eu (ppm)	Gd (ppm)	Tb (ppm)	Dy (ppm)
20120809BG-1	48.2	101	10.85	35.5	7.13	0.5	5.92	0.92	4.73
20120809BG-2	25.4	50.6	5.47	17.9	3.69	0.33	3.13	0.49	2.66
20120809BG-3	45.6	92.3	9.95	32.6	6.12	0.4	4.61	0.67	3.75
20120809BG-4	3.6	7.1	0.84	3.1	1.16	0.09	1.61	0.34	2.21
20120809BG-5	32.4	68.7	7.17	24.3	5.32	0.35	4.51	0.66	3.64
20120809BG-6	30.3	68.1	6.86	22.7	5.06	0.4	4.49	0.82	5.53
20120824WS-D	5.3	15.5	2.47	11.9	3.74	1.03	3.92	0.6	3.48
20120824WS-E	148.5	285	30.9	103	15.9	1.9	9.8	1.13	4.77
20120824WS-F	3.7	7.02	1.05	4.2	1.27	0.35	1.56	0.32	2.04

Element	Ho (ppm)	Er (ppm)	Tm (ppm)	Yb (ppm)	Lu (ppm)	Sc (ppm)	Y (ppm)	Cumulative REE (ppm)
20120809BG-1	0.8	1.98	0.24	1.49	0.22	4	19.9	223.48
20120809BG-2	0.53	1.39	0.19	1.22	0.18	3	14.3	116.18
20120809BG-3	0.71	1.73	0.2	1.25	0.18	3	19.3	203.07
20120809BG-4	0.49	1.47	0.21	1.3	0.18	1	13.8	24.7
20120809BG-5	0.68	1.79	0.22	1.39	0.2	3	18.2	154.33
20120809BG-6	1.2	3.69	0.51	3.33	0.46	2	34.3	155.45
20120824WS-D	0.68	1.87	0.25	1.51	0.2	5.1	17.5	57.55
20120824WS-E	0.89	2.37	0.32	2.04	0.31	3.6	24.1	610.43
20120824WS-F	0.45	1.48	0.24	1.77	0.29	1.1	11.6	26.84

From Sutherland and others (2013)

for some REE concentrations, not all samples collected along it host notable REE. Eight other samples collected in 2012 by the WSGS did not contain elevated REE, although some contained elevated Th and/or U, and one hosted elevated Ag (table 18).

Mohawk claims 2 and 3, SE¼ sec. 20, T. 28 N., R. 90 W., Fremont County

These claims, along the South Granite Mountains Fault, contained greater than 0.10 percent U_3O_8 (Bromley, 1957), and the uranium phosphate mineral autunite is thought to be in fracture planes in Archean granite (Holmquist, 1956). One sample taken contained 150 ppm La, 150 ppm Y, 300 ppm Zn, and 70 ppm Zr. Sheared granite contained 237 ppm U, while unsheared granite contained 14 ppm U (Griffin and Milton, 1982). The Cody Shale located below the thrust sheet of Precambrian granite contained 0.010 percent uranium (Love, 1964). The origin of the REE enrichment is unknown (King and Harris, 2002).

Unnamed (Sample 201), SE¼SW¼ sec. 18, T. 28 N., R. 90 W., Fremont County

This unnamed location is near the Mohawk claims on the northeast side of Green Mountain about 2 km (1.25 mi) north of the South Granite Mountains Fault. Here, Archean quartz monzonite contained trace radioactive phosphates and 300 ppm La, <10 ppm Nb, 10 ppm Y, 100 ppm Zr, 221 ppm Th, and 2 ppm eU (Griffin and Milton, 1982; King and Harris, 2002).

Babbs mine, SE¼ sec. 26, T. 27 N., R. 88 W., Carbon County

The Babbs mine, also known as the Weidemeir mine or Cherry Creek prospect, is located near the crest of the Ferris Mountains (Wilson, 1955). It consisted of two adits, three open cuts, and multiple prospect pits that targeted mineralized quartz veins and silicified breccia within Precambrian granitic country rock (Hausel, 1997). The mine is reclaimed, but abundant cupriferous minerals remain in the dump piles. Malachite, chalcopyrite,

Table 19. Concentration of REE from the Babbs mine. Bold values indicate concentrations greater than five times the crustal abundance.

	Babbs mine								
Element	La (ppm)	Ce (ppm)	Pr (ppm)	Nd (ppm)	Sm (ppm)	Eu (ppm)	Gd (ppm)	Tb (ppm)	Dy (ppm)
FM8112010-2	3.1	5.58	0.74	3.8	1.92	1.33	3.83	0.98	9.54
	Ho (ppm)	Er (ppm)	Tm (ppm)	Yb (ppm)	Lu (ppm)	Sc (ppm)	Y (ppm)	Cumulative REE (ppm)	
	3.14	**16**	**3.71**	**37.5**	**7.06**	2.2	93.5	193.93	

From Sutherland and others (2013)

azurite, and bornite mineralization occurs in quartz veins and disseminated pyrite and chalcopyrite occur within brecciated granite and granodiorite with a silicified matrix (Wilson, 1955; Hausel, 1997). One sulfide-bearing-quartz vein is hosted by a mafic dike (Hausel, 1997). Scheelite and allanite are also reported at the mine site (Wilson, 1955). Massive crystalline epidote with some iron staining, quartz, and jasper (Sample FM8112010-2) is present below the portal of one of the reclaimed adits and is strongly enriched in erbium, thulium, ytterbium, and lutetium (table 19; Sutherland and others, 2013).

REE at the Babbs mine are noteworthy, but the site also hosts significant silver and copper occurrences. A silicified, brecciated granite present at the Babbs mine (Sample Babbs-2) contains 28 ppm (0.82 oz/ton) silver, and 0.43 percent copper; a copper-stained quartz vein (Sample Babbs-1) contains 4 ppm (0.12 oz/ton) silver and greater than one percent copper (Sutherland and others, 2013).

Omega claims, SE¼SE¼ sec. 17, T. 27 N., R. 83 W., Carbon County

The Omega claims are located on the southeast edge of the Pedro Mountains. This area was described by King and Harris (2002) as shattered, biotite-rich zones in an Archean quartz monzonite with one sample containing 700 ppm lanthanum. An older report claimed there were no rare-earth-bearing minerals (Griffin and Milton, 1982), but another claimed up to 30 times background radioactivity on a biotite- and quartz-bearing vein in the granitic rocks (Holmquist, 1955d). Three samples were taken from the Precambrian rock. One contained heavy epidotization in large pieces of float concentrated along the slope. Another was taken of quartz monzonite similar to what King and Harris (2002) described sans biotite, and the third was a partially stained, red rhyolite with large, translucent quartz grains. Of the three, the only sample exhibiting elevated REE was the rhyolite, Sample 20150803LC-7 (table 20). Neodymium, praseodymium, and samarium were elevated, but only cerium and lanthanum were present above five times the crustal average. Several other samples collected in this general area for previous studies by the WSGS failed to show any elevated concentrations of REE (Sutherland and others, 2013).

Pyramid Peak area, center T. 27–28 N., R. 84 W., Carbon County

Griffin and Milton (1982) reported a trace of allanite and less than 5 percent epidote in Archean granite and quartz monzonite from this area. Two samples contained 700 and 150 ppm La and 20 and 10 ppm Y. It is possible this is the same site as Holmquist's (1955c) Canyon claim #1 (sec. 34, T. 28 N., R. 84 W; King and Harris, 2002). There were no radioactive minerals reported, but 90 times background radiation was recorded along a quartz vein (Holmquist, 1955c). Many epidote-bearing sites in the area, including Pyramid Peak, appear to be enriched in REE (King and Harris, 2002).

A #1 claim and Beaver #1 claim, NW¼ sec. 3 and NE¼ sec. 4, T. 25 N., R. 82 W., Carbon County

The Precambrian granite at this locale in the Shirley

Table 20. Concentration of REE from the Omega claims. Bold values indicate concentrations greater than five times the crustal abundance.

	Omega claims								
Element	La (ppm)	Ce (ppm)	Pr (ppm)	Nd (ppm)	Sm (ppm)	Eu (ppm)	Gd (ppm)	Tb (ppm)	Dy (ppm)
20150803LC-7	**220**	**400**	39.9	135	23.3	4.72	15.45	1.91	9.09
	Ho (ppm)	Er (ppm)	Tm (ppm)	Yb (ppm)	Lu (ppm)	Sc (ppm)	Y (ppm)	Cumulative REE (ppm)	
	1.62	3.85	0.48	2.8	0.39	4	46.7	909.21	

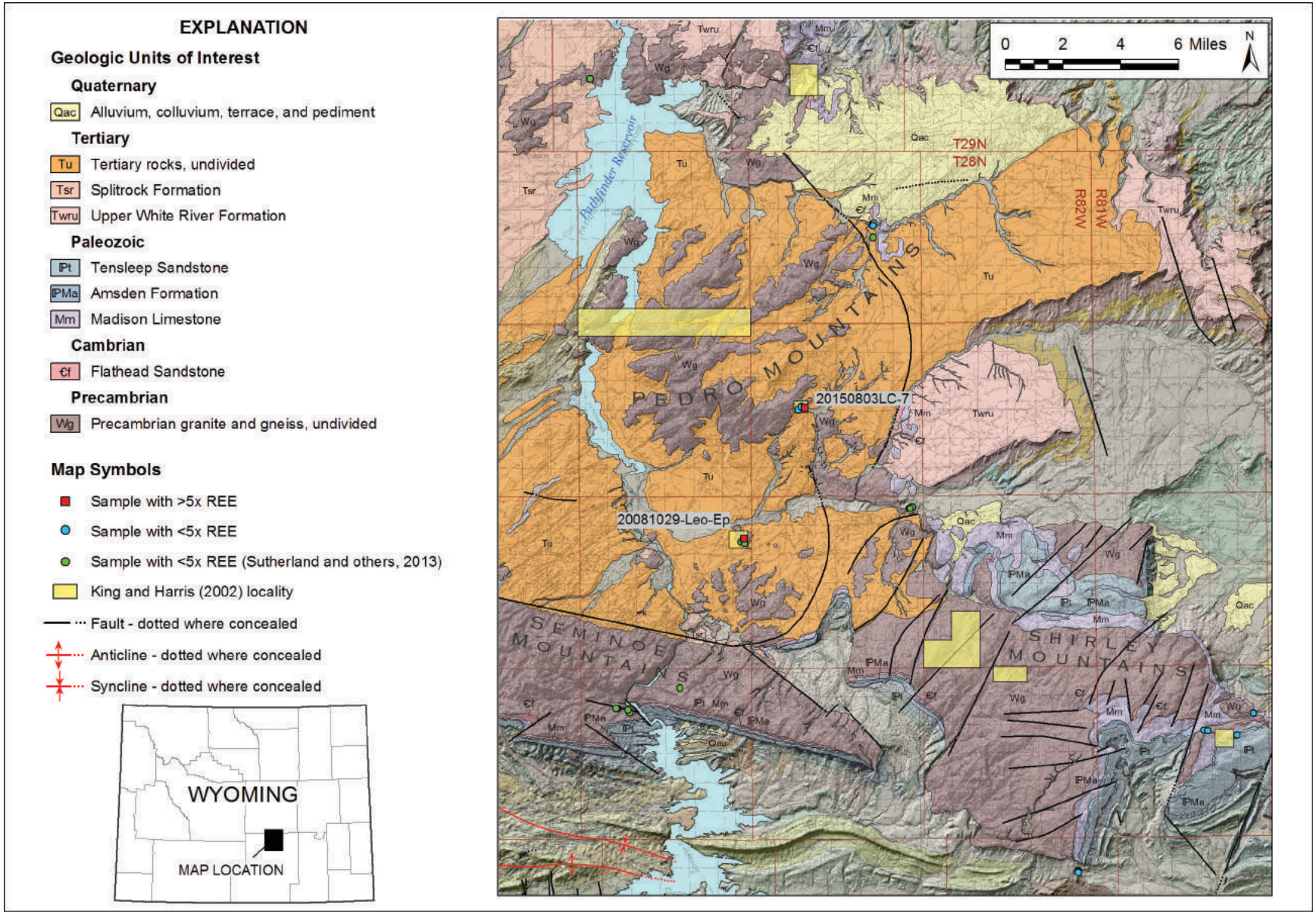


Figure 18. Sample locations and geology of the western Shirley and Pedro Mountains area. Sampling focused on Precambrian rocks and their neighboring units; these units are bold. Map modified from Jones and Gregory (2011).

Mountains exhibits 20 to 30 times the background radioactivity (Holmquist, 1955a, b). Samples were collected from an Archean diorite and quartz monzonite in the area and, respectively, contained 200 and 300 ppm La, <10 ppm Nb, 100 and 200 ppm Zr, 10 ppm Y each, 714 and 807 ppm eTh, and 2 and 11 ppm eU. A trace of allanite and apatite were also reported in a thin section of magnetite-bearing pegmatite (Griffin and Milton, 1982; King and Harris, 2002). The exact locations of the samples are unknown and much of the area is privately owned. Access was not obtained by the WSGS to investigate.

WL claims area, secs. 29, 31, and 32, T. 26 N., R. 82 W., Carbon County

The WL claims are near the A #1 and Beaver #1 claims. Unidentified, small, black, vitreous crystals are reported here in a 6 by 18 m (20 by 60 ft) highly radioactive zone, up to 50 times background. This area is in a 30 m (100 ft) wide, north-trending pegmatite that cuts Precambrian granite (Whalen, 1955). Griffin and Milton (1982) sampled the area, but none were taken in pegmatitic rock. Many of the samples were epidote-bearing, including Precambrian quartz monzonite and granite from the SW¼ of section 29. Samples of epidote-bearing Precambrian quartz diorite came from the section 32 and the SE¼ of section 29. A range of 6 ppm to 95 ppm eU and 192 ppm to 5,110 ppm eTh were reported in the area. One sample of epidosite contained 150 ppm La but less than 10 ppm Y. Traces of uranothorite were identified by SEM/EDS (Griffin and Milton, 1982; King and Harris, 2002). The WSGS did not visit this location as much of it is under private land ownership.

Jem claims area, center sec. 14, T. 25 N., R. 81 W., Carbon County

The Jem claims are a karst-hosted uranium deposit in the Shirley Mountains. A sample of granite in the area yielded 150 ppm La, 20 ppm Y, 100 ppm Zr, 58 ppm eTh, and 7 ppm eU. The granite is reddish near an unconformable contact with younger rocks, and iron oxide, calcite, traces of opaques, apatite, and zircon were reported. The feldspar in the granite is slightly altered, and biotite is almost entirely altered to chlorite (Griffin and Milton, 1982; King and Harris, 2002). Samples were collected by the WSGS near the Jem claim in the Flathead conglomerate and red to limonitic Amsden Formation as well as an outcrop with granitic gneiss, amphibolite mafic dikes, and pegmatites. None of these samples were enriched in REE. One sample (20150803LC-1C) of a fine-grained mafic dike did contain elevated scandium at 38 ppm, and the sample of Amsden Formation (20150803LC-3) contained elevated vanadium at 924 ppm as well as selenium at 12 ppm.

Bighorn Mountains

The Bighorn Mountains are a north- to northwest-trending Laramide uplift, mostly cored with Archean granite and gneiss, and unconformably overlain by Paleozoic sediments. The flanks of the uplift vary from gentle dip slopes in the southeastern part of the range to faulted and overturned sediments along the northwestern flank. The east-trending, left-lateral, oblique-slip Tensleep Fault separates the central Bighorn Mountains from the southern part of the range, which is split in a NNE direction by the basement-controlled right-lateral, oblique-slip Big Trails Fault System. Both faults are accompanied by subsidiary faults (Ver Ploeg and Greer, 1996; Ver Ploeg, 2004).

The core of the northern Bighorns is dominated by the granitic Bighorn batholith, which includes granite, granodiorite, quartz monzonite, and tonalite. The core of the central and southern part of the range is dominated by quartzofeldspathic gneisses and minor supracrustal rocks. Two generations of mafic dikes, Archean and Proterozoic, cross-cut the core of the range but are not common in the gneisses to the south (Frost and Fanning, 2006). Fault trends parallel and adjacent to these dikes provided evidence for basement control of major faults (Ver Ploeg and Greer, 1996).

Beaver Creek allanite prospect-Ramsbottom property, secs. 5 and 6, T. 46 N., R. 83 W.; sec. 31, T. 47 N., R. 83 W., Johnson County

At this location, near The Horn in the southern Bighorn Mountains (fig. 19), allanite is present in lenses, bands, and pods of metamorphic calc-silicate rocks. The rocks are composed of a complex assemblage of calcite, diopside, garnet, sodium-rich amphiboles, epidote, oligoclase, magnetite, and allanite. Allanite occurs as irregular masses that interfinger with epidote (Wilson, 1960). The bodies are generally concordant with the 300° trending foliation of the hosting Precambrian quartzofeldspathic gneiss and form a discontinuous zone varying from a few cm (in) to 1.8 m (6 ft) wide and 1,143 m (3,750 ft) long (King and Harris, 2002). Marble is adjacent to some of the calc-silicate bodies, and allanite tends to be more abundant in such areas. Individual allanite crystals are as long as 5 cm (2 in; King and Harris, 2002). This area is located near the projected intersection between a southeasterly splay of the Tensleep Fault and the northern end of a northeast linear trend, observable in satellite imagery, which may be an unmapped subsidiary of the Big Trails Fault.

Numerous prospect pits and trenches were cut in the site prior to 1960. In 1955, as much as 544 tonnes (600 tons) of allanite-bearing rock were removed from workings in section 31 (Bromley, 1955; Sargent, 1960). Assays reported

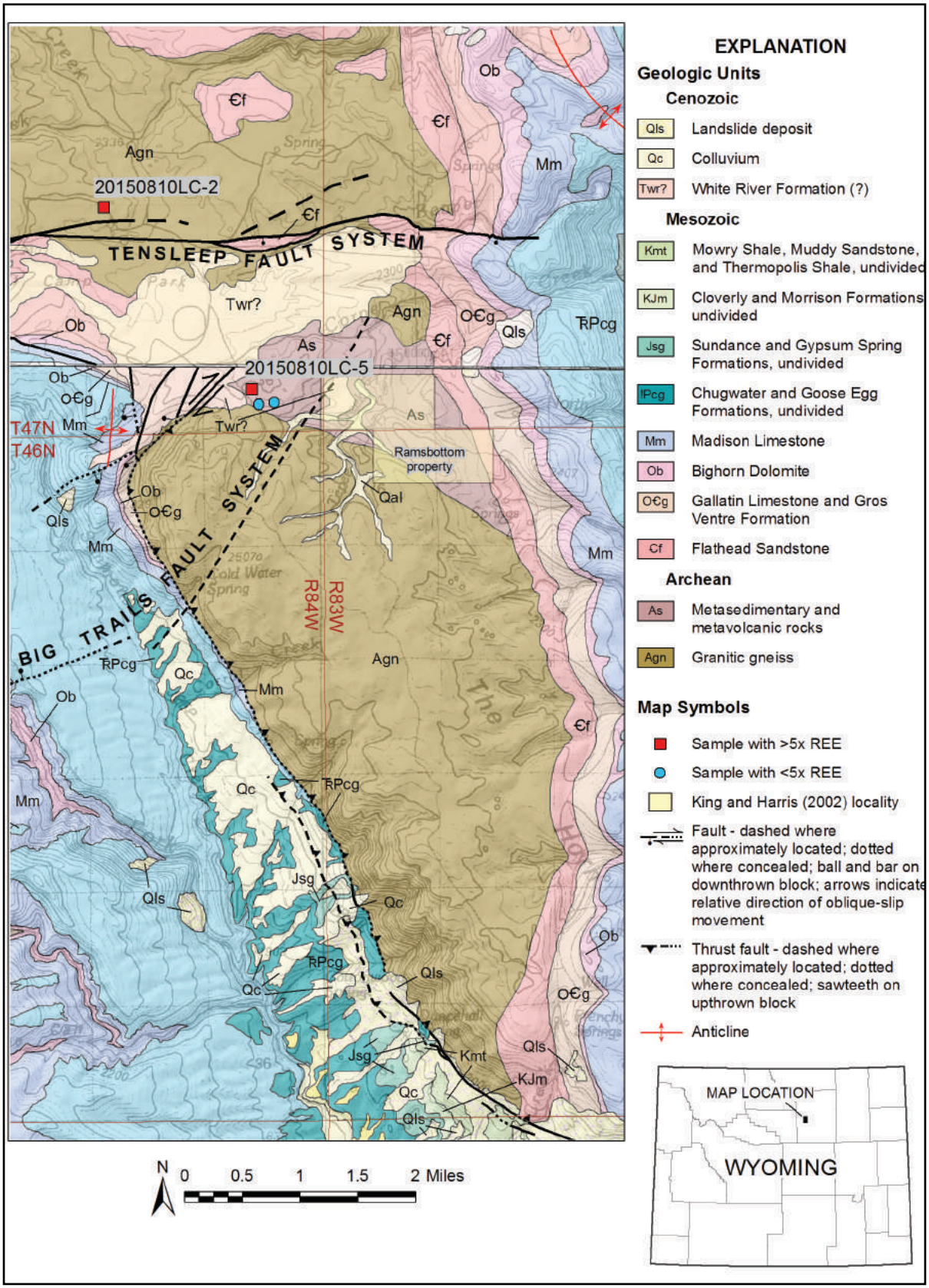


Figure 19. Sample locations and geology of The Horn area. Sampling focused in Precambrian rocks near the Ramsbottom property (King and Harris, 2002). Map modified from Ver Ploeg and Boyd (2002) and Ver Ploeg and others (2004).

by Wilson (1960) yielded up to 11 percent CeO_2, 0.7 percent thorium, and 1.5 percent other REO. Access to the Beaver Creek allanite prospect requires passage through private lands, and the WSGS was unable to gain permission for this investigation.

Bull Camp prospects, SW¼SW¼ sec. 23 and NW¼NW¼ sec. 26, T. 47 N., R. 84. W., Johnson County

These prospects are located on or adjacent to the eastern part of the Tensleep Fault (fig. 19), a few miles northwest of the Beaver Creek allanite locale. Historic reports indicate that these prospects were originally explored around 1900 or earlier for gold and copper (Hausel, 1997). The pits expose Archean granitic gneiss (Ver Ploeg and Boyd, 2002) and pegmatitic rock with varying degrees of deformation from extremely altered to granular. Rust and copper staining, including malachite and azurite mineralization, is prevalent. Some altered areas are epidote-rich, and vuggy quartz pockets can be found. Of the samples collected, the extremely rusty and epidote-rich rocks contained elevated REE, and between two samples (20150810LC-2D and 2E), only europium, lanthanum, praseodymium, and scandium were not significantly elevated (table 21). Other elements of economic interest present in this area are cobalt and copper. Sample 201508LC-2A, a copper-stained rock, contained 3.23 percent Cu and Sample 201508LC-2D, a very rusty rock, contained 818 ppm Co.

Stove Leg prospect, SE¼SW¼ sec. 36, T. 47 N., R. 84 W., Johnson County

This previously unnamed prospect (fig. 20A) lies to the southeast of the Bull Camp Prospects and to the west of the Beaver Creek allanite prospect. Light colored granitic gneiss and amphibolite comprise the majority of the exposed outcrop. The area is near the contact between Archean granitic gneiss with metasedimentary and metavolcanic rocks (Ver Ploeg and others, 2004). Massive, dense andradite garnet (Sample 20150810LC-5A; fig. 20B) occurs erratically across the area. Extensive epidotization (Sample 20150810LC-5B; fig. 20C) as well as silicification are also present. The silicified rocks include jasper and botryoidal quartz (Sample 20150810LC-5C; fig. 20D). All of the samples collected here contained elevated REE, and the silicified material contained higher concentrations overall (table 22).

In the northeastern part of the Bighorn Mountains, one NURE sample showed more than five times the average crustal abundance of Ce, about four times for La, and double the Y. However, no other NURE samples in the area approached REE enrichment concentrations (Smith, 2001). Similarly, none of the three samples collected in the northeastern Bighorn Mountains by the WSGS of , leopard rock (20150811LC-1), quartz-pegmatite with epidote (20150811LC-2), and hematite-rich and copper-stained quartz-pegmatite (20150811LC-3) hosted elevated REE.

Sample R49, SW¼NW¼ sec. 23, T. 53 N., R. 84 W., Johnson County

A 1976 report by Segerstrom and Weisner (1976) summarized an investigation of the mineral resources in areas adjacent to the Cloud Peak Primitive (now wilderness) area for its proposed expansion. They noted one sample (R49)from a metadiabase dike several miles southwest of Story, Wyo., which showed 200 ppm La, 30 ppm Sc, and 500 ppm Ni. The site is now inaccessible and within the Wilderness Area, but their sample may reflect on slightly elevated REE in similar dikes outside of the designated wilderness boundary.

Two samples of gneiss, collected about 13 km (8 mi) south of R49, also hosted lanthanum concentrations greater than five times the average. Samples R13 (sec. 34, T. 52 N., R. 84 W.) and R17 (sec. 32, T. 52 N, R. 84 W.) both contained 300 ppm La. However, no other rock samples in the vicinity contained similarly elevated REE.

Several stream sediment samples, also collected by Segerstrom and Weisner (1976) from a broad area, contained elevated La and Y. This, they explained, was due

Table 21. Concentration of REE from the Bull Camp prospects. Bold values indicate concentrations greater than five times the crustal abundance.

	Bull Camp prospects								
Element	La (ppm)	Ce (ppm)	Pr (ppm)	Nd (ppm)	Sm (ppm)	Eu (ppm)	Gd (ppm)	Tb (ppm)	Dy (ppm)
20150810LC-2D	38.7	65.9	8.08	30.5	9.9	1.14	17.3	3.71	23.9
20150810LC-2E	112	211	25.3	100.5	**33.1**	4.82	**53.8**	**11.1**	**72.9**

Element	Ho (ppm)	Er (ppm)	Tm (ppm)	Yb (ppm)	Lu (ppm)	Sc (ppm)	Y (ppm)	Cumulative REE (ppm)
20150810LC-2D	**5.66**	**16.05**	**2.85**	**19.95**	**3.05**	13	**164**	423.69
20150810LC-2E	17	**47.8**	**8.08**	**56.8**	**7.63**	17	**493**	**1,271.83**

Table 22. Concentration of REE from the Stove Leg prospect. Bold values indicate concentrations greater than five times the crustal abundance.

	Stove Leg prospect								
Element	La (ppm)	Ce (ppm)	Pr (ppm)	Nd (ppm)	Sm (ppm)	Eu (ppm)	Gd (ppm)	Tb (ppm)	Dy (ppm)
20150810LC-5A	26	59.1	9.7	73.4	**43.4**	**14.2**	**39.4**	**4.42**	19
20150810LC-5B	**173**	**436**	**55.2**	**222**	**33.9**	7.33	**20.3**	1.87	7.33
20150810LC-5C	**229**	**629**	**75.8**	**288**	**42**	**9.63**	**26.1**	2.57	10.1

Element	Ho (ppm)	Er (ppm)	Tm (ppm)	Yb (ppm)	Lu (ppm)	Sc (ppm)	Y (ppm)	Cumulative REE (ppm)
20150810LC-5A	3.29	7.73	0.97	6.15	0.9	9	85.8	402.46
20150810LC-5B	1.1	2.27	0.28	1.53	0.23	8	26.9	997.24
20150810LC-5C	1.51	3.18	0.36	1.93	0.29	12	36.1	**1,367.57**

to concentrations of monazite in the heavy-mineral fraction. Although details are lacking, the concentration of monazite in stream sediment samples might also explain some elevated REE values in many of the NURE samples from this area.

Bald Mountain area mafic dike, NE¼SE¼ sec. 22, T. 56 N., R. 91 W., Sheridan County

Sample 20110824WS-B is from a Precambrian mafic dike in brecciated and re-healed contact with the surrounding granitic rocks. The dike protrudes through part of the lower Flathead Sandstone, which is a known host of REE-bearing minerals in the region. The sample showed slightly elevated LREE values in the dike, which may have contributed to the later Cambrian paleoplacers.

Rainbow claims, estimated as T. 58 N., R. 92 W., Big Horn County

This location is an unverified occurrence (King and Harris, 2002). Euxenite was reported in a pegmatite on these claims by Parker (1963). However, the location given for the pegmatite is just east of Cookstove Basin in sedimentary rocks. This is likely an error. The location given above is where Archean granites are exposed (King and Harris, 2002). Harris reported monazite in pegmatites in the basin, but this is also unverified. Mapping of the area

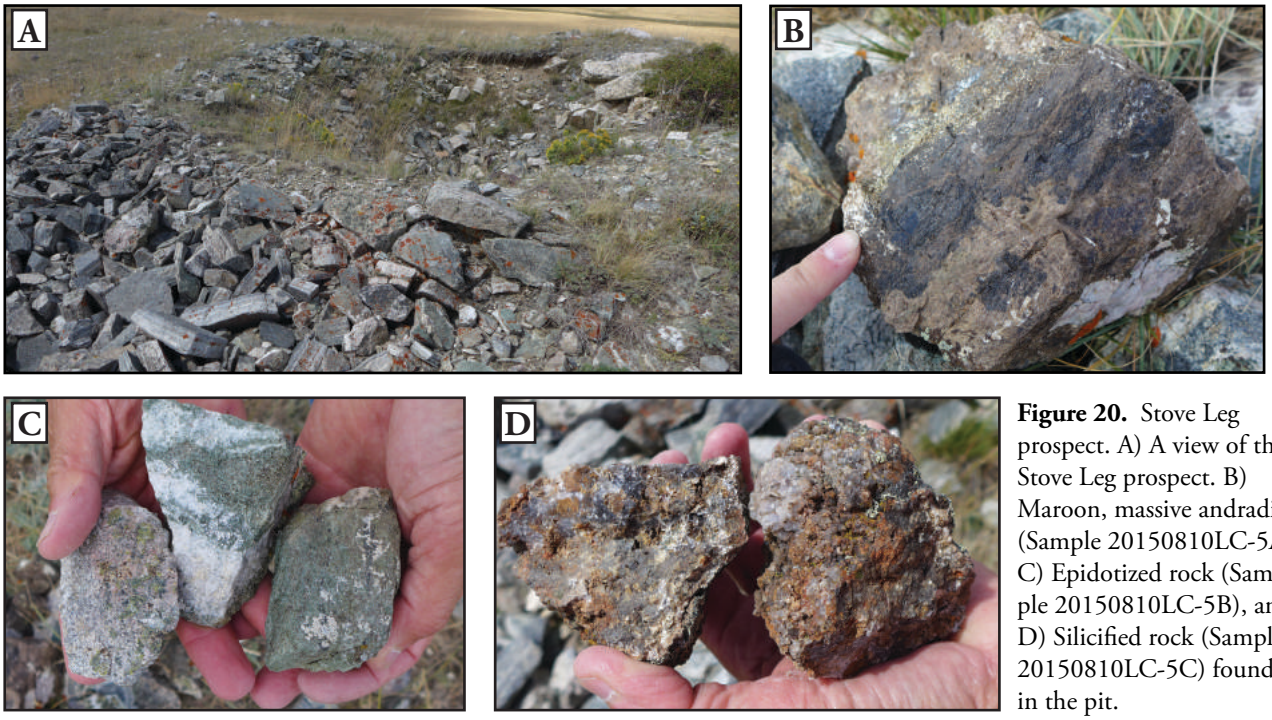


Figure 20. Stove Leg prospect. A) A view of the Stove Leg prospect. B) Maroon, massive andradite (Sample 20150810LC-5A), C) Epidotized rock (Sample 20150810LC-5B), and D) Silicified rock (Sample 20150810LC-5C) found in the pit.

by Taucher (1953) did not mention pegmatites. Harris and Hausel (1986) also report pegmatites in granitic gneiss containing trace REE in the Cookstove Basin. The pegmatites contain quartz and feldspar with rare occurrences of monazite, euxenite, and specularite. Again, no location was provided with the description. During this study, the WSGS traversed along the ridge on the east edge of the area listed by King and Harris (2002). Only sedimentary rocks were exposed, and no samples were taken. It is still possible there are REE-bearing pegmatites in Precambrian units in the area; the location remains unverified.

Wind River Mountains

Elevated LREE have been reported in the Precambrian Louis Lake Batholith (Condie and Lo, 1971) and Bear Ears pluton in the southern Wind River Range. Eight of 57 samples in the Louis Lake Batholith, one of 18 samples in the Bear Ears pluton, and three of 29 samples from miscellaneous crystalline rocks contained elevated REE (King and Harris, 2002). Table 23 displays sample information from a combination of sources from King and Harris (2002), and the correlating chemistry for these samples can be found in table 24. It is unlikely that REE in the Wind River Range would favor economic interest due to their widespread distribution and their location within national forest and wilderness areas.

Union Pass–Warm Spring Area

The Union Pass–Warm Spring area (fig. 21) is located on the north end of the Wind River Mountains, approximately 12 km (7.5 mi) due west of Dubois. The area is known to host placer deposits of gold, heavy minerals, and at least one vein- and breccia-hosted uranium deposit. Ullmer (1983) noted that a north-northwest-trending lineament intersects the Dubois claims uranium deposit, which is hosted in a brecciated quartz vein cutting a magnetite- and biotite-rich pod within Archean gneiss (Granger and others, 1971; Ullmer, 1983). Uranium mineralization within the Dubois claims was likely produced through hydrothermal alteration related to the emplacement of granitic dikes (Ullmer, 1983). Placer deposits in the area will be discussed in a later section.

Wildcat Road, SE¼SE¼ sec. 3, T. 41 N., R. 108 W., Fremont County

This site is exposed in a road-cut on Wildcat Road (fig. 22A), near the northwest end of Ullmer's (1983) lineament and is similar to the Dubois claims. The lineament is observable in aerial imagery.

The iron-rich pod here contains much less biotite than at the Dubois claims and is dominantly composed of iron-rich pyroxenes and olivine. These include hypersthene, ferroaugite, fayalite, magnetite, and quartz with minor plagioclase, biotite, and hornblende. Ullmer (1983) argues that the iron-rich composition and mineral assemblage of the relatively unaltered rocks at the northwest end of the lineament suggest the iron-rich pods are metamorphosed iron formation, rather than intrusive ultramafic rocks. Iron-rich float is present along the length of the lineament (Sutherland and others, 2013; Sutherland and Cola, 2015).

Granger and others (1971) and Ullmer (1983) refer to the iron-rich pods as biotite gneiss and mica schist, respectively. Samples collected by Sutherland and Cola (2015) were magnetite-rich and rusty to limonitic. Although many of the rocks were granular, some of the samples appeared to contain banding (fig. 22B), which would further suggest the presences of banded iron formation before heavy faulting and metasomatic alteration. No elevated rare earths were present in this banded rock (Sample 20141015WS-D); however, it did contain up to 50 percent Fe_2O_3.

The iron-rich pod (Sample 20121004JC-A) is cut by a very coarse-grained, biotite-rich granitic dike with abundant iron-staining (Sample 20121004JC-B; fig. 21A). Sample 20121004JC-B was split into two subsamples for analyses: unaltered granitic material (20121004JC-B.1) with radioactivity up to three times background when isolated in the lab, and altered, heavily limonite-stained granitic material (20121004JC-B.2) with no anomalous radioactivity. In the unaltered sample, zircon is present within biotite and is likely the source of the elevated radioactivity and the REE (Sutherland and others, 2013).

The presence of moderately radioactive granite supports Ullmer's (1983) assertion that mineralization within the Dubois claims is associated with the emplacement of granitic dikes. The unaltered radioactive granite is weakly enriched in the LREE as well as gadolinium and terbium. The altered granite, iron-rich pod, and altered BIF exhibit no notable REE enrichment (table 25; Sutherland and others, 2013; Sutherland and Cola, 2015).

Dubois claims, SW¼NW¼ sec. 12, T. 41 N., R. 108 W., Fremont County

Ullmer (1983) reported that uranium mineralization (up to 2.4 percent U_3O_8) in this area is hosted in a brittle deformation zone within an altered magnetite- and biotite-rich pod in Archean gneiss. The findings of Ullmer (1983) are in agreement with Granger and others (1971), who found pitchblende within a quartz, hematite, and magnetite cemented breccia zone cutting biotite gneiss. Ullmer (1983) interprets the magnetite- and biotite-rich pod as contact-metamorphosed iron formation that was hydro-

Table 23. Locations and host rock of samples from the Wind River Range.

Wind River Range			
Sample #	Location	Reported Host	Mapped Host
37	SW¼ T. 31 N., R. 101 W., Fremont Co.	Louis Lake*	Louis Lake
86	E½ T. 30–31 N., R. 103 W., Sublette Co.	Louis Lake*	Louis Lake
LLB-8	NW¼ T. 31 N., R. 101 W., Fremont Co.	Louis Lake	Louis Lake
PRM 1	SW¼ T. 30 N., R. 104 W., Sublette Co.	Louis Lake	Bear Ears
PRM 6	NE¼ T. 29 N., R. 104 W., Sublette Co.	Louis Lake	Bear Ears
BW 3	center E line T. 35 N., R 106–107 W., Sublette Co.	Louis Lake	Bear Ears
BW 7	center E line T. 35 N., R 106–107 W., Sublette Co.	Louis Lake	Bear Ears
BW 22	SE¼ T. 32 N., R. 104 W., Sublette Co.	Louis Lake	Bear Ears
BW 15	SW¼ T. 37 N., R. 108 W., Sublette Co.	Bear Ears	Bear Ears
BW 14	SW¼ T. 37 N., R. 108 W., Sublette Co.	Misc	Bear Ears
BW 48	NE¼ T. 37 N., R. 107 W., Sublette Co.	Misc	Migmatite
BW 49	NE¼ T. 37 N., R. 107 W., Sublette Co.	Misc	Migmatite

Adapted from King and Harris (2002)

Reported host units from Stuckless (1989)

* from Condie and Lo (1971)

Mapped host units from Stuckless (1989), Stuckless and others (1985), and Love and Christiansen (1985)

Table 24. Analyses of historic samples from the Wind River Range. Bold values indicate concentrations greater than five times the crustal abundances.

Wind River Range								
Element	La (ppm)	Ce (ppm)	Nd (ppm)	Sm (ppm)	Eu (ppm)	Gd (ppm)	Y (ppm)	Cumulative REE (ppm)
37*	156	291	-	22	3	-	-	472
86*	**207**	**376**	-	27	3	-	-	613
LLB 8	**213**	**410**	155	28	3	18	64	891
PRM 1	**171**	**315**	117	16	2	9	27	657
PRM 6	**242**	**472**	**194**	29	5	17	45	**1,004**
BW 3	168	**328**	133	20	3	15	48	715
BW 7	102	243	116	19	5	13	32	530
BW 22	166	**327**	139	21	3	16	30	702
BW 15	158	296	121	18	3	14	37	647
BW 14	**174**	**333**	128	19	4	15	30	703
BW 48	166	**321**	128	19	5	12	31	682
BW 49	168	271	97	12	2	6	17	573
Louis Lake Average	98	190	77	12	2	8	26	413
Bear Ears Average	78	144	52	8	1	6	17	306

Adapted from King and Harris (2002)

Sample chemistry from Stuckless (1989)

* from Condie and Lo (1971)

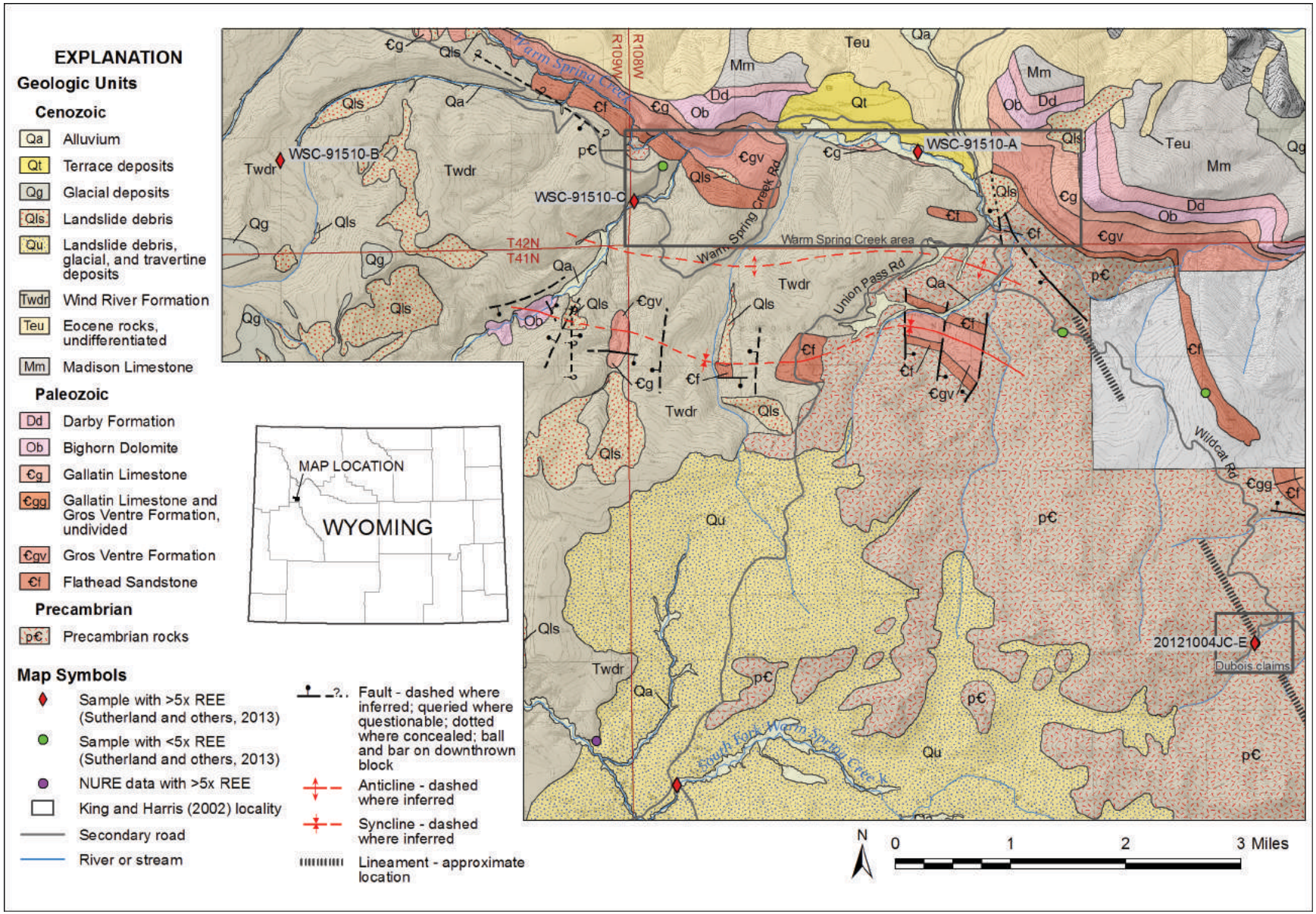


Figure 21. Sample locations and geology of the Union Pass-Warm Spring area. Samples displayed come from RI-65 (Sutherland and others, 2103) and NURE data. Most samples with elevated REE in this area are found in the Wind River Formation or Flathead Formation. Map modified from Keefer (1957), Dunnewald (1958), Rohrer (1968), Granger and others (1971), Ullmer (1983), and Sutherland and others (2013).

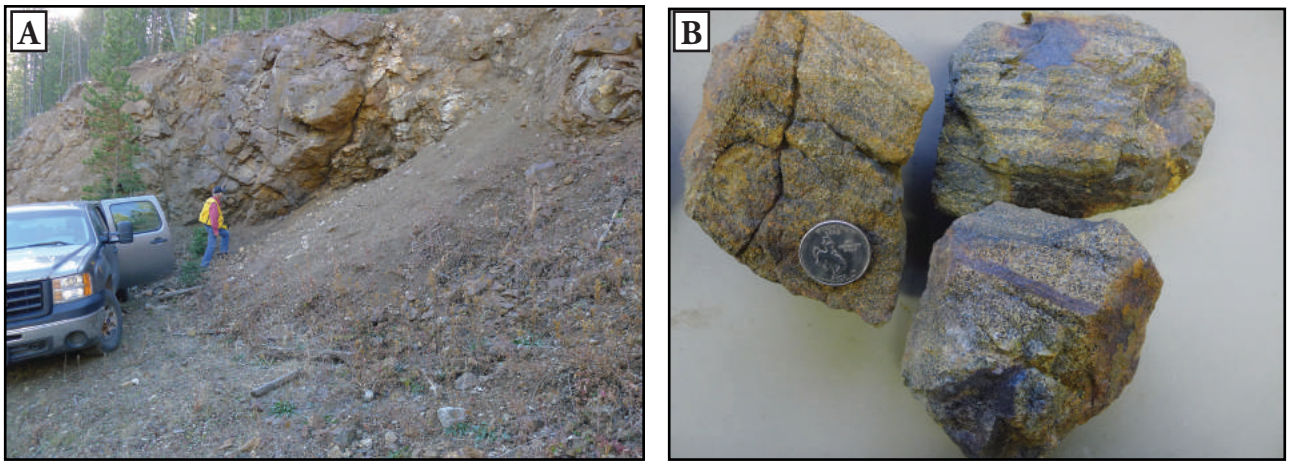


Figure 22. Wildcat Road. A) The exposed pegmatite and shear zone is exposed along the road. B) Altered rock with iron-rich bands reminiscent of banded iron formation (Sample 20141016WS-A; Sutherland and Cola, 2015).

thermally altered. Hydrothermal alteration resulted in chlorite and sericite as well as the growth of biotite, and it was likely the source of uranium enrichment (Ullmer, 1983).

The host rock at the surface at the mine site consists of a brecciated quartz vein with moderate biotite and hornblende, iron-staining, and the occurrence of minor to moderate opaque minerals (Sample 20121004JC-D). The vein cuts an altered black magnetite- and biotite-rich pod (Sample 20121004JC-E) that also contains quartz, hornblende, andradite, and allanite. The iron-rich rock is strongly enriched in LREE, moderately enriched in gadolinium and thorium, and weakly enriched in the remaining REE and yttrium. The brecciated quartz vein exhibits no significant enrichment of REE or other elements (table 25).

The presence of REE enrichment at two locations on the lineament described by Ullmer (1983) is significant, and

Table 25. Concentration of REE from the Union Pass-Warm Spring area. Bold values indicate concentrations greater than five times the crustal abundance.

	Union Pass - Warm Spring area								
Element	La (ppm)	Ce (ppm)	Pr (ppm)	Nd (ppm)	Sm (ppm)	Eu (ppm)	Gd (ppm)	Tb (ppm)	Dy (ppm)
20121004JC-A	32.6	57.8	5.92	19.2	3.19	0.64	3.63	0.86	7.39
20121004JC-B.1	100.5	**479**	18.6	61.1	9.19	1	6.23	0.73	3.16
20121004JC-B.2	3.1	4.9	0.57	1.9	0.34	0.04	0.24	0.04	0.22
20121004JC-D	12.3	29.7	3.09	11.2	2.46	0.45	1.85	0.43	2.88
20121004JC-E	**821**	**1,640**	**143**	**471**	**57.1**	3.01	**28.2**	2.87	12.35
20141015WS-D*	7.4	13.7	1.44	5.2	0.98	0.26	0.76	0.13	0.7

Element	Ho (ppm)	Er (ppm)	Tm (ppm)	Yb (ppm)	Lu (ppm)	Sc (ppm)	Y (ppm)	Cumulative REE (ppm)
20121004JC-A	2	6.94	1.24	8.71	1.47	51	52.7	255.02
20121004JC-B.1	0.49	1.17	0.15	0.91	0.14	10	12.3	704.67
20121004JC-B.2	0.04	0.13	0.02	0.16	0.03	6	1.2	18.93
20121004JC-D	0.59	1.85	0.32	2.22	0.36	14	12.4	96.1
20121004JC-E	2.31	6.29	0.95	6.07	1.05	13	50.8	**3,259**
20141015WS-D*	0.15	0.41	0.06	0.44	0.08	1	4.7	37.41

From Sutherland and others (2013)

*Sutherland and Cola (2015)

warrants further investigation along its length. In particular, the relationship between the three sampled rock types requires further study to fully characterize this deposit. Enrichment is variable within rock types and is apparently associated with hydrothermal activity in the case of the iron-rich rocks.

Gros Ventre Range

The Gros Ventre Range is a Precambrian-cored, irregular Laramide uplift situated between the Wind River Mountains and Jackson Hole. The range is cross cut by and bounded on the southwest by northwest-trending faults. Exposures across the range are generally dominated by Phanerozoic sedimentary rocks (fig. 23). King and Harris (2002) summarized the follow samples collected by Simons and others (1988) from Archean granite in the Gros Ventre Wilderness. The origin of the REE enrichment is unknown, but many are associated with metal oxide or sulfide mineralization. Since these samples are located within a wilderness area, access is limited and difficult. The WSGS did not visit this area, but high amounts of lanthanum and yttrium may warrant further study to determine the origin of REE and their possible relationship with other metals.

Unnamed (USGS Sample #3103), common corner secs. 28, 29, 32, and 33, T. 40 N., R. 114 W., Teton County

This sample is from an outcrop of Archean granite within a small, magnetite-bearing fault zone. The rock contains 1,000 ppm Y, 20,000 ppm Pb, 20 ppm Au, and 1 ppm Ag.

Unnamed (USGS Sample #3124), center secs. 28–33, T. 40 N., R. 114 W., Teton County

This Archean granite or granitic gneiss has no metal mineralization and contains 70 ppm La, 200 ppm Y, and 150 ppm V.

Unnamed (USGS Sample #3169), NE¼ sec. 34, T. 40 N., R. 113 W., Teton County

At this location, a quartz hematite veinlet in Archean granite contained 1,000 ppm Y and 150 ppm La.

Unnamed (USGS Sample #3181), center E½ sec. 2, T. 39 N., R. 113 W., Teton County

A sulfide veinlet in Archean granite contained 200 ppm La, 2,000 ppm Cr, 100 ppm Cu, and 100 ppm Ni.

Unnamed (USGS Sample #3190), N¼ secs. 11–12, T. 39 N., R. 113 W., Teton County

Magnetite veinlets in a fault within Archean granite contained >1,000 ppm La and 500 ppm V.

TERTIARY-AGED IGNEOUS OCCURRENCES

Tertiary-aged and younger igneous rocks that have potential to host REE in Wyoming include a wide variety of volcanics and intrusive rocks. These crop out in the Absaroka Mountains in northwestern Wyoming, the Black Hills in the northeastern part of the state, the Rattlesnake Hills in central Wyoming, Battle Mountain in south central Wyoming, the Leucite Hills, north of Rock Springs, and the Cedar Mountain breccia pipes in southwestern Wyoming.

Absaroka Mountains and Vicinity

The Absaroka Mountains host large expanses of calc-alkaline plutons, dikes, lava flows, and breccias that grade laterally into volcaniclastics (Hausel, 1997) and vary in age from Eocene to Miocene (Wilson, 1964). Some igneous rocks near the southern and western edges of the Absarokas are much younger and are related to the Yellowstone volcanics. Several samples from metalliferous deposits in the Kirwin area were analyzed for REE, but all contained less than five times the crustal abundance. The majority of the Absarokas are designated wilderness, making access difficult.

Pilot Knob, NW¼ sec. 3, T. 43 N., R. 110 W., Fremont County

Near Togwotee Pass, the Eocene Aycross Formation (fig. 24), part of the Absaroka volcanic super group, surrounds Pilot Knob (Love and Christiansen, 1985), which is described by Love and others (1982) as a vogesite lamprophyre of Tertiary age (or younger). A sample taken from the large talus pile at the base of Pilot Knob (figs. 25A, B) contained elevated LREE (table 26). The fine-grained, hard, tan to light-gray rock contains biotite, plagioclase-orthoclase, and greenish amphibole (fig. 25C). Given the broad expanse of Tertiary and younger volcanics in northwest Wyoming, there could be other locales with elevated REE.

Black Hills

Eocene alkalic intrusive rocks form the centers of several domes in the Black Hills (fig. 26) as well as numerous dikes that cut Precambrian rocks in the Mineral Hill area. These intrusions include the REE-rich carbonatites previously described in the Bear Lodge Mountains section. However, the carbonatites in the Bear Lodge Mountains host the only known significant REE enrichment in the area.

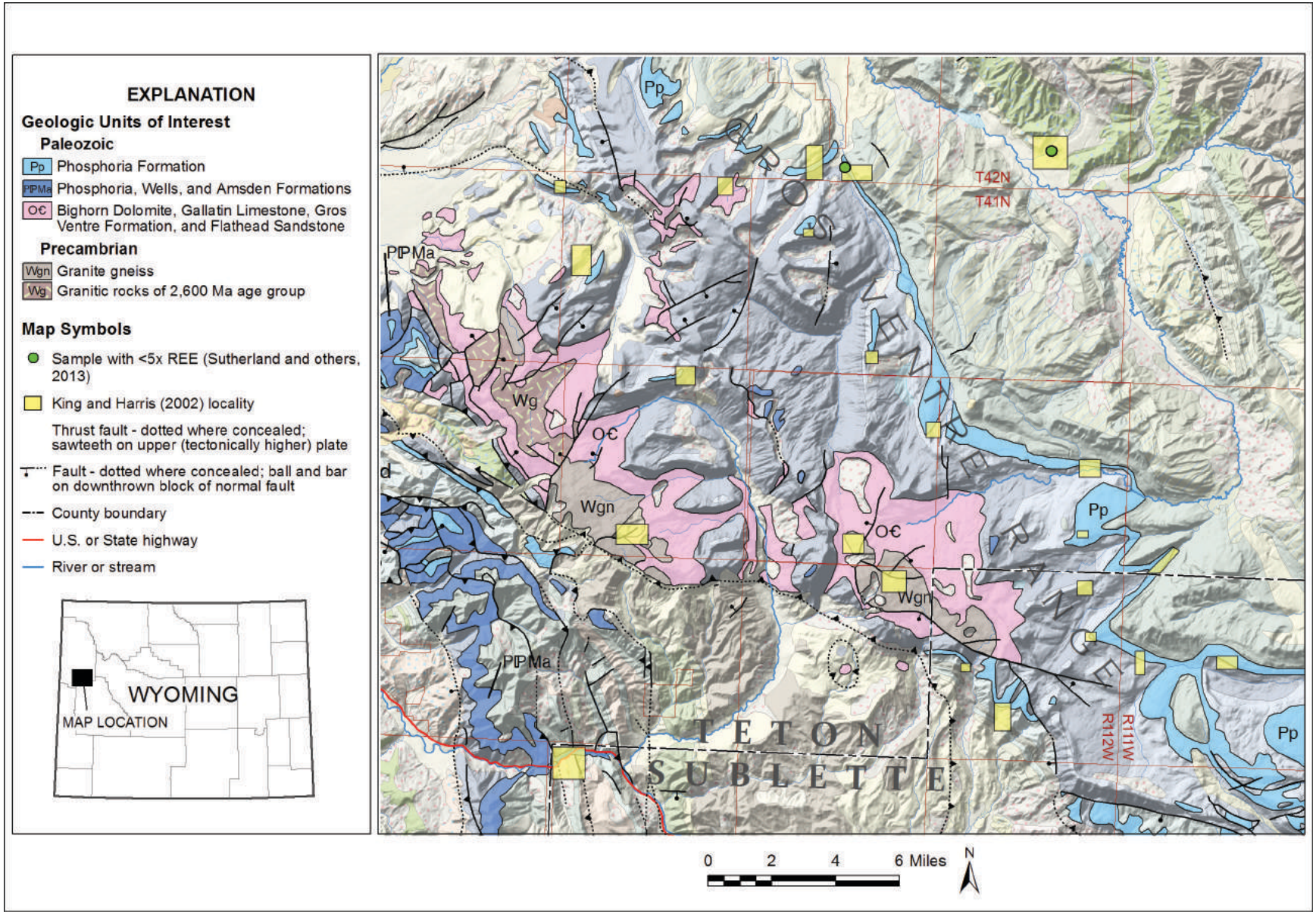


Figure 23. Geology of the Gros Ventre Range. No sampling was done during this study due to limited access in the wilderness area. One sample was taken during RI-65 (Sutherland and others, 2013). King and Harris (2002) indicate many locations bearing elevated REE, commonly in the Phosphoria Formation, Flathead Sandstone, and Precambrian rock. These units are bold compared to surrounding geology. Map modified from Love and Christiansen (1985).

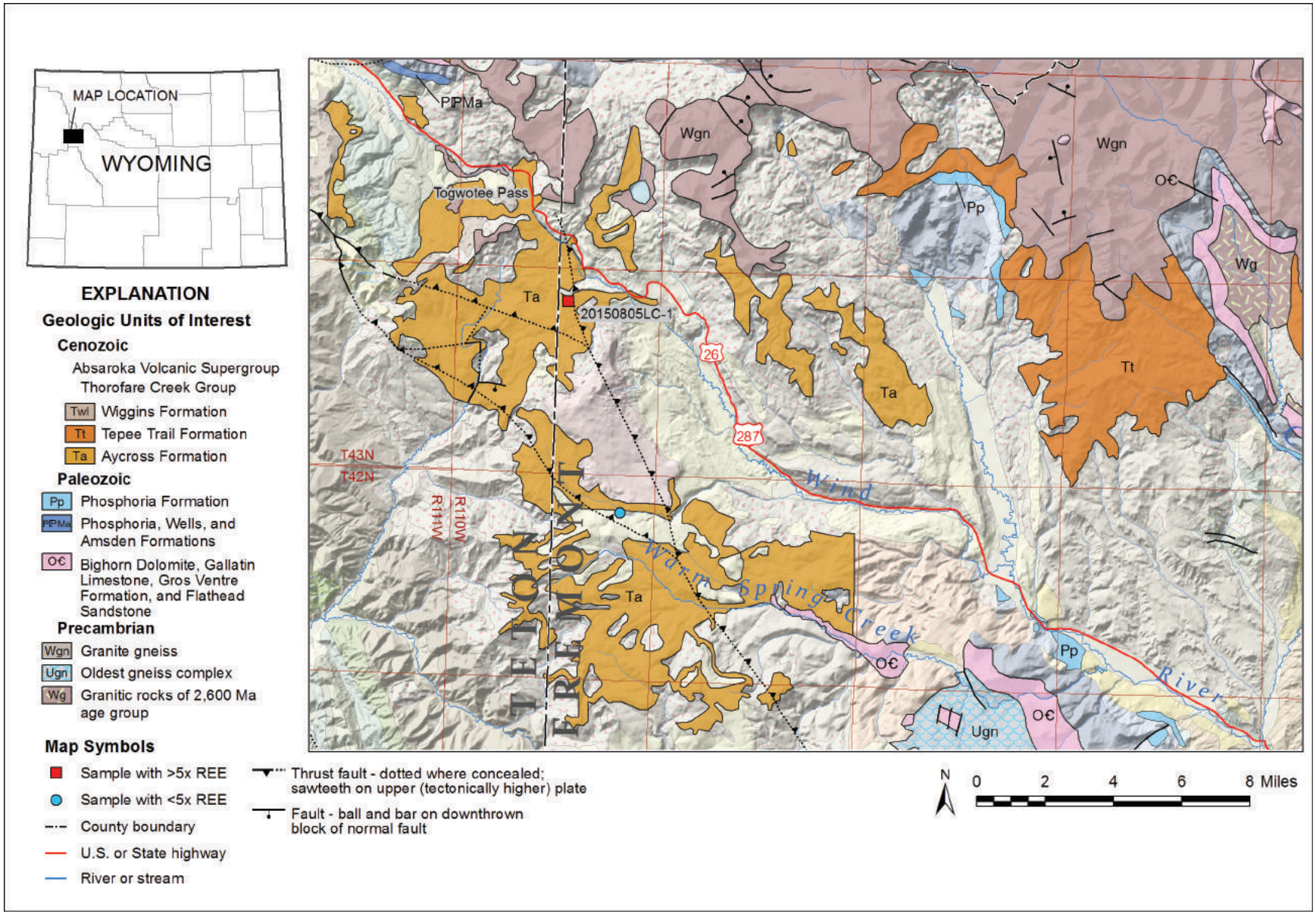


Figure 24. Sample locations and geology of the Pilot Knob area. The Tertiary volcanics, as well as Phosphoria Formation, Flathead Sandstone, and Precambrian rocks are bold compared to surrounding geology since they have higher potential of hosting elevated REE. Map modified from Love and Christiansen (1985).

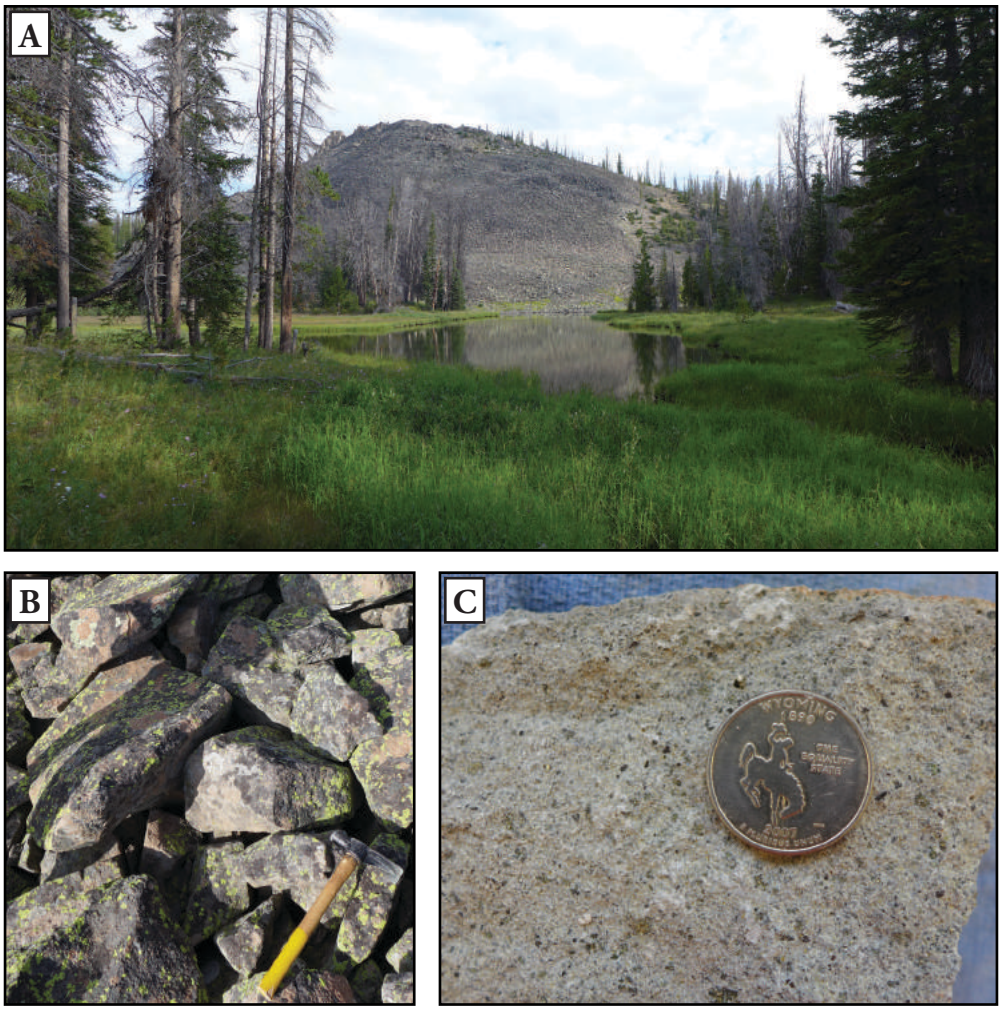


Figure 25. Pilot Knob. A) A view looking northwest toward Pilot Knob. B) Large blocks of the igneous rock which form a talus pile along the slope of Pilot Knob. C) Close-up of a fresh surface of the igneous rock (Sample 20150805LC-1).

Table 26. Concentration of REE from Pilot Knob. Bold values indicate concentrations greater than five times the crustal abundance.

	Pilot Knob								
Element	La (ppm)	Ce (ppm)	Pr (ppm)	Nd (ppm)	Sm (ppm)	Eu (ppm)	Gd (ppm)	Tb (ppm)	Dy (ppm)
20150805LC-1	**177.5**	**370**	**41.2**	152.5	19.6	4.36	9.32	1.02	4.35
	Ho (ppm)	Er (ppm)	Tm (ppm)	Yb (ppm)	Lu (ppm)	Sc (ppm)	Y (ppm)	Cumulative REE (ppm)	
	0.73	1.67	0.26	1.69	0.24	12	18.6	815.04	

Southern Bear Lodge Mountains, center E½E½ sec. 33, T. 52 N., R. 63 W., Crook County

See previous discussion of the Bear Lodge deposit for details. Phonolite from the area is shown in figure 27A.

Mineral Hill (Tinton, Negro Hill) area, T. 51 N., R. 60 W.; N½ T. 50 N., R. 60 W., Crook County

This area is a tertiary alkali-igneous complex that intruded Precambrian schists, parallel to host rock foliation, and lower Paleozoic sedimentary units (fig. 26; Welch, 1974; Smith and Page, 1941). Samples from Precambrian and Tertiary rocks were analyzed and con-

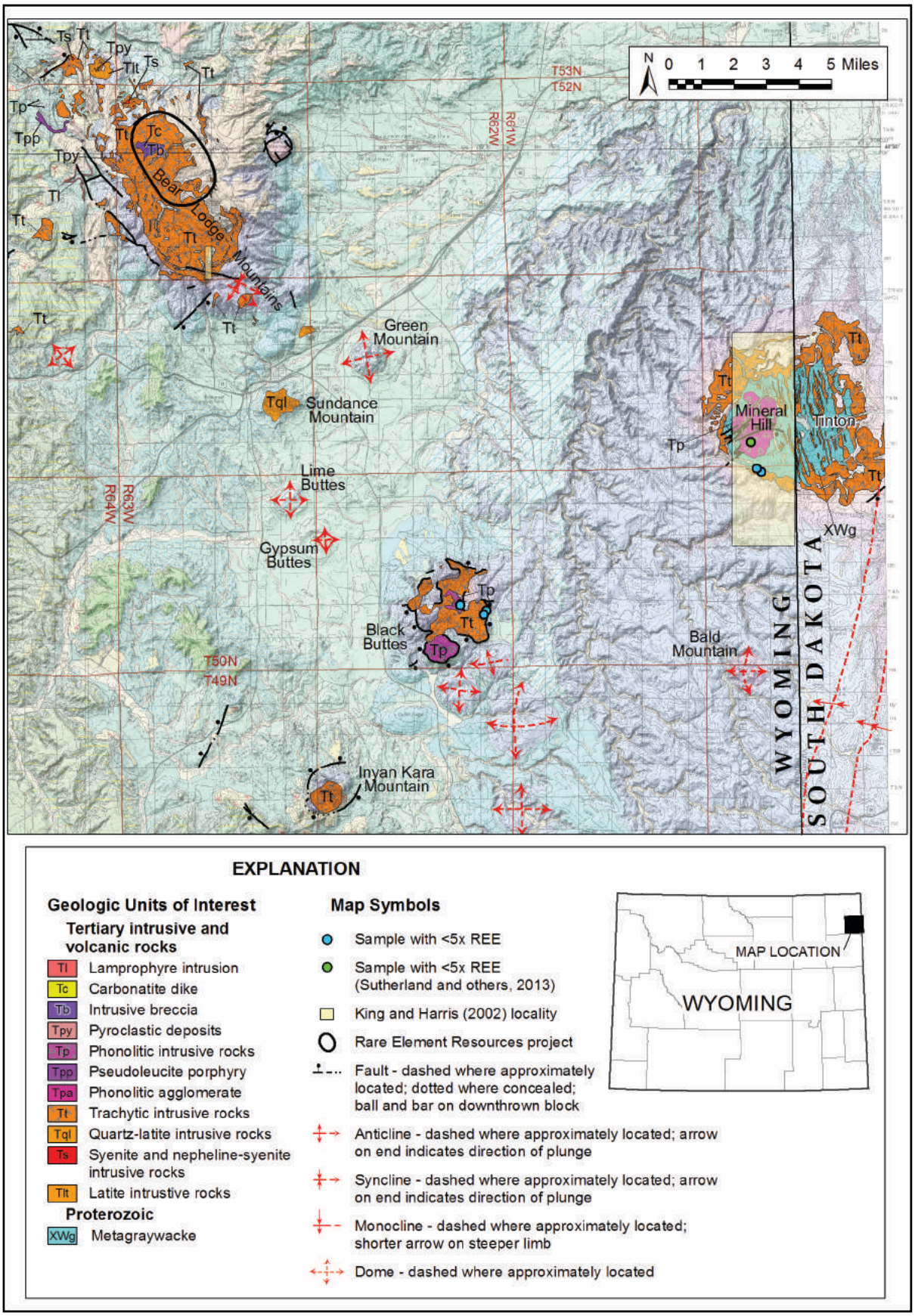


Figure 26. Sample locations and geology of northeastern Wyoming. Tertiary igneous rocks commonly contain elevated REE in this region. These units are bold compared to surrounding geology. Map modified from Sutherland (2007; 2008).

Table 27. Concentration of REE from the Mineral Hill area. Bold values indicate concentrations greater than five times the crustal abundance.

	Mineral Hill area								
Element	La (ppm)	Ce (ppm)	Pr (ppm)	Nd (ppm)	Sm (ppm)	Eu (ppm)	Gd (ppm)	Tb (ppm)	Dy (ppm)
20150717DB-1	119.5	253	30.9	126.5	20.5	5.28	14.2	1.75	8.04
20150717DB-2	120.5	238	26.3	103.5	22	6.64	17.45	1.56	5.62

Element	Ho (ppm)	Er (ppm)	Tm (ppm)	Yb (ppm)	Lu (ppm)	Sc (ppm)	Y (ppm)	Cumulative REE (ppm)
20150717DB-1	1.38	3.4	0.44	2.68	0.4	9	38.4	635.37
20150717DB-2	0.85	2.03	0.28	1.55	0.23	7	23.1	576.61

tained up to 124 ppm La, 473 ppm Ce, 74 ppm Y, 1,576 ppm Ba, 2,686 ppm F, 89 ppm Nb, 1,806 ppm Sr, 148 ppm Ta, 42 ppm Th, and 15 ppm U (Gersic and others, 1990; Welch, 1974). Stream sediment samples in the area also contained elevated rare earths (Warren, 1980). The area was originally mined for tin, and an interest was also taken in lithium, tantalum, and gold (Hess and Bryan, 1938). Between 1903 and 1927, about 47,630 kg (105,039 lbs) of tin were produced from the South Dakota potion of the area (Smith and Page, 1941).

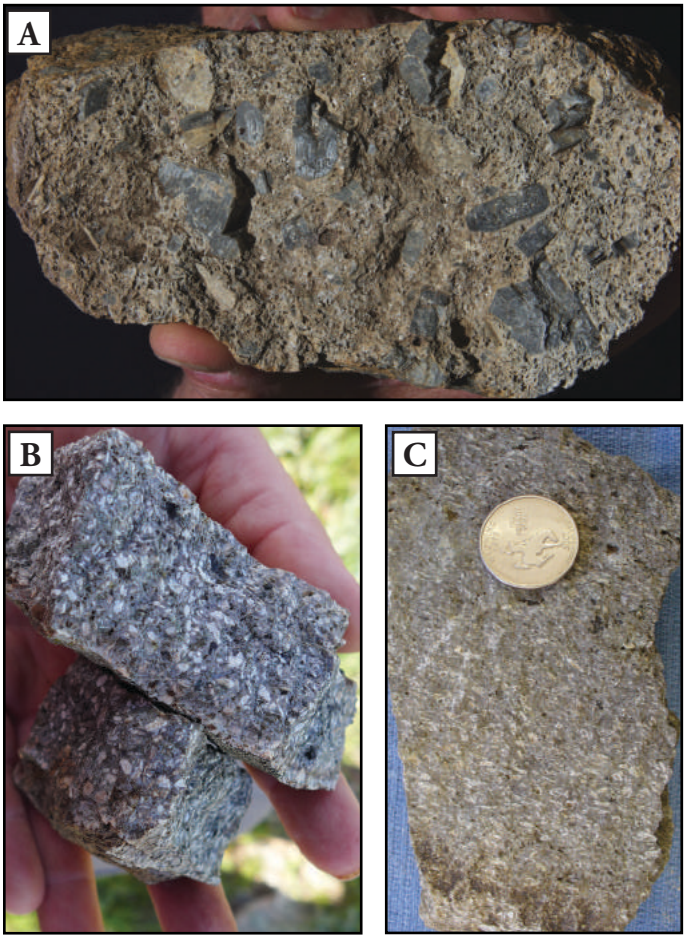


Figure 27. Phonolitic rocks from northeastern Wyoming. A) Phonolite with feldspar megacrysts from the Rare Element Resources, Ltd. Bear Lodge area. B) and C) Gray phonolitic rock with feldspar, hornblende, and small xenoliths at Cement Ridge (Sample 20150623LC-1).

Since REE are commonly associated with carbonatites and alkali igneous rocks (King and Harris, 2002), and the presence of the economic-grade Bear Lodge REE project is less than 32 km (20 mi) to the north-northwest, these intrusive units are worth evaluating. The WSGS sampled Cement Ridge and Mineral Hill as well as the Black Buttes area to the south-southwest. Along Cement Ridge (figs. 27 B, C), gray to tan trachyte or phonolite with feldspar and hornblende phenocrysts crops out with some limonitic stain and dark xenoliths. However, no elevated rare earths were present here. Two samples taken on Mineral Hill yielded elevated REE but did not exceed five times the crustal abundance (table 27). Sample 20150717DB-1 came from a very fractured, low-lying, hydrothermally altered, occasionally porphyritic phonolite containing abundant millimeter-sized vugs filled with iron oxides and silica. Sample 20150717DB-2, composed of a yellow-tan phonolite breccia, contained vugs filled with iron oxides, silica, pale-yellow crystals, and a fine-grained soft material.

In the Black Buttes area (fig. 26), more outcrops of gray, pink-weathering trachyte-phonolite with feldspar, and hornblende phenocrysts and megacrysts are found. Many of these outcrops exhibit fracturing, layering, and shearing, which indicates a possibility of intrusive dikes in the area. Cerium, strontium, and tellurium were slightly elevated in the samples (20140624LC-1, 2, 3), but most often, REE were not elevated.

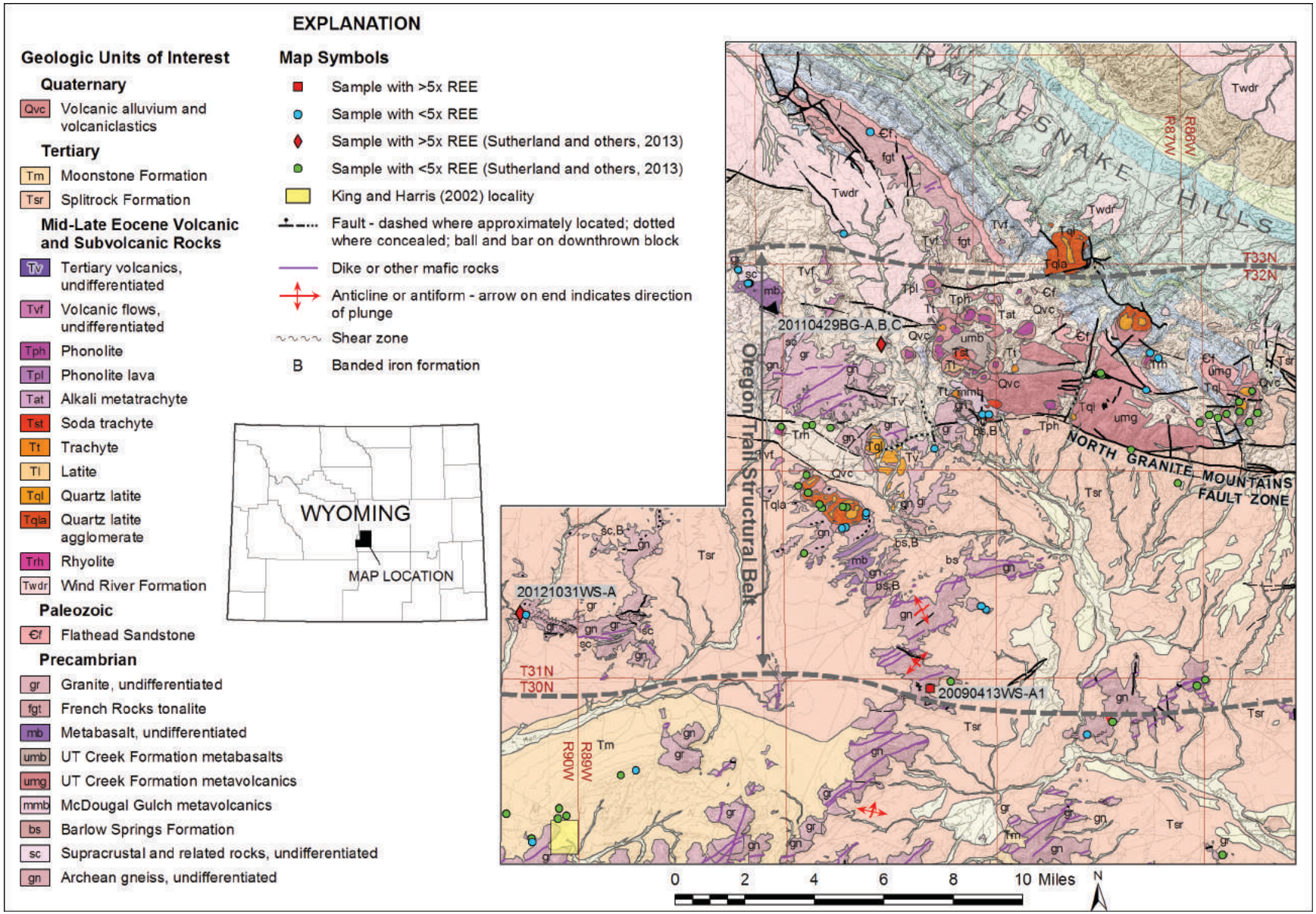


Figure 28. Sample locations and geology of the Rattlesnake Hills area. Samples from RI-65 (Sutherland and others, 2013), the current study, and King and Harris (2002) locales are shown. Sampling was focused in Tertiary volcanics and Precambrian igneous and metamorphic rock where elevated REEs are expected; these units are bold. The Oregon Trail structural belt and map are modified from Grace and others (2006) and Sutherland and Hausel (2003), respectively.

Rattlesnake Hills

Tertiary carbonatite dikes and veins are also a component of Middle-Late Eocene Rattlesnake Hills volcanic and subvolcanic rocks in central Wyoming (Autenrieth, 2012; Sutherland and Worman, 2013). The Rattlesnake Hills alkalic igneous rocks, which are in many ways comparable to those in the Bear Lodge Mountains (Hoch and Frost, 1993), straddle the east-trending North Granite Mountains Fault zone and the southern part of the northwest-trending Rattlesnake Hills anticline (fig. 28). Overall descriptions and mapping of these rocks were undertaken by Carey (1959) and Pekarek (1977). Pekarek and others (1974) dated feldspars from quartz latite and phonolite in the eastern Rattlesnake Hills at about 44 Ma; similar dates were obtained by Autenrieth (2012) in the central part of the volcanic/intrusive complex. The duration of volcanism is variably interpreted to have taken place over the course of about 10 million years (Rachou, 1951), about 5 to 8 million years (Van Houten, 1955; Carey, 1959), or possibly less than 2 million years, subject to additional dating of intrusives (Autenrieth, 2012).

Rattlesnake Hills carbonatites, T. 31 N., R. 88 W.; T. 32 N., R. 86–89 W.; and T. 33 N., R. 87 W., Natrona County

The petrography and petrochemistry of the Rattlesnake Hills volcanics were investigated in detail by Stupak (1984), who identified calcite of possible magmatic origin in some phonolites and alkali trachytes. Hoch and Frost (1993) focused on petrographic and geochemical characteristics of the sodium-rich trachytes and phonolites. They stated that carbonatites had, to that date, not been observed but acknowledged the possibility of their occurrence. Autenrieth (2012) mapped and described late-stage carbonatites, which are spatially associated with silica undersaturated igneous rocks, in the form of dikes and veins with well-developed flow structures that had intruded into brecciated wall rock. Sutherland and Worman (2013) mapped several small outcrops of fine-grained white carbonatite in the western part of the Rattlesnake Hills (fig. 29); these occur as large masses and thin dikes that cut both quartz latite and underlying Archean rocks. Anomalous amounts of carbonate are also found within phonolites and latites in both the western and eastern parts of the volcanic field and are accompanied by carbonate dikes that may or may not be igneous in origin but may relate to later hydrothermal activity.

REE analyses of carbonatites, associated alkalic rocks, and potentially related veins in or near the Rattlesnake Hills for this investigation and previous WSGS studies are shown in table 28. Neither WSGS analyses nor those published by Stupak (1984), Hoch and Frost (1993), or Autenrieth (2012) showed any REE enrichment within the carbonatites of the Rattlesnake Hills volcanic/intrusive complex or within associated igneous rocks. This remains an oddity as carbonatites often host economic grade REE deposits or are at least enriched in REE. More research must be done to determine why the carbonatites in the Rattlesnake Hills are essentially barren. If the carbonatites once contained REE, it is possible that faulting and hydrothermal activity could have remobilized them.

Split Rock Formation carbonate dikes, SE¼SW¼ and SW¼SE¼ sec. 18, T. 31 N., R. 85 W., Natrona County

East-trending carbonate dikes of unknown origin cut Tertiary sediments southeast of the Rattlesnake Hills about 11 km (7 mi) from the nearest Tertiary igneous outcrop. These have textures that vary from that of fine-grained limestone to tufa and are suspected to have derived from hydrothermal activity, possibly related to the Rattlesnake Hills volcanics. Other similar subparallel dikes crop out in this area, which is also cut by fractures or faults parallel to the dikes. Samples 20120824WS-A, B, and C are

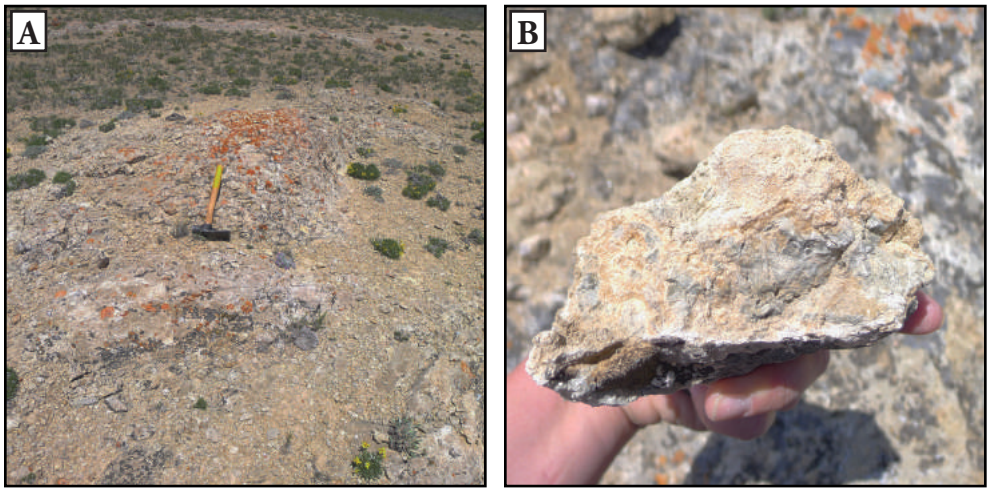


Figure 29. Carbonatitic rocks in the Rattlesnake Hills area. A) Low-lying outcrop of carbonatite with carbonatite veins and Precambrian breccia float nearby and within. B) Close-up of a carbonatite hand sample (Sample 20150608LC-5).

Table 28. Concentration of REE from carbonatite and potentially related rocks in the Rattlesnake Hills area. Bold values indicate concentrations greater than five times the crustal abundance. Results continue across the following page.

Rattlesnake Hills area carbonatites									
Element	La (ppm)	Ce (ppm)	Pr (ppm)	Nd (ppm)	Sm (ppm)	Eu (ppm)	Gd (ppm)	Tb (ppm)	Dy (ppm)
KA146974 (1)*	11.70	12.27	-	10.91	-	-	-	-	-
KA146974 (2)*	-	-	-	-	-	-	-	-	-
KA146933*	-	-	-	-	-	-	-	-	-
KA146983*	-	-	-	-	-	-	-	-	-
KA146937*	-	-	-	-	-	-	-	-	-
20121101WS-F	10.3	18.3	2.1	7.8	1.4	0.47	1.34	0.18	1.06
20150608LC-3	28.8	43.3	4.74	14.7	2.46	0.31	2.03	0.28	1.6
20150608LC-5	4.9	3.8	0.97	4	0.96	0.26	1.23	0.2	1.34
20150608LC-6	14.5	18.3	2.12	7.4	1.11	0.47	1.08	0.15	0.83
20120613WS-F	27.6	58.1	6.4	24.7	5.43	1.47	4.56	0.71	4.18
20120614WS-B	27	48.8	6.13	23.1	4.79	1.34	4.02	0.58	3.4
20110817WS-C	38.1	73.8	8.3	18	6.14	1.81	5.04	0.7	4.13
20120614WS-A	32.6	61.3	7.66	29.3	6.15	1.71	5.2	0.78	4.44
20110817WS-A	37	66.5	8.07	31.9	6.57	1.96	5.61	0.82	4.52
20110817WS-B	38.8	67.4	8.39	33.3	6.69	1.97	5.58	0.79	4.53
20110817WS-E	35.6	68.4	7.92	31.4	6.47	1.91	5.41	0.81	4.48
20110818WS-B	41.3	74.2	8.68	34.9	6.8	1.99	5.64	0.78	4.25
20120919WS-A	53.7	99.2	10.8	38	7.31	2.18	5.74	0.83	4.49
20120919WS-B	57.3	105	11.6	40.4	7.82	2.3	6.05	0.87	4.66
20120919WS-C	49.4	90.7	10.2	36.9	7.39	2.2	5.99	0.86	4.7
20121031WS-B	28.9	51.8	5.98	21.6	3.96	1.27	3.58	0.49	2.73
20121031WS-H	40.5	73	8.6	31.8	5.59	1.89	4.98	0.69	3.95
20120824WS-A	15.2	24.5	3.04	10.8	1.87	0.49	1.62	0.24	1.45
20120824WS-B	10.3	11.6	1.89	6.7	1.17	0.33	1.17	0.19	1.38
20120824WS-C	12.1	16.3	2.29	8.1	1.39	0.34	1.24	0.2	1.19
20120918WS-D	4.8	10.5	1.06	3.7	0.74	0.14	0.66	0.1	0.69
20120918WS-G	3.9	21	1.2	5.1	1.45	0.24	1.9	0.4	3.24

*From Autenrieth (2012)

from these carbonate dikes cutting the Miocene Split Rock Formation. None of these samples showed any enrichment in REE.

Moonstone Formation reefs, SW¼SE¼ sec. 24 and NE¼NW¼ sec. 25, T. 30 N., R. 90 W., Fremont County

In this area, sandy, calcareous, partly silicified tuffaceous knobs project above the relatively flat-lying Pliocene Moonstone Formation. Love (1961; 1970) suggested that these knobs were possible algal reefs. However, they contain no fossil material and appear to be hot-springs type tufa deposits, possibly related to the Rattlesnake Hills volcanics. Several small, historical prospect pits are dug into the mounds that exhibit radioactivity notably higher than the local background; this radioactivity appears to be concentrated along silicified fractures. Brecciation along fractures is evident in two of the largest knobs. Sample 20120918WS-D, collected in section 25, contains >1,000 ppm Thorium. Sample 20120918WS-G, collected in section 24, contains 213 ppm thorium. No anomalous REE were detected in any of these samples (Sutherland and others, 2013).

Element	Ho (ppm)	Er (ppm)	Tm (ppm)	Yb (ppm)	Lu (ppm)	Sc (ppm)	Y (ppm)	Cumulative REE (ppm)	Rock Type
KA146974 (1)*	-	-	-	-	-	0.00	14.54	49.42	Carbonatite
KA146974 (2)*	-	-	-	-	-	6.7	41.4	48.1	Carbonatite
KA146933*	-	-	-	-	-	8.3	18	26.3	Carbonatite
KA146983*	-	-	-	-	-	0.7	10.8	11.5	Carbonatite
KA146937*	-	-	-	-	-	4.4	24.9	29.3	Carbonatite
20121101WS-F	0.22	0.61	0.1	0.63	0.1	1	7.9	53.51	Carbonatite
20150608LC-3	0.31	0.8	0.13	0.58	0.1	1	8.5	109.64	Carbonatite
20150608LC-5	0.3	1.01	0.15	0.93	0.14	<1	13.5	33.69	Carbonatite
20150608LC-6	0.18	0.56	0.09	0.52	0.09	1	5.7	54.1	Carbonatite
20120613WS-F	0.85	2.58	0.39	2.48	0.39	-	27	166.84	Quartz Latite
20120614WS-B	0.68	1.96	0.31	2.06	0.32	-	19.6	144.09	Quartz Latite
20110817WS-C	0.8	2.31	0.37	2.48	0.4	2.5	25.6	190.48	Quartz Latite
20120614WS-A	0.9	2.55	0.4	2.62	0.4	-	24.4	180.41	Quartz Latite
20110817WS-A	0.96	2.69	0.41	2.85	0.45	-	27.2	197.51	Quartz Latite
20110817WS-B	0.93	2.67	0.4	2.67	0.44	-	26.8	201.36	Rhyolite
20110817WS-E	0.92	2.58	0.39	2.6	0.42	-	26.5	195.81	Quartz Latite
20110818WS-B	0.83	2.34	0.34	2.25	0.37	-	23.7	208.37	Quartz Latite
20120919WS-A	0.91	2.46	0.39	2.53	0.43	3	25.4	257.37	Quartz Latite
20120919WS-B	0.96	2.58	0.42	2.7	0.45	3	26.4	272.51	Rhyolite
20120919WS-C	0.96	2.61	0.42	2.64	0.44	5	25.6	246.01	Rhyolite
20121031WS-B	0.55	1.54	0.24	1.7	0.28	2	17	143.62	Carbonate Dike
20121031WS-H	0.79	2.22	0.34	2.29	0.37	3	23	203.01	Carbonate Dike
20120824WS-A	0.33	1.06	0.19	1.35	0.24	2	10.8	75.18	Carbonate Dike
20120824WS-B	0.35	1.19	0.2	1.43	0.24	1	13.7	52.84	Carbonate Dike
20120824WS-C	0.26	0.81	0.14	0.91	0.16	1	9.2	55.63	Carbonate Dike
20120918WS-D	0.25	1.41	0.38	3.42	0.95	1	9.6	39.4	Carbonate Dike
20120918WS-G	1.08	3.95	0.68	4.17	0.82	<1	43.8	92.93	Carbonate Dike

Leucite Hills

The Leucite Hills in the Green River Basin make up one of the largest lamproite fields in the world (Hausel, 2006). The 0.9 to 3.0 Ma (Lange and others, 2000) lamproites are ultrapotassic, mafic to ultramafic volcanic and subvolcanic rocks that can be extremely enriched in LREE (Kuehner, 1980; Ogden, 1979). Notable REE occurrences in the Leucite Hills are located on Zirkel Mesa, Pilot Butte, and South Table Mountain (table 29; Sutherland and others, 2013). Detailed descriptions of the geology and geochemistry of the Leucite Hills are available in WSGS RI-56 (Hausel, 2006).

Zirkel Mesa, NE¼NW¼ sec. 24, T. 22 N., R. 102 W., Sweetwater County

Zirkel Mesa is the largest exposure of lamproite in the Leucite Hills and is dominantly composed of orendite, a diopside-sanidine-phlogopite lamproite (Hausel, 2006). Wyomingite (diopside-leucite-phlogopite lamproite) from Zirkel Mesa (Sample ZM1-WY) is enriched in LREE, europium, gadolinium, terbium, and dysprosium; lanthanum and cerium are enriched greater than five times the crustal abundance (table 29; Sutherland and others, 2013).

Table 29. Concentration of REE from the Leucite Hills area. Bold values indicate concentrations greater than five times the crustal abundance.

	Leucite Hills								
Element	La (ppm)	Ce (ppm)	Pr (ppm)	Nd (ppm)	Sm (ppm)	Eu (ppm)	Gd (ppm)	Tb (ppm)	Dy (ppm)
EH-44*	149	283	-	120	-	3.4	-	<1	-
EH-46*	128	245	-	100	-	2.8	-	<1	-
EH-47*	**177**	**320**	-	120	-	3.5	-	<1	-
ZM1-WY	**185.5**	**375**	41.2	150.5	19.75	4.35	13.85	1.49	4.6
PB1-95	**355**	**700**	**75.4**	267	**33.4**	7.02	23.7	2.23	6.18
STM-1-2010	151	**308**	34	121.5	15.9	3.48	11.45	1.22	3.87

Element	Ho (ppm)	Er (ppm)	Tm (ppm)	Yb (ppm)	Lu (ppm)	Sc (ppm)	Y (ppm)	Cumulative REE (ppm)
EH-44*	-	-	-	1	<0.2	-	27	583.4
EH-46*	-	-	-	1	<0.2	-	27	503.8
EH-47*	-	-	-	1	<0.2	-	25	646.5
ZM1-WY	0.66	2.05	0.17	1.08	0.15	-	18.1	818.5
PB1-95	0.86	2.77	0.21	1.32	0.19	-	22.5	**1,497.8**
STM-1-2010	0.55	1.67	0.14	0.87	0.13	-	14.8	668.6

*From Hausel (2006)

Pilot Butte, SE¼NE¼ sec. 10, T. 19 N., R. 106 W., Sweetwater County

The Pilot Butte lamproite consists of a volcanic neck, a single lobate lava flow, and two associated small dikes exposed on the southwest flank of the butte. The volcanic and subvolcanic rocks on Pilot Butte are dominantly madupite (diopside-phlogopite-leucite lamproite) with Green River Formation xenoliths (Hausel, 2006). The Pilot Butte madupite is enriched in LREE, europium, gadolinium, terbium, and dysprosium; La, Ce, Pr, Nd, and Sm are all enriched greater than five times the average abundance (Sutherland and others, 2013).

South Table Mountain, SE¼SW¼ sec. 6, T. 22 N., R. 102 W., Sweetwater County

South Table Mountain is composed of olivine orendite and wyomingite. The olivine orendite is enriched in LREE, europium, gadolinium, and terbium; only cerium is enriched to greater than five times the average (Sutherland and others, 2013).

Other Tertiary-aged Igneous Occurrences

Battle Mountain, SE¼SE¼SW¼ sec. 4, T. 12 N., R. 88 W., Carbon County

Basaltic magmatism in the vicinity of Battle Mountain occurs at the southwestern edge of the Sierra Madre. These Late Miocene flows, pyroclastics, dikes, and plugs at Battle Mountain are dominated by basalt and represent the northwestern end of the Elkhead Mountains volcanic field. These volcanics both intrude and overlie the Browns Park Formation in the Battle Mountain area (Scott and others, 2011). A sample (BattleMtn-1-2010) collected in this area contained only slightly elevated REE.

Cedar Mountain breccia pipes, NW¼SE¼SE¼ sec. 36, T. 13 N., R. 113 W., Uinta County

Eocene breccia pipes, in the Cedar Mountain area near Lone Tree in southwestern Wyoming, host diamonds (Hausel, 1998). These rocks are related to kimberlites, which on average are elevated in LREE content (Hausel and others, 2003). A sample (CM-95) from one of the pipes showed only slightly elevated REE concentrations.

SEDIMENTARY OCCURRENCES

Important REE occurrences in Wyoming are hosted in a number of sedimentary environments. These include modern placers, fossil beach placers (or paleoplacers) within marginal marine sandstones, uranium- and phosphate-rich horizons in Eocene lacustrine deposits in southwestern Wyoming, and phosphorite beds in western Wyoming (King and Harris, 2002). Minor REE occurrences are also present within phosphate concretions in the Bighorn Basin and in alteration zones associated with reduction-oxidation fronts in central Wyoming (Sutherland and others, 2013).

Paleoplacers may host REE-bearing minerals, such as monazite, zircon, and apatite. The Cambrian Flathead Sandstone and the Cretaceous Mesaverde Formation are the most notable REE-bearing paleoplacers in Wyoming; minor paleoplacers are also found in numerous other formations (fig. 30). Quaternary alluvial deposits can often host placers downstream from older REE mineral concentrations (Sutherland and others, 2013). It should be noted however, that not all paleoplacers and black sandstones are enriched in REE. REE content is based on the mineralogical composition of erosional sources; samples from Bacon Ridge, Separation Rim, the Stump Formation, and Oakie Trail (Sutherland and others, 2013) are all examples of paleoplacer locales with no REE enrichment.

In addition to paleoplacers, sandstones can potentially host REE and other minerals in reduction-oxidation fronts associated with the interaction between oxidized groundwater and reducing geologic environments. Such deposits are known sources of uranium (e.g. Smith Ranch mine, Wyoming), silver, and copper (e.g. Paoli deposit in Oklahoma; Thomas and others, 1991). These geological environments potentially host other metals as well (Sutherland and others, 2013). Uranium-related REE occurrences will be discussed in a later section.

REE occurrences are hosted by phosphorite beds, phosphatic shale, and mudstone in western and southwestern Wyoming, most notably in the Phosphoria Formation and the Wilkins Peak Member of the Green River Formation. As mentioned earlier, phosphate concretions within black shale in northern Wyoming can also contain REE. There appears to be a positive relationship between phosphatic rocks and REE most likely due to the presence of apatite and other rare earth-bearing phosphate minerals. For example, phosphatic beds in the Meade Peak Member of the Phosphoria Formation are composed almost entirely of peloidal fluoroapatite and bioclastic fragments (Sheldon, 1963). Although no economic, phosphate-related REE deposits have been identified in Wyoming, mining for REE-rich phosphorite has occurred in southeast Idaho near Lincoln County, Wyoming. These were minor mines that focused more on phosphate extraction rather than REE and are either no longer operating or were operating with no REO production as of 1993 (Jackson and Christiansen, 1993). Each deposit reportedly amounted to less than 100,000 tonnes (110,200 tons) of contained

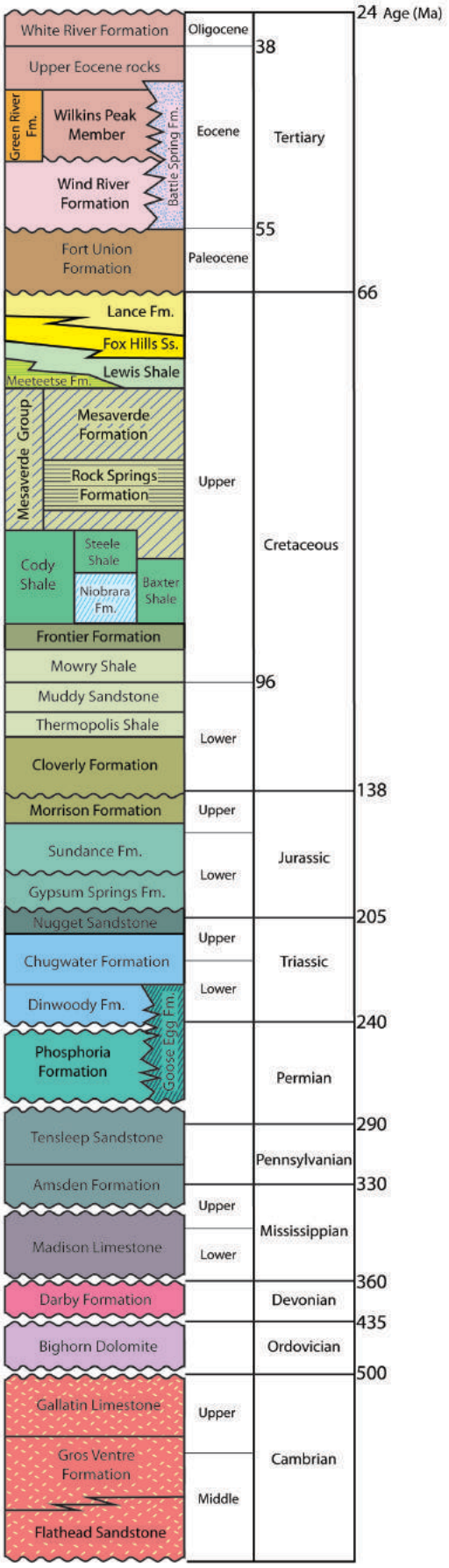


Figure 30. Generalized stratigraphic column of Wyoming. Rock units were compiled from Love and others (1993). Only units with widespread occurrence in the state are shown. Units where REE have been found are bold.

REO in total resources (Jackson and Christiansen, 1993). Phosphate production has occurred in Wyoming in the vicinity of Cokeville, York Canyon, South Mountain, and Leefe Mines (Jasinski and others, 2004; Carnes, 2015), but no evaluation was done for REE potential.

The following REE-bearing sedimentary occurrences are listed in stratigraphic order by formation from youngest to oldest.

Quaternary Placers

Quaternary alluvial deposits form downstream from either igneous sources of heavy minerals or below paleoplacers that have been reworked in modern streams. Although REE-bearing heavy minerals can be concentrated from these placers, the overall grade of the unconcentrated in-place material must be considered for any evaluation of potential economic recovery.

Bald Mountain Quaternary placers, S½ sec. 14 and sec. 20, T. 56 N., R. 91 W., Big Horn and Sheridan Counties

Quaternary alluvial placers, in drainages flowing away from Flathead Sandstone paleoplacers in the Bald Mountain area, reportedly host higher gold values than those found in the Flathead Sandstone due to further concentration of the paleoplacers (Hausel, 1989). They are also reported to host monazite (Wilson, 1951; King and Harris, 2002), but no historical estimates are known for the monazite concentrations in these modern placers.

Two placer samples were collected from Quaternary alluvium to test for the presence of REE. Sample 20120801WS-B came from Half Ounce Creek, northeast of Rooster Hill, and Sample 20120801WS-C was taken from upper Porcupine Creek, northwest of Rooster Hill (fig. 22). Although the concentrates showed cumulative REE of 5,489 ppm and 6,433 ppm, respectively, the unconcentrated cumulative REE values were about 46 ppm for Sample 20120801WS-B and 8 ppm for Sample 20120801WS-C (Sutherland and others, 2013).

Warm Spring Creek placers, secs. 28–34, T. 42 N., R. 108 W., and secs. 21–23, 25, 26, and 36, T. 42 N., R. 109 W., Fremont County

Placer deposits along Warm Spring Creek (fig. 22), also known as the Clarks Camp-Union Pass gold placers, include monazite-bearing gravels. These gravels are reported to extend 4.8 km (3 mi) up the South Fork and were at one point covered in claims (Wilson, 1960; Bolmer and Biggs, 1965; Osterwald and others, 1966; Rohrer, 1968; Hausel, 1989). These monazite-bearing gravel deposits range from 0.4 to 1 km (0.25 to 0.6 mi) wide, extend for about 4.8 km (3 mi) in length, and include high terraces more than 30 m (100 ft) above the stream bottom (Hausel, 1989).

The area was mapped by Rohrer (1968), at which time he sampled and mapped quartzite conglomerate layers in the Wind River Formation containing flour gold within a matrix of fine- to coarse-grained angular quartzite and tuffaceous sandstone. These conglomerate layers, dominated by percussion-marked pebbles to rounded, cobble-sized, quartzite stones, represent four eastward-trending channels about 1.6 to 3.2 km (1 to 2 mi) wide. He cited gold values of less than 0.009 to 1.777 g/cy (0.0003 to 0.06268 oz/cy as interpreted from the 1966 gold value of $35/oz) from the conglomerates as sampled by J.C. Antweiler but made no mention of monazite or other REE-bearing minerals within them. Rohrer (1968) stated that these auriferous deposits are derived from similar deposits in the Pinyon Conglomerate, occurring about 13 km (8 mi) to the West, which Love (1973) believed to have originated in the hypothetical, now vanished, Laramide (Late Cretaceous to Paleocene) Targhee uplift west of Jackson Hole (Sutherland and others, 2013).

Modern stream placers at four locations along Warm Spring Creek and the South Fork of Warm Spring Creek were sampled by the WSGS in 2010 and 2011. Monazite and xenotime grains identified in the pan samples were generally angular to subrounded, suggesting a relatively local source. Precambrian igneous rocks south of the Quaternary placers are the probable source of the monazite and xenotime.

Although analyses of placer concentrates showed high cumulative REE values, the calculated values for unconcentrated bank cubic yards (BCY) of placer material were all less than crustal abundances. Sample WSC-91510-*A* (NW¼NE¼ and NE¼NW¼ sec. 33, T. 42 N., R. 108 W.) showed a calculated total of REE at 37.28 g/BCY (1.32 oz/BCY), or about 27 ppm, with gold content calculated at 25.3 mg/BCY (0.0009 oz/BCY). Sample WSC-91510-B (NW¼SW¼ sec. 22, T. 42 N., R. 109 W.) showed a calculated total of REE at 3.84 g/BCY (0.136 oz/BCY), or about 3 ppm, with gold content calculated at 1.9 mg/BCY (0.00007 oz/BCY). Sample WSC-91510-C, from the South Fork of Warm Spring Creek (NW¼SW¼ sec. 31, T. 42 N., R. 108 W.) showed a calculated total of REE at 51.92 g/BCY (1.83 oz/BCY), or about 37 ppm, with gold content calculated at 2.9 mg/BCY (0.0001 oz/BCY).

Sample 20110921WS-B, near the upper end of the South Fork Warm Spring Creek (NE¼SW¼ sec. 30, T. 41 N., R. 108 W.) showed a calculated total of REE at 32.5 g/BCY (1.146 oz/BCY), or about 23 ppm, with no gold

(Sutherland and others, 2013). The presence of REE in this placer sample suggests a possible source in the Precambrian rocks to the south and east.

White River Formation

The Oligocene White River Formation consists of as much as 183 m (600 ft) of white to grayish-orange and brown, sandy tuffaceous siltstone, sandstone, and conglomerate, with local beds of altered volcanic ash (Love, 1970). The White River unconformably, and in some places angularly, overlies older rock units.

Hurda claims, sec. 7, T. 27 N., R. 77 W.; secs. 12 and 13, T. 27 N., R. 78 W., Carbon County

A carbonaceous shale in the White River Formation exhibits 10 times the background radioactivity. Uranium minerals are not found at the surface, and ore grade rock is not encountered in drill holes (Whalen, 1954a). Silty, arkosic sandstone from an outcrop of Wind River Formation in section 7 contained 300 ppm La, 100 ppm Y, 50 ppm Zr, and 52 ppm cU_3O_8 (Griffin and Milton, 1982). Harshman (1968) also calls this area White River Formation. The origin of REE enrichment is unknown but is hypothesized by King and Harris (2002) as related to paleoplacer deposits found in the Shirley Basin area. Although this occurrence is in the White River Formation, rather than in the underlying Wind River Formation, it is closely associated with Wind River-hosted, classic roll-front uranium deposits in the Shirley Basin uranium mining district (Gregory and others, 2010; Bailey and Gregory, 2011). Consequently, rather than a paleoplacer, this could be a residual deposit left behind due to changes in site specific redox conditions where REE were deposited, and uranium moved on further in solution to form a roll-front deposit.

Green River Formation: Wilkins Peak Member

The Green River Formation in southwestern Wyoming, as described by Bradley (1964), is an accumulation of lenses of lacustrine sediments that intertongue and interfinger with shallow basin-filling fluviatile sediments of the Bridger and Wasatch Formations. The lake sediments deposited in Lake Gosiute include sandstone, claystone, shale, dolomitic marlstone, oil shale, numerous thin beds of volcanic tuff, and thick layers of evaporites dominated by trona and halite. The majority of these were deposited in a closed basin with no outlet (Dyni, 1997).

The Green River Formation is subdivided into several subunits (fig. 31); the main subunits, from top to bottom, are the Laney Shale Member, Wilkins Peak Member, and Tipton Shale Member or Tipton Tongue. The Wilkins Peak Member is as much as 412 m (1,350 ft) thick (Dyni, 1997) and hosts the world's largest known deposits of trona in multiple mineable beds near Green River. The Wilkins Peak is characterized by its abundance of saline minerals and a general lack of vegetation on its brilliant white outcrops (Zeller and Stephens, 1969; Sutherland and Luhr, 2011).

Thirty-two uraniferous phosphatic zones (UPZs) were identified by Love (1954) within the Wilkins Peak Member in the Green River Basin. He also described in detail the lower 32.6 m (107 ft) of the Wilkins Peak in a measured section on Lulu claim #2. It included 13 lithologically distinct horizons, one unit within the underlying Tipton Shale Member, and four UPZs in the NE¼SW¼ sec. 10, T. 17 N., R. 106 W. (table 30). The UPZs in the lower part of the Wilkins Peak tend to be more enriched in uranium and phosphate (up to 0.15 percent uranium and 18.2 percent P_2O_5) than those higher in the member (Love, 1964). Scarce, dark-green to black, REE-bearing carbonate minerals within the Wilkins Peak Member include burbankite, mckelveyite, and ewaldite (Milton and others, 1965; Milton, 1971). Love (1964) noted the presence of REE-bearing minerals in his UPZs 1, 2, and 2a (numbered from the bottom) as well as in trona beds. The lower UPZs commonly host greater than 0.1 percent REE, but the enrichment is not homogenous and significant lateral variation is observed (King and Harris, 2002).

UPZs are not lithologically distinct from the surrounding rocks and are best identified through the use of radiation detecting equipment (Sutherland and others, 2013). When a Geiger counter was not available, field identification at those sites was based entirely on descriptions of field relations provided by Love (1964).

I-80 On-ramp area, Exit 91, east of Green River, NW¼SE¼ sec. 23, T. 18 N., R. 107 W., Sweetwater County

Mudstone and limestone of the Wilkins Peak Member crop out at this location between the on-ramp and eastbound driving lane of I-80. The units exposed here match the descriptions of horizons 6 through 10 on Lulu claim #2 (Love, 1964), which include UPZ 2 and UPZ 2a. UPZ 2 is hosted within a green, blocky, calcareous mudstone (Sample 20120928JC-A) about 1 m (3.3 ft) below the base of the overlying tan to gray, thin-bedded to laminated marlstone. UPZ 2a is hosted within a green, blocky, calcareous siltstone and shale (Sample 20120928JC-B) about 1 m (3.3 ft) below the overlying tan, slabby, dolomitic marlstone. Neither of these samples are significantly enriched in REE or other elements of economic interest (Sutherland and others, 2013).

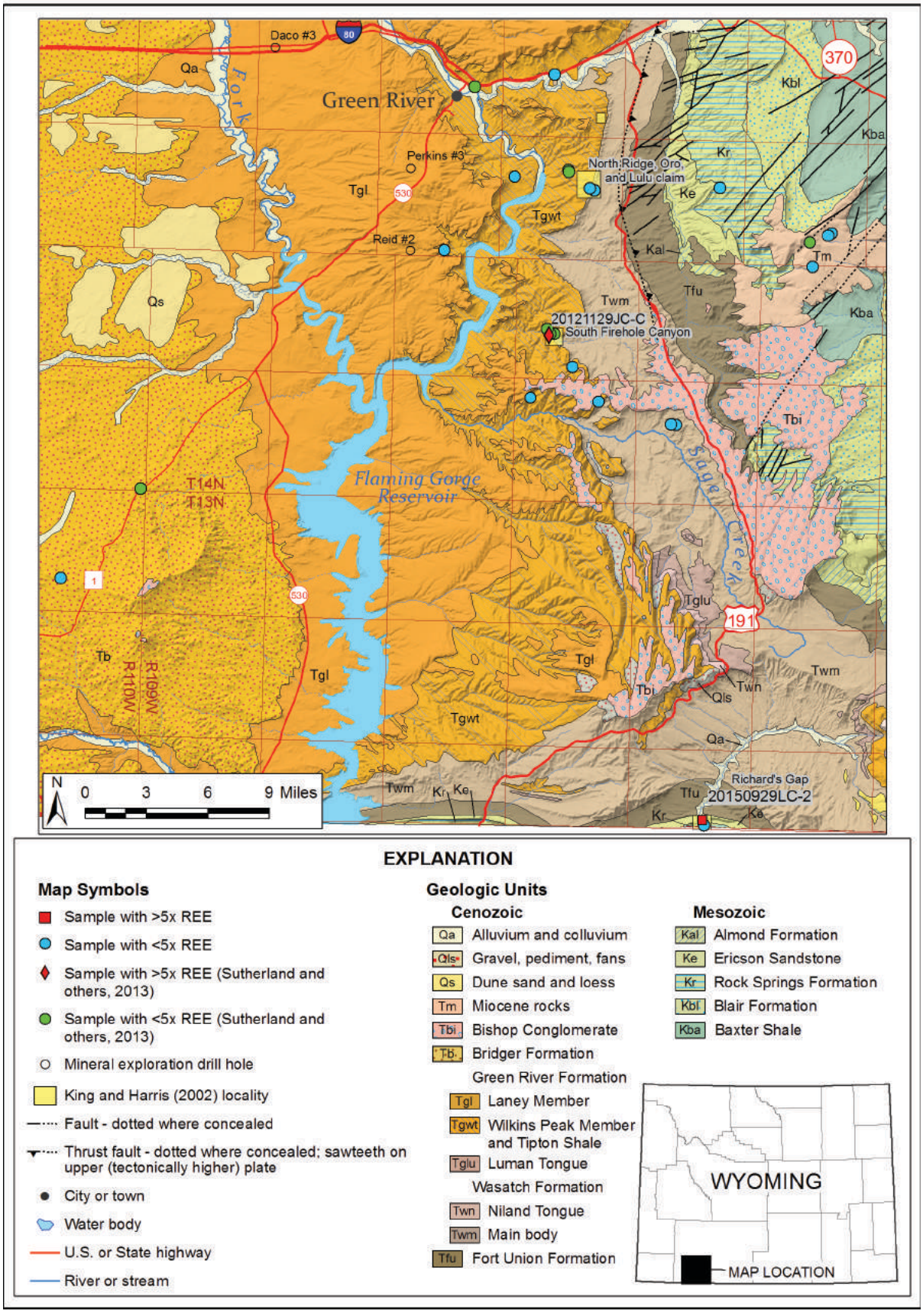


Figure 31. Sample locations and geology of southeast Green River Basin. Sampling focused on the Wilkins Peak Member of the Green River Formation. Map modified from Love and Christiansen (1985).

Table 30. Measured section of the lower part of the Wilkins Peak Member of the Green River Formation by Love (1964) at the Lulu claim #2, southwest of Rock Springs.

Bed	Description	Thickness (m)	Thickness (ft)
14	Oil shale, dark-brown, laminated, hard; weathers white; **UPZ 3**	0.15	0.5
13	Shale, gray, soft, fissile	3.35	11.0
12	Gray, very hard, massive, medium-grained sandstone; weathers rusty-brown; outcrops as ledge that breaks into angular blocks that are conspicuous down slope; regionally identifiable, known as the Firehole bed.	0.12	0.4
11	Shale, claystone, and siltstone, gray to greenish-gray, chippy; moderately hard but forms slope	4.88	16.0
10	Dolomitic marlstone, tan, slabby, hard, fissile; forms ledge	0.61	2.0
9	Claystone and siltstone, green, blocky, slightly radioactive near top; **UPZ 2a** occurs about 1 m below the top but is not lithologically distinct	2.74	9.0
8	Dolomitic marlstone, tan, hard, slabby, fissile; weathers gray; forms ledge	1.52	5.0
7	Claystone and siltstone, green, blocky; forms slope; **UPZ 2** occurs about 1 m below top but is not litholigically distinct	3.35	11.0
6	Shale and marlstone, greenish-gray, hard, fissile; forms slope	1.52	5.0
5	Dolomitic marlstone, gray, hard, thin-bedded, fissile; weathers tan; interbedded with gray, soft, fissile calcareous shale; forms slope broken by thin ledges	9.14	30.0
4	Dolomitic marlstone, bluish-gray; weathers rusty-brown at top; top 1.5 m forms widespread hard brown ledge that comprises most radioactive part of **UPZ 1**	2.44	8.0
3	Shale, gray, marly, soft, fissile	0.91	3.0
2	Marly sandy siltstone, gray, hard, slabby, fissile; weathers brown, forms weak ledge; base of Wilkins Peak Member	1.83	6.0
1	Oil shale, dark-brown, fissile, thin bedded; weathers gray; top of Tipton Shale	4.3+	14+

From Love (1964)

Lulu claims, NE¼SW¼ sec. 10, T. 17 N., R. 106 W., Sweetwater County

In this area, the uppermost Tipton Shale Member and lower Wilkins Peak Member of the Green River Formation are exposed. The Tipton Shale is composed of brown to gray, well-indurated oil shale. The lower 3 m (10 ft) of the Wilkins Peak Member consists of marly, sandy siltstone and marly shale (horizons 2 and 3 of Love, 1964). UPZ 1 is hosted in the upper 2 m (6.6 ft) of horizon 4, which includes a lower gray to red, irregularly bedded, blocky, slope-forming, dolomitic marlstone with a white powdery mineral coating fractures (Sample 20120928JC-E) and an upper gray to brown, interlayered, sandy siltstone and marlstone (Sample 20120928JC-C). A blocky, green mudstone to siltstone (Sample 20120928JC-D) that may contain UPZ 2 or 2a crops out about 15 m (50 ft) above horizon 4; this layer is similar to the two rock units of Samples 20120928JC-A and 20120928JC-B. REE enrichment is not present in any of these samples, but all three are enriched in lithium 5 to 6.5 times the crustal abundance (Sutherland and others, 2013).

Localities L-24, L-24B, and L-25 (Ridge and North Ridge), sec. 11, T. 17 N., R. 106 W., Sweetwater County

Here, the uraniferous phosphatic zone 1 varies from 0.3 to 2.1 m (1 to 7 ft) thick and contains 0.001 to 0.15 percent cU and 0.15 to 18.2 percent P_2O_5. Love (1964) concluded that the average rare earth enrichment is greater than 1,000 ppm total REE in zone 1 by spectrographic analyses (King and Harris, 2002).

Locality L-28 (Oro claim no. 1), SW¼NW¼ sec. 14, T. 17 N., R. 106 W., Sweetwater County

UPZ 1 at this location contains 0.024 to 0.12 percent cU and 1.6 to 4.44 percent P_2O_5. It varies from 15 to 91 cm (6 in to 3 ft) thick and contains an average enrichment of greater than 1,000 ppm total REE (Love, 1964). During this study, the WSGS took a sample (20150929LC-9) near this area in a rusty-orange shale. There were no elevated elements of any interest.

South Firehole Canyon, NW¼SE¼, sec. 20, T. 16 N., R. 106 W., Sweetwater County

At South Firehole Canyon, Love (1964) reported the presence of UPZs 1, 2, 2a, 3, 3a, and possibly 4, with up to 0.016 percent eU, 0.009 percent uranium, and 10.56 percent P_2O_5 in UPZ 2a. The Wilkins Peak Member here is similar to the section described by Love (1964) at Lulu claim #2, except that beds 2 through 6 (Love, 1964) are replaced by about 11.9 m (39 ft) of resistant ridge-forming, gray to tan, platy to fissile, dolomitic siltstone, with thin interbeds of non-resistant mudstone and shale. This unit exhibits lateral variations in color, including bright red and rusty areas. Background radioactivity at the site was 560 cpm (Sutherland and others, 2013).

About 3 m (10 ft) above the base of the Wilkins Peak Member is a radioactivity anomaly up to 2.5 times the background (1,400 cpm). The anomaly is within gray to tan, weathered, thin-bedded, about 1 cm (0.4 in), to fissile, limonite-bearing dolomitic siltstone (Sample 20121129JC-A); the stratigraphic position of the anomaly is equivalent to bed 4 (table 31; Love, 1964), which contains UPZ 1. Bedding at the sample site strikes 295° and dips 4° SW (Sutherland and others, 2013).

A radioactivity anomaly up to 2.3 times background (1,300 cpm) occurs within bed 7 (table 30), about 15 m (50 ft) above the base of the Wilkins Peak. Bed 7 consists of green, slope-forming, interbedded mudstone and shale. The radioactivity anomaly is associated with UPZ 2, which is hosted in a layer of green, weakly calcareous shale (table 31; Sample 20121129JC-B) about 51 cm (20 in) below the base of bed 8, which is composed of gray to tan, fissile, dolomitic siltstone.

UPZ 2a, hosted in bed 9 (table 30), is associated with a radioactivity anomaly up to 10.6 times background (5,900 cpm) about 19 m (62 ft) above the base of the Wilkins Peak. Bed 9 consists of green, slope-forming, interbedded mudstone and shale; UPZ 2a occurs within green, blocky, noncalcareous mudstone (table 31; Sample 20121129JC-C) about 51 cm (20 in) below the base of the gray to tan, fissile, calcareous siltstone of bed 10.

The next 64.9 to 70.1 m (213 to 230 ft) above bed 9 consist of interbedded, ridge-forming, gray to tan siltstone and dolostone as well as slope-forming, green shale and mudstone with no anomalous radioactivity. About 88 to 90 m (289 to 295 ft) above the base of the Wilkins Peak Member, higher than the uppermost unit in Love's (1964) measured section (table 30), is a succession of ridge-forming, interbedded, green, calcareous mudstone and limestone, and green to gray, laminated to cross-laminated siltstone overlain by a medium- to coarse-grained, cross-bedded sandstone. UPZ 4 is associated with a radioactivity anomaly up to 5.9 times background (3,300 cpm) and occurs about 1.5 m (5 ft) above the base of this interbedded succession within a green, well-indurated, bulbous, thin-bedded calcareous mudstone (Sample 20121129JC-D).

REE enrichment is only found in UPZ 2a (Sample 20121129JC-C) and is restricted to HREE and yttrium. This is similar to Love's (1964) results, in which he reported high concentrations of yttrium and neodymium. Notably, the enrichment of neodymium in UPZ 2a, reported by Love (1964), is not present in Sample 20121129JC-C. This indicates that relative enrichment between LREE and HREE may vary laterally or vertically across UPZ 2a in the Firehole Canyon area (table 31; Sutherland and others, 2013).

More sampling was done by the authors, south of the coordinates for the area above, in order to further characterize the Firehole Canyon area. In the Wasatch Formation, a reddish-purple, cross-bedded, easily weathered sandstone (20150929LC-3) and a variegated clay with limonitic and rusty bands (20150929LC-4) were sampled. In the Wilkins Peak Member, an area with tan, rippled shale and a greenish claystone with rusty spots (20150929LC-5) was sampled as well as an outcrop of red shale with ripples and concretionary iron (20150929LC-6). Another locale with

Table 31. Concentration of REE from South Firehole Canyon. Bold values indicate concentrations greater than five times the crustal abundance.

	South Firehole Canyon								
Element	La (ppm)	Ce (ppm)	Pr (ppm)	Nd (ppm)	Sm (ppm)	Eu (ppm)	Gd (ppm)	Tb (ppm)	Dy (ppm)
20121129JC-A	41	83.4	10	38.9	7.93	1.6	7.18	1.18	6.87
20121129JC-B	42.5	80.6	9.29	33.1	5.8	1.14	4.73	0.8	5.05
20121129JC-C	55.4	131.5	18.65	87	25.4	6.44	**32.5**	**6.67**	**44.1**
20121129JC-D	24	49	6.01	22.8	4.35	0.91	4.46	0.97	8.28

Element	Ho (ppm)	Er (ppm)	Tm (ppm)	Yb (ppm)	Lu (ppm)	Sc (ppm)	Y (ppm)	Cumulative REE (ppm)
20121129JC-A	1.33	3.63	0.52	2.9	0.42	9	41.3	257.2
20121129JC-B	1.12	3.44	0.54	3.08	0.44	8	36.4	236.0
20121129JC-C	**9.75**	**29.7**	**4.67**	**28.2**	**4.25**	13	**300**	797.2
20121129JC-D	2.39	8.49	1.42	7.71	1.01	7	79.5	228.3

From Sutherland and others (2013)

a slumped section containing a slag-like black material (20150929LC-7A), maroon-purple slate with yellow bands and spots (20150929LC7-B), and tan shale with black spots reminiscent of oil shale (20150929LC-7C) was sampled. None of these contained elevated REE, which strengthens an argument for variability of composition within the Wilkins Peak Member.

Tronox (formerly FMC) Westvaco Mine, sec. 15, T. 19 N., R. 110 W., Sweetwater County

A green mineral, associated with labuntsovite and leucosphenite, was reported within trona bed 17 in three cores of the Green River Formation (Love, 1964). The green mineral is similar to that reported in uraniferous phosphatic zone 1, and the trona bed directly overlies UPZ 5 (Love, 1964). The specific sample site and analytical results are unknown. Milton and others (1965) suggested that the rare earth mineral is mckelveyite, and Donnay and Donnay (1971) identified intergrown mckelveyite and ewaldite from a sample with a green mineral in the mine's waste dump. This may or may not be the same mineral and could have been modified by the mining process (King and Harris, 2002).

Diamond Alkali Co. DACO 3, NW¼NW¼ sec. 17, T. 18 N., R. 108 W., Sweetwater County

At a depth of 417 m (1,369 ft), UPZ 1 contained 0.006 percent cU and 1.25 percent P_2O_5 (Love, 1964). A rare earth-bearing mineral was reported as mckelveyite (Milton and others, 1965) or intergrown mckelveyite and ewaldite (Donnay and Donnay, 1971). Mckelveyite is rare and forms in Wyoming trona beds and in association with the unique alkaline intrusion of the Khibiny massif in Russia. Diamond Alkali Co. DACO 3 is also considered the type locality for mckelveyite-(Y) (fig. 31; Milton and others, 1965; Mineral Data Publishing, 2001-2005).

J.M. Perkins Green River no. 3, SW¼ sec. 8, T. 17 N., R. 107 W., Sweetwater County

A sample taken from UPZ 1 in the Green River Formation at a depth of 544 m (1,784 ft) contained a rare earth mineral, 0.001 percent cU and <0.05 percent P_2O_5 (fig. 31; Love, 1964). As with many of the samples in this area, Milton and others (1965) report the REE-bearing mineral to be mckelveyite, while Donnay and Donnay (1971) report the mineral as intergrown mckelveyite and ewaldite. Fitzpatrick and Pabst (1977) identified the rare earth mineral as burbankite (King and Harris, 2002).

Diamond Alkali Co. Reid no. 2, SE¼SE¼ sec. 32, T. 17 N., R. 107 W., Sweetwater County

At a depth of 433.7 m (1,422.5 ft), UPZ 1 contained 0.005 percent cU, 0.22 percent P_2O_5, and a rare earth mineral. Uraniferous phosphatic zone 2a was sampled at 1,331 feet and contained 0.021 cU and 5.34 percent P_2O_5. Spectrographic analyses indicate an average of >150 ppm Y and Nd were present in zone 2a (Love, 1964). The REE-bearing mineral is thought to be mckelveyite (Milton and others, 1965) or intergrown mckelveyite and ewaldite (Donnay and Donnay, 1971). The WSGS sampled to the east of this location where more outcrop is exposed in canyons (fig. 31). Sample 20150928LC-3 was taken down section in bluish-tan to gray shale with rusty layers and veins of pinkish-translucent, acicular evaporite. The veins, confirmed as gypsum by XRD, run both parallel to bedding and cross-cut bedding. Although REE are associated with trona and other evaporite minerals in the area, no elevated REE were encountered.

Mountain Fuel Supply Company- John Hay Jr. no. 1, SW¼NW¼ sec. 2, T. 18 N., R. 110 W., Sweetwater County

This is an unverified occurrence due to inconsistencies in reporting (King and Harris, 2002). A green mineral, similar to the previous sites, was reported here (Milton and others, 1965). Milton and others (1965) place this location at the Westvaco Mine, and Love (1964) does not mention a green mineral at the Hay no. 1 well. Milton and others (1965) also place their sample near the main trona bed at 475 m (1,557 ft). However, the main trona bed is actually at 484.6 to 487.7 m (1,590 to 1,600 ft) depth with a brown organic trona beginning at 474.6 m (1,557 ft; Fahey, 1962).

Locality L-5 (Old Log Inn), NW¼NW¼NE¼ sec. 12, T. 18 N., R. 106 W., Sweetwater County

UPZ 1 is about 1.2 m (4 ft) thick with 0.081 percent cU and 15.4 percent P_2O_5 at this location. Semi-quantitative spectrographic analyses indicate an average of greater than 1,000 ppm REE (Love, 1964).

Locality L-14 (northeast Wilkins Peak), SE¼NW¼SW¼ sec. 25, T. 18 N., R. 106 W., Sweetwater County

At this location, uraniferous phosphatic zone 1 contains 0.009 to 0.068 percent cU and 0.42 to 6.5 percent P_2O_5. Spectrographic analysis indicated the average rare earth enrichment is greater than 1,000 ppm total REE (Love, 1964).

White Mountain no. 1, NW¼SW¼ sec. 7, T. 18 N., R. 106 W., Sweetwater County

Three horizons within the Wilkins Peak Member of the Green River Formation were uraniferous in this well. A 0.5 m (1.8 ft) thick mudstone at a depth of 253.4 m (831.5 ft) also contained 100 ppm La and 200 ppm Y, along with 60 ppm U and 2.95 percent P_2O_5 (Mott, 1978).

UP corehole 41-23, NE¼NE¼ sec. 23, T. 17 N., R. 109 W., Sweetwater County

Similar to the White Mountain no. 1 well, this well also encountered three uraniferous (>50 ppm U) horizons in the Wilkins Peak Member. One 12.2 cm (4.8 in) sample of mudstone and oil shale at a depth of 572.4 m (1,878 ft) also contained 500 ppm Y, <20 ppm La as well as 195 ppm U, 1.35 percent P_2O_5, and 3.36 percent organic carbon (Mott, 1978). King and Harris (2002) suggest the yttrium content may be a typographical error, 50 not 500 ppm, based on the low amount of lanthanum.

Wind River Formation

The Early Eocene Wind River Formation is dominated by variegated to drab claystone and siltstone with interbedded lenticular to sheet-like sandstone beds (Soister, 1968). These are accompanied by lenses and beds of arkosic conglomerate with several widespread white tuff beds (Love, 1970). The overall thickness of the formation is variable since it was deposited on a surface of considerable local relief, but it may be as much as 305 m (1,000 ft) in the central Wind River Basin (Soister, 1968) and more than 549 m (1,800 ft) at the northwestern end of the basin (Rohrer, 1968). The Wind River Formation hosts roll-front uranium deposits in the Gas Hills area of the Wind River Basin and in Shirley Basin.

Southwest Pine Mountain, SE¼SE¼ sec. 31, T. 53 N., R. 84 W., Natrona County

At this location (fig. 32), the Wind River Formation (Hunter and others, 2005) is yellowish-brown, medium- to coarse-grained, quartz-rich sandstone with limonite stain, black manganese oxide, and monazite. The sample, WGS-0501, contains cerium, gadolinium, lanthanum, neodymium, praseodymium, and samarium at concentrations greater five times the average crustal abundance. It also contains other REE at slightly elevated concentrations (table 32). This locale is the most northwestern of a northwest-southeast trend including the Ranger claims in the Lance Formation and the Poison Spider claim in the Lewis Shale. This sample also contained elevated amounts of other elements such as 57.7 percent Fe_2O_3, 2,500 ppm V, >10,000 ppm Zr, and 248 ppm Hf.

About 2.4 km (1.5 mi) to the east-southeast of this location in T. 34 N., R. 84 W., petrified wood and silicified bones (20150610LC-4) hosted by the variegated Wind River Formation can be found in the NW¼SW¼NW¼ corner of section 4. Septarian concretions (20150610LC-3) of varying size are also present in the variegated rock units in the SW¼NE¼SW¼ of the same section.

Northern Wind River Basin, NE¼SE¼NE¼ sec. 19, T. 39 N., R. 93 W., Fremont County

This locale is just south of the Owl Creek Mountains and east of Wind River Canyon. The Wind River Formation (Love and Christiansen, 1985) exhibits variegated units throughout the basin and has a particularly strong limonitic stain here. The unit is conglomerate ranging from fine- to coarse-grained with mostly rounded clasts. The finer grained matrix crumbles easily, and the limonite stain penetrates beyond the surface of the unit. Cerium is the only REE present above five times the average (Sample 20150804LC-5), but lanthanum, neodymium, and praseodymium were also elevated (table 33).

Deacon's Prayer group claims, NW¼NW¼ and SW¼NE¼ sec. 17; SE¼SE¼ sec. 18, T. 32 N., R. 82 W., Natrona County

Griffin and Milton (1982) reported 90 ppm cU_3O_8, 250 ppm lanthanum, 70 ppm yttrium, 3,000 ppm titanium, and 300 ppm zirconium within a coarse-grained to conglomeratic arkosic sandstone in the basal Wind River Formation. The area sampled by Griffin and Milton (1982) is located on private land, but the Wind River Formation crops out on adjacent public land to the north (Hunter and others, 2005).

Sutherland and others (2013) sampled a coarse-grained arkosic sandstone, interbedded with a cobble- to boulder-conglomerate supported by a coarse-grained arkosic matrix, along a ridge trending about 320°. The clasts in the conglomerate are dominantly felsic igneous rocks,

Table 32. Concentration of REE from Southwest Pine Mountain. Bold values indicate concentrations greater than five times the crustal abundance.

	Southwest Pine Mountain								
Element	La (ppm)	Ce (ppm)	Pr (ppm)	Nd (ppm)	Sm (ppm)	Eu (ppm)	Gd (ppm)	Tb (ppm)	Dy (ppm)
WGS-0501	**299**	**575**	**59.1**	**216**	**35.9**	2.46	**27.6**	3.57	17.5
	Ho (ppm)	Er (ppm)	Tm (ppm)	Yb (ppm)	Lu (ppm)	Sc (ppm)	Y (ppm)	Cumulative REE (ppm)	
	3.47	10.9	1.61	12.55	2.34	21	102.5	**1,390.50**	

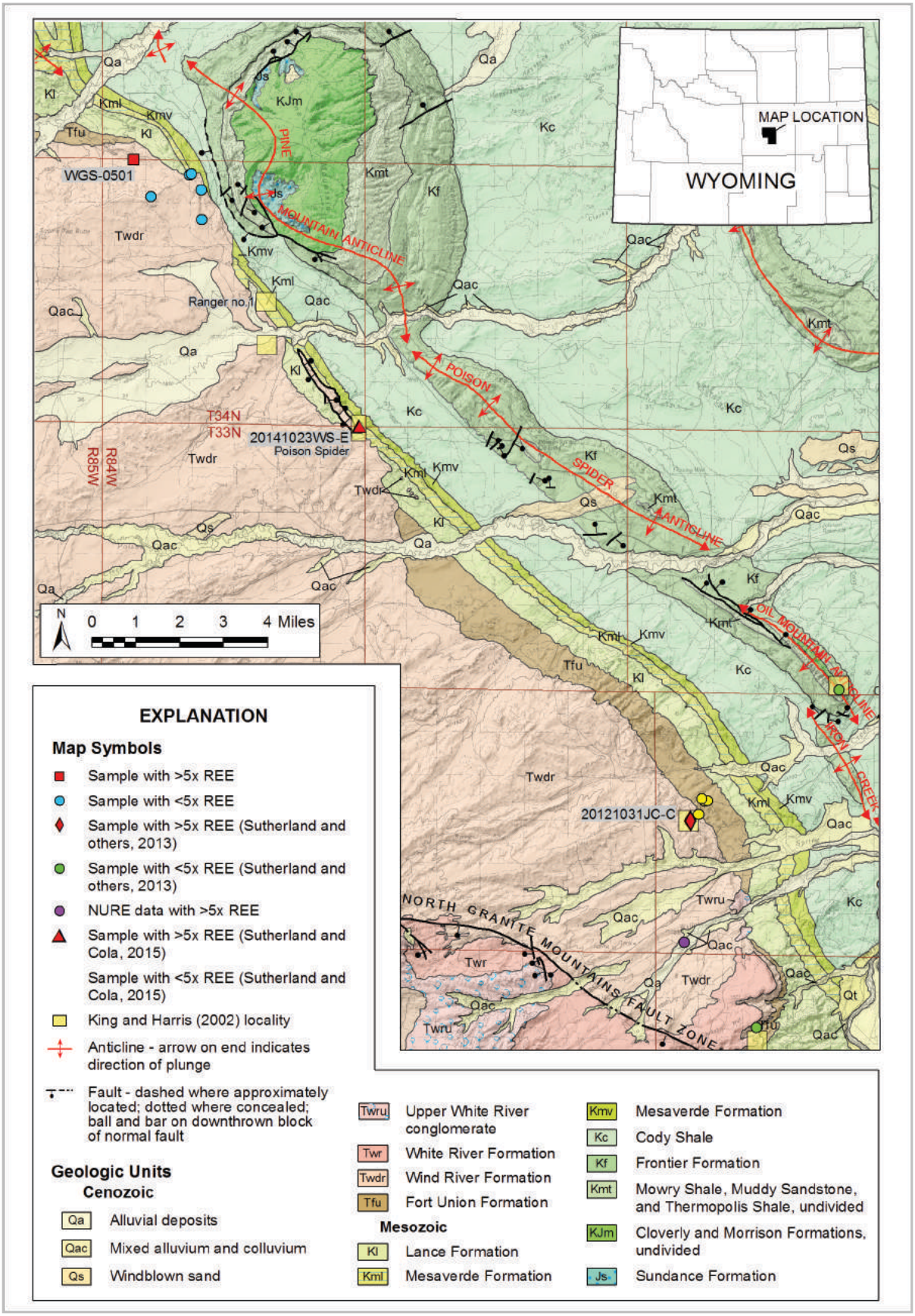


Figure 32. Sample locations and geology along the southwestern edge of the Casper Arch. Samples with elevated REE appear to follow along a stratigraphic trend in or near the Wind River Formation. Map modified from Sutherland and Hausel (2003).

but mafic, metamorphic, and sedimentary clasts are also present. The sandstone hosts large iron concretions greater than 1.8 m (6 ft) across with dark-brown, coarse-grained, subangular, limonite-cemented, lithic arkose rinds 10 to 20 cm (4 to 8 in) thick (Sample 20121031JC-C). The insides of the concretions are tan to yellow, very coarse grained, subangular, calcite cemented, limonitic lithic arkose (Sample 20121031JC-D). The interiors of the concretions are not significantly enriched in any of the REE or any other elements of economic interest. However, the concretionary rind (Sample 20121031JC-C) contains 152.2 ppm yttrium, greater than five times its crustal abundance (table 34), and is weakly enriched in all of the naturally occurring REE except europium and scandium (Sutherland and others, 2013). In addition, the rind contains nearly 63 ppm uranium and 0.094 percent titanium. When compared to the results of Griffin and Milton (1982), recent sampling indicates that high concentrations of REE, yttrium, titanium, and uranium within the Deacon's Prayer group claim may be isolated occurrences (Sutherland and others, 2013).

More sampling was done in the area near the contact of the Wind River and Fort Union Formations by Sutherland and Cola (2015). The area has heavily iron-stained, vertical to subvertical, undulating layers and is disrupted by folds and faults. The dark, blackish-brown layers (20141023WS-A), magnetite-rich iron concretions (Samples 20141023WS-B, C), and red hematitic sandstone with metallic banding (20141023WS-D) were sampled. Although slight elevations of REE were found here in previous studies, these samples contained no elevated REE. It is suggested that the folding and faulting in the area may have thickened iron-rich mineralization at this locality, and subsequent fluid movement through porous sandstones or along faults and fractures could have allowed pathways for remobilization of ions (Sutherland and Cola, 2015). Thus, the concentrations of REE in the area may be sporadic and highly variable.

Bates Hole area, T. 27 N., R. 78, 80, 81 W., Carbon County

Aerial surveys detected high radioactivity along the south rim of Bates Hole and the northwestern rim of Shirley Basin. Surface examination concluded that thorium-rich monazite in sandy and conglomerate beds in the Wind River and White River Formations were the source of radioactivity (Harshman, 1972; Roehler, 1958; Vine and Denson, 1954). The amount of monazite present varies from a few hundredths to 1.43 pounds of monazite per ton of sand (Harshman, 1972), and it is suggested the occurrences are fluvial placers (King and Harris, 2002). The WSGS visited and sampled (20150610LC-6) the upper part of the Wind River Formation, or possibly the lower part of the White River Formation, in this area and found no

Table 33. Concentration of REE from the northern Wind River Basin. Bold values indicate concentrations greater than five times the crustal abundance.

	Northern Wind River Basin								
Element	La (ppm)	Ce (ppm)	Pr (ppm)	Nd (ppm)	Sm (ppm)	Eu (ppm)	Gd (ppm)	Tb (ppm)	Dy (ppm)
20150804LC-5	156.5	292	30.5	106.5	18.65	1.35	12.9	1.73	8.54
	Ho (ppm)	Er (ppm)	Tm (ppm)	Yb (ppm)	Lu (ppm)	Sc (ppm)	Y (ppm)	Cumulative REE (ppm)	
	1.75	4.49	0.61	3.84	0.55	8	42.8	690.71	

Table 34. Concentration of REE from the Deacon's Prayer group claims. Bold values indicate concentrations greater than five times the crustal abundance.

	Deacon's Prayer group claims								
Element	La (ppm)	Ce (ppm)	Pr (ppm)	Nd (ppm)	Sm (ppm)	Eu (ppm)	Gd (ppm)	Tb (ppm)	Dy (ppm)
20121031JC-C	66.1	111.5	13.8	48.1	11.25	1.82	19.35	3.03	18.8
20121031JC-D	32.1	53.1	6.42	21.4	4.64	0.68	5.23	0.77	4.44
Element	Ho (ppm)	Er (ppm)	Tm (ppm)	Yb (ppm)	Lu (ppm)	Sc (ppm)	Y (ppm)	Cumulative REE (ppm)	
20121031JC-C	4.11	12.05	1.52	8.34	1.33	12.3	**152.5**	485.9	
20121031JC-D	0.85	2.43	0.32	1.91	0.3	7.9	26.2	168.7	

From Sutherland and others (2013)

Samples from Deacon's Prayer in Sutherland and Cola (2015) contained no elevated REE.

elevated REE. The only outcrops exposed were along the rim and the majority of this large area showed no outcrops for sampling.

Gafco placer claims and Shirley #22 lode claims, sec. 3, T. 27 N., R. 81 W., Carbon County

This location is near the western edge of the Shirley Basin uranium mining district and contains monazite within heavy-mineral concentrates in coarse-grained arkosic sandstone and conglomerate in the basal White River Formation, which unconformably overlies the Wind River Formation. A sample contained 0.12 percent Th and 0.003 percent U (Vine and Denson, 1954). A concentrate, 1/50th of the original sample, reportedly contained 25 percent REE, 6 percent ThO_2, and 0.25 percent U_3O_8 (Whalen, 1954b). A sample of gravel at the top of the Wind River Formation from the center of section 3 contained 9.7 percent heavy minerals, 23 percent of which were monazite. These gravels also contained 830 ppm eTh and 29 ppm eU (Griffin and Milton, 1982).

Unnamed, NE¼ sec. 5, T. 27 N., R. 81 W., Carbon County

Two samples from gravel in the upper part of the Wind River Formation at this location contained 700 and 1,000 ppm La, 70 and 200 ppm Y, 10 and 50 ppm Nb, 2,000 and 5,000 ppm Ti, and 500 ppm Zr. Another sandstone sample contained 150 ppm La, 1,500 ppm Ti, 20 ppm Y, and 300 ppm Zr (Griffin and Milton, 1982). This is probably a fluvial placer (King and Harris, 2002).

King and Harris (2002) list six other unnamed locations in the Shirley Basin-Bates Hole area by Griffin and Milton (1982), Love (1954a), Ellis (1977), and Harshman (1968). Many of these are described as low-grade, radioactive, monazite-bearing placers in the White River or Wind River Formations. No significant values of REE, thorium, or uranium were reported. These are considered unverified occurrences by King and Harris (2002).

Battle Spring Formation

The Eocene Battle Spring Formation consists of 1,006 m (3,300 ft) or more of light-gray to brown, coarse-grained to pebbly, arkosic sandstone and conglomerate, accompanied by greenish-gray sandy clay and mudstone. Locally, it contains large, sandy, iron-rich, spheroidal concretions (Sheridan and others, 1961; Bradley, 1964). The Battle Spring has gradational, interfingering contacts, both horizontally and vertically, with the Wasatch and Green River Formations (Denson and Pipiringos, 1974). The Battle Spring Formation is also the host for roll-front uranium deposits in the Crooks Gap-Green Mountain uranium district and the northeastern part of the Great Divide Basin. This is discussed further in the "REE Associated with Uranium Deposits" section.

Unnamed (Sample 44), NE¼ sec. 30, T. 28 N., R. 92 W., Fremont County

Gray, carbonaceous shale in the Battle Spring Formation contained 150 ppm La, 20 ppm Y, 1,400 ppm Ti, 200 ppm Zr, and 56 ppm cU_3O_8 (Griffin and Milton, 1982; King and Harris, 2002). This REE occurrence is located in the western part to the Crooks Gap-Green Mountain uranium mining district (Gregory and others, 2010). Its close proximity to roll-front uranium deposits suggests that it could be a residual deposit left behind due to changes in site specific redox conditions, where REE were deposited and uranium moved further on to be deposited under slightly different conditions. This interpretation is also supported by NURE samples with elevated REE in and adjacent to the uranium mining district (fig. 33).

Unnamed (Sample 52), NW¼ sec. 16, T. 24 N., R. 92 W., Sweetwater County

Sandstone in the Battle Spring Formation contained 300 ppm La, 20 ppm Y, 3,000 ppm Ti, 300 ppm Zr, and 6 ppm U_3O_8 (Griffin and Milton, 1982). King and Harris (2002) discussed this site and stated that the origin of the lanthanum enrichment is unknown. This location has similarities to the unnamed (Sample 44) site in that it is located in the general vicinity of known roll-front uranium deposition in the same formation. This site is in the eastern part of the Great Divide Basin uranium mining district. The Lost Creek uranium deposit also occurs about 8 km (5 mi) to the northwest, and redox uranium occurrences are known a few km (mi) to the west (Gregory and others, 2010). Four NURE samples that host elevated REE are also located nearby, 8 to 11 km (5 to 7 mi) to the north, suggesting that hydrologic conditions responsible for the uranium deposits may also have been responsible for local deposition of REE.

Unnamed (Sample 55), W½ sec. 6–7 line, T. 24 N., R. 93 W., Sweetwater County

Silty shale from the Battle Spring Formation contained 150 ppm La, 10 ppm Y, 2,000 ppm Ti, 200 ppm Zr, and 27 ppm cU_3O_8. A sandstone near here contained 525 ppm cU_3O_8 with no REE enrichment (Griffin and Milton, 1982). King and Harris (2002) stated that the source of REE is not a placer but is unknown. The location of this sample, in close proximity to redox uranium occurrences, is similar to that of unnamed (Sample 52) and may also be related to the movement of fluids responsible for the nearby roll-front uranium.

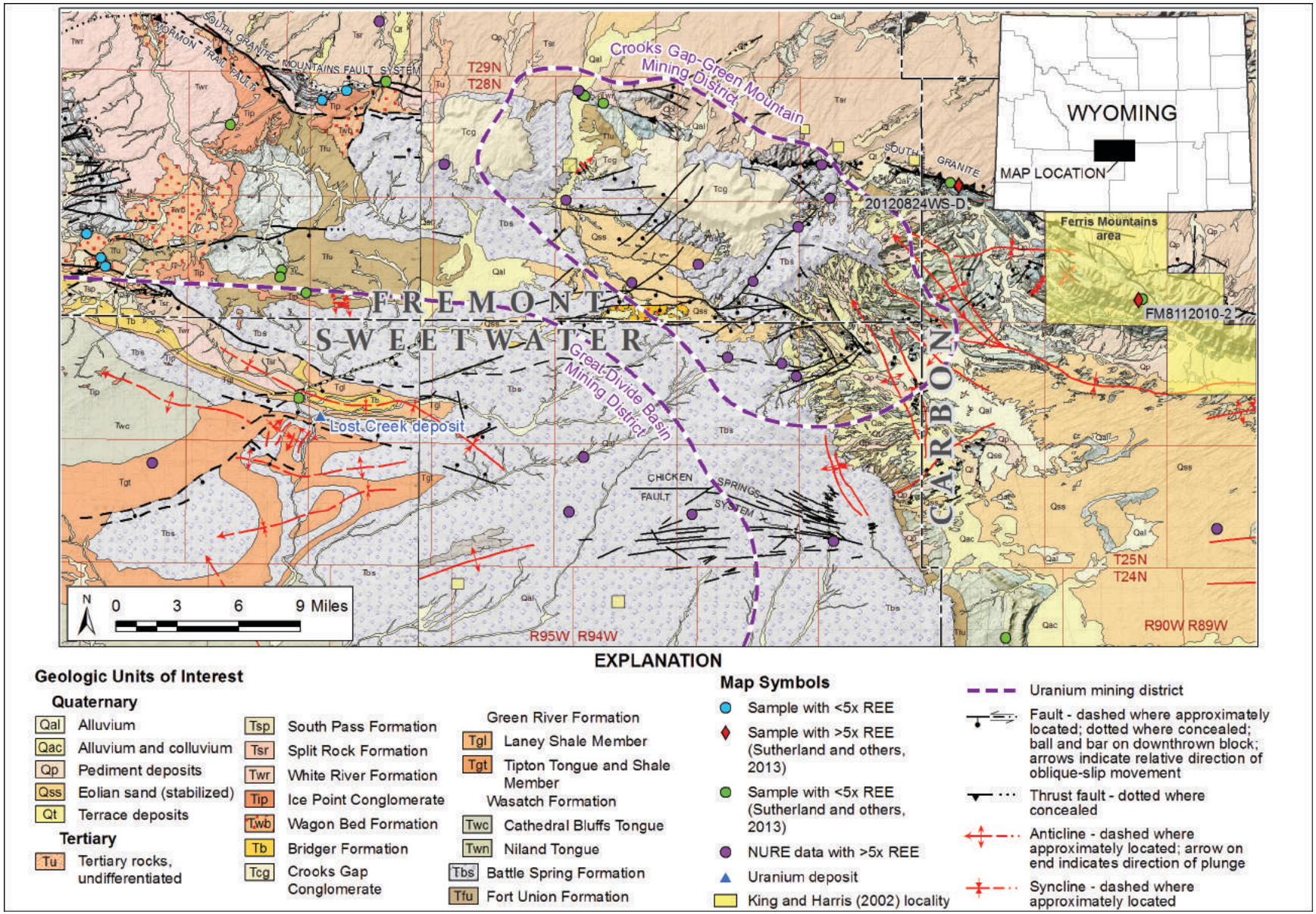


Figure 33. Sample locations and geology of the northern Great Divide Basin. King and Harris (2002) locales, east to west, include the Ferris Mountain area, Gap claims, Mohawk claims, and unnamed areas. Quaternary and Tertiary units are bold due to elevated REE in NURE samples. The Great Divide Basin and Crooks Gap-Green Mountain uranium mining districts are shown (Gregory and others, 2010). Map modified from Sutherland and Hausel (2006) and Jones and others (2011).

Lance Formation

The Late Cretaceous Lance Formation is a nonmarine sequence of interbedded, light colored, partly conglomeratic sandstone, gray to black shale and claystone, and brown to black carbonaceous shale and coal. It varies in thickness from about 90 m (300 ft) to more than 1,500 m (5,000 ft) in the northern and eastern Wind River Basin. The Lance is overlain by the Paleocene Fort Union Formation in a contact that varies from an erosional unconformity along the Wind River Basin margins to conformable in the center of the basin (Keefer, 1965).

Ranger no. 1 claim, NE¼ sec. 22, T. 34 N., R. 84 W., Natrona County

This fossil beach placer is in the Lance Formation but cuts an arkosic sandstone in the Lewis Shale. The black lens exhibits 20 times background radiation and is associated with limonite, carbonaceous material, and manganese oxides (Hadfield, 1954). A grab sample contained 0.319 percent cU_3O_8 (Geslin, 1954), which would indicate a roll-front-type deposition when combined with the mineralization description. Two samples of the arkosic sandstone contained 500 and 1,000 ppm La, 70 and 500 ppm Y, 1,000 and 5,000 ppm Ti, <10 ppm Nb, 50 ppm and 200 ppm Zr, 41 ppm eU, and 1,440 ppm eTh. Heavy-mineral analysis concluded magnetite, ilmenite, xenotime, and zircon were part of the placer (Griffin and Milton, 1982). This deposit is the only known occurrence of a black sandstone in the Lance Formation in Wyoming (King and Harris, 2002).

An additional sample from a black sandstone, thought to be an extension of the Ranger claim to the southeast, contained 300 ppm La, 2,000 ppm Ti, 70 ppm Y, 100 ppm Zr, <10 ppm Nb, 13 ppm eU, and 195 ppm eTh (Griffin and Milton, 1982).

The Ranger claim also appears to be on trend with the Poison Spider deposit in the Lewis Shale (fig. 32), described below, and the Southwest Pine Mountain locale in the Wind River Formation described earlier. Further investigation would be required to identify a possible relationship between these black sandstone deposits.

Fox Hills Sandstone and Lewis Shale

The Upper Cretaceous Fox Hills Sandstone in the Powder River Basin is 46 to 61 m (150 to 200 ft) of light-gray to yellowish-gray, friable, very fine- to medium-grained, soft, thin-bedded marine sandstone. The unit is interbedded in places with gray sandy shale and is in gradational contact with the underlying Pierre Shale (Mapel and Pillmore, 1964; Sutherland, 2007). The upper part of the Pierre is equivalent to the Lewis Shale in central and southwestern Wyoming. The Lewis Shale consists of interbedded gray, olive-gray, and buff shale and fine- to medium- grained sandstone. The Lewis directly overlies the Mesaverde Formation, or in the southeastern Green River Basin, the Mesaverde Group. (Keefer, 1965; Love and others, 1993).

Salt Creek (north), secs. 24–26, T. 39 N., R. 78 W.; sec. 31, T. 39 N., R. 77 W., Natrona County; Salt Creek (south) secs. 19 and 30, T. 38 N., R. 77 W., Natrona County

Two segments of titaniferous black sandstones occur in the Fox Hills Sandstone on the east edge of the Salt Creek anticline. The northern segment is at least 2,743 m (9,000 ft) long, and the southern segment is at least 1.6 km (1 mi) long and 229 m (750 ft) wide (Houston and Murphy, 1970; 1977). REE enrichment has not been confirmed but is suspected based on the commonality of REE in black sandstones (King and Harris, 2002).

Seminoe, sec. 35, T. 25 N., R. 85 W.; secs. 15 and 28, T. 24 N., R. 85 W., Carbon County

The extent of this radioactive, titaniferous black sandstone, paleo-beach placer is unknown (Houston and Murphy, 1970). Houston and Murphy (1977) determined it is within the Fox Hills Sandstone but did not check for REE enrichment. Thus, this is a suspected but unverified REE locality based on the mineralogy of black sandstone deposits (King and Harris, 2002).

Poison Spider, NE¼NE¼ sec. 1, T. 33 N., R. 84 W.; SE¼SE¼ sec. 35, T. 34 N., R. 84 W., Natrona County

This magnetite-ilmenite-bearing sandstone deposit is located in the Lewis Shale (fig. 32). The deposit is up to

Table 35. Concentration of REE from the Poison Spider deposit. Bold values indicate concentrations greater than five times the crustal abundance.

	Poison Spider								
Element	La (ppm)	Ce (ppm)	Pr (ppm)	Nd (ppm)	Sm (ppm)	Eu (ppm)	Gd (ppm)	Tb (ppm)	Dy (ppm)
20141023WS-E	**346**	**635**	**65.9**	**226**	**38.3**	2.15	24.5	3.02	14.65
	Ho (ppm)	Er (ppm)	Tm (ppm)	Yb (ppm)	Lu (ppm)	Sc (ppm)	Y (ppm)	Cumulative REE (ppm)	
	2.56	7.54	1.23	8.87	1.69	13	72.7	**1,463.11**	

From Sutherland and Cola (2015)

2 m (7 ft) thick and extends about 91 m (300 ft). A prospect at this location exposes rusty-maroon, magnetite-rich rock in a highly faulted area (Sutherland and Cola, 2015). The deposit contains more than 60 percent Fe_2O_3 and is enriched in LREE (Sample 20141023WS-E). Some HREE are elevated but not more than five times the average crustal abundance as the LREE are (table 35).

Fiddlers Green, sec. 21, T. 21 N., R. 80 W., Sweetwater County

This is a radioactive, titaniferous black sandstone, paleobeach placer in the Lewis Shale. The deposit is up to 3.9 m (13 ft) thick and exposed for 793 m (2,600 ft; Houston and Murphy, 1970). Radioactivity reached 2.5 times the background, and the sample contained 49 ppm eTh (Dribus and Nanna, 1982). This is a suspected but unverified REE locality based on its similarity to other Wyoming Mesozoic black sand placers (King and Harris, 2002).

Mesaverde Formation

The Upper Cretaceous Mesaverde Formation is predominantly a nonmarine sequence of gray and brown, fine- to medium-grained, cross-bedded sandstone interbedded with shale, carbonaceous shale, and coal (Love, 1970). It occurs throughout Wyoming, except in the northeastern part of the state (Love and others, 1993), and is separated into a number of formations called the Mesaverde Group in some areas, particularly in the Rock Springs Uplift in southwestern Wyoming. Among others, the Rock Springs Formation is included within the Mesaverde Group.

The thickness of the Mesaverde is variable and ranges from about 90 m (300 ft) in some areas to more than 1,500 m (5,000 ft) in the Green River Basin (Roehler, 1990). It overlies and partially intertongues with black shale of the Cody Shale and its equivalent formations. Together, the Cody and the Mesaverde represent a generally regressive sequence that transitioned from a deep marine to nearshore terrestrial environment over the depositional history of the two units. The black shale, that in places overlies the basal sandstone of the Mesaverde, represents a short-lived transgressive event (Houston and Murphy, 1962).

Titaniferous black sandstones at, or near, the top of the basal sandstone of the Mesaverde Formation are thought to be fossil beach placers analogous to modern heavy-mineral-rich black sand beaches found in Australia (Houston and Murphy, 1962; 1970). The titaniferous black sandstone horizons are relatively common in the lower part of the Mesaverde Formation across Wyoming, Colorado, and New Mexico or in the Mesaverde Group in Arizona (Houston and Murphy, 1962, 1970). The Wyoming deposits (fig. 34) occur at the top of the formation's basal sandstone (Houston and Murphy, 1962), which is typically tan to buff and fine-grained. It is overlain by a succession of interbedded sandstone, shale, carbonaceous shale, and coal or, in some areas, by black shale.

The heavy minerals within the titaniferous black sandstones of the Mesaverde Formation (fig. 34) were studied in detail by Houston and Murphy (1962; 1970) and are dominantly volcanic in origin. The heavy-mineral fraction of the black sandstone consists of 79 to 97 percent opaque minerals, mostly iron-titanium oxides, but a radioactive niobium-bearing mineral may also be present. The remaining heavy-mineral fraction is composed of varying amounts zircon, monazite, garnet, rutile, tourmaline, amphiboles, spinel, sphene, epidote, biotite, chlorite, staurolite, and apatite. Zircon and garnet are the most abundant of the translucent heavy minerals (Houston and Murphy, 1962). Many of the following sites sampled from the Mesaverde Formation in Wyoming were collected during WSGS RI-65 and 67. Analyses of the samples collected by this and previous studies (Sutherland and others, 2013; Sutherland and Cola, 2015) are included in appendices 1 and 2.

Grass Creek area, (north deposit) E½SE¼ sec. 8, SW¼SW¼ sec. 9, NW¼NW¼ sec. 16, T. 46 N., R. 98 W.; (south deposit) S½NE¼ sec. 33, S½NW¼ sec. 34, T. 46 N., R. 98 W., Hot Springs County

The Grass Creek area is reported by Houston and Murphy (1962) to host the largest known titaniferous black sandstone deposit in Wyoming. It is exposed in two outcrops, 4.4 km (2.75 mi) apart, on the northeast and south flanks of the Grass Creek anticline. Like many other black sandstone deposits in the Mesaverde Formation, the Grass Creek black sandstone is hosted near the top of the basal sandstone of the Mesaverde Formation. However, this deposit differs from other Mesaverde black sandstones in that it is not overlain by marine sediments (Houston and Murphy, 1962).

In the northern exposure, the black sandstone has a maximum width of about 207 m (680 ft), a maximum thickness of about 4.9 m (16 ft), and an average thickness close to 3.4 m (11 ft). Bedding in the northern outcrop strikes 315° with a 15° NE dip. The southern outcrop strikes 100° and dips 30° to 35° S along the south flank of the anticline. The black sandstone of the southern outcrop is poorly and sporadically exposed, but it can be traced for more than 488 m (1,600 ft) and has a maximum thickness of at least 1.5 m (5 ft; Houston and Murphy, 1962).

During the RI-65 investigation (Sutherland and others, 2013), a fine-grained, black to red, opaque mineral-rich sandstone (WMS-GC1-2010), sampled from the south-

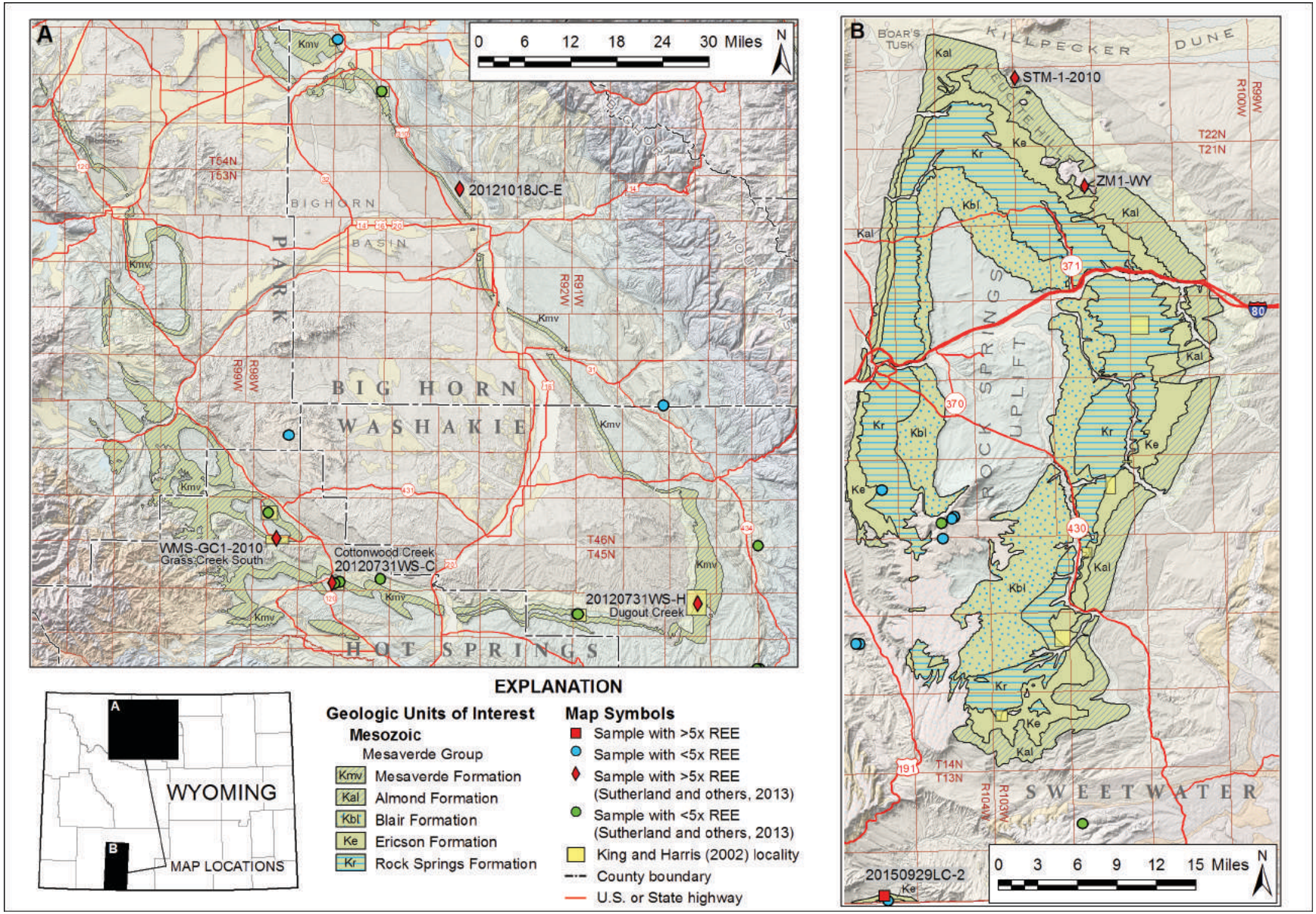


Figure 34. Sample locations and geology focusing on black sandstone deposits in Wyoming. Black sandstones are most commonly found in Mesaverde Group formations across Wyoming; these units are bold compared to surrounding geology in (A) the Bighorn Basin and (B) the Rock Springs Uplift area. Maps modified from Love and Christiansen (1985).

Table 36. Concentration of REE from black sandstone deposits. Bold values indicate concentrations greater than five times the crustal abundance.

	Black sandstone deposits								
Element	La (ppm)	Ce (ppm)	Pr (ppm)	Nd (ppm)	Sm (ppm)	Eu (ppm)	Gd (ppm)	Tb (ppm)	Dy (ppm)
20120731WS-C*	**597**	**972**	**108**	**350**	**46.8**	5.64	**29.6**	4.07	22.1
20120731WS-H*	**408**	**669**	**74.9**	**247**	**35.2**	3.44	23.7	3.53	20.4
WMS-GC1-2010*	**850**	**1,505**	**169.5**	**551**	**80.3**	6.67	**76.8**	**10.35**	**55.8**
20141015WS-D†	**1,340**	**2,490**	**267**	**894**	**30**	**9.05**	**73.3**	**9.52**	**50.9**

Element	Ho (ppm)	Er (ppm)	Tm (ppm)	Yb (ppm)	Lu (ppm)	Sc (ppm)	Y (ppm)	Cumulative REE (ppm)
20120731WS-C*	4.42	12.85	1.98	13.95	2.42	15	129.5	**2,315.33**
20120731WS-H*	4.25	12.9	2.12	14.95	2.7	31	121.5	**1,674.59**
WMS-GC1-2010*	**12.5**	**42.8**	**6.93**	**50.9**	**8.99**	43.3	**331**	**3,801.84**
20141015WS-D†	**10.15**	**30.9**	**5.29**	**39.2**	**7.55**	40	**292**	**5,588.86**

*Selected samples from Sutherland and others (2013)

†From Sutherland and Cola (2015)

ern Grass Creek outcrop (fig. 34A), is enriched to greater than five times the crustal abundance in all of the naturally occurring REE, except for europium; yttrium and niobium are also present at significant levels of enrichment. A red to orange, botryoidal-appearing sandstone (Sample WMS-GC2-2010), collected from the northern outcrop, exhibits no significant enrichment of REE or other elements of economic interest. On the other hand, a sample (20141015WS-D) collected during RI-67 (Sutherland and Cola, 2015) exceeded the quintupled abundance of all the rare earths except scandium, which was only slightly elevated (table 36). Also present was 28.5 percent TiO_2, 748 ppm Nb, 23 ppm Sn, 605 ppm Th, 931 ppm V, and >10,000 ppm Zr.

Cottonwood Creek, SE¼SE¼ sec. 26 and NE¼NE¼ sec 35, T. 45 N., R. 97 W., Hot Springs County

The titaniferous black sandstone in the Mesaverde Formation at Cottonwood Creek is a dark-brown to black and rusty-brown, fine- to medium-grained, cross-bedded sandstone in discontinuous outcrops (Sutherland and others, 2013). Detailed descriptions and analyses of the deposit are found in Houston and Murphy (1962). King and Harris (2002) summarize those findings and include information from more recent studies. The maximum thickness of the black sandstone is reported to be 2.7 m (9 ft), with zircon accounting for 18.5 percent of the heavy-mineral fraction and monazite making up 1 percent. Madsen (1978) reported that one sample from this deposit contained 1,687 ppm lanthanum.

The black sandstone (Sample 20120731WS-C) is enriched in all of the REE as well as yttrium and niobium. La, Ce, Pr, Nd, Sm, and Gd are all present above five times the average abundance (table 36). Several dark-brown, iron-rich, fine- to medium-grained, lenticular sandstone bodies are also present in this area. However, two samples (20120731WS-A and 20120731WS-B) showed no significant enrichment in any of the REE or titanium (Sutherland and others, 2013).

Mud Creek, NW¼NE¼ sec. 19, T. 44 N., R. 91 W., Washakie County

The black sands just north of Mud Creek were initially described by Houston and Murphy (1962) with additional details from King and Harris (2002). The titaniferous black sandstone occurs in the uppermost part of the basal sandstone of the Mesaverde and has a maximum thickness of 2.3 m (7.5 ft) with an exposure width of about 457 m (1,500 ft). Houston and Murphy (1962) reported that the heavy-mineral suite contains 5 percent zircon. Another sample, collected by Madsen (1978), contained 500 ppm lanthanum.

Samples collected from the upper part of the Mesaverde outcrop, about 0.5 km (0.3 mi) northeast of the 1962 and 1978 samples, showed no REE enrichment (Sutherland and others, 2013). Apparently, these were stratigraphically higher in the formation than the titaniferous black sandstone described by Houston and Murphy (1962). One sample appeared to be an iron-rich sandstone, however the dark coloration was primarily due to a surficial coating. This darker sandstone is overlain by a thick, white, cross-bedded sandstone near the top of the

Mesaverde Formation that also showed no REE enrichment (Sutherland and others 2013).

Dugout Creek, NE¼SW¼ sec. 11, T. 44 N., R. 89 W., Washakie County

The titaniferous black sandstone in the Dugout Creek deposit is in the upper part of the basal Mesaverde Formation and is radioactive in some outcrops. The black sandstone crops out across several sections, and its thickness varies from about 0.9 to 7.6 m (3 to 25 ft) but averages 3 to 4.6 m (10 to 15 ft; Houston and Murphy, 1962). This is the most extensive exposure of Mesaverde black sandstone in Wyoming (Sutherland and others, 2013).

Zircon makes up 5 percent of the total heavy-mineral content in the black sandstone here, and monazite accounts for 1 percent. Uranium content reportedly varies from 0.001 to 0.021 percent eU, depending on which earlier investigation is cited (King and Harris, 2002). Madsen (1978) reported one sample that contained 312 ppm lanthanum.

A recent WSGS sample from this location (Sample 20120731WS-H) consists of fine- to medium-grained, dark-brown to purple and orange, cross-bedded sandstone about 3 ft thick that overlies a yellowish-brown sandstone. The dark-brown sandstone outcrop is about 0.40 km (0.25 mi) in length at this locality. A similar layer is noted about 1.6 km (1 mi) to the north and appears to be continuous for 0.4 to 0.8 km (0.25 to 0.5 mi). Several prospect pits are found near the sample site. The sample is composed of 12 percent TiO_2 and is slightly elevated in all the REE except dysprosium and holmium. The LREE, ytterbium, and niobium are enriched more than five times the average crustal abundance (table 36; Sutherland and others, 2013).

Lovell deposit, secs. 7 and 12, T. 55 N., R. 95 W., Big Horn County

This slightly radioactive, titaniferous, black sandstone deposit averages 0.9 m (3 ft) thick, with a maximum thickness of 1.2 m (4 ft). The outcrop extends along an 11° SW dipping hogback for 914 to 1,524 m (3,000 to 5,000 ft; King and Harris, 2002). Houston and Murphy (1962) reported zircon in the heavy-mineral fraction but an absence of monazite. A sample from this deposit by Garrand and others (1982) showed 50 ppm lanthanum, >20 ppm niobium, 40 ppm yttrium, 200 ppm zircon, and 8 ppm cU_3O_8 (20 ppm eU_3O_8). Madsen (1978) reported 316 ppm lanthanum in a sample from this deposit.

The WSGS sampled this deposit for RI-65 (20120801WS-A) and RI-67 (20141015WS-A1, A2). The area has a dark-brown to purple, thin-bedded, fine-grained sandstone up to 1.2 m (4 ft) thick. Magnetite nuggets along with weathered pieces of sandstone cover the ground. Analyses of these samples showed 3 to 12 percent TiO_2 and weak enrichment in the LREE, gadolinium, and niobium.

Cowley deposit, center sec. 1, T. 56 N., R. 97 W., Big Horn County

Radioactive, titaniferous, black sandstone is exposed for 274 m (900 ft) with an average thickness of 0.3 m (1 ft) and a maximum of 1.1 m (3.5 ft); it is unknown how large the deposit is due to alluvium coverage. The deposit has a northwest trend with a strike of N 60° W and a dip of 9° SW. Zircon, but not monazite, is present in this paleobeach placer (Houston and Murphy, 1962). Samples contained <20 and 400 ppm La, 30 and <20 ppm Nb, <10 ppm Y, 2,000 and 60,000 ppm Ti, 100 and 800 ppm Zr, and 3 and 35 ppm cU_3O_8 (Garrand and others, 1982). Madsen (1978) reported a sample contained 135 ppm La, and Dow and Batty (1961) reported 0.01 percent eTh.

Unnamed (Sample 86), SW¼ sec. 5, T. 40 N., R. 78 W., Natrona County

At this location, a black sandstone in the Teapot Member of the Mesaverde Formation contains magnetite, 1 percent sphene, and 6 percent allanite. The sample also contained 67 ppm eTh and a maximum of 8 ppm cU (Damp and Brown, 1982). This is an unverified REE locality since no analyses were completed for rare earths, and it is unknown if the allanite was correctly identified (King and Harris, 2002).

Unnamed (Sample 83), S½ sec. 27, T. 40 N., R. 78 W., Natrona County

Damp and Brown (1982) reported a heavy-mineral concentration in the Teapot Member at this location. The sample contained <100 ppm La, 195 ppm Nb, 51,400 ppm Ti, 622 ppm W, <40 ppm Y, 907 ppm Zr, 11 ppm eTh, and 22 ppm eU. Although the REE do not appear elevated, this is an unverified locale by King and Harris (2002) based on the deposit type.

Coalbank Hills, center sec. 5, T. 34 N., R. 88 W., Natrona County

This radioactive, titaniferous, black sandstone is about 427 m (1,400 ft) long with a maximum thickness of 1.5 m (5 ft). The bedding strikes N 40° W and dips 23° NE (Houston and Murphy, 1962; Loomis and Holmquist, 1954). Samples contained as much as 1.170 ppm eTh and 160 ppm eU, but no analyses were done for REE (Dow and Batty, 1961). Griffin and Milton (1982) note the presence of xenotime and zircon. Nonetheless, this is an unverified occurrence.

Clarkson Hill, NE¼NE¼NE¼ sec. 20, T. 31 N., R. 82 W., Natrona County

A radioactive, titaniferous, black sandstone is exposed in a 46 m (150 ft) long by 6 m (20 ft) wide outcrop in the Parkman Sandstone Member of the Mesaverde Formation. The maximum thickness is about 1.7 m (5.6 ft). Houston and Murphy (1962) reported 0.001 percent cU and 0.004 percent eU, while Dow and Batty (1961) reported 0.04 eTh. No analyses were done for REE, but zircon, monazite, xenotime, apatite, and possibly allanite are present in the deposit (Griffin and Milton, 1982). Thus, this is an unverified occurrence of REE.

Unnamed (Sample 96), sec. 22, T. 43 N., R. 81 W., Johnson County

This is another heavy-mineral concentration located in the Parkman Sandstone Member of the Mesaverde Formation (Damp and Brown, 1982). The sample contained 98 ppm eTh and 20 ppm eU. No rare earth analyses were completed, making this an unverified REE occurrence (King and Harris, 2002).

Shotgun Bench, sec. 18, T. 5 N., R. 1 E., (Wind River Meridian), Fremont County

This black sandstone is reported as 91 m (300 ft) wide and no more than 1.5 m (5 ft) thick (Houston and Murphy, 1970). This is an unverified REE locale based only on the common occurrence in heavy-mineral deposits (King and Harris, 2002).

Sheep Mountain, SE¼ sec. 10 and NW¼NW¼ sec. 14, T. 15 N., R. 77 W., Albany County

Radioactive, ilmenite-bearing, black sandstone crops out in the lower Mesaverde Formation (Houston and Murphy, 1962). The deposit is exposed intermittently along strike near the northeastern flank of Sheep Mountain for about 1,311 m (4,300 ft). The trend ranges between N 30° W to N 45° W, with a dip of 25° NE (Hausel and Jones, 1982), but magnetic data suggests the deposit does not extend down dip (Hausel and Jones, 1982). The outcrop width is about 15 m (50 ft), and a prospect near the southeastern end exposes a maximum thickness of 5.2 m (17 ft) tapering to about 0.6 m (2 ft) thick (Houston and Murphy, 1962). Of six samples collected, an average composition of 63 percent heavy minerals included 84.2 percent opaques, 10.3 percent zircon, and 1 percent monazite. These samples vary from less than 0.001 percent to 0.007 percent cU (Houston and Murphy, 1962). The Crescent lode #1 property on this black sandstone contained 8 to 43 ppm cU_3O_8, 88 to 357 ppm eTh, <100 ppm La, <40 ppm Y, 32,300 ppm Ti, 7,170 ppm Zr, and 262 ppm Nb, plus monazite and thorite (Dribus and Nanna, 1982). Madsen (1978) reported a sample with 706 ppm La.

Rock Springs Formation

The Rock Springs Formation, of the Mesaverde Group in southwestern Wyoming, is 488 m (1,600 ft) thick in the northern part of the Rock Springs Uplift and comprises interbedded shale, carbonaceous shale, coal, siltstone, and delta-plain sandstone. It thins to the southeast as it intertongues with marine shale, sandstone, and siltstone of the upper part of the Blair Formation, also within the Mesaverde Group. Toward the southern end of the uplift, the Rock Springs Formation at Richard's Gap is less than 91 m (300 ft) thick and is dominated by interbedded sandstone and shale accompanied by minor thin beds of carbonaceous shale and coal (Roehler, 1989).

Heavy-mineral sands found in the McCourt Sandstone Tongue of the Rock Springs Formation are similar to those in the Mesaverde Formation in other parts of Wyoming. The Rock Springs Formation deposits are elongated lenses of dark-brown to black, fine to medium-grained, ferruginous sandstones as much as 2 m (6.6 ft) thick and 610 m (2,000 ft) long. These placers were deposited along a single shoreline during one stage of the interior Cretaceous sea's regression. The source for most of the heavy minerals was probably in the Sevier orogenic belt, 240 to 400 km (150 to 250 mi) to the west (Roehler, 1989).

Richard's Gap (Red Creek deposit), SE¼NW¼SE¼ sec. 22, T. 12 N., R. 105 W., Sweetwater County

This location, referred to as the Red Creek deposit by Houston and Murphy (1962), is about nine miles west of the common intersection of the Wyoming-Utah-Colorado borders and accessed by the Clay Basin road (Co. Rd. 62). This radioactive, titaniferous, black sandstone in the McCourt Sandstone Tongue of the Rock Springs Formation was described by Houston and Murphy (1962) and Roehler (1989). Outcrop of the black sandstone lens is elongated in the east-west direction with approximate dimensions of 457 m (1,500 ft) long, 244 m (800 ft) wide, and a thickness of 2 m (6.6 ft) tapering to 1.2 m (4 ft). However, the dense concentration of heavy minerals only covers about 38 m (125 ft) in length of this outcrop (Houston and Murphy, 1962; Roehler, 1989). Houston and Murphy (1962) reported abundant zircon and only minor monazite, while Madsen (1978) reported a sample with 700 ppm lanthanum (King and Harris, 2002).

Roehler (1989) describes two other minor lenses of heavy minerals at Richard's Gap. One is a 12 cm (4.8 in) thick lens of dark-brown, ferruginous, heavy-mineral sandstone less than 76 m (250 ft) long that tapers out in both

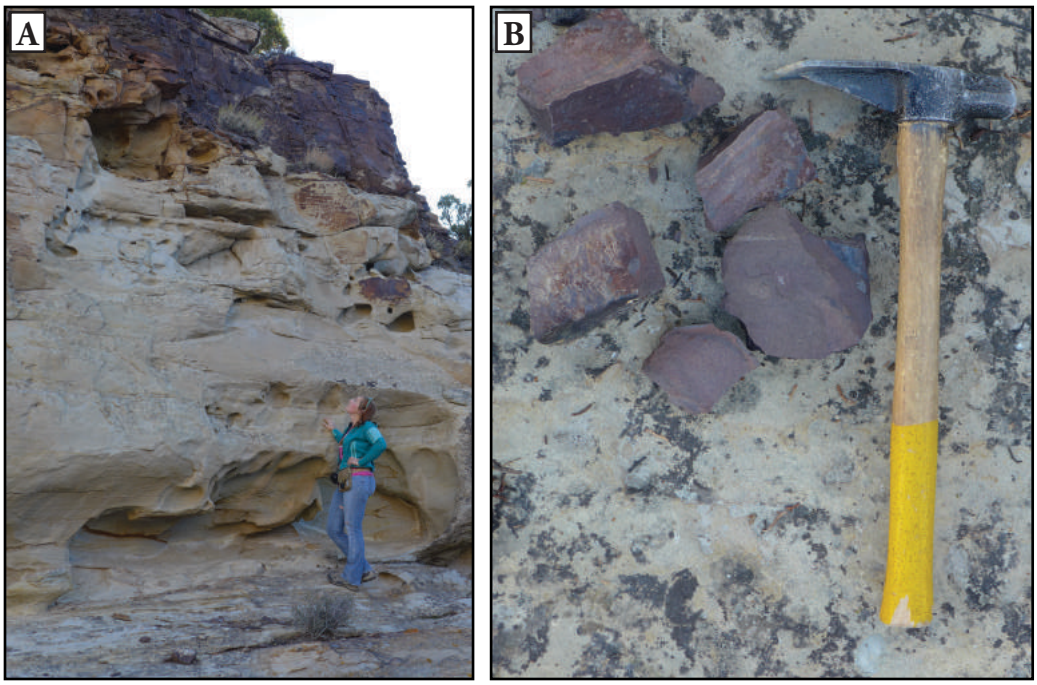


Figure 35. Richard's Gap. A) Outcrop of the McCourt Sandstone Tongue in the Rock Springs Formation with a layer of black sandstone above. B) Hand samples of the magnetitic, dense black sandstone containing elevated REE (Sample 20150929LC-2).

Table 37. Concentration of REE from Richard's Gap. Bold values indicate concentrations greater than five times the crustal abundance.

	Richard's Gap								
Element	La (ppm)	Ce (ppm)	Pr (ppm)	Nd (ppm)	Sm (ppm)	Eu (ppm)	Gd (ppm)	Tb (ppm)	Dy (ppm)
20150929LC-2	**483**	**927**	**99.9**	**356**	**55.8**	5.79	**38.2**	**5.53**	**30.4**
	Ho (ppm)	Er (ppm)	Tm (ppm)	Yb (ppm)	Lu (ppm)	Sc (ppm)	Y (ppm)	Cumulative REE (ppm)	
	6.78	**23.3**	**4.46**	**32.2**	**6.33**	83	**182**	**2,339.69**	

directions. The other is a small 18 cm (7 in) thick lens of unknown length in a trough of large-scale cross beds.

The thickest and most easily accessible exposure of the black sandstone was up a small gully in the Rock Springs Formation, east of the road. The surrounding rock is tan, cross-bedded sandstone with concretionary iron and huecos of various sizes. The color of the sandstone transitions from tan to rusty-brown near the contact with the iron-rich unit (fig. 35A). The rock composing the black sandstone (Sample 20150929LC-2) is dense, hard, and magnetic (fig. 35B). Each of the REE were elevated in the sample, and many of them were elevated much more than five times the average abundance. In fact, 15 times the average abundance of cerium was present as well as 14 times the lanthanum, and 11 times the lutetium, praseodymium, and ytterbium (table 37). Other elevated elements at this locale include 44.2 percent Fe_2O_3, 33.9 percent TiO_2, 785 ppm Hf, 434 ppm Nb, 1,200 ppm V, and >10,000 ppm Zr.

Salt Wells Creek (Titsworth Gap; Murphy no. 1), center SE¼ sec. 7, T. 14 N., R. 103 W., Sweetwater County

Here, a radioactive, titaniferous, black sandstone crops out near the top of the McCourt Tongue of the Rock Springs Formation near the southern end of the Rock Springs Uplift. The lenticular deposit, east of and about 91 m (300 ft) above the road, is 76 m (250 ft) long in the northeast-southwest direction and no more than 0.9 m (3 ft) thick (Houston and Murphy, 1962). However, Roehler (1989) describes the deposit as 610 m (2,000 ft) long. Samples contained monazite and zircon as well as 0.003 percent cU (Houston and Murphy; 1962), up to 0.04 percent eTh (Dow and Batty, 1961), 500 ppm La, and 100 ppm Y (Morris and Stanley, 1982).

Pretty Water Creek (Camel Rock; Murphy no. 2), SW¼ and W½SE¼ sec. 8, T. 16 N., R. 102 W., Sweetwater County

This northeast-trending outcrop of titaniferous, black sandstone is on the east flank of the Rock Springs Uplift. It is

located near the top of the McCourt Tongue at the base of gray cliffs in the overlying Ericson Sandstone (Roehler, 1989). Dow and Batty (1961) described the outcrop as 0.9 m (3 ft) thick and 137 m (450 ft) long. Roehler (1989) described a maximum thickness of 1.3 m (4.2 ft) near the north end of the deposit, which tapers progressively southward until pinching out. Samples collected by Dow and Batty (1961) contained up to 0.04 percent eTh, but analyses were not done for REE. Since REE are common in Wyoming black sandstones, this is an unverified rare earth locality (King and Harris, 2002). This site was visited by Sutherland and Cola (2015), but it was only possible to sample from the talus at the base of the extremely steep slope. Much of the material that appeared iron-rich was only sandstone coated with desert varnish (Sample 20141017WS-D). No elevated REE, or other elements of interest, were found.

Beacon (UPRR #1), sec. 19, T. 19 N., R. 101 W., Sweetwater County

The location of this radioactive, titaniferous, black sandstone deposit indicates that it is within the McCourt Tongue of the Rock Springs Formation. It is exposed for a length of 823 m (2,700 ft), with an average thickness of 2.1 m (7 ft) and average width of 46 m (150 ft; Dow and Batty, 1961). Samples contained 500 and 700 ppm La, 100 and 300 ppm Y, with 28 and 40 ppm cU_3O_8 (Morris and Stanley, 1982; King and Harris, 2002).

Bradley Road (Honnes Ranch; UPRR #2), SW¼ sec. 11 and N½NW¼ sec. 14, T. 17 N., R. 102 W., Sweetwater County

This tan to dark-brown, titaniferous sandstone, in a 17.4 m (57 ft) thick section of the McCourt Tongue, caps a ridge for 762 m (2,500 ft). It is between 15 and 30 m (50 and 100 ft) wide and averages 1.2 m (4 ft) thick (Dow and Batty, 1961). Samples contained 55 ppm cU_3O_8, 1,000 ppm La, and 100 ppm Y (Morris and Stanley, 1982). The magnetite-ilmenite-bearing deposit was investigated for economic iron potential by Wilson (1976) who collected samples from a shaft that contained 20.2 percent iron and 21.2 percent TiO_2. This area has been cut by a normal fault that dropped the northeasterly third of the mineralized zone about 18 m (60 ft) below the southwestern part of the deposit (Sutherland and Cola, 2015). The occurrence of REE in this deposit remains unverified.

Cooper Ridge, NE¼NW¼SE¼ sec. 1, T. 17 N., R. 102 W., Sweetwater County

This heavy-mineral deposit occurs in two thin beds within the McCourt Tongue of the Rock Springs Formation. The deposit is poorly exposed but visible from the road as a thin black streak within sandstone outcrops near the base of Cooper Ridge. The lower of the two dark-brown, heavy-mineral sandstones is thinner, and they are separated by a thin, extensively iron-stained sandstone that contains lesser amounts of heavy minerals. Maximum combined thickness of both heavy-mineral and intervening beds is 1 m (3.3 ft) with an overall length of 37 m (120 ft; Roehler, 1989). Love and Murphy (1962) reported 0.015 percent eU and 28.0 percent TiO_2. No analyses have been done for REE, so this remains an unverified occurrence of REE-bearing minerals.

Black Butte (Zalenka deposit), sec. 30, T. 18 N., R. 101 W.; sec. 1, T. 17 N., R. 102 W., Sweetwater County

This well exposed deposit is at the top of a bench-forming sandstone along the lower part of a slope in the McCourt Tongue. The dark-brown to black, heavy-mineral sandstone forms thin and lenticular layers that pinch and swell. Light-gray, quartzose sandstone laminae separate these layers (Roehler, 1989). The deposit trends northeast for about 457 m (1,500 ft) and has a thickness of 0.9 to 1.2 m (3 to 4 ft; Houston and Murphy, 1962). Samples contained an average 14.0 percent TiO_2, <0.001 to 0.003 percent cU (Houston and Murphy, 1962), 0.06 percent eTh (Dow and Batty, 1961), 1,000 and 1,500 ppm La, and 100 and 500 ppm Y (Morris and Stanley, 1982). A smaller, poorly exposed deposit, about 0.3 m (1 ft) thick, caps a low ridge about 3.2 km (2 mi) south-southwest of this deposit (Houston and Murphy, 1962).

Yenko deposit (Dans Creek), sec. 13, T. 15 N., R. 103 W., Sweetwater County

The Yenko deposit is a magnetite-ilmenite-bearing black sandstone reported in the basal part of the Ericson Sandstone; but, based on the stratigraphy of similar deposits in the Rock Springs Uplift, it is likely in the top of the McCourt Sandstone Tongue of the Rock Springs Formation. The deposit crops out on the west wall of a mesa and trends northeast until disappearing under a 61 m (200 ft) thick cover of younger sediments. It has a width of 76 m (250 ft) and an average thickness of 1.7 m (5.5 ft). The average composition of four samples from the deposit included 16.3 percent iron and 22.4 percent TiO_2 (Dow and Batty, 1961). No REE analyses are known for this deposit, but their speculative occurrence is based on the similarity to other heavy-mineral paleoplacers within the Rock Springs Formation.

Frontier Formation

The Upper Cretaceous Frontier Formation is dominated by dark-gray to black marine shale interbedded with siltstone and persistent beds of fine- to coarse-grained sandstone. Thin beds of white to yellow bentonite, porcellanite, and impure coal are found in the lower part (Love and others, 1979), and some sandstones are interpreted to be

paleo-beach placers (Houston and Murphy, 1962). The Frontier Formation is overlain by the Cody Shale, or the stratigraphic equivalent, and lies on top of the Mowry Shale (Love and others, 1993).

Spring Gap, SE¼NW¼ sec. 30, T. 16 N., R. 117 W., Uinta County

Madsen and Reinhart (1982) reported up to 1,000 ppm lanthanum, 80 ppm yttrium, <100 ppm niobium, and 660 ppm eTh within altered sandstone in the Cretaceous Frontier Formation. This sandstone exhibits an elemental assemblage typical of beach placer deposits and contains limonite, pyrite, leucoxene, and an unidentified REE-bearing mineral. The stratigraphy of samples reported by Madsen and Reinhart (1982) is ambiguous (King and Harris, 2002), but recent mapping (M'Gonigle and Dover, 2004) and field investigations (Sutherland and others, 2013) show that this sandstone is within the lower third of the Frontier Formation.

Near the area sampled by Madsen and Reinhart (1982), an exploration trench exposes light-green to yellow weathering, angular to subangular, medium- to coarse-grained sandstone, with approximately 25 percent weathered plagioclase, 40 percent quartz, 35 percent mafic minerals, 5 percent biotite, and minor limonite and hematite staining (table 38; Sample 20121128JC-E). This weathered sandstone unit is overlain by a dark-green to dark-brown, angular, medium- to coarse-grained laminated sandstone with approximately 40 percent mafic minerals, 25 percent limonite, 20 percent weathered plagioclase, 10 percent quartz, 5 percent black opaques, and calcite-filled fractures (Sample 20121128JC-D). In places, the mafic minerals in the upper portion of the exposure appear to have grown around plagioclase. Background radioactivity in the area is 900 cpm, and the upper mafic-rich unit exhibits up to three times the background at 2,600 cpm; the lower unit exhibits no anomalous radioactivity. The bedding here strikes 202° and dips 55° NW. The lower, light-green sandstone (Sample 20121128JC-E) is not significantly enriched in any of the REE. However, the upper, dark-green to dark-brown sandstone (Sample 20121128JC-D) is enriched in all of the REE as well as scandium, yttrium, and niobium; only europium, lutetium, and scandium are enriched less than five times the average crustal abundance (table 38; Sutherland and others, 2013).

Frontier Formation-Spring Gap, NE¼SW¼ sec. 8, T. 16 N., R. 117 W., Uinta County

The same altered Frontier Formation sandstone, as that sampled in section 30, crops out here and is reported by Madsen and Reinhart (1982) to contain 650 ppm lanthanum, 50 ppm yttrium, 120 ppm niobium, 600 ppm eTh, 25 ppm eU, and an elemental assemblage typical of beach placer deposits. The sandstone exposed in a prospect pit at this locality is similar to Sample 20121128JC-D. It is dark-green to dark-brown, angular, and medium- to very coarse grained, with approximately 40 percent mafic minerals, 20 percent limonite, 20 percent weathered plagioclase, 10 percent quartz, 2.5 percent black opaque minerals, 2.5 percent hematite, and calcite filled fractures (Sample 20121128JC-F). Some mafic minerals appear to have grown around plagioclase grains making them probable products of alteration (Sutherland and others, 2013). Background radioactivity at this location was 650 cpm away from the outcrop, 1,000 cpm near the outcrop, and up to five times background (3,300 cpm) at the point of sampling. This sample (20121128JC-F) is enriched in all of the naturally occurring REE as well as scandium, yttrium, and niobium; the LREE are all enriched to greater than five times the average abundance (table 38). Monazite is identifiable in thin-section within Sample 20121128JC-F and is likely present in Sample 20121128JC-D (Sutherland and others, 2013).

Table 38. Concentration of REE from Spring Gap area and Frontier Formation. Bold values indicate concentrations greater than five times the crustal abundance.

	Spring Gap-Frontier Formation								
Element	La (ppm)	Ce (ppm)	Pr (ppm)	Nd (ppm)	Sm (ppm)	Eu (ppm)	Gd (ppm)	Tb (ppm)	Dy (ppm)
20121128JC-D	**2,430**	**4,110**	**395**	**1,225**	**145.5**	5.39	**69.9**	**8.35**	**41.1**
20121128JC-E	40.8	72.8	8.49	32.7	6.4	1.7	5.66	0.85	4.88
20121128JC-F	**990**	**1,650**	**160.5**	**499**	**57.4**	3.06	**25.7**	**2.73**	**12.55**

Element	Ho (ppm)	Er (ppm)	Tm (ppm)	Yb (ppm)	Lu (ppm)	Sc (ppm)	Y (ppm)	Cumulative REE (ppm)
20121128JC-D	**7.23**	**18.1**	**2.54**	**14.75**	2.26	85	**184**	**8,744.12**
20121128JC-E	0.98	2.76	0.41	2.38	0.36	10	29.1	220.27
20121128JC-F	2.09	5.1	0.73	4.29	0.67	37	53.8	**3,504.62**

From Sutherland and others (2013)

Cumberland Gap, SE¼ sec. 25, T. 18 N., R. 117 W.; W¼ sec. 18 and NW¼ sec. 30, T. 18 N., R. 116 W., Uinta County

Monazite was found in this radioactive, titaniferous, black sandstone in the lower part of the Frontier Formation. The radioactivity of the area is nearly five times the background, and uranium content ranges 0.001 to 0.002 percent cU. The longest exposure of the deposit is 183 m (600 ft) but is estimated as being more than 4,023 m (13,200 ft) long and 61 m (200 ft) wide (Houston and Murphy, 1962). Samples taken at the northeast and southwest ends of the deposit yielded 0.01 and 0.02 percent eTh, respectively (Dow and Batty, 1961). This REE occurrence is unverified, and its inclusion here is based on similarity to other deposits in the absence of chemical analyses (King and Harris, 2002).

Thermopolis Shale

The Lower Cretaceous Thermopolis Shale is dominantly soft black shale with thin bentonite layers near the top and bottom (Love and others, 1979). A few thin, silty sandstones are sometimes found in the middle part, and large iron stone concretions are common (Skipp, 1957; Sutherland and Cola, 2015). The Thermopolis is directly beneath the Muddy Sandstone, and overlies the Cloverly Formation (Love and others, 1993).

dahllite concretions, NW¼NE¼ sec. 14, T. 53 N., R. 94 W., Big Horn County

The Thermopolis Shale at the Wyo-Ben bentonite mine near Greybull is 76 to 91 m (250 to 300 ft) thick and consists of black to gray, bentonitic shale interbedded with thin yellow to brown siltstone which grades to sandstone beds near its base (Kozimko, 1985; Ladd, 1985). Dahllite [$Ca_5(PO_4,CO_3)_3(OH,O)$] concretions (fig. 36) are present near the base of the Thermopolis Shale in the Bighorn Basin (Moberly, 1962) and have also been noted in southwestern Montana (Dyman and others, 2000). The concretions are gray, spheroidal, have a rough surface, and have a radial fibrous texture in cross-section. A sample of these concretions (20121018JC-E) is enriched in all of the REE plus yttrium; of these, gadolinium, terbium, and yttrium are all enriched greater than five times the crustal abundance (table 39; Sutherland and others, 2013).

Table 39. Concentration of REE in dahllite near the Wyo-Ben Mine. Bold values indicate concentrations greater than five times the crustal abundance.

	Wyo-Ben Mine dahllite								
Element	La (ppm)	Ce (ppm)	Pr (ppm)	Nd (ppm)	Sm (ppm)	Eu (ppm)	Gd (ppm)	Tb (ppm)	Dy (ppm)
20121018JC-5	65.4	135	20.1	93.2	24.4	6.32	**31.9**	**4.83**	26.7
	Ho (ppm)	Er (ppm)	Tm (ppm)	Yb (ppm)	Lu (ppm)	Sc (ppm)	Y (ppm)	Cumulative REE (ppm)	
	4.96	10.8	1.15	5.56	0.72	9	**187.5**	627.5	

From Sutherland and others (2013)

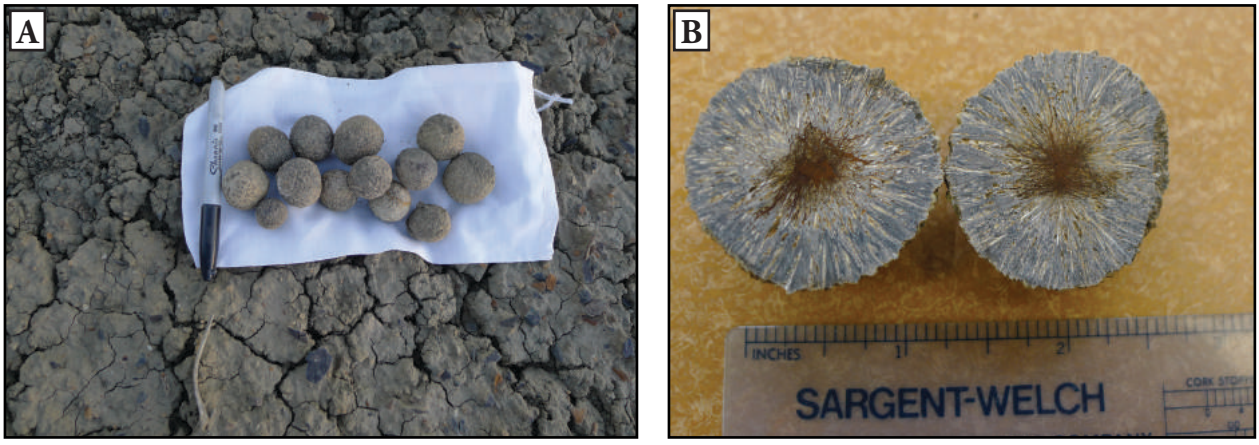


Figure 36. Dahllite concretions from the Cretaceous Thermopolis Shale near the Wyo-Ben bentonite mine, northwest of Greybull. A) Sample 20121018JC-E collected during RI-65 (Sutherland and others, 2013). B) Interior of a dahllite concretion.

Cloverly-Morrison Formations

The Lower Cretaceous Cloverly Formation unconformably overlies the Upper Jurassic Morrison Formation, and their combined thickness varies regionally from about 30 to 152 m (100 to 500 ft). Because of the relative thinness in many areas and difficulty in picking their mutual contact in the field, the two formations are often combined. The top of the Cloverly is a white to gray, fine-grained, cross-bedded, slabby quartz sandstone that forms a quartzite in some areas. The top sandstone is underlain by lenticular variegated shale and claystone in the middle of the formation, and hosts a hard, brown to gray and buff, quartz and chert pebble conglomerate at the base (Pekarek, 1977; Love and others, 1979; Sutherland and Hausel, 2005). The Morrison Formation is variegated, silty, siliceous claystone and siltstone interbedded with gray to white silty sandstone. These beds are occasionally accompanied by marlstone and limestone lenses (Pekarek, 1977; Love and others, 1979). The Cloverly-Morrison Formations lie beneath the Thermopolis Shale and conformably overlies the Jurassic Sundance Formation (Love and others, 1993).

Crooked Creek group claims, sec. 27 and 28, T. 58 N., R. 95 W., Big Horn County

Radioactive, uranium roll-front type mineralization occurs along the contact between the Morrison and Cloverly Formations as well as in limonite stained channel sandstones in these formations (Hart, 1955b). Sample analyses were reported to contain 40 to 100 ppm La, 100 ppm Zr, 3,000–4,000 ppm Ti, and at least 100 ppm Y. The sample collected with the highest chemical uranium showed 500 ppm Y and 100 ppm La, while the sample with the highest radiometric uranium was not enriched in REE (Garrand and others, 1982). The origin of the yttrium enrichment is not known since it is uncommon to find abundant rare earths in roll-fronts. It is possible the value is a typographical error, 50 not 500, and the high titanium could indicate an additional, local, heavy-mineral deposit (King and Harris, 2002).

North Sheldon Gulch, NW¼SE¼ sec. 33, T. 53 N., R. 91 W., Big Horn County

This locale is characterized by variegated layers of the Cloverly-Morrison Formations (fig. 37; Love and Christiansen, 1985), which can be found along the gulch to the northwest and southeast (fig. 38A). Dense calcium phosphate concretions (fig. 38B), iron concretions, belemnites, crystalline gypsum, and gastroliths (fig. 38C) are scattered throughout gray bentonitic clay at the sample site. Hail (1954) reported radioactive iron stone concretions within a bentonitic shale, and later analysis of the concretions by Damp and Jennings (1982) found elevated yttrium, at 167 ppm, and 17 percent P_2O_5. Rare earth enrichment was associated with the phosphatic nature of the concretions (King and Harris, 2002). Sample 20150812LC-3A, composed of the dense calcium phosphate concretions (fig. 38B), exhibited significant REE concentrations and 18.4 percent P_2O_5. All the REE except scandium were enriched above the quintupled crustal average. Many even reach 10 times the crustal abundance, and gadolinium was present at almost 30 times the crustal abundance (table 40). Selenium was also elevated in the calcium phosphate concretions at 21.1 ppm, and barium was elevated to 5,870 ppm in the bentonitic layer (20150812LC-3B).

Shell Creek prospect (Reeves Ranch), sec. 11, T. 52 N., R. 92 W., Big Horn County

At this location, high radioactivity, 25 to 30 times background, is attributed to occasionally pyritic, black, silicified bones in the Morrison Formation. These are primarily found at the base of a 12 foot thick lens of gray, medium-grained sandstone (Osterwald, 1950). Silicified wood and carbonaceous material in the area are not radioactive (Reyner, 1950). Mudstone in the area contained little uranium and no rare earth enrichment. However, the pyritic dinosaur bones contained 230 ppm La, 298 ppm Nb, 96,200 ppm P, 1,050 ppm Sr, 645 ppm Ti, 307 ppm W, 384 ppm Y, 299 ppm Zr, 1 ppm eTh, and 2,026 ppm eU (Damp and Jennings, 1982). The REE enrichment is probably due to the elevated phosphates (King and Harris, 2002). During this study, sampling of the area did not produced elevated REE. Samples of calcite-rich nodules (20150812LC-2A) and blue-gray chert nodules (20150812LC-2C), taken from a dark-grayish-purple bentonitic clay layer, contained 4,340 and 4,120 ppm Ba, respectively.

Bobcat Gulch-Hyattville area, sec. 31, T. 49 N., R. 89 W., Big Horn County

Damp and Jennings (1982) report dinosaur bones in alluvium. An assayed sample contained 749 ppm U, 2 ppm eTh, 110 ppm La, 628 ppm Nb, >100,000 ppm P, 5,350 ppm Sr, 126 ppm Y, and 619 ppm Zr. Enriched REE is probably due to the phosphatic nature of the bones (King and Harris, 2002). During this study, sampling was done near Bobcat Gulch and although no elevated rare earths were present, other elements of economic interest were found. Iron concretions (Sample 20150812LC-4B) scattered within cross-bedded sandstone contained >250 ppm As, 19.2 ppm Se, and 3.1 ppm Ag. A fine-grained, grayish-white quartzite (20150812LC-4C) capping the area contained 96.5 percent SiO_2. This chemical content could be of interest for high purity silica usages.

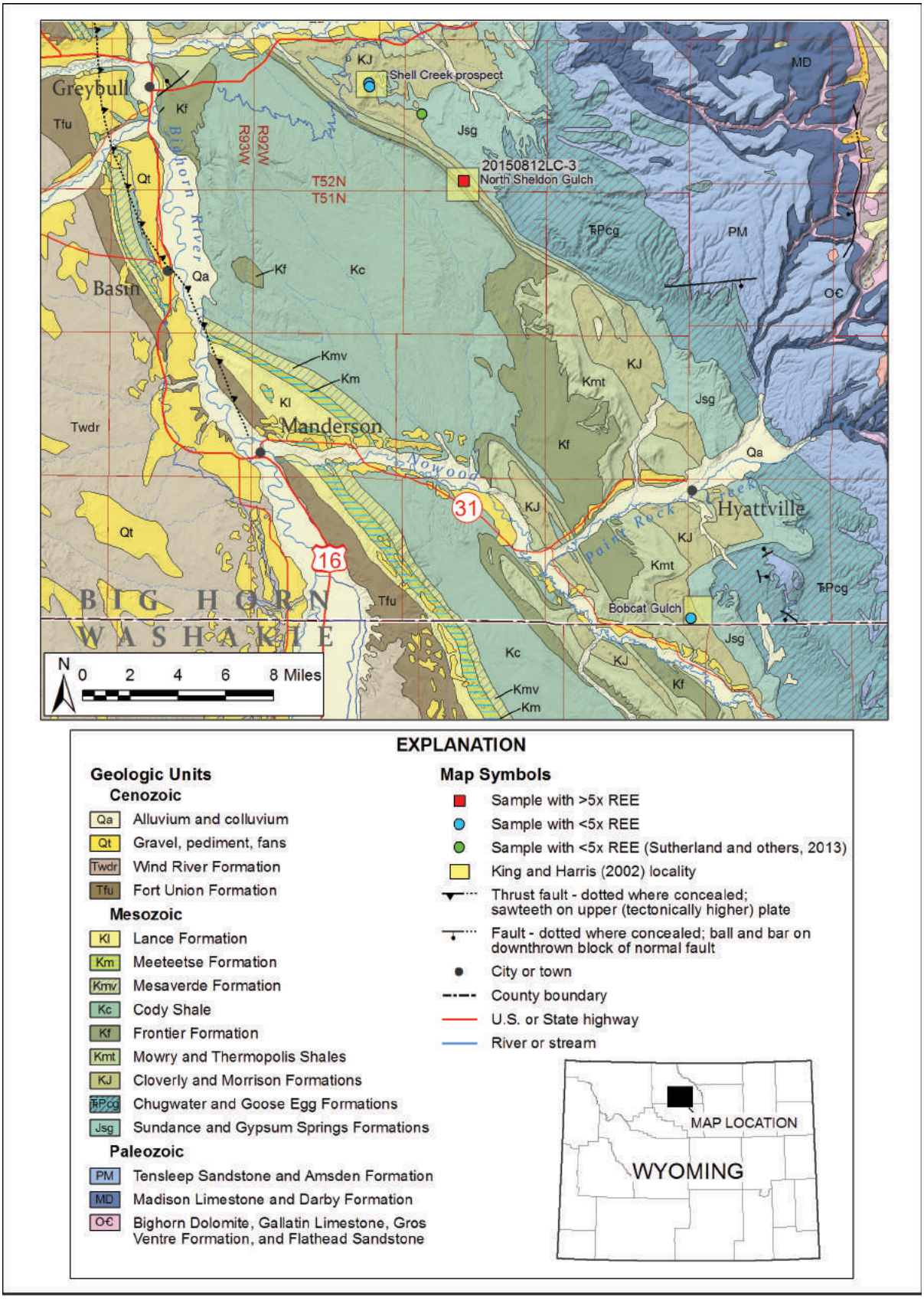


Figure 37. Sample locations and geology of northeast Bighorn Basin. One sample contained extremely elevated REE in the Morrison-Cloverly Formations. Map modified from Love and Christiansen (1985).

Table 40. Concentration of REE from North Sheldon Gulch. Bold values indicate concentrations greater than five times the crustal abundance.

	North Sheldon Gulch								
Element	La (ppm)	Ce (ppm)	Pr (ppm)	Nd (ppm)	Sm (ppm)	Eu (ppm)	Gd (ppm)	Tb (ppm)	Dy (ppm)
20150812LC-3A	**170.5**	**498**	**72.5**	**387**	**110**	**23**	**129.5**	**17.45**	**89**
	Ho (ppm)	Er (ppm)	Tm (ppm)	Yb (ppm)	Lu (ppm)	Sc (ppm)	Y (ppm)	Cumulative REE (ppm)	
	15.05	**39.7**	**5.2**	**32.8**	**4.27**	6	**430**	**2,029.97**	

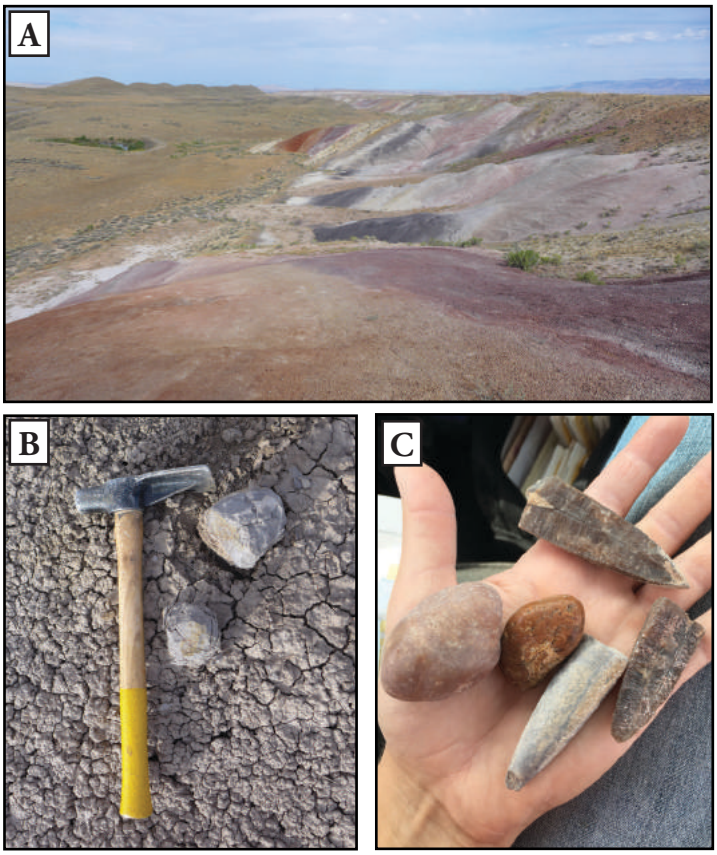


Figure 38. North Sheldon Gulch. A) A view of the variegated Cloverly-Morrison Formations to the northwest from the North Sheldon Gulch locale. B) Calcium phosphate concretions containing extremely elevated REE within the Cloverly-Morrison Formations (Sample 20150812LC-3A). C) Belemnite fossils and gastroliths from this locale.

Poison Creek, NE¼SW¼SW¼ sec. 36, T. 48 N., R. 83 W., Johnson County

Dinosaur bones in the Jurassic Morrison Formation at this location contained 962 ppm eU, 0 ppm eTh, 58 ppm La, >100,000 ppm P, 1,190 ppm Sr, 729 ppm W, 123 ppm Y, 217 ppm Zn, and 822 ppm Zr (Damp and Jennings, 1982). The yttrium enrichment is attributed to the high amount of phosphate in the bones (King and Harris, 2002).

Phosphoria Formation

In central Wyoming, the Permian Phosphoria Formation consists of about 107 m (350 ft) of interbedded chert, limestone, dolomite, siltstone, very fine sandstone, thin beds of phosphate rock, and shale as well as a thin basal conglomerate present at many localities. The Phosphoria is interbedded with and grades into the lower part of the Goose Egg Formation, causing complex relationships between the two (Zeller and others, 1956; Carey, 1959; Keefer, 1966). In western Wyoming, the Phosphoria is much thicker and subdivided into five units from bottom to top: a lower chert unit, the Meade Peak Member, the Rex Chert Member, the Retort Member, and the Tosi Chert Member (Sheldon, 1963; Carnes, 2015). The Phosphoria Formation lies unconformably beneath the Triassic Dinwoody Formation and unconformably overlies the Pennsylvanian Tensleep Sandstone or its equivalent (Love and others, 1993). As mentioned earlier, the Phosphoria has been mined in Wyoming and Idaho for phosphates, and although REE were reported in Idaho mines, little or no REE production has occurred. Sample locations below are grouped by their vicinity in the Wyoming Range (fig. 39) and the Gros Ventre Range (fig. 23). Although the Gros Ventre Range has REE potential, samples are typically located within the Gros Ventre Wilderness area, making them isolated and difficult to access, which limits economic feasibility.

Teton Pass, sec. 23, T. 41 N., R. 118 W., Teton County

A phosphate unit with 2.34 percent P_2O_5 and 0.013 percent U_3O_8 was reported west of Teton Pass (Benham, 1984). This area also contained 170 ppm La, 220 ppm Y, and 36 ppm Ce as reported by Motooka and others (1984; King and Harris, 2002).

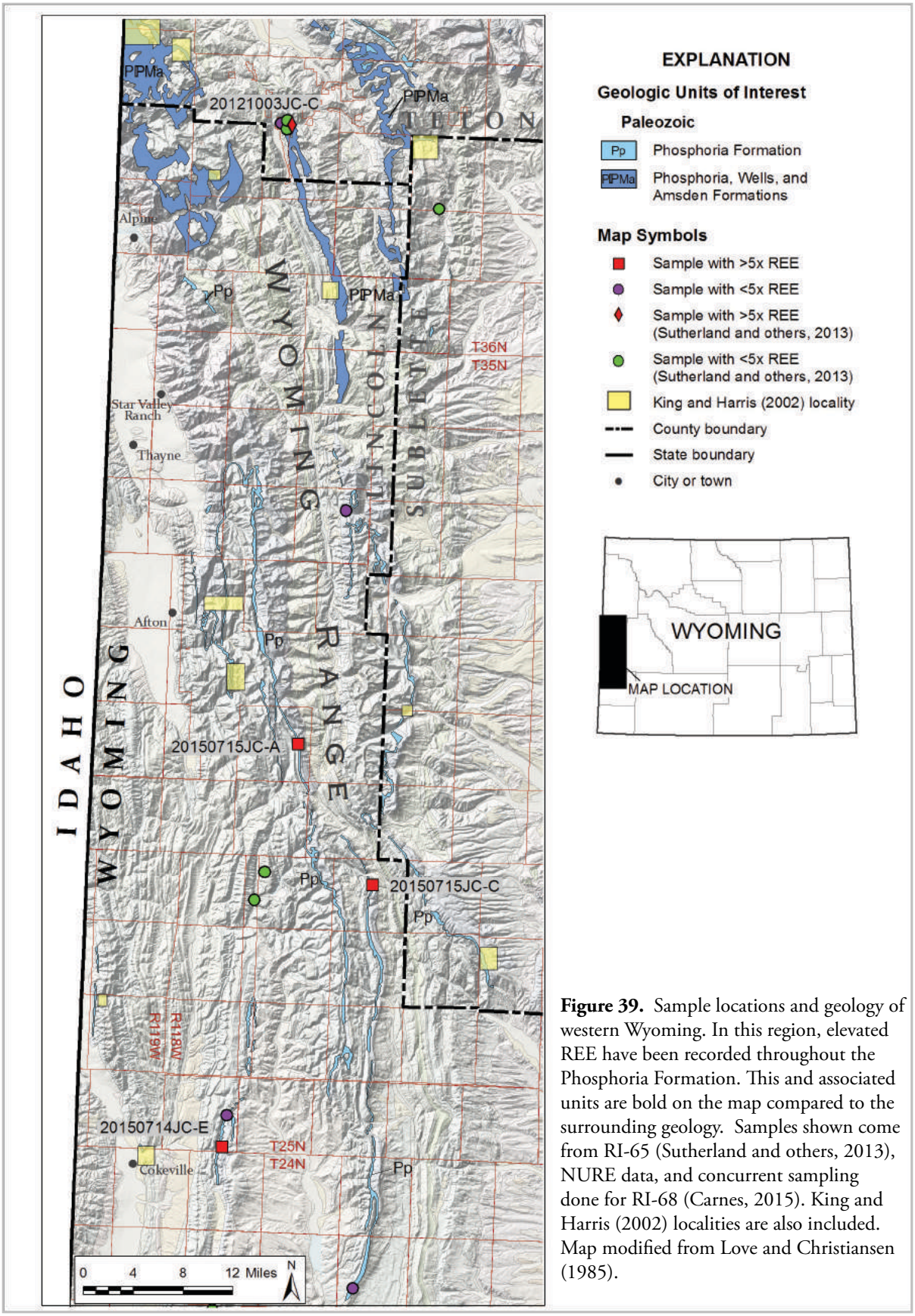


Figure 39. Sample locations and geology of western Wyoming. In this region, elevated REE have been recorded throughout the Phosphoria Formation. This and associated units are bold on the map compared to the surrounding geology. Samples shown come from RI-65 (Sutherland and others, 2013), NURE data, and concurrent sampling done for RI-68 (Carnes, 2015). King and Harris (2002) localities are also included. Map modified from Love and Christiansen (1985).

Siddoway Fork, sec. 8, T. 1 N., R. 46 E. (Idaho); T. 40 N., R. 118 W., Teton County

Sampling in a stratigraphic section of Phosphoria Formation yielded 110 to 180 ppm La, 150 to 200 ppm Y, 21 to 44 ppm Ce, and 8.4 to 17 percent P (Motooka and others, 1984). Sampling by Benham (1984) could not be correlated with these (King and Harris, 2002).

Smokey Hollow, S½ sec. 33, T. 40 N., R. 118 W., Teton County

Phosphorite and phosphate-rich rock were sampled from a stratigraphic section in the Phosphoria Formation at this locale (Benham, 1984; Motooka and others, 1984). Samples contained 130 to 220 ppm La, 130 to 270 ppm Y, 32 to 59 ppm Ce, and 6.6 to 9.6 percent P (Motooka and others, 1984).

North Fork Big Elk Creek, sec. 11, T. 39 N., R. 118 W., Teton County

Phosphate-rich rock and phosphorite sampled here contained 97 to 520 ppm La, 150 to 520 ppm Y, 26 to 140 ppm Ce, and 7.1 to 14 percent P (Motooka and others, 1984; Benham, 1984; King and Harris, 2002).

Hoback, SW¼NE¼ sec. 32, T. 39 N., R. 116 W., Teton County

The Phosphoria Formation crops out in extensively folded and faulted terrain along U.S. Hwy 89, near the historic town site of Hoback, and was the target of a phosphate exploration trench (Albee, 1968). The Phosphoria overlays the Mississippian and Pennsylvanian Wells Formation and is overlain by the Triassic Dinwoody Formation. The northeastern margin of this outcrop is cut by a high-angle fault that places the Phosphoria Formation in fault contact with the Wells Formation (Albee, 1968). The Astoria mineral hot spring is located 335 m (1,100 ft) east-southeast of this outcrop (Breckenridge and Hinckley, 1978) and indicates that the overall area may have experienced hydrothermal activity at some point in the past.

The Phosphoria Formation in this area (fig. 39) includes the Meade Peak Phosphatic Shale Member and an overlying, unnamed, tan mudstone interbedded with chert-bearing limey mudstone (Sample 20121003JC-A). The Meade Peak is composed of black, moderately- to well-indurated, massive mudstone (Sample 20121003JC-B) interbedded with black, fissile, poorly indurated shale (Sample 20121003JC-C). The Meade Peak Member is about 15 m (50 ft) thick at this locality, and the overall thickness of the Phosphoria Formation is about 55 m (180 ft). Bedding within the Phosphoria strikes 288˚ and dips 21˚ NW. The upper black shale of the Meade Peak Member is the most phosphatic unit sampled at this location, with 10.4 percent P_2O_5. Significant REE enrichment is only observed here within the black phosphatic shale; lanthanum and yttrium are the only REE enriched greater than five times the average abundance (table 41). The black shale is also enriched in various metals, most notably chromium, nickel, cadmium, and molybdenum. Also, a sample of mudstone in the area (20150716JC-B), that had no elevated REE, contained 95.9 ppm Se, 8.7 ppm Ag, and 1,550 ppm Zn.

Wolf Creek, SW¼ sec. 28, T. 38 N., R. 117 W., Lincoln County

Nine separate phosphorite units in the Phosphoria Formation were sampled at this location. They contained 140 to 320 ppm La, 170 to 440 ppm Y, and 48 to 90 ppm Ce (Motooka and others, 1984). Sampling by Benham (1984), which yielded 0.004 to 0.016 percent U_3O_8, 2.45 to 2.90 percent F, and 27.73 to 33.44 percent P_2O_5, probably correlates with this area (King and Harris, 2002).

Bear Creek Gulch-Hoback Canyon, sec. 6, T. 38 N., R. 114 W., Sublette County

A sample taken here contained 196 ppm Y, 160 ppm La, 34 ppm Pr, 96 ppm Nd, 24 ppm Sm, 5.8 ppm Eu, 3.5 ppm Tb, 3.9 ppm Ho, 2.09 ppm Tm, and 11 ppm Yb (Schofield and Haskin, 1964; King and Harris, 2002).

Steer Creek, sec. 9, T. 36 N., R. 116 W., Lincoln County

Two samples of pellet phosphorite in the Meade Peak Member contained 0.012 and 0.015 percent cU, 29.6 and 25.0 percent P_2O_5, 3.03 and 2.33 percent F, and rare earth enrichment in the form of 100 and 300 ppm La, 300 ppm Y, 300 ppm Nd, and 10 ppm Yb (Gulbrandsen, 1966; Cheney and others, 1953; King and Harris, 2002).

Middle Piney Lake, NE¼NW¼ sec. 8, T. 30 N., R. 115 W., Sublette County

At this location, pellet phosphorite in the Meade Peak Member contained 0.004 and 0.12 percent cU, 28.9 and 25.0 percent P_2O_5, 2.92 and 3.10 percent F, 300 ppm La, 100 and 300 ppm Y, 300 ppm Nd, and 10 ppm Yb (Gulbrandsen, 1966; Sheldon and others, 1953; King and Harris, 2002).

Poison Creek, SW¼SE¼ sec. 13, T. 30 N., R. 117 W., Lincoln County

This locale, as well as the following two, were sampled for a recent study on phosphate rock in Wyoming (Carnes, 2015). Sample 20150715JC-A (fig. 40), located a little more than 6.4 km (4 mi) east of Mount Wagner along Forest Road 10072, is a non-calcareous mudstone in the Phosphoria Formation with fine- to medium-grained

Table 41. Concentration of REE from the Phosphoria Formation. Bold values indicate concentrations greater than five times the crustal abundance.

	Phosphoria Formation								
Element	La (ppm)	Ce (ppm)	Pr (ppm)	Nd (ppm)	Sm (ppm)	Eu (ppm)	Gd (ppm)	Tb (ppm)	Dy (ppm)
20121003JC-A*	5.7	3.7	85	3.2	0.52	0.14	0.62	0.1	0.64
20121003LC-B*	37.4	53.2	7.48	28.3	5.6	1.1	5.09	0.81	4.69
20121003JC-C*	**218**	67.9	26.8	105.5	17.1	3.62	19.65	2.85	18.7
20150714JC-E	142	116.5	28.3	115	20.4	6.11	22.8	3.17	18.3
20150715JC-A	**283**	88.4	37.1	141.5	24.1	5.06	**30.7**	**4.14**	**28.8**
20150715JC-C	**198.5**	53.8	19.8	73.7	11.4	2.49	15.5	2.06	14.7
20150715JC-E	**491**	88.5	**75.9**	**296**	**48.6**	**11.4**	**61.4**	**7.69**	**50.3**
20150714JC-A	154	109	26.6	105	17.4	5.45	21.2	2.92	17.85

Element	Ho (ppm)	Er (ppm)	Tm (ppm)	Yb (ppm)	Lu (ppm)	Sc (ppm)	Y (ppm)	Cumulative REE (ppm)
20121003JC-A*	0.14	0.47	0.07	0.45	0.08	<1	8.8	109.63
20121003LC-B*	1.02	3.1	0.47	3.32	0.54	8	34.6	194.72
20121003JC-C*	4.59	14.1	2.07	12.05	2.01	9	**306**	829.94
20150714JC-E	3.86	10.65	1.35	7.92	1.14	5	**202**	704.50
20150715JC-A	**7.4**	**22.8**	**3.13**	**18.2**	**2.99**	7	**525**	**1,229.32**
20150715JC-C	3.91	12.3	1.77	10.9	1.85	8	**310**	740.68
20150715JC-E	**12.15**	**35.8**	**4.7**	**27.3**	**4.27**	4	**790**	**2,009.01**
20150714JC-A	1.16	10.55	1.54	7.89	1.16	6	**207**	694.72

*Samples from Sutherland and others (2013)

Other samples from Carnes (2015)

apatite pellets and a strong sulfur odor. Yttrium was the only element enriched five times above the average abundance, but many other REE were elevated to some extent (table 41).

Shafer Creek, SW¼NE¼NW¼ sec. 15, T. 28 N., R. 116 W., Lincoln County

A similar sample (20150715JC-C) taken east of Bull Mountain near Forest Road 10166, with a slightly calcareous matrix and apatite pellets, was slightly elevated in most REE. Both lanthanum and yttrium were present at greater than five times average crustal abundance (table 41). In addition, Tl was present greater than 10 times and Se greater than 180 times the crustal abundance.

Middle Fork Pine Creek, NW¼NE¼SE¼ sec. 35, T. 25 N., R. 118 W., Lincoln County

Again, Sample 20150714JC-E was similar to the above samples but had a limonite-rich matrix. It contained many elevated REE as well as 1,130 ppm Cr, 31.8 ppm U, and 6.2 ppm Se. Another sample at this location (20150715JC-E) bearing elevated REE, selenium, and 53.4 ppm U was a weak to non-calcareous packestone with fine- to medium-grained apatite pellets and coarse to very coarse grained concentrically ringed apatite "ooids." While multiple REE and selenium were elevated quintuple the average in the Phosphoria Formation, yttrium was often elevated 7, 18, and even 27 times the crustal abundance (table 41).

Cokeville section, NW¼ sec. 4, T. 24 N., R. 119 W., Lincoln County

Samples of pellet phosphorite from the Meade Peak Member of the Phosphoria Formation contained 0.004 and 0.021 percent cU, 23.0 and 32.4 percent P_2O_5, and 2.03 and 3.55 percent F. Rare earth enrichment included 300 ppm Y, 300 ppm Nd, 100 ppm La, and 10 ppm Yb (Gulbrandsen, 1966; Sheldon and others, 1953; King and Harris, 2002).

Raymond Canyon, NW¼NE¼ sec. 6, T. 26 N., R. 119 W., Lincoln County

Thirty-one samples of phosphorite and phosphate-rich rock were taken across 106 stratigraphic feet in the Meade Peak

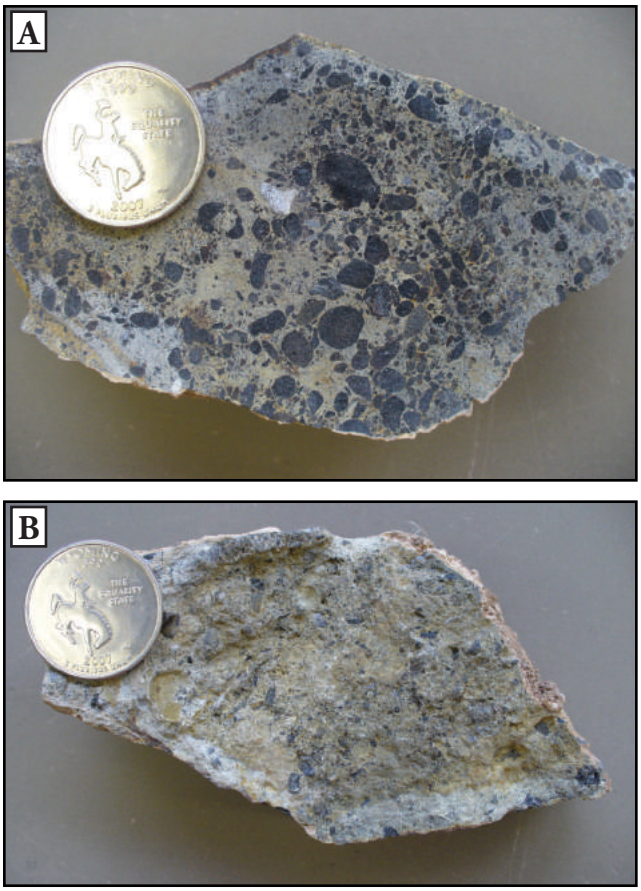


Figure 40. Sample of Phosphoria Formation from the Poison Creek area with coarse-grained, rounded to subrounded clasts of dark mudstone in a fine-grained, limonite-stained matrix as A) A fresh cut surface. B) The naturally weathered appearance (Sample 20150715JC-A).

Member here. The section contained 0.002 to 0.30 eU, 10.73 to 36.32 percent P_2O_5, 50 to 700 ppm La, 50 to 1,000 ppm Y, and up to 700 ppm Nd (Vine, 1966; Sheldon and others, 1953; King and Harris, 2002).

Deadline Ridge, sec. 8, T. 27 N., R. 114 W., Sublette County

Two samples of pellet phosphorite and oolitic pellet-phosphorite, from the Retort Member of the Phosphoria Formation, contained 0.003 and 0.002 percent cU, 31.6 and 28.0 percent P_2O_5, 3.15 and 3.08 percent F, 300 and 100 ppm La, and 300 ppm Y (Gulbrandsen, 1966; Sheldon and others, 1953; King and Harris, 2002).

Snow King Mountain, NE¼NE¼ sec. 9, T. 40 N., R. 116 W., Teton County

Phosphate-rich rock was sampled by Gere and others (1966) from a stratigraphic section of the Phosphoria Formation. Composition ranged from 15.07 to 30.98 percent P_2O_5, 200 to 1,000 ppm Y, up to 700 ppm Nd, 100 to 700 ppm La, and up to 50 ppm Yb (King and Harris, 2002).

Flat Creek (USBM Samples #58–61), NE¼SE¼ sec. 1, T. 41 N., R. 115 W., Teton County

Phosphorite sampled from chips across 15 to 76 cm (6 to 30 in) of outcrop contained 200 to 300 ppm Y, up to 200 ppm La, 25.7 to 40.0 percent P_2O_5, 0.006 to 0.006 percent U, 2.3 to 3.2 percent F, 500 to 1,000 ppm Cr, 60 to 1,000 ppm V, and up to 1,000 ppm Sr (Simons and others, 1988; King and Harris, 2002).

Table Mountain area (USGS Sample #54), E½ sec. 18, T. 41 N., R. 114 W., Teton County

This 15 cm (6 in) sample of phosphorite contained 500 ppm La, 500 ppm Y, 12 percent P, 115 ppm U, 1,000 ppm Cr, and 500 ppm V (Simon and others, 1988; King and Harris, 2002).

East Miners Creek (USGS Sample #370), NW¼ sec. 1, T. 41 N., R. 114 W., Teton County

This sample was reportedly taken from a shale in the Phosphoria Formation. The shale contained 200 ppm La, 500 ppm Y, 86 ppm U, 300 ppm Cr, and 300 ppm V (Simons and others, 1988; King and Harris, 2002).

Crystal Creek (USGS Samples #15–17), sec. 32–33 line, T. 42 N., R. 113 W., Teton County

Phosphorite samples #15 and #17 contained 500 and 1,000 ppm La, 700 and 1,000 ppm Y, 12 and 9 percent P, 1,500 ppm Cr, 500 and 70 ppm V, up to 3 ppm Ag, and 100 ppm Zn. Sample #16 was collected from black shale in the Phosphoria Formation and contained 150 ppm La, 200 ppm Y, 5 ppm Ag, 100 ppm Cr, and 700 ppm Zn (Simons and others, 1988; King and Harris, 2002).

Crystal Creek Canyon, NW¼SW¼ sec. 34, T. 42 N., R. 113 W., Teton County

Simons and others (1988) reported samples with up to 700 ppm lanthanum, 300 ppm yttrium, and 31.5 percent P_2O_5 from the Phosphoria Formation in the Crystal Creek Canyon area. The Meade Peak Phosphatic Shale Member of the Phosphoria Formation does not appear to crop out in this area. Instead, the outcrop consists of gray to tan, extensively fractured limestone and limey mudstone with nodules of chert and yellow to brown, radiating-bladed, carbonate crystals (Sample 20121003JC-F). This unit is not significantly enriched in any REE or other elements of economic interest (Sutherland and others, 2013).

Crystal Creek area (USBM Samples #10–14), S½ sec. 34, T. 42 N., R. 113 W., Teton County

Phosphorite chips sampled across 23 cm to 1 m (0.75 to 3.3 ft) of Phosphoria Formation outcrop contained 100 to 300 ppm Y, up to 700 ppm La, 27.5 to 31.5 percent P_2O_5, 0.007 to 0.012 percent U, 2.6 to 3.2 percent F, 100 to 500 ppm Cr, <60 to 500 ppm C, and up to 1,000 ppm Sr (Simons and others, 1988; King and Harris, 2002).

Unnamed (USGS Samples #1002 and 1003), NE¼SE¼ sec. 8, T. 41 N., R. 113 W., Teton County

These samples of phosphorite and phosphate-rich rock contained 500 ppm La, 500 ppm Y, 9 and 4.5 percent P, 1,200 and 1,000 ppm Cr, and 200 and 70 ppm V (Simons and others, 1988; King and Harris, 2002).

Crystal Peak (USGS Sample #34), NW¼NW¼ sec. 35, T. 41 N., R. 113 W., Teton County

This 0.6 m (2 ft) sample of phosphorite contained 500 ppm La, 500 ppm Y, 12 percent P, 1,000 ppm Cr, and 500 ppm V (Simon and others, 1988; King and Harris, 2002).

Granite Creek area (USGS Samples #80–82), NE¼ sec. 3, T. 40 N., R. 114 W., Teton County

Samples 80 and 81 came from 6 to 10 cm (2.4 to 3.9 in) samples of phosphorite. They contained 100 and 500 ppm La, 1,000 and 700 ppm Y, 12 percent P, 500 and 700 ppm Cr, and 300 and 100 ppm V. Only 62 ppm U was recorded from phosphorite Sample #82 (Simon and others, 1988; King and Harris, 2002).

The Six Lakes area (USGS Samples #178 and 179), SE¼ sec. 12, T. 40 N., R. 113 W., Teton County

These two samples of phosphorite contained 500 and 300 ppm La, 300 and 200 ppm Y, 9 percent P, 70 ppm and no data U, 500 and 700 ppm Cr, and 70 and 200 ppm V (Simon and others, 1988; King and Harris, 2002).

Bear Cabin Creek (USGS Sample #103), SE¼ sec. 14, T. 40 N., R. 112 W., Teton County

Simon and others (1988) collected this sample of phosphorite that contained 500 ppm La, 700 ppm Y, 12 percent P, 700 ppm Cr, and 300 ppm V (King and Harris, 2002).

Unnamed (USGS Sample #124), center N½ sec. 26, T. 40 N., R. 112 W., Teton County

This sample of phosphate-rich rock contained 700 ppm La, 700 ppm Y, 3 percent P, 1,000 ppm Cr, and 300 ppm V (Simon and others, 1988; King and Harris, 2002).

Unnamed (USGS Sample #302), S½SW¼SE¼ sec. 26, T. 40 N., R. 112 W., Teton County

Simon and others (1988) reported phosphorite that contained 200 ppm La, 300 ppm Y, 12 percent P, 300 ppm Cr, and 150 ppm V (King and Harris, 2002).

Clear Creek (USGS Samples #204, 205, 406; USBM Sample #57), NE¼NE¼NE¼ sec. 6, T. 39 N., R. 111 W., Sublette County; down valley to W½NE¼ sec. 32, T. 40 N., R. 111 W., Teton County

Four samples of phosphorite and phosphate-rich rock, respectively, contained 500, 300, 200, and 300 ppm Y; 200, 150, <200, and 200 ppm La; 9 and 6 percent P, 28.6 percent P_2O_5, and 6 percent P; 500, 500, 600, and 700 ppm Cr; and 200, 70, <60, and 70 ppm V. Sample #57 was a collection of chips across 0.8 m (2.5 ft) of outcrop and also contained 0.002 percent U and 2.0 percent F (Simons and others, 1988; King and Harris, 2002).

Triangle Peak area (USGS Sample #290), center sec. 2, T. 39 N., R. 112 W., Sublette County

A 3 m (10 ft) sample of phosphorite at this location contained 200 ppm La, 300 ppm Y, 12 percent P, 87 ppm U, 300 ppm Cr, and 100 ppm V (Simon and others, 1988; King and Harris, 2002).

Unnamed (USGS Samples #308 and 309), NW¼NW¼ sec. 20, T. 39 N., R. 112 W., Sublette County

An 18 cm (7 in) sample of phosphate-rich rock (#308) yielded 300 ppm La, 300 ppm Y, 6 percent P, 1 ppm Ag, 300 ppm Cr, 50 ppm V, and 700 ppm Zn. A black shale in the same area (#309) contained 150 pp La, 150 ppm Y, 5 ppm Ag, 1,000 ppm Cr, and 1,000 ppm Zn (Simons and others, 1988; King and Harris, 2002).

Dell Creek (USBM Sample #41), center W½ sec. 28, T. 39 N., R. 112 W., Sublette County

This sampling of phosphorite chips across 46 cm (18 in) of outcrop contained 300 ppm Y, <200 ppm La, 29.8 percent P_2O_5, 0.009 percent U, 3.0 percent F, 500 ppm Cr, <60 ppm V, and 1,000 ppm Sr (Simons and others, 1988; King and Harris, 2002).

Wilderness boundary (USGS Samples #296, 298, 300), N¼ sec. 13–14 line, T. 39 N., R. 112 W., Sublette County

Three samples of phosphorite and phosphate-rich rock, respectively, contained 200, 300, and 200 ppm of both La and Y; 6, 9, and 12 percent P; 72, no data, and 95 ppm U; 300, 500, and 500 ppm Cr; and 50, 20, and 200 ppm V (Simons and others, 1988; King and Harris, 2002).

Tosi Creek (USGS Samples #327–329), E½SE¼ sec. 18, T. 39 N., R. 111 W., Sublette County

Simons and others (1988) Samples 327 and 328 of phosphate-rich rock contained 500 and 200 ppm La, 150 and 500 ppm Y, 6 and 12 percent P, and 1.5 and 2 ppm Ag. Sample #329 was taken from a black shale in the Phosphoria Formation and contained 150 ppm La, 150 ppm Y, no data for phosphorus, and 5 ppm Ag (King and Harris, 2002).

West Tosi Creek (USGS Sample #319), center W½ sec. 15, T. 39 N., R. 111 W., Sublette County

Phosphate-rich rock at this location contained 200 ppm La, 300 ppm Y, 6 percent P, 68 ppm U, 500 ppm Cr, and 70 ppm V (Simons and others, 1988; King and Harris, 2002).

Flathead Sandstone

The Middle Cambrian Flathead Sandstone, known earlier as the Deadwood Conglomerate, is the oldest sedimentary formation above the Precambrian in Wyoming and has a maximum thickness of about 171 m (560 ft; Kanizay, 1978). The Flathead is dominantly quartz-rich, subangular, medium- to coarse-grained sandstone with large scale cross-bedding. Aside from quartz, abundant feldspar and crystalline lithic fragments typical of the underlying granite are common. Most of the formation is thin- to thick-bedded and well-cemented, with a predominant reddish-brown color that grades to purple, rusty-orange, yellow, or gray (Sutherland and others, 2013). The sandstone is interrupted by thin layers of greenish-gray siltstone and shale, particularly in the upper part of the formation. The Flathead represents a fluvial-marine transition zone along a north-south oriented shoreline with braided stream deposits in the conglomeratic base of the formation (Middleton, 1980). The Flathead commonly contains elevated REE primarily due to paleoplacers within the sandstones and conglomerates that make up the formation. Many of the occurrences containing REE discussed below attribute the enrichment to increased monazite and zircon. Depending on the fluvial depositional history of the area, the Flathead may or may not contain such paleoplacers or REE enrichment.

The basal conglomerate varies from 6 to 15 m (20 to 50 ft) in thickness (McKinney and Horst, 1953a). These braided stream deposits are quartz-rich, arkosic conglomerates with subangular to rounded clasts indicative of both a nearby source and a lack of reworking (Middleton, 1980). Clast sizes are up to 5 cm (2 in) in diameter with cementation varying from moderately silicic or limonitic to localized areas of quartzite.

Rawlins Red deposit, NW¼NE¼NE¼ sec. 8, T. 21 N., R. 83 W., Carbon County

This is a red to brown, fine- to medium-grained, arkosic sandstone rich with iron oxide. The iron appears dark-brown to black and metallic but not magnetic. This sample was taken from an old pit and represents some of the more concentrated high-grade hematite (Sutherland and Cola, 2015). It is common for samples to contain 30 to 90 percent Fe_2O_3. However, one sample also contained LREE and strontium greater than five times the crustal abundance. In fact, cerium was present at more than 15 times the crustal abundance (table 42).

Bald Mountain paleoplacers, T. 56 N., R. 91 W., Big Horn and Sheridan Counties

The Bald Mountain area sits along the upper part of the west flank of the northwest-trending, northern Bighorn Mountains at elevations between 2,621 and 2,865 m (8,600 and 9,400 ft). This part of the Bighorn Mountains is an asymmetric, Laramide, anticlinal uplift characterized by west-dipping monoclines. Near-horizontal to east-dipping exposures of Lower Paleozoic formations unconformably overlie medium- to coarse-grained, pink to gray, Archean plutonic rocks that generally vary from granitic to quartz dioritic in composition. The granitic rocks locally contain minor pegmatites and are cut by more than one generation of hornblende-diorite, mafic dikes (Osterwald, 1959; Hausel, 1989; Cardinal, 1958).

Precambrian rocks in the Bald Mountain area are not known to host significant precious metal deposits. However, gold paleoplacers within the Middle Cambrian Flathead conglomerates attracted attention around 1900. The gold rush was short lived when gold values proved insufficient to support commercial operations (McKinney and Horst, 1953a; Hausel, 1989).

Gold in the basal Flathead Sandstone in the Bald Mountain area occurs as fine-grained, flat flakes with jagged edges that suggest a nearby source (Sutherland and others, 2013), and the paleoplacer also contains other heavy minerals, including ilmenite, magnetite, zircon, and monazite. The monazite attracted interest as a source for thorium in 1951 (Wilson, 1951; McKinney and Horst, 1953a; Hausel, 1989; King and Harris, 2002). Heavy-mineral concentrates from some of the higher grade samples contained 38.3 percent ilmenite, 8.7 percent monazite, 4.0 percent magnetite, 0.2 percent zircon, and 48.8 percent other impurities (McKinney and Horst, 1953a).

The monazite occurs as reddish-brown grains up to a few millimeters (< 0.1 in) across within a limonitic matrix of the basal quartz-pebble conglomerate. The dense sand-

stones overlying the basal conglomerate also host notable monazite but at much lower concentrations than the basal conglomerate (Wilson, 1951). Although the entire Flathead Sandstone contains some monazite, the only significant concentrations are found in lower sections. Monazite concentrations within the basal Flathead are highly variable laterally, ranging from trace amounts of scattered grains to more than 9.5 kg/tonne (19 lbs/ton). Greater amounts of monazite are generally associated with poorly cemented areas, an abundance of large quartz pebbles, and a deep yellowish-red color resulting from the strong presence of hematite or limonite (McKinney and Horst, 1953a).

The USBM drilled 92 exploration holes in 1952 to test the monazite-bearing conglomerates (fig. 41). Drilling totaled 2,020 ft (616 m) from which 24,140 kg (53,214 lbs) of samples were collected for analyses. Depth of drilling was limited by the underlying Precambrian basement. The deepest hole was 14.8 m (48.5 ft), but the average depth was only 6.7 m (22 ft). Some holes were essentially barren, but numerous holes east of Rooster Hill encountered higher-grade, monazite-enriched zones at more than one depth, with apparent gradations between them. This reinforced the concept of a three-dimensional, braided stream, depositional environment (Sutherland and others, 2013).

From drilling, the USBM estimated a resource of 18 million tonnes (20 million tons) that averaged 1.25 kg/tonne (2.5 lbs/ton) of monazite (McKinney and Horst, 1953a; Borrowman and Rosenbaum, 1962). A high-grade zone was estimated to contain 612,000 tonnes (675,000 tons) of conglomerate that averaged 6.6 kg/tonne (13.2 lbs/ton) of monazite (Borrowman and Rosenbaum, 1962). The average chemical assay value for pure monazite showed 8.8 percent ThO_2 and 0.12 percent U_3O_8. Gold assays taken from six drill holes in the high-grade monazite area varied from 0.034 to 0.172 ppm (0.001 to 0.005 oz/ton) and averaged 0.103 ppm (0.003 oz/ton; McKinney and Horst, 1953b; Hausel, 1989). Ilmenite, which accounted for as much as 38.3 percent of concentrates from higher-grade portions of the deposit, was suggested by Wilson (1951) and by McKinney and Horst (1953a) as providing additional economic potential for the paleoplacers. At the time, no analyses were done for REE, and it was suggested that economic conditions were not conducive to a mining operation. However, it was also noted as a possibly valuable deposit, as the USBM and USAEC were concerned with the availability of REE and thorium (McKinney and Horst, 1953b).

Using the paleoplacer resource estimations reported by McKinney and Horst (1953a; b) and the typical value of 61 percent REO in monazite (Long and others, 2010), the estimated Bald Mountain paleoplacer resource would be 0.7630 kg REO/tonne (1.525 lbs REO/ton), or 0.076 percent REO. The high-grade paleoplacer material would be around 4.02 kg REO/tonne (8.05 lbs REO/ton), or 0.40 percent REO. This is based on an interpretation that the paleoplacers are relatively uniform layers enriched with monazite, and the likely depositional environment of erratic braded streams would deem these estimates as inaccurate (King and Harris, 2002; Sutherland and others, 2013).

In 2011, five samples were collected by the WSGS from east of Rooster Hill and three from the west end of Bald Mountain (Sutherland and others, 2013). Three samples (20110824WS-C, -D, and -F) showed significant REE with total REE contents of 4,714.68 ppm, 6,815.69 ppm, and 2,309 ppm, respectively (table 43). These samples were high in most LREE and showed elevated values for HREE and yttrium. There were also significantly amounts of thorium, and Samples 20110824WS-C and 20110824WS-D were high in uranium. Some of the other samples showed slightly elevated LREE values but were not considered as enriched. WSGS sampling demonstrated the presence of significant REE concentrations, particularly the LREE, associated with thorium-bearing monazite investigated by the USBM and USAEC in 1952 (Sutherland and others, 2013).

The following sample information from the Bald Mountain area comes from RI-65 (Sutherland and others, 2013). No further sampling was done for this report.

Table 42. Concentration of REE from the Rawlins Red deposit. Bold values indicate concentrations greater than five times the crustal abundance.

	Rawlins Red								
Element	La (ppm)	Ce (ppm)	Pr (ppm)	Nd (ppm)	Sm (ppm)	Eu (ppm)	Gd (ppm)	Tb (ppm)	Dy (ppm)
CC134	**337**	**946**	**64.9**	**209**	**33.1**	4.91	15.2	1.3	4.78
	Ho (ppm)	Er (ppm)	Tm (ppm)	Yb (ppm)	Lu (ppm)	Sc (ppm)	Y (ppm)	Cumulative REE (ppm)	
	0.72	1.84	0.23	1.49	0.25	3	18.2	**1,641.92**	

From Sutherland and Cola (2015)

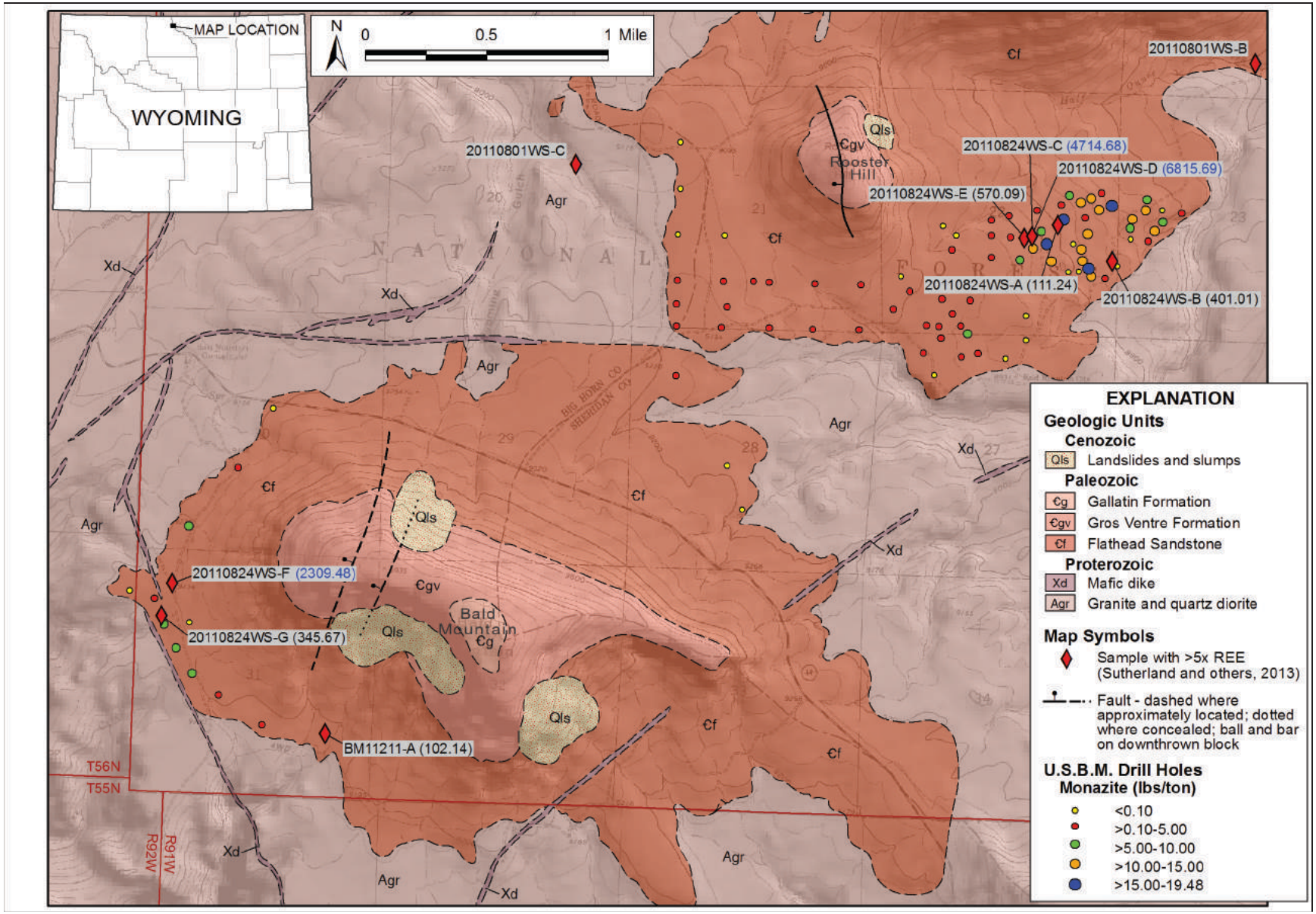


Figure 41. Geology and sample and drill hole locations near Bald Mountain. Locations of 1952 USBM drill holes (McKinney and Horst, 1953) and samples (Sutherland and others, 2013) show the abundance of REE and monazite in the Flathead Sandstone. Numbers next to sample names indicate the total REE in ppm; blue numbers indicate REE at five times the crustal abundance. Map modified from Cardinal (1958), Love and Christiansen (1985), and Sutherland and others (2013).

Sample 20110824WS-A is an iron-stained and partially white-banded, cross-bedded, coarse-grained, arkosic sandstone and conglomerate representative of the bottom of the Flathead Sandstone in what appears to be a paleochannel cut between low outcrops of Precambrian granite and a mafic dike. Only thorium was slightly elevated (table 43).

Sample 20110824WS-C is a poorly cemented, limonitic layer in the basal Flathead Sandstone located at an unknown distance above the contact with Precambrian crystalline rocks. The sample was collected just below a coarse conglomeratic layer exposed on the west side of an old, north-trending, exploration trench about 6 m (20 ft) deep. LREE values were significant in this sample, and HREE and yttrium values were also elevated (table 43).

Sample 20110824WS-D was collected near the east side of the same trench as the previous sample but about 18 m (60 ft) further south. It is a coarse, limonitic, quartz-pebble conglomerate (fig. 42) representative of the layer above Sample 20110824WS-C. It showed the greatest amount of REE and thorium of any sample taken in the area. HREE and yttrium values were also elevated (table 43).

Sample 20110824WS-E is a purple, iron-rich sandstone and conglomerate collected at the west end of an east-trending trench. This locale is west of the previous two samples and about 6 m (20 ft) higher in the Flathead Sandstone than Sample 20110824WS-D. This sample hosted elevated LREE values, but none exceeded five times the crustal abundance. Thorium was notably higher at more than 15 times the average crustal values.

Sample BM11211-A, taken from the middle part of the Flathead Sandstone on the lower southwestern slope of Bald Mountain, showed no anomalous REE but had slightly elevated thorium values.

Sample 20110824WS-F was collected from the east end of an old exploration trench about 43 m (140 ft) long, 8 m (25 ft) wide, and 3.7 m (12 ft) deep. The basal Flathead Sandstone exposed in this trench is a heavily iron-stained, partly limonitic, coarse sandstone to conglomerate with some very angular clasts. Non-magnetic, rounded, black pebbles up to 1.27 cm (0.5 in) diameter are common here and easily crush into a limonitic-brown powder. These were later identified as goethite [$Fe_3(OH)$] by X-ray diffraction. The raw sample contained

Table 43. Concentration of REE from Bald Mountain. Bold values indicate concentrations greater than five times the crustal abundance.

	Bald Mountain								
Element	La (ppm)	Ce (ppm)	Pr (ppm)	Nd (ppm)	Sm (ppm)	Eu (ppm)	Gd (ppm)	Tb (ppm)	Dy (ppm)
20110824WS-A	27.5	49.8	4.9	15.7	2.2	0.4	1.4	0.2	1.0
20110824WS-B	94.7	169.5	18.1	61.5	9.6	4.1	7.2	0.9	4.2
20110824WS-C	**1,220.0**	**2,230.0**	**220.0**	**695.0**	**103.5**	4.6	**62.0**	**6.6**	27.9
20110824WS-D	**1,790.0**	**3,190.0**	**329.0**	**1,045.0**	**150.0**	5.0	**77.6**	**7.8**	**36.2**
20110824WS-E	145.5	260.0	27.0	87.6	12.8	0.8	6.7	0.7	3.9
20110824WS-F	**613**	**1,090.0**	**109.5**	**360.0**	**48.3**	1.7	24.1	2.4	10.6
20110824WS-G	89.6	159.0	16.0	53.0	7.3	0.7	4.0	0.4	2.2
BM11211-A	21.6	43.7	4.3	15.2	2.4	0.5	1.6	0.2	1.3

Element	Ho (ppm)	Er (ppm)	Tm (ppm)	Yb (ppm)	Lu (ppm)	Sc (ppm)	Y (ppm)	Cumulative REE (ppm)
20110824WS-A	0.2	0.6	0.1	0.6	0.1	0.8	6.0	111.5
20110824WS-B	0.8	1.9	0.3	1.4	0.2	7.9	18.8	401.1
20110824WS-C	4.6	10.3	1.4	7.3	1.1	4.0	116.5	**4,714.8**
20110824WS-D	5.3	11.9	1.3	8.0	1.1	4.1	**153.5**	**6,815.8**
20110824WS-E	0.6	1.6	0.2	1.3	0.2	1.5	19.7	570.1
20110824WS-F	1.5	3.2	0.3	1.8	0.3	1.9	40.9	**2,309.5**
20110824WS-G	0.3	0.8	0.1	0.7	0.1	2.1	9.5	345.8
BM11211-A	0.3	0.8	0.1	0.9	0.2	1.6	7.6	102.3

From Sutherland and others (2013)

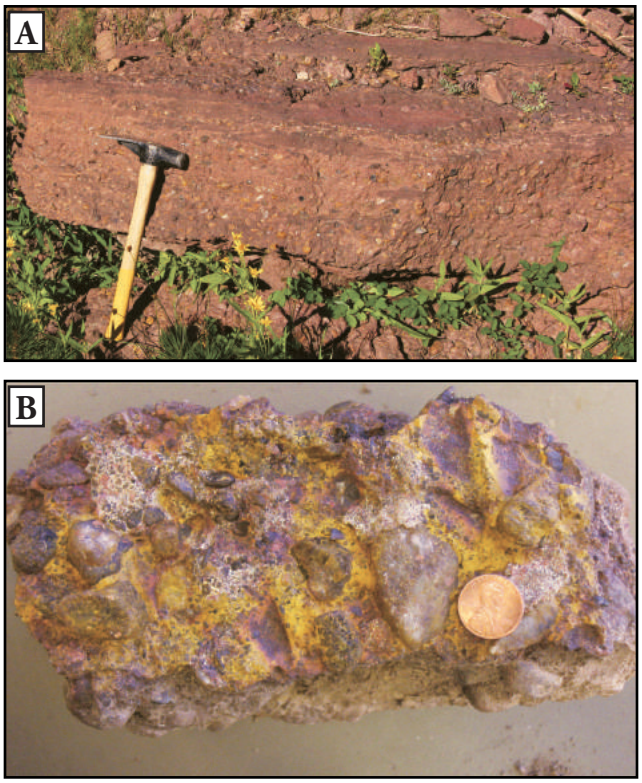


Figure 42. Conglomerate of the lower Flathead Sandstone. A) Outcrop of basal conglomerate in the Flathead Sandstone. B) Close-up of the conglomerate sample collected during RI-65 (Sample 20110824WS-D; Sutherland and others, 2013).

2,309 ppm REE, more than 10 times background crustal values. This would be an estimated TREO of about 0.27 percent. The sample was particularly enriched in La, Ce, Pr, Nd, and Sm. Although not as high, values for Eu, Gd, Tb, Dy, and Ho are elevated as well. The sample also contained more than 65 times the average crustal abundance of thorium.

Sample 20110824WS-G was collected from excavated material near the center of a 70 m (230 ft) long by 1.2 m (4 ft) wide by 1.2 m (4 ft) deep trench. The sample of iron-stained and limonitic sandstone and conglomerate was from the lower part of the Flathead Sandstone. It contained nine times the average crustal abundance of thorium but did not show any significant REE above background crustal values (table 43).

Western Rattlesnake Hills, NE¼ sec. 16, T. 32 N., R. 88 W., Natrona County

The basal Flathead Sandstone crops out at this locality in the Rattlesnake Hills as tan to pink conglomerate. Sample 20110429BG-A is enriched more than five times the average crustal abundance in lanthanum and cerium and is weakly to moderately enriched in the rest of the LREE: gadolinium, terbium, dysprosium, and holmium. Five feet above the base of the Flathead is a red conglomerate (Sample 20120429BG-B) that contains comparable enrichment to Sample A in the LREE and weak to moderate enrichment of the HREE and yttrium. Immediately overlying the red conglomerate is dark-purple conglomerate (Sample 20120429BG-C) enriched in the LREE: gadolinium, terbium, dysprosium, and holmium. Lanthanum, cerium, praseodymium, and neodymium are also enriched to greater than five times the average (table 44).

Union Pass–Warm Spring area, N½NE¼NE¼ sec. 31, T. 42 N., R. 108 W.; NE¼NE¼NE¼ sec. 12, T. 41 N., R. 108 W., Fremont County

Sites in the Union Pass-Warm Spring area (fig. 22) contained REE in Precambrian rock but were also thought to have potential for paleoplacers in the Flathead Sandstone, similar to those in the Bald Mountain area in the Bighorns. Samples 20110920WS-A and 20121004JC-C of the Flathead were collected in the area and analyzed for

Table 44. Concentration of REE from the western Rattlesnake Hills. Bold values indicate concentrations greater than five times the crustal abundance.

	Western Rattlesnake Hills								
Element	La (ppm)	Ce (ppm)	Pr (ppm)	Nd (ppm)	Sm (ppm)	Eu (ppm)	Gd (ppm)	Tb (ppm)	Dy (ppm)
20110429BG-A	**165**	**333**	38.1	145	22.6	1.02	13.5	1.62	7.7
20110429BG-A	**255**	**525**	**59.9**	**229**	**36.5**	1.5	19.75	2.45	11.7
20110429BG-A	**195**	**395**	**45**	**170**	27.2	1.18	14.8	1.79	8.3

Element	Ho (ppm)	Er (ppm)	Tm (ppm)	Yb (ppm)	Lu (ppm)	Sc (ppm)	Y (ppm)	Cumulative REE (ppm)
20110429BG-A	1.22	2.95	0.39	2.51	0.41	2.6	33.8	771.42
20110429BG-A	1.82	4.18	0.56	3.45	0.57	4.0	50.9	**1,176.28**
20110429BG-A	1.28	2.87	0.39	2.35	0.4	2.7	36.3	904.56

From Sutherland and others (2013)

REE. No elevated values for REE, thorium, or uranium were detected for Sample 20121004JC-C. Sample 20110920WS-A was only slightly elevated in thorium but not in REE (Sutherland and others, 2013).

Little Basin area, sec. 21, SW¼SW¼ sec. 22, and NW¼NW¼NW¼ sec. 27, T. 29 N., R. 83 W., Natrona County

Within sandstone and pebble conglomerate of the Flathead, a paleo-beach placer contains high concentrations of thorium, up to 10,300 ppm eTh. The deposit contains monazite, zircon, and xenotime. Griffin and Milton (1982) reported 73 to 6,882 ppm eTh, and Malan (1972) reported lower concentrations of 194 and 273 ppm Th. No analyses were done for REE; however, the beach placer may contain elevated concentrations, and the variety of thorium levels in the area may indicate the extent of the deposit (King and Harris, 2002).

Dilworth Bench, sec. 8, T. 56 N., R. 104 W., Park County

A sample taken in Flathead Sandstone along Barrus Creek on Dilworth Bench contained 1,000 ppm La, 3,000 ppm Ti, only 40 ppm Y, 200 ppm Zr, and 4 ppm cU_3O_8 (Garrand and others, 1982). This could be a paleoplacer deposit or a typographical error, 100 not 1,000 ppm La (King and Harris, 2002).

Prospect Creek area, E½SW¼NW¼ sec. 26, T. 48 N., R. 86 W., Washakie County

A paleoplacer in a Flathead conglomerate reportedly contained high thorium concentrations. Further analysis yielded 215 ppm La, 40 ppm Y, 11,100 ppm Ti, 1,650 ppm Zr, 366 ppm eTh, and 18 ppm eU (Damp and Jennings, 1982). Wilson (1960) references an anomalous radioactivity in the same section that may relate to the paleoplacer. This is an unverified occurrence of REE due to the type of deposit and vicinity to Bald Mountain, which is known to contain elevated REE (King and Harris, 2002). The WSGS sampled Flathead (20150810LC-6) along Forest Road #436 near the Prospect Creek area. The quartz-pebble conglomerate was heavily silicified in part and varied from tan to maroon and rusty. No elevated REE or other elements of economic interest were observed.

Unnamed, NW¼SE¼ sec. 22, and NW¼SE¼ sec. 23, T. 32 N., R. 101 W., Fremont County

Sandstone with trace monazite and zircon occurs in the Flathead at this location. No analyses were done for REE, zircon, or titanium, but an assay yielded 446 ppm eTh and 21 ppm eU (Gebhardt and others, 1982). This is a possible paleoplacer that may contain elevated rare earths (King and Harris, 2002).

Unnamed, SW¼ sec. 29, T. 30 N., R. 99 W., Fremont County

Gebhardt and others (1982) sampled Flathead Sandstone that contained 312 ppm eTh and 17 ppm eU. Although no analyses were done for REE, zircon, or titanium, it is suggested the site is a paleoplacer and an unverified occurrence of REE (King and Harris, 2002).

Unnamed, sec. 24, T. 2 S., R. 3 W., (WRM) Fremont County

A conglomerate in the Flathead contained 366 ppm Th and 11 ppm U (Malan, 1972). Similar to the above locations, this is a suggested paleoplacer and possibly enriched in REE, although no analyses were done for REE, Zr, or Ti (King and Harris, 2002).

Unnamed (Sample 243), center W½ sec. 18, T. 47 N., R. 85 W., Johnson County

This quartz-pebble conglomerate contained 324 ppm eTh, 15 ppm eU, <100 La, <100 ppm Nd, <40 ppm Y, 8,650 ppm Ti, and 2,650 ppm Zr (Damp and Brown, 1982). This locale is possibly a paleoplacer and could have enrichment of REE elsewhere in the deposit (King and Harris, 2002).

REE ASSOCIATED WITH URANIUM DEPOSITS

REE are associated with various uranium deposits worldwide (Long and others, 2010; Lottermoser, 2015; Mercadier and others, 2011; Damascena and others, 2015). The common occurrence of REE within uranium ores results in part from the similar ionic radii of the elements (Shannon, 1976) and the probable co-emplacement of these from a common source fluid (Lottermoser, 2015). REE leached from uranium minerals during uranium processing may result in REE concentrations of several percent in some mill tailings (Lottermoser, 2015).

Lottermoser (2015) described several uranium ore bodies in Australia that are also enriched in REE. The Olympic Dam Cu-U-Au-Ag deposit in South Australia hosts 48 million tonnes (53 million tons) of 0.2 percent La and 0.3 percent Ce but remains an uneconomic REE resource (Long and others, 2010; Lottermoser, 2015). Even so, Lottermoser (2015) speculates that mill tailings from Olympic Dam may host significant REE concentrations. He further notes that the long-closed Mary Kathleen uranium mine, a uranium-bearing skarn in northwest Queensland, hosts approximately 3 percent TREO in 6.35 million tonnes (7 million tons) of mill tailings. To date, there has not been an efficient method identified or developed for REE recovery. This situation suggests that significant chemical processing challenges need to be addressed before REE extraction becomes practical from uranium tailings.

REE are less sensitive to redox changes than uranium and readily substitute for uranium in post-crystallization alterations (Mercadier and others, 2011). Within the solutional environments that created Wyoming roll-front uranium deposits, it is reasonable that variations within sedimentary units would prompt a variety of redox conditions. Those variations might favor either precipitation of uranium, REE, or both. WSGS samples collected from across Wyoming show no general correlation between uranium and REE. Relatively high REE concentrations are occasionally associated with both high and low uranium concentrations.

In contrast to the thousands of loose-sediment NURE samples, a much smaller number of rock samples were collected for this study. Due to the wide dispersion and the relatively low number of these samples, little correlation can be shown between elevated REE and proximity to sedimentary uranium districts. No WSGS samples were collected from uranium mine or mill tailings.

None of the NURE samples had complete REE analyses. Therefore, the cutoff of five times the crustal average was used per individual REE in evaluation of the NURE samples rather than total REE content. Of 2,366 NURE samples from Wyoming, 113 had analyses showing one or more REE exceeding five times the average crustal abundance (fig. 43). Some of the samples with anomalously elevated REE concentrations are hosted by the same sedimentary units that have been or are being mined for uranium. These samples also cluster geographically in and around the general area of active or abandoned uranium mines. Other NURE samples with REE elevated above average, but still less than five times their average abundance, similarly occur near uranium mining areas. The clustering of elevated REE samples is particularly noticeable in the northeastern Great Divide Basin, Shirley Basin, and to a lesser extent in the Gas Hills uranium district (fig.43). These sediment-hosted REE concentrations may have differentially precipitated from the same or similar solutions to those that concentrated the economic uranium deposits in response to variable redox conditions.

Some elevated REE concentrations referred to by King and Harris (2002) are similarly associated with sandstone uranium deposits. For example, as mentioned earlier, the White River Formation-hosted Hurda claims are within the Shirley Basin uranium mining district (Gregory and others, 2010). King and Harris (2002) also described elevated REE concentrations at unnamed locations in the Battle Spring Formation adjacent to the Lost Creek uranium mine in the northeastern Great Divide Basin (fig. 33) and within the Crooks Gap-Green Mountain uranium mining district (fig. 43; Gregory and others, 2010).

NURE samples with elevated REE concentrations in other areas are not as easily explained. Those located in Tertiary sediments in the Washakie Basin, in south central Wyoming, and southwest of the Wind River Mountains may represent solution-front deposits in the absence of uranium or possible paleoplacers. Others within the Wind River Mountains and the Laramie Mountains may be related to pegmatites, while those in or near Yellowstone are probably related to Tertiary and Quaternary volcanic rocks.

REE ASSOCIATED WITH COAL

Trace elements, including REE, vary significantly both regionally and within individual coal beds (Stricker and Flores, 2003; Hower and others, 2013; Hower and others, 2015; Deonarine and others, 2015). Elevated concentrations of REE plus Y in some coals are related to the source of the fine sedimentary components in the coal sequence, commonly volcanic ash (Hower and others, 2015). Thus, the greatest concentrations of REE in coal are generally found within or adjacent to zones with higher ash content. This may be associated within clay and shale partings or the sedimentary units that cap or underlie the coal seams (Stricker and others, 2007; Hower and others, 2015). Carbonaceous shales immediately adjacent to the roof and floor rock of coal beds often contain higher concentrations than the coal bed itself.

The WSGS collected a small number of coal samples, as well as related carbonaceous shale and claystones, for analyses. Table 45 includes these samples along with previously published data from several sources regarding coal in Wyoming. To compare, REE analyses of coals, whole ash, and related rocks from locations other than Wyoming are also included in tables 46 and 47. Concentrations of cumulative REE plus Y or of individual elements were related back to their average crustal abundances to put them in perspective, because published data does not often address all REE or only addressed particular elements.

In 2015, six samples were collected by the WSGS in conjunction with two mapping projects along the west side of the Rawlins uplift. Sample 20150702CC-1B was collected from the lowest Paleocene Fort Union Formation coal bed in the Hadsell Draw area, within the Rawlins Peak SW 7.5' quadrangle (Carroll and others, 2015a; Carroll and others, 2015b). This sample of the Honey T-9 coal bed, near the Cretaceous–Paleogene boundary, shows 4 ppm Sc and 10.4 ppm Y (0.15 and 0.36 times average crustal abundance, respectively). Cumulative REE plus Y is 86.99 ppm, or about 0.45 times the average crustal REE plus Y content. The Honey T-9 coal bed hosts REE at less than half of the average crustal concentration.

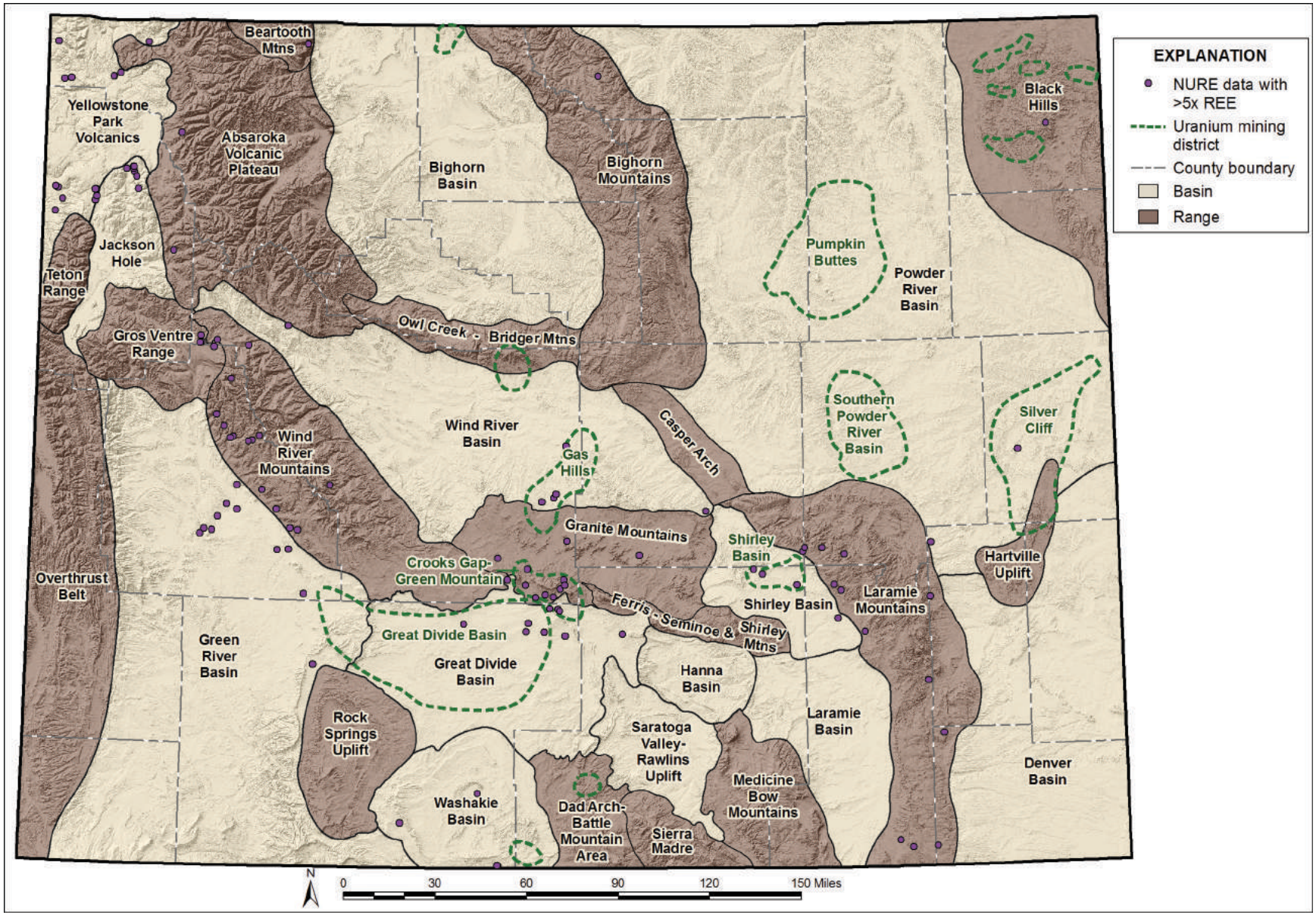


Figure 43. NURE sample localities across Wyoming. Only samples with five times the crustal concentration of REE are shown. Uranium mining districts are modified from Gregory and others (2010), and larger districts are labeled in green.

Sample 20150702CC-1A was collected from the carbonaceous shale roof above the coal and showed a higher REE plus Y content, 152.08 ppm, than the underlying coal. The claystone floor underlying the coal (Sample 20150702CC-1C) showed 135.39 ppm. REE concentration in the roof is 0.79 times the average crustal REE plus Y content, while the claystone floor is 0.7 times the average crustal REE plus Y. Both the roof and floor values are elevated above those found in the main coal but are still less than average crustal abundances.

Sample 20150715RL-1A was collected from a Cretaceous Lance Formation coal bed within the Shamrock Hills 7.5' quadrangle (Lynds and others, 2015; Carroll and others, 2015a). It showed 1 ppm Sc and 4.1 ppm Y, with a cumulative REE plus Y of 28.95 ppm; these values, respectively, represent about 0.04, 0.14, and 0.15 times average crustal abundances. An adjacent carbonaceous shale (Sample 20150715RL-2) in the Lance Formation hosted 9 ppm Sc, 12.7 ppm Y, and 104.61 ppm cumulative REE plus Y. This equates to 0.35, 0.44, and 0.54 times the average crustal abundances, respectively. Sample 20150715RL-3, from another nearby carbonaceous shale in the Battle Spring Formation, hosted 5 ppm Sc, 39.2 ppm Y, and 306.22 ppm REE plus Y, or 0.19, 1.35, and 1.60 times average crustal abundances, respectively.

Within the Cretaceous Rock Springs Formation, a four-foot thick coal bed was sampled (20150930LC-1) from an abandoned mine referred to as the Kent mine no. 1. Analysis of this coal showed <1 ppm Sc, 2.8 ppm Y, and a cumulative REE plus Y of 8.43 ppm; this is only <0.04, 0.10, and 0.04 times the average crustal abundances, respectively.

Stricker and others (2007) cited an average Sc content of 1.0 to 1.4 ppm for multiple coal samples from the mid-lower Wyodak and Big George coal seams in the Powder River Basin (PRB) and a Y content of 1.7 to 2.6 ppm for the same samples. These values roughly represent REE concentrations of about 0.04 to 0.05 times average crustal abundances for Sc, and 0.06 to 0.09 times average crustal abundances for Y. Jones (2010) showed an average content for 48 Wyoming Tertiary coal samples of 1.5 ppm Sc and 5 ppm Y, equaling 0.06 and 0.17 times average crustal abundances, respectively. This compares to an average of 3 ppm Sc and 10 ppm Y (0.12 and 0.34 times average abundances) of United States coals. Jones (2010) also noted an average content in the same Wyoming coal samples of <20 ppm Ce, <15 ppm Nd, 7 ppm La, and 0.5 ppm Yb, which, respectively, represents <0.33, <0.45, 0.21, and 0.18 times the average crustal abundances.

REE concentrations within Wyoming coal beds, based on both WSGS samples and published analyses, are notably less than average crustal abundances. A comparison can be made with a coal from China that hosts a REE content near the crustal average (table 46; Hower and others, 2013). However, that coal also has a relatively high ash content, and REE concentrations within carbonaceous shales and claystones related to the coal beds are variable but generally greater than those within the coal.

REE and Y are not volatile elements that are vulnerable to loss with flue gas during the combustion of coal (Hower and others, 2015). Thus, these elements are concentrated, retrievable by-products derived from combustion. However, since the concentration of REE plus Y in a feed coal is projected to be proportional to that in the coal combustion by-products (CCB), only coals with high REE plus Y contents will create by-products that are also high in REE plus Y (Hower and others, 2015). Hower and others (2013) presented REE plus Y content for coal ash from various power plants in China, Bulgaria, Turkey, and Kentucky (table 46 and 47). REE plus Y concentrations in these ashes varied from 140.4 ppm to 639.8 ppm, or 0.73 to 3.32 times the average abundance of REE plus Y. In some eastern Kentucky coals, the REE plus Y varied from 39.9 ppm to 102.4 ppm on a whole coal basis (Hower and others, 2015), or 0.21 to 0.53 times the average crustal REE plus Y abundances (table 47). The ash from these same coals showed concentrated REE plus Y to vary from 550.5 ppm to 921.9 ppm, or 2.85 to 4.78 times the average crustal abundances. These coal ashes show a notable increase in REE plus Y concentration over that found in the coal.

The vast majority of currently mined Wyoming coal comes from the PRB. Of the 356.3 million tonnes (392.7 million tons) mined in Wyoming in 2014, slightly less than 12.7 million tonnes (14 million tons), or 3.5 percent, came from outside of the PRB (C. Carroll, personal communication, 2015). All of the most recent WSGS coal and related samples came from the Greater Green River Basin and show somewhat higher REE content for the individual elements measured than for those from within the PRB, as cited by Stricker and others (2007). These WSGS coal samples also appear to host higher average REE concentrations in comparison with the few individual element averages noted in Jones (2010), which included coals within as well as outside of the PRB.

Jones (2010) described Wyoming coals as having ash contents that vary widely from only a few percent to more than 50 percent. He explained that a typical, persistent, Wyoming coal of mineable thickness generally contains less than 10 percent ash. Jones (2010) samples were from

Table 45. Concentration of REE from coal and coal-related rocks in Wyoming. No values exceed concentrations greater than five times the crustal abundance.

	Wyoming coal and coal-related rocks																	
Element	La (ppm)	Ce (ppm)	Pr (ppm)	Nd (ppm)	Sm (ppm)	Eu (ppm)	Gd (ppm)	Tb (ppm)	Dy (ppm)	Ho (ppm)	Er (ppm)	Tm (ppm)	Yb (ppm)	Lu (ppm)	Sc (ppm)	Y (ppm)	Cumulative REE (ppm)	Rock Type
20150702CC-1A	27.3	52.6	6.39	23.8	4.43	0.92	4.09	0.6	3.53	0.74	2.29	0.32	2.17	0.3	8	22.6	160.08	Hadsell Draw shale roof
20150702CC-1C	23.2	41.5	4.98	18.5	3.63	0.64	3.62	0.56	3.88	0.89	3.01	0.41	2.93	0.44	5	27.2	140.39	Hadsell Draw, claystone floor
20150715RL-2	23.1	37.7	4.3	15.1	2.58	0.47	2.1	0.34	2.16	0.46	1.45	0.2	1.71	0.24	9	12.7	113.61	Shamrock Hills, Lance Fm. Carb. Sh
20150715RL-3	52.2	99.9	13.75	53.9	12.15	2.06	9.22	1.47	8.54	1.66	4.71	0.76	5.92	0.78	5	39.2	311.22	Shamrock Hills, Battle Spring Fm. Carb. Sh
20150702CC-1B	18.9	30.5	3.69	13.3	2.57	0.47	2.1	0.32	1.8	0.38	1.09	0.14	1.16	0.17	4	10.4	90.99	Hadsell Draw, Honey T-9 coal bed
20150715RL-1	7.1	10.2	1.04	3.8	0.78	0.13	0.51	0.1	0.45	0.1	0.33	0.04	0.24	0.03	1	4.1	29.95	Shamrock Hills, Lance Fm. coal bed
20150930LC-1	0.8	2	0.27	1.1	0.23	0.05	0.34	0.05	0.37	0.07	0.16	0.03	0.13	0.03	<1	2.8	8.43	Kent Mine No.1, Rock Springs Fm. coal
Stricker and others, 2007				1.2											1.1	2.2	4.5	PRB, Mid/Lower Wyodak, 79 core samples*
Stricker and others, 2007				0.83											1.4	1.7	3.93	PRB, Big George, 50 core samples*
Stricker and others, 2007				1.3											1.0	<1.8	2.3	PRB, Mid/Lower Wyodak, 39 core samples*
Stricker and others, 2007				1.0											<1.2	2.6	3.6	PRB, Mid/Lower Wyodak, 40 core samples*
Jones, 2010	7.0	<20		<15									0.5		1.5	5.0		Avg. of 48 Wyoming Coals
Jones, 2010	NR	NR		3.0									1.0		3.0	10.0		U.S. Avg. for Coal

*Trace Elements "reported on a whole coal dry basis", but determined on coal ash

NR = Not Recorded

Table 46. Concentration of REE from coal and coal-related rocks internationally. No values exceed concentrations greater than five times the crustal abundance.

Element	Ash %	La (ppm)	Ce (ppm)	Pr (ppm)	Nd (ppm)	Sm (ppm)	Eu (ppm)	Gd (ppm)	Tb (ppm)	Dy (ppm)	Ho (ppm)	Er (ppm)	Tm (ppm)	Yb (ppm)	Lu (ppm)	Sc (ppm)	Y (ppm)	Cumulative REE (ppm)
Chinese coal ash																		
69405	91.64	94.0	199.0	23.0	90.0	18.0	3.5	17.6	2.5	14.1	2.8	8.0	1.1	7.5	1.1	25.0	77.0	584.2
69406	89.09	96.0	206.0	24.0	93.0	18.0	3.7	18.6	2.6	15.1	3.0	8.6	1.2	8.0	1.2	25.0	83.0	607
69407	91.72	100.0	210.0	25.0	97.0	19.0	3.9	18.9	2.6	15.1	3.0	8.6	1.2	8.0	1.1	23.0	82.0	618.4
69408	91.29	110.0	225.0	27.0	106.0	20.0	4.1	20.1	2.8	15.8	3.1	9.0	1.3	8.4	1.2	26.0	86.0	665.8
69409	86.08	107.0	219.0	23.0	81.0	15.0	2.3	16.2	2.3	12.9	2.5	7.2	1.0	6.6	0.9	17.0	67.0	580.9
69410	84.01	107.0	218.0	23.0	81.0	15.0	2.4	16.1	2.3	13.0	2.5	7.3	1.0	6.6	1.0	17.0	67.0	580.2
Jungar Power Plant, China																		
Coal (avg.)	32.98	41.2	71.8	8.1	27.6	5.2	0.9	4.7	0.7	4.2	0.8	2.4	0.3	2.3	0.3	NR	20.4	190.9
Economizer fly ash (avg.)	95.43	85.4	141.0	17.3	58.5	10.6	1.8	9.1	1.4	8.6	1.7	4.9	0.7	4.8	0.7	NR	42.1	388.6
Wet fly ash (avg.)	96.16	104.3	178.0	21.5	72.5	13.5	2.4	11.7	1.8	10.8	2.1	6.2	0.9	6.0	0.9	NR	54.2	486.8
Bottom ash (avg.)	82.62	67.3	117.4	13.9	46.8	8.7	1.5	7.5	1.1	6.9	1.3	4.0	0.6	3.9	0.6	NR	33.8	315.3
Bulgarian coal ash																		
93516	NR	37.7	82.4	9.3	35.3	7.2	1.7	7.3	1.0	5.4	1.1	3.0	0.4	2.8	NR	NR	32.7	227.3
93517	NR	40.2	87.1	9.8	37.1	7.6	1.8	7.7	1.1	5.8	1.1	3.2	0.5	3.0	NR	NR	34.8	240.8
93518	NR	39.0	87.6	9.6	36.7	7.6	1.8	7.7	1.1	5.8	1.2	3.3	0.5	3.1	NR	NR	35.1	240.1
93520	NR	39.1	85.6	9.4	35.0	7.1	1.6	7.3	1.0	5.4	1.1	2.9	0.4	2.8	NR	NR	30.9	229.6
93521	NR	39.1	86.2	9.4	34.8	7.0	1.6	7.2	1.0	5.4	1.1	3.0	0.4	2.8	NR	NR	30.7	229.7
93522	NR	38.4	84.2	9.3	34.7	7.1	1.6	7.3	1.0	5.4	1.1	3.0	0.4	2.9	NR	NR	31.3	227.7
Turkish coal ash																		
NR	NR	36.0	72.0	8.5	32.0	6.2	1.7	6.4	1.0	5.4	1.0	2.9	0.4	2.7	NR	NR	33.0	209.2
NR	NR	38.0	85.0	9.4	38.0	7.2	1.8	7.3	1.1	6.5	1.3	3.8	0.5	3.4	NR	NR	40.0	243.3
NR	NR	37.0	75.0	8.5	31.0	6.4	1.7	6.3	0.9	5.3	1.0	3.0	0.4	2.7	NR	NR	32.0	211.2
NR	NR	41.0	80.0	9.0	34.0	6.1	1.6	5.7	0.8	4.4	0.9	2.5	0.4	2.3	NR	NR	26.0	214.7

Data from Hower and others (2013; 2015)

NR = Not Reported

Table 47. Concentration of REE from coal and coal-related rocks in Kentucky. No values exceed concentrations greater than five times the crustal abundance.

Element	Ash %	La (ppm)	Ce (ppm)	Pr (ppm)	Nd (ppm)	Sm (ppm)	Eu (ppm)	Gd (ppm)	Tb (ppm)	Dy (ppm)	Ho (ppm)	Er (ppm)	Tm (ppm)	Yb (ppm)	Lu (ppm)	Sc (ppm)	Y (ppm)	Cumulative REE (ppm)
Kentucky coal ash																		
93438	NR	21.9	48.2	5.7	21.4	4.4	0.9	4.6	0.7	3.8	0.8	2.2	0.3	2.1	NR	NR	23.4	140.4
93446	NR	36.0	83.2	9.2	34.5	6.9	1.4	7.2	1.1	6.2	1.3	3.7	0.5	3.5	NR	NR	40.1	234.8
93447	NR	41.9	96.5	10.6	40.1	8.1	1.8	8.7	1.3	7.6	1.6	4.7	0.7	4.3	NR	NR	49.5	277.4
93448	NR	43.4	100.9	11.1	42.0	8.6	1.9	9.2	1.4	8.2	1.7	5.0	0.7	4.7	NR	NR	53.4	292.2
93469	NR	29.1	65.3	7.5	28.5	5.8	1.2	6.1	0.9	5.0	1.0	2.9	0.4	2.7	NR	NR	30.5	186.9
93295	NR	86.1	188.5	20.7	80.7	16.8	4.0	19.9	2.9	15.2	3.0	8.7	1.2	7.9	NR	NR	88.2	543.8
93297	NR	80.5	175.7	19.5	77.0	16.2	3.9	19.1	2.8	14.7	2.9	8.4	1.1	7.6	NR	NR	86.0	515.4
93299	NR	61.9	131.8	15.1	60.1	12.9	3.1	15.3	2.3	12.1	2.4	6.8	0.9	6.2	NR	NR	70.6	401.5
93304	NR	46.2	98.4	11.5	46.2	10.0	2.5	12.1	1.8	9.5	1.9	5.4	0.7	4.8	NR	NR	55.8	306.8
93307	NR	49.8	105.3	12.0	47.6	9.6	2.2	11.5	1.6	8.2	1.6	4.8	0.7	4.7	NR	NR	47.1	306.7
93310	NR	50.9	107.3	12.2	48.2	9.8	2.3	11.7	1.6	8.4	1.7	4.9	0.7	4.8	NR	NR	47.6	312.1
93312	NR	50.8	108.5	12.2	48.0	9.7	2.3	11.6	1.6	8.1	1.6	4.8	0.7	4.7	NR	NR	46.6	311.2
93314	NR	50.3	106.3	12.1	47.2	9.5	2.2	11.3	1.5	7.8	1.6	4.7	0.7	4.5	NR	NR	44.7	304.4
93316	NR	49.7	104.6	12.0	46.8	9.3	2.2	11.3	1.5	7.6	1.5	4.5	0.6	4.4	NR	NR	44.1	300.1
93382	NR	88.2	188.9	21.6	86.2	17.9	4.1	21.2	3.0	15.0	2.9	8.5	1.2	7.9	NR	NR	86.1	552.7
93385	NR	87.1	186.1	21.6	86.9	18.3	4.3	22.2	3.2	16.3	3.2	9.3	1.3	8.6	NR	NR	95.2	563.6
93387	NR	89.8	194.8	22.6	91.3	19.6	4.7	23.4	3.5	17.9	3.5	10.3	1.4	9.4	NR	NR	106.7	598.9
Kentucky coal																		
Coalburg Bed (avg)	11.28	11.1	21.2	6.5	11.3	1.9	0.4	1.7	0.4	2.1	0.6	1.0	0.4	1.2	0.2	NR	8.7	68.7
Leatherwood Bed (avg)	11.02	13.1	24.7	6.0	13.8	2.2	0.5	1.8	0.4	2.2	0.6	1.1	0.4	1.4	0.2	NR	10.0	78.4
Fire Clay Bed (avg)	11.46	17.9	33.9	7.1	17.9	2.9	0.5	2.7	0.6	2.8	0.6	1.4	0.4	1.7	0.2	NR	11.8	102.4
Pond Creek Bed (avg)	7.24	6.4	12.2	4.2	6.0	1.1	0.3	1.1	0.2	1.3	0.4	0.6	0.2	0.8	0.1	NR	5.0	39.9
Clintwood Bed (avg)	6.89	7.2	13.1	3.6	6.9	1.2	0.3	1.4	0.2	1.2	0.3	0.6	0.2	0.8	0.1	NR	5.4	42.5

Data from Hower and others (2013; 2015)

NR = Not Reported

"run-of-mine" coal, which is considered the "sales coal" to power plant customers.

Assuming that a generic Wyoming coal bed contains about 50 ppm REE plus Sc and Y, a reasonably high average considering values cited above, and the lowest average amount of ash at about 5 percent (Jones, 2010), the CCB (such as fly ash) could most efficiently concentrate REE content by a factor of about 20 times. This would increase the REE concentration from 50 ppm in the highly uniform and fictitious coal to 1,000 ppm in the combustion products. It should be stated that this is an unlikely scenario. If the REE was recovered at 99.999 percent, as in the proprietary process used in Rare Element Resources' Bear Lodge Project, which is tailored to the specific chemistry of that deposit, then approximately 999.9 ppm could be recovered from the ash product. If the chemistry of the CCB is variable, then REE recovery could drop well below this idealized number. If beneficiation and/or blending occurred to bring the coal into specification for a particular power plant, the REE concentration would likely be lowered significantly.

In attempting to assess the potential economics of extraction of relatively low REE concentrations from CCB, other factors should be considered. U.S. utilities produced 61.4 million tonnes (67.7 million tons) of fly ash during 2010, but only 22.7 million tonnes (25.0 million tons) were put to use. That left 38.7 million tonnes (42.7 million tons) as unused with the amount of waste projected to grow over time (Hower and others, 2013). Currently, approximately 43 percent of the coal ash is reused, according to the American Coal Ash Association (Deonarine and others, 2015). Aside from this amount, other factors affect the REE potential of CCB. Beneficiation for power plants, often removes undesirable rock and high ash material from the coal, which may also remove REE, and blending coals from other areas may have a similar effect (Hower and others, 2015). Wyoming coal is not washed at the mine as are all other coals in the U.S. that have higher sulfur contents (C. Carroll, personal communication, 2015). As REE are removed or diluted through these processes, the potential for economic REE recovery from the combustion products correspondingly decreases.

Sutherland and others (2013) suggested that a total REE content greater than 3,000 ppm may be indicative of potential for an economic deposit but did not address REE content in CCB. A review of REE advanced exploration projects in carbonatite and peralkaline intrusion host rocks, described in Verplanck and others (2014), shows 3,000 ppm TREO as the lowest cut-off grade for any project and 5,120 ppm as the lowest reported average ore grade. Seredin and Dai (2012) suggest 900 ppm REE plus Y within coal ash as a possible low-end concentration for economic development in China. If the hypothetical calculations made earlier for Wyoming coal, which assumed the best case scenario of REE recovery just under 1,000 ppm, are considered under these circumstances, it would not likely be deemed economical with currently available technology.

Although coal resources are relatively large, extensive variation can occur across a region. The small particle size of ash would circumvent the costs of mining and crushing, and the particular chemistry for a coal bed would need consideration for chemical processing. The more uniform the original material is, the more efficient processing and recovery will be. Favorable chemistry for metal extraction must also be coupled with long-term projected use to ensure that an REE processing facility could produce an economic product. In addition, shipping of coal ash from widely dispersed power plants to a central processing plant is another expense.

Thus, the low REE concentrations typically found in Wyoming coals, combined with the factors discussed above, do not appear to indicate an economic potential for REE extraction.

It should be noted that advances in research and technology may make REE in coal economical in the future. In fact, a recent news release (Jamasmie, 2016b) indicates that the USDOE, in collaboration with Pennsylvania State University, has found an economic and environmentally friendly process for extraction of REE from CCB using an ion exchange process. The process involves rinsing the coal with a solution that separates REE bound to the coal. However, concentrations of REE appear to be related more to the ash content than to the coal itself. Given this, the previously mentioned economic factors would still need to be considered before a large-scale operation using new technology can be demonstrated.

OCCURRENCES OF OTHER ELEMENTS AND MINERALS

During this investigation, chemical analyses for each sample included a full suite of major, trace, and REE (appendices 1 and 2). While REE were the target of the study, significant concentrations of other elements and minerals were present in some samples and are described in this section. Samples categorized as such from WSGS RI-65 (Sutherland and others, 2013) are also included, and the following samples are ordered alphabetically by county.

Blanche mine, SE¼SE¼SE¼ sec. 32, T. 15 N., R. 79 W., Albany County

A sample (20150822LC-1) collected from the mine dump

is a dark colored pyroxinite containing pyroxene, olivine, plagioclase, and minor pyrrhotite. The subhedral pyroxene shows moderate chloritization and olivine is largely serpentinized. Rock chemistry revealed only one elevated REE (scandium) at 40 ppm as well as 0.005 ppm Au, 0.007 ppm Pt, and 0.005 ppm Pd. Access was granted by the private land owner.

Duchess mine, SW¼SW¼ sec. 32, T. 15 N., R. 79 W., Albany County

Dump piles near the Duchess mine location contain a mixture of mafic and felsic rock. Quartz veins are prevalent and are commonly vuggy with rusty-orange coatings. Some epidote and copper mineralization is present. Multiple samples were taken, but only the vuggy quartz (20150818LC-7B) and the very rusty quartz (20150818LC-7C) contained elevated elements of any interest. Samples 7B and 7C yielded 0.042 and 0.002 ppm Au, 0.006 and <0.005 ppm Pt, 0.003 Pd each, 1,050 and 209 ppm V, >250 ppm As each, and 20.1 and 17 percent Fe_2O_3, respectively.

New Rambler mine, center SW¼SW¼ sec. 33, T. 15 N., R. 79 W., Albany County

Initially, this area was investigated because of placer gold in the mid-1800s, and the New Rambler mine opened as a gold prospect just before the year 1900. Over the next few years, copper and platinum were discovered, and eventually more than 5,443 tonnes (6,000 tons) of ore containing Cu, Au, Ag, Pt, and Pd was produced. Much of the area is composed of hydrothermally altered mafic rocks in a mylonitic shear zone. In 1910, a concentrating mill was built, and minor production continued until a fire destroyed the mill and mine buildings in 1918 (McCallum and Orback, 1968).

Samples were collected from the reclaimed mine dump. Felsic rock, comprised of k-feldspar, plagioclase, quartz, and some amphibole, is the host of ore material (20150822LC-2). Ore, from the supergene enrichment zone, contains chalcocite with lesser chrysocolla, cuprite, copper oxides, and iron oxides. The chalcocite and chrysocolla occur separately or together in veins as well as disseminated in the rock. This sample contains 1.31 ppm Au, 6.2 ppm Pt, 3.15 ppm Pd, 3.33 percent Cu, 1.52 ppm Te, and 8.3 ppm Ag.

A sulfide-bearing pyroxenite from the mine dump contains moderately altered pyroxene, serpentinized olivine, pyrrhotite, and chalcopyrite (20150822LC-3). The sulfides display minor to moderate oxidation and occur as disseminated and net-textured segregations in the rock. This sample contained 0.2119 ppm Au, 0.808 ppm Pt, 1.69 ppm Pd, 1,150 ppm Cr, 24.2 ppm Se, 3.23 ppm Te, 3.3 ppm Ag, and 6,500 ppm Cu. Access was granted by private land owners.

Strong mine, sec. 4, T. 16 N., R. 71 W., Albany County

The original mine included a 110 m (360 ft) shaft with five levels totaling at least 399 m (1,308 ft) of tunnels by 1907 (Beeler, 1907). The shaft was sunk into fractured diabasic and gabbroic dikes hosted by layered gneiss and schist surrounded by granite and anorthosite (Hausel, 1997). Tungsten was targeted in scheelite deposits at the 107 m (350 ft) level. Scheelite ore, totaling 90.7 tonnes (100 tons), was shipped to Boulder, Colo. and yielded 0.2 to 0.6 percent WO_3 (Hausel, 1997). Gold, silver, and nickel were also recovered from the mine (Beeler, 1942). A grab sample of scheelite- and pyrite-bearing quartz-potassium feldspar-biotite gneiss (Sample 19710416ST-3) contains 5,820 ppm tungsten but no REE enrichment (Sutherland and others, 2013).

Taylor deposit, SE¼SE¼ sec. 2, T. 20 N., R. 71 W., Albany County

A large quarry exists at this location. Dark anorthosite, with bleaching in some areas, hosts a massive titaniferous-magnetite deposit. This deposit, related to the Laramie Anorthosite Complex, is thought to have accumulated by magmatic segregation (Sutherland and Cola, 2015). A sample of magnetite yielded 62.9 percent Fe_2O_3, 18.25 percent TiO_2, and 3,410 ppm V.

Chalk Bluff, center S½NW¼NE¼ sec. 11, T. 24 N., R. 82 W., Carbon County

Several layers of volcanic material of unknown origin crop out here in the northern part of the Hanna Basin (J. Lillegraven, personal communication, 2014). Samples of rhyolite, ash flows, iron oxide-rich layers, silicified ash, and welded tuffs were collected during an earlier investigation. Of these samples a slight elevation of REE was found in a 1.5 m (5 ft) thick iron oxide-rich ash layer (20140822WS-B) in the form of 134 ppm Ce and 88.4 ppm La. Vanadium was also elevated to 1,640 ppm. Another sample of rhyolitic cobbles (20140822WS-A) contained 1,215 ppm V and 17 ppm Se.

Eureka mine, NE¼SE¼NW¼ sec. 22, T. 14 N., R. 84 W., Carbon County

The Eureka mine area is located within the Grand Encampment district in the Sierra Madre. In the region, faulting and shearing from the Mullen Creek-Nash Fork shear zone is prevalent in Precambrian igneous and metamorphic rocks. By 1901, thousands of prospects had been dug in the area, claims had been staked, and over more than 200 mining companies were operating (Hausel, 1997). However, the exact history of this particular locale is unknown.

The reclaimed location of the Eureka mine is made up of mafic dike material with some rusty quartzite and concretionary iron, which may be granular, brecciated, or vesicular (20150917LC-1). Chemical analysis revealed 0.02 ppm Au, 74.3 percent Fe_2O_3, 1,015 ppm V, 6.9 pp, Se, 2.91 ppm Te, 1,050 ppm Co, 3,770 ppm Cu, and 1,590 ppm Ni.

Many small prospects can be found in the area, but one of interest, in the SW¼NE¼SW¼ of the same section, contains quartzite and schist with some silicification and jasperization as well as heavy copper mineralization in the form of malachite and azurite. The rock can vary from quite dense to light and porous. In some places, the rock is very altered, "punky," and a rusty- to dark-brown color. Two samples taken from the pit (20150825LC-8A, 8B) contained 0.24 and 0.55 ppm Au, 13.8 and 62.7 percent Fe_2O_3, 211 and 1,840 ppm V, 2.27 and 0.869 ppm In, 10.4 and 5.5 ppm Se, and 9.3 and 1.335 percent Cu. Outside of the excavated area, the outcrop is not well exposed; therefore, the size of this deposit is unknown.

Gold Coin mine, SW¼ sec. 11, T. 15 N., R. 87 W., Carbon County

The Gold Coin mine targeted copper, lead, gold, and silver mineralization within a 0.3 m (1 ft) wide quartz vein (Beeler, 1902; Hausel, 1997). The vein is concentrated within a fissure that trends 75° and dips to the south at a high angle (Spencer, 1904). The vein cuts the regional foliation of the hosting Late Archean black diorite (Beeler, 1902; Spencer, 1904). A sample of vein quartz with abundant limonite (possibly replacing sulfides), galena, chalcopyrite with chalcocite rims, and minor malachite (Sample 20121203WSGS-B) from the Gold Coin mine yielded 318 ppm (9.27 oz/ton) silver, 0.11 ppm (0.003 oz/ton) gold, 0.11 percent copper, and 14.6 percent zinc (Sutherland and others, 2013).

Hub prospect, E½NE¼ sec. 6, T. 15 N., R. 87 W., Carbon County

The Hub prospect targeted a 0.5 m (1.5 ft) thick quartz vein that cuts sheared amphibolite of the Late Archean Silver Lake Metavolcanics. Hausel (1986) reported a sample of this quartz vein that yielded 0.41 percent copper, 150.8 g/tonne (3.99 oz/ton) silver, and no gold. Visible gold was reported in a separate sample (Hausel, 1997), and a sample of limonite-stained vein quartz, mineralized with chalcopyrite, pyrite, bornite, malachite, and hematite, analyzed for this report, yielded 17.25 ppm (0.50 oz/ton) gold, 41.3 ppm (1.20 oz/ton) silver, and 2.62 percent copper (Sutherland and others, 2013). A sample (20150918LC-1) collected for this study from intensely sheared rock with quartz veins, copper mineralization, vuggy quartz, and actinolite contained 1.4 ppm Ag, 2,010 ppm Cu, and 2.83 ppm Au.

Nature's Mint mine, S½N½ sec. 30, T. 14 N., R. 80 W., Carbon County

This historic gold mine, located on private property, still has original structures in place. A granitic gneiss with rusty pyrite in a waste pile (20150818LC-10A) had 1.32 ppm Au, >250 ppm As, 34.2 ppm Bi, 34.9 ppm Ag, 7,740 ppm Cu, and 1,150 ppm Pb. A second sample (20150818LC-10B), taken from altered mafic material in another mine dump, contained elevated REE, 35 ppm Sc, and 0.24 ppm Au. A prospect to the north of the mine, locally referred to as a "rhodochrosite prospect," contained 0.49 ppm Au in rusty, quartz-rich pegmatite float.

Section 8 mine, S½SE¼ sec. 8, T. 14 N., R. 85 W., Carbon County

The Section 8 mine targeted copper mineralization hosted in pyritized banded chert within amphibolite of the Silver Lake Metavolcanics; the exact field relationship between the amphibolite and chert is unknown. In addition to the amphibolite, chlorite-garnet schist is also present in the Silver Lake Metavolcanics in the vicinity of the Section 8 mine. The banded chert has a trend of 81° and dips 52° SE. Mineralization is concordant with the local banding in the chert. A sample from the mine yielded 2.61 percent copper but no detectable gold (Hausel, 1986; 1997); silver was not reported. A sample of pyrite- and chalcopyrite-bearing banded chert (Sample 20121203WSGS-D) yielded 27.4 ppm (0.80 oz/ton) silver and 6.75 percent copper (Sutherland and others, 2013).

Unnamed mine, N½SE¼SW¼ sec. 35, T. 15 N., R. 80 W., Carbon County

Just north of the Savage Run Wilderness boundary in the Medicine Bow Mountains, several interconnected prospects cover a 137 by 85 m (450 by 280 ft) area. Most of the rock is extremely altered, punky, rusty material with vuggy quartz and prevalent copper mineralization. Material is both mafic and felsic in origin, but heavy shearing and brecciation make it impossible to discern any details of the host rock. Samples (20150818LC-8A-D) contained up to 0.237 ppm Au, <0.005 ppm Pt, 0.004 ppm Pd, 24.2 percent Fe_2O_3, >250 ppm As, 2,200 ppm Sr, 7.5 ppm Se, 37.6 ppm Ag, and 11.65 percent Cu. The area does not appear to be mined-out, so the elevated amount of gold and copper may warrant further investigation.

Bison Basin area, NW¼NW¼NW¼ sec. 17, T. 27 N., R. 96 W., Fremont County

The Tensleep Sandstone crops out within and adjacent to a canyon at this location. Rather than the typical sandstone lithology, it is heavily silicified into a quartzite. A grab sample (20150713LC-6) revealed a composition of

99.1 percent SiO_2 and only 0.28 percent Fe_2O_3 (table 48). According to Harris (1988), a silica (SiO_2) content of 95 percent or greater is primary raw material in the manufacture of glass. A silica content of greater than 98 percent is necessary for the manufacture of ferrosilicon, and a purity of greater than 99 percent SiO_2 is necessary for production of silicon metal (Murphy and Brown, 1985). This high purity silica may be of possible industrial interest if its purity extends over a significant area.

Bison Basin area, NE¼NE¼SE¼ sec. 20, T. 27 N., R. 96 W., Fremont County

A limonitic, rusty, nodular layer (20150713LC-4), in either the Bridger or Fort Union Formations (Sutherland and Hausel, 2006), contains highly polished, agatized, and silicified float as well as 33.4 percent Fe_2O_3, >250 ppm As, and 17.5 ppm Tl. This site is located near the poorly exposed, east-trending Flat Top fault. A second sample (20150713LC-5) taken in a similar, concretion-rich, limonitic layer in the SE¼NW¼NE¼ of sec. 20, contained >250 ppm As and 11.9 ppm Se. This sample is in the Wagon Bed Formation and is located along a northwest-trending, poorly exposed splay of the Flat Top fault.

Black Rock Gap prospect, SE¼SW¼ sec. 32, T. 31 N., R. 91 W., Fremont County

The Black Rock Gap prospect is located along an east-trending shear zone in the north-central Granite Mountains. Intensive potassic and propylitic alteration surrounds the prospect that has a 4.6 m (15 ft) long adit in the center of a north-trending antiformal structure just west of Black Rock Gap. The adit follows a 95˚ trending, near vertical shear zone, which cuts granitic gniess, mafic, and ultramafic rocks. Brecciation accompanies shearing in some areas. Abundant jasper and epidote are present near the adit as well as copper staining. Epidotization is spread across a wide area near the prospect and is easily seen in aerial imagery. A sample of sheared ultramafic rock with copper staining (20121009WS-A) yielded 0.5 ppm (0.015 oz/ton) gold, 318 ppm cobalt, 516 ppm chromium, and 1.15 percent copper. A sample of iron-stained fault gouge from the shear zone (20121009WS-B) yielded 0.51 ppm (0.015 oz/ton) gold, 318 ppm cobalt, 515 ppm chromium, and 1.575 percent copper. Two additional samples from the prospect of brecciated mafic rock with $CaCO_3$ cement (20121009WS-C) and severely altered and brecciated felsic gneiss (20121009WS-D) yielded 1,200 ppm and 1,630 ppm chromium, respectively (Sutherland and others, 2013).

Ore Road quarry, center N½ sec. 6, T. 30 N., R. 91 W.; center S½ sec. 31, T. 31 N., R. 91 W., Fremont County

A variety of rocks are exposed in the Ore Road quarry north of Jeffrey City. Sheared amphibolite, mafic and felsic pegmatites and dikes, and quartz veins cross-cut granitic gneiss. Sampling focused on syenitic gneiss and pegmatite that primarily contained k-feldspar, quartz, muscovite, biotite, occasionally garnet, and a dark, dull, blocky mineral (20150602LC-1, 2). Although there were no elevated REE, 803 ppm Rb, >250 ppm As, and 31 ppm Bi were observed. A prospect just to the north of this location contained a welded tuff with varying degrees of silicification and opalization. A sample (20150602LC-3) contained >250 ppm As and 0.02 ppm Au.

Owl Creek Mountains, sec. 28, T. 40 N., R. 93 W., Fremont County

Along the southern flanks of Owl Creek Mountains, many prospects and mines have been developed in search of gemstones, copper, iron formation, and more. Many of the areas sampled contained beryl, apatite, garnet, and tourmaline. At one prospect, in the SE¼SE¼NW¼ of the section, pegmatites with bands of garnets form soft-sediment deformation-like patterns; sections of pegmatite contain milky feldspars (20150804LC-2B) and copper staining (20150804LC-2C). Alone, the feldspar contains 108.5 ppm Cs and 2,960 ppm Rb. The copper-rich sample contained 96.8 ppm Ga, 848 ppm Rb, and 117 ppm Sn.

In the SW¼NE¼ part of section 28, rusty granitic gneiss host pegmatites with beryl, tourmaline, and muscovite. Epidotized rock (20150804LC-4B) contained elevated Cs at 128 ppm and Rb at 2,170 ppm.

Southeast Wind River Basin, SW¼NE¼ sec. 18, T. 34 N., R. 89 W., Fremont County

An intense orange to limonitic exposure of possibly Fort

Table 48. Major element oxide composition of the Tensleep Sandstone in Bison Basin. Bold values indicate concentrations greater than five times the crustal abundance.

	Bison Basin							
Element	SiO_2 (%)	Al_2O_3 (%)	Fe_2O_3 (%)	CaO (%)	MgO (%)	Na_2O (%)	K_2O (%)	Cr_2O_3 (%)
20150713LC-6	**99.1**	0.7	0.28	0.47	0.09	0.04	0.49	<0.01
Element	TiO_2 (%)	MnO (%)	P_2O_5 (%)	SrO (%)	BaO (%)	C (%)	S (%)	Total (%)
20150713LC-6	0.02	<0.01	0.12	0.01	0.01	0.09	0.01	101.43

Union Formation contains elevated selenium at 35.7 ppm (Sample 20150803LC-11). In this area, the ground is also covered in petrified wood and polished, silicified to agatized, well-rounded material.

Unnamed-South Pass area, SE¼ sec. 23, T. 29 N., R. 98 W., Fremont County

A sample of black, very fine- to fine-grained quartz biotite schist, cut by a white, fine-grained quartz vein with epidote, chlorite, and scheelite (Sample 20121212WSGS-B) contains 5,190 ppm tungsten, 0.15 ppm gold (0.004 oz/ton), and 0.23 ppm (0.007 oz/ton) silver (Sutherland and others, 2013).

Unnamed, SE¼SE¼NE¼ sec. 26, T. 29 N., R. 98 W., Fremont County

A quartz vein with iron-oxidation and copper staining was sampled at this location in a previous WSGS investigation. The sample (20140925WS-B) contained 0.37 ppm Au, >250 ppm As, >250 ppm Bi, 2.16 ppm In, 1.8 ppm Ag, and 4,340 ppm Cu.

Garnet Hill, E½NW¼NE¼ sec. 26, T. 28 N., R. 65 W., Goshen County

Many prospects in this area expose very altered, crumbly, purplish-black rock with limonitic and rusty stain. Some parts of the rock appear brecciated and dense while others are porous and light. Goethite was found in float, and jasperization varies between prospects but indicates heavy silicification occurred in the area. The iron-rich, purplish-black rock (20150923LC-1) contained 68.6 percent Fe_2O_3 and 1,005 ppm V.

Another set of adits with mine dumps can be found along the drainage to the west. Here, folded and faulted, sulfur-rich shale and slatey to schistose rock with a white fibrous mineral hosts sulfur-rich, bowling ball-like, iron concretions. The bowling ball concretions (20150923LC-4B) contained 0.04 ppm Au, 38.8 percent Fe_2O_3, 24.1 percent S, 14.4 ppm Se, and 3.2 ppm Ag.

This area is mapped as primarily Precambrian Haystack Range Granite and quartzofeldspathic schist with pegmatites. Metamorphism attained sillimanite-grade as garnet, andalusite, and sillimanite have been found in the area. Although mapping on the 1:100,000 scale does not show detailed structure in the immediate vicinity of Garnet Hill, folding and faulting related to the Hartville Uplift are abundant just to the west (McLaughlin and Harris, 2005).

Black Mountain, NW¼NW¼SW¼ sec. 1, T. 32 N., R. 89 W., Natrona County

Black Mountain is composed primarily of McDougal Gulch Metavolcanics and mafic dikes. Prospect pits dotting the northwest side of the peak also reveal quartz and spodumene-rich veins; the largest exposure reaching almost 7.6 m (25 ft) wide with unknown length and depth. The greenish-gray spodumene forms large euhedral-massive crystals and is accompanied by black and dark-green tourmaline and bluish apatite in varying amounts. One prospect also exposes slickenlines, indicating some fault movement in the immediate area. Four samples (20150609LC-1, 3, 4, 5) were taken from the various spodumene pits and contained up to 210 ppm Cs, 283 ppm Sn, 1,870 ppm Ta, and 7,000 ppm Li. One prospect differed in that it exposed rusty quartzite with some jasperization. This sample (20150609LC-2), thought to be in the Barlow Springs Formation, contained >250 ppm As but <0.01 ppm Au.

UT Creek – Lost Muffler fault prospects, NW¼NW¼ sec. 22, T. 32 N., R. 87 W., Natrona County

The UT Creek Formation is generally east-trending and inclined steeply south to near vertical in the northern part of the Saddle Rock quadrangle (Sutherland and others, 2012). The Archean formation is dominated by fine- to medium-grained metagreywackes and tuffaceous metagreywackes separated by a relatively thick metavolcanic member that is locally dominated by foliated to massive, black, fine-grained to aphanitic metabasalts (Hausel, 1996).

The Lost Muffler fault parallels the general east trend of the UT Creek Formation and carries anomalous gold values west of UT Creek (Hausel, 1996) where it is dotted with small prospects. Adjacent to a minor outcrop of black schist near the north side of the fault, east of UT Creek, and near a contact between metabasalt and metagraywacke, a prospect pit is dug into sheared metabasalt cut by iron-stained quartz veins. Sample 20120607WS-B is representative of the sheared metabasalt and associated quartz veins. Analysis of this sample showed 1.84 ppm (0.05 oz/ton) gold and no anomalous REE (Sutherland and others, 2013).

Wagon Bed Formation ash layer, NE¼SE¼ sec. 32, T. 32 N., R. 87 W., Natrona County

The Wagon Bed Formation crops out in this vicinity, where it is dominated by conglomerates, sandstones, and ash layers, along with minor silicified limestone. Conglomerate typical of the Wagon Bed Formation caps the ridge above and immediately to the northwest of this location. A tufa deposit from a paleo-hot spring (Sample 20120613WS-A) is underlain by a 1.5 to 3.0 m (5 to 10 ft) thick ash layer (Sample 20120613WS-B). The tufa (Sample 20120613WS-A) contains 3.68 ppm (0.11 oz/ton) gold, but the ash layer

contains no gold. No anomalous REE were detected in either sample (Sutherland and others, 2013).

Wagon Bed Formation, NW¼SE¼ sec. 30, T. 32 N., R. 88 W., Natrona County

The Wagon Bed Formation crops out south of the North Granite Mountains Fault in the northern part of the Blackjack Ranch 7.5' quadrangle. Regionally, it varies from pale-olive and greenish-gray, tuffaceous sandstone, siltstone, and mudstone with some ash layers to a highly variable coarse conglomerate. Outcrops of the Wagon Bed in this area are poorly exposed due to weathering and slope wash. However, ground disturbances, such as excavations or drill holes, provide opportunities to examine the lithology of the formation. At this site, a recent (2012) drill hole provided subsurface material from the Wagon Bed Formation. Three samples were collected here (20121031WS-E, F, and G). Cream to greenish and rusty-orange, very-fine grained sandstone and ash (Sample 20121031WS-F) contained 3.15 ppm (0.09 oz/ton) gold (Sutherland and others, 2013).

Leopard Rock mine, S¼NW¼SW¼ sec. 19, T. 56 N., R. 87 W., Sheridan County

A small excavation at this locale exposes "leopard rock" decorative stone. A dark, fine-grained, mafic matrix surrounds light colored, megacrystic plagioclase. The plagioclase is often subhedral or rounded and commonly has a reaction rim (Sample 20150811LC-1). The appearance of the rock is reminiscent of the pattern on a leopard, hence the name.

Southwest Lookout Mountain, NE¼NE¼SW¼ sec. 16, T. 54 N., R. 87 W., Sheridan County

In this area, many rehabilitated prospects and trenches dot the land. One of these is covered in abundant iron-rich float as well as iron-stained quartz veins, botryoidal hematite, and vuggy, crumbling, copper-stained rock. Sample 20150811LC-3 contained 57.2 percent Fe_2O_3 and 0.002 ppm Au.

Aspen Mountain area, sec. 4, T. 16 N., R. 104 W.; sec. 6, T. 17 N., R. 104 W., Sweetwater County

Sampling in the Aspen Mountain area revealed heavily silicified material and tufa-like deposits, suggesting the presence of paleo-hot springs and related faulting. Although outcrop is sparse, silicified, banded rock (20150930LC-2) was encountered on the east side of Aspen Mountain in the SE¼NW¼ of section 26. It is composed of 98.1 percent SiO_2; the low amount of impurities in this quartzite may be of interest for industrial silica uses.

Many carbonate-rich rocks with irregular layering indicate a hot spring origin, which has not been previously suggested for this region. Various carbonate-rich samples, taken from rock exposed by blasting for power line installation in the NW¼SW¼ of section 26, are somewhat silicified but also have a caliche coating, oolitic-branching textures, and vugs filled with a calcium-rich mineral (20150930LC-A, B). More outcrop of tufa-like rock is exposed near the north-central border of section 4. This possible paleo-hot spring is rich in calcium carbonate and exhibits layering, high porosity, and silicification. Radiating, milky to translucent calcite crystals fill layers and veins throughout (20150930LC-4). It also contains 4,790 ppm Sr. Further investigation of the area for more evidence of paleo-hot springs is necessary and could lead to more information on the geological history of south-central Wyoming.

Tiger Stripe chert, sec. 29, T. 14 N., R. 110 W., Sweetwater County

In this area, a tan, silty unit just above the Robins Egg Blue Tuff in the Wasatch Formation contains Tiger Stripe chert scattered throughout (20150928LC-2). Some pieces display alternating tan and black layers while others are predominately black (fig. 44). In south-central Wyoming and northwestern Utah, this material was used by paleo-indians for arrowheads and tools.



Figure 44. Tiger Stripe chert from the Wasatch Formation.

CONCLUSIONS

Rare earth elements are encompassed in everyday life whether in cell phones or energy provided by wind turbines. The importance of REE to national defense and the continuously advancing technology sector is immense. It is vital to the United States, and globally, that more REE resources be found and made available for use.

Localities of REE enrichment occur in Wyoming within pegmatites, Precambrian igneous and metamorphic rocks, paleoplacer black sandstone deposits, coarse-grained sandstones and conglomerates, and phosphatic units. Carbonatites in the state have been known to be both enriched and barren in rare earths.

REE have also been found concentrated in the same sedimentary units that host uranium deposits, whether accompanied by uranium or not. These occurrences are clustered in the northeastern Great Divide Basin uranium district, Shirley Basin uranium district, and to a lesser extent in the Gas Hills uranium district. These sediment-hosted REE concentrations may have differentially precipitated from the same solutions that concentrated the economic uranium deposits because of changing redox conditions. Significant chemical processing challenges need to be addressed before REE extraction becomes practical from uranium tailings.

Recently, the ability to extract REE from coal has become a rising interest. However, REE concentrations within most Wyoming coals are notably less than average crustal abundances. Although REE will concentrate in residual waste products derived from coal combustion, the low amounts typically found in Wyoming coals combined with processing and transportation factors do not indicate economic potential for the extraction of REE from the coal under current conditions.

Even though many of the areas in Wyoming with REE enrichment do not appear to have economic potential, the Bear Lodge deposit in northeastern Wyoming has great promise of becoming an active REE mine. A lull in the current market has slowed the progress made toward establishing a mine and processing center, but the excellent quality and substantial amount of REE may justify its future development.

This continued investigation of REE in Wyoming expanded upon previously known sites and established new locations of enrichment in a variety of geologic settings across the state.

Large amounts of accessible analytical data can be found on the WSGS's online database Wyo-DOG. The information provided here will hopefully foster exploration and lead to greater knowledge and better understanding of REE and other potentially economic minerals in Wyoming.

ACKNOWLEDGEMENTS

The authors thank the following people and organizations for their support and contribution throughout the creation of this report. The Wyoming State Legislature for initiating this project and allocating the funds for it; State Geologist and WSGS Director Tom Drean as well as Alan Ver Ploeg, David Lucke, and Seth Wittke for their management oversight; Kathy Olson for keeping the project on budget and moving forward; and Suzanne Luhr for editing the various maps and figures in the report. Many thanks are given to Judy Sutherland and Mat Dunlop for their support and patience over a long field season; and Robert Gregory, Davin Bagdonas, Christopher Carroll, Ranie Lynds, Rachel Toner, and Jacob Carnes for sharing samples and data. Special thanks to Robert Gregory, Christopher Carroll, Jacob Carnes, Andrea Loveland, and Christina George for editorial review of the publication.

We especially thank all of those who allowed us access and sampling on several sites of private land, including John Voight of New Sunrise LLC, Gary Vakotnic of the Rock Springs Grazing Association, Jim Purdy, Shelley and John Ellis, Robert Logan, Wayne Turcato, Nancy Bath, Rex Cue of the Fischer Ranch, and Hugh Hageman. It was a pleasure to get your perspective on the local areas, and we are grateful for your help. A big thanks also goes to Dick Larsen at Rare Element Resources, Ltd. for insightful conversations regarding the rare earth industry and the Bear Lodge deposit as well as James Hower at the University of Kentucky for assistance on coal-related rare earth occurrences. A special thanks also goes to XRD specialist Kriss Leftwich for helping refine the more puzzling diffraction patterns.

All maps were compiled using data from the following sources: USBLM, U.S. Census Bureau, USGS, the Wyoming Geographical Information Science Center, and the WSGS. We appreciate the use of this data.

REFERENCES

Adams, J.W., Arengi, J.T., and Parrish, I.S., 1980, Uranium- and thorium-bearing pegmatites of the United States: U.S. Department of Energy Report GJBX-166(80), 476 p.

Albee, H.F., 1968, Geologic map of the Munger Mountain quadrangle, Teton and Lincoln Counties, Wyoming: U.S. Geological Survey Geologic Quadrangle Map GQ-705, scale 1:24,000.

Anthony, J.W., Bideaux, R.A., Bladh, K.W., and Nichols, M.C., eds., 2001, Handbook of Mineralogy, Mineralogical Society of America, Chantilly, VA, accessed May 2015, at http://www.handbookofmineralogy.org/.

Autenrieth, K.D., 2012, Geologic setting of gold mineralization in the Rattlesnake Hills, Wyoming: Pocatello, Idaho State University, M.S. thesis, 259 p., 2 pls., scale 1:12,000.

Bailey, R.V., and Gregory, R.W., 2011, The Shirley Basin mine and the development of the roll front model of uranium ore deposition: An historical perspective: Wyoming State Geological Survey Memoir 6, 36 p.

Beeler, H.C., 1907, A report on the Strong mine, Leslie, Albany County, Wyoming: Office of the State Geologist [Wyoming State Geological Survey] Mineral Report 07-87, 16 p.

Beeler, H.C., 1942, A brief statement on conditions noted at the Strong mine 16 miles northeast of Laramie, Albany County, Wyoming: Geological Survey of Wyoming [Wyoming State Geological Survey] Mineral Report 42-1, 8 p.

Benham, J.R., 1984, The Meade Peak phosphatic shale member of the Permian Phosphoria Formation in the Snake River Range, Bonneville and Teton Counties, Idaho, and Lincoln and Teton Counties, Wyoming: Cheney, Eastern Washington University, M.S. thesis, 80 p.

Blackstone, D.L., and Hausel, W.D., 1992, Field guide to the Seminoe Mountains, *in* Frost, B.R., and Roberts, S., eds., Mineral resources of Wyoming, Wyoming Geological Association 42nd annual field conference guidebook: Geological Survey of Wyoming [Wyoming State Geological Survey], Reprint 48, p. 201–210.

Blatt, H., and Tracy, R.J., 1997, Petrology (2nd ed.), New York: Freeman, 66 p.

Bolmer, R.L., and Biggs, P., 1965, Mineral resources and their potential on Indian Lands, Wind River Reservation, Fremont and Hot Springs Counties, Wyoming: U.S. Bureau of Mines Preliminary Report 159, 103 p.

Borrowman, S.R., and Rosenbaum, J.B., 1962, Recovery of thorium from a Wyoming ore: U.S. Bureau of Mines Report of Investigations 5917, 8 p.

Borzone, G., Raggio, R., and Ferro, R., 1999, Thermochemistry and reactivity of rare earth metals: Physical Chemistry Chemical Physics, v. 1(7), p. 1487–1500.

Bradley, W.H., 1964, Geology of the Green River Formation and associated Eocene rocks in southwestern Wyoming and adjacent parts of Colorado and Utah: U.S. Geological Survey Professional Paper 496-A, p. A1–A86, scale 1:250,000.

Bradsher, K., 2010, China said to widen its embargo of minerals: The New York Times, 19 October 2010, accessed October 2010, at http://www.nytimes.com/2010/10/20/business/global/20rare.html?_r=1.

Breckenridge, R.M., and Hinckley, B.S., 1978, Thermal springs of Wyoming: Geological Survey of Wyoming [Wyoming State Geological Survey] Bulletin 60, 104 p.

Bromley, C.P., 1955, U.S. Atomic Energy Commission Preliminary Reconnaissance Report, DEB-S-2-1023, 1 p.

Bromley, C.P., 1957, Location of uranium occurrences in southcentral Wyoming and northeastern Colorado: U.S. Atomic Energy Commission Technical Report TM-D-1-23, 15 p.

Business Wire, 2015, Rare Element Resources Reports First Quarter Results: Business Wire, 11 May 2015, accessed May 2015, at http://www.businesswire.com/news/home/20150511005228/en#.VVZeDJOrFoO.

Cardinal, D.F., 1958, Geology of the Crystal Creek-Bald Mountain area, Big Horn and Sheridan Counties, Wyoming: Laramie, University of Wyoming, M.A. thesis, 114 p., 2 pls., scale 1:20,000.

Carey, B.D., 1959, Geology of the Rattlesnake Hills Tertiary volcanic field, Natrona County, Wyoming: Laramie, University of Wyoming, Ph.D. dissertation, 247 p., scale 1:63,360.

Carnes, J.D., 2015, Phosphate Rock in Wyoming: Wyoming State Geological Survey Report of Investigations 68, 34 p.

Carnes, J.D., Lynds, R.M., Gregory, R.W., and Ver Ploeg, A.J., 2013, Preliminary geologic map of the Dale Creek quadrangle, Albany County, Wyoming: Wyoming State Geological Survey Open File Report 13-2, 31 p., scale 1:24,000.

Carroll, C.J., Lynds, R.M., Ratigan, D.R., and Palkovic, M.J., 2015a, Report on the preliminary geologic maps of the Shamrock Hills and Rawlins Peak SW quadrangles, Carbon County, Wyoming: Wyoming State Geological Survey Open File Report 2015-08, 33 p.

Carroll, C.J., Ratigan, D.R., Lynds, R.M., and Palkovic, M.J., 2015b, Preliminary Geologic Map of the Rawlins Peak Southwest Quadrangle, Carbon County, Wyoming: Wyoming State Geological Survey Open File Report 2015-06, scale 1:24,000.

Castor, B., and Hedrick, J.B., 2006, Rare Earth Elements, *in* Kogel, J.E., Trivedi, N.C., Barker, J.M., and Krukowsk, eds., Industrial minerals and rocks: commodities,

markets, and uses (7th ed.): Littleton, Colorado, Society for Mining, Metallurgy and Exploration, Inc., p. 769-792.

Chamberlain, K.R., and Frost, B.R., 1995, Mid-Proterozoic mafic dikes in the central Wyoming Province: evidence for Belt-age extension and supercontinent breakup [abs.]: Proceedings of the Geological Association of Canada–Mineralogical Association of Canada 40th annual conference, Victoria, BC, v. 20, p. A-15.

Chamberlain, K.R., Frost, C.D., and Frost, B.R., 2003, Early Archean to Mesoproterozoic evolution of the Wyoming Province–Archean origins to modern lithospheric architecture: Canadian Journal of Earth Sciences, v. 40, no. 10, p. 1357–1374.

Chamberlain, K.R., Sears, J.W., Frost, B.R., and Doughty, P.T., 2000, Ages of Belt Supergroup deposition and intrusion of mafic dikes in the central Wyoming Province: evidence for extension at ca. 1.5 Ga and 1.37 Ga and potential piercing points for Rodinia reconstructions [abs.]: Geological Society of America Abstracts with Programs, v. 32, no. 7, p. A-319.

Cheney, T.M., Sheldon, R.P., Waring, R.G., and Warner, M.A., 1953, Stratigraphic sections of the Phosphoria Formation in Wyoming, 1951: U.S. Geological Survey [Atomic Energy Commission] Trace Elements Investigations Report TEI-377, 28 p.

Condie, K.C., and Lo, H.H., 1971, Trace element geochemistry of the Louis Lake batholith of Early Precambrian age, Wyoming: Geochimica et Cosmochimica Acta, v. 35, p. 1099–1119.

Cordier, D.J., 2011, Rare Earths, in Mineral commodity summaries 2011: U.S. Geological Survey, p. 128–129.

Damascena, K.F.R, Amaral, R.S., Santos Junior, J.A., Genezini, F.A., Silva, A.A., and Menezes, R.S.C., 2015, Rare-earth elements in uranium deposits in the municipality of Pedra, Pernambuco, Brazil: Journal of Radioanalytical and Nuclear Chemistry, v. 304(3), p. 1053-1058.

Damp, J.N., and Brown, L., 1982, National Uranium Resource Evaluation Arminto Quadrangle, Wyoming: U.S. Department of Energy Report PGJ/F-18(82), 61 p., 7 sheets microfiche.

Damp, J.N., and Jennings, M.D., 1982, National uranium resource evaluation Sheridan Quadrangle, Wyoming and Montana: U.S. Department of Energy Report PGJ/F-127(82), 63 p., 6 sheets microfiche.

Davis, K., 2011, Supply of Critical Rare-earth Elements About to Expand: IDG News-PCWorld, 31 October 2011, accessed November 2011, at http://www.pcworld.com/businesscenter/article/242892/supply_of_critical_rareearth_elements_about_to_expand.html.

Deer, W.A., Howie, R.A., and Zussman, J., 1967, Rock-forming minerals, Non-silicates: London, Longmans, Green, and Co., v. 5, 371 p.

DeNault, K.J., 1967, Geology and distribution of copper, lead, and zinc in streams and soil–Broadway mine area, Carbon County, Wyoming: Laramie, University of Wyoming, M.S. thesis, 45 p.

Denson, N.M., and Pipiringos, G.N., 1974, Geologic map and sections showing areal distribution of Tertiary rocks near the southeastern terminus of the Wind River Range, Fremont and Sweetwater Counties, Wyoming: U.S. Geological Society Miscellaneous Investigations Series Map I-835, scale 1:48,000.

Deonarine, A., Kolker, A., and Doughten, M., 2015, Trace Elements in Coal Ash: U.S. Geological Survey Fact Sheet 2015–3037, 6 p.

DeWitt, E., Redden, J.A., Wilson, A.B., and Buscher, D., 1986, Mineral resource potential and geology of the Black Hills National Forest, South Dakota and Wyoming: U.S. Geological Survey Bulletin 1580, 135 p., 4 pls., scale 1:250,000.

Donnay, G., and Donnay, J.D.H., 1971, Ewaldite, a new barium calcium carbonate: Tschermaks Mineralogische und Petrographische Mittelungen, v. 15, no. 3, p. 185–200.

Dow, V.T., and Batty, J.V., 1961, Reconnaissance of titaniferous sandstone deposits in Utah, Wyoming, New Mexico, and Colorado: U.S. Bureau of Mines Report of Investigations 5860, 52 p.

Dribus, J.B., and Nanna, R.F., 1982, National uranium resource evaluation, Rawlins quadrangle, Wyoming and Colorado: U.S. Department of Energy Report PGJ/F19(82), 116 p., 21 sheets microfiche.

Duke, G.I., 2005, Geochemistry of Paleocene-Eocene alkalic igneous rocks, northern Black Hills, South Dakota and Wyoming: Rapid City, South Dakota School of Mines and Technology, Ph.D. dissertation, 291 p.

Dunnewald, J.B., 1958, Geology of the Fish Lake Mountain area, Fremont County, Wyoming: Laramie, University of Wyoming, M.S. thesis, 1 pl., scale 1:24,000.

Dyman, T.S., Porter, K.W., Tysdal, R.G., Cobban, W.A., and Obradovich, J.D., 2000, Late Albian Blackleaf and Thermopolis-Muddy sequence in southwestern Montana and correlation with time-equivalent strata in west-central Montana [abs.], *in* Schalla, R.A., and Johnson, E.H., eds., Montana Geological Society 50th Anniversary Symposium Montana/Alberta Thrust Belt and Adjacent Foreland, v. 2, p. 65–82.

Dyni, J.R., 1997, Sodium carbonate resources of the Green River Formation, *in* Jones, R.W., and Harris, R.E., eds., 1997, Proceedings of the 32nd annual forum on the geology of industrial minerals: Wyoming State Geological Survey Public Information Circular 38, p. 123–143.

El-Etr, H.A., 1963, Pegmatites of the Anderson Ridge Quadrangle, Fremont County, Wyoming: Rolla, Missouri School of Mines, M.S. thesis, 102 p.

Ellis, J.R., 1977, Chemical and physical analyses of selected soil samples in Wyoming, 1967–1969: U.S. Department of Energy Report GJBX-45(77), 315 p.

Elmquist, S., 2011, Rare earths fall as GE, Toyota find alternatives: Bloomberg News, 2 October 2011, accessed November 2011, at http://www.pittsburghlive.com/x/pittsburghtrib/business/s_759771.html.

Els, F., 2015, Rare earth price rally evaporates: Mining.com, 13 April 2015, accessed April 2015, at http://www.mining.com/rare-earth-price-rally-evaporates/?utm_source=digest-en-mining-150413&utm_medium=e-mail&utm_campaign=digest.

Fahey, J.T., 1962, Saline minerals of the Green River Formation: U.S. Geological Survey Professional Paper 405, p. 5–12.

Fladager, G., 2015, Digging in: rare element mine moves forward: Casper Journal, 9 February 2015, accessed May 2015, at http://casperjournal.com/business/article_d836fa31-4c45-5e7c-b4a9-fd5ee357bd49.html.

Fitzpatrick, J., and Pabst, A., 1977, Burbankite from the Green River Formation, Wyoming: American Mineralogist, v. 62, no. 1 and 2, p. 158–163.

Frost, C.D., and Fanning, C.M., 2006, Archean geochronological framework of the Bighorn Mountains, Wyoming: Canadian Journal of Earth Sciences, v. 43, no. 10, p. 1399–1418.

Frost, C.D., Frost, B.R., Chamberlain, K.R., and Edwards, B.R., 1999, Petrogenesis of the 1.43 Ga Sherman batholith, SE Wyoming, USA—A reduced, rapakivi-type anorogenic granite: Journal of Petrology, v. 40, no. 12, p. 1771–1802.

Frost, C.D., Frost, B.R., Chamberlain, K.R., and Hulsebosch, T.P., 1998, The Late Archean history of the Wyoming province as recorded by granitic magmatism in the Wind River Range, Wyoming: Precambrian Research, v. 89, p. 145–173.

Frost, B.R., and Frost, C.D., Lindsley, D.H., Scoates, J.S., and Mitchell, J.N., 1993, The Laramie Anorthosite Complex and Sherman batholith: geology, evolution, and theories of origin, *in* Snoke, A.W., Steidtmann, J.R., and Roberts, S.M., eds., Geology of Wyoming: Wyoming State Geological Survey Memoir 5, p. 118–161.

Frost, C.D., Fruchey, B.L., Chamberlain, K.R., and Frost, B.R., 2006, Archean crustal growth by lateral accretion of juvenile supracrustal belts in the south-central Wyoming Province: Canadian Journal of Earth Sciences, v. 43, p. 1533–1555.

Gambogi, J., 2014, Rare Earths: U.S. Geological Survey Mineral Commodity Summaries, 2 p.

Gambogi, J., 2015a, Rare Earths: U.S. Geological Survey Mineral Commodity Summaries, 2 p.

Gambogi, J., 2015b, Yttrium: U.S. Geological Survey Mineral Commodity Summaries, 2 p.

Gambogi, J., 2016, Rare Earths: U.S. Geological Survey Mineral Commodity Summaries, 2 p.

Garrand, M.S., Kopp, R.S., and Cohenour, R.E., 1982, National uranium resource evaluation, Cody quadrangle, Wyoming: U.S. Department of Energy report PGJ/F-43(82), 63 p., 7 sheets microfiche.

Gebhardt, R., Jennings, M., and Fiscus, D., 1982, National uranium resource evaluation Lander quadrangle, Wyoming: U.S. Department of Energy Report PGJ/F-50(82), 37 p., 5 sheets microfiche.

Gere, W.C., Schell, E.M., and Moore, K.P., 1966, Stratigraphic sections and phosphate analyses of Permian rocks in the Teton Range and parts of the Snake River and Gros Ventre Ranges, Idaho and Wyoming: U.S. Geological Survey Open File Report 66-47, 67 p.

Gersic, J., Peterson, E.K., and Schreiner, R.A., 1990, Appraisal of selected mineral resources of the Black Hills National Forest, South Dakota and Wyoming: U.S. Bureau of Mines Mineral Land Assessment Open File Report MLA 5-90, 255 p.

Geslin, H.E., 1954, U.S. Atomic Energy Commission Preliminary Reconnaissance Report DEB-RRD-1315, 1 p.

Grace, K.M., 2010, A rare find in rare earths–Commerce Resources' Eldor project could help break the Chinese monopoly: Resource Clips, 15 December 2010, accessed December 2010, at http://resourceclips.com/2010/12/15/a-rare-find-in-rare-earths/?.

Grace, R.L.B., Chamberlain, K.R., Frost, B.R., and Frost, C.D., 2006, Tectonic histories of the Paleoarchean to Mesoarchean Sacawee block and Neoarchean Oregon Trail structural belt of south-central Wyoming Province: Canadian Journal of Earth Sciences, v. 43, no. 10, p. 1445–1466.

Graff, P.J., 1978, Geology of the lower part of the Early Proterozoic Snowy Range Supergroup, Sierra Madre, Wyoming: Laramie, University of Wyoming, Ph.D. dissertation, 85 p.

Graff, P.J., and Houston, R.S., 1977, Radioactive conglomerate in Proterozoic (Precambrian X) metasedimentary rocks of the Sierra Madre, Wyoming: U.S. Geological Survey Open-File Report 77-830, 8 p.

Granger, H.C., McKay, E.J., Mattick, R.E., Patten, L.L., and McIlroy, P., 1971, Mineral resources of the Glacier Primitive Area, Wyoming: U.S. Geological Survey Bulletin 1391-F, 113 p., scale 1:62,500.

Gregory, R.W., Jones, R.W., and Cottingham, K.D., 2010, Uranium map of Wyoming: Wyoming State Geological Survey Map Series 94, scale 1:500,000.

Griffin, J.R., and Milton, E.J., 1982, National uranium resource evaluation, Casper quadrangle, Wyoming: U.S. Department of Energy Report PGJ/F-33(82), 65 p., 10 sheets microfiche.

Griffin, J.R., and Warner, A.J., 1982, National uranium resource evaluation, Cheyenne quadrangle, Wyoming: U.S. Department of Energy Report PGJ/F-115(82), 63 p., 5 sheets microfiche.

Grushkin, D., 2011, Alaska's billion dollar mountain: Bloomberg Businessweek, 27 October 2011, accessed November 2011, at http://www.businessweek.com/magazine/alaskas-billion-dollar-mountain-10272011.html.

Gulbrandsen, R.A., 1966, Chemical composition of phosphorites of the Phosphoria Formation: Geochimica et Cosmochimica Acta, v. 30, p. 769–778.

Gulbrandsen, R.A., 1977, Byproduct resources in phosphate ore of southeastern Idaho [abs.]: Geological Society of America Abstracts with Programs, v. 9, no. 6, p. 728.

Gupta, C.K. and Krishnamurthy, N., 2005, Extractive metallurgy of rare earths, Boca Raton, FL: CRC Press, 506 p.

Hadfield, J.P., Jr., 1954, U.S. Atomic Energy Commission Preliminary Reconnaissance Report DEB-RRD-1383, 1 p.

Hals, T., 2016, Creditors of bankrupt rare earths miner Molycorp reach deal: Reuters, 23 February 2016, accessed February 2016, at http://www.reuters.com/article/molycorp-bankruptcy-idUSL2N1621G0.

Harris, R.E., 1988, The Casa silica rock deposit, Platte County, Wyoming: Wyoming State Geological Survey Report of Investigations 42, 38 p.

Harris, R.E., and Hausel, W.D., 1986, Wyoming Pegmatites, *in* Modreski, P.J., ed., Colorado Pegmatites: abstracts, short papers, and field guides, Proceedings of the Colorado Pegmatite Symposium, May 30–June 2, 1986, Denver, Colorado: Friends of Mineralogy, Colorado Chapter, p. 101–108.

Harshman, E.N., 1968, Geologic map of the Shirley Basin area, Albany, Carbon, Converse, and Natrona Counties, Wyoming: U.S. Geological Survey Miscellaneous Geologic Investigations Map I-539.

Harshman, E.N., 1972, Geology and uranium deposits, Shirley Basin area, Wyoming: U.S. Geological Survey, Professional paper 745, 82 p.

Hart, O.M., 1955b, U.S. Atomic Energy Commission Preliminary Reconnaissance Report BH-B-95, 1 p.

Hausel, W.D., 1986, Mineral deposits of the Encampment district, Sierra Madre, Wyoming-Colorado: Geological survey of Wyoming [Wyoming State Geological Survey] Report of Investigations 37, 31 p.

Hausel, W.D., 1989, The geology of Wyoming's precious metal lode and placer deposits: Geological Survey of Wyoming [Wyoming State Geological Survey] Bulletin 68, 248 p.

Hausel, W.D., 1991, Economic geology of the South Pass granite-greenstone belt, southern Wind River Range, western Wyoming: Geological Survey of Wyoming [Wyoming State Geological Survey] Report of Investigations 44, 129 p., scale 1:48,000.

Hausel, W.D., 1992, Zinc-lead-copper-silver-gold-massive sulfide mineralization at the Broadway mine, Sierra Madre, Wyoming: Geological Survey of Wyoming [Wyoming State Geological Survey] Mineral Report MR92-4, 6 p.

Hausel, W.D., 1994, Economic geology of the Seminoe Mountains mining district, Carbon County, Wyoming: Wyoming State Geological Survey Report of Investigations 50, 31 p., scale 1:24,000.

Hausel, W.D., 1996, Geology and gold mineralization of the Rattlesnake Hills, Granite Mountains, Wyoming: Wyoming State Geological Survey Report of Investigations 52, 28 p., scale 1:24,000.

Hausel, W.D., 1997, Copper, lead, zinc, molybdenum, and associated metal deposits of Wyoming: Wyoming State Geological Survey Bulletin 70, 229 p.

Hausel, W.D., 1998, Diamonds and mantle source rocks in the Wyoming craton, with a discussion of other U.S. occurrences: Wyoming State Geological Survey Report of Investigations 53, 93 p.

Hausel, W.D., 2006, Geology and Geochemistry of the Leucite Hills Volcanic Field: Wyoming State Geological Survey Report of Investigations 56, 76 p., 1 pl., scale 1:100,000.

Hausel, W.D., 2007, Revised geologic map of the South Pass City 7.5' Quadrangle, Fremont County, Wyoming: Wyoming State Geological Survey Map Series MS-74, scale 1:24,000.

Hausel, W.D., Graff, P.J., and Albert, K.G., 1985, Economic geology of the Copper Mountain supracrustal belt, Owl Creek Mountains, Fremont County, Wyoming: Geological Survey of Wyoming [Wyoming State Geological Survey] Report of Investigations 28, 33 p., scale 1:24,000.

Hausel, W.D., Gregory, R.W., Motten, R.H., and Sutherland, W.M., 2003, Geology of the Iron Mountain kimberlite district and nearby kimberlitic indicator mineral anomalies in southeastern Wyoming: Wyoming State Geological Survey Report of Investigations 54, 42 p., 3 pls., scale 1:100,000.

Hausel, W.D., and Jones, S., 1982, Geological reconnaissance report of metallic deposits for in situ and heap leaching extraction research possibilities: Geological Survey of Wyoming [Wyoming State Geological Survey] Open File Report 82-4, 51 p., 3 pls.

Hausel, W.D., and Sutherland, W.M., 1988, The geology and mineral resources of the Black Hills uplift, Wyoming: Wyoming Geological Association 39th annual field conference guidebook, p. 285–293.

Haxel, G.B., Hedrick, J.B., and Orris, G.J., 2002, Rare earth elements–critical resources for high technology: U.S. Geological Survey Fact Sheet 087-02, 4 p.

Hedrick, J.B., 1985, Rare-earth elements and yttrium, in Mineral facts and problems: U.S. Bureau of Mines Bulletin 675, p. 647–664.

Hedrick, J.B., 2004, Rare earths in selected U.S. defense applications, *in* proceedings of the 40th forum on the Geology of Industrial Minerals, May 2-7, 2004, Bloomington, Indiana, 13 p.

Hedrick, J.B., 2010, Rare-earth industry overview and defense applications: Presentation by Hedrick Consultants Inc., Burke, Virginia, *in* the 2010 Society for Mining, Metallurgy, and Exploration annual meeting and exhibit, March 1, 2010.

Hedrick, J.B., and Templeton, D.A., 1988, Rare earth minerals and metals, *in* U.S. Bureau of Mines Minerals Yearbook, v. 1, p. 779–789.

Hess, F.L., and Bryan, B., Jr., 1938, The Pegmatites at Tinton, South Dakota.: U.S. Bureau of Mines Report of Investigations 3404, 19 p.

Hills, F.A., and Houston, R.S., 1979, Early Proterozoic tectonics of the central Rocky Mountains, North America: University of Wyoming Contributions to Geology, v. 17, no. 2, p. 89–109.

Hoch, A.R., and Frost, C.D., 1993, Petrographic and geochemical characteristics of mid-Tertiary igneous rocks in the Rattlesnake Hills, central Wyoming, with a comparison to the Bear Lodge intrusive suite of northeastern Wyoming, *in* Snoke, A.W., Steidtmann, J.R., and Roberts, S.M., eds., Geology of Wyoming: Wyoming State Geological Survey Memoir 5, p. 508–528.

Hoffman, J.D., and Buttleman, K., 1994, National Geochemical Data Base: National Uranium Resource Evaluation data for the conterminous United States, with MAPPER display software by R.A. Ambroziak and MAPPER documentation by C.A. Cook: U.S. Geological Survey Digital Data Series DDS-0018-A, CD-ROM.

Hoffman, J.D., and Buttleman, K., 1996, National Geochemical Data Base: 1. National Uranium Resource Evaluation (NURE) Hydrogeochemical and Stream Sediment Reconnaissance (HSSR) data for Alaska, formatted for GSSEARCH data base search software, 2. NURE HSSR data formatted as dBASE files for Alaska and the conterminous United States, 3. NURE HSSR data as originally compiled by the Department of Energy for Alaska and the conterminous United States, with MAPPER display software by R.A. Ambroziak and MAPPER documentation by C.A. Cook: U.S. Geological Survey Digital Data Series DDS-0018-B, CD-ROM.

Holmquist, G.V., 1955a, U.S. Atomic Energy Commission Preliminary Reconnaissance Report DEB-P-2-2606, 1 p.

Holmquist, G.V., 1955b, U.S. Atomic Energy Commission Preliminary Reconnaissance Report DEB-P-2-2607, 1 p.

Holmquist, G.V., 1955c, U.S. Atomic Energy Commission Preliminary Reconnaissance Report DEB-P-2-2282, 1 p.

Holmquist, G.V., 1955d, U.S. Atomic Energy Commission Preliminary Reconnaissance Report DEB-P-2-2281, 1 p.

Holmquist, G.V., 1956, U.S. Atomic Energy Commission Preliminary Reconnaissance Report DEB-P-2-2788, 1 p.

Houston, R.S., 1961, The Big Creek pegmatite area, Carbon County, Wyoming: Wyoming State Geological Survey Preliminary Report 1, 11 p.

Houston, R.S., 1993, Late Archean and Early Proterozoic geology of southeastern Wyoming, *in* Snoke, A.W., Steidtmann, J.R., and Roberts, S.M., eds., Geology of Wyoming: Wyoming State Geological Survey Memoir 5, p. 78–116.

Houston, R.S., and Karlstrom, K.E., 1981, A summary of the geology and uranium potential of Precambrian conglomerates in southeastern Wyoming, *in* Karlstrom, K.E., Houston, R.S., Flurkey, A.J., Coolidge, C.M., Kratochvil, A.L., and Sever, C.K., eds., Summary of the geology and uranium potential of Precambrian conglomerates in southeastern Wyoming: U.S. Department of Energy Report GJBX-139(81), p. 25–193.

Houston, R.S., Karlstrom, K.E., and Graff, P.J., 1978, Radioactive quartz-pebble conglomerates of the Sierra Madre and Medicine Bow Mountains, southeastern Wyoming: Geological Survey of Wyoming [Wyoming State Geological Survey] Open File Report 78-3, 49 p., 3 pls., scale 1:50,000.

Houston, R.S., Karlstrom, K.E., and Graff, P.J., 1979, Progress report on the study of radioactive quartz-pebble conglomerate of the Medicine Bow Mountains and Sierra Madre, southeastern Wyoming: U.S. Geological Survey Open File Report 79-1131, 43 p.

Houston, R.S., Karlstrom, K.E., Hills, F.A., and Smithson, S.B., 1979, The Cheyenne belt–a major Precambrian crustal boundary in the western United States: Geological Society of America Special Paper 11, p. 446.

Houston, R.S., and Love, J.D., 1956, Titaniferous sandstone in marine rocks of Late Jurassic age, northwestern Wyoming: Wyoming Geological Association 11th annual field conference guidebook, p. 7–74.

Houston, R.S., and Murphy, J.F., 1962, Titaniferous black sandstone deposits of Wyoming: Geological Survey of Wyoming [Wyoming State Geological Survey] Bulletin 49, 55 p.

Houston, R.S., and Murphy, J.F., 1970, Fossil beach placers in sandstones of Late Cretaceous age in Wyoming and other Rocky Mountains states: Wyoming Geological Association 22nd annual field conference guidebook, p. 241–249.

Houston, R.S., and Murphy, J.F., 1977, Depositional environment of Upper Cretaceous black sandstones of the western interior: U.S. Geological Survey Professional Paper 994-A, 29 p.

Hower, J.C., Dai, S., Seredin, V.V., Zhao, L., Kostova, I.J., Silva, L.F.O., Mardon, S.M., and Gurdal, G., 2013, A note on the occurrence of Yttrium and rare earth elements in coal combustion products: Coal combustion and gasification products, v. 5, p. 39-47.

Hower, J.C., Groppo, J.G., Henke, K.R., Hood, M.M., Eble, C.F., Honaker, R.Q., Zhang, W., and Qian, D., 2015, Notes on the Potential for the Concentration of Rare Earth Elements and Yttrium in Coal Combustion Fly Ash: Minerals, v. 5, p. 356–366.

Hsu, J., 2010, U.S. sitting on mother lode of rare tech-crucial minerals: LiveScience, 8 March 2010, accessed December 2011, at http://www.livescience.com/6179-sitting-mother-lode-rare-tech-crucial-minerals.html.

Hunter, J., Ver Ploeg, A.J., and Boyd, C.S., 2005, Geologic map of the Casper 30' x 60' quadrangle, Natrona and Converse Counties, Central Wyoming: Wyoming State Geological Survey Map Series 65, scale 1:100,000.

Jackson, W.D., and Christiansen, G., 1993, International strategic minerals inventory summary report–rare-earth oxides: U.S. Geological Survey Circular 930-N, 68 p.

Jamasmie, C., 2015a, US Gov't offers $20 million to projects aimed at recovering rare earths from coal: Mining.com, 1 July 2015, accessed July 2015, at http://www.mining.com/us-govt-offers-20-million-to-projects-aimed-at-recovering-rare-earths-from-coal/?utm_source=digest-en-mining-150701&utm_medium=email&utm_campaign=digest.

Jamasmie, C., 2015b, US company to begin recovering rare earths from old electronics: Mining.com, 26 August 2015, accessed August 2015, at http://www.mining.com/us-company-to-begin-recovering-rare-earths-from-old-electronics/?utm_source=digest-en-mining-150826&utm_medium=email&utm_campaign=digest.

Jamasmie, C., 2016a, China gets tougher on illegal mining, exporting of rare earths: Mining.com, 2 February 2016, accessed February 2016, at http://www.mining.com/china-gets-tougher-on-illegal-mining-exporting-of-rare-earths/?utm_source=digest-en-mining-160202&utm_medium=email&utm_campaign=digest.

Jamasmie, C., 2016b, US scientists figure cost-effective way to extract rare earths from coal: Mining.com, 4 February 2016, accessed February 2016, at http://www.mining.com/us-scientists-figure-cost-effective-way-to-extract-rare-earths-from-coal/?utm_source=digest-en-mining-160204&utm_medium=email&utm_campaign=digest.

Jasinski, S.M., Lee, W.H., and Causey, J.D., 2004, The history of the Western Phosphate Field, *in* Hein, J.R., ed., Life cycle of the Phosphoria Formation: Handbook of Exploration and Environmental Geochemistry: Amsterdam, Elsvier, v. 8, p. 45–61.

Jones, N.R., 2010, Wyoming coal geology, in Keystone coal industry manual: New York, Mining Information Services of the McGraw-Hill Mining Publications, p. 310–631.

Jones, N.R., and Gregory, R.W., 2011, Preliminary Geologic Map of the Shirley Basin 30' x 60' Quadrangle, Carbon, Natrona, Albany, and Converse Counties, Wyoming: Wyoming State Geological Survey Open File Report 11-8, scale 1:100,000.

Kaiman, J., 2014, Rare earth mining in China: the bleak social and environmental costs: The Guardian, 20 March 2014, accessed May 2015, at http://www.theguardian.com/sustainable-business/rare-earth-mining-china-social-environmental-costs.

Kanizay, S.P., 1978, Preliminary geologic map of the Sheridan area, northwestern Powder River Basin, Wyoming: U.S. Geological Survey Map MF-1043, scale 1:50,000.

Karlstrom, K.E., Houston, R.S., Flurkey, A.J., Coolidge, C.M., Kratochvil, A.L., and Sever, C.K., 1981a, A summary of the geology and uranium potential of Precambrian conglomerates in southeastern Wyoming: U.S. Department of Energy Report GJBX-139(81), v. I, 541 p.

Karlstrom, K.E., Houston, R.S., Schmidt, T.G., Inlow, D., Flurkey, A.J., Kratochvil, A.L., Coolidge, C.M., Sever, C.K. Quimby, W.F., 1981b, Drill hole data, drill-site geology, and geochemical data from the study of Precambrian uraniferous conglomerates of the Medicine Bow Mountains and the Sierra Madre of southeastern Wyoming: Department of Energy Open File report GJBX-139(81), v. 2, 682 p.

Keefer, W.R., 1957, Geology of the Du Noir area, Fremont County, Wyoming: U.S. Geological Survey Professional Paper 294-E, p. 155-221, 2 pls., scale 1:48,000.

Keefer, W.R., 1965, Stratigraphy and geologic history of the uppermost Cretaceous, Paleocene, and lower Eocene rocks in the Wind River Basin, Wyoming: U.S. Geological Survey Professional Paper 495-A, 77 p.

Keefer, W.R., 1966, Paleozoic formations in the Wind River Basin, Wyoming: U.S. Geological Survey Professional Paper 495-B, 60 p.

King, J.K., 1991, Rare earth elements and yttrium in Wyoming: Wyoming State Geological Survey Industrial Mineral Report 91-3 [supersedes 87-8], 125 p.

King, J.K., and Harris, R.E., 1987, Rare earth elements and yttrium in Wyoming: Wyoming State Geological Survey Open File Report 87-8, 43 p.

King, J.K., and Harris, R.E., 2002, Rare earth elements and yttrium in Wyoming [Revised]: Wyoming State Geological Survey Industrial Mineral Report 91-3 [supersedes 87-8], 125 p.

Kline, M.H., and Winkel, W.W., 1952, Bald Mountain conglomerates (Deadwood Formation), Sheridan and Big Horn Counties, Wyoming: U.S. Atomic Energy Commission Technical Report RMO-784, 14 p.

Kozimko, L.M., 1985, Geologic map of the Greybull North quadrangle, Wyoming: Wyoming State Geological Survey Map Series 19, scale 1:24,000.

Kuehner, S.M., 1980, Petrogenesis of ultrapotassic rocks, Leucite Hills, Wyoming: London, Ontario, University of Western Ontario, M.S. thesis, 197 p.

Ladd, R.E., 1985, Geologic map of the Sheep Canyon quadrangle, Wyoming: Wyoming State Geological Survey Map Series 20, scale 1:24,000.

Lange, R.A., Carmichael, I.S.E., and Hall, C.M., 2000, $^{40}Ar/^{39}Ar$ chronology of the Leucite Hills, Wyoming: Eruption rates, erosion rates, and an evolving temperature structure of the underlying mantle: Earth and Planetary Science Letters, v. 174, p. 329–340.

Langstaff, G.D., 1995, Archean geology of the Granite Mountains: Golden, Colorado School of Mines, Ph.D. dissertation, 671 p., scale 1:24,000.

Linnen, R.L., Van Lichtervelde, M., Cerny, P., 2012, Granitic pegmatites as sources of strategic metals: Elements, v. 8, p. 275–280.

Long, K.R., Van Gosen, B.S., Foley, N.K., and Cordier, D., 2010, The principal rare earth elements deposits of the United States–A summary of domestic deposits and a global perspective: U.S. Geological Survey Scientific Investigations Report 2010-5220, 96 p.

Long, K.R., Van Gosen, B.S., and Johnson, K., 2010, Rare earth elements in U.S. not so rare, significant deposits found in 14 States: U.S. Geological Survey News Release, November 17, 2010.

Loomis, T.H.W., and Holmquist, G.V., 1954, U.S. Atomic Energy Commission Preliminary Reconnaissance Report ED-R-1493, 1 p.

Lottermoser, B.G., 2015, Rare earth elements in Australian uranium deposits *in* Merkel, B.J., and Arab, A., eds., Uranium–Past and future challenges: proceedings of the 7th international conference on uranium mining and hydrogeology: Springer International Publishing Switzerland, 2015, 870 p.

Love, J.D., 1961, Splitrock Formation (Miocene) and Moonstone Formation (Pliocene) in central Wyoming: U.S. Geological Survey Bulletin 1121-I, 39 p.

Love, J.D., 1964, Uraniferous phosphatic lake beds of Eocene age in intermontane basins of Wyoming and Utah: U.S. Geological Survey Professional Paper 474-E, 66 p.

Love, J.D., 1970, Cenozoic geology of the Granite Mountains area, central Wyoming: U.S. Geological Survey Professional Paper 495-C, 154 p., 4 pls., scale 1:125,000.

Love, J.D., 1973, Harebell Formation (Upper Cretaceous) and Pinyon Conglomerate (Uppermost Cretaceous and Paleocene), Northwestern Wyoming–Geology of gold-bearing conglomerates in Northwestern Wyoming: U.S. Geological Survey Professional Paper 734-A, 54 p.

Love, J.D., 1984, Gold, silver and other selected trace elements in the Phosphoria Formation of western Wyoming: Wyoming Geological Association 35th annual field conference guidebook, p. 383–388.

Love, J.D. and Christiansen, A.C., 1985, Geologic Map of Wyoming: U.S. Geological Survey [Wyoming State Geological Survey release 2014], 3 pls., scale 1:500,000.

Love, J.D., Christiansen, A.C., Earle, J.L., and Jones, R.W., 1979, Preliminary geologic map of the Casper 1 x 2 degree quadrangle, central Wyoming: U.S. Geological Survey Open File Report 79-961, scale 1:250,000.

Love, J.D., Christiansen, A.C., and Ver Ploeg, A.J. 1993, Stratigraphic chart showing Phanerozoic nomenclature for the State of Wyoming: Wyoming State Geological Survey Map Series 41, 1 p.

Love, J.D., McKenna, M.C., Bergquist, H.R., Taylor, D.W., and Jordan, M.E., 1982, Geologic map of the Lava Mountain quadrangle [unpublished]: Wyoming State Geological Survey, scale 1:24,000.

Lynas Corporation Ltd., 2011, accessed December 2012, at http://www.lynascorp.com/page.asp?category_id=1&page_id=25.

Lynds, R.M., Palkovic, M.J., Carroll, C.J., and Ratigan, D.R., 2015, Preliminary geologic map of the Shamrock Hills quadrangle, Carbon County, Wyoming: Wyoming State Geological Survey Open File Report 2015-07, scale 1:24,000.

Madsen, M., 1978, A statistical analysis of heavy mineral variations in Upper Cretaceous black sandstone deposits of the Rocky Mountain states: Laramie, University of Wyoming, M.S. thesis, 139 p.

Madsen, M.E., and Reinhart, W.R., 1982, National uranium resource evaluation Ogden quadrangle, Utah and Wyoming: U.S. Department of Energy Report PGJ/F-124(82), 53 p., 3 sheets microfiche.

Malan, R.C., 1972, Summary report-distribution of uranium and thorium in the Precambrian of the western United States: U. S. Atomic Energy Commission AEC-RD-12, 59 p.

Mapel, W.J., and Pillmore, C.L., 1964, Geology of the Upton Quadrangle, Crook and Weston Counties, Wyoming: U.S. Geological Society Bulletin 1181-J, p. J1–J54, scale 1:48,000.

Marzell, J.G., 1932, Sixteenth biennial report of the state geologist: Office of the State Geologist, Cheyenne, Wyoming [Wyoming State Geological Survey], 123 p.

McCallum, M.E., and Kluender, S.E., 1983, Mineral resources potential of the Savage Run Wilderness, Carbon and Albany Counties, Wyoming: U.S. Geological Survey Miscellaneous Field Studies Map MF-1638A, 10 p.

McCallum, M.E., and Orback, C.J., 1968, The New Rambler copper-gold-platinum district, Albany and Carbon Counties, Wyoming: The Geological Survey of Wyoming [Wyoming State Geological Survey] Preliminary Report 8, 12 p.

McDermott, M., 2009, Goodbye fossil fuel dependence, hello rare earth dependence: Treehugger.com, 5 June 2009,

accessed August 2009, at http://www.treehugger.com/files/2009/06/goodbye-fossil-fuel-dependence-hello-rare-earth-dependence.php.

McKinney, A.A., and Horst, H.W., 1953a, Deadwood conglomerate, Bald Mountain deposit, Sheridan and Big Horn Counties, Wyoming: U.S. Atomic Energy Commission Technical Report RMO-1546, 47 p.

McKinney, A.A., and Horst, H.W., 1953b, Deadwood conglomerate monazite deposit, Bald Mountain area, Sheridan and Bighorn Counties, Wyoming: U.S. Atomic Energy Commission Technical Report RME-3128, 40 p.

McLaughlin, J.F, Bagdonas, D.A., Frost, C.D., and Frost, B.R., 2013, Geologic Map of the Stampede Meadow Quadrangle, Fremont County, Wyoming: Wyoming State Geological Survey Map Series 102, scale 1:24,000.

McLaughlin, J.F., and Harris, R.E., 2005, Geological map of the Torrington 30' x 60' quadrangle, Goshen and Platte Counties, Wyoming, and Sioux and Scotts Bluff Counties, Nebraska: Wyoming State Geological Survey Map Series 66, 1 sheet, scale 1:100,000.

Metal-Pages, 2015, Rare Earths: Metal-Pages.com, accessed June 2015, at http://www.metal-pages.com/metalprices/rareearths/.

Metal Prices, 2015, Rare Earth: Metalprices.com, accessed June 2015, at http://www.metalprices.com/p/metal_index.

Mercadier, J., Cuney, M., Lach, P., Boiron, M.C., Bonhoure, J., Richard, A., Leisen, M., and Kister, P., 2011, Origin of uranium deposits revealed by their rare earth element signature: Terra Nova, v. 23, no. 4, p. 264-269.

M'Gonigle, J.W., and Dover, J.H., 2004, Geologic map of the Kemmerer 30' x 60' quadrangle, Lincoln, Uinta, and Sweetwater Counties, Wyoming: Wyoming State Geological Survey, Open File Report 04-7, scale 1:100,000.

Middleton, L.T., 1980, Sedimentology of the Middle Cambrian Flathead Sandstone, Wyoming: Laramie, University of Wyoming, Ph.D. dissertation, 182 p.

Milton, C., 1971, Authigenic minerals in the Green River basin: University of Wyoming Contributions to Geology, v. 10, no. 1, p. 57–64.

Milton, C., Ingram, B., Clark, J.R., and Dwornik, E.J., 1965, McKelveyite, a new hydrous sodium barium rare-earth uranium carbonate mineral from the Green River Formation, Wyoming: American Mineralogist, v. 50, p. 593–612.

MinDat.org, 2016, Online mineral database, accessed March 2016, at http://www.mindat.org, accessed.

Mineral Data Publishing, 2016, Ewaldite $Ba(Ca,Y,Na,K)(CO_3)_2 \bullet nH_2O$, and McKelveyite $NaCa(Ba,Sr)_3(Y,REE)(CO_3)_6 \cdot 3H_2O$, accessed March 2016, at http://www.handbookofmineralogy.org/pdfs/ewaldite.pdf.

Mineral Prices, 2015, Rare earth metals HEFA rare earth: Mineralprices.com, accessed June 2015, at http://www.mineralprices.com/default.aspx#rar.

Mining.com, 2015, Researchers develop method to recover rare earth elements from discarded EV engines: Mining.com, 5 October 2015, accessed October 2015, at http://www.mining.com/researchers-develop-method-to-recover-rare-earth-elements-from-discarded-ev-engines/.

Moberly, R., 1962, Lower Cretaceous history of the Bighorn Basin, Wyoming: Wyoming Geological Association 17th annual field conference guidebook, p. 94–101.

Molycorp, 2013, Project Phoenix: Molycorp, accessed March 2013, at http://www.molycorp.com/about-us/project-phoenix.

Molycorp, 2015a, Rare Earth Recycling: Molycorp, accessed May 2015, at http://www.molycorp.com/technology/rare-earth-recycling/.

Molycorp, 2015b, News Release: Molycorp, Inc., Files Restructuring Plan: Molycorp, 3 November 2015, accessed November 2015, at http://www.molycorp.com/molycorp-inc-files-restructuring-plan/.

Molycorp, 2015c, Molycorp Mountain Pass: Molycorp, accessed September 2015, at http://www.molycorp.com/about-us/our-facilities/molycorp-mountain-pass/.

Morris, A.V., and Stanley, D.R., 1982, National uranium resource evaluation, Rock Springs Quadrangle, Wyoming and Colorado: U.S. Department of Energy Report PGJ/F-80(82), 42 p., 5 sheets microfiche.

Motooka, J.M., Wilson, W.R., Church, S.E., and Grunzensky, A.L., 1984, Analytical data and sample locality map for phosphate rocks from the East and West Palisades roadless areas, Idaho and Wyoming: U.S. Geological Survey Open File Report 84-163, 22 p.

Mott, L.V., 1978, Origin of the uraniferous phosphatic zones in the Wilkins Peak Member of the Green River Formation, Wyoming: Laramie, University of Wyoming, M.S. thesis, 114 p.

Murphy, G.F., and Brown, R.E., 1985, Silicon, *in* Mineral facts and problems: U.S. Bureau of Mines Bulletin 675, p. 713–728.

Mussard, D.E., 1982, Petrology and geochemistry of selected Precambrian felsic plutons, southern Medicine Bow Mountains, Wyoming: Fort Collins, Colorado State University, M.S. thesis, 245 p.

Niles, T., 2012, REE dragon–Western rare earths discoveries may just feed China: Resource Clips, 7 February 2012, accessed February 2012, at http://resourceclips.com/2012/02/07/ree-dragon/.

The Northern Miner, 2010, Midland Exploration explores Ytterby REE project: The Northern Miner Daily News, 7 October 2010, accessed October 2010, at http://www.northernminer.com/issues/

story.aspx?aid=1000388151&link_source=aypr_NM&issue=10072010&link_targ=DailyNews.

Ogden, P.R., Jr., 1979, The geology, major element geochemistry, and petrogenesis of the Leucite Hills volcanic rocks, Wyoming: Laramie, University of Wyoming, PhD dissertation, 137 p.

Osterwald, F.W., 1947, Report of geologic investigation of the Broadway lead-zinc claim, Carbon County, Wyoming: Geological Survey of Wyoming [Wyoming State Geological Survey] Mineral Report 47-2, 4 p.

Osterwald, F.W., 1950, Notes on occurrence of uranium in Morrison Formation near Greybull, Wyoming [unpublished]: Geological Survey of Wyoming [Wyoming State Geological Survey] Mineral Report MR 50-4, 4 p.

Osterwald, F.W., 1959, Structure and petrology of the northern Big Horn [sic] Mountains, Wyoming: Wyoming State Geological Survey Bulletin 48, 47 p.

Osterwald, F.W., Osterwald, D.B., Long, L.S., Jr., and Wilson, W.H., 1966, Mineral resources of Wyoming: Geological Survey of Wyoming [Wyoming State Geological Survey] Bulletin 50, 287 p.

Overstreet, W.C., Lovering, T.G., Rosenblum, S., and Day, G.W., 1978, Minor elements in magnetic concentrates from Alaska: U.S. Geological Survey Report USGS-GD-77-827, 596 p.

Overstreet, W.C., Mousa, H., and Matzko, J.J., 1985, Composition of coarse-grained magnetite from pegmatite dikes related to plutons of quartz monzonite in the Jabal Lababa area, Kingdom of Saudi Arabia: U.S. Geological Survey Open-File Report 85-2, 25 p.

Parker, R.L., 1963, Niobium and tantalum in the United States: U.S. Geological Survey, Miscellaneous Investigations Resource Map MR-36, 8 p., 1 pl.

Pekarek, A.H., 1977, Structural geology and volcanic petrology of the Rattlesnake Hills, Wyoming: Wyoming Geological Association Earth Science Bulletin, v. 10, no. 4, p. 3–30.

Pekarek, A.H., Marvin, R.F., and Mehnert, H.H., 1974, K-Ar ages of the volcanics in the Rattlesnake Hills, central Wyoming: Geology, v. 2, p. 283–285.

Peterman, Z.E., and Hildreth, R.A., 1978, Reconnaissance geology and geochronology of the Precambrian of the Granite Mountains, Wyoming: U.S. Geological Survey Professional Paper 1055, 22 p.

Proctor, P.D., and El-Etr, H.A., 1968, Layered Pegmatites, Southern Wind River Mountains, Fremont County, Wyoming: Economic Geology, v. 63, p. 595–611.

Qin, S., Zhao, C., Li, Y., and Zhang, Y., 2015, Review of coal as a promising source of lithium: International Journal of Oil, Gas and Coal Technology, 2015, v. 9, no. 2, p. 215–229.

Quest Rare Minerals, 2013, Strange Lake rare earth project: Quest Rare Mineral Ltd., accessed March 2013, at http://www.questrareminerals.com/strange_lake.php.

Rachou, J.F., 1951, Tertiary stratigraphy of the Rattlesnake Hills, central Wyoming: Laramie, University of Wyoming, M.A. thesis, 70 p.

Rare Earth Salts, 2014, Rare earth salts announces joint development agreement with mining major: Rare Earth Salts, 28 October 2014, accessed May 2015, at http://rareearthsalts.com/rare-earth-salts-announces-joint-development-agreement/.

Rare Earth Salts, 2015, Rare earth salts approaches near term commercialization of rare earth separation technology: Rare Earth Salts, 7 May 2015, accessed May 2015, at http://rareearthsalts.com/rare-earth-salts-approaches-term-commercialization-rare-earth-separation-technology/.

Rare Element Resources, Ltd., 2011, Various summaries and press releases, accessed December 2011, at http://www.rareelementresources.com/s/Home.asp.

Rare Element Resources, Ltd., 2012, Various summaries and press releases, accessed March 2012, at http://www.rareelementresources.com/s/Home.asp.

Rare Element Resources, Ltd., 2013a, News Release: Rare element bench scale metallurgical processing tests produce a 90+ percent REO concentrate: Rare Element Resources, 4 March 2013, accessed March 2013, at http://www.rareelementresources.com/investor-information/news-releases/2013-archive/2013/03/04/rare-element-bench-scale-metallurgical-processing-tests-produce-a-90-reo-concentrate#.VV9-9karFoM.

Rare Element Resources, Ltd., 2013b, News Release: Rare element reports additional drilling results high in critical rare earth elements: Rare Element Resources, 11 March 2013, accessed March 2013, at http://www.rareelementresources.com/investor-information/news-releases/2013-archive/2013/03/11/rare-element-reports-additional-drilling-results-high-in-critical-rare-earth-elements#.VV9-mkarFoM.

Rare Element Resources, Ltd., 2014, Bear Lodge Project Canadian NI 43-101 Pre-Feasibility Study Report on the Reserves and Development of the Bull Hill Mine, Wyoming: Rare Element Resources, 9 October 2014, accessed May 2015, at http://www.rareelementresources.com/App_Themes/NI43-101PreFeasibilityStudyReport/HTML/.

Rare Element Resources, Ltd., 2015a, Bear Lodge Project: Rare Element Resources, accessed December 2015, at http://www.rareelementresources.com/bear-lodge-project#.Vl8ckL-rFoM.

Rare Element Resources, Ltd., 2015b, Rare Element Resources' Proprietary Separation Technology Successfully Delivers Multiple, High-Purity Rare Earth Products in an Efficient and Environmentally Sound Process: Rare Element Resources, 3 June 2015, accessed February 2016, at http://www.rareelementresources.com/investor-information/news-releases/2015-archive/2015/06/03/rare-element-resources-propri-

etary-separation-technology-successfully-delivers-multiple-high-purity-rare-earth-products-in-an-efficient-and-environmentally-sound-process#.Vst-P-arFoN.

Rare Element Resources, Ltd., 2015c, Rare Element Resources Expands on Advantages of its Patent-Pending, Zero-Discharge SX Separation Technology in Pilot Plant Testing: Rare Element Resources, 16 December 2015, accessed February 2016, at http://www.rareelementresources.com/investor-information/news-releases/2015-archive/2015/12/16/rare-element-resources-expands-on-advantages-of-its-patent-pending-zero-discharge-sx-separation-technology-in-pilot-plant-testing#.VsuGkuarFoM.

Rare Element Resources, Ltd., 2016, News Release: Rare Element Resources Announces Suspension of Permitting Activities: Rare Element Resources, 22 January 2016, accessed January 2016, at http://www.rareelementresources.com/investor-information/news-releases/2016/01/22/rare-element-resources-announces-suspension-of-permitting-activities#.VruOVKrFoM.

Reyner, M.L., 1950, U.S. Atomic Energy Commission Preliminary Reconnaissance Report U-1, 1 p.

Robinson, C.S., Mapel, W.J., and Bergendahl, M.H., 1964, Stratigraphy and structure of the northern and western flank of the Black Hills uplift, Wyoming, Montana, and South Dakota: U.S. Geological Survey Professional Paper 404, 134 p., scale 1:96,000.

Roehler, H.W., 1958, Geology of the Bates Hole, Wyoming: Laramie, University of Wyoming, M.A. thesis, 57 p., 2 pls.

Roehler, H.W., 1989, Origin and Distribution of six heavy-mineral placer deposits in coastal-marine sandstones in the Upper Cretaceous McCourt Sandstone Tongue of the Rock Springs Formation, southwest Wyoming: U.S. Geological Survey Bulletin 1867, 34 p., 1 pl.

Roehler, H.W., 1990, Stratigraphy of the Mesaverde Group in the central and eastern Greater Green River Basin, Wyoming, Colorado, and Utah: U.S. Geological Survey Professional Paper 1508, 52 p.

Rohrer, W.L., 1968, Geologic map of the Fish Lake quadrangle, Fremont County, Wyoming: U.S. Geological Survey Geologic Quadrangle Map GQ-724, scale 1:24,000.

Russell, R.T., and DeVore, G.W., 1948, Report on field examination of allanite deposits, Natrona County, Wyoming: Geological Survey of Wyoming [Wyoming State Geological Survey] Mineral Report 48-2, 11 p.

Saefong, M.P., 2015, Rare-earth elements are poised for a recovery: Marketwatch, 19 August 2015, accessed August 2015, at http://www.marketwatch.com/story/rare-earth-elements-are-poised-for-a-recovery-2015-08-19.

Sargent, K.A., 1960, Allanite occurrences in the Horn area, Bighorn Mountains, Wyoming: Iowa City, University of Iowa, Ph.D. dissertation, 136 p., 5 pls.

Saywell, T., 2011, Molycorp's Mountain Pass: A made-in-America solution, The Northern Miner, v. 97, no. 41, 1 p.

Schofield, A., and Haskin, L., 1964, Rare-earth distribution patterns in eight terrestrial materials: Geochimica et Cosmochimica Acta, v. 28, p. 437–446.

Scott, J.E., Sutherland, W.M., Johnson, J., and McLaughlin, J.F., 2011, Geologic map of the Baggs 30' x 60' quadrangle, Carbon and Sweetwater Counties, Wyoming, and Moffat and Routt Counties, Colorado: Wyoming State Geological Survey Map Series 95, 33 p., 1 sheet, scale 1:100,000.

Segerstrom, K., and Weisner, R.C., 1976, Mineral resources of areas adjacent to the Cloud Peak Primitive Area, Wyoming: U.S. Geological Survey Bulletin 1391-D, 37 p., scale 1:63,360.

Seredin, V.V., and Dai, S., 2012, Coal deposits as potential alternative sources for lanthanides and yttrium: International Journal of Coal Geology, v. 94, p. 67–93.

Shannon, R.D., 1976, Revised effective ionic radii and systematic studies of interatomic distances in halides and chalcogenides: Acta Crystallography, v. A32, p. 751–767.

Sheldon, R.P., 1963, Physical stratigraphy and mineral resources of Permian rocks in western Wyoming: U.S. Geological Survey Professional Paper 313-B, p. 49–273.

Sheldon, R.P., Waring, R.G., Warner, M.A., and Smart, R.A., 1953, Stratigraphic sections of the Phosphoria Formation in Wyoming, 1949-1950: U.S. Geological Survey Circular 301, 45 p.

Shen, H., 2015, Chinese rare earths exports dramatically decrease while global demand for rare earth products increase: Investor Intel, 29 March 2015, accessed June 2015 at http://www.investorintel.com/technology-metals-intel/chinese-rare-earths-exports-dramatically-decrease-while-global-demand-for-rare-earth-products-increase/.

Sheridan, D.M., Maxwell, D.H., and Collier, J.T., 1961, Geology of the Lost Creek schroeckingerite deposits, Sweetwater County, Wyoming: U.S. Geological Survey Bulletin 1087-J, p. 391–478, scale 1:63,360.

Simons, F.S., Love, J.D., Keefer, W.R., Harwood, D.S., Kulik, D.M, and Bieniewski, C.L., 1988, Mineral resources of the Gros Ventre Wilderness study area, Teton and Sublette Counties, Wyoming: U.S. Geological Survey Bulletin 1591, 65 p.

Skipp, W.L., 1957, Stratigraphy of the Thermopolis shale and the Muddy sandstone in the southwestern Wind River Basin: Wyoming Geological Association 12th annual field conference guidebook, p. 63–65.

Smith, E.W., 1953a, U.S. Atomic Energy Commission Preliminary Reconnaissance Report DEB-RRD-732, 1 p.

Smith, E.W., 1953b, U.S. Atomic Energy Commission Preliminary Reconnaissance Report DEB-RRD-731, 1 p.

Smith, E.W., 1953c, U.S. Atomic Energy Commission Preliminary Reconnaissance Report DEB-RRD-730, 1 p.

Smith, E.W., 1954, Reconnaissance for uraniferous deposits in the Laramie Mountains, Wyoming: U.S. Atomic Energy Commission Technical Report RME-1048, 17 p.

Smith, S.M., 2001, National Geochemical Database: Reformatted data from the National Uranium Resource Evaluation (NURE) Hydrogeochemical and Stream Sediment Reconnaissance (HSSR) Program, Version 1.30: U.S. Geological Survey Open-File Report 97-492, also accessible at http://pubs.usgs.gov/of/1997/ofr-97-0492/index.html.

Smith, W.C., and Page, L.R., 1941, Tin-bearing pegmatites of the Tinton district, Lawrence County, South Dakota [sic]: U.S. Geological Survey Bulletin 922-T, p. 595–630, 4 pls.

Spencer, A.C., 1904, Copper deposits of the Encampment district, Wyoming: U.S. Geological Survey Professional Paper 25, 107 p.

Soister, P.E., 1968, Stratigraphy of the Wind River Formation in south-central Wind River Basin, Wyoming; U.S. Geological Survey Professional Paper 594-A, 50 p., 5 pls., scale 1:63,360.

Staatz, M. H., 1983, Geology and description of thorium and rare-earth deposits in the southern Bear Lodge Mountains, northeastern Wyoming: U.S. Geological Survey Professional Paper 1049-D, 52 p., scale 1:24,000.

Stricker, G.D., and Flores, R.M., 2003, Factors controlling trace elements of environmental concerns for Powder River Basin coal, Wyoming [abs.]: Geological Society of America Abstracts with Programs Paper 92-7, v. 35, no. 6, p. 229.

Stricker, G.D., Flores, R.M., Trippi, M.H., Ellis, M.S., Olson, C.M., Sullivan, J.E., and Takahashi, K.I., 2007, Coal quality and major, minor, and trace elements in the Powder River, Green River, and Williston basins, Wyoming and North Dakota: U.S. Geological Survey Open File Report 2007-1116, 31 p.

Stuckless, J.S., Hedge, C.E., Worl, R.G., Simmons, K.R., Nkome, I.T., and Wenner, D.B., 1985, Isotopic studies of the Late Archean plutonic rocks of the Wind River Range, Wyoming: Geological Society of America Bulletin, v. 96, p. 850–860.

Stupak, W.A., 1984, The petrography and petrochemistry of the Eocene volcanics, Rattlesnake Hills, central Wyoming: Fredericton, University of New Brunswick, M.S. thesis, 318 p.

Sutherland, W.M., 2007, Geologic map of the Sundance 30' x 60' quadrangle, Crook and Weston Counties, Wyoming and Lawrence and Pennington Counties, South Dakota: Wyoming State Geological Survey Map Series 78, 26 p., scale 1:100,000.

Sutherland, W.M., 2008, Geologic map of the Devils Tower 30' x 60' quadrangle, Crook County, Wyoming; Butte and Lawrence Counties, South Dakota; and Carter County, Montana: Wyoming State Geological Survey Map Series 81, 29 p., scale 1:100,000

Sutherland, W.M., and Cola, E.C., 2015, Iron resources of Wyoming: Wyoming State Geological Survey Report of Investigations 67, 92 p.

Sutherland, W.M., Gregory, R.W., Carnes, J.D., and Worman, B.N., 2013, Rare earth elements in Wyoming: Wyoming State Geological Survey Report of Investigations 65, 82 p.

Sutherland, W.M., and Hausel, W.D., 2003, Geologic map of the Rattlesnake Hills 30' x 60' quadrangle, Fremont and Natrona Counties, Wyoming: Wyoming State Geological Survey Map Series 61, 28 p., scale 1:100,000.

Sutherland, W.M., and Hausel, W.D., 2005, Preliminary geologic map of the Saratoga 30' x 60' quadrangle, Carbon and Albany Counties, Wyoming and northern Colorado: Wyoming State Geological Survey Open File Report 04-10, 34 p., scale 1:100,000.

Sutherland, W.M. and Hausel, W.D., 2006, Geologic map of the South Pass 30' x 60' quadrangle, Fremont and Sweetwater Counties, Wyoming: Wyoming State Geological Survey Map Series 70, 23 p., scale 1:100,000.

Sutherland, W.M., and Luhr, S.C., 2011, Preliminary geologic map of the Farson 30' x 60' quadrangle, Sweetwater, Sublette, and Fremont Counties, Wyoming: Wyoming State Geological Survey Open File Report 11-6, 32 p., 1 sheet, scale 1:100,000.

Sutherland, W.M., and Worman, B.N., 2013, Preliminary geologic map of the Blackjack Ranch quadrangle, Natrona County, Wyoming: Wyoming State Geological Survey Open File Report 13-3, 24 p., scale 1:24,000.

Taucher, L.M., 1953, Geology of the Cookstove Basin area, Big Horn County, Wyoming: Laramie, University of Wyoming, M.A. thesis, 88 p., 2 pls., scale 1:31,680.

Thaden, R.E., 1980, Geologic map of the Guffy Peak quadrangle showing chromolithofacies in the Wind River Formation, Fremont and Hot Springs Counties, Wyoming: U.S. Geological Survey Geologic Quadrangle Map GQ-1527, scale 1:24,000.

Taylor, S.R., and McLennan, S.M., 1985, The continental crust–its composition and evolution: Blackwell, Oxford, England, 312 p.

Thomas, H.D., 1951, Monazite–Sundance, Crook County, telephone conversation record with C.C. Towle, U.S. Atomic Energy Commission: Wyoming State Geological Survey Mineral Report 51-7, 1 p.

Thomas, C.A., Hagni, R.D., and Berendsen, P., 1991, Ore microscopy of the Paoli silver-copper deposit, Oklahoma: U.S. Geological Survey Ore Geology Reviews 6, p. 229–244.

Uda, T., Jacob, K.T., and Hirasawa, M., 2000, Technique for Enhanced Rare Earth Separation: Science, v. 289, no. 5488, p. 2326–2329.

Ullmer, E., 1983, Precambrian iron-rich pods and uranium mineralization near Warm Spring Creek, Fremont County, Wyoming: Contributions to Geology, University of Wyoming, Laramie, v. 22, no. 2, p. 75–82.

U.S. Department of Energy, 2010, Critical materials strategy: U.S. Department of Energy, 166 p., accessed December 2010, at http://energy.gov/sites/prod/files/edg/news/documents/criticalmaterialsstrategy.pdf.

U.S. Geological Survey, 2013, Mineral commodity summaries 2013, Rare Earths: U.S. Geological Survey, p. 128–129.

Van Houten, F.B., 1955, Volcanic-rich Middle and Upper Eocene sedimentary rocks northwest of Rattlesnake Hills central Wyoming: U.S. Geological Survey Professional Paper 274-A, 14 p.

Van Houton, F.B., 1964, Tertiary geology of the Beaver Rim area Fremont and Natrona Counties, Wyoming: U.S. Geological Survey Bulletin 1164, 99 p., 8 pls.

Verplanck, P.L., Van Gosen, B.S., Seal, R.R, and McCafferty, A.E., 2014, A deposit model for carbonatite and peralkaline intrusion-related rare earth element deposits: U.S. Geological Survey Scientific Investigations Report 2010–5070-J, 58 p.

Ver Ploeg, A.J. 2004, Geologic map of the Nowater Creek 30' x 60' quadrangle, northcentral Wyoming: Wyoming State Geological Survey Map Series 39, scale 1:100,000.

Ver Ploeg, A.J., Bagdonas, D., and McLaughlin, J.F., 2011, Preliminary geologic map of the Best Ranch quadrangle, Albany County, Wyoming: Wyoming State Geological Survey Open File Report 11-7, scale 1:24,000.

Ver Ploeg, A.J., and Boyd, C.S., 2002, Geologic map of the Buffalo 30' x 60' quadrangle, Johnson and Campbell Counties, Wyoming: Wyoming State Geological Survey Map Series 59, scale 1:100,000.

Ver Ploeg, A.J., Boyd, C.S., and Mulbay, J.M., 2004, Geologic map of the Kaycee 30' x 60' quadrangle, Johnson and Campbell Counties, Wyoming: Wyoming State Geological Survey Map Series 63, scale 1:100,000.

Ver Ploeg, A.J., and Greer, P.L., 1996, Evidence for right-oblique-slip on a northern segment of the Big Trails fault system, southern Bighorn Mountains, Wyoming: Wyoming Geological Association 47th annual field conference guidebook, p. 179–188.

Vine, J.D., 1966, Analyses of some upper Paleozoic black shales and associated rocks: U.S. Geological Survey Open File Report 66-147, 1 sheet microfiche.

Vine, J.D., and Denson, N.M., 1954, U.S. Atomic Energy Commission Preliminary Reconnaissance Report F-1141, 1 p.

Warren, R.G., 1980, Uranium hydrogeochemical and stream sediment reconnaissance of the Gillette NTMS quadrangle, Wyoming, including concentrations of forty-two additional elements: U.S. Department of Energy report GJBX-234(80), 129 p.

WebElements.com, 2012, WebElements periodic Table, accessed November 2011, at http://www.webelements.com/.

Webmineral.com, 2016, Mineralogy Database, accessed March 2016, at http://webmineral.com/.

Welch, C.M., 1974, A preliminary report on the geology of the Mineral Hill area, Crook County, Wyoming: Rapid City, South Dakota School of Mines and Technology, M.S. thesis, 83 p., 2 pls.

Whalen, J.F., 1954a, U.S. Atomic Energy Commission Preliminary Reconnaissance Report DEB-RRD-1358, 1 p.

Whalen, J.F., 1954b, U.S. Atomic Energy Commission Preliminary Reconnaissance Report DEB-RRD-1390, 1 p.

Whalen, J.F., 1955, U.S. Atomic Energy Commission Preliminary Reconnaissance Report DEB-P-2-2252, 1 p.

Wilburn, D.R., 2012, Byproduct Metals and Rare-Earth Elements Used in the Production of Light-Emitting Diodes–Overview of Principal Sources of Supply and Material Requirements for Selected Markets: U.S. Geological Survey Scientific Investigations Report 2012–5215, 15 p.

Wilmarth, V.R., and Johnson, D.H., 1953, Preliminary reconnaissance survey for thorium, uranium, and rare-earth oxides, Bear Lodge Mountains, Crook County, Wyoming: U.S. Geological Survey Trace Elements Investigations Report 172, 26 p., scale 1:500.

Wilson, W.H., 1951, A monazite deposit in the Big Horn [sic] Mountains, Sheridan and Big Horn Counties, Wyoming [unpublished]: Geological Survey of Wyoming [Wyoming State Geological Survey] Mineral Report 51-6, 3 p.

Wilson, W.H., 1955, Cherry Creek copper prospect, Carbon County, Wyoming: Geological Survey of Wyoming [Wyoming State Geological Survey] Mineral Report 55-3, 10 p.

Wilson, W.H., 1960, Radioactive mineral deposits of Wyoming: Wyoming State Geological Survey Report of Investigations 7, 41 p.

Wilson, W.H., 1964, The Kirwin mineralized area, Park County, Wyoming: Wyoming State Geological Survey Preliminary Report 2, 20 p., scale 1:24,000.

Wilson, W.H., 1976, Wyoming iron resources summary report [unpublished]: U.S. Bureau of Mines Contract No. J0265005, 56 p.

Zeller, H.D., and Stephens, E.V., 1969, Geology of the Oregon Buttes area, Sweetwater, Sublette, and Fremont Counties, southwestern Wyoming: U.S. Geological Society Bulletin 1256, 60 p., scale 1:48,000.

Zeller, H.D., Soister, P.E., and Hayden, H.J., 1956, Preliminary geologic map of the Gas Hills uranium district, Fremont and Natrona Counties, Wyoming: U.S. Geological Survey Mineral Investigation Field Studies Map MF-83.

Index

A

Absaroka Mountains 59
Absaroka volcanic super group 59
Albany area 42
alkalic igneous rocks 16, 66
allanite 1, 12, 13, 21, 23, 26–27, 30–34, 38, 42, 44, 49, 51, 53, 58, 86–87
Allie claims 21, 38
ancylite 13
Anderson Ridge 34–36
Aspen Mountain area 117
Australia 7–8, 83, 105
Aycross Formation 59

B

Bald Mountain 16, 54, 71, 100,–105
bastnasite 12–13, 16, 18, 19
Bates Hole 79–80
Battle Mountain 59, 69
Battle Spring Formation 44, 80, 106–108
Beacon 89
Bear Cabin Creek 99
Bear Creek Gulch-Hoback Canyon 96
Bear Ears pluton 55
Bear Lodge deposit 7, 10, 15–16, 19, 118
Bear Lodge Mountains 1, 15, 18, 59, 62, 66
belemnites 92
beryl 27–28, 30, 36, 38, 115
BIF 55
Big Creek 13, 16, 21, 29–32
Bighorn Basin 69, 84, 91–93
Bighorn Mountains 1, 16, 21, 51–53, 100
Big Trails fault 51
Black Butte 89
Black Buttes 18, 64
Blackhall Mountain 21, 31–34
Black Hills 18, 59
Black Mountain 116
Black Rock Gap prospect 115
Blanche mine 112
Bobcat Gulch-Hyattville area 92
Bow River Quartzite 39
Bradley Road 89
Bridger Formation 72, 115
Broadway mine 41
Bull Camp prospects 49, 53
Bull Hill 18–19

C

Camel Rock. *See* Pretty Water Creek
carbonatite 1, 2, 12, 13–19, 59, 64, 66–67, 112
Carbon target 18–19
Carrico Ranch 41
Cedar Mountain 59, 69
Cement Ridge 64
cerianite 19
Chalk Bluff 113
Cheyenne belt 21, 23, 28–30, 43
China 1, 7–10, 12, 108, 112
Clarence Wood lode claims 16, 44
Clarkson Hill 87
Clear Creek 99
Cloverly Formation 91–92
Cloverly-Morrison Formation 92
coal 2, 4, 9, 82–83, 87, 89, 106–112, 118
Cody Shale 48, 83, 90
Cokeville section 97
Cookstove Basin 54–55
Cooper Creek area 39
Cooper Ridge 89
Cottonwood Creek 16, 85
Cowley deposit 86
Crooked Creek group claims 92
Crooks Gap-Green Mountain uranium district 80
Crystal Creek 98
Crystal Creek Canyon 98
Crystal Peak 99
crytolite 25
Cumberland Gap 91

D

dahllite concretions 91
Dans Creek. *See* Yenko deposit
Deacon's Prayer group claims 77–79
Deadline Ridge 98
Deep Gulch Conglomerate 41
Dell Creek 99
Devils Tower 18
Dexter Peak 41
Diamond Alkali Co. DACO 3 76
Diamond Alkali Co. Reid no. 2 76
Dilworth Bench 105
dinosaur bones 92
Dubois claims 55
Duchess mine 113
Dugout Creek 16, 86

E

East Miners Creek 98
Elkhead Mountains volcanic field 69
Emigrant Trail Thrust Fault 44
Eureka mine 113
euxenite 12, 16, 21, 27–28, 30, 32–33, 55

ewaldite 12–13
Extraction of REE 10

F

Ferris-Seminoe Mountains 44
Fiddlers Green 83
Fiesta #2 prospect 46
Flat Creek 98
Flathead Sandstone 16, 54, 60–61, 70–71, 100–105
FMR 18–20
Fort Union Formation 79, 82, 106, 115
Fox Hills Sandstone 82
Frontier Formation 16, 89–91
Frontier Formation-Spring Gap 90

G

Gafco placer claims 80
Gaps Trondhjemite 42
garnet 30, 31, 33, 36, 51, 83, 114–116
Garnet Hill 116
gastroliths 92
General Geology of REE 12
Geologic Occurrences of Wyoming REE 16
Gold Coin Mine 114
Granite Creek 99
Granite Mountains 44–48, 66, 115–117
Grass Creek 16, 83–85
Great Divide Basin 80–81, 106, 118
Green Mountain 18, 44–46, 48, 80–81, 106
Green River Basin 68, 72–73, 82–83, 108
Green River Formation 12, 69–76
Gros Ventre Range 59, 94

H

Heart Formation 41
Heavy Rare Earth Elements 4
Hoback 16, 96
Holiday Place pegmatite 16, 26–27
Honnes Ranch. *See* Bradley Road
Hubbell Ditch area 39
Hub prospect 114
Hurda claims 72, 106

I

I-80 On-ramp area, Exit 91, east of Green River 72
Inyan Kara Mountain 18

J

Jack Creek Quartzite 41
jade 39–47
J.M. Perkins Green River no. 3 76

K

Keystone quartz diorite 42
kimberlites 69

L

Lance Formation 77, 82, 108
Laramie Anorthosite Complex 21
Laramie Mountains 21–23, 27, 106
LCT pegmatites 21
Leopard Rock mine 117
Leucite Hills 59, 68–69
Lewis Shale 77, 82, 83
Light Rare Earth Elements 4
Lindsey Quartzite 39
Little Basin area 105
Louis Lake Batholith 55
Lovell deposit 16, 86
Lulu claims 74

M

magnetite 15, 23, 30–32, 36, 51, 55, 58–59, 79, 82–83, 86, 89, 100, 113
Magnolia Formation 39
Manning Ranch 41
Many Values 21, 28, 30
McCourt Sandstone Tongue 87–89
McKelveyite 12–13, 72, 76
Meade Peak Member 70, 94–97
Medicine Bow Mountains 16, 21–23, 28, 30, 38–43, 114
Medicine Peak Quartzite 39
Mesaverde Formation 16, 70, 82–87
Middle Fork Pine Creek 97
Middle Piney Lake 96
Mineral Hill 18, 59, 62–64
Missouri Buttes 18
Mohawk claims 48, 81
Molycorp 1, 7–10
monazite 1, 12–18, 30–33, 41, 54–55, 70–71, 77–80, 83–88, 100–102, 105
Moonstone Formation 46, 67
Moonstone Formation reefs 67
Morrison Formation 92–94
Mountain Fuel Supply Company-John Hay Jr. no. 1 76
Mountain Pass 1, 9–10
Mud Creek 85
Mullen Creek area 42
Mullen Creek complex 30, 34
Mullen Creek-Nash Fork shear zone 28, 30, 113
Murphy no. 1. *See* Salt Wells Creek
Murphy no.2. *See* Pretty Water Creek

N

Nature's Mint mine 114
New Rambler mine 113
northeast Wilkins Peak 76
North Fork Big Elk Creek 96
North Sheldon Gulch 2, 92–94
NURE 2–4, 17, 33, 46, 53–54, 57, 80–81, 95, 106–107
NYF pegmatites 21

O

Old Log Inn 76
Omega claims 44, 49
Onemile Creek area 39–40
Oregon Trail structural belt 39, 44–45, 65
Ore Road Quarry 115
Oro claim no. 1 74
Owl Creek Mountains 37–38, 77, 115

P

paleoplacer 12, 16, 70–72, 100–101, 105, 118
  black sandstone 16, 82–91, 118
parisite 13, 19
Parkman Sandstone Member 87
Parlett-Adams claim. *See* Allie claims
Pedro Mountains 44
Pegmatites 21
petrified wood 77
Phantom Lake Group 42
Phosphoria Formation 16, 60–61, 70, 94–100
Pierre Shale 82
Pilot Butte 68–69
Pilot Knob 59–62
Platt Mine 13, 16, 30–33
Poison Creek 94–96
Poison Spider deposit 77, 82
Politics and Supplies 7
Precambrian Occurrences 21
Pretty Water Creek 88
Prospect Creek area 105

Q

Quaternary Placers 71

R

Rainbow claims 54
Ranger claims 77
Ranger no. 1 claim 82
Rare Earth Oxide 4
Rare Earth Salts Separations and Refining, LLC 12
Rare Element Resources, Ltd 1, 4, 7, 10, 13–20, 64, 118
Rattlesnake Hills 16, 59, 65–67, 104
Rawlins Red deposit 100–101
Raymond Canyon 97
recycling 9
Red Creek deposit. *See* Richard's Gap
REE Associated with Coal 106
REE Associated with Uranium Deposits 105
REE Minerals 12
REE Prices 10
REE Uses 7
Reeves Ranch. *See* Shell Creek prospect
Rhoads Jade mine 46
Richard's Gap 87–88
Ridge and North Ridge area 74
Rock Creek 39
Rock Mountain Conglomerate 39
Rock Springs Formation 83, 87–89, 108
Rock Springs uplift 83, 87–89

S

Sage Creek prospect 44
Salt Creek 82
Salt Wells Creek 88
samarskite 1, 13, 16, 32
Section 8 mine 114
Seminoe (paleoplacer) 82
septarian concretions 77
Shafer Creek 97
Sheep Mountain 87
Shell Creek prospect 92
Sherman Granite 21–24, 27–30, 42
Shirley Basin 72, 77–80, 106, 118
Shirley Mountains 44
Shotgun Bench 87
Siddoway Fork 96
Sierra Madre 21, 28, 33, 38–41, 69, 113
silicified bones 77
Smokey Hollow 96
Snow King Mountain 98
Southeast Wind River Basin 115
South Firehole Canyon 16, 74–75
South Pass area 116
Southwest Lookout Mountain 117
Southwest Pine Mountain 77, 82
Split Rock Formation 66–67
Spring Gap 16, 90
Steer Creek 96
Stove Leg prospect 53–54
Strong mine 113
Sundance Mountain 18
synchysite 19

T

Table Mountain area 98
Taylor deposit 113

Taylor target 19–20
Teapot Member 86
Tensleep Fault 51–53
Tertiary aged Igneous Occurrences 59
Teton Pass 94
Thermopolis Shale 91–92
The Six Lakes area 99
Threemile Creek. *See* Rock Creek
Tie Siding 16, 21–27
  Tie Siding pegmatite 23–26
Tiger Stripe Chert 117
Tin Cup Mine 46
Tinton 18, 62
Tipton Shale Member 72, 74
Titsworth Gap. *See* Salt Wells Creek
Tosi Creek 100
Total Rare Earth Oxides 4
tourmaline 30, 36, 38, 46, 83, 115–116
Triangle Peak area 99
Tronox Westvaco Mine 76

U

Union Pass-Warm Spring 16, 55, 104
UPRR #1. *See* Beacon
UPRR #2. *See* Bradley Road
uranium 1–3, 9, 13–16, 23, 27–30, 33, 46–48, 55, 58–74, 77–81, 91–92, 101, 105–106, 118
Uranium King Mine 32
U.S. Atomic Energy Commission (USAEC) 1
U.S. Bureau of Land Management (USBLM) 2–3, 118
U.S. Bureau of Mines (USBM) 1
U.S. Rare Earths, Inc. 9
UT Creek – Lost Muffler Fault prospects 116

V

Vagner Formation 39

W

Wagon Bed Formation 117
Warm Spring Creek placers 71
Wasatch Formation 75, 117
Weddle claims 21, 27–28
Western Rattlesnake Hills 16, 104
West Tosi Creek 100
Whippet mine 36
White Mountain no. 1 76
White River Formation 72, 79–80, 106
Whitetail Ridge 19
Wildcat Road 55
Wilderness boundary 99
Wilkins Peak Member 70–77
Wind River Basin 37, 77–82, 115
Wind River Formation 37, 57, 71–72, 77–82
Wind River Indian Reservation 2
Wind River Mountains 55, 59, 106
Wolf Creek 96
Wyo-Ben Mine 16, 91
Wyo-DOG 1–3, 18, 118

X

xenotime 12, 15, 21, 71, 82, 86–87, 105

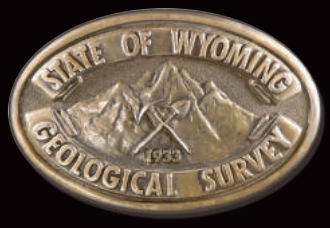
Y

Yenko deposit 89

Z

Zalenka deposit. *See* Black Butte
Zimmerman mine 38
Zirkel Mesa 68

NOTES



Interpreting the past , providing for the future

APPENDIX 1: RI-71 DATA

Shading = Greater Than 5X Crustal Abundance
Shading= elevated but less than 5X
*oxides based on weighted average of lithosphere abundance (not 5X) by Parker, 1
Shaded Sample # = overall contains elevated REEs

RE15069003 - Finalized
CLIENT : TKT - Wyoming State Geological Survey
of Samples : 30
DATE RECEIVED : 2015-05-12 DATE FINALIZED : 2015-05-26
PROJECT : April 2015- Sample List
CERTIFICATE COMMENTS :
PO NUMBER :

Sample #	Location	Type of Deposit/Category
20110818WS-B	SR Rhyolite	Ti
20110818WS-C	SR Wagon Bed 20110818WS-C	T-s
20120608WS-A	SR Flathead 20120608WS-A	Cf
WGS-0203	Broadway mine	PC-i; epidote
WGS-0273	Lake Owen complex	PC-i
WGS-0315	Odell prospect	PC-p; PC-i; epidote
WGS-0323	Jade Prospect, N1/2, Sec. 30, T30N, R92	PC-p
WGS-0490	Rattlesnake Hills, SW 1/4, NE 1/4, Sec. 2	PC-f; PC-p; PC-m; Ti
WGS-0493	Rattlesnake Hills, SE 1/4, NE 1/4, Sec. 25	PC-f; PC-p; PC-m
WGS-0501	Southwest Pine Mountain, Natrona Count	M-sed; T-sed
WGS-0508	Charter Oak mine	PC-i
WGS-0550	Squaw Teats	T-sed
WGS-0599	No. 1 Wilson Well, SE1/4, SW1/4, Sec. 6,	P-sed; M-sed
20140822WS-A	Chalk Bluff	Ti
20140822WS-B	Chalk Bluff	T-sed
20140822WS-C	Chalk Bluff	T-sed; ash flow
20140822WS-D	Chalk Bluff	T-i
20140822WS-F	Chalk Bluff	T-sed; T-s
20140822WS-H	Chalk Bluff	T-sed; T-con
20140822WS-I	Chalk Bluff	Ti; welded tuff
20140822WS-J	Dry Creek Road	Ti; lapilli tuff
20140822WS-K	Dry Creek Road	Ti; flow
20140616WS-A	Moonstone concretion	T-sed; T-con
20140630WS-B	iron stained qtz vein	PC-p
20140711WS-A	limonitic faulted area	T-sed; f
20140715WS-A	calcite vein	T-sed; f; vein
20140924WS-D	iron stained qtz vein	PC-p; PC-m
20140925WS-B	Cu and Fe stained qtz vein	PC-p; PC-m
20141014WS-C	Belle Fourche satin spar	M-sed; M-con
20141016WS-D	Sheep Creek Iron	P-sed; P-con

RE15099827 - Finalized
CLIENT : TKT - Wyoming State Geological Survey

of Samples : 80
DATE RECEIVED : 2015-07-08 DATE FINALIZED : 2015-07-24
PROJECT : July 2015-Sample List Page 1
CERTIFICATE COMMENTS : Full Project: July 2015-Sample List Page 1 of 5
PO NUMBER :

Sample #	Location	Type of Deposit/Category
20021010WS-1	20021010WS-1	PC-f; epidote
20080611WS-B	Owl Creek Mountains nephrite	PC-p; epidote/jade
20081029WS-A1	Imperial prospects	PC-p; epidote/jade
20081029WS-A2	Imperial prospects	PC-p; alteration/jade
20081029WS-A3	Imperial prospects	PC-p; alteration/jade
20081029WS-A4	Imperial prospects	PC-p; alteration/jade
20081029WS-A5	Imperial prospects	PC-p; alteration/jade
20081029-Leo-Ep	Sage Creek Prospect	PC-p; epidote
20090413WS-A1	Fiesta #2 (epidote)	PC-p; epidote/jade
20090622WS-A	Imperial prospects [20090622WS-A]	PC-p; alteration/jade
20090819WS-A1	Rhoads jade pit	PC-p; epidote
20090819WS-A2	Rhoads jade pit	PC-p; epidote/jade
20121010WS-B	Thulite-jade prospect	PC-p; epidote/jade
20150612WS-A	WY jade float (office sample)	PC-p; jade
1994-AVP	Miners Delight/ Lewiston area (LD82-1)	PC-p
20150602LC-1	Ore Road Quarry	PC-p
20150602LC-2	Ore Road Quarry	PC-p
20150602LC-3	Granite Mountains area	Ts
20150602LC-4	Granite Mountains area	PC-i
20150602LC-5	Granite Mountains area	PC-i
20150603LC-1	Tin Cup Mountain area	PC-f
20150603LC-2	Tin Cup Mountain area	PC-p
20150603LC-3	Tin Cup Mountain area	PC-m
20150603LC-4	Tin Cup Mine	PC-p
20150603LC-5	Tin Cup Mountain area	PC-p
20150603LC-6	Tin Cup Mountain area	PC-p
20150603LC-6A	Tin Cup Mountain area	PC-m; PC-p
20150603LC-7	Tin Cup Mountain area	PC-m
20150603LC-8	Tin Cup Mountain area	PC-i; epidote
20150603LC-9	Jasper Prospect	PC-m; jasper; PC-f
20150603LC-9A	Jasper Prospect	PC-f; PC-m; jasper
20150603LC-10	Red Boy-Sutherland Mine	PC-m; PC-f
20150603LC-11	Red Boy-Sutherland Mine	PC-p; PC-m; PC-f
20150604LC-1	Curtis-Marion Jade Mine	PC-p; epidote/jade
20150604LC-2	Jade Prospect	PC-p; epidote/jade
20150604LC-3	Jade Prospect	PC-p; epidote/jade
20150604LC-4	Jade Prospect	PC-p; epidote/jade
20150604LC-5	Jade Prospect	PC-p; epidote/jade
20150604LC-6	Jade Prospect	PC-p; epidote/jade
20150608LC-1	Crilly Gap Pegmatite	PC-p
20150608LC-2	Crilly Gap Pegmatite	PC-p
20150608LC-3	BlackJack Ranch-Barlow Gap Quads	Tc
20150608LC-4	BlackJack Ranch-Barlow Gap Quads	PC-i
20150608LC-5	BlackJack Ranch-Barlow Gap Quads	Tc
20150608LC-6	BlackJack Ranch-Barlow Gap Quads	Tc
20150609LC-1	Black Mountain area	PC-p
20150609LC-2	Black Mountain area	PC-m
20150609LC-3	Black Mountain area	PC-m

20150609LC-4	Black Mountain area	PC-m
20150609LC-5	Black Mountain area	PC-p
20150610LC-1	SW Pine Mountain area	M-con
20150610LC-2	SW Pine Mountain area	M-con
20150610LC-3	SW Pine Mountain area	T-sed
20150610LC-4	SW Pine Mountain area	M,T-sed; f
20150610LC-4A	SW Pine Mountain area	M,T-sed; f
20150610LC-4B	SW Pine Mountain area	M,T-sed; f
20150610LC-5	SW Pine Mountain area	M,T-con
20150610LC-6	Shirley Rim	T-sed
20150618LC-1	Elmers Rock area	PC-f; PC-i; epidote
20150618LC-2	Elmers Rock area	PC-p
20150618LC-3	Elmers Rock area	PC-p; PC-f
20150618LC-4	Elmers Rock area	PC-i
20150618LC-5	Halleck Canyon	PC-m; PC-p
20150618LC-6	Halleck Canyon	PC-m; PC-f
20150618LC-7	Halleck Canyon	PC-i
20150618LC-8	Halleck Canyon	PC-f
20150618LC-9	Halleck Canyon	PC-i
20150618LC-10	Hwy 34	PC-p; PC-f
20150618LC-11A	Hwy 34	PC-i; epidote
20150618LC-11B	Hwy 34	PC-p; PC-i
20150619LC-1	Taylor Deposit	PC-i
20150619LC-2	Taylor Deposit	PC-i
20150622LC-1A	Sunrise Mine	Chert
20150622LC-1B	Sunrise Mine	Clay
20150622LC-1C	Sunrise Mine	Chert
20150623LC-1	Cement Ridge Lookout (Black Hills)	Ti
20150623LC-2	Cement Ridge Lookout (Black Hills)	Ti
20150624LC-1	Black Buttes area (Black Hills)	Ti
20150624LC-2	Black Buttes area (Black Hills)	Ti; f
20150624LC-3	Black Buttes area (Black Hills)	Ti

RE15134836 - Finalized
CLIENT : TKT - Wyoming State Geological Survey
of Samples : 148
DATE RECEIVED : 2015-09-05 DATE FINALIZED : 2015-09-22
PROJECT : Sept 2015 - Sample List Page
CERTIFICATE COMMENTS : Full project name: Sept 2015 - Sample List Page 1 of 9 ALL:NSS is non-s
PO NUMBER :

Sample #	**Location**	**Type of Deposit/Category**
20150702CC-1A	Hadsell Draw Coal Bed	Coal; shale roof
20150702CC-1B	Hadsell Draw Coal Bed	Coal bed; Honey T-9
20150702CC-1C	Hadsell Draw Coal Bed	Coal; claystone floor
20150713LC-1	Rawlins Area	P-con
20150713LC-2	Rawlins Area	P-sed
20150713LC-3	Rawlins Area	P-sed; f
20150713LC-4	Bison Basin	T-sed; f
20150713LC-5	Bison Basin	T-sed; con
20150713LC-6	Bison Basin	P-sed; s
20150714LC-1	Anderson Ridge area	PC-p
20150714LC-2	Anderson Ridge area	PC-p
20150714LC-3	Anderson Ridge area	PC-f

20150714LC-4	Anderson Ridge area	PC-i
20150714LC-5	Anderson Ridge area	PC-p
20150714LC-6	Anderson Ridge area	PC-m; PC-p
20150714LC-7A	Anderson Ridge area	PC-p
20150714LC-7B	Anderson Ridge area	PC-p
20150714LC-8	Anderson Ridge area	PC-m
20150714LC-9A	Max Long Jade mine	PC-p; epidote/jade
20150714LC-9B	Max Long Jade mine	PC-p; jade
20150714LC-10	Anderson Ridge area	PC-p
20150714LC-11	Anderson Ridge area	PC-p
20150714LC-12	Anderson Ridge area	PC-p
20150714LC-13	Anderson Ridge area	PC-p
20150714LC-14	Anderson Ridge area	PC-p
20150714LC-15	Anderson Ridge area	PC-p
20150715LC-1	Crooks Mountain West area, South Granit	M-sed; s, f
20150715LC-2	Crooks Mountain West area, South Granit	Cf
20150715LC-3A	Fort Ridge area	PC-p; PC-i; epidote
20150715LC-3B	Fort Ridge area	PC-p; PC-i; epidote
20150715LC-3C	Fort Ridge area	PC-p; PC-i; epidote
20150715RL-1	Shamrock Hills - Lance Fm	Coal
20150715RL-2	Shamrock Hills - Lance Fm	P-sed; Coal
20150715RL-3	Shamrock Hills - Battle Spring Fm	Coal
20150803LC-1A	Jem Claims	PC-p; PC-i; epidote
20150803LC-1B	Jem Claims	PC-i
20150803LC-1C	Jem Claims	PC-p; PC-I
20150803LC-1D	Jem Claims	PC-p
20150803LC-2	Shirley Mountains	Cf
20150803LC-3	Shirley Mountains	P-sed
20150803LC-4	Shirley Mountains	PC-i
20150803LC-5	Omega Claims	PC-i; epidote
20150803LC-6	Omega Claims	PC-i
20150803LC-7	Omega Claims	PC-I; PC-m
20150803LC-8	Pedro Mountains	Cf
20150803LC-9	SE Wind River Basin	T-sed; U
20150803LC-10	SE Wind River Basin	T-sed
20150803LC-11	SE Wind River Basin	T-sed
20150804LC-1	Owl Creek Mountains	PC-p
20150804LC-2A	Owl Creek Mountains	PC-p; PC-m
20150804LC-2B	Owl Creek Mountains	PC-p
20150804LC-2C	Owl Creek Mountains	PC-p
20150804LC-3	Owl Creek Mountains	PC-p; PC-m
20150804LC-4A	Owl Creek Mountains	PC-p
20150804LC-4B	Owl Creek Mountains	PC-p; epidote; PC-m
20150804LC-5	Northern Wind River Basin	T-sed
20150804LC-6A	Northern Wind River Basin	T-sed
20150804LC-6B	Northern Wind River Basin	T-sed
20150804LC-6C	Northern Wind River Basin	T-con
20150804LC-7	Northern Wind River Basin	T-sed
20150804LC-8A	Northern Wind River Basin	T-sed; s
20150804LC-8B	Northern Wind River Basin	T-sed
20150805LC-1	Pilot Knob	Ti (or Quat?)
20150805LC-2	Lava Mountain	Ti (or Quat?)
20150810LC-1	Slope Road, Southern Big Horn Mountain	P-sed
20150810LC-2A	Bull Camp Prospects, Southern Big Horn	PC-p; Pci; epidote
20150810LC-2B	Bull Camp Prospects, Southern Big Horn	PC-p; Pci; epidote
20150810LC-2C	Bull Camp Prospects, Southern Big Horn	PC-p; Pci; epidote

20150810LC-2D	Bull Camp Prospects, Southern Big Horn	PC-p; Pci; epidote
20150810LC-2E	Bull Camp Prospects, Southern Big Horn	PC-p; Pci; epidote
20150810LC-3	Ramsbottom area, Southern Big Horn Mo	PCi; PC-p
20150810LC-4	Ramsbottom area, Southern Big Horn Mo	PC-p
20150810LC-5A	"Stove Leg" prospect, Southern Bighorns	PC-p
20150810LC-5B	"Stove Leg" prospect, Southern Bighorns	PC-p; epidote
20150810LC-5C	"Stove Leg" prospect, Southern Bighorns	PC-i; silicified
20150810LC-6	Prospect Creek area, Southern Bighorn M	Cf
20150811LC-1	Northern Bighorn Mountains	PC-p; PC-i
20150811LC-2	Black Mountain area, Northern Bighorns	PC-p; epidote
20150811LC-3	SW Lookout Mountain area, Northern Bigl	PC-p
20150812LC-1	Shell Sheep prospect, Reeves Ranch, Ea	M-sed
20150812LC-2A	Shell Sheep prospect, Reeves Ranch, Ea	M-con
20150812LC-2B	Shell Sheep prospect, Reeves Ranch, Ea	M-sed
20150812LC-2C	Shell Sheep prospect, Reeves Ranch, Ea	M-s
20150812LC-2D	Shell Sheep prospect, Reeves Ranch, Ea	M-sed
20150812LC-3A	North Sheldon Gulch, Eastern Bighorn Ba	M-con
20150812LC-3B	North Sheldon Gulch, Eastern Bighorn Ba	M-sed
20150812LC-3C	North Sheldon Gulch, Eastern Bighorn Ba	M-con
20150812LC-4A	Bobcat Gulch, Eastern Bighorn Basin	M-sed; s
20150812LC-4B	Bobcat Gulch, Eastern Bighorn Basin	M-con
20150812LC-4C	Bobcat Gulch, Eastern Bighorn Basin	M-sed
20150818LC-1	Albany area	PC-i; PC-f
20150818LC-2	Albany area	PC-i; PC-f
20150818LC-3	Albany area-Sherman Granite Quarry	PC-i
20150818LC-4	Albany area	PC-I; epidote
20150818LC-5	Albany area	PC-p
20150818LC-6A	New Rambler Mine dump (Duchess Mine?	PC-i
20150818LC-6B	New Rambler Mine dump (Duchess Mine?	PC-i; epidote
20150818LC-7A	New Rambler Mine dump (Duchess Mine?	PC-i; epidote
20150818LC-7B	New Rambler Mine dump (Duchess Mine?	PC-p
20150818LC-7C	New Rambler Mine dump (Duchess Mine?	PC-p
20150818LC-7D	New Rambler Mine dump (Duchess Mine?	PC-p
20150818LC-8A	Medicine Bow Mountains	PC-i;PC-f
20150818LC-8B	Medicine Bow Mountains	PC-i; PC-f
20150818LC-8C	Medicine Bow Mountains	PC-p
20150818LC-8D	Medicine Bow Mountains	PC-i; PC-f; epidote
20150818LC-9	Medicine Bow Mountains	PC-i; epidote
20150818LC-10A	Nature's Mint Mine	PC-i; epidote
20150818LC-10B	Nature's Mint Mine	PC-i
20150818LC-11A	Medicine Bow Mountains	PC-p
20150818LC-11B	Medicine Bow Mountains	PC-i; epidote
20150818LC-11C	Medicine Bow Mountains	PC-i
20150818LC-12	Medicine Bow Mountains	PC-i; epidote
20150819LC-1	Big Creek Pegmatite area	PC-p; PC-f
20150819LC-2A	Big Creek Pegmatite area	PC-i; epidote
20150819LC-2B	Big Creek Pegmatite area	PC-i
20150819LC-3	Big Creek Pegmatite area- Platte Mine pit	PC-i; PC-p
20150819LC-4	Big Creek Pegmatite area	PC-i; PC-p; PC-f
20150819LC-5	Big Creek Pegmatite area	PC-p
20150819LC-6A	Big Creek Pegmatite area	PC-p
20150819LC-6B	Big Creek Pegmatite area	PC-p
20150819LC-7	Big Creek Pegmatite area	PC-p; PC-i
20150819LC-8	Big Creek Pegmatite area	PC-p; PC-i
20150819LC-9	Big Creek Pegmatite area	PC-p; PC-i; PC-f
20150819LC-10	Big Creek Pegmatite area	PC-i; PC-p; PC-f; epidote

20150819LC-11A	Big Creek Pegmatite area	PC-p
20150819LC-11B	Big Creek Pegmatite area	PC-p
20150819LC-11C	Big Creek Pegmatite area	PC-p; PC-i
20150819LC-11D	Big Creek Pegmatite area	PC-p; PC-i
20150819LC-12	Big Creek Pegmatite area	PC-p
20150822LC-1	Blanche Mine	PC-I
20150822LC-2	New Rambler Mine	PC-I
20150822LC-3	New Rambler Mine	PC-I
20150823WS-A	Red Oxide prospect	PC-p
20150825LC-1	Sierra Madre	PC-i; PC-f; epidote
20150825LC-2A	Sierra Madre	PC-p; PC-i
20150825LC-2B	Sierra Madre	PC-i; PC-f; epidote
20150825LC-3A	Sierra Madre	PC-f
20150825LC-3B	Sierra Madre	PC-f; epidote
20150825LC-4A	Sierra Madre-Blackhall Mountain	PC-p
20150825LC-4B	Sierra Madre-Blackhall Mountain	PC-p; PC-i
20150825LC-5A	Sierra Madre-Blackhall Mountain	PC-p
20150825LC-5B	Sierra Madre-Blackhall Mountain	PC-p
20150825LC-6	Sierra Madre	PC-f; PC-p; PC-m
20150825LC-7	Sierra Madre	PC-f; PC-p; PC-m
20150825LC-8A	Eureka Mine, Sierra Madre	PC-m
20150825LC-8B	Eureka Mine, Sierra Madre	PC-p
20150715JC-A	Phosphoria Formation	P-sed
20150826WS-1	Flathead	Cf

RE15114315 - Finalized
CLIENT : TKT - Wyoming State Geological Survey
of Samples : 23
DATE RECEIVED : 2015-07-31 DATE FINALIZED : 2015-08-18
PROJECT : Wyoming Phosphates
CERTIFICATE COMMENTS : ME-XRF26: High total was obtained due to partial Sulphur being calculat
PO NUMBER :

Sample #	Location	Type of Deposit/Category
20150623JC-B	Phosphate rock	P-sed; Phosphoria Fm
20150714JC-E	Phosphate rock	P-sed; Phosphoria Fm
20150715JC-C	Phosphate rock	P-sed; Phosphoria Fm
20150715JC-E	Phosphate rock	P-sed; Phosphoria Fm
20150716JC-B	Mudstone	P-sed; Phosphoria Fm

RE15158301 - Finalized
CLIENT : TKT - Wyoming State Geological Survey
of Samples : 66
DATE RECEIVED : 2015-10-15 DATE FINALIZED : 2015-11-15
PROJECT : Oct 2015 - Sample List Page 1
CERTIFICATE COMMENTS : Full Project: Oct 2015 - Sample List Page 1 of 5
PO NUMBER :

Sample #	Location	Type of Deposit/Category
20150903LC-1A	Muddy Mtn Rim	M-sed
20150903LC-1B	Muddy Mtn Rim	M-sed

20150907LC-1	Miners Delight area	PC-p
20150917LC-1	Eureka Mine, Sierra Madre	PC-p
20150917LC-2	Finley Mine, Sierra Madre	PC-p
20150917LC-3	Newton Group, Sierra Madre	PC-p
20150917LC-4	Rambler area, Sierra Madre	PC-p
20150917LC-5	Sierra Madre	PC-p
20150917LC-6	Sierra Madre	PC-p
20150917LC-7	Sierra Madre	PC-p
20150917LC-8A	Sierra Madre	PC-p
20150917LC-8B	Sierra Madre	PC-p
20150917LC-9	Sierra Madre	PC-p
20150918LC-1	Hub Prospect, Sierra Madre	PC-p
20150922LC-1A	Tie Siding area	PC-p
20150922LC-2	Tie Siding area	PC-p
20150922LC-3	Tie Siding area	PC-p
20150922LC-4	Tie Siding area	PC-p
20150922LC-5	Tie Siding area	PC-p
20150922LC-6A	Tie Siding area	PC-p
20150922LC-7A	Tie Siding area	PC-p
20150922LC-7B	Tie Siding area	PC-p
20150922LC-9	Tie Siding area	PC-p
20150922LC-10A	Tie Siding area	PC-p
20150922LC-10B	Tie Siding area	PC-p
20150922LC-11	Tie Siding area	PC-p
20150923LC-1	Garnet Hill area	PC-f
20150923LC-2	Garnet Hill area	PC-f
20150923LC-3	Garnet Hill area	PC-f
20150923LC-4A	Garnet Hill area	PC-f
20150923LC-4B	Garnet Hill area	PC-f
20150928LC-1	Wilkins Peak Member	T-sed
20150928LC-2	Wilkins Peak Member	T-sed
20150928LC-3	Wilkins Peak Member	T-sed
20150928LC-4	Wilkins Peak Member	T-sed
20150929LC-1	Wilkins Peak Member	T-sed
20150929LC-2	Wilkins Peak Member	T-sed
20150929LC-3	Wilkins Peak Member	T-sed
20150929LC-4	Wilkins Peak Member	T-sed
20150929LC-5	Wilkins Peak Member	T-sed
20150929LC-6	Wilkins Peak Member	T-sed
20150929LC-7A	Wilkins Peak Member	T-sed
20150929LC-7B	Wilkins Peak Member	T-sed
20150929LC-7C	Wilkins Peak Member	T-sed
20150929LC-8	Firehole Canyon area	T-sed
20150929LC-9	Oro Claim	T-sed
20150930LC-1	Kent Mine No.1	coal
20150930LC-2	Aspen Mountain area	Qh
20150930LC-3A	Aspen Mountain area	Qh
20150930LC-3B	Aspen Mountain area	Qh
20150930LC-4	Aspen Mountain area	Qh
20150925RL-5	Ervay Basin	T-sed, Wagon Bed Fm.
20150925WS-1	Ervay Basin	french rocks tonalite
20150925WS-7	Ervay Basin	Cf
WGS-0533-TC34-95	Granite Mountains	M, quartzite
RSWS92601-2	Granite Mountains	PC-p, ep
20150624JC-E	Phosphoria Fm	P-sed; Phosphoria Fm
20150713JC-A.1	Phosphoria Fm	P-sed; Phosphoria Fm

20150714JC-A	Phosphoria Fm	P-sed; Phosphoria Fm
20150622JC-C	Phosphoria Fm	P-sed; Phosphoria Fm
20150925RL-01		T-sed, Wagon Bed Fm. volcaniclastics
20150925RL-03		T-sed, Wagon Bed Fm. volcaniclastics
20150925RL-04		T-sed, Wagon Bed Fm. volcaniclastics

RE15179176 - Finalized
CLIENT : TKT - Wyoming State Geological Survey
of Samples : 23
DATE RECEIVED : 2015-11-19 DATE FINALIZED : 2015-12-04
PROJECT : 2015-Zeo
CERTIFICATE COMMENTS :
PO NUMBER :

Sample #	Location	Type of Deposit/Category
20150604DB-3		T-sed, Split Rock Fm.
20150604DB-4		T-sed, Moonstone Fm.
20150604BG-1		T-sed, Moonstone Fm.
20150604BG-2		T-sed, Moonstone Fm.
20150701DB-1		T-sed, Moonstone Fm.
20150701DB-2		T-sed, Moonstone Fm.
20150701DB-4		T-sed, Moonstone Fm.
20150701DB-5		T-sed, Moonstone Fm.
20150701DB-6		T-sed, Moonstone Fm.
20150701DB-7		T-sed, Moonstone Fm.
20150701BG-2		T-sed, Moonstone Fm.
20150702DB-1		T-sed, Moonstone Fm.
20150819DB-2	Lysite Mountain	T-sed; Ti
20150820DB-2	Lysite Mountain	T-sed; Ti
20150819BG-1	Lysite Mountain	T-sed; Ti
20150819BG-2	Lysite Mountain	T-sed; Ti
20150819BG-3	Lysite Mountain	T-sed; Ti
20150819BG-4	Lysite Mountain	T-sed; Ti
20150918DB-1		T-sed, Wagon Bed Fm.
20150930DB-2		T-sed, Blue Point Conglomerate
20150717DB-1	Mineral Hill	Ti
20150717DB-2	Mineral Hill	Ti

	REEs	other
	REEs	other

1967 (USGS paper 440-D)

			5x crust
		PGM-ICP24 Au	PGM-ICP24 Pt
Latitude	**Longitude**	ppm	ppm
42.7437	-107.2189		
42.7415	-107.2143		
42.7282	-107.2211		
41.0489	-106.7530		
41.1875	-106.0630		
42.6017	-107.9090		
42.5474	-107.8840		
42.7182	-107.3140		
42.7182	-107.3100		
42.9534	-106.9520		
41.2535	-106.9030		
44.1083	-108.5810		
44.8558	-108.4640		
42.06857	-106.604426		
42.06854	-106.604440		
42.06847	-106.604437		
42.06833	-106.604410		
42.06821	-106.604474		
42.06792	-106.604444		
42.06792	-106.604444		
42.70392	-107.340774		
42.70392	-107.340774		
42.57007	-107.509734		
42.63498148	-107.5717928		
42.71635	-107.620580		
42.72280446	-107.581726		
43.41223	-108.062563		
42.46040	-108.503130		
44.83770	-104.899365		
42.85283	-110.660449		

Latitude	Longitude	PGM-ICP24 Au ppm	PGM-ICP24 Pt ppm
41.2029	-106.2900		
43.405478	-107.991054		
42.5948	-107.9197		
42.5948	-107.9197		
42.5948	-107.9197		
42.5948	-107.9197		
42.5948	-107.9197		
42.2365	-106.8285		
42.6041	-107.3436		
42.602	-107.9103		
42.594918	-107.830577		
42.594918	-107.830577		
42.5402	-107.568		
-	-		
42.411902	-108.520194		
42.6086737	-107.7662587		
42.60863414	-107.7660444		
42.61740153	-107.7615495		
42.62771672	-107.7422882		
42.63098415	-107.7422886		
42.63576502	-107.9244194		
42.63589117	-107.9229395		
42.63548817	-107.9168128		
42.650163	-107.908479		
42.65393414	-107.8889818		
42.65222792	-107.8893014		
42.652508	-107.889394		
42.64931462	-107.8935916		
42.64468194	-107.8836548		
42.64706316	-107.8866303		
42.647141	-107.887124		
42.62241315	-107.9019343		
42.62460862	-107.897075		
42.57388218	-107.893584		
42.57617849	-107.8992915		
42.60999679	-107.9020569		
42.56794226	-107.9097661		
42.59701598	-107.8211541		
42.597305	-107.820081		
42.63681485	-107.3119967		
42.63823425	-107.3149109		
42.67607125	-107.3797678		
42.67730271	-107.3795471		
42.67136724	-107.3914445		
42.67087983	-107.3933207		
42.77293352	-107.4454533		
42.77321943	-107.4453123		
42.77310552	-107.4458859		

42.77289329	-107.4463013
42.77868728	-107.4516573
42.941223	-106.944196
42.93356901	-106.9212901
42.94355571	-106.9216169
42.94842468	-106.92688
42.94866	-106.926694
42.948687	-106.9268
42.94883891	-106.9260443
42.323761	-106.446281
41.93213727	-105.3943435
41.93260029	-105.394405
41.93241379	-105.3970743
41.92663757	-105.3948573
41.85411751	-105.3362532
41.85562952	-105.3278801
41.8565864	-105.3265885
41.85551352	-105.326009
41.85675094	-105.3170355
41.77324095	-105.3531532
41.77253938	-105.3548229
41.77253938	-105.3548229
41.73116262	-105.310984
41.730832	-105.309425
42.33152339	-104.707993
42.33152339	-104.707993
42.33152339	-104.707993
44.3548543	-104.0765965
44.35649221	-104.0795283
44.29422556	-104.2487549
44.29680686	-104.2647557
44.2923647	-104.2502416

sufficient sample.

		PGM-ICP24 Au	PGM-ICP24 Pt
Latitude	**Longitude**	ppm	ppm
41.796167	-107.403313		
41.796167	-107.403313		
41.796167	-107.403313		
41.81024219	-107.3134066		
41.80782552	-107.3112865		
41.79599823	-107.3004532		
42.29851621	-108.3001372		
42.30468437	-108.3050194		
42.32162654	-108.3182325		
42.43892105	-108.8706034		
42.44904136	-108.8719814		
42.47208422	-108.8983911		

42.47109834	-108.9032111
42.46891955	-108.9038053
42.45670334	-108.9609751
42.46234654	-108.9719908
42.46234654	-108.9719908
42.44838246	-108.9698285
42.53690466	-109.1360892
42.53690466	-109.1360892
42.42491288	-108.9250239
42.43537291	-108.9344672
42.43851461	-108.9317185
42.43777164	-108.9311618
42.43074752	-108.9253209
42.42976726	-108.9604944
42.417402	-108.094678
42.42445045	-108.0716321
42.44491755	-107.1290365
42.44491755	-107.1290365
42.44491755	-107.1290365
41.9258511	-107.4470406
41.9258511	-107.4470406
41.95978297	-107.4998199
42.13867	-106.51849
42.13867	-106.51849
42.13867	-106.51849
42.13867	-106.51849
42.13821676	-106.5153363
42.13585859	-106.4958252
42.14677854	-106.4842821
42.303772	-106.789053
42.303281	-106.789276
42.30326691	-106.7873095
42.3942388	-106.7387602
42.87120069	-107.5044891
42.92159605	-107.5509893
42.92239325	-107.5488357
43.41056518	-108.0145034
43.40817349	-108.0063376
43.40817349	-108.0063376
43.40817349	-108.0063376
43.40498828	-107.9991915
43.40798238	-108.0021583
43.40798238	-108.0021583
43.337649	-108.0343652
43.29728125	-108.0167889
43.29728125	-108.0167889
43.29728125	-108.0167889
43.35578685	-107.8731394
43.40558223	-107.7424883
43.40558223	-107.7424883
43.71206107	-110.0446503
43.62306126	-110.0108203
43.85490898	-106.9532198
44.01997782	-106.9255062
44.01997782	-106.9255062
44.01997782	-106.9255062

44.01997782	-106.9255062		
44.01997782	-106.9255062		
43.99563577	-106.895648		
43.99535045	-106.8983319		
43.99731257	-106.8995373		
43.99731257	-106.8995373		
43.99731257	-106.8995373		
44.09312602	-107.1397806		
44.80924197	-107.4015271		
44.72830128	-107.4124261		
44.6528639	-107.3879359		
44.49403161	-107.8720307		
44.49190051	-107.8717458		
44.49190051	-107.8717458		
44.49190051	-107.8717458		
44.49190051	-107.8717458		
44.43470174	-107.7917297		
44.43470174	-107.7917297		
44.43470174	-107.7917297		
44.17005379	-107.5992367		
44.17005379	-107.5992367		
44.17005379	-107.5992367		
41.17886762	-106.1324826		
41.18129485	-106.1382923		
41.18786953	-106.1639074		
41.2026123	-106.1610187		
41.20174829	-106.1831736		
41.22019426	-106.2994441		
41.22019426	-106.2994441		
41.21939312	-106.3024138	<0.001	<0.005
41.21939312	-106.3024138	0.042	0.006
41.21939312	-106.3024138	0.002	<0.005
41.21939312	-106.3024138	0.01	<0.005
41.22011782	-106.353355	0.237	<0.005
41.22011782	-106.353355	0.007	<0.005
41.22011782	-106.353355	0.203	<0.005
41.22011782	-106.353355	0.005	<0.005
41.14681019	-106.4331107		
41.1545016	-106.4271164		
41.1545016	-106.4271164		
41.15732051	-106.4294839		
41.15732051	-106.4294839		
41.15732051	-106.4294839		
41.12511138	-106.2436625		
41.09239656	-106.4810603		
41.09911759	-106.4811673		
41.09911759	-106.4811673		
41.11963724	-106.4685539		
41.11208179	-106.4610061		
41.11012311	-106.4557598		
41.10251435	-106.4521466		
41.10267931	-106.4510245		
41.0970631	-106.440042		
41.0905268	-106.4363831		
41.07846617	-106.4259971		
41.07813014	-106.4273544		

41.07828319	-106.4321469		
41.07828319	-106.4321469		
41.07828319	-106.4321469		
41.07828319	-106.4321469		
41.0794953	-106.4294024		
41.21891	-106.284759	0.005	0.007
41.219593	-106.281684	1.31	6.2
41.219593	-106.281684	0.219	0.808
41.381626	-106.262551		
41.03006311	-106.5250594		
41.0311525	-106.5297231		
41.0311525	-106.5297231		
41.0284718	-106.522021		
41.0284718	-106.522021		
41.04509538	-106.6953249		
41.04509538	-106.6953249		
41.03262663	-106.6843941		
41.03262663	-106.6843941		
41.15314473	-106.8304952		
41.14709417	-106.8037363		
41.16457866	-106.8309017		
41.16457866	-106.8309017		
42.57966	-110.72222		
42.57586584	-108.0104862		

ed twice (in individual data and also in LOI data). SF (Sulphur Free) Total is below 102%.

		PGM-ICP24 Au	PGM-ICP24 Pt
Latitude	**Longitude**	ppm	ppm
42.598806	-108.637803		
42.10757	-110.81721		
42.41886	-110.59631		
42.10757	-110.81721		
43.30166	-110.78041		

		PGM-ICP24 Au	PGM-ICP24 Pt
Latitude	**Longitude**	ppm	ppm
42.681281	-106.260035		
42.681281	-106.260035		

42.526815	-108.690362
41.17006428	-106.8277725
41.17048387	-106.8246015
41.16387047	-106.9030033
41.16347359	-107.0064383
41.24649273	-107.1102607
41.27482784	-107.0909075
41.2488281	-107.0686677
41.24948558	-107.0195622
41.24948558	-107.0195622
41.21695323	-106.9337457
41.30503354	-107.2159487
41.020856	-105.471262
41.03397436	-105.4616332
41.03591896	-105.4589347
41.01404051	-105.4210894
41.01943033	-105.4265304
41.06548377	-105.5036211
41.06247325	-105.5021465
41.06247325	-105.5021465
41.06248397	-105.5058853
41.06194736	-105.4341431
41.06194736	-105.4341431
41.01967743	-105.4156888
42.37644712	-104.6213519
42.3771787	-104.6230387
42.37713	-104.62271
42.37677377	-104.6235093
42.37677377	-104.6235093
41.53260497	-109.3766863
41.16713463	-109.8296211
41.406435	-109.47689
41.45963355	-109.412
41.0041611	-109.222122
41.00593002	-109.2227842
41.28630543	-109.2556175
41.28644331	-109.260234
41.30298047	-109.392765
41.30127635	-109.3287272
41.32538656	-109.3536408
41.32538656	-109.3536408
41.32538656	-109.3536408
41.45092542	-109.3367719
41.45244288	-109.3413493
41.45477163	-109.2185182
41.42411121	-109.1123351
41.42213082	-109.1160318
41.42213082	-109.1160318
41.40019052	-109.1301871
42.79369114	-107.3919162
42.83605102	-107.3767793
42.836468	-107.376672
42.5474	-107.884
42.58459	-107.255047
43.588555	-107.954546
41.94811343	-110.6044012

42.1441	-110.81088
42.62441	-108.485264
42.74990961	-107.397874
42.755016	-107.408226
42.780536	-107.399575

		PGM-ICP24 Au	PGM-ICP24 Pt
Latitude	**Longitude**	ppm	ppm
42.54422	-107.47437		
42.54397	-107.47548		
42.54329	-107.472006		
42.54317	-107.472383		
42.57465	-107.49902		
42.57398	-107.49886		
42.5732	-107.49797		
42.57234	-107.49768		
42.5495	-107.52831		
42.54981	-107.52808		
42.54998	-107.52788		
42.6244	-107.1806		
43.54103	-107.60372		
43.56726	-107.62424		
43.53839	-107.60946		
43.53828	-107.60956		
43.53828	#VALUE!		
43.54182	-107.60361		
42.70736	-108.17963		
43.68711	-109.7197		
44.3707	-104.08089		
44.37017	-104.08115		

Type of Deposit/Category
Precambrian
PC-p = Pegmatites, veins, dikes, & alterations (epidote where noted)
PC-f = Faults and shear zones
PC-c = Metacarbonate rocks
PC-d = Disseminated minerals in alkalic igneous rocks
PC-m = Metasediments including paleoplacers
PC-l = Igneous bodies & gneisses

Pz & Mz Paleoplacers
Cf = Cambrian Flathead Ss
Kmv = Cretaceous Mesaverde Fm
PPd = Permian Phosphoria Fm Disseminations within phosphate rock
Con = Concretions (may include Tertiary)

al abundance*:	0.0155	59.07*	15.22*	3.10*	5.10*	3.45*	3.71*
PGM-ICP24	Au-AA25	ME-ICP06	ME-ICP06	ME-ICP06	ME-ICP06	ME-ICP06	ME-ICP06
Pd	Au	SiO2	Al2O3	Fe2O3	CaO	MgO	Na2O
ppm	ppm	%	%	%	%	%	%
	<0.01	66.9	15.55	3.44	2.8	0.81	5.27
	0.01	75.8	8.74	4.67	2.57	2.04	2.15
		89.4	1.69	6.14	0.06	0.06	0.04
		52.8	8.57	17.75	12.85	3.91	0.41
		51.1	18.3	5.76	12.35	8.05	2.5
		60.4	16.55	2.46	11	2.8	1.91
		47.1	31.5	0.53	6.61	1.14	1.95
		90.7	0.34	4.02	2.51	0.07	0.03
		67.2	0.52	26	1.54	0.18	0.68
		4.67	2.26	57.7	2.9	2.13	0.03
		18.6	1.69	67.4	0.08	0.14	0.06
		63.5	8.37	1.82	11.2	0.57	1.17
		38.8	2.86	1.25	16.85	11.35	0.07
	<0.01	87.1	4.69	1.64	0.55	0.34	0.08
	<0.01	71.5	12.35	3.61	0.51	0.97	0.08
		88.4	4.99	1.09	0.27	0.46	0.08
	<0.01	91.9	3.42	1.31	0.12	0.17	0.11
		91.3	2.13	0.62	0.15	0.11	0.25
	<0.01	79.3	7.69	1.48	0.72	0.78	0.71
		82.8	0.41	0.37	3.46	4.46	0.11
		60.7	16.3	4.44	3.02	1.12	4.47
	<0.01	65.4	13.65	5.63	1.67	0.14	1.52
	<0.01	85.9	5.32	1.72	1.53	0.51	0.94
	<0.01	91.1	1.75	3.24	1	0.26	0.07
	<0.01	73.9	13.95	1.27	0.47	0.33	3.94
		17.8	3.32	0.58	41.3	0.2	0.92
	<0.01	89.8	2.6	3.25	0.17	1.07	0.04
	0.37	86.2	1.1	5.74	0.86	0.04	0.06
		1.41	0.53	2.34	52.8	0.27	0.03
	<0.01	80.4	1.72	1.33	7.58	0.78	0.04

PGM-ICP24	Au-AA25	ME-ICP06	ME-ICP06	ME-ICP06	ME-ICP06	ME-ICP06	ME-ICP06
Pd	Au	SiO2	Al2O3	Fe2O3	CaO	MgO	Na2O
ppm	ppm	%	%	%	%	%	%
		49.6	13.45	11.35	11	6.97	1.5
		64.3	15.8	1.56	8.33	3.37	4.07
		46.8	21.6	3	14.45	5.87	1.35
		43	31.5	0.86	14.5	0.69	0.49
		56.4	1.51	3.7	13.45	21.8	0.12
		54.9	18.1	1.6	11.45	6.13	2.18
		51.1	4.59	9.46	8.99	22.5	0.14
		52	16.75	7.77	17.15	0.52	0.48
		49.4	22	5.7	13.6	1.33	4.49
		73.9	8.2	2.09	9.13	4.03	0.24
		43.9	21.9	6.54	12.85	4.19	2.81
		45.5	23.9	6.38	16.95	0.05	3.37
		45.1	33.1	0.28	8.43	1.06	1.43
		54.7	1.73	6.8	13.05	19.85	0.15
		62.4	0.31	16.1	1.03	0.08	0.05
		69.1	15.8	0.71	0.26	0.22	3.03
		73.5	14.45	0.9	0.48	0.11	6
	0.02	47.1	0.36	0.33	25.7	1.86	0.09
		65.3	17.55	1.43	0.18	0.53	3.94
	<0.01	93.7	2.66	1.5	0.08	0.75	1.08
	<0.01	48.3	16.85	12.3	7.65	5.89	2.63
	0.06	82.3	0.57	13.6	0.23	0.13	0.06
	<0.01	96.7	0.39	2.22	0.05	0.1	0.09
		98.9	0.08	0.51	0.07	0.02	0.03
		77.7	12.05	1.15	0.38	1.36	0.28
		80.9	9.25	2.73	0.49	2.2	0.5
		34.8	18.05	17.55	0.52	16.15	0.1
		79.6	0.2	12.9	0.23	5.95	0.04
		63.6	12.35	5.2	12.1	3.15	0.41
	<0.01	40.7	8.81	33	0.51	0.55	0.28
	<0.01	37.5	3.87	38.8	2.89	0.79	0.65
	<0.01	73.2	2.85	14.3	1.86	4.8	0.12
	<0.01	60.9	9.33	12.15	4.99	2.96	1.61
		49.7	6.43	8.83	14.55	14.75	0.29
		44.8	29.8	3.35	13.15	0.58	1.79
		55.8	19.65	3.94	13.9	1.57	1.17
		48.9	3.21	5.94	0.35	31.7	0.02
		50.4	22.5	6.04	13.85	0.49	4
		49.9	5.65	3.97	9.78	24.4	0.09
		67.4	18.5	3.28	0.39	0.3	7.85
		76.6	14.2	0.53	0.47	0.07	6.68
	<0.01	13.45	1.26	0.96	46	0.95	0.2
		72.4	14.75	2.29	2.2	0.39	3.4
		1.5	0.31	0.21	54.5	0.41	0.05
		22.8	4.11	0.91	37.9	0.7	0.69
		80.5	12.35	0.95	0.42	0.21	3.04
	<0.01	77.5	0.4	20.3	0.25	0.12	0.02
		72.1	16.4	0.87	1.29	0.08	7.35

		86.5	9.05	0.46	0.14	0.01	5.03
		78.8	13.8	0.88	0.3	0.11	5.18
		50.7	6.72	10.85	14.3	0.32	1.46
		7.86	1.57	0.54	49	0.38	0.05
		69.9	13.25	4.09	0.71	1.19	0.64
	<0.01	30.4	3.33	7.36	28.9	1.23	0.11
		45.8	16.7	12.85	1.62	2.4	1.36
		55.1	7.93	5.32	13.55	0.45	0.75
		26.6	4.1	27.5	16.3	1.13	0.14
		66.6	14	6.25	0.69	0.82	0.45
		73.3	12.9	2.8	3.78	0.45	3.48
		47.1	9.7	11.95	10.25	13.4	1.24
		74	12.95	0.44	0.15	0.05	1.81
		74.9	13.25	0.58	0.1	0.07	1.37
		47.2	16.1	13.6	5.77	6.69	2.89
		84.3	8.65	1.14	0.06	0.38	0.11
		73.9	12.2	1.88	0.41	0.15	3.05
	<0.01	64	6.37	17.15	0.85	2.23	0.15
		65.7	15.15	5.28	2.16	0.17	3.96
	<0.01	50	27.6	2.16	11.5	1.05	3.93
		54.8	23.5	2.37	8.82	0.36	5.68
	<0.01	39.1	14.7	19.8	8.43	3.06	2.8
		1.78	3.33	62.9	0.15	2	0.04
		55.4	26.2	1.07	8.95	0.17	5.3
		98.6	0.18	0.73	0.08	0.03	0.04
		42.7	1.06	47.2	0.32	0.59	0.04
		47.2	0.38	48.4	0.1	0.04	0.03
		62.6	18.15	4.36	1.63	0.93	5.68
		55.9	16.65	7.75	5.52	2.48	4.06
		61.2	19.5	2.28	1.31	0.17	6.88
		59.8	20.8	1.99	0.82	0.09	8.79
		60.6	18.8	4.4	2.9	0.52	6.01

PGM-ICP24	Au-AA25	ME-ICP06	ME-ICP06	ME-ICP06	ME-ICP06	ME-ICP06	ME-ICP06
Pd	Au	SiO2	Al2O3	Fe2O3	CaO	MgO	Na2O
ppm	ppm	%	%	%	%	%	%
		36	10.5	3.86	1.96	0.97	0.09
		16.9	5.48	2.78	1.99	0.35	0.03
		78.7	8.56	0.94	0.18	0.33	0.07
		59	4.1	2.38	9.49	6.87	0.02
		55.2	5.67	26.7	4.95	0.18	0.04
		31.6	3.28	20.7	20.8	0.68	0.03
		41.7	6.59	33.4	0.4	0.25	0.94
		65.9	8.37	13.75	0.3	0.12	1.45
		99.1	0.7	0.28	0.47	0.09	0.04
		73.5	14.6	0.89	0.46	0.09	2.85
		64.3	15.1	8.68	0.15	0.14	1.42
	0.15	75.6	5.56	10.6	0.25	2.37	0.32

0.01	65	18.65	2.6	0.27	0.19	9.68
	65.7	20.1	2.11	0.29	0.22	8.61
	74.5	14.55	1.39	0.45	0.08	4.46
	64.6	19.75	2.74	0.09	0.46	2.19
0.46	49.1	14.2	8.87	3.01	0.02	2.56
	65.4	16.65	4.01	2.1	1.93	2.61
	46	3.45	5.87	3.68	30.4	0.12
	64.9	20.1	0.64	5.69	0.25	5.06
<0.01	99.3	0.2	0.42	0.05	0.06	0.03
	67.7	17.6	1.39	0.71	0.24	9.43
	66	19.4	1.11	0.31	0.06	8.88
	79	13.65	0.57	0.07	0.05	5.93
1.05	27.2	8.31	20.7	1.5	0.04	0.88
	77.3	12.7	1.96	0.4	0.69	3.82
<0.01	97.5	0.38	0.64	0.66	0.05	0.06
	95.4	1.62	0.53	0.07	0.02	0.04
	64	15.9	5.31	8.52	0.24	4.38
	73.7	14	1.6	1.41	0.29	3.65
	48.6	13.75	14.55	9.8	6.32	2.2
	2.48	1.86	0.57	0.71	0.24	0.03
	52.9	10.75	10.2	0.09	0.6	0.1
	77.4	5.71	2.25	1.55	0.38	0.25
	68.2	8.87	13.45	0.12	2.85	1.08
	72.1	14	1.45	0.16	0.36	3.44
	47.9	14	14	8.77	6.81	1.64
	61.8	13.6	8.07	3.53	3.9	4.29
	96.7	1.31	0.4	0.03	0.04	0.04
	76.7	4.64	15.05	0.18	0.21	0.04
	72.8	13.1	1.32	0.29	0.28	2.17
	68	12.1	6.09	10.7	0.2	0.37
	76.2	12.8	1.68	0.99	0.11	3.37
	66.8	12.65	6.49	11.2	0.31	0.28
	97.1	1.14	1.32	0.07	0.09	0.02
	61.9	8.98	16.45	1.29	0.43	1.96
	79.3	5.66	6.04	0.12	0.04	0.71
	67.4	6.54	15.25	0.44	0.21	0.69
	78.1	13.3	0.64	0.55	0.01	7.14
	74	14.6	1.92	0.2	0.03	6.86
	66.2	18.5	0.39	0.19	0.01	1.18
	59.9	23.6	1.99	0.47	0.39	6.88
	72	16.15	0.49	0.93	0.02	9.18
	66	19.15	0.59	1.45	0.05	9.39
	71.7	17	1.36	0.06	0.7	0.94
	70.1	12.55	5.04	1.73	0.9	2.74
	62.4	8.64	3.03	10.1	1.12	1.59
	51.5	16.6	9.2	1.09	3.77	0.92
	6.31	1.97	1.06	48.1	1.07	0.07
	66.1	10.8	3.06	4.54	1.86	1.33
	78.6	7.71	3.04	1.1	0.84	0.85
	62.8	12.65	4.05	6.4	0.82	2.25
	53.4	15.9	6.23	7.34	5.79	2.61
	58.1	15.15	7.09	6.46	4.76	2.89
	93.9	0.83	2.33	0.51	0.06	0.02
	80	5.06	9.15	0.36	0.28	0.29
	68.1	17.6	1.08	0.07	0.08	6.51
	83.7	5.95	4.4	0.27	0.95	0.94

		42.3	15.8	24.8	0.24	3.08	1.94
		53.8	15.2	10.8	3.44	2.83	0.29
		72.8	14.6	1.23	0.31	0.06	3.75
		73.6	13.9	1.05	1.65	0.13	4.91
		42.5	13.1	13.55	26.5	0.45	1.72
		47.8	6.19	6.15	21.3	8.65	1.91
	<0.01	91.3	0.65	4.54	0.43	1.32	0.07
		92.9	2.81	1.86	0.13	0.12	0.07
		47	21.5	8.22	10.4	4.24	2.12
		52.2	25.8	3.06	2.9	1.8	0.07
	0.02	33.2	2.75	57.2	0.06	0.07	0.02
		93.7	0.44	3.43	1.01	0.56	0.04
		1.71	0.17	0.08	54.2	0.28	0.06
		58.9	15.05	4.62	1.68	2.36	1.38
		97.2	0.45	1.05	0.27	0.05	0.1
		89.8	4.15	1.95	0.67	0.14	0.04
		40.8	4.95	1.03	26.8	0.17	0.67
		62.2	14.85	3.67	1.61	1.48	0.74
		58.4	1.68	24.7	3.91	0.3	0.21
		99	0.16	0.93	0.36	0.02	0.02
		63.4	0.78	27.2	1.62	0.21	0.06
		96.5	0.69	2.43	0.14	0.04	0.02
		62.7	17.35	4.76	1.78	0.86	4.58
		74.1	13.85	1.64	0.51	0.34	4.07
		72.2	13.05	3.97	1.18	0.39	3.34
		63.5	14	7.2	8.97	0.14	0.09
		95.8	2.23	2.07	0.07	0.18	0.19
	<0.01	45.8	16.05	14.05	6.35	8.26	2.54
	<0.01	68.2	14.25	3.41	5.6	0.03	3.21
<0.001		67	14	5.45	6.72	0.91	3.64
0.003		75.5	0.14	20.1	0.12	0.09	0.05
0.003		52.7	11.3	17	4.93	0.38	0.14
0.001		58.6	14.1	7.97	5.27	4.82	2.95
0.004		47.4	2.91	24.2	0.18	0.65	0.4
0.001		70.4	3.79	22.4	0.15	0.4	0.73
0.001		91.1	2.58	5.2	0.09	0.47	0.12
0.003		66	11.4	7.63	10.85	0.2	0.27
	<0.01	67	14.95	3.94	4.32	0.16	4.07
	1.32	88.4	0.21	7.11	0.04	0.01	0.04
	0.24	48.7	16.1	14.15	9.19	4.67	3.11
	0.49	77.8	10.8	4.85	0.25	0.16	4.46
	0.02	53.5	15	10.15	16.2	0.12	0.09
	0.03	49.7	19.1	8.46	8.7	4.23	3.57
	<0.01	58.5	16.4	7.96	3.9	3.57	3.8
		75.4	14.75	0.65	0.43	0.09	4.78
		80.9	12.15	0.68	0.42	0.04	6.37
		78.5	12.15	1.3	0.69	0.06	3.98
	0.03	93.9	0.07	5.07	0.07	0.02	0.02
		81.9	10.05	0.86	1.04	0.06	4.53
		76.3	13.8	2.49	1.67	0.05	4.33
		62.8	15.15	6.93	0.93	3.11	4.55
		72.2	14.75	2.14	0.94	0.15	3.45
		70	10.55	13.55	2.33	0.08	3.46
		80.7	10.3	1.75	0.39	0.47	1.52
		82.3	9.54	1.93	0.91	0.1	1.92
		76.3	12.7	1.95	1.08	0.08	2.77

	<0.01	98.2	0.09	1.11	0.04	0.01	0.01
		94.9	0.09	1.77	0.03	0.02	0.01
		66.3	21.9	0.39	3.08	0.02	8.15
		75.1	14.25	2.19	1.35	0.05	4.93
		72.6	17.75	0.51	3.26	0.03	6.81
0.005		47.1	8.53	10.45	11.95	17.8	0.55
3.15		52.8	16.65	11.2	4.04	2.83	4.13
1.69		39.8	8.61	18	8.04	14.75	0.64
	0.01	55.6	22.7	9.27	0.11	0.14	0.03
		67	11.75	8.11	10.9	0.35	0.57
		69.9	15.6	1.01	1.44	0.08	2.61
		55.3	14.25	10.35	8.35	4.44	1.52
	0.02	43.7	20.3	14.1	17.65	0.87	0.81
	0.03	40.8	21.8	16	11	2.9	1.32
		52.8	15.4	14.7	6.53	3.21	3.16
		67.3	14.75	6.61	0.94	0.16	2.81
		75.5	14.8	1.72	3.07	0.41	4.57
		75.6	13.85	0.47	1.13	0.03	2.83
		94.4	1.4	1.38	0.06	0.94	0.1
	<0.01	46.8	3.54	26.7	8.26	0.46	0.38
	0.24	68.8	0.86	13.8	0.17	0.24	0.01
	0.55	15.6	2.63	62.7	0.34	0.23	0.01
		37.7	3.99	2.65	28.5	0.35	0.38
	<0.01	88.1	4.33	1.41	0.34	0.04	0.07

PGM-ICP24	Au-AA25	ME-XRF26	ME-XRF26	ME-XRF26	ME-XRF26	ME-XRF26	ME-XRF26
Pd	Au	SiO2	Al2O3	Fe2O3	CaO	MgO	Na2O
ppm	ppm	%	%	%	%	%	%
		17.96	3.1	1.68	38.7	1.06	1.02
		11.04	1.66	1	44.5	0.17	0.93
		11.01	1.69	0.67	44.5	0.19	1.1
		7.79	0.59	0.29	49	0.08	0.84
		67.17	10.79	3.75	1.62	0.67	0.13

PGM-ICP24	Au-AA25	ME-ICP06	ME-ICP06	ME-ICP06	ME-ICP06	ME-ICP06	ME-ICP06
Pd	Au	SiO2	Al2O3	Fe2O3	CaO	MgO	Na2O
ppm	ppm	%	%	%	%	%	%
		98.4	0.34	2.01	0.12	0.03	0.03
		96.4	0.54	2.04	0.05	0.03	0.02

<0.01	95	0.18	3.66	0.11	0.06	0.03
0.02	7.16	0.81	74.3	3.13	0.21	0.07
0.04	87.4	0.35	8.38	0.32	0.08	0.01
	67.2	16.3	4.6	0.3	0.77	7.01
<0.01	86.3	0.26	10.85	0.04	0.05	0.07
0.02	98.7	0.15	0.75	0.04	0.09	0.02
0.03	81.9	4.28	1.67	4.16	0.75	0.2
0.08	93.3	0.07	6.81	0.04	0.02	0.03
	50.2	4.86	13.5	5.65	23.7	0.64
	51	7.51	11.35	5.59	22.8	0.71
<0.01	43.5	16.9	9.24	5.46	9.9	3.48
2.83	91.9	1.08	4.29	0.54	0.56	0.09
	73.4	13.9	3.41	0.7	0.16	5.2
	60.8	14.05	7.51	9.03	0.86	2.08
	43.3	5.93	31.2	5.77	2.33	1.16
0.41	56.7	0.05	37.5	0.04	0.06	0.02
	60.1	17.35	5.4	0.36	1.22	3.77
	68	11.3	8.83	0.66	2.34	4.93
	39.5	18.2	11.95	22.6	1.76	0.04
	60	13.9	10.1	3.37	1.94	7.15
	59.4	14.35	8.3	4.34	2.41	4.65
	67.3	12.45	6.74	9.65	0.27	1.01
	75.2	13.05	0.74	0.09	0.03	2.18
	64.3	16.5	5.46	1.3	0.13	4.48
<0.01	13.1	2.18	68.6	0.34	0.13	0.04
0.02	72.3	0.61	18.35	0.09	0.11	0.02
	60.6	13	7.42	0.32	0.27	1.3
	68.2	0.99	19.8	0.18	0.11	0.09
0.04	25.2	4.25	38.8	0.71	2.01	0.33
	33.9	7.22	3.41	14.7	11.25	1.7
	55	13.15	6.48	7.55	2.61	2.4
	54.9	12.9	4.84	5.99	1.43	3.04
	57.1	16.45	6.26	2.57	2.05	3.95
	52.4	3.9	12.1	7.64	0.98	0.71
	4.14	1.08	44.2	1.36	1.84	0.02
	78.1	6.56	2.92	3.63	1.73	1.16
	60.8	15.85	5.84	1.6	2.47	0.78
	58.4	10.25	3.81	10.2	1.53	2.89
	31.5	7.81	2.52	24.7	4.25	2.01
	55.7	16.85	9.24	4.91	4.51	6.09
	54.2	16.1	7.02	6.54	6.88	5.01
	53.2	14.65	5.04	11.35	4.37	4.16
	79.9	7.5	6.33	0.79	0.94	1.29
	37.7	7.7	2.51	24.7	1.27	2.73
	0.7	0.39	0.15	0.45	0.07	0.03
	98.1	0.2	0.72	0.2	0.03	0.02
	84.3	0.61	0.36	6.18	0.51	0.06
	96.5	0.2	0.4	0.24	0.06	0.02
	0.76	0.11	0.09	54.8	0.14	0.09
	69.4	13.55	2.17	1.33	0.53	1.12
	92.5	3.23	0.86	0.05	0.06	0.06
	62.4	16.05	5.33	5.24	2.82	4.52
	46.6	32.1	0.91	3.69	3.73	1.51
	53.1	26.1	1.3	8.23	3.23	2.98
	2.07	0.22	0.12	31.6	18.55	0.04
	9.87	1.11	0.47	46.1	0.3	1.26

		38.1	4.4	4.78	26.6	0.39	0.44
		15.2	2.71	1.45	36	6.57	0.15
		68.5	14.5	3.72	3.03	0.96	4.26
		60.3	16.9	5.01	4.36	1.76	4.59
		64.7	17.1	4.17	3.72	0.98	5.18

PGM-ICP24	Au-AA25	ME-ICP06	ME-ICP06	ME-ICP06	ME-ICP06	ME-ICP06	ME-ICP06
Pd	Au	SiO2	Al2O3	Fe2O3	CaO	MgO	Na2O
ppm	ppm	%	%	%	%	%	%
		70.7	11.85	2.34	1.08	0.48	1.68
		55.8	12.2	3.07	2.2	1.9	3.04
		58.6	13.1	3	4.08	2.79	0.56
		75.4	11	2.35	1.88	0.76	2.15
		63.3	10.05	2.26	8.05	1.76	1.78
		68.5	10.85	2.33	5.15	1.2	1.98
		68.4	10.35	1.41	4.88	0.95	0.9
		70.6	10.2	2.23	3.02	1.64	1.47
		69.7	11.45	1.29	2.43	1.29	2.23
		69	9.96	2.12	3.35	2.06	1.42
		51.2	6.3	1.45	18.65	0.77	1.01
		56.4	9.58	0.93	12.4	0.88	1.54
		54.8	11.65	1.86	11.05	1.5	1.33
		64.2	15.35	1.86	1.36	1.43	1.75
		75.4	8.67	1.5	2.06	1.26	0.7
		62.9	12.9	1.31	2.96	1.81	0.63
		63.3	13.5	1.75	2.57	2.23	1
		72.2	10.1	2.07	2.1	1.32	0.85
		79	4.24	2.08	0.78	3.77	0.1
		60.9	15.9	5.72	3.39	2.15	3.72
		48.1	16.55	15.7	0.58	0.36	0.35
		56.3	19.75	3.37	0.22	0.42	0.4

Pz & Mz & Tert

P, M, or T-con = Concretionary material
P, M, or T-sed = Sedimentary unit
P, M, or T-s = Silicified

Other

Chert = Chert & related nodules with various c
Coal = Coal bed (or roof or floor)
U = Associated with uranium prospect

Tertiary alkali igneous rocks & related:

Tc = Carbonatite veins/dikes,
Th = Hydrothermal zones
Ti = Intrusive or extrusive igneous rocks

Quaternary alluvium:

Qpp = Placers & paleoplacers
Qh = Possibly in hotsprings & paleo-hotsprings

3.13*	.05*	1.03*	.11*	.30*	.02*	.05*	.04*	.06*
ME-ICP06	ME-ICP06	ME-ICP06	ME-ICP06	ME-ICP06	ME-ICP06	ME-ICP06	C-IR07	S-IR08
K2O	Cr2O3	TiO2	MnO	P2O5	SrO	BaO	C	S
%	%	%	%	%	%	%	%	%
3.15	<0.01	0.36	0.08	0.21	0.17	0.09	0.11	0.01
1.26	0.01	0.38	0.1	0.17	0.05	0.05	0.05	0.02
1.08	<0.01	0.11	0.04	0.06	0.01	0.02	0.05	0.01
0.47	<0.01	0.12	0.5	1.1	0.05	0.01	0.11	0.02
0.11	0.01	0.13	0.12	0.02	0.08	0.01	0.1	0.01
0.82	0.16	1.36	0.02	0.12	0.1	0.01	0.05	0.01
5.82	<0.01	0.11	0.02	0.02	0.05	0.06	0.04	<0.01
0.05	<0.01	<0.01	0.09	0.01	<0.01	<0.01	0.58	<0.01
0.18	0.01	0.12	0.18	0.07	<0.01	0.02	0.44	0.03
0.05	0.14	12.95	0.67	0.59	0.02	0.06	0.99	0.07
0.49	0.03	0.14	0.38	0.04	<0.01	0.01	0.12	0.01
1.61	0.01	0.2	0.14	0.07	0.02	0.06	2.43	0.09
1.44	<0.01	0.15	0.02	0.04	0.02	0.05	7.42	0.8
0.64	<0.01	0.41	0.01	0.01	<0.01	0.03	0.08	0.23
0.97	0.01	0.44	0.01	0.06	0.03	0.04	0.09	0.14
0.63	<0.01	0.41	0.01	0.02	<0.01	0.03	0.07	0.02
0.95	<0.01	0.64	0.01	0.01	<0.01	0.04	0.06	0.01
0.94	<0.01	0.66	0.01	0.01	0.01	0.06	0.02	0.01
1.76	0.01	0.58	0.04	0.02	0.01	0.12	0.03	0.02
0.12	<0.01	0.02	0.01	0.01	0.01	0.02	0.82	0.04
1.88	<0.01	0.43	0.07	0.23	0.17	0.08	0.02	<0.01
9.34	<0.01	0.31	0.19	0.16	0.04	0.09	0.28	0.02
2.37	<0.01	0.17	0.03	0.05	0.03	0.08	0.22	0.2
1.23	<0.01	0.02	0.02	0.02	<0.01	0.01	0.3	0.01
5.09	<0.01	0.17	0.01	0.03	0.01	0.09	0.02	<0.01
1.06	<0.01	0.03	0.38	0.03	0.01	0.02	9.39	<0.01
0.6	0.01	0.09	0.02	0.04	<0.01	0.01	0.06	0.01
0.3	<0.01	0.02	0.01	0.08	0.07	0.01	0.04	0.2
0.04	<0.01	0.01	0.29	0.03	0.03	0.01	12.1	<0.01
0.65	<0.01	0.09	0.01	0.01	<0.01	<0.01	1.75	<0.01

ME-ICP06 K2O %	ME-ICP06 Cr2O3 %	ME-ICP06 TiO2 %	ME-ICP06 MnO %	ME-ICP06 P2O5 %	ME-ICP06 SrO %	ME-ICP06 BaO %	C-IR07 C %	S-IR08 S %
0.85	0.08	0.7	0.22	0.18	0.05	0.03	0.08	0.01
0.07	<0.01	0.49	0.01	0.17	0.1	<0.01	0.03	0.01
1.98	0.41	0.45	0.02	0.08	0.08	0.02	0.02	<0.01
4.46	<0.01	0.13	0.02	0.12	0.08	0.04	0.02	<0.01
0.06	0.01	0.05	0.05	<0.01	<0.01	<0.01	0.05	0.01
0.72	0.89	0.63	0.02	0.07	0.07	0.01	0.04	0.02
0.05	0.27	0.24	0.22	<0.01	<0.01	<0.01	0.02	<0.01
0.01	0.01	1.16	0.02	0.4	0.14	<0.01	0.02	<0.01
0.23	0.11	0.72	0.03	0.03	0.17	0.01	0.02	<0.01
0.04	0.44	0.52	0.01	0.06	0.06	<0.01	0.06	<0.01
1.03	1.14	0.28	0.04	0.08	0.13	0.01	0.04	<0.01
0.05	0.01	0.17	0.02	0.03	0.16	<0.01	0.02	<0.01
5.48	<0.01	0.09	0.03	0.01	0.06	0.04	0.03	<0.01
0.11	0.01	0.05	0.08	<0.01	<0.01	<0.01	0.19	<0.01
0.13	<0.01	0.02	0.01	0.01	0.01	<0.01	0.06	3.85
9.16	<0.01	0.01	0.01	0.25	<0.01	0.05	0.02	0.01
3.21	<0.01	0.01	0.18	0.1	<0.01	0.02	0.03	<0.01
0.1	<0.01	0.01	0.02	0.02	0.02	<0.01	5.57	0.05
9.51	<0.01	0.21	0.02	0.05	<0.01	0.14	0.04	0.01
0.09	<0.01	0.03	0.02	0.01	<0.01	<0.01	0.03	<0.01
0.57	0.01	1.44	0.18	0.11	0.02	0.01	0.05	0.02
0.08	<0.01	0.09	0.02	0.02	<0.01	<0.01	0.12	0.02
0.13	<0.01	0.02	0.01	0.01	<0.01	<0.01	0.03	0.01
0.04	<0.01	0.05	0.01	0.03	<0.01	<0.01	0.03	<0.01
3.36	<0.01	0.23	0.02	0.27	<0.01	0.03	0.16	<0.01
0.04	<0.01	0.23	0.01	0.03	<0.01	<0.01	0.02	0.01
2.85	0.02	1.24	0.19	0.05	<0.01	0.01	0.17	0.01
0.07	<0.01	0.01	0.08	0.02	<0.01	<0.01	0.04	0.01
0.39	<0.01	0.94	0.05	0.15	0.07	0.01	0.11	0.01
1.05	0.02	0.08	0.03	0.1	0.09	0.02	0.14	1.87
1.46	0.01	0.23	0.89	0.03	0.01	0.01	2.47	0.04
0.06	0.02	0.09	0.13	0.08	<0.01	<0.01	0.04	0.85
4.73	<0.01	0.09	0.18	0.62	0.02	0.12	0.15	0.02
0.15	0.22	1.68	0.08	0.33	0.05	<0.01	0.05	0.01
3.26	<0.01	0.11	0.05	0.05	0.18	0.03	0.03	<0.01
0.4	0.04	0.14	0.02	0.05	0.1	0.01	0.02	<0.01
0.03	0.31	0.11	0.06	0.01	<0.01	<0.01	0.07	<0.01
0.13	0.01	0.23	0.03	0.05	0.14	<0.01	0.06	<0.01
0.03	0.68	0.21	0.06	0.03	<0.01	<0.01	0.09	0.01
1.02	<0.01	0.01	1.24	0.1	<0.01	<0.01	0.05	<0.01
1.1	<0.01	0.01	0.01	0.02	<0.01	0.01	0.09	0.01
0.35	<0.01	0.04	0.04	0.06	0.03	0.01	9.71	0.03
4.03	<0.01	0.22	0.03	0.1	0.03	0.29	0.3	<0.01
0.08	<0.01	0.01	0.03	0.05	0.02	0.01	11.3	0.02
1.64	<0.01	0.09	0.04	0.07	0.06	0.04	7.98	0.05
0.64	<0.01	0.02	0.07	0.18	0.01	0.02	0.09	0.01
0.05	0.01	0.22	0.02	0.05	0.01	0.01	0.08	0.02
0.77	<0.01	0.01	0.1	0.92	0.01	0.01	0.11	0.01

0.19	<0.01	<0.01	0.01	0.13	<0.01	<0.01	0.02	<0.01
2.2	<0.01	0.02	0.04	0.15	<0.01	<0.01	0.05	<0.01
1.53	<0.01	0.14	0.09	0.14	0.02	0.05	3.1	0.05
0.25	<0.01	0.06	0.17	0.07	0.02	0.04	10.3	0.05
1.93	0.01	0.59	0.01	0.04	0.02	0.05	0.11	0.11
0.67	0.01	0.16	0.5	0.24	0.03	0.03	6.48	0.04
0.58	<0.01	0.43	0.03	0.24	0.03	0.04	0.21	0.15
1.54	<0.01	0.28	1.12	0.06	0.02	0.05	3.04	0.02
0.75	<0.01	0.21	1.21	1.6	0.06	0.06	3.51	0.11
3.26	0.01	0.52	0.02	0.09	0.01	0.06	0.13	<0.01
2.22	<0.01	0.16	0.04	0.04	0.03	0.04	0.13	0.01
0.37	0.16	0.7	0.18	0.06	0.01	0.01	0.26	<0.01
8.32	<0.01	0.01	<0.01	<0.01	0.01	0.11	0.18	<0.01
9.22	<0.01	0.05	0.01	0.02	0.01	0.17	0.06	<0.01
0.43	0.04	1.67	0.18	0.43	0.01	0.02	0.04	<0.01
2.34	0.02	0.56	0.01	0.02	<0.01	0.09	0.02	<0.01
5.55	<0.01	0.11	0.01	0.02	<0.01	0.04	0.17	0.01
0.49	0.01	0.19	0.03	0.05	<0.01	0.01	0.61	0.06
5.23	<0.01	0.42	0.09	0.1	0.02	0.22	0.02	<0.01
0.38	<0.01	0.14	0.03	0.03	0.14	0.03	0.25	<0.01
1.23	<0.01	0.17	0.03	1.27	0.1	0.09	0.03	0.01
0.63	<0.01	5.04	0.17	0.63	0.07	0.05	0.13	0.38
<0.01	0.02	18.25	0.36	0.03	0.01	<0.01	0.11	<0.01
1.01	<0.01	0.2	0.01	0.04	0.12	0.07	0.05	<0.01
0.01	<0.01	0.05	0.01	0.01	0.01	0.04	0.02	0.01
0.08	<0.01	0.2	0.04	0.25	0.08	0.14	0.04	0.14
0.02	<0.01	0.01	0.06	0.1	0.03	0.03	0.02	0.09
3.83	<0.01	0.55	0.15	0.24	0.2	0.1	0.15	0.01
2.82	0.01	0.82	0.16	0.45	0.19	0.07	0.51	0.01
5.63	<0.01	0.19	0.18	0.03	0.1	0.05	0.13	0.01
5.29	<0.01	0.1	0.15	<0.01	0.02	0.01	0.07	0.02
4.65	<0.01	0.51	0.12	0.22	0.27	0.12	0.2	0.01

ME-ICP06 K2O %	ME-ICP06 Cr2O3 %	ME-ICP06 TiO2 %	ME-ICP06 MnO %	ME-ICP06 P2O5 %	ME-ICP06 SrO %	ME-ICP06 BaO %	C-IR07 C %	S-IR08 S %
1.08	0.01	0.42	0.07	0.11	0.03	0.05	21.6	0.13
0.26	<0.01	0.29	0.05	0.05	0.03	0.04	36	0.43
0.93	0.01	0.71	0.01	0.02	0.01	0.02	3.62	0.04
2.01	<0.01	0.2	0.07	0.01	<0.01	0.01	4.05	<0.01
0.29	0.01	0.21	0.04	0.03	0.01	<0.01	1.09	<0.01
2.13	<0.01	0.11	0.66	0.51	0.01	0.02	4.29	0.01
2.58	<0.01	0.23	0.02	0.6	0.02	0.05	0.17	1.58
3.74	<0.01	0.09	<0.01	0.23	0.01	0.07	0.24	0.72
0.49	<0.01	0.02	<0.01	0.12	0.01	0.01	0.09	0.01
7.7	<0.01	0.03	0.01	0.04	0.02	0.04	0.02	<0.01
6.49	<0.01	0.01	2.73	0.16	<0.01	0.01	0.05	<0.01
0.3	0.01	0.34	0.04	0.11	<0.01	0.01	0.02	0.02

1.28	<0.01	0.01	0.01	0.14	0.01	0.01	0.09	<0.01
0.91	<0.01	0.01	0.04	0.17	0.01	0.01	0.01	<0.01
5.08	<0.01	0.01	0.24	0.03	<0.01	0.01	0.05	<0.01
7.4	<0.01	0.03	0.06	0.11	<0.01	<0.01	0.01	<0.01
8.63	<0.01	<0.01	0.01	0.24	0.02	0.02	0.02	<0.01
3.77	0.01	0.62	0.06	0.1	0.03	0.07	0.02	<0.01
0.09	0.4	0.11	0.13	0.01	<0.01	<0.01	0.08	<0.01
1.5	<0.01	0.02	0.04	0.03	0.06	0.02	<0.01	<0.01
0.04	<0.01	0.01	<0.01	0.01	<0.01	0.02	0.04	<0.01
0.23	<0.01	0.01	0.02	0.2	0.01	0.01	0.01	<0.01
2.53	<0.01	<0.01	0.49	0.23	<0.01	0.01	0.1	<0.01
1.24	<0.01	<0.01	0.01	0.17	0.01	<0.01	0.18	<0.01
5.66	<0.01	0.01	<0.01	0.19	0.03	0.01	0.02	0.15
0.39	<0.01	0.05	0.03	0.04	<0.01	<0.01	0.09	<0.01
0.09	0.01	0.01	0.01	0.36	<0.01	<0.01	0.04	<0.01
0.98	<0.01	0.44	0.01	0.04	0.01	0.02	0.29	<0.01
0.1	<0.01	0.18	0.02	0.04	0.1	<0.01	0.02	<0.01
4.23	<0.01	0.14	0.01	0.04	0.02	0.11	0.05	<0.01
0.45	0.02	1.35	0.22	0.13	0.02	0.04	0.11	0.02
0.08	<0.01	0.05	<0.01	<0.01	0.01	0.05	49.6	0.59
2.34	0.01	0.56	<0.01	0.08	0.01	0.04	4.8	2.37
1.43	<0.01	0.23	<0.01	0.03	0.02	0.15	3.81	0.08
2.98	<0.01	0.01	0.06	0.05	<0.01	0.03	0.06	<0.01
5.79	<0.01	0.08	0.01	0.04	0.01	0.07	0.05	<0.01
1.34	0.03	1.24	0.19	0.1	0.02	0.02	0.03	0.01
1.18	<0.01	0.56	0.1	0.04	0.01	0.03	0.02	<0.01
0.87	<0.01	0.33	0.01	0.03	0.01	0.01	0.04	<0.01
1.2	0.01	0.46	0.01	0.05	<0.01	0.01	0.15	0.02
6.42	<0.01	0.12	0.01	0.04	0.01	0.08	0.03	<0.01
0.17	<0.01	0.23	0.02	0.02	0.08	<0.01	0.09	<0.01
4.64	<0.01	0.09	0.02	0.04	0.01	0.03	0.15	<0.01
0.15	<0.01	0.25	0.03	0.01	0.11	0.01	0.04	<0.01
0.4	<0.01	0.05	0.01	0.02	<0.01	<0.01	0.08	<0.01
3.22	0.01	0.18	0.04	0.67	0.04	0.1	0.11	0.05
2.7	<0.01	0.04	0.01	0.07	0.01	0.04	0.04	1.29
2.67	<0.01	0.15	0.01	0.08	0.01	0.05	0.19	0.64
0.19	<0.01	<0.01	0.01	0.09	<0.01	<0.01	0.11	<0.01
0.72	<0.01	<0.01	0.76	0.08	<0.01	<0.01	0.02	0.01
14.05	<0.01	<0.01	0.01	0.22	<0.01	<0.01	0.03	<0.01
3.47	<0.01	0.02	0.03	0.1	<0.01	0.01	0.04	<0.01
0.24	<0.01	<0.01	0.07	0.72	<0.01	<0.01	0.12	<0.01
0.28	<0.01	<0.01	0.01	0.69	<0.01	<0.01	0.18	<0.01
5.16	<0.01	<0.01	0.08	<0.01	<0.01	0.02	0.02	<0.01
3.3	0.01	0.55	0.04	0.07	0.02	0.1	0.13	0.01
2.41	0.01	0.32	0.05	0.05	0.01	0.04	2.08	<0.01
4.24	0.03	0.73	0.05	0.06	0.02	0.05	0.07	<0.01
0.46	<0.01	0.07	0.27	0.03	0.01	0.02	10.4	0.02
5.39	0.01	0.34	0.08	0.12	0.04	0.11	0.83	<0.01
3.42	<0.01	0.29	0.01	0.07	0.06	0.13	0.05	0.01
3.53	<0.01	0.47	0.03	0.29	0.12	0.23	0.84	0.05
4.03	0.03	0.79	0.09	0.59	0.27	0.29	0.22	<0.01
1.98	0.03	0.74	0.1	0.24	0.07	0.16	0.03	<0.01
0.36	<0.01	0.14	0.01	0.33	0.03	<0.01	0.1	<0.01
1.61	<0.01	0.57	0.02	0.38	<0.01	0.01	0.29	0.01
5.7	<0.01	0.02	<0.01	0.01	<0.01	0.02	0.02	<0.01
2.03	<0.01	0.2	0.02	0.19	<0.01	0.01	0.04	<0.01

3.92	<0.01	0.44	0.03	0.16	<0.01	0.03	0.07	0.02
3.4	0.01	1.47	0.04	2.7	<0.01	0.02	0.06	<0.01
6.67	<0.01	0.02	0.01	0.02	0.01	0.02	0.23	<0.01
2.13	<0.01	0.05	0.01	0.04	0.03	0.05	0.1	<0.01
0.41	<0.01	0.4	0.26	0.06	0.07	0.02	0.12	<0.01
0.97	<0.01	0.06	0.18	4.93	0.12	0.02	0.06	0.01
0.2	<0.01	0.09	0.09	0.07	<0.01	0.08	0.28	0.01
1.73	<0.01	0.23	0.01	0.01	0.01	0.03	0.07	<0.01
1.19	0.02	0.66	0.13	0.08	0.03	0.02	0.05	0.01
7.38	<0.01	0.21	0.04	0.06	0.08	0.16	0.04	<0.01
0.12	<0.01	0.09	0.01	0.11	<0.01	0.01	0.11	0.06
0.12	<0.01	0.13	0.01	0.08	<0.01	0.02	0.3	0.04
0.03	<0.01	<0.01	0.15	0.01	0.06	0.45	11.3	0.16
1.06	<0.01	0.47	0.04	0.04	0.03	0.12	0.21	0.08
0.03	<0.01	0.01	0.01	0.01	0.01	0.41	0.09	0.09
0.27	<0.01	0.18	0.01	0.02	0.01	0.06	0.06	0.31
0.09	<0.01	0.48	0.06	18.4	0.13	0.04	0.49	0.6
0.27	<0.01	0.5	0.03	0.11	0.05	0.61	0.23	0.11
0.36	<0.01	0.17	0.39	0.56	0.04	0.09	0.81	0.42
0.03	0.01	0.37	0.01	0.06	<0.01	0.01	0.15	0.04
0.12	<0.01	0.28	0.08	0.08	0.01	0.02	0.51	0.06
0.04	<0.01	0.08	0.01	0.01	<0.01	<0.01	0.2	<0.01
6.35	<0.01	0.28	0.16	0.25	0.11	0.19	0.03	<0.01
5.27	<0.01	0.15	0.04	0.04	0.02	0.06	0.03	<0.01
5.13	<0.01	0.33	0.05	0.06	0.01	0.12	0.02	<0.01
4.7	<0.01	0.19	0.08	0.06	0.15	0.08	0.05	<0.01
0.06	<0.01	0.04	0.01	0.02	<0.01	<0.01	0.03	<0.01
1.88	0.02	0.53	0.24	0.15	0.04	0.08	0.02	<0.01
2.96	<0.01	0.23	0.04	0.06	0.07	0.1	0.03	<0.01
0.3	<0.01	0.63	0.09	0.18	0.06	0.01	0.02	<0.01
0.03	<0.01	0.01	0.17	0.16	<0.01	0.02	0.08	<0.01
3.31	0.01	0.56	0.22	0.18	0.01	0.09	1.09	<0.01
1.23	0.03	0.57	0.14	0.15	0.05	0.05	0.04	<0.01
0.34	<0.01	0.23	0.03	0.09	0.01	0.18	0.81	0.08
0.72	<0.01	0.16	0.03	0.05	<0.01	0.02	0.02	0.01
0.22	<0.01	0.09	0.04	0.05	<0.01	0.01	0.09	<0.01
1.06	<0.01	1.07	0.11	0.34	0.27	0.01	0.02	<0.01
3.24	<0.01	0.34	0.05	0.04	0.1	0.25	0.03	<0.01
0.06	<0.01	0.01	0.01	0.01	<0.01	<0.01	0.02	5.17
0.35	0.01	1.59	0.22	0.69	0.1	0.04	0.02	<0.01
1.27	<0.01	0.08	0.02	0.05	0.03	0.03	0.04	0.01
0.02	0.01	0.88	0.07	0.27	0.3	<0.01	0.02	<0.01
1.14	0.01	0.6	0.14	0.14	0.13	0.05	0.04	<0.01
1.58	0.01	0.68	0.14	0.24	0.06	0.05	0.02	<0.01
5.23	<0.01	0.02	0.01	0.01	0.02	0.04	0.02	<0.01
0.97	<0.01	0.01	0.01	0.02	0.01	0.01	0.04	<0.01
2.7	<0.01	0.01	0.21	0.01	0.01	0.01	0.03	<0.01
0.01	<0.01	0.02	0.01	0.02	<0.01	<0.01	0.02	<0.01
0.26	<0.01	0.01	0.16	0.01	<0.01	<0.01	0.05	<0.01
2.2	<0.01	0.03	0.44	<0.01	0.01	<0.01	0.04	<0.01
2.5	0.01	0.62	0.1	0.17	0.02	0.04	0.09	<0.01
5.29	<0.01	0.01	0.64	0.02	0.01	0.02	0.02	<0.01
0.28	<0.01	0.13	0.09	0.01	0.02	0.01	0.2	<0.01
5.53	<0.01	0.14	0.02	0.02	0.03	0.19	0.03	<0.01
3.38	<0.01	0.03	0.97	0.01	0.01	0.02	0.02	<0.01
5.93	<0.01	0.1	0.03	0.02	0.02	0.09	0.11	<0.01

0.01	<0.01	0.01	0.01	<0.01	<0.01	<0.01	0.11	<0.01
0.02	<0.01	<0.01	0.1	0.01	<0.01	<0.01	0.07	<0.01
1.43	<0.01	<0.01	0.01	0.01	0.01	0.01	0.02	<0.01
2.89	<0.01	0.04	0.06	<0.01	<0.01	<0.01	0.02	<0.01
0.27	<0.01	<0.01	0.12	0.01	0.02	<0.01	0.07	<0.01
0.19	0.1	0.29	0.16	0.02	0.03	0.01	0.18	<0.01
0.17	0.01	0.58	0.14	0.4	0.07	0.01	0.02	<0.01
0.16	0.15	0.39	0.16	0.06	0.01	0.01	0.02	3.87
0.01	0.05	1.45	0.02	0.08	<0.01	<0.01	0.16	0.01
0.32	<0.01	0.44	0.07	0.13	0.16	0.01	0.02	<0.01
7.03	<0.01	0.02	0.01	0.01	0.06	0.45	0.05	<0.01
3.3	0.04	0.61	0.17	0.19	0.06	0.11	0.14	<0.01
0.07	0.02	0.69	0.26	0.3	0.12	<0.01	0.03	0.03
2.46	0.03	0.8	0.21	0.28	0.08	0.05	0.04	<0.01
1.91	<0.01	1.88	0.25	0.7	0.05	0.28	0.05	<0.01
5.84	<0.01	0.36	0.03	0.03	0.05	0.37	0.12	<0.01
0.88	<0.01	0.22	0.02	0.02	0.06	0.07	0.03	<0.01
5.66	<0.01	0.03	<0.01	0.02	0.06	0.44	0.15	<0.01
0.1	<0.01	0.05	0.02	0.01	<0.01	<0.01	0.03	<0.01
0.92	<0.01	0.23	0.48	0.05	<0.01	0.04	1.98	<0.01
0.02	<0.01	0.08	0.01	0.02	<0.01	0.08	0.29	0.02
0.14	<0.01	0.03	0.02	0.27	0.01	0.02	0.11	0.09
1.15	0.03	0.28	0.05	15.95	0.07	0.02	1.58	0.35
3.55	<0.01	0.2	0.01	0.11	0.01	0.05	0.1	<0.01

ME-XRF26	ME-XRF26	ME-XRF26	ME-XRF26	ME-XRF26	ME-XRF26	ME-XRF26	S-IR08	C-IR07
K2O	Cr2O3	TiO2	MnO	P2O5	SrO	BaO	S	C
%	%	%	%	%	%	%	%	%
1.4	0.05	0.18	0.05	21.6	0.1	0.04	0.87	2.83
0.58	0.16	0.16	0.03	30.7	0.11	0.06	1.03	0.7
0.49	0.16	0.17	0.01	30.8	0.07	0.03	1.42	1.75
0.16	0.07	0.05	0.01	34.5	0.1	0.02	1.03	1.3
3.13	0.07	0.73	0.01	0.92	0.05	0.04	0.65	4.43

ME-ICP06	ME-ICP06	ME-ICP06	ME-ICP06	ME-ICP06	ME-ICP06	ME-ICP06	C-IR07	S-IR08
K2O	Cr2O3	TiO2	MnO	P2O5	SrO	BaO	C	S
%	%	%	%	%	%	%	%	%
0.05	0.01	0.05	0.01	0.03	0.02	0.04	0.1	0.01
0.04	<0.01	0.06	0.03	0.04	0.01	0.02	0.07	<0.01

0.03	<0.01	<0.01	0.01	<0.01	<0.01	<0.01	0.05	<0.01
0.23	0.01	0.04	0.2	0.13	0.02	0.04	0.77	0.48
0.1	<0.01	0.01	0.58	0.03	<0.01	0.05	0.27	<0.01
1.33	0.01	0.49	0.04	0.1	0.01	0.02	0.02	<0.01
0.04	<0.01	0.01	0.07	0.03	<0.01	<0.01	0.03	<0.01
0.01	<0.01	<0.01	0.01	<0.01	<0.01	<0.01	0.01	<0.01
2.81	0.02	0.08	0.05	0.01	<0.01	0.05	0.86	<0.01
0.04	<0.01	<0.01	0.01	0.03	<0.01	0.02	0.01	0.95
0.09	0.36	0.49	0.21	0.03	0.01	<0.01	0.06	0.01
0.06	0.35	0.21	0.18	<0.01	0.01	<0.01	0.02	<0.01
0.5	0.03	0.68	0.07	0.34	0.02	0.02	1.11	<0.01
0.06	<0.01	0.02	0.02	<0.01	<0.01	<0.01	0.03	<0.01
3.2	<0.01	0.1	0.04	<0.01	0.01	0.02	0.01	<0.01
2.4	<0.01	0.7	0.13	0.17	0.11	0.06	0.02	<0.01
1.43	<0.01	3.45	0.47	1.1	0.01	0.05	0.04	<0.01
0.02	<0.01	0.01	0.01	<0.01	<0.01	0.04	0.03	0.02
9.09	<0.01	0.49	0.04	0.05	<0.01	0.13	0.09	<0.01
0.26	<0.01	1.11	0.09	0.43	<0.01	0.02	0.05	<0.01
0.01	<0.01	0.34	0.2	0.06	0.24	<0.01	0.79	<0.01
0.1	<0.01	1.49	0.06	0.4	0.01	<0.01	0.13	<0.01
2.33	<0.01	1.49	0.12	0.68	0.04	0.09	0.04	<0.01
0.71	<0.01	0.14	0.1	0.04	0.06	0.02	0.02	<0.01
8.45	<0.01	0.02	0.01	<0.01	<0.01	0.03	0.02	<0.01
6.89	<0.01	0.39	0.06	0.03	0.01	0.13	0.01	<0.01
0.73	0.01	0.3	0.01	0.25	0.01	0.03	0.24	0.89
0.18	<0.01	0.25	0.02	0.05	<0.01	0.01	3.99	0.11
7.09	0.01	0.3	0.02	0.07	0.02	0.1	4.44	0.25
0.7	<0.01	0.24	0.01	0.08	<0.01	<0.01	0.39	2.51
0.66	0.01	0.4	0.18	0.1	<0.01	<0.01	1.68	24.1
2.4	0.01	0.27	0.07	0.58	0.11	0.04	4.95	0.22
3.62	0.02	0.87	0.1	0.24	0.09	0.12	0.88	0.67
4.34	0.03	0.56	0.02	0.06	0.05	0.08	0.09	3.18
5	0.01	0.68	0.03	0.07	0.03	0.07	0.53	0.02
1.27	<0.01	0.26	0.04	0.1	0.01	0.03	0.6	4.97
0.03	0.04	33.9	0.69	0.17	0.02	0.07	0.57	0.04
1.88	0.01	0.57	0.06	0.14	0.02	0.04	1.19	<0.01
4.45	0.01	0.65	0.03	0.97	0.02	0.06	0.22	0.2
2.97	<0.01	0.45	0.06	0.06	0.05	0.06	2.42	0.06
2.99	<0.01	0.33	0.07	0.09	0.11	0.2	6.43	0.08
3	0.01	0.53	0.06	0.17	0.06	0.07	0.09	0.17
4.15	0.01	0.55	0.06	0.1	0.06	0.07	0.09	0.15
4.46	0.01	0.59	0.08	0.18	0.09	0.08	0.46	0.19
1.92	0.01	0.26	0.05	0.06	0.01	0.05	0.13	<0.01
1.78	<0.01	0.29	0.04	0.07	0.09	0.04	5.71	0.01
0.02	<0.01	0.02	<0.01	0.01	<0.01	<0.01	>50	0.62
0.03	0.01	0.26	0.01	0.09	<0.01	0.08	0.16	0.02
0.31	<0.01	0.39	<0.01	0.02	0.03	0.03	1.54	0.02
0.03	<0.01	0.76	<0.01	0.01	0.01	0.06	0.13	0.01
0.02	<0.01	0.01	0.02	0.02	0.59	<0.01	12	0.02
2	<0.01	0.29	0.02	0.01	0.02	0.09	0.16	0.05
1.88	<0.01	0.48	0.02	0.03	0.01	0.04	0.23	0.04
1.79	0.01	0.55	0.08	0.28	0.09	0.09	0.23	<0.01
7.09	<0.01	0.08	0.05	<0.01	0.04	0.07	0.05	<0.01
3.79	<0.01	0.21	0.03	<0.01	0.07	0.05	0.03	<0.01
0.04	<0.01	0.01	0.01	0.15	0.01	<0.01	12.7	<0.01
0.44	0.06	0.08	<0.01	30.9	0.13	0.03	1.54	1.4

1.24	0.04	0.29	0.04	19.05	0.09	0.03	0.58	0.42
1.09	0.03	0.13	0.06	2.66	0.02	0.01	9.11	0.11
2.57	<0.01	0.36	0.08	0.2	0.13	0.1	0.04	<0.01
2.3	<0.01	0.5	0.12	0.38	0.18	0.08	0.07	0.01
2.98	<0.01	0.41	0.1	0.27	0.17	0.09	0.05	<0.01

ME-ICP06 K2O %	ME-ICP06 Cr2O3 %	ME-ICP06 TiO2 %	ME-ICP06 MnO %	ME-ICP06 P2O5 %	ME-ICP06 SrO %	ME-ICP06 BaO %	C-IR07 C %	S-IR08 S %
5.81	<0.01	0.28	0.03	0.03	0.01	0.07	0.25	0.01
4	<0.01	0.32	0.03	0.03	0.05	0.29	0.38	0.37
2.28	<0.01	0.36	0.03	0.05	0.04	0.02	0.38	0.02
3.72	<0.01	0.33	0.03	0.07	0.05	0.07	0.19	0.02
2.66	<0.01	0.3	0.04	0.04	0.05	0.07	1.4	0.01
3.4	<0.01	0.31	0.04	0.04	0.05	0.07	0.91	0.02
2.98	<0.01	0.28	0.01	0.06	0.13	0.1	0.67	0.01
3	<0.01	0.32	0.02	0.07	0.07	0.07	0.33	0.03
3.87	<0.01	0.26	0.01	0.02	0.12	0.09	0.38	0.01
3.34	<0.01	0.32	0.03	0.07	0.06	0.06	0.41	0.01
1.89	<0.01	0.2	0.05	0.03	0.08	0.06	3.85	0.01
3.89	<0.01	0.14	0.07	0.03	0.02	0.06	2.5	0.01
2.77	0.01	0.29	0.08	0.22	0.22	0.19	1.87	0.01
7.69	<0.01	0.19	0.02	0.11	0.09	0.18	0.05	0.06
1.72	<0.01	0.2	0.01	0.02	0.2	0.36	0.05	<0.01
2.72	<0.01	0.1	<0.01	0.02	0.32	0.64	0.08	0.1
3.74	<0.01	0.22	0.01	0.02	0.25	0.42	0.15	0.02
2.6	0.01	0.31	0.01	0.03	0.1	0.17	0.04	<0.01
2.97	<0.01	0.21	0.17	0.15	0.01	0.1	0.19	0.01
4.78	<0.01	0.74	0.06	0.31	0.1	0.25	0.05	0.03
11.2	<0.01	1.78	0.09	0.8	0.13	0.09	0.26	0.01
12.4	<0.01	1.43	0.02	0.31	0.22	0.12	0.06	0.4

origins

1700	300	700	9.5	31	15	9	95	26
ME-MS81	ME-MS81	ME-MS81	ME-MS81	ME-MS81	ME-MS81	ME-MS81	ME-MS81	ME-MS81
Ba	Ce	Cr	Cs	Dy	Er	Eu	Ga	Gd
ppm	ppm	ppm	ppm	ppm	ppm	ppm	ppm	ppm
840	71.3	10	2.64	4.06	2.11	1.8	21.5	5.09
418	36.1	80	3.44	2.51	1.35	0.91	11.2	2.87
220	33.2	20	0.37	1.31	0.8	0.34	2.2	1.73
45.7	1860	10	0.08	49.8	21.4	10	30	71.4
77	3.3	40	0.22	0.65	0.32	0.31	13.2	0.49
78.3	110.5	1180	0.28	7.83	4.79	1.48	18	8.76
512	11.8	20	0.68	0.34	0.16	0.06	10.4	0.55
39.1	2.7	10	0.2	0.43	0.36	0.11	0.8	0.41
135	3	60	0.25	0.39	0.62	0.07	9.2	0.24
547	575	1070	0.15	17.5	10.9	2.46	67.7	27.6
76.9	3.3	180	0.12	2.07	1.48	0.26	3.6	0.97
564	27.7	40	0.66	1.69	0.88	0.55	8.1	1.84
464	13.8	20	1.39	1.14	0.74	0.28	3.7	1.26
281	17.1	20	1.78	1.13	0.9	0.21	5.8	1
606	134	70	5.66	3.34	2.34	0.81	20.2	3.02
267	17.3	20	1.36	1.43	1.12	0.24	5.5	1.28
348	14.1	30	0.92	1.65	1.36	0.18	3.9	1.28
528	12.7	20	0.97	0.96	0.93	0.18	4.4	0.75
1105	85.6	30	4.61	4.13	2.55	0.76	9.6	4.54
171	2.2	10	0.12	0.09	0.14	0.04	1	0.18
748	96.7	10	4.52	4.69	2.56	2.09	21.7	5.85
780	71.2	10	2.03	4.11	2.16	1.68	18	5.04
696	53.2	20	1.34	1.67	0.75	0.46	8.1	2.64
89.8	22.2	10	0.41	0.95	0.62	0.21	4.8	1.07
764	40.5	10	1.13	1.99	1.19	0.39	15.2	2.24
218	30.3	10	0.35	4.65	3.15	0.76	4.5	4.01
67.5	24.3	60	0.47	1.06	0.61	0.35	3.3	1.29
130.5	31.7	20	0.1	0.62	0.33	0.34	2.1	0.96
78.7	14.2	<10	0.18	1.28	0.72	0.17	0.9	1.48
25.6	12.7	30	0.91	1.24	0.69	0.31	2	1.06

ME-MS81 Ba ppm	ME-MS81 Ce ppm	ME-MS81 Cr ppm	ME-MS81 Cs ppm	ME-MS81 Dy ppm	ME-MS81 Er ppm	ME-MS81 Eu ppm	ME-MS81 Ga ppm	ME-MS81 Gd ppm
232	19.9	580	0.37	2.95	1.8	0.85	15	2.92
25.3	59.9	30	0.03	2.12	1.07	0.73	17.2	2.71
176.5	27	2860	0.21	2.27	1.21	1.09	32.4	2.76
350	1.4	20	0.35	0.46	0.31	0.04	17.2	0.36
4.5	<0.5	70	0.05	0.11	0.09	<0.03	3	0.08
82	62.6	6210	0.19	11.6	5.08	1.35	18.6	11.85
4.3	5.4	1870	0.06	1.74	0.96	0.22	7.2	1.71
30.9	410	40	0.04	16.2	8.55	3.21	55.1	20
67.9	298	780	0.11	22.4	12.95	3.22	53.7	20
3.7	18.4	3070	0.02	2.31	1.15	0.35	16.8	2.59
106.5	215	7930	0.13	38	23	6.84	53.7	28.8
11.1	157	50	0.03	7.88	4.07	2.61	53.6	10.65
315	0.8	10	1.21	0.74	0.8	<0.03	19.8	0.29
9.4	2.1	60	0.14	0.24	0.18	0.04	4	0.21
24.6	2.1	20	0.1	0.12	0.05	0.04	1.5	0.1
408	2	20	31.9	0.24	0.08	0.12	30	0.2
157	6.4	10	4.44	2.68	0.89	0.1	22.4	1.82
30.7	2.3	10	0.09	0.2	0.11	0.04	1.4	0.18
1135	3.5	10	0.42	1.19	0.86	0.14	12.2	0.88
31.6	19.7	20	0.11	1.04	0.59	0.22	4.5	1.17
83.8	9.7	210	0.38	3.27	2.01	0.94	21.8	3.22
26.9	1.4	10	0.13	0.34	0.2	0.05	6.4	0.34
20	0.7	20	0.1	0.2	0.12	<0.03	2	0.15
2.2	0.6	20	0.04	0.13	0.08	<0.03	1	0.17
261	156.5	20	7.34	5.84	3.07	0.89	20.2	6.35
4.8	7.3	30	0.16	0.4	0.23	0.5	14.1	0.53
96.5	31.3	280	98.3	4.7	2.9	0.92	23.1	3.9
13.1	1.7	20	0.14	0.36	0.29	0.03	1.4	0.4
83.5	61.3	20	0.09	4.01	2.48	1.05	19.1	4.15
130	16.7	120	0.2	0.59	0.34	0.25	11.3	0.63
96.9	86.9	60	1.08	6.78	3.85	2.1	9.3	5.79
7.6	21.7	160	0.1	4.72	2.93	0.9	5.2	5.06
1045	41.5	20	1.12	8.71	5.33	1.7	15.6	8.51
18.1	33.1	1540	0.27	2.67	1.82	0.81	14.5	2.56
292	4.1	20	0.23	0.19	0.16	0.05	16	0.21
49.4	35.6	270	0.12	2.72	1.61	1.16	31.5	2.84
7.9	0.6	2140	0.07	0.2	0.14	<0.03	4.9	0.15
23.2	184	50	0.09	9.28	4.46	3.42	53.8	12.5
5.5	1.6	4770	0.24	0.93	0.66	<0.03	6.8	0.64
28.4	11.2	20	2.67	14.05	6.25	0.08	39.1	6.51
67.8	5.5	20	1.27	1.5	0.52	0.09	25.1	1.23
60.8	43.3	20	9.29	1.6	0.8	0.31	2.8	2.03
2600	63.4	10	2.22	2.21	1.44	1.05	15.8	2.88
49.3	3.8	20	3.16	1.34	1.01	0.26	0.6	1.23
336	18.3	10	2.34	0.83	0.56	0.47	5.1	1.08
155.5	1.7	10	209	0.08	0.04	0.03	72.8	0.15
122.5	6.1	90	2.97	0.15	0.1	0.07	10.1	0.23
69.5	1.2	10	210	<0.05	0.03	0.23	53.8	0.07

23.8	<0.5	10	16.4	<0.05	0.03	<0.03	46.1	<0.05
23.5	3.6	20	12.9	0.7	0.27	0.07	55.3	0.58
422	26.9	20	1.04	2.49	1.8	0.55	8.7	2.41
304	13.5	10	0.84	1.38	0.82	0.3	2.5	1.46
467	46.4	70	7.41	2.59	1.82	0.64	16.4	2.77
255	45.2	50	1.79	4.03	2.44	1.03	5.8	4.78
352	91	10	2.46	8.47	4.95	2.21	22.4	11.05
393	55.9	30	3.23	6.45	4.28	1.32	10.8	6.47
514	67.7	20	1.9	4.45	2.85	1.14	7.8	5.47
477	130.5	40	2.32	4.29	1.97	1.19	19.7	5.89
356	61.7	30	0.17	0.96	0.44	0.42	22.8	1.65
111	8.6	1240	0.28	2.29	1.32	0.64	12.9	2.36
974	5.8	10	0.3	0.12	0.05	0.24	12.3	0.21
1445	45.9	10	0.48	1.17	0.49	0.8	11.8	2.03
207	81.3	270	0.76	7.38	4.54	2.02	20.6	8.25
751	42.5	150	1.07	1.13	0.68	0.36	11.7	1.66
308	77.7	10	0.61	12.9	7.46	0.59	30.8	10.35
92.9	10.5	40	2.92	0.8	0.51	0.18	10	0.98
1830	121.5	10	0.79	7.25	4.05	3.41	29	8.95
269	5.9	10	0.09	0.19	0.09	0.76	17.6	0.33
761	120.5	10	0.32	6.52	2.84	2.97	25.9	10.05
422	44.1	50	0.05	4.07	2.21	2.15	27.8	5.72
18.3	2.1	260	0.01	0.23	0.12	0.07	54.3	0.28
617	6.4	10	0.01	0.11	0.06	1.7	23.4	0.28
337	0.9	30	0.09	<0.05	0.03	0.04	0.7	0.13
1220	22.3	30	0.51	3.78	2.23	1.53	2.9	6.3
298	5	10	0.28	0.52	0.28	0.36	1.3	1.42
887	141.5	10	0.96	4.55	2.14	2.86	24.4	7.81
612	148	60	0.74	5.66	2.85	3.41	23.7	8.98
420	164.5	10	6.36	4.03	2.9	1.7	30.7	5.4
51	156	<10	11.95	0.33	0.18	0.39	41	0.87
1105	182.5	20	3.31	5.67	2.61	3.51	24.1	9.07

ME-MS81 Ba ppm	ME-MS81 Ce ppm	ME-MS81 Cr ppm	ME-MS81 Cs ppm	ME-MS81 Dy ppm	ME-MS81 Er ppm	ME-MS81 Eu ppm	ME-MS81 Ga ppm	ME-MS81 Gd ppm
440	52.6	40	4.55	3.53	2.29	0.92	12.9	4.09
338	30.5	20	1.22	1.8	1.09	0.47	8.9	2.1
221	41.5	50	7.41	3.88	3.01	0.64	15.7	3.62
61.7	10.7	30	2.82	1.66	0.98	0.38	4.5	1.47
36.9	60.7	100	0.85	9.63	4.49	2.76	11.2	15.5
163.5	88.7	20	3.24	5.61	3.59	1.34	8.4	7.09
459	111.5	30	5.4	5.89	3.42	1.17	10.3	6.61
644	47.4	20	2.38	1.71	1.25	0.34	11.1	2.28
121.5	3.1	20	0.43	0.3	0.15	0.05	0.8	0.41
317	35	<10	3.4	5.74	3.97	0.42	15.9	3.96
78.1	3.1	10	7.61	21	9.61	0.04	25.5	4.59
53.6	41.8	90	0.18	1.77	0.85	0.8	22.2	2.69

53.3	3.6	<10	0.51	1.66	0.65	0.34	29.9	1.46
46.4	3.1	<10	0.67	1.43	0.4	0.12	46.4	1.21
50.9	4.4	10	1.9	4.76	4.49	0.06	23.1	0.92
36.9	3.1	<10	88.4	1.03	0.27	<0.03	64.1	1.46
164.5	10.8	30	22.1	3.45	0.89	0.15	24.2	5.2
613	96	70	8.01	4.49	2.61	1.36	22.9	5.8
18.5	8	2870	0.28	2.51	1.38	0.26	7.8	2.38
172.5	27	10	0.51	0.69	0.28	1.04	21.1	1.07
164.5	2	10	0.21	0.12	0.05	<0.03	0.4	0.19
71.8	6	10	0.57	0.9	0.29	0.69	24.3	1.14
62	1.2	<10	5.18	0.55	0.22	0.05	35.3	0.41
21	0.9	10	8.51	0.13	0.03	<0.03	37.2	0.18
53	0.5	<10	12.55	<0.05	<0.03	<0.03	9.2	0.07
12	19.4	10	0.31	4.13	2.2	0.08	26.7	3.15
34.6	3.1	40	0.34	1.08	0.71	0.26	0.7	1.32
208	72.5	20	0.33	4.37	2.63	0.69	2.1	4.75
18.9	15.6	10	0.09	2.17	1.19	0.9	34.5	1.96
979	46.4	<10	0.95	1.04	0.5	0.6	17.1	1.89
352	22.2	170	0.7	4.68	2.72	1.18	19.2	4.45
474	10.2	10	0.21	0.45	0.33	0.13	1.6	0.51
380	37.7	60	8.09	2.16	1.45	0.47	18.9	2.1
1380	99.9	30	1.85	8.54	4.71	2.06	17.5	9.22
251	23.5	10	0.29	1.82	1	0.25	13.8	1.51
630	31.1	<10	0.9	3.01	1.71	0.35	17.1	2.62
163.5	17.2	190	1.01	4.2	2.43	1.02	17.8	3.99
288	12.1	20	0.33	3.03	2.07	0.49	16.5	2.27
102	116.5	20	0.35	4.39	2.29	0.44	1.8	5.78
59	19.7	100	1.85	1.85	1.41	0.33	8.1	1.6
734	82.5	10	2.15	4.9	2.25	0.44	17.1	5.62
33.1	36.9	10	0.11	1.25	0.93	0.51	32.1	1.88
304	80.3	10	0.7	1.79	0.7	0.59	16.3	3.03
97.1	400	20	0.09	9.09	3.85	4.72	55.5	15.45
36.8	24.6	10	0.44	0.79	0.42	0.21	1.6	0.96
897	28.7	70	1.74	4.04	2.06	1.02	10.3	4.12
404	33.3	10	0.81	0.88	0.55	0.2	8.8	0.93
429	27.5	30	1.37	2.15	1.42	0.43	12	2.06
19.8	1.4	10	7.47	0.06	0.03	<0.03	26.8	0.11
9.8	10	10	5.28	4.6	1.56	<0.03	37.8	3.58
43.4	2	10	108.5	0.21	0.04	<0.03	31.8	0.41
92.7	7.1	<10	76.2	0.56	0.26	0.16	96.8	0.68
9.1	3.8	<10	6.38	1.29	0.16	0.17	48.5	1.32
39.7	1.1	10	92.8	0.26	0.11	0.12	48.9	0.31
177	<0.5	10	128	0.05	<0.03	<0.03	27.7	<0.05
942	292	100	1.47	8.54	4.49	1.35	16.1	12.9
405	25.6	70	6.37	2.2	1.18	0.52	11.3	2.41
424	69	180	28.7	5.24	2.8	1.42	22.9	5.88
161	42	20	2.45	7.05	4.56	1.41	3.3	6.83
1050	68.1	50	2.21	1.37	0.74	0.73	14.2	2.14
1265	47.5	20	5.2	1.38	0.7	0.53	11.6	1.89
2170	61.7	40	1.92	2.01	1.06	0.97	15.7	3.21
2870	370	200	0.37	4.35	1.67	4.36	21.3	9.32
1475	113.5	210	0.49	4.43	2.49	1.79	18.5	5.52
42.4	57.2	10	0.31	2.67	0.97	0.94	1.7	3.71
113.5	82.2	20	1.59	6.37	4.33	1.24	13.5	7.2
186.5	9.2	10	1.48	3.42	2.69	0.2	21.1	2.45
124.5	25.2	10	0.45	4.28	2.78	0.37	11.4	3.93

261	65.9	20	5.53	23.9	16.05	1.14	42.5	17.3
161.5	211	40	1.52	72.9	47.8	4.82	41.3	53.8
152.5	7.2	10	1.1	9.2	5.63	0.26	24.5	5.9
430	3.4	10	1.7	0.65	0.39	0.32	17.4	0.86
144	59.1	10	0.31	19	7.73	14.2	40.5	39.4
225	436	<10	0.4	7.33	2.27	7.33	14.6	20.3
791	629	20	1.53	10.1	3.18	9.63	5.9	26.1
318	32	20	1.13	1.44	0.79	0.45	3.7	1.83
213	14.3	140	0.51	2.45	1.61	0.82	17.4	2.33
1470	54.2	10	3	1.97	0.94	0.48	40.1	2.36
54.6	8.2	10	0.09	0.65	0.5	0.13	18.9	0.65
130.5	9.4	10	0.33	0.6	0.54	0.13	1.9	0.65
4340	9.3	10	0.06	2.49	1.84	0.38	0.4	2.61
1165	70.8	20	3.24	6.3	4.55	1.28	17.8	7.62
4120	5.3	20	0.13	0.49	0.26	0.16	1	0.94
590	23	20	0.66	1.41	1.12	0.26	4	1.43
326	498	20	0.55	89	39.7	23	9.4	129.5
5870	34.6	20	1.38	7.93	5.28	1.34	17.4	8.48
800	21.2	20	0.46	1.87	1.34	0.49	2.4	2.34
70.7	6	40	0.11	1.06	1.11	0.14	0.7	0.84
193	16.5	20	0.27	3.19	2.79	0.56	1.6	3.57
47	5.2	10	0.17	0.33	0.25	0.08	2.1	0.41
1705	584	10	3.51	5.72	3.05	3.8	14.2	11.2
526	245	10	1.22	3.4	2.13	1.24	14.3	5.25
1155	145.5	10	4.46	9.68	6.22	1.5	22.2	10.85
706	116	10	1.04	6.8	4.82	0.98	45.3	6.94
14.2	7.7	10	0.58	1.13	0.74	0.12	5.3	0.94
713	16.6	150	0.7	1.98	1.19	0.74	15.2	2.4
973	46.5	10	0.27	2.9	1.74	1.15	21.4	3.39
109.5	62.1	10	0.18	3.24	2.01	1.86	19.3	4.74
170	4.5	30	0.18	2.07	1.52	0.62	1	2.68
878	24.1	70	0.79	2.46	1.71	0.73	12.6	2.71
447	26.6	240	0.59	2.46	1.54	0.73	14.1	2.53
1780	9.8	20	1.57	3.27	2.48	0.54	5.7	2.74
151	57.1	20	1.46	2.58	1.51	0.68	5.9	2.6
61	15.3	30	1.03	2.33	1.13	0.73	3.4	2.85
105.5	61.5	20	0.5	7.52	4.87	1.54	23.2	8.28
2560	43.5	10	0.24	4.99	3.78	2.63	24.3	6.17
25	0.8	20	0.21	0.05	0.08	0.03	0.5	0.07
347	46.5	40	0.3	4.1	2.35	1.8	20.2	6.05
251	63.5	10	1.15	7.93	5.06	0.66	8.8	7.41
11.2	42.6	60	0.06	4.04	2.53	1.63	24.3	5.12
467	27	50	2.15	2.17	1.38	1.08	19	2.88
475	32.3	40	0.67	4	2.69	0.96	18.5	4.56
369	2.9	10	0.36	2.68	2.31	0.36	16.7	1.98
65.5	8.9	10	1.12	3.77	2.27	0.36	7.2	2.83
93.6	3.4	10	1.71	7.22	14.05	0.28	11.4	1.89
15.2	4.2	10	0.04	0.3	0.19	0.13	0.4	0.39
20.1	4	10	0.38	13.15	8.84	0.11	16.7	7.22
31.9	0.9	10	2.25	14.45	22.8	0.2	16.9	2.21
359	44.9	70	0.37	3.48	2.25	0.94	22.9	3.74
138	6.7	10	2.05	15.5	12.45	0.31	20.4	6.15
56.8	6.8	10	0.59	6.41	4.63	0.62	26.3	3.9
1655	1.2	10	1.65	0.28	0.22	0.18	8.5	0.3
201	11.8	10	0.55	32.1	63.9	0.37	12.4	4.8
721	110.5	10	0.87	3.52	1.96	1	19	4.69

13.6	1.3	10	0.07	0.88	0.68	0.09	0.3	0.55
25.9	4.7	10	0.07	1.79	1.18	0.24	0.3	1.54
57.2	1.2	10	0.75	0.38	0.16	0.3	43.5	0.41
37.7	4.3	10	1.76	15.65	6.08	0.42	33.9	9.46
11	0.7	10	0.24	3.22	3.92	0.36	27.1	0.99
67	7.5	750	0.21	1.41	0.83	0.45	8.3	1.48
83.9	16.3	70	0.22	1.53	0.86	0.59	14.1	1.68
115.5	6.8	1150	0.13	1.35	0.77	0.5	9	1.4
16.2	5.8	340	0.03	1.33	0.71	0.28	23.9	1.01
66.6	57.8	20	0.03	5.85	3.88	1.88	28.2	5.64
4440	1.4	50	0.48	0.12	0.09	0.56	11	0.08
987	24.4	330	0.29	6.98	5.15	1.48	18.6	5.46
25.9	43.4	170	0.05	3.68	2.35	1.49	36.4	4.01
447	33.5	210	0.68	4.1	2.43	2.15	36.8	4.48
2750	107.5	20	0.2	12.1	7.09	4.05	23.8	14.45
3630	31.9	10	0.16	0.31	0.16	1.15	21.8	0.61
676	873	10	0.1	2	0.47	2.25	20.4	7.68
4210	14.1	10	0.08	0.11	0.03	1.14	13.2	0.21
34.9	3.9	30	0.05	0.63	0.32	0.19	2.2	0.56
399	16.2	30	0.32	4.35	2.77	1.14	4.9	3.83
747	4.8	10	<0.01	0.41	0.28	0.07	4.7	0.42
184	10.7	30	0.69	3.62	2.13	0.81	8.4	4.22
225	116.5	230	1.41	18.3	10.65	6.11	5.4	22.8
429	53.2	20	0.67	2.75	1.82	0.74	5.4	3.19

ME-MS81	ME-MS81	ME-MS81	ME-MS81	ME-MS81	ME-MS81	ME-MS81	ME-MS81	ME-MS81
Ba	Ce	Cr	Cs	Dy	Er	Eu	Ga	Gd
ppm	ppm	ppm	ppm	ppm	ppm	ppm	ppm	ppm
211	59.6	350	1.83	7.96	5.41	1.68	4.7	8.92
406	88.4	1130	3.42	28.8	22.8	5.06	3.8	30.7
111.5	53.8	1120	1.3	14.7	12.3	2.49	3.9	15.5
50.8	88.5	450	0.26	50.3	35.8	11.4	3.6	61.4
334	50.8	440	5.49	3.84	2.47	0.85	9.4	4.26

ME-MS81	ME-MS81	ME-MS81	ME-MS81	ME-MS81	ME-MS81	ME-MS81	ME-MS81	ME-MS81
Ba	Ce	Cr	Cs	Dy	Er	Eu	Ga	Gd
ppm	ppm	ppm	ppm	ppm	ppm	ppm	ppm	ppm
316	33	70	0.06	1.19	0.51	0.62	1.3	2.25
184.5	27.7	30	0.17	1.18	0.75	0.4	1.3	1.46

11.1	3.4	20	0.06	0.54	0.36	0.2	0.6	0.66
299	8.8	80	0.03	1.18	0.54	0.5	5.3	1.76
431	8.4	20	0.08	7.1	5.08	1	1.5	5.57
185	22.7	100	0.65	1.76	1.36	0.53	15.9	1.82
46.8	11.2	20	0.29	0.91	0.47	0.07	1	0.5
6.2	0.8	10	0.05	0.09	<0.03	<0.03	0.5	0.1
459	3.9	100	0.48	0.59	0.36	0.14	3.5	0.58
172	0.8	20	0.11	0.09	0.03	<0.03	0.4	0.07
23.5	5.6	2570	0.07	1.65	1.02	0.4	7.3	1.49
25.8	1.8	2550	0.15	0.76	0.46	0.21	6.9	0.8
139	16.6	230	0.33	1.48	0.84	0.46	20.3	2.04
36.9	0.9	20	0.11	0.32	0.22	0.08	1.8	0.38
199	21.3	20	2.32	1.68	1.13	0.54	25.6	1.57
529	99.9	10	0.19	6.24	3.62	2.56	33.7	7.49
429	504	10	0.72	45.5	24.8	1.85	24.2	52.7
363	1.7	10	0.06	0.56	0.35	<0.03	0.9	0.43
1155	182.5	10	6.39	11.35	7.31	1.71	28.8	9.74
169	69.8	10	0.97	7.52	4.52	1.35	13.8	6.37
12.1	84.7	10	0.07	5.61	3.01	4.9	47.7	6.26
36.2	127	10	0.07	11.65	6.78	2.91	19.2	13.35
807	238	30	0.22	11.3	6	3.08	24.3	14.7
154	38.1	10	0.2	5.02	3.59	0.38	35.9	4.3
271	3	10	0.92	0.44	0.34	0.08	18.4	0.28
1135	149	10	0.53	10.7	6.01	2.23	26.1	11.6
235	10.4	50	0.83	0.52	0.26	0.14	14.5	0.42
59.1	7.7	30	0.26	0.95	0.75	0.12	2.7	0.69
882	68.9	50	3.38	3.32	2.22	1.04	16.3	3.41
19.5	15.3	20	0.97	1.11	0.64	0.2	2.8	1.07
17.7	17.7	90	2.3	1.75	0.98	0.37	8.2	1.81
344	34.8	40	4.06	2.3	1.96	0.46	9.7	2.1
1055	74.6	160	3.51	3.71	1.84	1.48	17.8	4.84
654	10.8	50	5.51	0.52	0.39	0.16	16.8	0.53
586	58.6	70	7.72	1.81	0.94	0.64	21.9	2.51
265	30.8	20	1.44	1.87	1.13	0.43	4.6	2.08
628	927	250	0.1	30.4	23.3	5.79	15.1	38.2
383	49.5	40	1.21	3.18	2.05	0.65	7.6	3.13
546	99.9	70	10.9	7.32	4.14	1.8	20.9	8.25
519	78.2	40	2.87	2.66	1.62	0.82	13.7	3.28
1750	126.5	40	1.51	7.41	3.91	1.95	11.4	9.06
580	100.5	80	4.97	4.23	2.11	1.26	21.8	5.51
646	67.5	80	7.88	3.02	1.62	0.85	21.4	3.72
725	86.6	70	4.52	4.68	2.46	1.3	18.1	5.51
463	40.4	40	2.35	2.84	1.63	0.71	9.6	3.19
374	81.4	30	1.5	3.94	2.4	0.77	12.9	3.68
29.9	2	<10	0.06	0.37	0.16	0.05	0.8	0.34
700	15.5	40	0.08	0.76	0.62	0.16	0.8	0.89
262	26.6	10	0.27	0.61	0.38	0.16	1.9	0.68
494	28.5	20	0.32	1.19	0.95	0.2	1.8	1.15
34.4	1.2	<10	0.34	1	0.63	0.15	0.4	0.95
814	69.1	10	4.94	2.62	1.41	0.65	16.9	3.18
350	49	30	1.33	1.6	0.92	0.49	4.1	2.21
795	101.5	80	0.63	2.43	1.05	1.54	19.4	4.32
623	17.5	20	0.69	0.29	0.12	0.04	10.6	0.51
457	47.1	10	0.73	3.23	2.02	0.32	16.4	3.12
20.1	1.1	10	0.05	0.08	0.06	<0.03	0.4	0.06
268	28.7	400	0.38	8.14	6.71	1.44	2	9.19

233	109	280	1.51	17.85	10.55	5.45	6.2	21.2
77.5	10.5	200	1.43	1.54	1.12	0.31	3.8	1.62
869	76.2	20	4.25	4.1	2.3	1.59	18.7	5.13
679	80.5	10	2.4	4.39	2.4	1.98	21.6	6.18
797	74.2	10	1.56	4	2.39	1.85	20.8	5.22

ME-MS81	ME-MS81	ME-MS81	ME-MS81	ME-MS81	ME-MS81	ME-MS81	ME-MS81	ME-MS81
Ba	Ce	Cr	Cs	Dy	Er	Eu	Ga	Gd
ppm	ppm	ppm	ppm	ppm	ppm	ppm	ppm	ppm
642	149.5	10	4.02	8.28	4.96	0.78	18.7	8.96
2700	123	10	3.22	9.91	7.67	0.77	20.2	7.19
207	220	10	2.13	11.85	6.58	0.92	16.9	12.45
640	54.4	20	2.06	2.46	1.37	0.82	13.5	3.23
579	69.3	10	2.18	5.32	3.24	0.99	13.3	5.49
633	73	20	2.55	4.23	2.61	0.88	14.4	4.9
917	59.6	20	2.58	3.04	1.68	0.71	12.6	3.61
638	71.9	20	2.33	3.8	2.41	0.87	14.1	4.5
836	63	10	2.81	1.96	0.84	0.65	13.7	2.84
528	52	20	4.04	3.07	1.78	0.71	13.9	3.3
533	48.5	10	1.35	3.7	2.51	0.64	9.2	4.16
564	44.5	10	2.94	1.47	0.91	0.47	11.9	1.98
1685	69.1	30	2.14	3.11	1.76	1.01	14.5	3.79
1565	65.3	10	3.08	1.54	0.67	0.57	16.3	2.51
3340	67	20	2.02	1.71	0.67	0.34	15.3	2.64
5850	124	10	1.34	3.99	1.37	0.43	22.6	7.08
3830	87.6	30	1.89	3.71	1.25	0.47	22.5	5.61
1520	59.3	30	3.43	3.02	1.37	1.01	13.1	4.32
922	16.5	30	1.93	0.89	0.52	0.24	6.1	1.23
2280	80.7	10	0.7	2.02	1.07	1.25	19.1	3.12
780	253	<10	0.95	8.04	3.4	5.28	26.2	14.2
1040	238	<10	1.19	5.62	2.03	6.64	31.5	17.45

7	16.5	6	170	2.8	85	165	43.5	300
ME-MS81	ME-MS81	ME-MS81	ME-MS81	ME-MS81	ME-MS81	ME-MS81	ME-MS81	ME-MS81
Ge	Hf	Ho	La	Lu	Nb	Nd	Pr	Rb
ppm	ppm	ppm	ppm	ppm	ppm	ppm	ppm	ppm
<5	5.4	0.72	38	0.31	18.4	32.9	8.15	76.7
<5	2.3	0.47	18	0.21	7.2	17.7	4.16	36
<5	2	0.25	16.6	0.09	2.1	14.4	3.55	18.3
6	1.2	8.42	937	1.86	7.1	713	198.5	3.9
<5	<0.2	0.15	1.6	0.04	<0.2	2.3	0.45	1.7
<5	4.2	1.55	62.2	0.6	28.5	44.5	11.7	33.5
<5	1.4	0.06	5.9	0.02	3.1	4.3	1.22	227
<5	<0.2	0.1	1.4	0.03	<0.2	1.4	0.35	1.9
<5	8.2	0.12	1.8	0.23	38.8	1.3	0.31	4.6
<5	248	3.47	299	2.34	156.5	216	59.1	1.9
<5	0.7	0.44	1.9	0.28	1.4	1.4	0.33	9.9
<5	3.2	0.31	15.1	0.11	3.7	11.8	3.11	45.7
<5	4.1	0.25	7.7	0.12	2.7	7.1	1.84	28
<5	7.2	0.25	9.3	0.18	9.7	6.3	1.71	25
<5	13.2	0.71	88.4	0.43	21.4	32.8	11	74.1
<5	7.1	0.32	8.9	0.19	11.5	7.3	1.82	24.5
<5	13.1	0.38	7.9	0.28	16.7	5.5	1.56	30.3
<5	11.9	0.21	7	0.17	17.9	5	1.41	26.2
<5	11.4	0.83	37.6	0.46	17	27.6	7.5	83.1
<5	0.5	0.03	1.3	0.01	0.6	1	0.28	2.7
<5	5.3	0.91	54.1	0.38	21.9	40.4	10.45	50.7
11	4.3	0.81	39.1	0.35	16.5	30.6	7.9	193
<5	3.8	0.32	26.8	0.12	9.2	21.7	5.95	44.6
<5	0.6	0.19	13	0.09	3.2	6.7	2	24.4
<5	4.6	0.41	22.4	0.16	6.8	16.1	4.43	135.5
<5	1	1.1	14	0.33	1.1	14.5	3.59	30.7
<5	1.3	0.22	11.6	0.08	0.9	9.1	2.44	11.7
<5	0.2	0.09	10	0.02	0.4	10	2.52	2.7
<5	0.2	0.28	8.8	0.06	0.2	6	1.48	1.4
<5	0.6	0.23	6.3	0.07	1.4	5.5	1.53	14.5

ME-MS81 Ge ppm	ME-MS81 Hf ppm	ME-MS81 Ho ppm	ME-MS81 La ppm	ME-MS81 Lu ppm	ME-MS81 Nb ppm	ME-MS81 Nd ppm	ME-MS81 Pr ppm	ME-MS81 Rb ppm
<5	1.8	0.66	9.6	0.26	3.1	11.8	2.66	20.2
<5	11.2	0.41	32.9	0.23	11.6	18	5.54	1.2
<5	1.2	0.46	16.5	0.18	5	10.6	2.94	77.1
<5	4.7	0.1	0.8	0.07	2.7	0.7	0.17	191
<5	0.4	0.02	<0.5	0.04	0.2	0.2	0.03	1.6
<5	1.3	2.12	27.7	0.84	7.9	35.7	8.05	29.8
<5	0.7	0.36	1.6	0.13	3.6	4.3	0.91	1
<5	14.6	3.14	242	0.91	39	135.5	39.9	0.3
<5	27.7	4.49	163	1.9	38.5	102.5	29.2	4.7
<5	1.2	0.44	7.5	0.16	7.1	9.9	2.43	1
6	1.6	8.16	144.5	2.79	8.8	78.6	21.4	35.4
<5	7.1	1.51	105	0.48	7.7	53	15.05	0.4
<5	3.8	0.24	1.1	0.11	10.5	0.8	0.15	181
<5	0.3	0.05	1.2	0.12	0.5	1	0.24	2.3
<5	0.2	0.02	1.2	0.01	0.4	0.9	0.23	1.9
<5	0.9	0.03	2	0.01	14	1.4	0.37	803
<5	3.6	0.38	3.6	0.18	7.7	3.1	0.92	188
<5	0.3	0.04	1.4	0.01	0.4	1.2	0.31	2.1
<5	5.3	0.3	1.4	0.15	11.9	1.7	0.4	236
<5	0.7	0.24	8.9	0.07	2	5.8	1.7	1.8
<5	2.8	0.7	4.2	0.29	9.3	7.7	1.55	21.6
<5	0.2	0.07	0.7	0.04	4.1	0.9	0.17	1.3
<5	<0.2	0.04	0.6	0.02	2.9	0.4	0.11	4.5
<5	<0.2	0.03	0.6	<0.01	0.3	0.5	0.15	0.3
<5	5.9	1.18	83.7	0.33	21.7	52.4	15.6	113.5
<5	0.5	0.08	4.4	0.02	0.3	2.9	0.75	1
<5	4.2	1.02	15.9	0.43	6.4	15	3.74	290
<5	<0.2	0.09	1.5	0.05	0.2	1.1	0.27	1.6
<5	5.1	0.87	35.7	0.39	9.1	24	6.67	7.8
<5	0.6	0.11	10.3	0.05	1.2	5.6	1.63	2.2
<5	1.1	1.32	14.6	0.48	3.2	22.9	5.06	19.4
<5	0.4	1.03	14.9	0.39	1.1	14.5	3.43	1.3
<5	0.6	1.81	18.5	0.76	18	34	7.16	60.7
<5	2.8	0.54	19.1	0.31	27	13.7	3.55	11.4
<5	1.5	0.04	2.5	0.03	3.6	1.7	0.51	129
<5	1.6	0.56	23	0.23	5.9	12.1	3.46	15.5
<5	0.3	0.04	<0.5	0.05	0.7	0.3	0.09	1.3
<5	1.5	1.75	111.5	0.46	11.6	61.9	18.4	3.1
<5	0.8	0.2	0.5	0.1	7.6	1.4	0.28	2
13	0.6	2.09	4.8	1.57	163	4.7	1.37	78.2
<5	0.2	0.21	4.3	0.11	56.3	3.1	0.92	69.1
<5	1.7	0.31	28.8	0.1	1.9	14.7	4.74	30.6
<5	4.3	0.47	33.5	0.24	7	19.9	5.97	70.8
<5	<0.2	0.3	4.9	0.14	0.7	4	0.97	6.6
<5	1.8	0.18	14.5	0.09	3.3	7.4	2.12	37.1
9	20.9	0.01	1.1	<0.01	175.5	1.1	0.27	146
8	0.7	0.02	3.9	0.01	7.5	2.4	0.73	10
7	2.9	<0.01	1	<0.01	30.1	0.4	0.13	314

11	0.5	<0.01	<0.5	<0.01	5.2	0.1	<0.03	89.2
<5	2	0.09	1.5	0.05	101.5	1.8	0.48	275
<5	2.2	0.52	15.3	0.23	3.3	11.2	3.01	37.6
<5	0.8	0.28	8.3	0.12	1.8	6.2	1.65	12.2
<5	5.9	0.61	26.2	0.3	13.6	17.7	5.14	106.5
<5	2.7	0.89	24	0.32	3.9	21.4	5.51	28.5
<5	5.6	1.8	41.9	0.6	11.8	42	10.7	35.3
<5	5.2	1.37	25.8	0.56	8.5	27.3	6.87	59.2
<5	2.4	0.98	42.1	0.34	4.8	25.8	7.14	30.8
<5	5.6	0.77	66.7	0.27	12.9	47.8	14.3	102
<5	3.2	0.16	31.4	0.06	3.9	16.7	5.44	71.2
<5	1.2	0.47	3.3	0.16	1.8	5.7	1.24	24.6
<5	0.3	0.02	2.5	0.01	0.5	1.4	0.41	261
<5	2	0.19	26.3	0.06	2.6	14.4	4.27	289
<5	6.6	1.5	41.9	0.62	14.7	37.1	9.54	12.4
<5	8.7	0.23	25.1	0.15	10.9	12.2	4.04	81.9
<5	9	2.59	29.6	0.87	108	30.8	8.26	199.5
<5	0.8	0.18	5.1	0.08	3.4	5	1.3	59.2
<5	14.1	1.43	59.6	0.67	48.6	53.1	14.15	142.5
<5	0.4	0.03	3.3	0.01	0.6	2.4	0.64	2.4
<5	8.8	1.17	55.4	0.27	4.8	65.6	15.25	19.7
<5	7	0.79	18.9	0.26	16.2	28.8	6.06	4.1
<5	3.5	0.05	1.6	0.03	26.6	1.3	0.31	0.6
<5	<0.2	0.02	4	0.01	0.5	2.6	0.68	2.9
<5	<0.2	0.02	0.5	0.01	0.3	0.6	0.11	0.6
<5	0.3	0.77	12	0.33	11.2	15.1	2.65	2.2
<5	<0.2	0.09	2.6	0.05	2.7	3.7	0.6	0.7
<5	6.7	0.81	76.9	0.35	25.3	61.3	16.1	86.9
<5	6	1.09	78	0.38	17.3	68	17.05	65
<5	10.1	0.88	96.6	0.57	49.6	49.7	15.5	198.5
<5	14.9	0.05	89.8	0.04	80.9	34.6	13.9	263
<5	6.2	1	98	0.32	38.9	80.9	21.3	109.5

ME-MS81 Ge	ME-MS81 Hf	ME-MS81 Ho	ME-MS81 La	ME-MS81 Lu	ME-MS81 Nb	ME-MS81 Nd	ME-MS81 Pr	ME-MS81 Rb
ppm	ppm	ppm	ppm	ppm	ppm	ppm	ppm	ppm
<5	3.5	0.74	27.3	0.3	9.7	23.8	6.39	50.4
<5	2.5	0.38	18.9	0.17	6.2	13.3	3.69	11
7	7.4	0.89	23.2	0.44	16.3	18.5	4.98	60.1
<5	2.4	0.35	4.5	0.14	3.2	5.8	1.35	35.6
<5	1.7	1.78	24.5	0.39	3.8	32.1	6.75	5.9
<5	2.7	1.21	20.6	0.46	5.2	32.3	7.57	60.2
<5	6.9	1.15	55.7	0.41	5.6	31.9	10.6	137.5
<5	4.9	0.37	37.2	0.16	2.4	12.2	3.85	109
<5	0.5	0.06	1.6	0.02	0.2	1.5	0.38	7.7
<5	0.9	1.35	17.6	0.5	1.8	14.4	4.25	176
11	1	3.66	2	1.42	5.9	1.4	0.42	237
<5	1.8	0.29	38.5	0.13	2.9	27.3	7.46	2.1

<5	0.6	0.29	1.8	0.14	15.1	2.8	0.57	44.7
<5	33.9	0.18	1.4	0.05	16.9	1.6	0.41	57.3
<5	2.2	1.13	2.7	1.3	2.3	1.9	0.55	163
5	1	0.12	1.2	0.06	12.2	2.7	0.6	844
<5	0.2	0.43	4.8	0.1	0.8	8.9	2.02	984
<5	6.4	0.9	50.6	0.37	11.7	38.9	10.9	135.5
<5	0.7	0.49	2.7	0.19	3.1	6.4	1.31	2.7
<5	2.1	0.1	16.7	0.07	0.6	9.3	2.87	60
<5	<0.2	0.03	1.1	0.02	<0.2	1.1	0.26	1.4
<5	3.1	0.15	3.3	0.05	3.3	3.7	0.86	7
<5	3.8	0.07	1	0.02	26.6	1	0.26	195.5
5	<0.2	0.03	0.7	0.01	80.5	0.6	0.17	267
<5	<0.2	0.01	<0.5	0.02	1	0.2	0.05	635
<5	1.8	0.77	8.1	0.58	0.4	9.8	2.62	8.3
<5	0.4	0.26	8.1	0.08	0.4	6	1.41	3.1
<5	16.5	0.98	36.5	0.48	7.8	24.5	6.93	19.7
<5	2.3	0.45	9	0.2	3.4	5.8	1.61	3.4
<5	5.1	0.2	26.2	0.09	4.4	15	4.52	84
<5	2.9	1.01	9.6	0.45	5.5	13.9	2.95	19.1
<5	0.6	0.1	7.1	0.03	1.2	3.8	1.04	3
<5	3.8	0.46	23.1	0.24	12.8	15.1	4.3	144.5
5	5.1	1.66	52.2	0.78	6.5	53.9	13.75	47.6
<5	0.2	0.39	5.5	0.14	0.6	5.1	1.34	37.5
<5	4.6	0.63	17.5	0.3	8.9	12.7	3.68	179.5
<5	2.6	0.97	7.5	0.39	4.8	11.3	2.38	67
<5	1.5	0.7	6.3	0.36	5.8	6	1.5	33.9
<5	8.9	0.86	61	0.3	5.4	43.6	12.65	17.4
5	11.2	0.48	11	0.27	8	8.5	2.18	21
<5	5.5	0.9	45.8	0.26	9.1	29.6	8.82	257
<5	10.4	0.3	21.8	0.18	3.4	12.8	3.81	5.4
<5	1.2	0.3	42	0.09	6.5	29.4	8.77	134.5
6	3	1.62	220	0.39	8.5	135	39.9	6
<5	1.4	0.17	11	0.07	1.1	8.4	2.4	8.5
<5	2	0.88	13.5	0.28	5.1	18.5	4.18	75.9
<5	1.7	0.2	23.5	0.08	2.3	6.9	2.57	81.9
5	3.8	0.48	14.4	0.21	4.9	12	3.23	90.3
<5	<0.2	0.03	1.1	0.01	261	0.5	0.15	19
5	3.5	0.69	3.9	0.36	43.6	5	1.38	159
6	<0.2	0.01	0.9	<0.01	0.9	0.9	0.26	2960
<5	0.2	0.07	4.7	0.03	92.4	2.4	0.68	848
7	3.5	0.09	1.8	0.02	87	1.6	0.45	22.8
5	1.6	0.04	0.6	0.01	5	0.6	0.13	48.3
<5	<0.2	<0.01	<0.5	<0.01	8.3	0.1	0.05	2170
<5	6.2	1.75	156.5	0.55	12.9	106.5	30.5	83.9
<5	1.9	0.5	15.5	0.18	5.7	11.5	3.13	130.5
<5	4	1.14	32.2	0.45	11.7	28.8	7.33	225
<5	0.5	1.78	26.1	0.64	1.6	21.2	5	26.9
<5	2.9	0.27	39.9	0.1	7.3	23.9	7.29	136
<5	3	0.26	25.2	0.1	7.8	17.8	5.07	103.5
<5	3	0.4	33.5	0.13	6.8	26	6.98	73.8
<5	8.9	0.73	177.5	0.24	9.5	152.5	41.2	52.5
<5	4.8	0.93	58.8	0.36	13.2	48	13	36.3
<5	7.8	0.51	24.3	0.14	2.7	22.2	5.87	6.2
<5	6	1.44	51.1	0.74	22.5	41.9	11.2	81.4
<5	0.6	0.91	5.9	0.51	3	4.7	1.24	201
<5	2.2	0.99	14.4	0.53	15.6	11.9	3.07	51.2

<5	3.6	5.66	38.7	3.05	23.1	30.5	8.08	122
<5	12.9	17	112	7.63	81.1	100.5	25.3	155.5
<5	4.5	2.13	3.7	0.88	18.5	5	1.04	356
<5	1.4	0.13	2.7	0.03	1.3	2.3	0.56	98.7
12	3.7	3.29	26	0.9	14.2	73.4	9.7	35.1
<5	3.2	1.1	173	0.23	9	222	55.2	40.1
<5	0.8	1.51	299	0.29	6.2	288	75.8	10.5
<5	5.7	0.3	15.2	0.14	4.9	12.2	3.38	30.7
<5	1.3	0.56	6.4	0.27	2.4	7.7	1.87	51.4
<5	4	0.33	19.5	0.15	5.8	15.9	4.49	324
<5	1	0.14	4	0.05	3.4	3	0.85	4.8
<5	2.5	0.13	4.7	0.07	2.3	4.1	1.02	3.8
<5	<0.2	0.6	8.9	0.29	<0.2	7.5	1.83	1.1
<5	7.9	1.31	35.8	0.61	10.9	32.8	8.34	54.6
<5	0.3	0.07	7	0.04	0.2	5.6	1.45	1
<5	7.4	0.31	14.6	0.18	4.1	9.4	2.57	9.5
<5	8.4	15.05	170.5	4.27	9.6	387	72.5	4.8
<5	6.6	1.72	14.4	0.82	12.4	23.7	4.9	12.4
<5	5.4	0.41	9.8	0.2	3.4	10.2	2.66	11.1
<5	20.3	0.28	3.3	0.26	8.1	2.9	0.69	0.6
<5	16.9	0.79	8.2	0.44	6	11.7	2.39	4.3
<5	4.2	0.09	3.1	0.05	1.6	2	0.57	1.6
<5	12	0.99	280	0.45	23.9	164	49.9	136
<5	6.4	0.65	102.5	0.38	36.4	57.3	17.9	139.5
<5	11.9	2.01	75.6	0.8	20.8	61.7	16.65	178
9	7.2	1.52	46.6	0.78	13.8	35.9	10.45	194.5
<5	0.7	0.25	2.6	0.1	1.2	2.9	0.66	4.6
<5	0.8	0.38	7.7	0.16	1.4	11	2.25	46.8
<5	4.5	0.57	22.9	0.28	7.7	21.6	5.54	43.6
<5	5.6	0.61	29	0.26	9.7	28.4	7.11	5.5
<5	<0.2	0.44	6.9	0.28	0.2	8.4	1.93	0.7
<5	2	0.56	10.6	0.27	4.3	13.4	3	74.2
<5	2.6	0.51	14	0.25	5.3	13.3	3.23	32.1
<5	1.2	0.72	5.9	0.31	2.3	8.6	1.89	16
<5	1.8	0.53	16.2	0.22	3.2	16.8	4.4	24.4
<5	0.5	0.41	13.5	0.15	1.3	15.5	3.89	12
5	6	1.51	25.5	0.65	11.3	33.3	8.04	24.7
<5	31.8	1.06	21.7	0.78	8.1	30.1	6.5	39.4
<5	<0.2	0.01	0.7	<0.01	<0.2	0.3	0.12	1.5
<5	0.8	0.83	21.3	0.31	7.9	29.8	6.5	4.4
<5	3.3	1.58	30.7	0.62	14.3	30.2	7.59	27.7
<5	1.9	0.79	18.4	0.33	5.5	25.3	5.7	0.4
<5	2.5	0.44	12.3	0.22	4.4	15.5	3.65	21.3
<5	3.7	0.81	13.2	0.44	10	21.4	4.69	48.6
<5	4.7	0.6	2.9	0.62	14.1	3.4	0.74	91.6
<5	2.3	0.8	5.1	0.4	4.1	6.1	1.44	24.8
<5	7.6	2.87	1.4	4.98	1.4	2.2	0.46	79.2
<5	<0.2	0.07	2.3	0.03	0.3	2	0.43	0.2
<5	6.3	2.81	2.2	2.1	158.5	3.7	0.66	12.2
<5	9.2	5.2	0.5	7.12	3.9	0.5	0.12	81.6
<5	4	0.77	21.7	0.41	12	22.5	5.85	54.6
<5	4.7	3.71	3.8	3.41	7.1	4.2	1	135
<5	18.9	1.42	3.6	0.94	2.6	5.7	1.14	6.1
<5	0.7	0.06	0.8	0.05	4.1	0.9	0.18	97.3
<5	1.9	13.55	6.8	19.95	2	6.5	1.77	74.8
<5	4.2	0.71	48.5	0.34	9	41.2	11.3	129.5

5	<0.2	0.18	1.2	0.1	1	1.1	0.26	0.7
6	<0.2	0.42	3.2	0.16	0.6	3.9	0.86	0.8
<5	<0.2	0.08	1.5	0.02	0.7	1.1	0.26	42.4
<5	5.5	2.77	1.7	0.67	154	3.2	0.54	116
<5	1.8	0.99	<0.5	0.95	4.6	0.5	0.11	5.3
<5	0.7	0.32	2.9	0.12	1.6	5.5	1.2	3
<5	1.5	0.34	7.5	0.13	3.5	8.9	2.1	4.4
<5	0.5	0.28	2.7	0.1	1.1	5.5	1.06	2
<5	2.6	0.25	2.6	0.15	4.3	3.9	0.89	0.5
5	2.8	1.35	30.1	0.6	10	25.3	6.93	6.4
<5	0.2	0.03	1.1	0.01	0.5	0.5	0.13	101.5
<5	1.8	1.67	10.7	0.83	7.9	16.6	3.53	82.6
<5	1.6	0.78	22.8	0.35	3.7	21.9	5.39	1.7
<5	1.8	0.84	18.2	0.4	4.3	20.8	4.7	78.2
<5	19.7	2.62	50.7	1.03	18.1	69.1	15.6	19.9
<5	4.2	0.05	17.6	0.03	1.9	9.9	2.91	75.6
<5	1.7	0.31	490	0.03	3	241	79.1	19.6
<5	0.4	0.02	7.6	0.01	0.5	3.7	1.26	69.9
<5	0.5	0.12	1.9	0.04	1.1	1.8	0.46	3.8
<5	0.9	0.93	8.3	0.41	2.2	9.6	2.3	29.2
<5	0.8	0.1	4.3	0.05	0.7	2.1	0.55	0.3
<5	0.8	0.8	14.1	0.27	0.7	18.5	4.21	7.5
<5	4.8	3.86	142	1.14	5.7	115	28.3	35.4
<5	7.9	0.51	20.7	0.29	4.9	19.9	5.16	67.2

ME-MS81 Ge ppm	ME-MS81 Hf ppm	ME-MS81 Ho ppm	ME-MS81 La ppm	ME-MS81 Lu ppm	ME-MS81 Nb ppm	ME-MS81 Nd ppm	ME-MS81 Pr ppm	ME-MS81 Rb ppm
<5	1.5	1.83	107	0.66	3.6	48.5	13.25	36.3
<5	3.4	7.4	283	2.99	2.2	141.5	37.1	22.3
<5	3.6	3.91	198.5	1.85	2.4	73.7	19.8	15.9
<5	1.1	12.15	491	4.27	0.4	296	75.9	5.2
<5	9.7	0.86	38.5	0.43	12.9	26.2	7.06	84.3

ME-MS81 Ge ppm	ME-MS81 Hf ppm	ME-MS81 Ho ppm	ME-MS81 La ppm	ME-MS81 Lu ppm	ME-MS81 Nb ppm	ME-MS81 Nd ppm	ME-MS81 Pr ppm	ME-MS81 Rb ppm
<5	1.7	0.2	17.5	0.08	1	18.7	4.37	1.3
<5	6.7	0.24	14.8	0.12	1.3	13.4	3.41	1.7

<5	<0.2	0.12	2	0.06	0.2	1.9	0.52	0.8
<5	<0.2	0.2	10.1	0.1	0.2	10.8	2.43	0.4
<5	<0.2	1.57	6	0.72	0.2	10.9	2.15	3.5
<5	6.7	0.41	11	0.26	7.4	11.1	2.78	43.8
<5	<0.2	0.19	8.2	0.08	0.2	3.6	1.1	1.8
<5	<0.2	0.01	<0.5	<0.01	<0.2	0.3	0.08	0.3
<5	0.4	0.13	2.6	0.04	0.6	2.8	0.67	122.5
<5	<0.2	0.01	0.6	0.01	<0.2	0.4	0.1	0.6
<5	0.7	0.38	2.4	0.15	1.3	3.7	0.78	2.7
<5	0.3	0.19	1.4	0.06	0.4	2.2	0.45	1.6
<5	3.2	0.32	6.3	0.13	4.3	11.3	2.43	14.8
<5	<0.2	0.07	1.2	0.05	<0.2	1.3	0.27	1.9
<5	1.4	0.37	11.1	0.24	32.9	9.7	2.66	131.5
<5	9.6	1.31	48.1	0.5	15.4	46.7	11.7	44.9
<5	85.2	9.13	194	3.36	123	301	68	32.4
<5	<0.2	0.11	1.3	0.04	0.5	1.8	0.4	0.6
<5	27.6	2.4	73.9	1.21	46.2	67.9	17.4	233
<5	6.8	1.57	28	0.58	12.3	35.4	8.26	9.5
6	1.7	1.17	61.3	0.51	5.6	51.3	13.6	0.6
<5	10.1	2.46	55.3	0.93	25.7	67.6	15.85	2.7
<5	16.4	2.25	98.5	0.76	35.1	99.6	26	57.9
<5	4.1	1.17	14	0.64	6.4	18.1	4.39	21.5
<5	0.3	0.11	1.7	0.07	0.9	1	0.3	256
<5	19.8	2.18	69.1	0.85	33.3	72.7	18.1	151.5
<5	1.5	0.11	6.6	0.05	4	2.8	0.9	28
<5	0.9	0.24	5	0.14	3	3.3	0.92	7
<5	4.3	0.71	37.3	0.4	15.4	27.1	7.8	184.5
<5	1.8	0.23	7.3	0.1	16.7	7.7	1.9	32.9
<5	2.8	0.35	8.7	0.18	19.5	9	2.21	38.8
<5	1.5	0.6	17.6	0.3	6.4	15.2	3.85	77.8
<5	5.5	0.66	39.6	0.24	14.9	32.4	8.51	128
<5	4.9	0.12	8.7	0.09	14	3.1	0.92	118
<5	5.3	0.33	31.3	0.17	17.8	23.6	6.7	142.5
<5	8.3	0.42	16.7	0.21	6.1	13.9	3.55	33.8
<5	785	6.78	483	6.33	434	356	99.9	1.4
<5	8.7	0.67	26.1	0.3	11.2	19.8	5.45	44.5
<5	4.4	1.52	51	0.51	13.9	44.3	11.6	180
<5	7.1	0.54	39.6	0.32	10.9	32.6	8.99	87.6
<5	3.1	1.37	59.8	0.59	7.1	56.1	14.05	50.3
<5	3.7	0.79	54.5	0.25	12.4	40.2	10.85	92.1
<5	3	0.59	35.5	0.22	12.5	27.8	7.58	114.5
<5	3.3	0.95	40.5	0.32	13.5	35.8	9.26	86.8
<5	2.8	0.6	21.3	0.25	6.1	17.1	4.73	56.8
<5	3.5	0.82	42.3	0.3	6.6	23.7	7.18	42.9
<5	0.3	0.07	0.8	0.03	2.1	1.1	0.27	0.5
<5	4.1	0.19	9	0.12	6.5	6.2	1.68	1.3
<5	5.2	0.13	16.6	0.09	7	8.3	2.58	7.3
<5	10.9	0.28	16.2	0.2	13.1	10.6	3.01	1.4
<5	<0.2	0.25	0.9	0.06	<0.2	1.6	0.32	1.3
<5	7.7	0.52	40.5	0.21	22.7	25.8	7.55	97.9
<5	6.7	0.32	22.9	0.13	7.7	18	4.99	36.2
<5	3.7	0.39	51.2	0.12	3.8	42.8	11.2	34.2
<5	1.2	0.05	9.3	0.02	2.8	5.9	1.77	270
<5	3.8	0.72	24.8	0.42	15.2	16.9	5.04	169
<5	0.2	0.02	0.8	<0.01	<0.2	0.4	0.14	1.5
<5	2	2.17	124.5	1.01	0.7	45.2	11.7	9.8

<5	3.7	3.85	154	1.16	5	105	26.6	35.9
<5	0.8	0.37	15.9	0.15	2.2	9.4	2.34	27.5
<5	4.6	0.81	40.7	0.34	17.2	32.2	8.23	64.4
<5	6	0.84	42.4	0.34	18	35.7	9.29	66.4
<5	5.3	0.8	41.1	0.34	19.8	32.7	8.41	62.3

ME-MS81	ME-MS81	ME-MS81	ME-MS81	ME-MS81	ME-MS81	ME-MS81	ME-MS81	ME-MS81
Ge	Hf	Ho	La	Lu	Nb	Nd	Pr	Rb
ppm	ppm	ppm	ppm	ppm	ppm	ppm	ppm	ppm
<5	9.3	1.65	77.8	0.7	36.7	53.8	15.55	199
<5	11.1	2.27	62.5	1.1	43.2	45	12.25	147.5
<5	10.8	2.28	101.5	0.93	45.8	73.2	20.7	89.9
<5	6.3	0.51	29.5	0.21	11.9	21.6	5.96	83.6
<5	8.5	1.08	33.3	0.47	12.7	29.9	7.69	84.6
<5	7.9	0.91	38.2	0.39	15.1	30	8.11	106
<5	6	0.62	32.5	0.25	11.6	23.7	6.53	84.8
<5	9.7	0.83	37.2	0.64	14.2	30.4	8.11	91.5
<5	5.7	0.32	31.9	0.16	14.3	25.1	7.07	115.5
<5	7	0.6	27.8	0.34	12.6	21.3	5.85	98.7
<5	3.9	0.85	22.6	0.36	8	20.7	5.08	56
<5	2.6	0.33	24.9	0.18	11.8	15	4.48	133
<5	4.3	0.66	37	0.24	10.4	27	7.13	61.3
<5	4.5	0.3	40.9	0.09	7	19.6	5.91	65.6
<5	6.9	0.3	34.4	0.08	22.6	21.6	6.54	47
<5	8.5	0.6	61.7	0.08	29	46.6	13.35	43.9
<5	8	0.57	44.7	0.1	35.8	31.8	8.83	63.3
<5	4.1	0.52	39.3	0.16	14.7	33.9	8.87	89.7
<5	1.4	0.18	10.9	0.07	5.2	7.4	2.15	44.8
<5	3.6	0.39	43.2	0.14	9.1	31.6	8.63	66.3
<5	8.8	1.38	119.5	0.4	46.4	126.5	30.9	208
<5	6	0.85	120.5	0.23	49.9	103.5	26.3	237

30	11	1800	8.5	4.7	30	2.25	9	950
ME-MS81	ME-MS81	ME-MS81	ME-MS81	ME-MS81	ME-MS81	ME-MS81	ME-MS81	ME-MS81
Sm	Sn	Sr	Ta	Tb	Th	Tm	U	V
ppm	ppm	ppm	ppm	ppm	ppm	ppm	ppm	ppm
6.12	1	1425	1	0.77	8.64	0.31	3.39	48
3.54	1	403	0.4	0.43	3.95	0.18	27.3	76
2.41	<1	73.8	0.2	0.23	21.7	0.11	2.91	191
112.5	11	456	0.3	9.53	404	2.59	28.7	34
0.53	<1	705	<0.1	0.09	0.37	0.05	0.11	86
9	3	848	2.2	1.33	23.8	0.61	7.75	67
0.74	<1	460	0.4	0.06	10.3	0.04	0.75	<5
0.37	1	25.4	<0.1	0.06	0.16	0.05	1.6	11
0.24	1	51.5	0.1	0.04	5.27	0.13	16.75	97
35.9	15	94.2	10.1	3.57	119	1.61	26.2	2500
0.42	<1	8.3	0.1	0.3	0.76	0.23	8.6	200
2.32	1	149.5	0.3	0.28	4.58	0.13	1.06	25
1.29	<1	154.5	0.2	0.2	2.14	0.11	1.72	23
1.16	1	49.1	0.6	0.16	4.73	0.17	31.2	1215
4.49	3	249	1.6	0.5	14	0.38	51.4	1640
1.31	1	37.2	0.8	0.22	5.38	0.16	10.25	394
1.02	1	39.6	1.2	0.24	10.15	0.23	4.11	48
0.86	1	53.2	1.3	0.17	9	0.15	4.63	111
5.18	1	120	1.3	0.72	11.6	0.39	5.16	66
0.21	<1	62.3	0.1	0.02	0.45	0.02	57.7	52
6.74	1	1455	1.2	0.9	11.85	0.38	2.87	74
5.44	1	290	0.9	0.73	11.45	0.35	12.05	139
3.4	1	208	0.4	0.34	4.23	0.13	22.9	40
0.93	1	16.3	0.1	0.16	5.46	0.09	11.15	59
2.91	1	98	0.7	0.36	17.6	0.16	2.32	20
3.58	<1	93.9	0.1	0.7	4.46	0.42	0.81	16
1.61	1	7	0.1	0.16	2.25	0.09	0.3	19
1.57	16	555	<0.1	0.12	0.85	0.03	5.12	200
1.25	<1	258	0.1	0.22	1.06	0.08	0.72	<5
1.07	<1	28	0.1	0.18	1.42	0.09	3.97	22

ME-MS81 Sm ppm	ME-MS81 Sn ppm	ME-MS81 Sr ppm	ME-MS81 Ta ppm	ME-MS81 Tb ppm	ME-MS81 Th ppm	ME-MS81 Tm ppm	ME-MS81 U ppm	ME-MS81 V ppm
2.75	1	394	0.2	0.49	1.66	0.27	0.94	285
3.18	2	820	0.9	0.37	41	0.18	7.86	60
2.41	2	635	0.2	0.43	1.46	0.18	2.51	135
0.22	<1	615	0.2	0.05	0.5	0.04	0.49	7
0.08	<1	7.6	0.1	0.02	0.2	0.02	0.11	70
10.2	2	534	0.5	2.08	1.11	0.71	9.4	116
1.25	1	6.6	0.2	0.28	0.56	0.14	0.17	130
23.6	5	1035	1.9	3	81.2	1.1	74.2	218
20.4	11	1335	4.1	3.53	33.8	1.96	47.9	130
2.37	2	433	0.3	0.4	1.58	0.16	2.02	91
20.5	7	1025	0.8	5.66	1.12	3.14	34.9	310
10.4	4	1200	0.7	1.49	4.76	0.49	18.75	151
0.21	<1	441	0.8	0.09	16.2	0.13	4.44	<5
0.25	<1	12	0.1	0.04	0.29	0.03	0.68	93
0.14	<1	49	<0.1	0.02	0.28	0.01	7.71	20
0.23	8	29.5	16.4	0.05	0.89	0.01	0.62	<5
1.75	5	23.8	3.8	0.45	6.8	0.17	2.39	9
0.17	<1	184	<0.1	0.03	0.44	0.02	17.25	7
0.68	1	30.2	1.1	0.15	37	0.13	2.11	13
1.15	1	10.7	0.2	0.2	3.12	0.09	0.5	14
2.44	1	117.5	3.4	0.53	1.36	0.3	2.23	381
0.25	1	10.5	1.6	0.05	0.22	0.04	3.18	224
0.16	<1	5.6	0.7	0.03	0.21	0.01	1.33	51
0.18	<1	1.5	<0.1	0.01	<0.05	0.01	0.08	<5
9.36	7	7.4	2.6	1.06	61.4	0.42	4.59	22
0.6	15	21.1	<0.1	0.08	2.1	0.03	0.21	196
3.48	13	7.2	0.5	0.65	4.12	0.44	1.25	271
0.19	<1	2.9	<0.1	0.05	0.24	0.06	2.07	77
4.54	2	569	0.6	0.65	12.9	0.37	2.95	300
0.95	1	701	0.1	0.11	3.27	0.06	42.7	238
5.61	4	72.1	0.2	1.08	6.26	0.5	33.7	308
4.23	<1	15.9	0.1	0.79	1.19	0.4	5.73	46
9.1	7	145	2.2	1.36	17.4	0.79	4.73	41
2.8	2	379	1.6	0.43	2.79	0.3	7.1	163
0.24	<1	1440	0.3	0.03	2.41	0.03	0.42	<5
2.47	1	879	1	0.42	6.92	0.25	5.26	84
0.08	1	5	0.3	0.03	0.2	0.03	0.17	82
12.6	4	1170	0.9	1.73	18.15	0.64	18.75	95
0.5	<1	7.7	0.7	0.13	0.35	0.12	0.31	74
3.4	13	11.7	136.5	2.26	13.95	1.43	8.1	<5
1.32	2	24.1	11.8	0.27	9.65	0.14	3.03	<5
2.46	1	260	0.3	0.28	6.06	0.13	1.52	11
3.08	1	212	1.1	0.37	7.38	0.23	0.92	18
0.96	<1	145	0.1	0.2	0.41	0.15	0.66	5
1.11	1	502	0.3	0.15	4.18	0.09	1.51	11
0.12	283	56.3	1870	0.02	21.6	0.01	6.17	12
0.38	14	60.8	3.6	0.03	1.91	0.02	11	341
0.09	75	73.3	44.7	0.01	3.35	0.01	1.67	5

<0.03	6	25.3	50.5	<0.01	0.23	<0.01	2.64	<5
0.56	60	18.2	27.4	0.13	5.54	0.05	1.25	<5
2.22	1	145	0.5	0.35	4.26	0.27	26.4	17
1.2	<1	141.5	0.6	0.22	1.32	0.13	1.69	25
3.09	2	159	1	0.44	9.54	0.31	3.73	149
4.56	1	249	0.4	0.73	4.25	0.36	2.79	70
8.75	2	220	1.1	1.42	14.95	0.75	3.4	50
5.6	1	146	0.6	0.98	6.54	0.68	2.33	32
4.82	1	485	0.4	0.79	3.52	0.4	4.2	54
8.72	2	94.3	0.9	0.77	37.9	0.32	6.99	79
2.65	1	239	0.3	0.18	28.7	0.06	8.86	39
1.81	1	77.6	0.2	0.36	0.79	0.2	0.26	234
0.28	<1	91.8	0.1	0.03	6.92	0.01	0.31	<5
2.81	<1	95.2	0.4	0.23	18.9	0.06	2.69	<5
8	1	130.5	0.9	1.24	6.14	0.68	1.34	225
2.2	5	7.6	1.4	0.2	8.76	0.13	1.41	63
8.94	5	24.7	4.4	1.96	50.3	1.18	7.25	<5
0.91	1	19.1	0.2	0.16	2.47	0.1	6.9	71
10.25	3	186.5	3.3	1.27	11.9	0.66	1.98	<5
0.36	<1	1105	0.1	0.03	0.19	0.02	0.07	11
11.95	<1	755	0.3	1.3	5.38	0.35	1.64	<5
6.49	1	526	0.9	0.86	0.87	0.27	0.37	422
0.31	1	8	1.4	0.04	0.1	0.02	0.34	3410
0.39	<1	978	<0.1	0.04	0.05	<0.01	0.06	10
0.15	<1	32.4	<0.1	0.01	<0.05	<0.01	3.9	11
5.42	<1	708	<0.1	0.72	0.51	0.33	11.05	397
1.39	<1	258	<0.1	0.13	0.06	0.04	9.36	174
11.1	1	1615	1.3	0.99	28.2	0.33	7.24	71
12.2	1	1550	0.9	1.16	17.1	0.4	3.74	117
7.36	1	820	1.7	0.75	36.6	0.48	9.67	17
2.36	1	175.5	1.9	0.1	83	0.02	32	12
13.5	1	2230	2	1.18	23	0.38	6.26	57

ME-MS81 Sm ppm	ME-MS81 Sn ppm	ME-MS81 Sr ppm	ME-MS81 Ta ppm	ME-MS81 Tb ppm	ME-MS81 Th ppm	ME-MS81 Tm ppm	ME-MS81 U ppm	ME-MS81 V ppm
4.43	1	219	0.5	0.6	8.38	0.32	3.17	75
2.57	1	268	0.4	0.32	6.72	0.14	6.14	62
3.63	2	62.8	1.1	0.56	7.73	0.41	3.87	66
1.8	1	24.4	0.2	0.31	2.26	0.14	0.87	35
10.3	1	75.3	0.2	1.9	3.35	0.53	1.53	457
7.4	1	78.5	0.3	1.04	7.13	0.44	7.01	58
6.6	1	119	0.4	1.06	20.2	0.43	20.6	45
2.6	<1	108.5	0.2	0.33	22.5	0.18	13.85	65
0.31	<1	23.5	<0.1	0.05	0.43	0.03	0.8	<5
3.68	4	151	0.2	0.83	18.7	0.56	2.35	7
1.13	12	11.2	2.7	2.52	0.34	1.74	1.6	19
4.38	1	17.6	0.2	0.35	2.79	0.1	1.64	100

1.21	13	47.3	4.6	0.32	6.43	0.11	7.77	25
1.23	9	40.8	5.2	0.32	14.2	0.06	4.84	<5
0.64	1	17.7	0.1	0.45	4.94	0.99	0.6	<5
2.07	32	18.6	0.9	0.25	7.32	0.04	1.24	<5
5.33	25	129	0.1	0.89	2.09	0.12	21.7	64
6.79	3	242	1	0.81	21.9	0.37	4.32	92
2.3	2	9.8	0.2	0.41	0.64	0.19	0.98	49
1.56	<1	579	0.1	0.12	12.1	0.05	2.15	<5
0.25	<1	7.9	<0.1	0.04	0.12	0.01	6.07	<5
1.31	4	83	3	0.19	5.85	0.05	2.58	44
0.33	7	30.6	20.3	0.09	1.36	0.03	0.57	<5
0.28	58	45.9	12.3	0.04	3.21	0.02	3.54	<5
0.13	6	160	0.3	0.01	0.12	<0.01	13.05	66
3.35	3	16.1	0.3	0.64	10.35	0.46	1.46	<5
1.16	<1	14.5	<0.1	0.19	0.43	0.09	1.23	16
5.04	<1	72.9	0.6	0.8	20.5	0.39	3.77	5
1.67	3	886	0.2	0.34	2.85	0.21	5.24	101
2.73	1	191	0.2	0.26	27.3	0.07	2.12	8
3.91	1	152	0.3	0.74	1.54	0.41	0.33	361
0.78	<1	115	0.1	0.1	1.12	0.04	0.48	5
2.58	2	98	1	0.34	12.65	0.2	4.63	135
12.15	1	168.5	0.4	1.47	7.16	0.76	16.15	39
1.63	1	18.9	0.1	0.3	12.05	0.14	1.57	110
2.81	1	69.2	0.9	0.46	31.6	0.25	3.37	8
3.08	1	150	0.3	0.63	1.21	0.41	0.47	337
1.98	3	122	1.6	0.46	4.12	0.34	2	209
8.07	<1	63.1	0.5	0.85	31.8	0.28	6.23	10
1.68	1	32.6	0.5	0.32	6.61	0.2	37.4	924
6.12	2	100.5	1.1	0.93	47.9	0.33	6.58	11
2.29	5	692	0.2	0.23	8.85	0.12	6.24	31
5.35	1	74.1	0.3	0.41	34.6	0.13	1.5	11
23.3	7	987	0.5	1.91	78.8	0.48	34.2	76
1.24	<1	19.7	0.1	0.12	2.59	0.05	1.22	8
4.52	1	329	0.4	0.66	7.86	0.31	82.6	269
1.16	1	79.9	0.2	0.16	9.87	0.09	2.2	6
2.65	1	73.5	0.4	0.34	14.1	0.22	26.2	83
0.12	1	13.4	169	0.02	2.15	<0.01	0.67	<5
3.41	18	2.1	18	0.86	10.6	0.32	4.92	<5
0.53	4	5.4	0.6	0.08	0.13	<0.01	0.13	<5
0.72	117	19.1	30.5	0.12	3.78	0.04	2.7	10
0.93	3	3	320	0.35	2.18	0.03	2.14	<5
0.27	2	22.8	29.1	0.06	0.83	0.02	2.94	<5
0.03	8	6.1	40.7	<0.01	0.1	<0.01	0.21	<5
18.65	2	163.5	1.8	1.73	102	0.61	9.83	56
2.42	3	94.6	1.8	0.39	3.65	0.16	1.09	54
5.71	5	168.5	1.7	0.88	11.9	0.47	2.99	158
5.43	1	86.1	0.2	1.19	1.76	0.63	1.23	21
3.2	1	291	0.5	0.28	6.74	0.1	1.95	67
2.71	1	502	0.6	0.24	6.62	0.09	0.99	55
4.22	1	966	0.4	0.41	5.87	0.14	5.51	79
19.6	2	2230	0.6	1.02	25.3	0.26	2.98	120
8.28	1	635	0.7	0.78	10.35	0.36	1.49	138
4.24	<1	200	0.2	0.51	4.76	0.19	0.92	10
9.05	2	12.2	1.3	1.13	12.1	0.73	48	175
1.32	<1	20.6	0.5	0.54	2.26	0.47	2.07	15
2.99	1	9.1	2.2	0.76	4.9	0.49	3.27	35

9.9	5	14.4	2	3.71	11.7	2.85	10.95	336
33.1	5	28.4	7.6	11.1	22.6	8.08	9.51	127
3.28	2	80	0.9	1.35	9.89	0.9	2.88	<5
0.8	1	238	0.1	0.12	1.95	0.04	0.65	6
43.4	71	528	1.7	4.42	1.8	0.97	5.07	451
33.9	5	1030	0.8	1.87	20.8	0.28	3.65	62
42	1	25.6	0.4	2.57	1.06	0.36	34.2	122
2.36	1	43.8	0.3	0.24	5.87	0.12	1.32	28
2.24	1	215	0.2	0.43	1.28	0.24	0.36	160
2.93	1	658	0.5	0.33	27.6	0.14	2.52	63
0.66	1	33.3	0.1	0.09	2.64	0.07	0.78	122
0.81	<1	28	0.2	0.11	1.22	0.05	0.57	14
1.9	<1	535	<0.1	0.38	0.23	0.28	4.76	16
7.55	2	201	0.9	1.12	8.52	0.61	2.26	54
1.17	<1	142.5	<0.1	0.12	0.43	0.02	1.67	8
1.89	1	88.1	0.3	0.28	3.02	0.15	0.86	20
110	2	1135	0.6	17.45	5.86	5.2	33.8	33
6.19	2	440	1	1.36	15.35	0.77	5.21	62
2.25	<1	306	0.3	0.32	3.13	0.2	14.15	39
0.63	1	16.2	0.5	0.17	1.28	0.16	1.54	7
2.69	1	36.9	0.5	0.5	2.57	0.37	33.7	93
0.43	<1	12.3	0.1	0.07	0.69	0.04	1.97	<5
21.3	1	867	0.8	1.19	42.3	0.41	5.97	36
8.26	1	174	1.5	0.66	63.3	0.33	6.76	8
13.35	4	125.5	1.3	1.6	19.3	0.84	3.56	11
7.34	3	1285	1.1	1.14	16.95	0.73	10.7	36
0.79	1	34.9	0.1	0.14	1.19	0.08	0.3	8
2.65	1	345	0.1	0.32	0.54	0.16	0.54	240
4.03	1	607	0.5	0.48	5.93	0.24	3.11	20
5.79	2	592	0.3	0.59	3.51	0.24	2.03	43
2.13	<1	37.2	<0.1	0.37	0.14	0.23	11.1	1050
3.11	1	53.3	0.3	0.4	1.51	0.25	3.19	209
2.97	1	394	0.4	0.38	11.05	0.21	1.64	179
2.38	1	82.2	0.1	0.5	1.72	0.34	14.85	167
3.37	1	18.2	0.2	0.43	2.97	0.24	3.6	109
3.56	<1	11.3	0.1	0.43	1.76	0.15	2.54	95
8.58	5	2200	0.6	1.2	4.68	0.7	3.18	104
7.33	1	879	0.3	0.83	2.87	0.57	3.73	10
0.06	<1	11.1	<0.1	0.01	0.12	<0.01	0.45	20
6.32	1	818	0.4	0.73	0.32	0.33	0.25	354
6.91	<1	218	2.5	1.21	22.7	0.66	1.25	170
6.06	1	2490	0.2	0.69	0.59	0.32	0.37	293
3.6	1	1115	0.2	0.44	0.54	0.17	0.37	211
5.27	1	491	0.8	0.73	4.43	0.43	2.85	163
1.35	<1	145.5	1.5	0.4	1.61	0.45	2.63	12
2.13	<1	124	2.3	0.55	3.64	0.34	7.09	12
1.14	<1	92.4	0.2	0.65	3.92	2.79	5.05	7
0.43	<1	7.8	<0.1	0.07	0.05	0.03	2.16	79
3.57	2	38.1	50.4	1.86	6.93	1.6	26.3	5
0.36	1	90.7	0.8	1.19	1.43	4.61	7.31	11
4.64	2	135.5	1.2	0.63	4.29	0.37	2.58	147
1.82	<1	95.8	1.7	2.01	3.86	2.39	2.14	7
3.15	1	215	0.6	0.86	40	0.75	9.38	139
0.31	<1	208	0.2	0.04	0.34	0.03	0.39	25
1.74	<1	77.9	0.1	2.35	3.45	12.65	1.43	8
6.83	1	202	<0.1	0.68	10.25	0.28	1.25	11

0.41	<1	1.4	1.8	0.11	0.29	0.11	0.59	21
1.24	<1	2.1	0.3	0.28	1.07	0.18	17.9	38
0.3	<1	139	0.1	0.07	0.24	0.03	0.15	<5
3.86	1	51.3	16	2.55	12.85	0.88	6.71	25
0.4	<1	156.5	0.5	0.31	1.24	0.72	0.64	<5
1.48	<1	248	0.1	0.24	0.53	0.12	0.32	167
2.03	1	603	0.3	0.23	2.13	0.13	89.9	149
1.61	1	101	<0.1	0.21	0.2	0.12	3.3	176
1.01	1	4.5	0.2	0.19	3.1	0.12	1.5	444
5.51	2	1410	2	0.92	2.27	0.6	7.74	144
0.07	<1	473	<0.1	0.02	0.1	0.02	0.36	9
5.35	2	556	0.5	1.05	1.53	0.86	0.76	216
4.31	3	1085	0.1	0.63	1.84	0.32	3.36	264
4.64	2	683	0.2	0.68	2.19	0.35	3.46	307
15.3	1	469	0.7	2.12	2.1	1.03	2.16	207
1.07	1	496	<0.1	0.06	2.39	0.03	0.37	37
23.3	<1	524	<0.1	0.63	63.4	0.05	0.68	13
0.43	<1	532	<0.1	0.03	0.73	<0.01	0.06	<5
0.46	<1	3.6	0.8	0.11	1.37	0.04	0.3	31
2.61	<1	46.3	0.2	0.69	2.25	0.4	9.72	484
0.36	9	46.4	<0.1	0.06	1.57	0.05	30.1	211
3.94	23	62.6	<0.1	0.57	7.56	0.29	14.45	1840
20.4	1	616	0.3	3.17	6.84	1.35	6.34	65
4.33	1	93	0.4	0.44	6.98	0.26	2.68	24

ME-MS81	ME-MS81	ME-MS81	ME-MS81	ME-MS81	ME-MS81	ME-MS81	ME-MS81	ME-MS81
Sm	Sn	Sr	Ta	Tb	Th	Tm	U	V
ppm	ppm	ppm	ppm	ppm	ppm	ppm	ppm	ppm
8.38	1	923	0.1	1.24	5.09	0.73	20.4	99
24.1	<1	1020	0.1	4.14	4.74	3.13	31.8	228
11.4	<1	617	0.1	2.06	3.64	1.77	129.5	521
48.6	<1	879	<0.1	7.69	1.88	4.7	53.4	205
4.96	2	410	0.9	0.6	8.99	0.4	12	381

ME-MS81	ME-MS81	ME-MS81	ME-MS81	ME-MS81	ME-MS81	ME-MS81	ME-MS81	ME-MS81
Sm	Sn	Sr	Ta	Tb	Th	Tm	U	V
ppm	ppm	ppm	ppm	ppm	ppm	ppm	ppm	ppm
3.6	<1	145	<0.1	0.26	0.76	0.09	2.86	28
2.11	<1	82.9	<0.1	0.22	1.42	0.12	2.3	31

0.59	<1	3.4	<0.1	0.09	0.11	0.07	0.42	12
1.88	<1	169.5	<0.1	0.21	0.41	0.08	2.43	1015
4.14	<1	12.3	<0.1	1.04	0.47	0.77	3.88	393
2.01	1	74.3	0.6	0.3	9.01	0.21	5.69	89
0.44	<1	11.1	<0.1	0.1	0.64	0.09	1.07	29
0.06	<1	1.6	<0.1	0.01	<0.05	0.01	0.07	6
0.62	<1	32.7	<0.1	0.11	0.51	0.06	0.2	69
0.06	<1	8.4	<0.1	0.01	0.1	0.01	0.89	10
1.16	<1	33.7	<0.1	0.24	0.41	0.16	0.11	222
0.65	<1	49.8	<0.1	0.13	0.14	0.08	0.05	149
2.41	<1	141	0.1	0.27	7.46	0.13	0.78	133
0.31	<1	3.8	<0.1	0.06	0.05	0.04	0.8	91
2	3	37.8	1.5	0.27	13.15	0.21	4.89	<5
9.02	2	933	0.7	1.16	17.1	0.47	7.82	112
61.5	3	45.2	5	8.04	15.5	3.4	14.15	58
0.38	<1	8.7	<0.1	0.07	0.14	0.05	112	11
12	3	29.6	1.9	1.65	13.3	1.14	6.12	10
7.13	2	19.5	0.4	1.16	6.44	0.64	3.93	72
7.3	3	2000	0.2	0.88	2.32	0.45	3.75	201
14.75	2	95	1.2	2.12	9.87	0.96	3.31	73
18.15	3	367	1.5	2.13	13.55	0.88	4.81	106
4.29	7	535	0.5	0.78	8.71	0.59	4.28	142
0.31	<1	13.5	<0.1	0.05	1.53	0.05	0.57	<5
14.15	2	79.8	1.5	1.81	13.8	0.9	4.41	5
0.56	1	25.4	0.1	0.08	3.03	0.04	2.93	1005
0.55	6	8	0.1	0.14	1.37	0.12	11.2	125
4.73	2	164	1.3	0.55	13.65	0.39	9.71	421
1.65	3	4	0.5	0.18	1.29	0.1	1.47	85
1.74	2	12.5	0.6	0.27	2.27	0.14	9.32	268
2.56	1	937	0.3	0.32	14.9	0.31	5.24	60
5.7	1	731	0.9	0.67	9.24	0.28	3.45	171
0.5	2	427	0.9	0.07	1.27	0.09	1.77	76
3.79	3	258	1.1	0.35	2.03	0.16	1.92	117
2.34	1	114.5	0.5	0.3	4.73	0.21	2.35	29
55.8	61	78.4	26.5	5.53	182.5	4.46	64.1	1200
3.31	1	130.5	0.9	0.47	7.74	0.34	2.01	37
8.87	3	192.5	1.1	1.29	14.9	0.63	7.42	106
4.43	2	428	0.8	0.47	2.97	0.27	3.21	49
10.9	1	953	0.5	1.34	23.6	0.61	8.8	60
6.83	4	525	0.9	0.76	18.65	0.29	6.95	151
4.94	2	494	0.9	0.57	10.05	0.25	4.73	155
6.98	1	770	0.9	0.83	19.45	0.35	9.2	87
3.27	1	97.2	0.5	0.47	4.88	0.27	3.84	63
3.85	1	778	0.5	0.63	6.03	0.37	3.21	48
0.23	<1	12.6	0.1	0.05	0.23	0.03	0.11	<5
0.89	<1	21.6	0.5	0.11	2.09	0.12	3.4	5
1.01	2	207	0.5	0.11	2.87	0.07	3.37	29
1.46	3	50.4	0.9	0.2	5.73	0.17	6.14	38
0.48	<1	4790	<0.1	0.16	0.1	0.09	0.91	16
4.38	3	186	1.7	0.5	12.2	0.24	3.72	21
2.87	<1	71.3	0.6	0.31	10.75	0.15	1.43	22
6.57	1	727	0.2	0.52	7.36	0.16	1.22	82
0.76	<1	337	0.5	0.06	26.6	0.03	0.99	5
3.38	2	581	1.5	0.53	15.85	0.37	5.05	17
0.03	<1	83	<0.1	0.01	0.15	0.01	0.98	5
6.46	<1	1065	0.1	1.2	1.01	0.97	40.5	73

17.4	1	694	0.4	2.92	6.54	1.54	7.72	99
1.53	<1	180	0.2	0.24	1.62	0.16	3.98	42
5.89	1	1060	1	0.75	9.17	0.37	2.62	56
6.61	1	1475	0.9	0.82	8.58	0.34	3.06	79
6.01	1	1355	1.1	0.72	8.8	0.36	2.9	79

ME-MS81	ME-MS81	ME-MS81	ME-MS81	ME-MS81	ME-MS81	ME-MS81	ME-MS81	ME-MS81
Sm	Sn	Sr	Ta	Tb	Th	Tm	U	V
ppm	ppm	ppm	ppm	ppm	ppm	ppm	ppm	ppm
9.89	7	88.2	2.8	1.42	35.4	0.77	7.12	14
8.27	8	398	3.2	1.38	35.1	1.36	24.5	83
13.9	8	352	3.2	2.02	50.8	0.97	5.6	418
3.79	2	396	0.8	0.42	6.31	0.2	3.54	51
6.03	2	395	0.9	0.92	16.65	0.49	5.81	48
5.78	2	370	1.1	0.77	11.55	0.42	5.13	56
4.27	2	1100	0.8	0.52	9.5	0.25	16.95	48
5.39	2	610	1	0.72	66.2	0.42	29.7	105
4.18	3	939	1.2	0.39	30.9	0.13	16.75	37
3.66	2	473	0.9	0.5	19.3	0.32	17.7	49
4.13	2	673	0.6	0.66	10.35	0.38	13.95	32
2.55	1	161	1.1	0.25	13.65	0.15	4.28	68
4.69	2	1765	0.8	0.52	7.06	0.28	3.98	92
3.18	1	769	1.6	0.29	5.89	0.09	0.87	31
3.42	3	1615	2.2	0.33	10.3	0.1	0.44	35
9.59	6	2610	4.5	0.96	19	0.15	0.77	26
7.14	5	1985	4	0.81	12.55	0.15	0.61	39
5.89	2	835	1	0.59	10.85	0.18	1.13	32
1.2	1	87.4	0.4	0.16	4.9	0.08	5.45	42
4.74	1	809	0.6	0.36	5.47	0.15	1.09	101
20.5	2	1005	2.4	1.75	21.5	0.44	5.64	564
22	2	1755	2	1.56	21.8	0.28	4.03	430

5.5	145	14	650	10.5	0.125	0.335	0.8	0.013
ME-MS81	ME-MS81	ME-MS81	ME-MS81	ME-MS42	ME-MS42	ME-MS42	ME-MS42	ME-MS42
W	Y	Yb	Zr	As	Bi	Hg	In	Re
ppm	ppm	ppm	ppm	ppm	ppm	ppm	ppm	ppm
1	20	2.18	204	1.4	0.08	0.017	0.028	<0.001
1	12.9	1.29	89	11.8	0.14	0.009	0.02	<0.001
9	7.3	0.66	79	119.5	0.03	0.039	0.019	0.001
2	214	14.95	21	49.6	0.46	0.027	0.102	0.001
1	3.1	0.32	4	0.6	0.03	0.012	0.012	<0.001
1	39.7	4.53	154	0.8	0.02	0.005	0.015	<0.001
<1	1.7	0.26	43	0.2	0.01	<0.005	0.007	<0.001
3	3.7	0.19	<2	6.8	0.09	0.036	0.009	<0.001
31	3.7	1.28	353	>250	1.1	0.239	0.033	0.002
5	102.5	12.55	>10000	2.7	0.18	0.049	0.216	0.001
7	12.1	2.04	27	23.8	0.18	0.027	0.392	<0.001
1	8.2	0.92	119	3.2	0.05	0.016	0.022	0.001
1	6.6	0.7	173	1.7	0.05	0.016	0.011	0.001
3	6.9	0.97	278	45.1	0.14	0.037	0.007	0.005
5	19.3	2.67	516	64.5	0.18	0.017	0.028	0.013
2	8.9	1.24	279	21.6	0.12	0.023	0.005	0.005
2	11.5	1.69	557	7.4	0.22	0.013	0.008	0.001
3	6.3	1.08	513	4.6	0.33	0.027	0.005	0.006
3	22.4	2.87	469	2.4	0.23	0.014	0.005	0.001
<1	0.8	0.06	22	3	0.01	0.023	<0.005	<0.001
1	23.6	2.42	210	0.6	0.15	<0.005	0.034	<0.001
61	22	2.31	173	51.5	0.17	0.017	0.025	0.001
1	8.9	0.75	178	16.7	0.07	0.01	0.012	0.003
4	4.2	0.57	56	19.3	0.05	0.009	0.015	0.001
2	11.9	1.2	148	7.5	0.05	<0.005	0.005	<0.001
1	39	2.28	37	4.1	0.02	0.007	0.005	0.001
2	5.8	0.49	52	2.6	0.05	<0.005	0.009	<0.001
126	3	0.2	8	>250	>250	0.013	2.16	0.001
1	11.7	0.55	5	46.2	0.68	0.007	0.014	0.001
1	7.2	0.49	23	12	0.21	<0.005	0.009	0.001

ME-MS81 W ppm	ME-MS81 Y ppm	ME-MS81 Yb ppm	ME-MS81 Zr ppm	ME-MS42 As ppm	ME-MS42 Bi ppm	ME-MS42 Hg ppm	ME-MS42 In ppm	ME-MS42 Re ppm
1	14.9	1.76	64	5.5	0.04	0.006	0.012	<0.001
<1	11.7	1.27	375	0.4	0.01	0.006	0.008	<0.001
<1	10.7	1.09	41	0.1	0.01	<0.005	<0.005	<0.001
1	2.9	0.36	176	0.5	0.01	0.006	<0.005	<0.001
1	0.8	0.19	12	0.1	<0.01	0.008	<0.005	<0.001
1	47.9	4.86	44	1.3	0.03	0.013	<0.005	<0.001
<1	8.8	0.94	25	3.6	0.02	0.009	0.006	<0.001
1	81.6	6.34	633	1.1	0.03	0.009	0.036	<0.001
1	127.5	12.95	1085	1.1	0.06	0.009	0.134	<0.001
<1	9.3	1.09	40	0.1	0.01	<0.005	<0.005	<0.001
<1	227	19.75	50	2.5	0.03	0.007	0.067	<0.001
<1	45.7	3.09	242	0.1	0.02	<0.005	0.038	<0.001
<1	6.5	0.94	113	0.3	0.08	<0.005	<0.005	<0.001
1	1.3	0.48	7	4.4	0.03	0.01	<0.005	0.001
33	0.7	0.04	7	>250	>250	0.057	0.109	0.001
1	1	0.05	7	>250	2.71	<0.005	<0.005	<0.001
1	12.1	1.29	42	41.3	31	<0.005	<0.005	<0.001
1	1	0.08	12	>250	2.2	0.012	<0.005	<0.001
1	8.2	0.88	185	36.1	0.31	0.005	<0.005	<0.001
1	5.1	0.45	23	20.5	0.19	0.007	<0.005	<0.001
2	17.2	1.99	97	83.9	0.68	<0.005	0.016	<0.001
4	1.9	0.26	8	157.5	4.05	0.011	0.048	0.001
2	1.2	0.08	2	24.4	0.25	0.006	0.005	<0.001
1	0.8	0.09	<2	78.5	0.5	<0.005	<0.005	<0.001
8	29.3	2.62	205	5.1	0.04	0.006	<0.005	<0.001
<1	2.1	0.15	15	4	0.19	<0.005	<0.005	<0.001
1	23.8	3.02	152	4.7	0.56	0.007	0.067	<0.001
9	3.3	0.34	2	103	0.14	<0.005	<0.005	<0.001
6	22.3	2.42	192	3	0.07	<0.005	0.011	<0.001
5	2.5	0.25	21	98.4	2.76	0.013	0.45	0.01
18	34.7	3.17	49	152.5	8.03	0.018	0.366	0.002
1	38.1	2.49	15	21.1	0.37	<0.005	0.077	0.005
1	49.4	5.43	17	5.9	0.07	<0.005	0.095	<0.001
1	14.1	2.14	117	2.4	0.05	<0.005	0.007	<0.001
<1	1.2	0.22	55	1.4	0.02	<0.005	<0.005	<0.001
<1	14.9	1.41	47	7.4	0.06	<0.005	0.008	<0.001
<1	1.1	0.17	8	1.3	0.01	0.005	0.009	<0.001
<1	48.3	3.26	43	1.5	0.03	<0.005	0.047	<0.001
1	5.2	0.66	26	1.8	0.02	0.007	0.005	<0.001
8	67.5	10.9	6	3.4	0.28	0.008	0.006	<0.001
1	4.3	0.65	4	2.1	0.15	0.005	0.006	<0.001
1	8.5	0.58	68	3.6	0.12	0.034	0.007	<0.001
4	12.2	1.36	166	3.8	0.14	0.007	0.012	<0.001
1	13.5	0.93	3	3.7	0.02	0.059	<0.005	<0.001
2	5.7	0.52	60	4.6	0.04	0.036	0.008	<0.001
9	<0.5	<0.03	32	16.4	0.79	<0.005	<0.005	<0.001
16	0.7	0.07	20	>250	0.55	0.009	0.576	<0.001
1	<0.5	<0.03	9	18.6	0.33	0.005	<0.005	<0.001

1	<0.5	<0.03	2	5.9	11	<0.005	<0.005	<0.001
9	3.3	0.25	19	4.5	0.04	<0.005	<0.005	<0.001
1	17.4	1.49	81	110	0.04	0.007	0.009	0.002
<1	10.8	0.67	30	2.1	0.1	0.019	0.006	<0.001
2	14.7	1.9	219	5.8	0.25	0.079	0.032	<0.001
1	26	2.18	100	38.7	0.16	0.046	0.016	<0.001
2	48.1	3.82	211	7.8	0.28	0.037	0.028	0.001
1	44.4	3.9	199	1.9	0.16	0.034	0.029	<0.001
1	35.8	2.04	97	9.7	0.1	0.044	0.013	0.001
1	19.6	1.82	195	11	0.1	0.075	0.02	<0.001
1	4.1	0.3	99	0.9	0.02	<0.005	0.008	<0.001
1	11.7	1.13	39	1.8	0.04	0.006	0.01	<0.001
<1	0.6	<0.03	7	0.3	0.01	<0.005	<0.005	<0.001
<1	4.8	0.36	46	0.5	0.01	<0.005	0.005	<0.001
<1	38.6	3.97	263	1.5	0.03	0.005	0.021	<0.001
3	5.7	0.83	320	2.3	0.06	<0.005	<0.005	<0.001
1	62.1	6.67	178	0.8	0.03	<0.005	0.026	<0.001
2	5.2	0.43	29	12.6	1.05	0.006	0.043	0.001
2	35.9	4.02	648	1.6	0.04	<0.005	0.043	<0.001
<1	0.8	0.06	12	0.4	0.01	<0.005	<0.005	<0.001
1	29.8	1.97	425	1.1	0.04	<0.005	0.009	<0.001
<1	19.7	1.51	313	0.2	0.02	<0.005	0.018	<0.001
<1	1.2	0.14	132	0.2	0.01	0.008	0.03	<0.001
<1	0.6	0.03	5	0.5	0.01	<0.005	<0.005	<0.001
1	<0.5	<0.03	4	1.6	0.01	0.118	<0.005	<0.001
33	26.2	1.85	16	148	0.05	0.434	0.039	<0.001
11	2.1	0.29	4	84.2	0.01	0.309	0.014	0.001
2	22.8	2.36	289	2.8	0.13	0.011	0.027	<0.001
1	29.2	2.62	241	2	0.08	<0.005	0.036	<0.001
2	27.7	3.38	490	2.5	0.44	<0.005	0.013	<0.001
1	2.4	0.17	796	8.4	1.75	0.006	<0.005	0.001
2	26.3	2.13	257	2.4	0.32	<0.005	0.027	<0.001

ME-MS81 W	ME-MS81 Y	ME-MS81 Yb	ME-MS81 Zr	ME-MS42 As	ME-MS42 Bi	ME-MS42 Hg	ME-MS42 In	ME-MS42 Re
ppm	ppm	ppm	ppm	ppm	ppm	ppm	ppm	ppm
2	22.6	2.17	137	9.9	0.29	0.066	0.029	0.002
1	10.4	1.16	90	5	0.23	0.056	0.02	0.008
2	27.2	2.93	297	0.9	0.22	0.018	0.014	<0.001
1	8.7	0.96	105	3.1	0.1	<0.005	0.033	<0.001
2	65.5	3.21	61	9.5	0.19	<0.005	0.288	<0.001
4	32.2	3.43	113	5.8	1.7	<0.005	0.06	0.001
4	21.9	3.26	265	>250	0.07	0.021	0.043	0.023
3	10.2	1.17	162	>250	0.03	0.068	0.053	0.006
<1	1.6	0.18	18	4.1	0.01	<0.005	<0.005	<0.001
1	39.4	3.59	20	10.3	0.15	<0.005	<0.005	<0.001
2	138.5	13.7	13	9.8	0.55	0.006	0.006	<0.001
2	8.9	0.83	79	15	1.22	<0.005	0.011	<0.001

2	9.2	1.01	12	71.7	3.79	<0.005	0.338	0.001
1	7.8	0.62	358	3.8	0.62	<0.005	<0.005	<0.001
1	36.8	9.04	35	1.9	0.75	<0.005	<0.005	<0.001
4	4.8	0.35	19	95.4	1.25	<0.005	<0.005	<0.001
16	18.2	0.65	5	>250	>250	0.015	0.021	0.001
2	24.5	2.59	235	83.3	0.68	<0.005	0.022	0.001
1	13.9	1.3	22	146.5	0.81	0.005	0.009	<0.001
<1	3.4	0.25	58	>250	2.42	<0.005	<0.005	<0.001
1	0.8	0.05	4	34.3	0.11	<0.005	<0.005	<0.001
1	4.5	0.23	39	128	0.34	<0.005	0.03	<0.001
1	2.8	0.19	30	46.6	0.39	<0.005	<0.005	<0.001
11	0.7	0.05	4	229	0.29	<0.005	<0.005	<0.001
1	<0.5	<0.03	2	>250	>250	<0.005	0.079	0.004
1	25.7	4.05	28	>250	1.79	<0.005	<0.005	<0.001
1	11.7	0.58	17	139.5	0.26	0.041	<0.005	0.001
2	26.1	3.07	662	>250	8.39	0.042	<0.005	<0.001
<1	13	1.28	77	27.4	0.16	<0.005	0.025	<0.001
<1	5.1	0.46	183	9.4	0.05	<0.005	<0.005	<0.001
<1	26.4	3.04	108	80.2	0.52	<0.005	0.018	<0.001
1	4.1	0.24	20	11.1	0.11	0.013	0.009	0.004
2	12.7	1.71	130	26.5	0.32	0.119	0.047	0.001
1	39.2	5.92	188	64.6	0.22	0.188	0.018	0.001
1	10.2	1.02	6	11.6	0.1	<0.005	0.017	<0.001
<1	17.1	1.88	134	5.2	0.03	<0.005	<0.005	<0.001
<1	23.1	2.52	86	18.7	0.1	0.006	0.009	<0.001
<1	20.4	2.28	40	4.1	0.06	<0.005	0.018	<0.001
1	24.5	2.05	326	2.1	0.03	<0.005	<0.005	<0.001
2	12.8	1.66	486	69.1	0.08	<0.005	0.019	<0.001
1	25.7	1.74	156	2.4	0.03	0.005	0.005	<0.001
<1	9.1	1.14	276	1.8	0.02	<0.005	0.011	<0.001
<1	8.4	0.68	30	2.1	0.03	<0.005	<0.005	<0.001
<1	46.7	2.8	90	1.7	0.03	<0.005	0.059	<0.001
1	3.7	0.43	55	1	0.04	<0.005	<0.005	<0.001
1	20.1	2.14	81	>250	0.05	0.005	0.013	<0.001
1	5.5	0.7	59	31.7	0.05	<0.005	0.01	<0.001
1	12.1	1.63	145	86.6	0.07	0.065	0.032	0.002
6	0.6	0.06	4	1.7	0.78	0.005	<0.005	<0.001
4	24.3	3.04	46	1.9	24.6	<0.005	<0.005	<0.001
<1	0.9	<0.03	2	1.4	6.03	<0.005	<0.005	<0.001
12	3.2	0.27	7	2	1.12	<0.005	0.006	<0.001
2	5.7	0.12	23	1	0.75	<0.005	<0.005	<0.001
1	1.4	0.06	14	1.1	1.83	<0.005	<0.005	<0.001
1	<0.5	<0.03	2	1.4	2.07	<0.005	<0.005	<0.001
1	42.8	3.84	236	133.5	0.15	0.038	0.012	0.002
2	12.5	1.12	69	0.9	0.62	0.008	0.018	<0.001
8	27.4	3.07	158	0.9	1.65	0.054	0.044	<0.001
1	54.4	4.27	19	1.6	0.24	0.014	0.006	<0.001
1	7.1	0.68	113	4.1	0.12	<0.005	0.01	<0.001
1	6.1	0.9	179	3.1	0.09	0.007	0.014	<0.001
1	9.8	0.98	141	1.1	0.06	0.007	0.02	<0.001
1	18.6	1.69	326	0.8	0.08	<0.005	0.02	<0.001
1	22.9	2.32	182	0.5	0.03	<0.005	0.009	<0.001
1	12.9	0.93	365	3.6	0.13	0.01	<0.005	0.006
5	41.3	5.31	249	25.3	0.66	0.008	0.514	0.001
1	25.4	3.5	14	3	0.14	<0.005	0.019	<0.001
1	27.6	3.92	77	3.1	0.06	0.005	0.047	<0.001

3	164	19.95	145	86.3	6.15	0.026	0.071	<0.001
1	493	56.8	537	4.4	0.24	0.007	0.068	<0.001
2	56.3	5.9	79	1.4	0.04	<0.005	0.005	<0.001
<1	3.7	0.32	47	0.8	0.05	<0.005	<0.005	<0.001
2	85.8	6.15	132	1.8	0.09	<0.005	0.138	<0.001
1	26.9	1.53	153	20.1	0.45	0.006	0.065	<0.001
3	36.1	1.93	45	15.1	0.08	0.009	0.017	<0.001
1	7.7	0.86	228	1	0.05	<0.005	0.007	<0.001
<1	13.9	1.7	54	1.3	0.02	<0.005	0.011	0.001
<1	8.8	1.03	152	0.5	0.01	<0.005	<0.005	<0.001
13	3	0.47	39	6.1	2.96	<0.005	<0.005	<0.001
<1	3.5	0.49	91	3.1	0.04	<0.005	<0.005	0.001
<1	21.6	2.01	4	5.7	0.04	<0.005	<0.005	0.001
2	39.4	4.14	255	14.3	0.26	0.005	0.041	<0.001
<1	2.5	0.2	13	0.8	0.02	<0.005	<0.005	<0.001
1	8.3	1.21	303	5.2	0.05	<0.005	0.01	<0.001
2	430	32.8	322	2.8	0.22	0.017	0.034	0.002
2	51.3	5.07	230	1	0.3	<0.005	0.072	<0.001
1	11.8	1.3	214	74.3	0.03	0.01	0.016	0.001
1	8	1.37	829	1	0.03	<0.005	<0.005	<0.001
1	34.1	2.59	720	>250	0.05	1.64	0.006	0.001
<1	2.7	0.51	160	23.3	0.02	<0.005	<0.005	<0.001
3	28.3	2.77	742	31.5	0.05	<0.005	0.037	<0.001
1	21.1	2.45	264	7.1	0.03	<0.005	0.017	0.001
1	53.8	5.58	433	1.2	0.06	<0.005	0.049	<0.001
2	46.5	5.27	248	2.5	0.08	<0.005	0.051	<0.001
<1	5.9	0.62	23	1.8	0.02	<0.005	<0.005	<0.001
1	10.5	1.08	23	2.9	0.03	<0.005	0.008	<0.001
1	15.3	1.65	149	1.7	0.03	<0.005	0.018	0.001
1	15.7	2.01	207	2.3	0.07	<0.005	0.025	0.001
30	12.2	1.73	12	>250	0.01	0.06	0.117	0.001
1	13.7	1.84	69	>250	0.05	0.007	0.101	<0.001
1	13.1	1.55	93	13.4	0.04	<0.005	0.008	<0.001
24	16.9	2.16	39	>250	0.33	0.421	0.022	0.001
45	12.9	1.61	57	17.3	0.21	<0.005	0.026	<0.001
5	9.8	1.05	19	63.8	0.1	0.023	0.01	<0.001
5	41.6	4.52	202	7.1	0.15	<0.005	0.089	<0.001
1	27.6	4.4	1625	1.6	0.01	<0.005	0.047	<0.001
1	<0.5	0.07	5	>250	34.2	0.066	0.099	<0.001
<1	21.7	2.21	26	3.3	0.17	<0.005	0.02	<0.001
6	49.2	4.39	68	83.2	0.17	0.037	0.02	<0.001
2	22	2.13	65	5.4	0.03	0.006	0.015	<0.001
<1	12.6	1.55	100	3.9	0.03	0.008	0.009	<0.001
1	23.5	2.87	126	3.3	0.03	<0.005	0.011	<0.001
<1	16.6	3.51	55	1.7	0.03	0.005	0.007	<0.001
<1	25	2.34	46	2.3	0.27	<0.005	0.007	<0.001
1	73.2	25.4	188	4.8	0.1	0.006	<0.005	<0.001
7	1.9	0.19	14	>250	0.3	0.009	<0.005	0.001
3	105	13.75	58	4.2	0.1	<0.005	0.01	<0.001
1	168	40.2	190	6.5	0.05	<0.005	<0.005	<0.001
2	21.1	2.82	162	29.6	0.09	<0.005	0.028	<0.001
<1	127.5	21.1	63	2.1	0.05	<0.005	<0.005	<0.001
1	29.7	5.88	558	2.8	0.03	0.006	0.005	<0.001
1	1.9	0.26	17	13.4	0.01	<0.005	<0.005	<0.001
1	350	110	46	2.1	0.01	<0.005	<0.005	0.001
<1	19.3	2.19	146	5.3	0.01	<0.005	0.02	<0.001

1	6.3	0.68	4	16.4	0.04	0.005	<0.005	<0.001
1	13.3	1.18	5	54.6	0.02	0.01	<0.005	<0.001
<1	2.7	0.17	2	1.1	0.01	<0.005	<0.005	<0.001
2	65.2	5.65	58	5.9	0.49	0.005	<0.005	<0.001
<1	28.3	5.99	34	1.2	0.04	<0.005	<0.005	<0.001
1	7.6	0.88	22	1.9	0.03	0.005	0.007	<0.001
3	8.4	0.92	46	4.8	2.07	0.011	0.025	0.001
1	6.8	0.63	15	34.4	0.92	0.014	0.037	0.015
1	5.2	0.89	98	21.3	0.19	0.01	0.081	<0.001
3	37.1	4.16	76	2.1	0.13	<0.005	0.037	<0.001
1	0.9	0.13	7	0.4	0.01	<0.005	<0.005	<0.001
1	44.8	5.77	65	1.3	0.03	0.007	0.022	<0.001
1	21.5	2.39	65	1.9	0.55	<0.005	0.02	<0.001
1	24.4	2.69	73	0.8	0.7	0.023	0.039	<0.001
<1	65.8	6.95	917	0.7	0.01	<0.005	0.034	<0.001
<1	1.7	0.19	178	0.5	0.01	<0.005	<0.005	<0.001
<1	5.6	0.25	75	0.1	0.01	<0.005	0.011	<0.001
<1	0.6	0.04	16	0.1	0.01	<0.005	<0.005	<0.001
3	3.3	0.29	19	6.1	0.09	<0.005	0.019	<0.001
10	23.7	3.06	36	>250	0.04	0.041	0.071	<0.001
3	3.1	0.29	34	96.8	4.21	0.051	2.27	0.001
26	22.2	1.72	67	>250	16.45	0.128	0.869	0.001
4	202	7.92	197	70.2	0.23	0.083	0.023	0.002
4	15.5	1.85	314	11.8	0.12	0.011	0.015	<0.001

ME-MS81	ME-MS81	ME-MS81	ME-MS81	ME-MS42	ME-MS42	ME-MS42	ME-MS42	ME-MS42
W	Y	Yb	Zr	As	Bi	Hg	In	Re
ppm	ppm	ppm	ppm	ppm	ppm	ppm	ppm	ppm
1	129.5	4.35	76	13.6	0.19	0.047	0.031	0.002
10	525	18.2	145	67.2	0.06	0.119	0.017	0.003
1	310	10.9	164	6.6	0.04	0.174	0.013	0.073
<1	790	27.3	64	5.8	0.02	0.261	0.008	0.093
6	32	2.86	376	35.6	0.2	0.253	0.021	0.155

ME-MS81	ME-MS81	ME-MS81	ME-MS81	ME-MS42	ME-MS42	ME-MS42	ME-MS42	ME-MS42
W	Y	Yb	Zr	As	Bi	Hg	In	Re
ppm	ppm	ppm	ppm	ppm	ppm	ppm	ppm	ppm
1	5.2	0.54	71	8.7	0.02	0.006	<0.005	<0.001
1	5.7	0.76	274	7	0.02	0.005	<0.005	<0.001

1	3.5	0.33	<2	41.4	2.06	0.006	<0.005	<0.001
25	5	0.48	2	184.5	4.24	0.038	0.024	0.001
9	44.6	5.21	6	196.5	0.13	0.084	0.086	0.001
2	11.2	1.53	255	13.8	3.46	0.013	0.011	<0.001
1	4.6	0.58	5	12.1	0.08	0.005	0.139	<0.001
1	<0.5	<0.03	<2	2.8	0.1	<0.005	0.009	<0.001
1	3.4	0.36	12	1.2	1.05	0.012	0.006	<0.001
1	<0.5	<0.03	2	6.6	0.24	0.005	<0.005	0.001
<1	8.9	0.94	29	0.3	0.01	<0.005	0.006	0.001
<1	4.3	0.42	10	0.2	0.01	0.007	<0.005	<0.001
1	8.5	0.87	123	0.9	0.03	0.006	0.016	<0.001
95	1.8	0.2	4	14.5	1.38	<0.005	0.897	<0.001
3	11.4	1.47	40	1	0.18	0.005	0.028	<0.001
1	34.9	3.34	371	0.4	0.03	<0.005	0.028	<0.001
3	229	22.8	3670	1.5	0.17	0.012	0.194	0.002
3	3.5	0.3	6	19.8	>250	0.046	0.038	<0.001
3	54.4	8	1180	1.7	0.75	0.01	0.15	<0.001
2	40.5	4.35	273	1.4	0.36	0.007	0.041	<0.001
1	36.4	3	62	0.8	0.81	<0.005	0.079	0.001
2	63.9	6.23	390	0.5	0.11	<0.005	0.046	<0.001
2	61.5	5.35	724	0.9	0.11	0.006	0.066	<0.001
1	32.1	4.48	121	0.7	0.53	0.01	0.025	<0.001
1	3	0.42	10	0.3	0.06	<0.005	<0.005	<0.001
1	54.8	5.9	846	0.8	0.07	0.008	0.051	<0.001
1	2.6	0.31	57	30.6	0.16	0.008	0.136	0.001
5	6.5	0.89	30	47.8	5.18	0.019	0.052	0.016
4	20.1	2.68	132	23.9	0.47	0.041	0.028	0.003
2	5.9	0.74	70	8.4	0.65	0.044	0.03	0.024
3	9.5	0.94	128	1	2.4	0.014	0.056	0.057
1	17.2	2.23	56	4.1	0.16	0.011	0.024	0.003
2	17.3	1.7	232	10.5	0.14	0.043	0.025	<0.001
1	3	0.58	180	10.6	0.32	0.028	0.038	0.014
2	8.1	1.1	194	8.4	0.34	0.013	0.054	0.001
1	11.2	1.3	341	4.4	0.07	0.014	0.01	<0.001
8	182	32.2	>10000	0.3	0.32	0.033	0.235	<0.001
2	18.1	1.87	352	8.8	0.09	0.006	0.018	0.02
3	42.8	3.49	164	29.2	0.54	0.056	0.041	0.008
1	15.6	1.86	281	8.4	0.19	0.015	0.023	0.02
1	41	3.62	108	9.6	0.29	0.013	0.029	0.005
2	20.2	1.79	148	84	2.26	0.008	0.045	0.006
2	15.2	1.47	103	14.2	0.1	0.009	0.013	0.024
2	24.6	2.15	120	11.3	0.07	0.008	0.015	0.019
1	15.2	1.53	105	2.1	0.08	0.012	0.015	0.001
1	25.3	2.02	147	11.1	0.35	0.011	0.022	0.001
1	2.8	0.13	13	0.2	0.06	0.016	<0.005	<0.001
6	5.4	0.85	166	1.4	0.05	0.037	<0.005	<0.001
33	3.6	0.54	216	3.5	0.11	0.012	<0.005	<0.001
47	7.3	1.17	459	1.4	0.12	0.01	<0.005	<0.001
1	8.6	0.49	7	2.2	0.02	0.011	<0.005	<0.001
2	13.3	1.45	288	1.1	0.14	0.021	0.012	<0.001
1	8.4	0.86	269	3.8	0.03	0.029	0.063	<0.001
<1	10.8	0.9	157	0.5	0.05	0.005	0.01	<0.001
1	1.5	0.15	39	0.1	0.01	<0.005	<0.005	<0.001
1	18.9	2.23	140	0.3	0.03	0.005	0.005	<0.001
<1	0.5	0.04	7	1.3	0.03	0.006	<0.005	0.001
<1	151	5.9	95	19.9	0.05	0.185	0.01	0.003

6	207	7.89	151	111	0.15	0.066	0.017	0.002
1	19.5	1.02	33	4.5	0.05	0.018	0.015	0.001
1	21.7	2.23	185	1.5	0.2	<0.005	0.017	<0.001
1	23.3	2.26	243	0.9	0.15	0.006	0.019	<0.001
1	21.6	2.27	211	1.3	0.07	0.005	0.023	<0.001

ME-MS81	ME-MS81	ME-MS81	ME-MS81	ME-MS42	ME-MS42	ME-MS42	ME-MS42	ME-MS42
W	Y	Yb	Zr	As	Bi	Hg	In	Re
ppm	ppm	ppm	ppm	ppm	ppm	ppm	ppm	ppm
2	47	4.75	327	1.7	0.44	0.017	0.022	<0.001
<1	43.6	8.69	407	10.8	0.57	0.02	0.061	0.012
1	70.5	6.35	384	7.7	0.36	0.014	0.054	0.001
1	12.7	1.29	239	2	0.09	0.015	0.021	<0.001
1	29.5	3.29	331	2.5	0.09	0.016	0.04	<0.001
1	24.3	2.53	312	2.9	0.09	0.014	0.029	0.001
1	15.6	1.61	236	3.2	0.14	0.009	0.023	0.001
1	20.5	3.65	417	4.3	0.07	0.007	0.026	<0.001
<1	8.7	1.01	208	5.4	0.12	0.007	0.024	0.001
1	15.4	2.06	289	4	0.11	0.007	0.028	0.015
1	25.4	2.55	164	2.1	0.08	0.008	0.028	0.001
1	9.9	1.1	90	0.6	0.02	0.007	0.006	<0.001
<1	16.7	1.63	165	1.9	0.14	0.116	0.024	<0.001
1	7.6	0.64	172	2.5	0.49	0.012	0.014	<0.001
3	6.8	0.59	229	<0.1	0.14	0.012	0.037	<0.001
2	13.5	0.85	230	14.8	0.29	0.017	0.076	0.009
1	12.5	0.84	214	0.3	0.28	0.01	0.068	0.003
2	13.4	1.26	155	0.2	0.16	0.01	0.023	<0.001
2	5.7	0.47	52	3	0.07	0.041	0.016	<0.001
2	10	0.91	142	0.1	<0.01	0.014	0.01	<0.001
27	38.4	2.68	394	15.3	0.7	0.015	0.089	0.002
30	23.1	1.55	278	5.2	0.79	0.048	0.026	0.001

1	0.25	0.005	2.65			0.4	0.75	150
ME-MS42	ME-MS42	ME-MS42	ME-MS42	OA-GRA05	TOT-ICP06	ME-4ACD8	ME-4ACD8	ME-4ACD8
Sb	Se	Te	Tl	LOI	Total	Ag	Cd	Co
ppm	ppm	ppm	ppm	%	%	ppm	ppm	ppm
0.12	0.2	0.01	0.04	1.06	99.89	<0.5	<0.5	4
0.39	0.3	0.08	0.22	3.28	101.27	<0.5	<0.5	12
5.89	0.4	0.01	0.05	1.02	99.73	1.5	0.7	17
13.5	7.7	0.02	0.04	1.38	99.92	<0.5	42.6	10
0.09	<0.2	0.11	<0.02	0.63	99.17	<0.5	<0.5	28
0.09	0.3	0.01	0.02	1.52	99.23	<0.5	<0.5	2
0.07	<0.2	0.01	0.06	3.52	98.43	<0.5	<0.5	<1
0.55	<0.2	0.04	0.03	2.32	100.14	<0.5	<0.5	4
1.33	2.2	0.4	0.57	4.22	100.92	<0.5	0.7	1
0.38	1.3	0.01	0.02	12.8	96.97	<0.5	2.1	85
0.09	<0.2	<0.01	0.02	10.25	99.31	<0.5	0.6	31
0.06	0.2	0.01	0.07	11.2	99.94	<0.5	<0.5	3
0.16	0.4	<0.01	0.06	25.5	98.4	<0.5	<0.5	1
0.14	17	0.02	1.18	5.27	100.77	<0.5	<0.5	<1
0.21	5.4	0.03	0.19	10.3	100.88	<0.5	<0.5	2
0.11	2.8	0.01	0.1	4.92	101.31	<0.5	<0.5	<1
0.1	<0.2	0.01	0.05	2.52	101.2	<0.5	<0.5	<1
0.17	<0.2	0.02	0.03	4.86	101.11	<0.5	<0.5	<1
0.1	0.8	0.05	0.38	8.01	101.23	<0.5	<0.5	2
0.17	<0.2	0.02	0.04	8.78	100.58	<0.5	<0.5	1
0.07	0.4	0.01	0.12	7.2	100.11	<0.5	<0.5	6
2.07	1.6	0.05	0.28	2.57	100.71	<0.5	<0.5	6
0.51	1.9	<0.01	0.22	2.95	101.6	<0.5	<0.5	2
1.94	<0.2	0.09	0.02	2.37	101.09	<0.5	<0.5	5
0.15	<0.2	<0.01	0.06	1.17	100.43	<0.5	<0.5	<1
0.12	0.4	0.01	0.02	33.2	98.85	<0.5	<0.5	<1
0.09	<0.2	0.02	0.02	1.31	99.01	<0.5	<0.5	9
19.35	3	0.4	0.02	1.9	96.39	1.8	1.9	3
0.08	<0.2	<0.01	<0.02	42.2	99.99	<0.5	<0.5	<1
0.2	0.7	0.01	0.02	7.3	99.91	<0.5	<0.5	3

ME-MS42	ME-MS42	ME-MS42	ME-MS42	OA-GRA05	TOT-ICP06	ME-4ACD8:	ME-4ACD8:	ME-4ACD8:
Sb	Se	Te	Tl	LOI	Total	Ag	Cd	Co
ppm	ppm	ppm	ppm	%	%	ppm	ppm	ppm
1.14	0.3	0.02	0.03	2.08	98.06	<0.5	0.5	48
0.12	<0.2	0.01	<0.02	0.9	99.17	<0.5	<0.5	2
0.09	<0.2	<0.01	0.02	2.43	98.54	<0.5	<0.5	4
0.05	<0.2	<0.01	0.04	3.02	98.91	<0.5	<0.5	1
0.05	<0.2	<0.01	<0.02	2.52	99.67	<0.5	<0.5	17
0.06	0.2	0.09	0.02	1.7	98.47	<0.5	<0.5	4
0.05	<0.2	<0.01	<0.02	3.62	101.18	<0.5	<0.5	57
0.08	1.3	<0.01	<0.02	1.66	98.07	<0.5	<0.5	2
0.16	2.3	0.01	<0.02	1.74	99.56	<0.5	<0.5	1
0.1	<0.2	0.02	<0.02	1.08	99.8	<0.5	<0.5	2
0.09	1.6	<0.01	<0.02	3.38	98.28	<0.5	<0.5	4
0.05	0.2	<0.01	<0.02	1.66	98.25	<0.5	<0.5	<1
<0.05	<0.2	<0.01	0.04	3.58	98.69	<0.5	<0.5	1
0.24	<0.2	0.02	<0.02	1.88	98.41	<0.5	<0.5	32
83.7	19.1	5.4	0.03	18.9	99.05	3.8	0.6	19
0.35	<0.2	0.02	0.11	0.34	98.94	<0.5	<0.5	<1
0.14	<0.2	0.02	0.05	0.4	99.36	<0.5	<0.5	1
0.34	0.2	0.04	0.02	22.9	98.51	<0.5	<0.5	1
0.12	0.2	0.01	0.04	0.92	99.78	<0.5	<0.5	9
0.08	<0.2	0.01	<0.02	0.76	100.68	<0.5	<0.5	3
0.26	0.4	0.07	0.09	4.17	100.13	<0.5	0.5	35
0.85	8.7	2.57	0.03	2.12	99.22	<0.5	<0.5	35
0.31	0.5	0.07	0.05	0.3	100.02	<0.5	<0.5	8
0.11	<0.2	0.01	<0.02	0.13	99.87	<0.5	<0.5	1
0.07	0.6	0.01	0.1	2.37	99.2	<0.5	<0.5	<1
0.07	<0.2	<0.01	<0.02	0.96	97.34	<0.5	<0.5	5
<0.05	0.6	0.02	2.28	7.43	98.96	<0.5	<0.5	59
0.36	<0.2	<0.01	<0.02	1.2	100.3	<0.5	<0.5	5
0.1	0.2	0.01	<0.02	1.76	100.18	<0.5	<0.5	6
0.44	3.9	0.69	<0.02	13.85	99.09	1.2	0.9	32
0.71	2.4	2.53	0.1	11.2	98.34	1.1	5.4	218
0.08	1.1	0.15	0.02	3.37	100.88	<0.5	<0.5	27
0.14	0.9	0.03	0.04	1.34	99.04	<0.5	<0.5	13
0.06	0.2	0.03	0.07	2.42	99.48	<0.5	<0.5	38
<0.05	<0.2	0.01	0.03	2.77	99.92	<0.5	<0.5	2
0.09	<0.2	<0.01	<0.02	1.68	98.47	<0.5	<0.5	1
<0.05	<0.2	<0.01	<0.02	8.5	99.14	<0.5	<0.5	63
0.08	0.4	<0.01	<0.02	1.61	99.48	<0.5	<0.5	2
0.05	<0.2	<0.01	<0.02	5.1	99.9	<0.5	<0.5	11
0.12	1	0.01	0.05	0.54	100.63	<0.5	<0.5	<1
0.06	0.3	<0.01	0.03	0.54	100.24	<0.5	<0.5	<1
0.09	0.4	0.01	1.02	36.9	100.25	<0.5	0.5	3
0.43	0.3	<0.01	0.14	1.21	101.34	<0.5	<0.5	3
0.08	0.4	<0.01	0.08	43.2	100.38	<0.5	1	<1
0.13	0.3	0.01	0.06	31	100.05	0.7	<0.5	1
1.82	<0.2	0.02	0.26	0.55	98.96	<0.5	<0.5	<1
3.15	2.9	0.09	0.08	2.52	101.48	<0.5	1	15
4.7	<0.2	0.01	0.16	0.47	100.38	<0.5	<0.5	1

1.95	<0.2	0.01	0.05	0.14	101.66	<0.5	<0.5	<1
0.11	<0.2	<0.01	0.07	0.44	101.92	<0.5	<0.5	<1
0.57	1.1	<0.01	0.08	13.95	100.27	<0.5	<0.5	6
0.13	0.4	0.01	0.09	39.5	99.51	<0.5	3	1
0.27	0.4	0.03	0.29	8.3	100.73	<0.5	<0.5	8
0.9	1.4	0.06	0.08	26.4	99.37	<0.5	5.3	12
0.58	2.5	0.01	0.37	17.05	99.13	<0.5	<0.5	16
0.16	1.1	0.02	0.15	14.55	100.72	<0.5	<0.5	7
0.72	4.7	0.03	0.1	19.75	99.41	<0.5	1.3	31
0.11	0.7	0.01	0.13	8.76	101.54	<0.5	<0.5	11
0.15	0.3	<0.01	0.02	1.05	100.29	<0.5	<0.5	3
0.09	0.2	0.01	0.04	1.76	96.89	<0.5	<0.5	68
0.07	<0.2	0.01	0.04	0.55	98.4	<0.5	<0.5	2
<0.05	0.2	<0.01	0.04	0.42	100.17	<0.5	<0.5	1
0.09	0.5	0.01	0.07	3.02	98.05	<0.5	<0.5	47
0.14	0.6	0.01	0.03	1.26	98.94	<0.5	<0.5	6
0.07	2	0.01	0.03	0.81	98.13	<0.5	<0.5	1
0.17	3.3	0.26	0.22	7.48	99.01	<0.5	<0.5	40
0.06	0.8	0.01	0.06	0.3	98.8	<0.5	<0.5	3
<0.05	<0.2	0.01	<0.02	2.32	99.31	<0.5	<0.5	7
0.08	1.1	0.01	<0.02	0.85	99.27	<0.5	<0.5	11
0.07	0.6	0.01	<0.02	0.3	94.78	<0.5	<0.5	46
0.08	0.2	<0.01	<0.02	-2.86	86.01	<0.5	2.3	165
<0.05	<0.2	<0.01	<0.02	0.67	99.21	<0.5	<0.5	1
0.57	0.2	<0.01	<0.02	1.6	101.39	<0.5	<0.5	1
6.57	0.9	0.1	0.13	6.9	99.6	<0.5	<0.5	15
4.56	0.3	0.01	0.86	3.6	100	2.2	<0.5	22
0.08	0.6	<0.01	0.05	2.35	100.77	<0.5	<0.5	6
0.33	0.8	<0.01	0.03	3.57	100.45	<0.5	<0.5	15
0.09	0.3	0.01	0.22	2.83	100.35	<0.5	<0.5	2
0.29	<0.2	0.03	1.79	3.53	101.39	<0.5	<0.5	2
0.1	0.6	<0.01	0.12	1.65	100.77	<0.5	<0.5	4

ME-MS42	ME-MS42	ME-MS42	ME-MS42	OA-GRA05	TOT-ICP06	ME-4ACD8	ME-4ACD8	ME-4ACD8
Sb	Se	Te	Tl	LOI	Total	Ag	Cd	Co
ppm	ppm	ppm	ppm	%	%	ppm	ppm	ppm
1.18	1.8	0.06	0.05	44.6	99.75	<0.5	0.7	10
0.95	2.7	0.06	0.14	70.5	98.75	<0.5	0.7	4
0.85	0.8	0.03	0.13	9.86	100.35	<0.5	<0.5	4
0.13	0.7	0.02	0.02	15.7	99.86	<0.5	<0.5	5
1.52	1	0.02	0.03	6.36	99.69	<0.5	1.3	11
0.33	1.4	0.16	0.83	18.6	99.13	<0.5	1.5	14
14.3	3	0.04	17.5	12.35	99.13	<0.5	0.6	11
79.9	11.9	0.03	0.65	6.23	100.26	<0.5	0.6	2
0.72	0.2	0.02	0.02	0.51	101.84	<0.5	<0.5	<1
0.19	0.4	0.02	0.15	0.46	100.69	<0.5	<0.5	1
0.36	0.8	0.02	0.15	0.77	99.96	<0.5	0.8	<1
0.25	0.8	0.08	0.02	3.85	99.36	<0.5	<0.5	15

0.27	1.2	0.07	0.02	1.39	99.24	<0.5	<0.5	40
0.06	<0.2	0.03	0.02	0.4	98.58	<0.5	<0.5	<1
0.05	<0.2	0.03	0.02	0.27	101.07	<0.5	<0.5	1
0.44	<0.2	0.02	0.06	0.69	98.12	<0.5	<0.5	<1
21.4	1	0.75	0.04	2.15	88.83	0.9	1.1	3
0.05	0.7	0.03	0.58	1.25	98.61	<0.5	<0.5	16
0.08	<0.2	0.06	<0.02	8.09	98.35	<0.5	0.6	96
0.15	0.2	0.04	0.13	1.09	99.4	<0.5	<0.5	2
0.09	<0.2	0.03	<0.02	0.93	101.07	<0.5	<0.5	<1
0.27	0.2	0.05	0.02	0.75	98.3	<0.5	<0.5	4
0.05	<0.2	0.02	0.03	0.3	99.32	<0.5	<0.5	<1
<0.05	<0.2	0.02	0.07	0.56	101.26	<0.5	<0.5	<1
2.48	4.1	5.08	0.08	16	80.53	5.8	<0.5	<1
0.05	0.2	0.02	<0.02	0.68	98.06	<0.5	<0.5	<1
1.49	0.3	0.02	0.04	0.46	100.23	<0.5	<0.5	<1
0.12	<0.2	0.06	0.03	1.11	100.29	<0.5	<0.5	<1
<0.05	0.2	0.02	<0.02	0.93	99.72	<0.5	<0.5	<1
<0.05	0.2	0.02	0.19	0.65	99.85	<0.5	<0.5	<1
0.05	0.9	0.03	0.08	0.57	98.02	<0.5	<0.5	42
0.1	1.1	0.02	0.08	93.6	99.68	<0.5	<0.5	1
0.36	1.6	0.05	0.67	22	99.68	<0.5	<0.5	<1
2.23	6.3	0.04	0.07	10.7	100.1	<0.5	<0.5	3
0.05	0.2	0.02	0.02	2.01	99.71	<0.5	<0.5	24
<0.05	0.4	0.02	0.02	1.11	98.62	<0.5	<0.5	1
<0.05	0.4	0.01	0.19	2.54	98.6	<0.5	<0.5	49
<0.05	<0.2	<0.01	0.02	2.17	99.28	<0.5	<0.5	25
<0.05	0.4	0.01	0.03	0.35	100.13	<0.5	<0.5	1
0.24	12	0.01	0.32	2.11	100.67	<0.5	<0.5	<1
<0.05	0.6	0.01	0.05	1.38	98.02	<0.5	<0.5	1
0.05	0.2	0.01	0.02	1.17	99.15	<0.5	<0.5	<1
0.06	0.3	0.01	0.19	0.81	100.79	<0.5	<0.5	<1
<0.05	0.7	0.01	<0.02	1.35	99.64	<0.5	<0.5	<1
0.08	<0.2	0.02	0.03	0.48	100.7	<0.5	<0.5	<1
0.25	1	0.01	0.2	4.97	100.24	<0.5	<0.5	2
0.13	0.7	0.01	0.09	5.67	100.41	<0.5	<0.5	<1
1.98	35.7	0.05	0.32	6.68	100.18	<0.5	<0.5	2
0.05	<0.2	<0.01	0.03	0.43	100.46	<0.5	<0.5	<1
<0.05	0.4	0.03	0.1	0.29	99.46	<0.5	<0.5	<1
0.05	<0.2	0.01	0.65	0.39	101.14	<0.5	<0.5	<1
0.09	0.2	0.01	0.45	2.15	99.01	<0.5	<0.5	4
<0.05	0.3	<0.01	0.03	0.43	100.23	<0.5	<0.5	<1
<0.05	<0.2	0.02	0.05	0.94	98.55	<0.5	<0.5	<1
<0.05	<0.2	0.01	0.85	2.23	99.25	<0.5	<0.5	<1
1.22	1.4	<0.01	0.38	2.59	99.74	<0.5	<0.5	4
0.05	0.3	0.01	0.11	9.28	99.05	<0.5	<0.5	7
0.05	0.8	0.03	0.48	10.2	98.46	<0.5	<0.5	31
<0.05	1.6	0.01	0.08	39.9	99.34	<0.5	0.8	<1
<0.05	<0.2	0.01	0.11	7.06	100.84	<0.5	<0.5	3
0.09	<0.2	0.01	0.16	3.78	99.9	<0.5	<0.5	8
0.06	0.8	0.01	0.08	6.75	100.39	<0.5	<0.5	5
<0.05	0.5	0.02	0.05	1.84	99.2	<0.5	<0.5	24
<0.05	0.4	<0.01	<0.02	0.69	98.46	<0.5	<0.5	20
0.29	0.7	0.01	0.02	0.42	98.94	<0.5	<0.5	<1
1.33	2.1	0.02	0.03	3.62	101.35	<0.5	<0.5	<1
0.23	<0.2	0.02	0.02	0.49	99.68	<0.5	<0.5	19
0.18	0.2	0.01	0.02	1.11	99.77	<0.5	<0.5	3

0.58	4.4	0.23	0.04	5.47	98.21	0.7	<0.5	818
0.23	1.6	0.03	0.07	4.21	98.21	<0.5	<0.5	13
0.08	0.8	0.01	0.07	0.81	100.31	<0.5	<0.5	<1
<0.05	<0.2	0.01	0.12	0.6	98.15	<0.5	<0.5	<1
0.05	2.5	0.01	0.04	0.84	99.88	<0.5	1.3	<1
0.06	1.7	0.03	0.05	0.94	99.22	<0.5	<0.5	13
0.4	2.4	0.02	0.11	2.65	101.49	<0.5	<0.5	11
0.07	0.2	0.02	0.1	0.69	100.6	<0.5	<0.5	1
<0.05	0.6	0.01	0.06	3.41	99.02	<0.5	<0.5	27
<0.05	0.4	0.01	0.09	4.5	98.26	<0.5	<0.5	2
0.12	2.6	0.63	<0.02	5.8	99.44	<0.5	<0.5	46
0.1	0.5	0.03	0.02	1.82	101.36	<0.5	<0.5	<1
<0.05	1.2	0.01	<0.02	42.8	100	<0.5	1	<1
0.1	1	0.02	0.08	14.05	99.8	<0.5	<0.5	7
0.07	<0.2	0.01	<0.02	1.27	100.87	<0.5	<0.5	<1
0.11	0.2	0.03	0.03	3.83	101.13	<0.5	<0.5	1
0.05	21.1	0.03	0.04	5.78	99.4	<0.5	0.9	<1
<0.05	1.8	0.03	0.04	14.45	100.57	<0.5	<0.5	4
1.24	2.4	0.03	0.31	8.59	99.4	<0.5	<0.5	6
0.11	0.2	0.02	<0.02	0.46	101.44	<0.5	<0.5	<1
4.32	19.2	0.14	0.57	5.63	99.49	3.1	5.8	126
0.21	1.2	0.02	0.04	1.07	101.03	<0.5	<0.5	<1
0.41	1.1	0.02	0.4	1.02	100.39	<0.5	<0.5	1
0.11	0.9	0.02	0.06	0.65	100.74	<0.5	<0.5	<1
0.1	1.7	0.01	0.36	0.56	100.39	<0.5	<0.5	2
0.28	1.3	0.01	0.05	1.13	100.29	<0.5	<0.5	<1
0.07	0.4	0.01	<0.02	0.25	100.92	<0.5	<0.5	<1
0.17	0.3	0.01	0.04	3.9	99.89	<0.5	<0.5	30
0.41	0.4	0.01	<0.02	0.76	98.92	<0.5	<0.5	<1
0.29	0.4	0.01	<0.02	1.3	100.29	<0.5	<0.5	2
16.1	0.7	0.07	0.02	4.23	100.62	<0.5	<0.5	15
1.41	1.1	0.01	0.04	7.71	98.54	1	<0.5	20
0.29	0.5	0.02	0.03	2.19	98.12	<0.5	<0.5	23
5.5	7.5	0.04	0.03	7.87	84.49	37.6	<0.5	7
2.4	0.8	0.02	0.04	1.18	100.03	<0.5	<0.5	2
1.65	1.6	0.05	0.04	1.96	101.93	0.6	<0.5	3
1.36	1.4	0.04	<0.02	1.22	100.43	<0.5	<0.5	<1
0.1	0.8	0.01	0.02	0.8	99.26	<0.5	<0.5	<1
0.43	3.6	0.33	<0.02	3.4	99.3	34.9	2.9	12
0.05	0.7	0.03	0.03	1.25	100.17	<0.5	<0.5	25
0.51	0.5	0.01	0.03	1.42	101.22	<0.5	<0.5	4
0.32	0.2	0.02	<0.02	1.48	98.09	<0.5	<0.5	5
0.11	0.2	0.02	0.02	2.65	98.62	<0.5	<0.5	22
0.18	0.4	0.01	0.02	2.9	99.79	<0.5	<0.5	17
0.08	0.3	0.02	0.02	0.42	101.85	<0.5	<0.5	<1
0.22	0.6	0.01	<0.02	0.41	102	<0.5	<0.5	<1
0.37	0.7	<0.01	0.04	0.61	100.24	<0.5	<0.5	<1
0.38	3.1	1.23	<0.02	0.91	100.12	0.9	<0.5	2
0.05	1.7	0.01	<0.02	0.32	99.2	<0.5	<0.5	<1
0.16	0.5	0.01	0.02	0.52	101.84	<0.5	<0.5	<1
0.25	0.6	0.01	0.03	3.05	99.98	<0.5	<0.5	18
0.11	0.7	0.01	0.02	0.45	100.07	<0.5	<0.5	<1
0.13	0.8	0.01	0.02	0.27	100.78	<0.5	<0.5	2
0.07	<0.2	<0.01	0.19	0.62	101.68	<0.5	<0.5	3
0.13	1.1	<0.01	0.02	0.29	101.41	<0.5	<0.5	<1
0.07	0.7	<0.01	0.04	0.6	101.67	<0.5	<0.5	<1

0.08	<0.2	<0.01	<0.02	0.32	99.81	<0.5	<0.5	<1
0.17	0.4	0.01	0.02	1.18	98.13	<0.5	<0.5	3
0.07	<0.2	<0.01	0.04	0.53	101.84	<0.5	<0.5	<1
0.15	3	<0.01	0.12	0.38	101.24	<0.5	<0.5	<1
0.09	<0.2	<0.01	<0.02	0.23	101.61	<0.5	<0.5	<1
0.18	0.2	0.02	0.05	3.46	100.64	<0.5	<0.5	67
0.29	0.3	1.52	0.06	5.85	98.88	8.3	0.9	69
0.61	24.2	3.23	<0.02	6.77	97.55	3.3	<0.5	137
1.12	0.5	0.06	<0.02	9.68	99.14	<0.5	<0.5	10
0.1	0.6	0.07	<0.02	1.3	101.11	<0.5	<0.5	6
0.05	<0.2	0.01	<0.02	0.55	98.77	<0.5	<0.5	<1
0.09	0.4	0.01	0.02	2.1	100.79	<0.5	<0.5	24
0.13	4	0.12	<0.02	1.77	100.66	<0.5	0.6	82
0.06	1.6	0.17	0.05	3.03	100.76	1.9	<0.5	49
<0.05	1	0.01	0.14	0.4	101.27	<0.5	<0.5	26
0.05	<0.2	<0.01	0.05	0.77	100.02	<0.5	<0.5	1
<0.05	0.3	0.01	0.11	0.41	101.75	<0.5	<0.5	1
<0.05	<0.2	<0.01	<0.02	0.56	100.68	<0.5	<0.5	<1
0.13	<0.2	0.02	<0.02	0.73	99.19	<0.5	<0.5	3
0.81	2	0.01	0.03	11.75	99.61	<0.5	0.5	78
0.53	10.4	0.18	<0.02	6.98	91.07	<0.5	<0.5	33
3.26	5.5	0.28	0.04	8.95	90.95	<0.5	1	36
2.35	6.8	0.05	0.24	7.07	98.19	<0.5	<0.5	5
0.93	0.4	0.04	0.03	0.4	98.62	<0.5	<0.5	1

ME-MS42	ME-MS42	ME-MS42	ME-MS42	OA-GRA05	ME-XRF26	ME-4ACD8	ME-4ACD8	ME-4ACD8
Sb	Se	Te	Tl	LOI 1000	Total	Ag	Cd	Co
ppm	ppm	ppm	ppm	%	%	ppm	ppm	ppm
0.16	2.4	0.02	0.38	10.14	99.35	<0.5	5	5
2.65	6.2	0.06	0.44	8.95	102.85	2.8	22.2	<1
1.19	9.3	0.03	5.66	5.07	99.64	2.9	84.3	<1
1.55	9	0.03	0.27	3.52	99.73	1.1	26.7	<1
9.04	95.9	0.37	0.09	9.57	100.7	8.7	21.8	2

ME-MS42	ME-MS42	ME-MS42	ME-MS42	OA-GRA05	TOT-ICP06	ME-4ACD8	ME-4ACD8	ME-4ACD8
Sb	Se	Te	Tl	LOI	Total	Ag	Cd	Co
ppm	ppm	ppm	ppm	%	%	ppm	ppm	ppm
0.27	0.5	<0.01	0.02	0.56	101.7	<0.5	<0.5	1
0.35	<0.2	0.08	0.03	0.47	99.75	<0.5	<0.5	2

0.33	<0.2	<0.01	<0.02	0.55	99.63	<0.5	0.6	2
3.58	6.9	2.91	0.32	12	98.35	<0.5	<0.5	1050
4.51	1	0.09	0.24	2.38	99.69	<0.5	<0.5	15
0.46	0.3	0.26	0.03	1.66	99.84	<0.5	<0.5	22
0.27	1.1	0.01	0.02	1.77	99.49	<0.5	<0.5	11
0.12	<0.2	0.54	<0.02	0.14	99.91	<0.5	<0.5	1
0.1	<0.2	0.01	0.04	3.66	99.64	<0.5	<0.5	6
0.07	6.2	0.26	<0.02	1.43	101.8	0.8	<0.5	124
0.05	<0.2	0.02	<0.02	-0.22	99.52	<0.5	<0.5	91
0.05	<0.2	<0.01	0.02	0.18	99.95	<0.5	<0.5	84
0.05	<0.2	<0.01	<0.02	8.92	99.06	<0.5	<0.5	24
0.24	1.6	0.96	<0.02	0.8	99.36	1.4	<0.5	20
0.11	0.2	<0.01	0.49	0.44	100.58	<0.5	<0.5	1
0.06	0.4	<0.01	0.02	1.21	99.11	<0.5	<0.5	9
0.11	3.7	0.01	0.11	2.1	98.3	<0.5	0.6	22
0.25	105.5	40.9	0.02	4.37	98.82	6.9	<0.5	45
0.2	1.7	0.1	0.12	1.82	99.82	<0.5	<0.5	3
0.07	0.7	0.02	0.02	1.8	99.77	<0.5	<0.5	16
0.05	0.4	0.08	<0.02	5.18	100.08	<0.5	<0.5	5
0.09	1.1	<0.01	<0.02	1.88	100.4	<0.5	<0.5	8
0.06	0.8	0.02	0.02	1.89	100.09	<0.5	<0.5	16
0.1	0.4	0.02	<0.02	1.2	99.69	<0.5	<0.5	3
0.05	<0.2	<0.01	0.04	0.21	100.01	<0.5	<0.5	1
<0.05	0.8	<0.01	0.03	0.61	100.29	<0.5	<0.5	3
0.37	0.4	0.01	0.06	13.3	99.03	<0.5	<0.5	<1
9.24	5.5	0.07	0.39	7.1	99.09	1	0.5	<1
1.07	6.9	0.05	0.76	7.87	98.39	0.7	1.4	3
0.69	10	0.1	1.36	8.92	99.32	1.7	0.8	7
3.63	14.4	0.22	0.54	23.4	96.05	3.2	2.7	125
0.23	0.4	0.01	0.26	23	98.66	<0.5	<0.5	7
0.18	0.6	0.01	0.26	8.48	100.73	<0.5	<0.5	20
0.58	0.4	0.04	0.44	11.95	100.19	<0.5	<0.5	6
0.55	0.5	0.04	0.55	7.61	101.88	<0.5	<0.5	9
0.25	0.3	0.01	0.1	13.15	92.59	<0.5	<0.5	1
0.27	1.7	<0.01	0.12	3.21	90.77	1.3	2.4	57
0.44	0.7	<0.01	0.06	4.88	101.7	<0.5	<0.5	7
0.83	2	0.07	0.4	7.5	101.03	<0.5	<0.5	14
0.68	0.8	0.02	0.27	10.4	101.13	<0.5	<0.5	8
0.71	2.3	0.03	0.13	24.2	100.78	<0.5	<0.5	4
4.5	0.5	0.01	0.02	0.57	101.77	<0.5	1.5	40
1.2	0.3	0.01	0.27	0.64	101.39	<0.5	<0.5	24
0.69	0.8	0.03	0.24	2.37	100.63	<0.5	<0.5	14
0.49	1.5	<0.01	0.14	2.63	101.74	<0.5	<0.5	9
0.83	1.1	0.06	0.22	21	99.92	<0.5	0.8	5
0.11	0.7	0.01	<0.02	98	99.84	<0.5	<0.5	2
0.28	0.2	0.01	<0.02	0.46	100.21	<0.5	<0.5	<1
0.42	<0.2	<0.01	<0.02	7.81	100.61	<0.5	<0.5	<1
1.39	<0.2	<0.01	<0.02	2.07	100.36	<0.5	<0.5	<1
0.13	0.4	0.02	0.03	43.4	100.05	<0.5	<0.5	<1
0.1	0.5	0.01	0.27	11.25	101.78	<0.5	<0.5	2
0.12	<0.2	<0.01	0.11	1.21	100.43	<0.5	<0.5	3
0.08	0.4	<0.01	0.13	1.25	100.5	<0.5	<0.5	16
0.07	<0.2	<0.01	0.06	4.85	100.72	<0.5	<0.5	<1
0.08	0.5	<0.01	0.05	2.59	101.68	<0.5	<0.5	1
0.11	0.7	0.01	<0.02	45.4	98.22	<0.5	<0.5	<1
2.25	7.4	0.04	0.05	5.22	95.97	3.3	9.3	<1

4.87	7.4	0.04	0.74	4.35	99.84	1.2	<0.5	15
0.14	1.5	<0.01	0.22	33.6	99.68	<0.5	6.1	<1
0.17	0.6	<0.01	0.13	1.74	100.15	<0.5	<0.5	5
0.13	0.4	0.01	0.11	4.09	100.57	<0.5	<0.5	8
0.13	0.6	<0.01	0.03	0.48	100.35	<0.5	<0.5	6

ME-MS42	ME-MS42	ME-MS42	ME-MS42	OA-GRA05	TOT-ICP06	ME-4ACD8	ME-4ACD8	ME-4ACD8
Sb	Se	Te	Tl	LOI	Total	Ag	Cd	Co
ppm	ppm	ppm	ppm	%	%	ppm	ppm	ppm
0.1	0.4	0.01	0.18	6.99	101.35	<0.5	<0.5	1
0.41	7.9	0.02	0.7	17.6	100.53	<0.5	<0.5	4
0.49	2.2	0.02	0.29	15.85	100.76	<0.5	<0.5	2
0.17	0.4	0.01	0.18	3.57	101.38	<0.5	<0.5	3
0.29	0.7	0.01	0.08	10.35	100.71	<0.5	<0.5	3
0.21	0.5	0.01	0.1	7.55	101.47	<0.5	<0.5	3
0.16	0.6	0.03	0.26	10.75	101.2	<0.5	<0.5	3
0.2	0.8	<0.01	0.09	8.12	100.83	<0.5	<0.5	2
0.75	0.5	0.01	1.38	8.65	101.41	<0.5	<0.5	<1
0.17	0.7	<0.01	0.25	9.18	100.97	<0.5	<0.5	5
0.15	0.8	0.02	0.13	17.8	99.49	<0.5	<0.5	1
0.08	0.2	<0.01	0.04	14.2	100.14	<0.5	<0.5	1
0.15	0.5	0.01	0.26	14	99.97	<0.5	<0.5	4
0.27	0.3	0.01	0.33	5.93	100.16	<0.5	<0.5	4
<0.05	0.4	0.01	0.18	8.81	100.91	<0.5	<0.5	3
0.39	0.7	0.02	0.98	14.05	100.36	<0.5	<0.5	1
0.07	0.6	0.02	0.76	11.25	100.26	<0.5	<0.5	4
0.08	0.5	0.02	0.23	8.11	99.98	<0.5	<0.5	2
0.13	0.2	0.01	0.11	6.7	100.28	<0.5	<0.5	13
<0.05	0.4	<0.01	0.04	1.94	99.96	<0.5	<0.5	18
0.91	1.1	0.09	0.36	2.66	98.39	0.6	1.1	15
0.39	1.2	0.06	0.46	4.12	99.08	<0.5	<0.5	4

340	85	5.5	450	50	130	395		130
ME-4ACD8	ME-4ACD8	ME-4ACD8	ME-4ACD8	ME-4ACD8	ME-4ACD8	ME-4ACD8	Cu-OG62	ME-MS42
Cu	Li	Mo	Ni	Pb	Sc	Zn	Cu	Sc
ppm	ppm	ppm	ppm	ppm	ppm	ppm	%	
3	10	1	2	15	4	74		
28	20	<1	31	22	9	60		
520	<10	2	22	103	2	120		
123	10	1	20	313	44	1865		
304	<10	<1	103	<2	35	45		
11	<10	1	143	7	20	12		
6	10	<1	<1	<2	1	19		
69	<10	2	20	<2	1	81		
227	20	9	11	7	2	51		
39	10	2	66	28	21	1065		
2580	10	3	147	<2	20	43		
34	10	<1	7	11	4	39		
9	10	1	9	<2	2	23		
20	20	18	1	9	2	22		
18	30	49	9	21	6	41		
9	20	15	1	9	2	17		
11	10	3	<1	17	2	11		
10	<10	5	<1	12	1	10		
11	30	1	2	66	2	22		
11	20	<1	5	<2	<1	8		
17	30	<1	4	16	5	83		
16	<10	1	6	19	4	136		
16	10	4	3	8	2	33		
56	10	4	9	5	1	21		
10	10	<1	3	14	2	15		
8	<10	<1	<1	4	1	8		
36	20	1	30	<2	2	25		
4340	<10	19	9	8	1	21		
35	<10	<1	<1	<2	<1	17		
9	30	<1	5	<2	2	13		

ME-4ACD8	ME-4ACD8	ME-4ACD8	ME-4ACD8	ME-4ACD8	ME-4ACD8	ME-4ACD8	Cu-OG62
Cu	Li	Mo	Ni	Pb	Sc	Zn	Cu
ppm	ppm	ppm	ppm	ppm	ppm	ppm	%
64	<10	<1	74	10	40	118	
1	<10	<1	36	14	5	<2	
2	10	<1	373	4	16	6	
<1	<10	<1	17	7	<1	3	
5	<10	<1	1010	2	9	34	
1	10	<1	394	9	41	10	
<1	<10	<1	932	5	18	48	
1	<10	<1	13	61	12	<2	
1	10	<1	56	40	15	5	
1	<10	<1	261	2	55	2	
<1	20	<1	78	28	13	13	
<1	<10	<1	<1	15	3	<2	
<1	30	<1	<1	37	<1	19	
6	<10	2	231	3	6	37	
102	<10	6	19	15	<1	15	
1	<10	<1	1	30	<1	8	
5	<10	<1	3	19	1	11	
12	20	<1	<1	4	<1	3	
2	<10	<1	8	17	1	9	
5	<10	1	9	3	2	7	
157	30	<1	102	12	36	172	
213	<10	35	22	3	4	8	
89	<10	1	11	2	1	3	
2	<10	1	1	2	<1	<2	
2	40	<1	2	26	3	10	
1	10	<1	2	4	4	13	
30	280	<1	144	5	40	209	
6	10	4	23	3	<1	35	
1	10	<1	6	6	29	8	
786	10	52	29	197	19	254	
1415	10	16	476	84	7	920	
336	<10	2	70	3	5	34	
442	<10	<1	18	12	9	89	
7	<10	<1	378	9	11	38	
6	<10	<1	2	9	<1	10	
2	<10	<1	29	9	4	6	
1	<10	<1	1150	3	19	50	
2	<10	<1	13	15	3	2	
2	20	<1	1230	<2	21	21	
2	20	<1	8	20	5	30	
1	<10	<1	2	36	2	4	
12	10	<1	11	2	1	18	
9	10	<1	2	25	2	21	
3	<10	<1	<1	2	<1	8	
8	10	<1	<1	8	1	11	
5	7000	<1	3	48	1	47	
142	20	5	8	6	2	165	
2	2420	<1	<1	11	<1	26	

1	70	<1	<1	8	<1	27
1	<10	<1	2	12	9	19
3	10	34	13	12	6	23
2	10	<1	1	9	2	30
21	50	<1	24	21	10	95
20	10	1	17	34	7	96
8	10	<1	23	14	5	119
10	10	<1	9	13	5	82
11	20	1	43	28	5	71
13	20	1	20	30	9	33
4	10	<1	10	11	2	13
32	<10	<1	393	4	31	81
2	<10	<1	1	30	<1	<2
8	<10	<1	1	21	1	2
61	20	<1	146	11	30	120
5	10	1	7	<2	7	3
3	<10	<1	1	32	1	45
148	40	11	35	14	9	57
5	20	<1	1	32	7	146
2	10	<1	13	<2	1	6
20	<10	<1	11	4	1	40
62	<10	2	46	3	26	199
17	<10	3	99	6	20	497
1	10	<1	<1	<2	<1	9
16	<10	3	3	<2	<1	10
1930	<10	12	127	152	1	264
788	<10	5	200	36	1	636
9	10	<1	8	18	4	124
25	30	<1	28	11	11	117
3	60	<1	<1	29	<1	134
1	80	<1	1	81	<1	204
4	20	1	1	24	3	104

ME-4ACD8	ME-4ACD8	ME-4ACD8	ME-4ACD8	ME-4ACD8	ME-4ACD8	ME-4ACD8	Cu-OG62
Cu	Li	Mo	Ni	Pb	Sc	Zn	Cu
ppm	ppm	ppm	ppm	ppm	ppm	ppm	%
24	20	2	25	33	8	80	
36	20	7	20	14	4	64	
14	20	1	17	13	5	38	
9	20	<1	9	3	8	18	
10	30	2	38	20	22	42	
7	10	<1	27	10	9	20	
29	10	10	13	14	6	343	
17	10	13	8	42	3	77	
1	30	<1	2	2	<1	<2	
4	10	<1	1	116	1	9	
3	60	2	<1	49	16	45	
4620	10	1	64	<2	8	38	

>10000	<10	2	12	58	3	7	1.085
30	<10	<1	2	3	<1	116	
50	<10	<1	1	49	7	4	
33	120	<1	<1	8	2	106	
7	<10	1	5	40	<1	6	
22	40	<1	43	29	12	89	
7	<10	<1	2040	<2	11	132	
4	<10	<1	18	16	<1	20	
4	<10	2	2	<2	<1	<2	
43	<10	<1	17	13	<1	21	
2	10	<1	<1	6	<1	17	
2	40	<1	<1	7	<1	24	
3	<10	1	1	16	<1	26	
2	<10	<1	<1	7	4	24	
4	20	9	4	<2	1	16	
3	10	<1	2	6	2	4	
2	<10	<1	2	4	5	4	
4	10	<1	<1	29	2	24	
140	<10	<1	90	<2	39	111	
7	<10	<1	15	3	1	53	
17	30	2	6	21	9	19	
35	10	2	22	38	5	60	
14	10	1	20	8	3	52	
2	10	<1	<1	26	2	3	
28	20	<1	105	3	38	99	
6	20	<1	26	2	23	55	
2	10	<1	1	5	1	3	
15	10	6	15	7	9	19	
3	10	<1	1	25	3	17	
5	<10	<1	1	7	1	9	
5	<10	<1	<1	41	1	18	
4	10	<1	1	31	4	4	
7	<10	1	2	3	1	6	
14	10	4	10	8	3	64	
5	10	4	1	18	1	6	
28	10	21	5	20	3	101	
2	20	<1	2	7	<1	5	
2	40	<1	<1	6	1	34	
1	20	<1	<1	23	<1	6	
2600	130	<1	5	36	<1	90	
9	10	<1	<1	<2	<1	3	
6	50	<1	6	4	<1	28	
18	270	<1	4	2	<1	34	
20	20	39	21	26	8	21	
19	40	<1	21	7	8	32	
112	100	<1	93	19	25	114	
24	10	<1	7	5	3	16	
18	20	<1	29	12	6	26	
13	20	<1	13	8	7	33	
22	10	<1	12	12	7	53	
42	10	<1	142	30	12	94	
28	10	<1	82	14	17	78	
7	10	<1	3	2	1	6	
>10000	10	2	2	5	8	7	3.23
397	<10	<1	1	8	2	4	
585	20	<1	9	2	5	10	

1850	50	1	54	<2	13	26	
2200	60	<1	15	6	17	21	
34	<10	<1	1	38	1	8	
30	10	<1	<1	20	1	13	
12	10	<1	3	4	9	24	
10	30	<1	7	10	8	218	
60	10	1	23	17	12	34	
11	10	<1	2	7	2	16	
70	20	<1	80	5	15	67	
9	10	<1	3	5	2	44	
19	<10	48	8	3	3	4	
12	10	<1	1	4	1	7	
36	<10	<1	3	<2	<1	3	
32	40	1	12	10	8	40	
17	20	1	2	<2	<1	5	
7	10	3	2	9	2	10	
33	20	8	9	71	6	21	
30	20	2	6	24	9	36	
26	10	14	14	12	2	74	
5	10	2	1	<2	1	2	
14	10	38	52	11	1	93	
6	10	4	<1	<2	<1	4	
4	10	<1	4	73	9	54	
1	10	<1	<1	16	3	16	
5	30	<1	1	22	5	92	
5	10	<1	<1	19	3	16	
1	<10	<1	2	2	4	25	
2	30	<1	81	<2	26	140	
1	<10	<1	<1	<2	5	5	
63	<10	<1	3	10	20	27	
593	<10	4	16	14	10	66	
5	<10	9	40	<2	17	96	
451	10	<1	45	10	19	86	
>10000	100	24	10	97	5	23	11.65
679	110	2	5	12	4	21	
1640	90	2	11	15	3	19	
40	10	<1	3	8	20	9	
50	<10	<1	<1	4	5	16	
7740	<10	5	4	1150	<1	79	
104	10	<1	27	6	35	132	
141	<10	3	6	8	3	18	
54	<10	<1	3	4	29	6	
76	10	<1	55	3	16	79	
57	20	<1	19	5	18	90	
11	<10	<1	<1	13	2	4	
10	<10	<1	<1	26	1	6	
5	<10	<1	<1	30	3	5	
187	<10	21	4	60	<1	3	
5	<10	<1	<1	44	10	5	
5	20	<1	<1	49	6	18	
15	30	<1	21	<2	18	81	
6	<10	<1	<1	43	8	4	
2	<10	<1	<1	152	2	80	
7	<10	<1	2	16	2	18	
8	<10	<1	<1	25	11	12	
4	<10	<1	1	16	1	14	

1	<10	1	1	2	<1	4	
3	<10	1	<1	6	1	13	
1	<10	<1	<1	29	<1	<2	
1	<10	<1	<1	64	4	5	
1	<10	<1	<1	25	2	2	
97	<10	<1	245	2	40	57	
>10000	10	1	778	6	17	41	3.33
6500	10	1	790	6	36	114	
295	110	<1	99	19	65	44	
143	<10	<1	8	13	16	11	
34	<10	<1	3	19	<1	6	
87	10	<1	36	6	35	60	
1520	<10	<1	26	12	22	19	
3200	10	<1	53	<2	31	115	
43	<10	<1	12	6	26	174	
29	<10	<1	3	17	1	83	
15	<10	<1	6	8	1	29	
5	<10	<1	<1	12	<1	5	
231	10	<1	8	2	1	7	
81	<10	12	104	3	17	100	
>10000	<10	3	499	21	1	4	9.3
>10000	10	8	80	49	4	9	1.335
170	20	1	31	85	5	49	
42	<10	<1	4	10	3	5	

ME-4ACD8	ME-4ACD8	ME-4ACD8	ME-4ACD8	ME-4ACD8	ME-4ACD8	ME-4ACD81	ME-MS42
Cu	Li	Mo	Ni	Pb	Sc	Zn	Sc
ppm	ppm	ppm	ppm	ppm	ppm	ppm	ppm
9	20	<1	16	27	6	552	4.5
15	20	1	51	10	7	644	6.3
42	10	16	31	13	5	969	4.6
25	10	18	29	12	4	362	3.7
50	60	43	154	17	8	1550	3.7

ME-4ACD8	ME-4ACD8	ME-4ACD8	ME-4ACD8	ME-4ACD8	ME-4ACD8	ME-4ACD81
Cu	Li	Mo	Ni	Pb	Sc	Zn
ppm	ppm	ppm	ppm	ppm	ppm	ppm
4	20	8	2	7	1	4
2	10	3	2	6	1	7

81	<10	3	2	90	<1	145
3770	<10	16	1590	31	5	188
1400	<10	6	42	6	8	11
688	10	7	28	2	8	11
54	<10	1	90	27	5	53
59	<10	2	2	5	<1	6
39	160	1	34	265	3	50
182	<10	3	57	6	<1	4
113	<10	1	844	<2	32	82
32	<10	<1	819	2	27	71
3	50	<1	125	3	11	74
2010	<10	1	23	344	3	54
15	10	<1	3	26	1	69
11	<10	<1	8	16	7	119
267	<10	9	9	45	49	774
1210	<10	819	2	472	<1	309
44	30	4	<1	27	7	96
25	30	1	3	3	15	84
10	30	3	<1	14	5	128
12	20	1	6	8	17	91
31	20	1	18	14	15	128
12	10	<1	<1	28	5	22
2	<10	<1	<1	14	<1	4
12	<10	<1	1	21	6	23
110	<10	1	4	12	2	93
165	<10	21	3	16	1	15
280	<10	54	30	83	10	162
45	<10	22	4	4	4	78
411	30	21	207	13	11	324
24	120	<1	25	13	7	65
18	70	<1	35	15	16	89
16	30	1	13	20	8	64
33	30	<1	26	27	10	120
4	10	<1	6	10	2	16
7	10	2	41	54	83	470
5	10	11	11	10	6	32
32	50	3	43	35	13	151
17	20	8	19	18	8	68
26	10	13	15	21	10	68
188	90	49	101	336	7	255
111	160	23	57	55	7	149
66	20	8	47	48	8	82
6	20	2	19	25	5	45
22	<10	5	18	42	8	61
4	<10	1	7	<2	<1	11
3	10	2	4	2	1	5
3	<10	1	1	7	1	2
1	10	2	2	11	2	2
1	10	<1	2	<2	3	7
5	20	1	5	24	4	42
4	10	<1	5	5	2	6
10	20	<1	45	9	9	70
5	30	<1	2	<2	1	27
1	10	<1	67	8	2	9
32	<10	1	2	3	<1	26
458	10	38	27	8	4	206

111	30	3	39	168	6	67
12	20	2	11	6	3	916
9	20	<1	7	20	5	64
41	20	<1	6	20	6	90
5	20	<1	3	18	5	70

ME-4ACD8:ME-4ACD8:ME-4ACD8:ME-4ACD8:ME-4ACD8:ME-4ACD8:ME-4ACD81

Cu	Li	Mo	Ni	Pb	Sc	Zn
ppm	ppm	ppm	ppm	ppm	ppm	ppm
5	10	3	1	30	4	53
8	30	<1	3	45	4	93
11	50	<1	4	40	5	73
6	20	<1	6	15	4	37
5	40	<1	6	19	5	49
7	20	1	7	19	4	44
7	10	1	5	14	4	30
5	30	<1	6	15	5	47
4	20	<1	3	13	4	17
8	40	<1	8	20	6	49
4	10	<1	3	15	3	27
4	20	1	4	14	2	29
10	30	<1	10	15	5	44
13	10	1	10	33	3	41
8	40	<1	10	17	3	51
10	10	2	12	29	2	58
14	20	<1	22	30	3	100
11	20	<1	11	17	5	45
21	80	<1	13	14	4	47
19	10	1	15	14	10	71
252	30	3	7	59	9	322
30	60	<1	5	158	7	111

TOTAL REEs ppm
197.51
111.41
84.89
4267.09
48.66
328.48
28.19
12.63
15.24
1388.16
47.24
78.83
45.01
49.26
309.76
53.54
50.59
38.7
204.67
6.37
256.79
197.43
129.01
53.89
108.18
123.04
61.12
62.48
48.21
40.59

113.31
145.08
95.64
7.91
10.64
272.8
46.61
1007.05
837.1
113.39
853.35
420.94
12.79
13.36
5.67
7.73
36.65
7.08
21.41
48.35
91.75
10.67
4.8
3.35
371.29
24.05
150.77
9.68
199.51
59.02
201.36
120.18
202.3
108.62
11.18
106.5
21.93
476.74
33.82
141.54
26.05
109.54
150.06
33.55
54.01
5.63
16.9
3.17

0.13
22.38
91.91
48.91
134.31
150.11
281.92
196.32
206.48
313.64
128.16
72.12
11.67
104.81
276.02
103.96
262.1
40.35
332.54
15.91
326.67
167.63
27.77
16.91
2.49
102.18
19.52
355.55
389.62
380.88
301.17
451.05

159.78
90.82
139.95
47.1
261.65
221.52
267.19
124.08
9.72
135.75
219.41
144.02

28.02
19.88
75.83
19.99
61.83
258.62
54.53
64.43
6
23.31
8.2
3.83
0.97
88.45
36.96
191.25
60.18
106.97
136.19
29.92
113.37
310.44
56.7
97.8
118.73
82.92
284.26
72.71
218.65
94.06
182.85
908.82
55.49
107.73
77.64
83.61
4.18
63.64
6.24
20.96
17.81
5.08
0.23
690.16
87.13
216.34
184.85
161.8
117.37
158.38
814.8
300.1
138.14
272.5
63.94
107.68

420.64
1264.2
108.79
17.29
401.56
997.01
1437.28
80.87
71.55
115.4
25.41
27.23
61.62
229.62
25.28
67.93
2025.7
176.04
68.18
27.65
90.94
15.78
1165.63
471.17
409.88
293.99
28.57
84.95
132.99
183.4
55.72
95.57
102.11
63.22
124.95
73.63
228.66
166.16
2.3
185.52
220
166.31
100.76
135.41
42.18
62.93
139.95
12.63
178.47
267.24
153.69
216.64
76.56
8.66
629.33
253.66

13.85
35.01
8.66
126.26
48.51
71.91
68.51
65.73
89.18
203.02
5.15
168.8
156.95
154.96
400.41
68.64
1726.64
29.27
15.08
96.88
17.89
91.81
703.36
133.35

408.85
1232.63
740.43
2008.44
187.36

TOTAL REEs ppm
89.11
73.37

14.34
49.06
112.25
76.97
37.13
1.46
19.36
2.19
60.97
40.91
65.08
10.2
66.64
284.01
1578.08
10.99
459.61
232.15
285.39
408.79
603.2
136.93
11.15
426.03
27.79
29.01
190.65
48.12
66.64
108.79
209.53
37.57
150.1
88.44
2339.69
140.92
300.42
199.26
348.21
257.07
177.83
230.29
118.49
206.66
8.43
43.49
62.46
74.58
19.88
175.41
115.15
244.5
39
131.08
3.25
408.29

697.41
68.7
207.54
223.35
206.97

TOTAL REEs ppm
389.81
338.96
549.15
142.46
202.01
201.03
158.49
196.34
152.25
144.69
145.22
110.17
179.62
152.19
149.52
286.25
209.08
178.09
51.69
198.28
635.37
576.61